J. A. CHRISTIANSEN

A HYPOTHESIS ON THE INTERACTION BETWEEN PERMANENT MOLECULAR QUADRUPOLES AND POLARIZED PHOTONS

Synopsis

It is assumed that a photon has an electrical field vector rotating in a plane perpendicular to its direction of propagation and a magnetic field vector in the same plane perpendicular to the electrical one. The hypothesis is based on the discovery in 1931 by A. KASTLER and other scientists that radiation can exchange angular momentum with matter. When now a photon traverses molecules which contain pairs of screw-like arranged permanent dipoles the electrical vector becomes twisted according to the chirality of the screw.

The hypothesis is tested on substances whose absolute configuration is known from other sources. In cases where there is no doubt about the chirality of the molecular quadrupole, *e.g.* *iso*-serine, the results concerning the connection between configuration and sense of optical rotation turns out to be correct. In other cases, *e.g.* serine, nothing definite can be said at present.

Application of the method to 1,2 XX-cyclohexane (X = OH or COOH) leads to a *cis-trans* assignment of the isomers which agrees with that arrived at in a preceding paper in these communications and disagrees with the currently accepted one.

In a theoretical investigation based on the then existing knowledge of quantum theory EINSTEIN[1] proved, in 1917, that radiation could exchange translational momentum with molecules. This lead him to designate the radiation as a "Nadelstrahlung". He even went so far as to state that "Kugelwellen gibt es nicht". His views were later confirmed experimentally by the discovery of the Compton-effect and it became custumary to denote the radiation corpuscles as photons.

In 1931 a number of authors, among which were the Nobel Prize winners A. KASTLER[2,3] and C. V. RAMAN[4], interpreted well established experimental evidence as meaning that photons not only had translational but also angular momentum. KASTLER and O. R. FRISCH[3] found, independently of each other, that the angular momentum had a component in the longitudinal direction but none in the transversal direction. To the writer this seems to make it natural or even necessary to assume that photons are endowed not only with mass as stated by EINSTEIN and confirmed by Compton's experiments, but that they also have some kind of structure.

As a reasonable structure the writer ventures to propose the following hypothesis: A photon posesses an electric field-vector which is perpendicular to its direction of propagation and rotates around that direction. It is therefore supposed to describe a screw surface which corresponds either to a right-handed (d-) or to a left-handed (l-) screw corresponding to the two kinds of circular polarized light. The pitch of the screws equals the wavelength of the light in question. Ordinary light is then considered to be a random mixture of d- and l-photons. In circular polarized light one of the two kinds is suppressed more or less completely. In linear polarized light d- and l- photons are pairwise coupled to each other so that the phases of their electrical vectors are always symmetric with respect to the plane of polarization. In stead of that one may just as well consider linearly polarized light as composed of photons whose electric field vectors are always in the plane of polarization and perpendicular to the direction of the light-ray,

1*

while their amplitudes oscillate. It should be remembered that the wavelength of light ordinarily used in polarimetry is roughly one thousand times as large as the cross sections of ordinary molecules. It follows from this that the phase of the rotating or oscillating electric field vector should remain nearly unchanged during the passage of a photon through a molecule provided that they do not interact with each other during the passage.

It should also be remembered that a photon can only interact with dipoles having vector-components perpendicular to the direction of its propagation. This follows from the circumstance mentioned above that it can only exchange angular momentum with the surroundings in the longitudinal but not in the transversal direction. This same circumstance makes the socalled Fischer-projection particularly well suited for discussions of the sense of optical rotation of molecules with one socalled asymmetry centre.

When now photons belonging to a linear polarized light ray pass a molecule which has a permanent dipole they may be exposed to orientating forces from the dipole and may exchange angular momentum with it. If, however, the ray has a macroscopic cross section and impinges on an ensemble of polar molecules performing independent rotational Brownian movements the orientating forces from the individual molecyles must cancel each other if the dipoles have not been regimented by an electrical field from the outside. Thus in case of molecules with only one permanent dipole there will be no net rotation of the plane of polarization when the ray passes the ensemble.

In the case of molecules which contain quadrupoles or, as we may also say, pairs of dipoles, the situation is different. We consider a dipole as a vector which points against the negative end of the dipole. A dipole around a carbon atom arises when negative electricity is displaced from the electronic cloud of an electropositive group or atom through that of the C atom unto the electronic cloud of the electronegative group or atom. This means that the vectors we have to consider roughly coincide with the edges of the classical tetrahedron. Thus, even in the case of only one asymmetric C atom, there may be two dipoles in a distance from each other. Such a pair of dipoles may be said to have the chirality of a lefthanded (*l*-) or a righthanded (*d*-) screw. The line which is perpendicular to both dipoles is the screw axis and from a figure it is easily seen whether the chirality is *d*- or *l*-. If now a photon belonging to a linear polarized ray of light traverses such a molecule its electric field vector must be twisted to the right or to the left according to whether the chirality of the quadrupole is *d*- or *l*-. But this means also that the plane of polarization is twisted either to the right or to the left. In the

former case the molecule is, by convention, designated as laevorotatory or (−), in the latter one as dextro-rotatory or (+).

The twist caused by permanent screw-like quadrupoles depends on the orientation of the screw axis relative to the direction of propagation of the photons or, which is the same, the direction of the light-ray. If the former is perpendicular to the latter the twist must be zero. But if the screw axis of the quadropole is orientated in parallel to the direction of the ray the twist has its maximum value, which is the same and has the same direction whether the photon enters the molecule from one end of the screw-axis or from the other. This means of course that there is no compensation of the twisting forces when a ray of macroscopic cross section impinges on an ensemble of molecules whose screw-like quadropoles are orientated at random, which they must be when the quadropoles are fixed relative to the skeleton of the molecule in the solution or in the gas in question when it is diluted enough to make the intermolecular forces to be of no account.

Some years ago J. H. BREWSTER[6] proposed "a useful model of optical activity" suggesting that a center of optical activity can usefully be described as a screw pattern of of electron polarizability. Patterns which can be described as left-handed screws are dextrorotatory (in the visible). He also presents empirical rules for predicting the rotatory effect of asymmetric atoms and conformations. To the present writer there is no doubt that patterns of polarizability may contribute to the optical activity of an asymmetric molecule, but it seems to him to be natural to compare the situation with that met with in the case of dielectric constants where both the permanent polarity and the polarizability of the molecule contribute to the polarization, the former one by orientation of the entire molecule in the electric field applied. Furthermore, DEBYE[7] and his numerous coworkers and followers have found by experience that so soon a molecule has a dipole-moment which can be estimated with reasonable accuracy the polraization by orientation outweighs the polarization by internal displacement of electrical charges due to the electrical field applied.

It seems therefore probable that, in cases where screwlike distinct quadrupoles are known to exist in the molecule, these must be assumed to be the main cause of the optical activity. It is only when it can be concluded from the constitution of the molecule, that the groups surrounding the active center cannot give rise to any sensible permanent quadropole that the pattern of polarizability can yield the main contribution to the rotation of the plane of polarization.

It follows that only in cases where both pairs in the quartet of groups

around the asymmetric carbon atom are known to be or can be seen to be dipoles will it be possible to predict the sense of optical rotation of the molecule. There may also be cases where intramolecular displacement of atoms or of ions tend to blur the result. But in clear-cut cases, where the dipole-moments of the two dipoles in the screwlike quadrupole are distinct the pre-edictions of the model are unambiguous and have been found to agree with knowledge concerning absolute configurations obtained from other sources. In the following a few samples shall be discussed. As well known E. FISCHER's arbitrary convention concerning the absolute configuration of glyceric alde-hyde has for many years served as basis for the assignment of configurati-ons to carbohydrates and also to a number of other organic compounds which can be prepared from that aldehyde without change of configuration. When the formula is written as (I)

$$CHO$$
$$\cdot$$
$$H \cdot C \cdot OH \qquad\qquad (I)$$
$$\cdot$$
$$CH_2OH$$
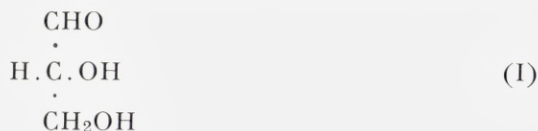
where the ligands in the horizontal line are meant to be located above the plane of the paper and those in the vertical line below the same plane, the molecule is said, according to Fischer's convention, to be a D-form. Fischer's glyceric aldehyde was dextro-rotatory, and this fact together with the assumption that the OH group is to the right is nowadays expressed by means of the symbol D (+). Many years after Fischer's time BIJVOET[8] and coworkers determined, by X-ray crystallography, the absolute configu-ration of sodium-rubidiumtartrate and thereby also that of glyceraldehyde.

Their result was that, fortunately, Fischer's convention was a true expression of the facts.

The question is, does the hypothesis discussed here yield the same result? The horizontal dipole in the D-form (I) points to the right if the direction from the positive to the negative end of the dipole is taken to be its direction. The vertical dipole is composed of two which both point outwards from the middle. According to measurements the moment of the CHO group is about $2.7 \ 10^{-18}$ electrostatic units or 2.7 D while that of the alcoholgroup is about 1.7 D. Consequently the vertical dipole points upwards. When there-fore the electric fieldvector of a photon traverses such a molecule it will be exposed to a pair of shearing forces with tend to twist it to the left and this will be the case whether the photon enters the asymmetric molecule from one end or from the other. Outside the asymmetric molecules the fieldvector may also be twisted but the 'twist'' resulting from interaction with asymmetric

or symmetric molecules must necessarily be zero by compensation as the directions of similar dipoles must be distributed at random. The plane containing the directions of the light-ray and the electrical vectors of the photons, which is the plane of polarization, must therefore as a result of all these forces be twisted to the left and the substance is then said to be dextro-rotatory or (+) in agreement with Bijvoet's result.

As another example we may mention *isoserine*. According to N. BJER-RUM[9] it is:

$$\begin{array}{c} CO_2^- \\ | \\ H.C.OH \\ | \\ CH_2NH_3^+ \end{array} \qquad \text{(II)}$$
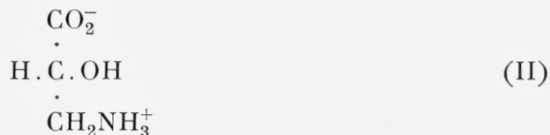
(II) shows that D-*iso*serine is D(+), in agreement with information from other sources[10].

Similarly, D-Alanine is (III)

$$\begin{array}{c} CO_2^- \\ | \\ H.C.NH_3^+ \\ | \\ CH_3 \end{array} \qquad \text{(III)}$$
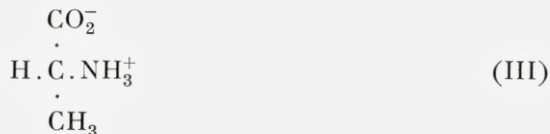
In (III) the negative end of the horizontal dipole points to the left, which shows that D-alanine is D(−) and the L-form L(+). The anion (IV) of D-lactic acid is

$$\begin{array}{c} CO_2^- \\ | \\ H.C.OH \\ | \\ CH_3 \end{array} \qquad \text{(IV)}$$

It is evident that the vertical dipole points upwards which implies that the solution of a salt with some strong base is *dextro* rotatory in agreement with results[11] arrived at in other ways. The D-lactic acid itself, however, is *laevo*rotatory[11].

This may have a rather natural explanation: like −NH₂ the group −OH is basic although not so strongly as the former. A fraction of the acid in aquous solution may therefore be in the form (V)

$$\begin{array}{c} CO_2^- \\ | \\ H.C.OH_2^+ \\ | \\ CH_3 \end{array} \qquad \text{(V)}$$
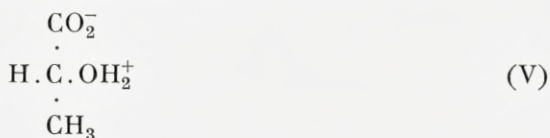
where the negative end of the horizontal dipole points to the left, which means that the substance is partially $(-)$, while a molecule of the configuration (VI) must be $(+)$.

$$
\begin{array}{c}
COOH \\
| \\
H.C.OH \\
| \\
CH_3
\end{array} \qquad \text{(VI)}
$$
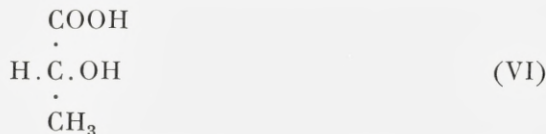
D glyceric acid is known to be $(-)$. In solution it is probably a mixture of (VII), (VIII), and (IX)

$$
\begin{array}{c}
COOH \\
| \\
H.C.OH \\
| \\
CH_2OH
\end{array} \qquad \text{(VII)}
$$

$$
\begin{array}{c}
CO_2^- \\
| \\
H.C.OH_2^+ \\
| \\
CH_2OH
\end{array} \qquad \text{(VIII)}
$$

$$
\begin{array}{c}
CO_2^- \\
| \\
H.C.OH \\
| \\
CH_2OH_2^+
\end{array} \qquad \text{(IX)}
$$
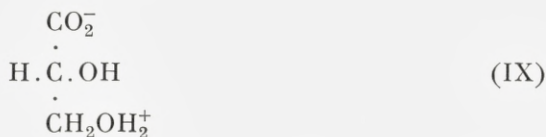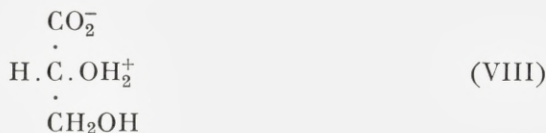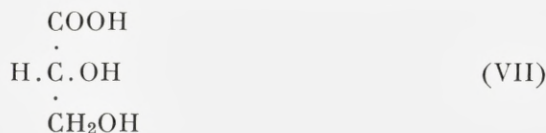
As the dipolemoment of $-COOH$ is only about 1 D while that of $-CH_2OH$ is about 1,7 D (VII) and (VIII) are both $(-)$, but (IX) must be $(+)$. Whether or not the sum of the contributions from the three forms (VII), (VIII) and (IX) will yield the result $(-)$ known from other sources cannot be told without knowledge of the specific rotations of the forms and their distribution. In this case therefore no prediction of the sense of rotation of the substance in question can be made. It can be predicted, however, that the rotation should be $(+)$ in a solution of a strong base, which agrees with the result from other sources.[13] L$(-)$ Serine serves, like glyceraldehyde, as a standard from which the absolute configurations of other optically active compounds are being derived chemically (by substitutions which do not affect the active centre). Klyne states[14] that its configuration is intercorrelated chemically with that of D$(+)$ glyceraldehyde (through a long series of reactions). On account of the CH_2OH group at the lower end of the three-carbon chain it

is, however, not by far so easy to treat by means of the present method as alanine. To this comes another difficulty: One is apt to believe that the NH_2-group is analogous to the HO-group in so far that both dipoles H_2N-CH and HO-CH point to the left with their negative ends. According to the measurements of J. ESTERMANN quoted by P. DEBYE in his book[7] this is, however, not so. He determined the dipolemoments of o, m and p amino-methylbenzoate and found that the o-compound had the smallest and the p-compound the greatest moment. This fact can hardly be interpreted otherwise than in the p-compouud the two dipoles H_2N-C and C-$COOCH_3$ must point in the same direction with their negative ends. The dipoles H_2N-CH and HO-CH must therefore point in opposite directions. The same conclusions must be drawn from the fact that p-chloroaniline and p-nitro-aniline have dipolements much greater than that of aniline itself.[15] L-serine written in the conventional way is (X). As the vertical

$$
\begin{array}{c}
COOH \\
\cdot \\
H_2N \cdot C \cdot H \\
\cdot \\
CH_2OH
\end{array}
\qquad (X)
$$
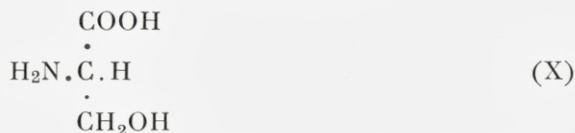
dipole in this points downwards, (X) is actually (−), but, according to N. BJERRUM[9], a more probable configuration is

$$
\begin{array}{c}
COO^- \\
\overset{+}{H_3N} \cdot C \cdot H \\
\cdot \\
CH_2OH
\end{array}
\qquad (XI)
$$

which, according to the present hypothesis should be (+), not (−).
    There is however a third possibility namely:

$$
\begin{array}{c}
COOH \\
\overset{+}{H_3N} \cdot C \cdot H \\
\cdot \\
CH_2O^-
\end{array}
\qquad (XII)
$$
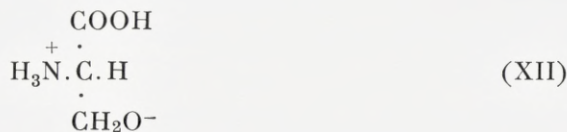
which is (−) .(XII) may seem to be a little too sophisticated. But, on the other hand, as CH_2OH according to the dipolemeasurements is more electronega-tive than COOH it cannot at all be excluded that the proton taken up by the

NH_2-group has migrated from the former rather than from the latter. But even so it is at the present state of affairs impossible to predict with any certainty the sense of the optical rotation of a mixture of the three forms of L-serine (X), (XI) and (XII). If, however, L-serine is dissolved in hydro-chloric acid in stead of in water the rotation becomes (+), which agrees with (XIII):

$$\begin{array}{c} COOH \\ \overset{+}{H_3N}.\overset{\cdot}{C}.H \\ \overset{\cdot}{CH_2OH_2^+} \end{array} \qquad\qquad (XIII)$$
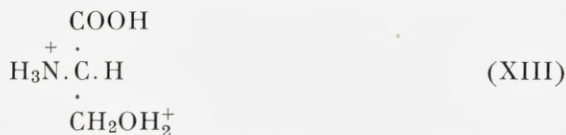
The whole question of the dependence of the rotatory power of L-serine as a function of the acidity of the solution should evidently be investigated experimentally before anything definite can be said on the question of agreement between the present hypothesis and the facts.

The results obtained in the preceding paragraphs seem sufficiently promising to justify an application of the same hypothesis to cases, where more than one carbon-atom comes into play. As will be seen from the fore-going pages there is no doubt that the hypothesis leads to the correct result when the configuration and the distribution of charges is unambiguous. In cases where a molecule containing two or more than two carbon-atoms bound in such a way to each other that the structure is rigid, the dipoles which are components of the screwlike quadrupole may be similar or identical. This latter extremely simple case may give rise to optical activity, which of course is impossible in the case of only one carbon-atom. Tartaric acid is the best known example of this kind of optical activity but the tartaric acid mole-cule is not rigid as the two carbon's can be twisted (although perhaps not quite freely) relatively to each other. Other important examples are XX vicinal disubstitutes of cyclohexane.

Configuration and Rotatory Power of Vicinal XX-substituted Cyclohexane

One of the most convenient ways of illustrating the structure of cyclo-hexane in the Sachse chair form and its derivatives is the socalled Newman-projection, in which two pairs of C-atoms are in the same plane while one C is above and the opposite one is below that plane. As cyclohexane deriva-
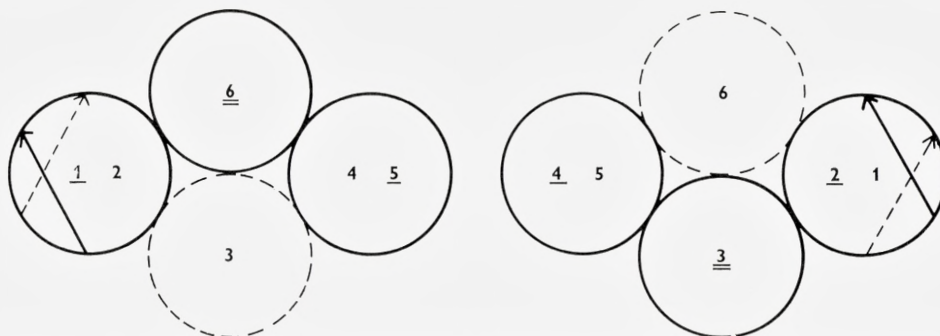
Fig. 1 shows a Newman-projection of 1,2 *cis*-cyclohexane XX where X is some eletronegative group. The arrows point to the negative ends of the dipoles. When drawn with heavy lines they are meant to be before the plane of the paper, when drawn broken they are behind the same plane. The same is true of the two circles which represent C_6 and C_3. The numerals in the circles denote the numbers of the six C-atoms. Numerals which relate to the foremost C-atoms are doubly underlined, those in the next plane are underlined with a single line and those behind the plane of the paper are not underlined. The diagram to the left is intended to show the molecule seen in the direction from C_6 to C_3, that to the right shows the same molecule seen in exactly the opposite direction. It is seen that the forces in the pair which tends to twist the electric field-vector of photons which impinges on an ensemble of molecules of the kind considered have the same direction throughout the molecule and that furthermore the contribution to the twist from the two situations illustrated in fig. 1 must be exactly equal because the two situations are equally probable. It is evident that the quadrupole has the character of a d-screw and that there-fore the substance must have (—) rotation. If both dipoles are inverted the optical rotation remains unchanged in direction.
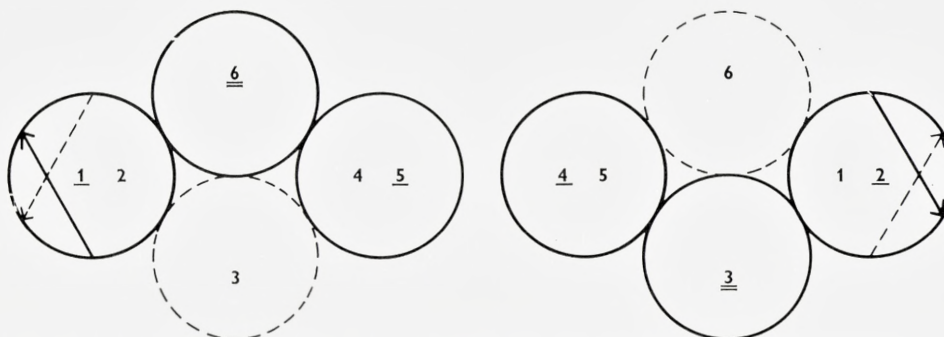

Fig. 2 shows a Newman-projection of a 1,2 cyclohexane XX molecule in *trans*(ee) configuration. The conventions from fig. 1 regarding positions relative to the plane of the paper and the meanings of the left and the right diagrams apply also here. Here again a photon has ecaxtly the same probality of meeting a molecule in the situation "left" and in the situation "right" when it impinges on an ensemble of molecules of the kind considered. But from this follows that the forces in the pairs which should tend to twist the electric vectors to the left compensate each other exactly throught the molecule so that the rotation becomes zero.

The same is evidently true, if both arrows are inverted, in which case the diagram would represent the *trans*(aa) configuration.

tives are stereochemically related to carbohydrates in pyranose-form, it is convenient to number the C-atoms similarly as it is done by convention in the pyranose sugars, C_6 corresponding to O_5 in the sugars while the carbons 1, 2, 4, and 5 are in one plane and C_6 above and C_3 below that plane.

Fig. 1 and fig. 2 are intended to illustrate the situation. A polarized electromagnetic wave-front or a bundle of polarized photons advancing in parallel, like the rows in a marching army, must meet molecules in the two kinds of orientation relative to the direction of propagation of the front, pictured respectively to the left and to the right, exactly equally often. In the case of fig. 1, the *cis*(ea), the field vectors of the photons will be exposed to shearing forces from "left" and "right" molecules which are pairwise equal and have pairwise the same direction. During the advancement of the front through the molecule the direction of the forces will perform a screwlike pattern which in this case corresponds to the pattern of a *d*-screw. Consequently the electric photon vectors will be exposed to a twist to the right during the passage of the front through the molecule.

In fig. 2, the *trans*-(ee) case, the situation is quite different, Also here the wavefront must pass corresponding planes in pairs of "left" and "right" molecules exactly equally often, and the forces to which the photon-vectors are exposed are equal in magnitude for the "left" and "right" molecules in the pair, but, their directions are opposite to each other in corresponding planes throughout the molecules. Consecuently the twisting forces will add up to zero and there will be no twist of the electrical vector of the photons and therefore no rotation of the plane of polarization.

If, in fig. 2, the arrows are inverted, fig. 2 visualizes a *trans*(aa) compound and it is seen that also this compound must be optically inactive. It follows that that isomer, which can be separated into optical antipodes must be the *cis*-form, and that (or those) which cannot must be *trans*-forms.

This result agrees with that arrived at in a group of papers[16] published in these communications, but it disagrees with the current assumption that the optically inactive form like the *meso*-tartaric acid is a *cis*-form.

It should be added, that if the two dipoles in the quadrupole corresponding to figures 1 and 2 are different, one must expect the rotation of the *trans*-form to be less than that of the *cis*-form, but not zero.

This allows a very natural interpretation of the finding of VAVON and PEIGNIER[17] quoted by ELIEL in his well known book[18]: A vicinal hexa-hydrophtalic acid, which is quoted by ELIEL as being *cis* but which the writer for several reasons believes to be *trans*(ee) has been prepared by

saponification under mild conditions from its monomethylester which was optically active while the acid itself became optically inactive. As will be seen, this behaviour is exactly what one should expect from the *trans*-acid if the writers arguments are correct.

References

1. EINSTEIN, A., *Physik. Zeitschr.* **18** (1917) 121
2. KASTLER, A., *Comptes Rendus* **193** (1931) 1075.
3. KASTLER, A., *Les Prix Nobel en 1966* Stockholm (1967) 119.
4. cf. ref. 3. p. 119.
5. van't HOFF, J. H. La Chimie dans l'éspace p. 35. Quoted from J. H. van't Hoff: Imagination in Science. *Molecular Biology, Biochemistry and Bio physics.* Springer Verlag **1** (1967) 7.
6. BREWSTER, J. H., *Journ. Am. Chem. Soc.* **81** (1959) 5475.
7. DEBYE, P., *Polare Molekeln*, Leipzig, 1929. Verlag von S. Hirzel.
8. BIJVOET, J. M., PEERDEMAN, A. F., and van BOMMEL, A. J. *Nature* **168** (1951) 271.
9. BJERRUM, NIELS. *Z. physik. Chem.* **104** (1923) 147.
10. KLYNE, W., *Progress in Stereochemistry* **1** (1954) 183.
11. Ref. 10. p. 195.
12. Ref. 10. p. 183.
13. MEYER-JACOBSEN, *Lehrbuch der organischen Chemie*, Erster Band, zweiter Teil, Leipzig (1913) 603.
14. Ref. 10, p. 178.
15. ARONEY, M. J., CALDERBANK, K. E., LE FÉVRE, J. W., and PIERENS, R. K., Journ., Chem. Soc. B (1968) 561.
16. CHRISTIANSEN, J. A., Mat. Fys. Medd. Dan. Vid. Selsk. **36**, 14 (1968).
17. VAVON, G., and PEIGNIER, P., *Bull. Soc. chim., France.* [4] **45** (1929) 293.
18. ELIEL, E. L. *Stereochemistry of Carbon Compounds*, MacGraw-Hill Book Company, New York, London. (1962) 184, 185.

MATEMATISK-FYSISKE

MEDDELELSER

BIND 36

INDHOLD

OLE J. HEILMANN

MATHEMATICAL POLYMERS I

Synopsis

The model introduced by VERDIER for the change of configuration of a polymer-molecule in solution has been examined and a new possibility for the motion of the polymer-segments has been tried. It is concluded that the long-ranged effect of the excluded-volume has almost no influence on the motion, while the rules chosen for changing bond-angles and bond-directions seems to be the determining factors. It is suggested that the relaxation-time for the change of configuration of a linear polymer with n segments should be proportional either to n^2 or to n^3, but the theory gives no possibility for preferring one possibility instead of the other.

The article includes a proposal for an extended least-squaremethod of estimation, which may be of general value, especially in Monte Carlo calculations.

This work has been inspired by an article by VERDIER and STOCKMAYER (1), which was later followed by two additional articles by VERDIER (2–3).

The polymers considered are assumed to consist of simple chains of n units (atoms). A cubic-lattice model is used for the configuration of the polymer. In a Cartesian reference-system this means that the atoms of the polymer are only allowed to be on points with integral coordinates, the distance between neighbouring atoms in the polymer being one. In models where the so called "excluded volume effect" is taken into consideration the further constraint that no two atoms are permitted to have identical coordinates is added. Within these restrictions all configurations are equally probable.

Several different models have been tried for the polymer changing its configuration, the general feature of all the models being the following: At equal time-intervals (t = 1, 2, 3, . . .) one of the n atoms of the polymer is chosen at random and moved according to the specific rules of the model, which may imply that no motion takes place. The philosophy behind these rules is that independent of the actual configuration of the polymer, any part of it has, within each unit of time, an equal probability of being affected by the surroundings (the solvent-molecules or other parts of the polymer) to such an extent that it changes its configuration significantly. If the time-unit of the model corresponds to this probability being $1/n$, the model should be a reasonable discrete analogue of the actual physical process. The time-unit of the model will then be α/n real time-units (seconds), where α is an unknown constant.

The detailed rules of the seven models, which have been tried are as follows:

Model I (which is identical with the model introduced by VERDIER and STOCKMAYER (1)) is a model with excluded volume. Let the chosen atom be numbered i. If it is not an end-atom ($i \neq 1 \wedge i \neq n$) then the local configuration is either as shown in Fig. 1 or as shown in Fig. 2. For the case shown in Fig. 1 no movement is possible. For the case shown in Fig. 2 the configuration

1*

is changed to the configuration shown in Fig. 3 (meaning that the directions from atom no. $i-1$ to atom no. i and from no. i to no. $i+1$ are interchanged) if the new configuration of the polymer does not conflict with the excluded-volume constraint. If on the other hand the chosen atom is an end-atom, the direction from the neighbouring atom to the end-atom is changed to one of the directions perpendicular to the original one, the choise being made at random between the four possibilities, and again the change is only carried out if it does not result in a conflict with the excluded volume constraint.

In Model II an additional type of motion is included, while the excluded-volume-effect is maintained. If the local configuration is as shown in Fig. 4a or Fig. 4b then no change occurs in Model I, while in Model II a 90°-rotation to either the configuration of Fig. 5a (respective 5b) or the configuration of Fig. 6a (respective 6b) is attempted, the choice between Fig. 5 and Fig. 6 being random and the actual decision, whether to move or not to move is made so that the structure remains consistent with the excluded-volume constraint. The physical significance of the difference between the two models seems quite small, from a mathematical viewpoint however the difference is very important. In Model I the number of "bonds" in any of the six possible directions is conserved except for the movement of the end-atoms, while this is not the case in Model II.

In the Models III–VI only the excluded-volume-effect among next-neighbouring atoms in the polymer is maintained, such that atoms being separated by more than one atom are allowed to occupy the same lattice point. Except for this difference, the rules in Model III are the same as those of Model I and the rules in Model IV are analogous to those of Model II. In Model IV the special question of how to treat a configuration like the one shown in Fig. 7 arises. It was arbitrarily decided to treat it as the configuration shown in Fig. 4a and not as the configuration shown in Fig. 4b.

In the Models V and VI the probability of the movement, which leads from the configurations shown in Fig. 4 to those shown in Fig. 5 and 6, is diminished as compared to Model IV. In Model V it is decreased by a factor 5/9 which is obtained by leaving out the movement if the configuration is the one shown in Fig. 5b.

In Model VI a further reduction by a factor 1/2 as compared to Model V is obtained by introducing a random choice of whether to move or not to move.

Finally in Model VII the effect of the excluded volume is totally neglected, the rules otherwise being the same as the rules of Model I and III except for a small change in the rules for moving the end-atoms. The choice for this movement is now made between all six possible directions of the bond to

Fig. 1

Fig. 4

Fig. 2

Fig. 5
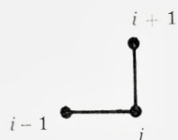
Fig. 3

Fig. 6
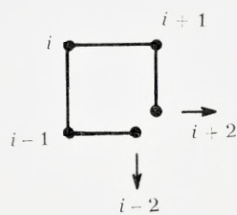
Fig. 7
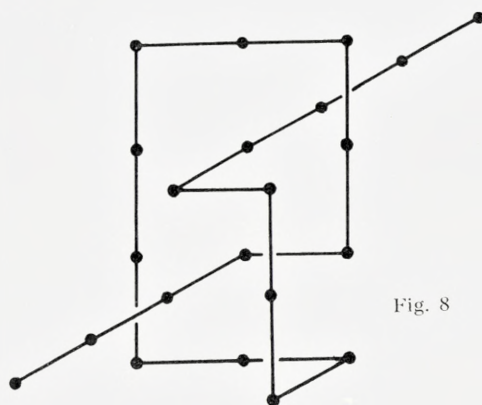
Fig. 8

the end-atoms. This change was introduced in the hope that it would then be possible to solve the model theoretically.

All the models for the movement of the polymer are Markovian, the process being discrete with the allowed configurations of the polymer as the states of the process. Taking configurations to be identical if they can be mapped onto each other by a simple translation (taking the numbering of the atoms into account), it is readily seen that the stochastic matrix for the Markov-process is symmetrical, and since not all atoms can be moved in all configurations not all the diagonal-elements of the matrix can be zero. The implication of this can be summarized as follows: The stochastic matrix is diagonalizable, all the eigenvalues are real, there are no transient states, there is no eigenvalue equal to -1 and the process is not cyclic. (See e. g. HOUSEHOLDER (4)). The configurations are numbered from 1 to N, where for a specific polymer N depends on the extend to which the excluded volume is taken into account. If p_{ji} is the conditional probability that a polymer which at time τ has configuration no. i will have configuration no. j at time $\tau + 1$, then the stochastical matrix is:

$$P = \{p_{ji}\}$$

Note that the matrix is transposed as compared to normal statistical nomenclature. When we introduce the probability-vector $p^{(\tau)}$ the i'th component of which is equal to the probability of finding the polymer in the configuration no. i to time τ and e as the vector having all unit components, the theory of Markov-processes gives as usual (the suffix T stands for transposing and all non-transposed vectors are taken to be column-vectors):

$$p^{(\tau)} = Pp^{(\tau-1)} = P^\tau p^{(0)} \tag{1}$$

$$e^T p^{(\tau)} = 1. \tag{2}$$

Numbering the eigenvalues by their numerical value:

$$|\lambda_1| \geq |\lambda_2| \geq |\lambda_3| \geq \ldots \geq |\lambda_N|; \quad \lambda_1 = 1$$

and numbering the eigenvectors, s_i, accordingly a suitable normalization gives:

$$s_i^T s_j = \delta_{ij} \tag{3}$$

$$s_1^T = \left(\frac{1}{\sqrt{N}}, \frac{1}{\sqrt{N}}, \frac{1}{\sqrt{N}}, \ldots, \frac{1}{\sqrt{N}} \right) \tag{4}$$

$$p^{(t)} = \sum_{i=1}^{N} (s_i^T p^{(0)}) \lambda_i^t s_i. \tag{5}$$

In the case where the polymer is able to change from any configuration to any other configuration in a finite number of steps, the eigenvalue 1 is non-degenerate, with the result that:

$$\lim_{t \to \infty} p^{(t)} = \frac{1}{N} e. \tag{6}$$

This means that the equilibrium-distribution of the Markov-process always would be identical to the static equilibrium distribution, where all configurations are equally probable.

This is not the case however, for the models I and II. Consider e. g. the configuration shown in Fig. 8 in which the polymer has tied itself in a tight knot, which it is not possible to untie by the movements allowed in the two models mentioned. (It should be noticed that it is essential that the knot is tight, and that the number of knots in general is not a constant of the motion.) On the other hand, since the knot consists of a total of 18 atoms, having very limited possibilities of moving, the number of configurations with tight knots is a very small fraction, only, of the total number of configurations. Therefore disregarding these configurations totally and changing N and the stochastic matrix accordingly, probably introduces only a negligible difference. In the following it will consequently be assumed that $|\lambda_2| < 1$ and that eqn. (6) is valid for the models.

We consider now a measurable property, f, for the polymer, which means that f is a stochastic variable for the Markov-process. Let f be the vector, the i'th component of which has the value assumed by f when the polymer is in configuration no. i, then the expectation-value of f at time t is given by:

$$E\{f(t)\} = f^T p^{(t)} = \sum_{i=1}^{N} (s_i^T p^{(0)}) \lambda_i^t (f^T s_i) \tag{7}$$

$$\lim_{t \to \infty} E\{f(t)\} = E\{f(\infty)\} = (f^T e)/N \tag{8}$$

$$E\{f(t)\} = E\{f(\infty)\} + \sum_{i=2}^{N} \alpha_i \lambda_i^t \tag{7a}$$

$$\alpha_i = (s_i^T p^{(0)})(f^T s_i).$$

As it stands eqn. (7) is an expression which is not particularly useful since N is of the order 5^n. If, however, one or two of the eigenvalues are much closer to one than any of the other eigenvalues ($-1/\ln |\lambda_2| \gg -1/\ln |\lambda_j|$ if $|\lambda_j| \neq |\lambda_2|$)then it would be possible to describe the process by one or two relaxation-times, meaning that the summation in (7) is cut off at 3 (if $|\lambda_3| \neq |\lambda_2|$).

It is of course a very queer assumption and at the present no attempt shall be made to defend it except that it is a very usual approximation (see ref. 5).

At a first glance eqn. (7) would give the impression that the relaxation-time does not depend on the chosen property. This need not to be the case, however, if $f^T s_2$ is zero for some properties and not for others. Considering the form of the stochastic matrix, it is found that the matrix must be invariant under the transformation-group obtained by taking the direct product of the full cubic-symmetry group (O_h) and a group with two elements corresponding to the possibility of renumbering the polymer-atoms from the other end. Normal group-theoretical arguments then show that only properties trans-forming in the same manner under this group can be expected to have equal relaxation-times. On the other hand it should not be unreasonable, among properties transforming in the same manner to choose that property, which it is most convenient to work with. Since $p^{(\infty)}$ is invariant under the group, all properties having no invariant component should converge to zero as t goes to infinity.

Another way of getting rid of some of the relaxation-times by making some of the α's zero, would be to make some of the scalar products ($s_i^T p^{(0)}$) zero. This could be obtained by choosing a starting configuration (or distribution of configurations) with a special symmetry. It will never be possible to exclude the eigenvalues having invariant eigenvectors in this manner, however.

Instead of attempting to press the theoretical considerations further it has been tried to get additional insight in the problems by a Monte-Carlo calcula-tion, using a direct simulation of the Markov-process. The calculations have been carried out on a GIER-computer and the programs have so far been written in GIER-Algol 3 with parts of the program in machine-code to keep the computing-time within days. The randomness has been introduced by using a pseudo-random-number-generator:

$$x_{n+1} = 23 x_n \mod (2^{39} + 1) \tag{9}$$

where x_n is the n'th random number (ZELEN and SEVERO (6)).

The detailed accomplishment of the simulation was as follows. For each model and each chosen n, a polymer was started several times in the same, fixed starting-configuration and allowed to move according to the rules of the model. At equal time-intervals (in model-time-units) the actual configura-tion was registered and the value of the selected property was calculated. Up till now only a single property has been tried, namely the square of the end-to-end distance of the polymer, which is invariant under the symmetry-group of the stochastic matrix. This property has the advantage of being

the most thoroughly examined property of the equilibrium distribution. A property depending more explicitly on the positions of all the atoms of the polymer, such as the radius of gyration would be expected to have a smaller variance on the average-values and thus give better estimates.

The starting-configuration has been rather close to a three-fold-axis in the cubic-lattice, consisting of alternating bonds in the directions $(1, 0, 0)$, $(0, 1, 0)$ and $(0, 0, 1)$. This configuration has the advantage of having a very high value of the end-to-end distance.

The decision of spacing the "observations" equally in time was made to simplify the administration in the programs, the smaller efficiency being compensated by a rather close spacing. The disadvantages of this strategy should be compensated for by the sophisticated method of estimation which was used (see Appendix).

Applying the hypothesis of two eigenvalues being sufficient, the squared end-to-end distance of the i'th registration, d_i, should have the expectation-value:

$$E\{d_i\} = d_{eq} + \alpha_2 e^{-\gamma_2 i\Delta} + \alpha_3 e^{-\gamma_3 i\Delta} \tag{10}$$

(where d_{eq} is the equilibrium-value of the squared end-to-end distance, and Δ is the time spacing between two consecutive registrations of d).

The estimation of the five parameters d_{eq}, α_2, α_3, γ_2 and γ_3 is exactly the kind of problem treated in the Appendix. To ensure the reliability of the result a graphical test was made.

In order to test whether the method of estimation outlined in the Appendix was applicable in the present case a presumably typical example was selected, Model II with n = 32, and this was thoroughly examined, using a material of all together 640 starts. Three problems were of special interest: Which of the three formulas (I. 12), (I. 15) and (I. 17) should be used to estimate the variance? Would the number of observations during a single start be important, if the spacing between the observations was adjusted to keep the total running-time of the starts constant? And would varying the number of starts used for estimation give the expected results?

To settle the first question both formula (I. 12) and formula (I. 17) were used in all the cases which were also used to answer the two other problems. Since the difference between the resulting standard deviations was of the order 10 $^0/_0$ and since q (formula (I. 3a)) also showed to be of that order, it was decided to use (I. 17), since it was the simplest formula. Consequently all standard deviations quoted will refer to this formula.

To see the influence of the number of observations, estimations were carried out with 8, 16 and 32 observations during the 8192 model-time-units

TABLE 1.

Number of observations	Number of starts	q	d_{eq}	α_2
8	160	$2.28_{10} - 2$	63 ± 4.1	$4.65_{10} - 4 \pm 6.1_{10} - 5$
16	160	$7.90_{10} - 2$	60 ± 4.2	$4.17_{10} - 4 \pm 4.6_{10} - 5$
32	160	$1.81_{10} - 1$	62 ± 3.2	$4.46_{10} - 4 \pm 3.4_{10} - 5$
8	640	$9.48_{10} - 3$	57 ± 1.3	$2.92_{10} - 4 \pm 1.6_{10} - 4$
16	640	$2.74_{10} - 2$	61 ± 2.9	$3.62_{10} - 4 \pm 2.7_{10} - 5$
32	640	$5.21_{10} - 2$	65 ± 2.0	$4.49_{10} - 4 \pm 2.0_{10} - 5$

Table 1 shows that the squared end-to-end distance at equilibrium, d_{eq}, and the reciprocal relaxation time, γ_2, are essentially independent of the number of observations.

in which each start was followed. To ensure that the conclusions would not depend strongly on the number of starts used, both the total of all 640 starts and a smaller group of 160 starts were used for the estimation. The results are shown in Table I. The differences do not seem to be significant. To use 8 observations for estimating 5 parameters is however rather unfavourable, and this leaves us with the choice between 16 and 32 observations. In general 16 has been used since this gives a smaller computation-time and a better numerical stability in finding the minimum for q. Finally, to see the effect of varying the number of starts, estimations were made on four groups of 40 starts each, on four groups of 160 starts each and on all 640 starts together. The results are shown in Table 2. It should be remarked that the estimations on the groups of 40 starts were made with 16 observations per start, while the others were made with 32 observations per start, meaning that the q's are not directly comparable. The two rows denoted mean give the mean of the four rows just above. The uncertainties quoted in these two rows are calculated from square-sums of the deviation from the mean, not using the uncertainties on the single estimates. The behaviour of the results seems satisfactory and especially it seems that the method of estimating the standard-deviation is reasonable.

For the general choice of the number of starts to use for estimation, the following considerations were essential. It was desirable to have approximately the same relative error on the estimates. If the number of starts was too low, it was extremely difficult to find minimum for q. The computation per start was however growing rapidly with the number of atoms in the polymer. It was found that when the number of atoms was equal to 8, 16, 32, 64 and 128 respectively, a reasonable compromise was something around 1200, 600, 300, 150 and 60 starts respectively.

TABLE 2.

	Numbers of starts	q	d_{eq}	α_2
	40	$2.68_{10} - 1$	48 ± 6.6	$3.28_{10} - 4 \pm 6.0_{10} - 5$
	40	$9.19_{10} - 2$	42 ± 95	$2.37_{10} - 4 \pm 7.0_{10} - 4$
	40	$1.28_{10} - 1$	72 ± 16	$7.70_{10} - 4 \pm 1.9_{10} - 4$
	40	$3.77_{10} - 2$	67 ± 21	$4.86_{10} - 4 \pm 1.7_{10} - 4$
mean	160	$1.32_{10} - 1$	57 ± 7.3	$4.55_{10} - 4 \pm 1.2_{10} - 4$
	160	$1.81_{10} - 1$	62 ± 3.2	$4.46_{10} - 4 \pm 3.4_{10} - 5$
	160	$2.36_{10} - 1$	60 ± 4.0	$3.80_{10} - 4 \pm 3.4_{10} - 5$
	160	$2.62_{10} - 1$	61 ± 3.0	$5.14_{10} - 4 \pm 3.4_{10} - 5$
	160	$1.94_{10} - 1$	67 ± 3.7	$5.08_{10} - 4 \pm 3.9_{10} - 5$
mean	640	$2.18_{10} - 1$	63 ± 1.6	$4.62_{10} - 4 \pm 3.1_{10} - 5$
	640	$5.21_{10} - 2$	65 ± 2.0	$4.49_{10} - 4 \pm 2.0_{10} - 5$

Table 2 shows that the estimated standard deviation is essentially proportional to the square root of the number of starts.

As a further check on the method the estimated values of d_{eq} were compared with the values known from equilibrium data:

$$d_{eq} = 1.067(n - 1)^{6/5} - 0.0915 \qquad (11)$$

for the models I and II (DOMB (7)),

$$d_{eq} = \frac{3}{2}(n - 1) - \frac{5}{8} + \frac{1}{8 \cdot 5^{n-2}} \qquad (12)$$

for the models III–VI, and

$$d_{eq} = n - 1 \qquad (13)$$

for model VII. As can be seen from table 3 the agreement is satisfactory. The method of estimation thus being confirmed, the results of the simulations will now be considered. Of the parameters estimated, γ_2 is the most interesting since γ_2^{-1} supposedly has some connection with the relaxation time in certain experiments on polymers. All the estimated values of γ_2 with the estimated standard deviations are shown in Table 4. (The values of γ_3 were generally larger by an order of magnitude.)

It is of course not really the absolute values of γ_2, but only the way in which it depends on n (the number of atoms in the polymer), which can be predicted by the simulations. Naturally the functional form to be chosen is open for discussion. It is easily seen that:

TABLE 3.

n	8	16	32	64	128
Formula (11)	10.8	27.2	65.5	154	358
Model I	$10 \pm .3$	$27 \pm .6$	67 ± 4	111 ± 20	489 ± 80
Model II	$12 \pm .3$	$27 \pm .9$	61 ± 3	166 ± 9	319 ± 24
Formula (12)	9.88	21.9	44.9	93.9	190
Model III	$10 \pm .3$	26 ± 1.6	62 ± 9	268 ± 20	990 ± 150
Model IV	$11 \pm .2$	22 ± 7.7	45 ± 1.3	98 ± 4	201 ± 10
Model V	$11 \pm .3$	$23 \pm .8$	45 ± 1.7	95 ± 4.3	190 ± 15
Model VI	$20 \pm .2$	19 ± 2	48 ± 2	101 ± 6	171 ± 25
Formula (13)	7	15	31	63	127
Model VII	$7 \pm .1$	$15 \pm .4$	30 ± 1.7	59 ± 5	107 ± 14

Table 3 shows that the values of the squared end-to-end distance at equilibrium, d_{eq}, estimated from the relaxation curves are essentially identical with values known from equilibrium data (formula (11), (12) and (13)).

$$\gamma_2 \approx an^{-\nu} \tag{14}$$

is a possibility, and that $\nu = 4$ for model I and III and $\nu = 3$ for the other five models would not be unreasonable. This is a result which for the models I and VII agrees with VERDIER (3). For the models II, IV, V and VI however the addition of a further term in eqn. (14) seems necessary to get agreement with the values for γ_2 for $n = 8$, so the forms shown in Table 5 are tentatively proposed as a representation of the values of γ_2. (The factors are least-square estimates and the uncertainties are standard deviations). It should be noticed that the time-unit for γ_2 is the model-time unit. To convert the results to real time-units, the values of γ_2 should be multiplied by n.

TABLE 4.

Model \ n	8	16	32	64	128
I	$(3.8 \pm .6)_{10} - 2$	$(2.2 \pm .2)_{10} - 3$	$(1.3 \pm .2)_{10} - 4$	$(5.5 \pm .9)_{10} - 6$	$(4.9 \pm .7)_{10} - 7$
II	$(4.5 \pm .7)_{10} - 2$	$(3.6 \pm .4)_{10} - 3$	$(3.6 \pm .3)_{10} - 4$	$(5.5 \pm .5)_{10} - 5$	$(5.0 \pm .4)_{10} - 6$
III	$(2.3 \pm .3)_{10} - 2$	$(2.1 \pm .3)_{10} - 3$	$(1.3 \pm .2)_{10} - 4$	$(1.2 \pm .1)_{10} - 5$	$(4.7 \pm .8)_{10} - 7$
IV	$(5.0 \pm .6)_{10} - 2$	$(3.9 \pm .3)_{10} - 3$	$(4.5 \pm .4)_{10} - 4$	$(5.6 \pm .3)_{10} - 5$	$(7.8 \pm .4)_{10} - 6$
V	$(4.7 \pm .6)_{10} - 2$	$(3.7 \pm .3)_{10} - 3$	$(3.5 \pm .2)_{10} - 4$	$(5.1 \pm .3)_{10} - 5$	$(5.3 \pm .3)_{10} - 6$
VI	$(2.3 \pm .3)_{10} - 2$	$(1.9 \pm .3)_{10} - 3$	$(3.1 \pm .2)_{10} - 4$	$(3.7 \pm .2)_{10} - 5$	$(4.2 \pm .2)_{10} - 6$
VII	$(4.4 \pm .4)_{10} - 2$	$(5.2 \pm .3)_{10} - 3$	$(5.9 \pm .3)_{10} - 4$	$(7.9 \pm .3)_{10} - 5$	$(8.9 \pm .3)_{10} - 6$

Table 4 shows the estimated valves of the reciprocal relaxation time, γ_2, in model-time-units.

TABLE 5.

Model	α_2
I	$(129 \pm 7)\, n^{-4}$
II	$(10.2 \pm .7)\, n^{-3} + (81 \pm 20)\, n^{-4}$
III	$(129 \pm 8)\, n^{-4}$
IV	$(14.8 \pm .6)\, n^{-3} + (35 \pm 18)\, n^{-4}$
V	$(10.8 \pm .5)\, n^{-3} + (74 \pm 18)\, n^{-4}$
VI	$(9.0 \pm .4)\, n^{-3} + (17 \pm 12)\, n^{-4}$
VII	$(19.8 \pm .4)\, n^{-3}$

Table 5 shows the estimated dependence of the reciprocal relaxation time, γ_2, on the number of atoms in the polymer. Remark that the time-unit is the model-time-unit.

It seems possible to draw the following three conclusions from the material shown in Table 4 and 5.

The real excluded volume has only an imperceptible influence on the relaxation (compare Model I and II with Model III and IV).

The possibility of a valence-angle equal to 0°, however, has an appreciable influence (compare Model III with Model VII)*).

The additional possibility of movement introduce in Models II and IV as compared with models I and III causes also a radical change in the relaxation behaviour.

The general result is then that it is the local structure of the polymer rather than the long-range effect of the excluded volume, which is of importance for understanding the movements of polymers.

Acknowledgements

* These conclusions should be compared with the analogous conclusions by Verdier (3).

Appendix

A General Least Square Method

Consider n uncorrelated observations $y^{(i)}$ ($i = 1, 2, \ldots, n$) of a p-dimensional stochastic variabel having the same p-variate distribution, F, with mean value μ given as a function of m parameters, $\beta_i (i = 1, 2, \ldots, m)$, where $m < p$:

$$\mu_j = g_j(\beta) \qquad\qquad j = 1, 2, \ldots, p \qquad\qquad (\text{I. 1})$$

The problem is that of finding reasonable estimates for the parameters, β_i, and for the variance of the estimators used.

The sample mean:

$$y = \frac{1}{n} \sum_{i=1}^{n} y^{(i)} \qquad\qquad (\text{I. 2})$$

will in general, following the central-limit theorem, be asymptotically ($n \to \infty$) normally distributed with mean μ and a dispersion matrix $\frac{1}{n} \Sigma$, Σ being the dispersion matrix of F. Argueing from this or from the general theory of least squares a good estimate of β should be the value of β that minimizes:

$$q' = (y_r - g_r(\beta))\sigma^{rs}(y_s - g_s(\beta)) \qquad\qquad (\text{I. 3})$$

(y_r without superscript stands for component of y defined in (I. 2), σ^{rs} are written for elements of Σ^{-1}, and here as well as in the following we use the convention that repeated indices in a product means summation over these indices, the limits of the summations being self-evident).

In order to be able to solve the problem of minimizing q it is indispensable to know Σ. Since Σ cannot be assumed known it is necessary to use an estimate of Σ.

An unbiased estimate for the elements of Σ is (conf. e. g. RAO (8))

$$s_{rs} = \frac{1}{n-1} \left[y_r^{(i)} y_s^{(i)} - n y_r y_s \right] \qquad\qquad (\text{I. 4})$$

Using this in (I. 3), the quadratic form to be minimized becomes:

$$q = (y_r - g_r(\beta))s^{rs}(y_s - g_s(\beta)) \qquad\qquad (\text{I. 3 a})$$

(superscripts on a matrix-element are again used to designate the elements of the inverse matrix).

We shall not here consider the intricate numerical problem of finding minimum for q if $g(\beta)$ is not linear in β. The solution, β^*, will in any case satisfy the equations:

$$-2\frac{\partial g_r(\beta)}{\partial \beta_1} s^{rs}(y_s - g_s(\beta)) = 0 \left.\begin{array}{c} \\ \\ l = 1, 2, \ldots, m \end{array}\right\} \quad (I.\,5)$$

β^* being an implicit function of y by (I. 5). A simple extension of the proof by CRAMER for variance of functions of moments (CRAMER (9) p. 353 ff.) gives:

$$C\{\beta_1^*, \beta_k^*\} = \frac{\partial \beta_1^*}{\partial y_r}(\sigma_{rs}/n)\frac{\partial \beta_k^*}{\partial y_s} + O(n^{-3/2}) = d'_{lk} \quad (I.\,9)$$

where σ_{rs} is an element of Σ.

By (I. 5):

$$\frac{\partial \beta_k^*}{\partial y_r} = 2a^{kl}(\beta^*)\frac{\partial g_s(\beta)}{\partial \beta_1}\bigg|_{\beta\,=\,\beta^*} s^{rs} \quad (I.\,10)$$

where

$$a_{kl}(\beta) = \frac{\partial^2 q}{\partial \beta_1 \partial \beta_k} = 2\frac{\partial g_r(\beta)}{\partial \beta_1}s^{rs}\frac{\partial g_s(\beta)}{\partial \beta_k} - 2\frac{\partial^2 g_r(\beta)}{\partial \beta_1 \partial \beta_k}s^{rs}(y_s - g_s(\beta)) \quad (I.\,11)$$

Hence using s_{sr} for σ_{sr} and neglecting terms of the order $n^{-3/2}$:

$$d'_{lk} = \frac{4}{n}a^{kj}(\beta^*)\frac{\partial g_s(\beta)}{\partial \beta_j}\bigg|_{\beta\,=\,\beta^*} s^{rs}\frac{\partial g_r(\beta)}{\partial \beta_i}\bigg|_{\beta\,=\,\beta^*} a^{il}(\beta^*). \quad (I.\,12)$$

To be correct it is not only y also s^{rs} that is estimated.

Making allowance for this is somewhat complicated. However, using the normal approximation, y and $\{s^{rs}\}$ becomes uncorrelated and the covariance of s_{rs} and s_{tu} becomes:

$$C\{s_{rs}, s_{tu}\} = (s_{ru}s_{st} + s_{rt}s_{su})/(n - 1). \quad (I.\,13)$$

The total-effect is then the addition of

$$d''_{lk} = \frac{n}{n - 1}qd'_{lk} \quad (I.\,14)$$

to d'_{lk} (For a proof see the end of the Appendix). Hence the total covariance-matrix is

$$d_{lk} = d'_{lk}\left(1 + \frac{n}{n-1}q\right). \tag{I. 15}$$

This should be compared with the analogous result by Rao (10, 11) for the case where $g(\beta)$ is linear in β.

Since q is of the order n^{-1} and the relative error of omitting terms of order $n^{-3/2}$ in (I. 9) is of the order $n^{-1/2}$, (I. 12) will actually do just as well as (I. 15).

However, reasonning this way (I. 12) can be simplified even more. As the second terms in (I. 11) is of the order $n^{-1/2}$ as compared to the first, $a_{lk}(\beta)$ can be approximated accurately enough by:

$$2b_{lk}(\beta) = 2\frac{\partial g_r(\beta)}{\partial \beta_l}s^{rs}\frac{\partial g_s(\beta)}{\partial \beta_k} \tag{I. 16}$$

and using this, (I. 12) becomes

$$d^+_{lk} = b^{kl}(\beta^*)/n. \tag{I. 17}$$

Finally a proof of eqn. (I. 14) under the assumption of a normal distribution shall be given.

Introducing $S^{(rs)}$ for the complement of s_{rs} i $S(S = \{s_{rs}\})$ and a double complement $S^{(rs)(tu)}$ being equal to the complement of s_{tu} in $S^{(rs)}$, if $r \neq t$ and $s \neq u$, and zero otherwise, and using $|S|$ for the determinant of S, straight-forward calculations give:

$$S^{(rs)(tu)} = S^{(ts)(ru)} = S^{(tu)(rs)} = S^{(ru)(ts)} \tag{I. 18}$$

$$s^{rs} = S^{(rs)}/|S| \tag{I. 19}$$

$$\frac{\partial s^{rs}}{\partial s_{tu}} = \frac{S^{(rs)(tu)}}{|S|} - \frac{S^{(rs)}S^{(tu)}}{|S|} \tag{I. 20}$$

$$S^{(rs)(tu)}s_{tu} = S^{(ru)}\delta_{sv}(1 - \delta_{su}) + S^{(rs)}\delta_{uv}(1 - \delta_{su}) \tag{I. 21}$$

(factors $(1 - \delta_{su})$ and $(0 - \delta_{su})$ will not cause summation irrespective of the indices s and u being repeated).

$$\frac{\partial s^{rs}}{\partial s_{tu}}s_{tv} = s^{ru}\delta_{sv}(1 - \delta_{su}) + s^{rs}\delta_{uv}(0 - \delta_{su}) \tag{I. 22}$$

$$\frac{\partial s^{rs}}{\partial s_{vw}}s_{vx}s_{wy}\frac{\partial s^{tu}}{\partial s_{xy}} = s^{ru}s^{ts}. \tag{I. 23}$$

Then on evaluating d''_{1k} in the same way as d'_{1k} we get:

$$
\left.
\begin{aligned}
d''_{ek} &= \frac{4}{n-1} a^{kj}(\beta^*) \frac{\partial g_r(\beta)}{\partial \beta_j}\bigg|_{\beta=\beta^*} (y_s - g_s(\beta^*)) \\[2mm]
&\quad \frac{\partial s^{rs}}{\partial s_{vw}}(s_{vx}s_{wy} + s_{vy}s_{wx})\frac{\partial s^{tu}}{\partial s_{xy}} \\[2mm]
&\quad (y_t - g_t(\beta^*))\frac{\partial g_u(\beta)}{\partial \beta_i}\bigg|_{\beta=\beta^*} a^{il}(\beta^*).
\end{aligned}
\right\} \quad (I.\,24)
$$

Using (I. 23), (I. 5), (I. 3 a) and (I. 12), (I. 24) can be transformed into (I. 14). The essential content of (I. 14), namely that d'_{1k} is smaller than d''_{1k} by a factor n, can of course be seen very easily by a direct comparison of (I. 24) with (I. 12), which shows that (I. 24) contains two extra factors of the form $(y_j - g_j(\beta^*))$, each being of the order $n^{-1/2}$.

Kemisk Laboratorium III
H. C. Ørsted Institutet
Københavns Universitet

References

1. P. H. VERDIER and W. H. STOCKMAYER, J. Chem. Phys. **36** 227 (1962).
2. P. H. VERDIER, J. Chem. Phys. **45** 2118 (1966).
3. P. H. VERDIER, J. Chem. Phys. **45** 2122 (1966).
4. A. S. HOUSEHOLDER, "The Theory of Matrices and Numerical Analysis", New York (1964).
5. See e. g. S. K. KIM, J. Chem. Phys. **28** 1057 (1958), K. E. SHULER, G. H. WEISS and K. ANDERSEN, J. Mat. Phys. **3** 550 (1962) and ref. 1.
6. M. ZELEN and N. C. SEVERO, "Probability Functions" in M. ABRAMOWITZ and I. A. STEGUN (ed.) "Handbook of Mathematical Functions", New York (1965).
7. C. DOMB, J. Chem. Phys. **38** 2957 (1963).
8. C. R. RAO, "Linear Statistical Inference and its Applications", New York (1965).
9. H. CRAMER, "Mathematical Methods of Statistics", Princeton (1946).
10. C. R. RAO, Biometrika **46**, 49 (1959).
11. C. R. RAO in L. Lecam & J. Neymann (Ed.) "Proceedings of the Fifth Berkeley Symposion on Mathematical Statistics and Probability". Vol I California (1967) p. 355.

ASGER AABOE

A COMPUTED LIST OF
NEW MOONS FOR 319 B.C. TO 316 B.C.
FROM BABYLON: B.M. 40094

Synopsis

B. M. 40094 is a computed ephemeris from Babylon giving the moment of conjunction of sun and moon for each month from S. E.–8, XII to S. E.–5, XII (i. e.,–318, Mar. 31 f.). It is the earliest lunar text belonging to System A that has come to light so far. Though otherwise in strict agreement with the procedures of the later texts of this system, this text is unique in incorporating the function Λ and three new related functions, Y, $\check{C}'$, and $\tilde{K}$. These new functions make it possible to solve several problems in the history of Babylonian lunar theory, particularly those concerning relations between mean values of Φ, G, and Λ.

Introduction

There are two final goals of Babylonian lunar theories: to foretell eclipses, and to predict the duration of various visibility phenomena near new and full moons, most importantly the time from sunset to moonset on the evening of first visibility of the new moon.

In the solution of either kind of problem the determination of the moment of syzygy, i. e., when the moon is either in conjunction or opposition to the sun, is of obvious significance. The fluctuations of the time interval between consecutive syzygies of the same kind are caused by the variation of the solar velocity, with the year as its period, conjointly with the variation of the lunar velocity, with the anomalistic month as its period. In the present paper[1] I shall be concerned with the lunar theory according to System A, in the terminology of ACT,[2] and here the combined effect of the two variable velocities is separated into two periodic additive terms, G and J, so that the time from syzygy to syzygy is

$$29^{\mathrm{d}} + \mathrm{G}^{\mathrm{H}} + \mathrm{J}^{\mathrm{H}},^{3}$$

where G's period is the anomalistic month and J depends on solar longitude.

G belongs to a family of periodic functions (Φ,F,G,Λ,X) from lunar System A, each of them with the anomalistic month as its period. Φ is a pure zig-zag function which runs uninterruptedly, as experience has shown so far, through the entire corpus of lunar System A texts. G is derived from Φ by a set of arithmetical rules of transformation which has long been under control, though it lacked astronomical justification; the meaning of Φ was

---

[2] ACT = O. NEUGEBAUER, *Astronomical Cuneiform Texts.* 3 vols., London, 1955. The reader is referred to this work for all details of theories, methods, and parameters.

[3] $1^{\mathrm{d}} = 6^{\mathrm{H}}$ (large hours) = 6,0 (time) degrees. The large hour is introduced for convenience in modern textual editions.

1*

not at all clear, though it was known that Φ is in precise phase with lunar velocity as represented by Column F.

In a recent article[4] I published some late-Babylonian texts which, in conjunction with a previously published text,[5] threw new light on this family of functions. X was found here for the first time; $\varLambda$ was already known from two procedure texts in ACT which had taught us how to derive $\varLambda$ from Φ, but nothing more, and the remaining three functions, Φ, F, and G, are in evidence in all the lunar ephemerides. These texts made it possible to identify all of the members of this family and to give astronomical sense to the established arithmetical rules for converting values of Φ into corresponding values of F, G, and $\varLambda$. We can now say that the values of these functions, associated with a given syzygy, have the following significance, beginning with the two that were identified already by KUGLER:[6]

daily progress of moon	$= \text{F}°$
length of preceding month	$= 29^\text{d} + \text{G}^\text{H}$
length of subsequent 223 months	$= 6585^\text{d} + \Phi^\text{H}$
length of preceding 12 months	$= 354^\text{d} + \varLambda^\text{H}$
difference between a constant year and the length of preceding 12 months	$= X^\text{d}$

All of these functions, save perhaps F, are artificial in the sense that they are not directly observable. They represent preliminary values, expressing only the effect of a variable lunar velocity. Indeed, they are not even necessarily correct in the mean, for G and, as we learn from the text published here, also $\varLambda$ receive corrections for solar anomaly, J and Y, respectively, neither of which has zero as its mean value.

There were two pieces of information in these texts that were crucial in making these identifications possible. The first was a pair of relations between differences in Φ and in G and $\varLambda$, respectively, or more precisely, letting Φ_n mean the value of Φ associated with syzygy number n in a certain sequence of syzygies of the same kind, and analogously for the other functions,

$$\Phi_n - \Phi_{n-1} = \text{G}_{n+223} - \text{G}_n \qquad (1)$$

and

$$\Phi_n - \Phi_{n-12} = \varLambda_{n+223} - \varLambda_n. \qquad (2)$$

[4] ASGER AABOE, *Some Lunar Auxiliary Tables and Related Texts from the Late Babylonian Period*. Mat. Fys. Medd. Dan. Vid. Selsk. **36**, no. 12 (1968).

[5] O. NEUGEBAUER, "*Saros*" *and Lunar Velocity in Babylonian Astronomy*. Mat. Fys. Medd. Dan. Vid. Selsk. **31**, no. 4 (1957). I shall refer to it as the Saros paper.

[6] F. X. KUGLER, *Die Babylonische Mondrechnung*. Freiburg im Breisgau, 1900.

The second was that when values of Φ were in active use, as in (1) and (2), then Φ was no longer a strict zig-zag function, but it was truncated at effective extrema ($2;13,20^{\mathrm{H}}$ and $1;58,31,6,40^{\mathrm{H}}$, to be exact). Incidentally, it turned out that F was treated similarly; its effective extrema are $15^{\circ/\mathrm{d}}$ and $11;15^{\circ/\mathrm{d}}$.

That relation (1) implies that Φ_n measures, but for a constant, the variable length of the 223 months (the "Saros")[7] following upon syzygy number n may be seen as follows:

If corresponding to syzygy number n the length of the subsequent Saros is called σ_n and that of the preceding lunation or month m_n, we have

$$\sigma_n = \sum_{i=n+1}^{n+223} m_i,$$

hence

$$\sigma_n - \sigma_{n-1} = m_{n+223} - m_n.$$

If we ignore all effects but that of lunar anomaly, i. e., assume that J is constant, or that syzygies are evenly spaced in longitude, we have:

$$m_{n+223} - m_n = G_{n+223} - G_n$$

so we obtain, using (1),

$$\sigma_n - \sigma_{n-1} = \Phi_n - \Phi_{n-1}$$

or

$$\sigma - \Phi = \text{constant.}$$

The size of Φ makes it plausible that the value of the constant is 6585^{d}.

Once Φ is identified, a similar argument shows that the relation (2) implies that Λ_n measures, but for a constant, the variable length of the 12 months (the "year") preceding syzygy number n. Let y_n be this year; we then have:

$$y_n = \sum_{i=n-11}^{n} m_i.$$

With notations as above, once again assuming a constant J, and using (2), we get:

[7] I shall use "Saros" to mean an interval of 223 synodic months; the importance of this time interval is that 223 synodic months are very nearly of the same length as 239 anomalistic months. In the texts, "18 years" is used as a technical term for 223 months (actually, 223 months exceed 18^{y} by some 10^{d}).

For a history of the use of "Saros" see O. Neugebauer, *The Exact Sciences in Antiquity.* 2nd edition. Providence, 1957, p. 141 ff.

$$\sigma_n - \sigma_{n-12} = \sum_{i=n+1}^{n+223} m_i - \sum_{i=n-11}^{n+211} m_i$$

$$= \sum_{i=n+212}^{n+223} m_i - \sum_{i=n-11}^{n} m_i$$

$$= y_{n+223} - y_n.$$

Since

$$\sigma_n - \sigma_{n-12} = \Phi_n - \Phi_{n-12}$$

we obtain, using (2),

$$\Lambda_{n+223} - \Lambda_n = y_{n+223} - y_n$$

or,

$$y - \Lambda = \text{constant.}$$

For the last step of the argument I used, strictly speaking, that 223 is relatively prime to 6247, the number period of Λ (and Φ).

The size of Λ makes it plausible that the value of the constant is 354^d.

A direct relation between G and Λ will be of importance in the following. We have:

$$y_n - y_{n-1} = \sum_{i=n-11}^{n} m_i - \sum_{i=n-12}^{n-1} m_i$$

$$= m_n - m_{n-12}.$$

Thus, arguing as before,

$$\Lambda_n - \Lambda_{n-1} = G_n - G_{n-12}. \tag{3}$$

Using the relations (1) and (2), and the truncated version of Φ, it is now possible to derive schemes for transforming Φ into G and Λ, if one provides an initial value for each. For details I refer to my previous publication; the resulting $\Phi - G$ table is, but for a few values near G's maximum, the one given in ACT.[8] The analogous $\Phi - \Lambda$ table appears as Table 3 below.

So far I have summarised, in slightly altered form, the relevant results of my previous article. However, there were then several questions that I had to leave unanswered. The most obvious one was about the relation between G and Λ—not their differences, for that is settled by (3)—but their actual values. One would expect, that

$$\sum_{i=n-11}^{n} (29^d + G_i^H)$$

would be precisely $354^d + \Lambda_n^H$, but that is not so. Thus the connexion between the initial values (or mean values) of G and Λ is not the obvious one, and

[8] ACT I, p. 60.

it was only when the text published here came under control that the proper relation became clear.

It appeared, as hinted above, that even as G receives a correction J for solar anomaly, so also should one apply a correction Y, as I call it, to $\varLambda$. With these corrections one has, indeed,

$$\sum_{i=n-11}^{n} (29^{\mathrm{d}} + G_i^{\mathrm{H}} + J_i^{\mathrm{H}}) = 354^{\mathrm{d}} + \varLambda_n^{\mathrm{H}} + Y_n^{\mathrm{H}}, \tag{4}$$

or, at least, very nearly (the small deviations may be explained, in part, by the adjustments of G near its maximum).

The relation (4) implies, that

$$\varLambda_n - \varLambda_{n-1} + Y_n - Y_{n-1} = G_n - G_{n-12} + J_n - J_{n-12}$$

which, together with (3), yields

$$Y_n - Y_{n-1} = J_n - J_{n-12}. \tag{5}$$

The relation (5) is satisfied exactly; further, we learn from our text that Y, as J, is zero on the arc of the ecliptic where the monthly progress of the sun is high $(30°/^{\mathrm{m}})$. I shall proceed to show in detail how the decision that Y vanish on the fast arc combined with relation (5) determines Y completely, if J is known.

At the base of J is the solar model of System A. The generating function (which here may be interpreted as the solar velocity in degrees per synodic month) is

$$\text{♓ } 27° \text{ to ♍ } 13°: \; w = 28;7,30°$$

$$\text{♍ } 13° \text{ to ♓ } 27°: \; W = 30°.$$

The monthly solar progress in longitude is then either W or w if the sun during the month remains entirely within the fast or the slow arc, respectively. If the place of discontinuity from high to low velocity must be crossed, the standard interpolation rule of System A is employed, i. e., if the distance p of the initial longitude from ♓ $27°$ is less than $W = 30°$, then the monthly progress $\varDelta\lambda$ of the sun is

$$\varDelta\lambda = p + q$$

where

$$\frac{p}{W} + \frac{q}{w} = 1,$$

and symmetrically for the other discontinuity. The period of this model is

$$P = \frac{46,23}{3,45} = 12;22,8$$

with

$$\Pi = 46,23 \text{ and } Z = 3,45,$$

i. e., the year has here the canonical value of $12;22,8$ synodic months, or, in whole numbers, $46,23$ months correspond to $3,45$ revolutions in the ecliptic, i. e., $3,45$ years.

  This solar model can advantageously be reduced to a distribution of $46,23$ intervals on the ecliptic,[9] $24,15$ of length $0;8°$ on the fast arc, and $22,8$ of length $0;7,30°$ on the slow; the monthly progress of the sun will then always be $3,45$ intervals, regardless of their length.

  Column J is closely and simply tied to this solar model. If λ_n is the solar longitude at syzygy number n, and the sun during the previous month has travelled the distance s within the slow arc $(0 \leqq s \leqq w)$, then

$$J_n = J(\lambda_n) = -\frac{s}{w} \cdot 0;57,3,45^H.$$

On most of the fast arc we have that $s = 0$, so $J = 0$; on most of the slow arc $s = w$, so $J = -0;57,3,45$. Only when a place of discontinuity of the solar velocity is passed in the course of the previous month, i. e., when λ_n is between $\mathcal{H}\ 27°$ and $\Upsilon\ 25;7,30°$ or between $\mathrm{I\!I\!\!\!P}\ 13°$ and $\underline{\Omega}\ 13°$, do we get intermediate values of J, and they depend linearly on λ_n (see Figure 1). I shall show later that this J-function makes very good sense and that it can be derived from the solar model and the lunar velocity, but for the moment we shall take it as given.

  If we now are to derive the analogous correction, Y, to Λ, we begin with relation (5) which states that the monthly difference in Y is the 12-monthly difference in J or, more precisely,

$$\Delta Y = Y_n - Y_{n-1} = J_n - J_{n-12}. \tag{5}$$

To advance 12 months means, in terms of the distribution version of the solar model, an advance in longitude of

$$12 \cdot Z = 12 \cdot 3,45 = 45,0 \equiv -1,23 \text{ intervals (mod. } \Pi)$$

  [9] ASGER AABOE, *On Period Relations in Babylonian Astronomy.* Centaurus 1964, vol. 10, pp. 213–231.
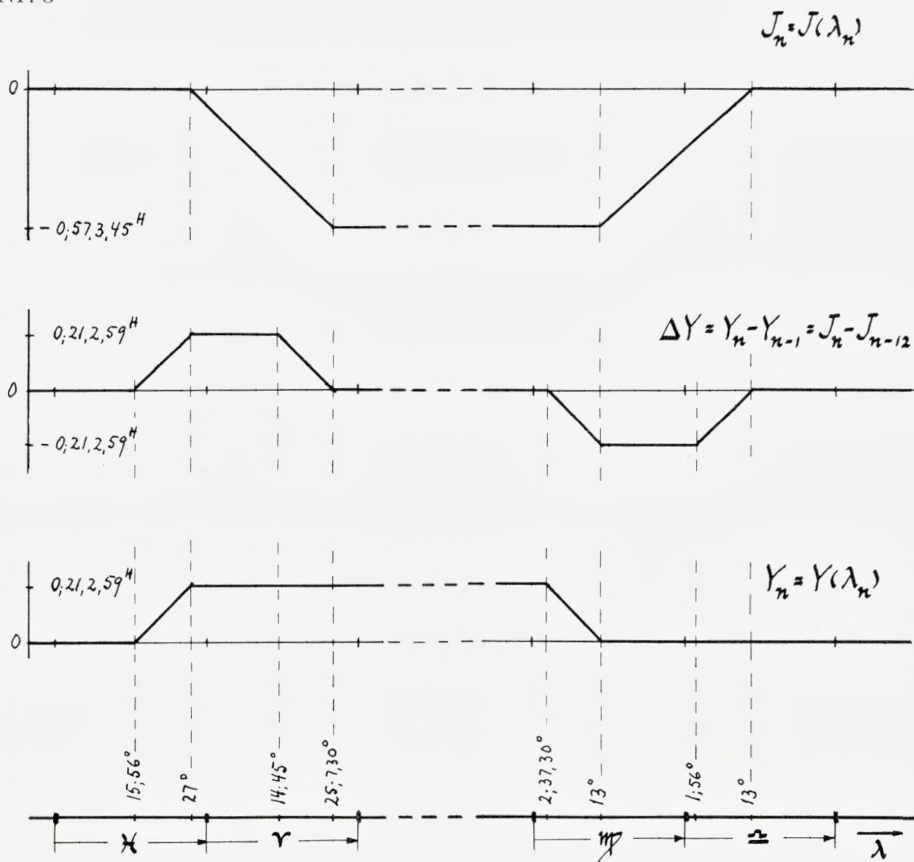
Fig. 1.

or a lag of 1,23 intervals; on the fast arc, 1,23 intervals amount to 11;4°, and on the slow to 10;22,30°. Thus, λ_{n-12} will always be 1,23 intervals ahead of λ_n in the ecliptic.

If λ_n and λ_{n-12} both lie on one of the predominant stretches of the ecliptic where J is constant, ΔY will be zero. If λ_n and λ_{n-12} both lie in one of the two transitional zones for J, both of length 3,45 intervals, ΔY will, but for its sign, be

$$|J_n - J_{n-12}| = \frac{1,23}{3,45} \cdot 0;57,3,45 = 0;21,2,59^H.$$

When we are moving into the slow arc, this contribution will be positive, and it is negative in the other transitional zone. When only one of the longitudes

λ_n and λ_{n-12} is in a transitional zone of J, ΔY will assume an intermediary value, and will depend linearly on λ_n, as shown in Figure 1.

If to this we now add the demand that Y itself be zero on the fast arc, or most of it, Y_n is completely determined as a function of λ_n (see again Figure 1). The value of Y will be

$$Y = +0;21,2,59^H$$

on most of the slow arc, but the jumps of the solar model will be preceded by short transitional zones, as is readily seen.

It is convenient and, as we shall see, useful to give Y_n directly as a function of λ_n, avoiding J as an intermediary:

λ_n between ♍ 13° and ♓ 15;56°: $Y_n = 0$
λ_n between ♓ 15;56° and ♓ 27°: $Y_n = 0;1,54,7,30 \cdot (\lambda_n - ♓ 15;56)$
λ_n between ♓ 27° and ♍ 2;37,30°: $Y_n = 0;21,2,59$
λ_n between ♍ 2;37,30° and ♍ 13°: $Y_n = 0;2,1,44 \cdot (♍ 13 - \lambda_n)$.

The zones of transition are so short for Y (1,23 intervals compared to the monthly advance of 3,45) that transitional Y-values are avoided more often than not.

I should emphasise that Y_n is not the same as

$$\sum_{i=n-11}^{n} J_i ;$$

Y agrees with J only in its differences, but the condition that Y be zero on the fast arc is entirely independent of J.

It is now possible to compute mean values, $\bar{J}$ and $\bar{Y}$, for J and Y. Since the values in one transitional zone complement those in the other, the non-zero values are effectively in play in 22,8 intervals (the number of intervals of the slow zone) out of the entire 46,23. Thus:

$$\bar{J} = -0;57,3,45 \cdot \frac{22,8}{46,23} = -0;27,13,45, \ldots^H$$

and

$$\bar{Y} = 0;21,2,59 \cdot \frac{22,8}{46,23} = 0;10,2,40, \ldots^H$$

Applying these mean corrections I can now get agreement where I failed earlier. In my previous publication I computed

$$\max \sum_{i=1}^{12} G_i \equiv 9;32,21,43, \ldots^{\mathrm{H}} \pmod{6^{\mathrm{H}}}$$

which did not agree with

$$\max \varLambda = 3;55,33,20^{\mathrm{H}},$$

even modulo 6^{H}. However,

$$\max \sum_{1}^{12} G + 12\,\bar{\mathrm{J}} = 9;32,21,43, \ldots - 5;26,45,6, \ldots$$
$$= 4;5,36,36, \ldots^{\mathrm{H}}$$

and

$$\max \varLambda + \overline{\mathrm{Y}} = 3;55,33,20 + 0;10,2,40, \ldots$$
$$= 4;5,36,0, \ldots^{\mathrm{H}}.$$

The slight deviation is, in part, due to the adjustment of G near its maximum. As said, it is in general so that

$$\sum_{i=n-11}^{n} (29^{\mathrm{d}} + G_i^{\mathrm{H}} + J_i^{\mathrm{H}}) = 354^{\mathrm{d}} + \varLambda_n^{\mathrm{H}} + Y_n^{\mathrm{H}},$$

at least to several sexagesimal places, so the rôle of $\varLambda$, when corrected by Y, can well be to provide a much needed control for the summation of G and J. I shall elaborate on this point below.

Further, I found in my previous paper that the sum of $\varLambda$, converted into days, and X was very constant, so

$$354^{\mathrm{d}} + \varLambda + X = 6,5;9,33, \ldots^{\mathrm{d}}$$

which is near a value of the year, though too small; thus I interpreted X as the variable epact, i. e., the difference between a constant year and the variable length of 12 months. Applying the correction $\overline{\mathrm{Y}}$ we now have:

$$354^{\mathrm{d}} + \varLambda + \overline{\mathrm{Y}} + X = 6,5;11,13, \ldots^{\mathrm{d}}$$

which is a better year value, though still too small.

It is now a reasonable guess that even as $\varLambda$ and G receive corrections for solar anomaly so also does $\varPhi$, though there is at present no textual evidence for it. Calling this hypothetical correction S we would then have for the length of the Saros

$$\sigma_n = 6585^{\mathrm{d}} + \varPhi_n + S_n = \sum_{i=n+1}^{n+223} (29^{\mathrm{d}} + G_i + J_i),$$

whence

$$\sigma_n - \sigma_{n-1} \;=\; \Phi_n - \Phi_{n-1} + S_n - S_{n-1}$$
$$=\; G_{n+223} - G_n + J_{n+223} - J_n$$

so

$$S_n - S_{n-1} \;=\; J_{n+223} - J_n.$$

An advance of 223 months corresponds to an advance in longitude of

$$3,43.Z \;=\; 13,56,15 \equiv 1,21 \text{ intervals (mod } \Pi)$$

(observe, that to go one Saros forward or 12 months back leads to solar positions within 2 intervals of each other). The 1,21 intervals amount to $10;7,30°$ on the slow arc and $10;48°$ on the fast.[9a] If the two longitudes λ_n and λ_{n+223} both lie in a transitional zone of J, the corresponding change in J will, but for its sign, be

$$|J_{n+223} - J_n| \;=\; \frac{1,21}{3,45} \cdot 0;57,3,45 \;=\; 0;20,32,33^{\mathrm{H}}.$$

When we move from the fast zone into the slow,

$$\Delta S \;=\; J_{n+223} - J_n$$

will be negative.

If we now require that S be zero on most of the fast arc, as are Y and J, an argument completely analogous to that for Y shows, that

$$S \;=\; -0;20,32,33^{\mathrm{H}}$$

on most of the slow arc. As for Y, there will be transitional zones for S, but they will be of length 1,21 intervals instead of 1,23 intervals.

The effective mean value of S, $\bar{S}$, will be

$$\bar{S} \;=\; -0;20,32,33 \cdot \frac{22,8}{46,23} \;=\; -0;9,48,9,\ldots^{\mathrm{H}} \;=\; -0;1,38,1,\ldots^{\mathrm{d}}.$$

It is very plausible, indeed, that Φ requires a correction of this sort. The mean value of Φ when not truncated is

$$\mu_{\Phi} \;=\; 2;7,26,23,20^{\mathrm{H}} \;=\; 0;21,14,23,\ldots^{\mathrm{d}};$$

but if one considers the effective Φ-function, truncated at $2;13,20$ and $1;58,31,6,40$, one can readily compute the effective mean value of Φ by finding the "area" under the truncated curve, to use modern terminology.

[9a] Cf. ACT No. 204, Section 7, where line 18 can now be restored.

It is
$$\overline{\varPhi} = 2;7,5,20,57, \ldots .^{\mathrm{H}} = 0;21,10,53, \ldots .^{\mathrm{d}}.$$

If we use the classical value for the mean synodic month of

$$\overline{m}_{\mathrm{B}} = 29;31,50,8,20^{\mathrm{d}}$$

which derives from System B, and which was used by HIPPARCHOS and PTOLEMY, we get for the mean Saros:

$$\overline{\sigma}_{\mathrm{B}} = 3,43 \cdot \overline{m}_{\mathrm{B}} = 1,49,45;19,20,48,20^{\mathrm{d}}.$$

There is no explicit value for the mean synodic month in System A; however, NEUGEBAUER derived one in the Saros paper from the value of the anomalistic month and the period relation of F and $\varPhi$, which relates the anomalistic to the synodic month, and he got

$$\overline{m}_{\mathrm{A}} = 29;31,50,19,11, \ldots .^{\mathrm{d}}.$$

This value yields a mean Saros of

$$\overline{\sigma}_{\mathrm{A}} = 1,49,45;20,1,17, \ldots .^{\mathrm{d}}.$$

For either of these values of the mean Saros, the fractional part is less than both $\mu_{\varPhi}$ and $\overline{\varPhi}$. However, if the latter values be corrected by the hypothetical $\overline{S}$ (in days), we get:

$$1,49,45 + \mu_{\varPhi} + \overline{S} = 1,49,45;19,36,22, \ldots .^{\mathrm{d}}$$

and

$$1,49,45 + \overline{\varPhi} + \overline{S} = 1,49,45;19,32,52, \ldots .^{\mathrm{d}}.$$

Though no perfect agreement is reached, it still seems reasonable that a correction like S should be applied to $\varPhi$.

Further, by brute numerical "integration" of G, NEUGEBAUER found the following effective "area" mean value of G:

$$\overline{G} = 3;38,15,1, \ldots .^{\mathrm{H}} = 0;36,22,30, \ldots .^{\mathrm{d}}$$

which, after application of the mean value $\overline{J}$ in days, implies a value for the mean synodic month of

$$\overline{m} = 29^{\mathrm{d}} + \overline{G} + \overline{J} = 29;31,50,12, \ldots .^{\mathrm{d}}.$$

Thus one gets the following value of the mean Saros:

$$3,43 \cdot (29^{\mathrm{d}} + \overline{G} + \overline{J}) = 1,49,45;19,36,42, \ldots .^{\mathrm{d}},$$

which, curiously enough, agrees better with the value derived from μ_Φ than with that derived from $\bar{\Phi}$.

All of the values of the mean Saros, and in particular the one derived from the reconstructed System A value of the mean synodic month, are close to

$$\bar{\sigma} = 6585\tfrac{1}{3}^{\text{d}}$$

which is assigned to the ancients by PTOLEMY,[10] and which he calls superficial. I cannot help suspecting that the relation

$$223 \text{ months} = 6585^{\text{d}} + \tfrac{1}{3}^{\text{d}}$$

somehow played a fundamental rôle in the construction of the more refined schemes, though I still cannot see what it was.

In these discussions of the various corrections for the effect of solar anomaly I have, as I said, taken J as given. However, I shall now show that once the solar model is agreed upon, J is essentially determined by the decision to let it vanish on the fast arc. On the slow arc, syzygies happen

$$30° - 28;7,30° = 1;52,30°$$

sooner in longitude than on the fast arc. If we now use $12;11,27°^{/\text{d}}$ as the difference velocity between the moon and the sun, i. e., assume a constant lunar velocity and ignore the relatively slight variation in solar velocity, then syzygies will happen, roughly,

$$\frac{1;52,30°}{12;11,27°^{/\text{d}}} \cdot 6^{\text{H/d}} = 0;55,22,10, \ldots^{\text{H}}$$

sooner in time on the slow arc than on the fast. If it is then decided that no correction to the time interval between consecutive syzygies is desired when both syzygies happen on the fast arc, a correction of the order of

$$- 0;55,22,10^{\text{H}}$$

should be applied when both syzygies occur on the slow arc. Further, it is readily seen that if one of the two consecutive syzygies is in the fast arc, and the other in the slow, then the required correction is found by precisely the same sort of rules that yield transitional J-values.

The correction we find in the texts is, of course, not this, but

$$J = - 0;57,3,45^{\text{H}},$$

[10] *Almagest* IV, 2.

yet it is of the right order of magnitude, and, as I just said, the rules for finding transitional J values are what one expects. The difference velocity between moon and sun that yields the actual J is, as a simple computation shows, $11;50, \ldots °/d$ which is rather low. I have sought, but in vain, for a derivation of precisely $-0;57,3,45$ which satisfied me, and I have failed to see the particular attractiveness of this number. It is, of course, nicely divisible by 3,45 (the Z of the solar model), but so are many other numbers of the same order of magnitude. That $0;57,3,45$ is too large obviously does not matter in the long run, for

$$29^d + \bar{G} + \bar{J}$$

is a very good value for the mean synodic month. I believe at present that this choice of a value for J may well be motivated by a desire for the pleasant initial value of G,

$$G = 2;40^H,$$

but it is clear that the order of magnitude is fixed, so the freedom of choice is quite restricted.

It is now possible to attempt a reconstruction of the theory and methodology underlying the procedures for predicting syzygies.

The basic decision is that the effect of lunar and solar anomaly be separated into independent, additive terms, so:

(i)   1 month $= 29^d + G^H + J^H$
(ii) 1 Saros $= 223$ months $= 6585^d + \Phi^H + S^H$
(iii)   12 months $= 354^d + \Lambda^H + Y^H$

where G, Φ, and Λ depend on lunar anomaly, and J, S, and Y on solar longitude.

The solar model, and the condition that J vanish on the arc of high monthly solar progress, combine to determine J, and hence $\bar{J}$, as we have just seen. Assuming that G, Φ, and Λ vary independently of J, S, and Y, or can be taken to be constant, we can now derive S and Y from J and the decision that they, too, be zero on the fast arc; thus $\bar{S}$ and $\bar{Y}$ are determined.

Turning now to Φ, we observe first that a value of the mean synodic month and S determine the mean value of Φ. Assuming next that J and S are constant, a theoretical argument shows that Φ is in phase with the lunar velocity F.[11] A value of Φ's amplitude, and the decision that Φ be a truncated

[11] For such an argument cf. loc. cit. in note 4, p. 10. If one wishes to check how successful the Babylonians were in bringing Φ and F into phase with the actual lunar velocity, it is particularly convenient to consider the conjunction which happened at the end of S.E. 80, VIII.

zig-zag function finally determine Φ completely. This last step raises several questions which I cannot answer satisfactorily; I shall return to them below.

As for G, a value of the mean synodic month and $\bar{J}$ determine the mean value of G, $\bar{G}$. Further, (i) and (ii), and the assumption that G and Φ vary independently of J and S, establish the fundamental relation between differences in G and Φ

$$\Phi_n - \Phi_{n-1} = G_{n+223} - G_n$$

which determines G but for an additive constant. Finally, $\bar{G}$ serves to fix that constant.

$\varLambda$ is treated as G.

It is clear that the remaining questions, except for those concerning arithmetical details of adjusting parameters to pleasant values, are raised by Φ. The central rôle of Φ is obvious, and it is now apparent that Φ was in continuous use—in the strong sense that its values computed month by month connect the earliest to the latest texts—since times already before the System A schemes reached their final form. However, I am still at a loss to explain in a satisfactory manner how the amplitude of Φ can be derived from the sort of observations which were recorded by the Babylonians, nor am I yet quite convinced of the desirability of truncating the zig-zag function which is chosen to represent it. And there is still the uncomfortable fact that Φ is found side by side with early and primitive solar models,[11a] while S as constructed above depends on the fully developed System A solar scheme. We can only hope that the appearance of new texts will help us solve these problems.

Text: B.M. 40094

B.M. 40094 (81–2–1, 59).

Provenance: Babylon (B.M. number).

Contents: K, M, $\varLambda$, Y, $\hat{C}$', K for new moons, month by month, for Philip Arrhidaeus 4, XII to 7, XII (= S.E.–8, XII to –5, XII).

Transcription: Table 2, complemented by Table 1.

Photograph: see Plate.

Here Φ_1 assumes precisely the value m_Φ, so one would expect the moon to be near its apogee. Dr. JOHN BRITTON drew my attention to the fact that there happens to be a solar eclipse at this conjunction (–231 Nov. 19, 7;44^h a.m. G.M.T.), so the desired information is readily available. It turns out that the moon is only about $1\frac{1}{2}°$ from its apogee at the moment of conjunction. Since their period relation is good, it is clear that F and Φ were very well in phase with the actual lunar velocity throughout the relevant period.

[11a] Cf. A. AABOE and A. SACHS, *Two Lunar Texts of the Achaemenid Period from Babylon.* To appear in Centaurus, 1969.

Description of Text

The text is a fragment belonging, as its curvature shows, to the right half of what was probably a very wide tablet of the shape characteristic of lunar ephemerides. Top and bottom, but no other, edges are preserved; the obverse has 20 lines, the reverse 18. The surface is crumbling rather badly. I am convinced that the text is a copy from a poorly preserved exemplar, for there is an unusual number of isolated errors of the sort readily committed in copying a bad text (e. g., 8 for 5, and 5 for 8).

Columns III and IV are run into each other, as are Columns V and VI. The scribe's hand is such that it is often difficult to distinguish between his "tab", "20", and ".", where "." denotes the separation mark consisting of two diagonal wedges, used for zero.

Critical Apparatus

Obv. I, 4.   [1,4]0,48: should be 1,40,45.
Obv. II, 6.   2,15,5: should be 2,17,5.
Obv. II, 8.   1,49,33: should be 1,49,43.
Obv. II, 9.   3,48,15: should be 3,48,25.
Rev. II, 8.   4],57,44: should be 4,57,46.
Rev. II,14.   1,49,5: should be 1,39,35.
Obv.III, 1.   3,5,10: copyist's error for 3,8,10; "tab" is followed by what may be "šá m[u]" (for the year) although the "šá" could be read "4".
Obv.III, 2.   3,40,45: should be 3,44,45.
Obv.III, 9.   18,29,16,42,46,40: should be 17,29,16,42,46,40.
Obv.III,10.   15,15: should be 18,15.
Obv.III,11.   6,27,54,53,20: should be 6,27,57,46,40.
Obv.III,15.   3,10,44,15,33,20: should be 3,10,54,15,33,20.
Obv.III,19.   3,34,12,2,13,20: should be 3,31,12,2,13,20.
Rev. III, 7.   1,33,25,53,58, . . .: should be 1,33,25,53,56,6,40.
Rev. III, 8.   1,23,36,45,47,13,20: should be 2,23,36,45,47,13,20.
Rev. III,13.   3,29,11,6,40: should be 3,29,11,40; a very natural slip of the stylus for a scribe accustomed to the frequently occurring endings of nice numbers.
Rev. III,18. Λ-value should be denoted lal.
Obv. IV,13.   Value should be 21,2,59, but traces in the second place look like ₍3₎ rather than ₍2₎.
Col. IV.   Except for the first four lines, the values are denoted lal instead of tab, perhaps in imitation of Col. J.

Table 1.

		[T₁]	[Φ₁]	[B₁]	[C₁]	[G₁]	[J₁]	[C'₁]
Obv.	1.	S.E. −8, XII	2, 7,53, 8,53,20	♈ 11;26,15	3, 0,57,30	3,42,20	− 29,17,31,30	− 9,40,45
		−7, I	2,10,39, 4,26,40	♉ 9;33,45	3,19,42,30	3,16,31,21,28,53,20	− 57, 3,45	− 9,22,30
		II	2,13,25	♊ 7;41,15	3,31, 4,30	2,50,48,20	− 57, 3,45	− 5,41
		III	2,16,10,55,33,20	♋ 5;48,45	3,35,26,30	2,40	− 57, 3,45	− 2,11
	5.	IV	2,15,12,46,40	♌ 3;56,15	3,32,48,30	2,40	− 57, 3,45	+ 1,19
		V	2,12,26,51, 6,40	♍ 2; 3,45	3,23,10,30	2,41,46, 6,40	− 57, 3,45	+ 4,49
		VI	2, 9,40,55,33,20	♎ 1;20	3, 5,46,40	3, 2,31,21,28,53,20	− 22,11,27,30	+ 8,41,55
		VII	2, 6,55	♏ 1;20	2,45,46,40	3,28,20		+ 10
		VIII	2, 4, 9, 4,26,40	♐ 1;20	2,31,28	3,54, 8,38,31, 6,40		+ 7, 9,20
	10.	IX	2, 1,23, 8,53,20	♑ 1;20	2,25, 9,20	4,19,57,17, 2,13,20		+ 3, 9,20
		X	1,58,37,13,20	♒ 1;20	2,26,50,40	4,45,45,55,33,20		− 50,40
		XI	1,59,44,37,46,40	♓ 1;20	2,36,32	4,55, 2,57,46,40		− 4,50,40
		XII	2, 2,30,33,20	♈ 1; 3,45	2,54, 2,30	4,32,30,51,51, 6,40	− 8,14,32,30	− 8,45,15
		XII₂	2, 5,16,28,53,20	♈ 29;11,15	3,12,47,30	4, 6,42,13,20	− 57, 3,45	− 9,22,30
	15.	−6, I	2, 8, 2,24,26,40	♉ 27;18,45	3,26,55,30	3,40,53,34,48,53,20	− 57, 3,45	− 7, 4
		II	2,10,48,20	♊ 25;26,15	3,34, 3,30	3,15, 4,56,17,46,40	− 57, 3,45	− 3,34
		III	2,13,34,15,33,20	♋ 23;33,45	3,34,11,30	2,49,33,20	− 57, 3,45	− 4
		IV	2,16,20,11, 6,40	♌ 21;41,15	3,27,19,30	2,40	− 57, 3,45	+ 3,26
		V	2,15, 3,31, 6,40	♍ 20;16	3,13, 9,20	2,40	− 43,14,26,30	+ 7, 5, 5
	20.	VI	2,12,17,35,33,20	♎ 20;16	2,53, 9,20	2,42,22,57,46,40		+ 10
Rev.	1.	VII	2, 9,31,40	♏ 20;16	2,35,53,36	3, 3,57,46,40		+ 8,37,52
		VIII	2, 6,45,44,26,40	♐ 20;16	2,26,37,52	3,29,46,25,11, 6,40		+ 4,37,52
		IX	2, 3,59,48,53,20	♑ 20;16	2,25,22, 8	3,55,35, 3,42,13,20		+ 37,52
		X	2, 1,13,53,20	♒ 20;16	2,32, 6,24	4,21,23,42,13,20		− 3,22, 8
	5.	XI	1,58,27,57,46,40	♓ 20;16	2,46,50,40	4,47, 9,11,51, 6,40		− 7,22, 8
		XII	1,59,53,53,20	♈ 18;48,45	3, 5,52,30	4,54,18,16,17,46,40	− 44,15,18,30	− 9,30,55
		−5, I	2, 2,39,48,53,20	♉ 16;56,15	3,22,46,30	4,31, 4,26,40	− 57, 3,45	− 8,27
		II	2, 5,25,44,26,40	♊ 15; 3,45	3,32,40,30	4, 5,15,48, 8,53,20	− 57, 3,45	− 4,57
		III	2, 8,11,40	♋ 13;11,15	3,35,34,30	3,39,27, 9,37,46,40	− 57, 3,45	− 1,27
	10.	IV	2,10,57,35,33,20	♌ 11;18,45	3,31,28,30	3,13,38,31, 6,40	− 57, 3,45	+ 2, 3
		V	2,13,43,31, 6,40	♍ 9;26,15	3,20,13,30	2,48,19,15,33,20	− 57, 3,45	+ 5,37,30
		VI	2,16,29,26,40	♎ 9;12	3, 0,32	2,40	− 7,13,40,30	+ 9,50,45
		VII	2,14,54,15,33,20	♏ 9;12	2,40,32	2,40		+ 10
		VIII	2,12, 8,20	♐ 9;12	2,28,19,12	2,43, 0,33,20		+ 6, 6,24
	15.	IX	2, 9,22,24,26,40	♑ 9;12	2,24, 6,24	3, 5,24,11,51, 6,40		+ 2, 6,24
		X	2, 6,36,28,53,20	♒ 9;12	2,27,53,36	3,31,12,50,22,13,20		− 1,53,36
		XI	2, 3,50,33,20	♓ 9;12	2,39,40,48	3,57, 1,28,53,20		− 5,53,36
		XII	2, 1, 4,37,46,40	♈ 8;26,15	2,58,57,30	4,22,50, 7,24,26,40	− 23,12,19,30	− 9,38,21

Rev. line 5. Col. IV,5 is empty; the Y-value should be 8,14,32,30 tab. In Col. V,5 the text has the value 8,12,35,30 tab; this should be 3,35,55 tab. In Col. VI,5 we read 3,36,45 with the final 5 damaged; this should be 0;7,29 tab. I believe that the scribe copied from an exemplar which, like his copy, occasionally

TABLE 2.

	I (K)		II (M)	III (Λ)	IV (Y)	V (C̃')	VI (K̃)	
Obv. 1.	[3, 3, 22]	29	5,29,46 šú	3, 5,10 tab šá⁽?⁾ mlu⁽?⁾	21, 2,59 tab	3,47,30 tab]	[3,32,40 tab]	1.
	[2,10].5	29	3,19,40 šú	3,40,45	21, 2,59 tab	2, 8 tab	[4, 7,56 tab]	
	[1]48.3	28	1,31,38 šú	3,55,33,20	21, 2,59 tab	1, . tab]	[4,17,36 tab]	
	[1,40,48	29	5,50,53 šú	3,54,15	21, 2,59 tab	8 lal	[4,15,10 tab]	
5.	1,44,15	29	4, 6,37 šú	3,33, 8,53,20		1,[19,30 lal]	[3,31,49 tab]	5.
	[1,49,31]	28	2,15, 5, šú	2,48, 1,52,16, 6,40		2,24 lal	[2,45,38 tab]	
	[2,49, 2]	[ ]	5,28, 3 šú	1,57,51, . ,25		3,41,[20 lal]	[1,54,10 tab]	
	[3,38,20]	[ ]	1,49,33 šú	1, 7,40, 8,33,53,20		3,22,[8 lal]	[1, 4, 18 tab]	
	[4, 1, 18]	[ ]	3,48,15 šú	18,29,16,42,46,40		1,53,40 lal]	[15,35 tab]	
10.	[4,23, 6]	[	5,2[5,19 šú	15, 15 lal		25, 4,[lal]	[18,40 lal]	10.
	[4,44,55]	[	40,24 šú	6,27,54,53,20 lal		1, 3, 28[tab]	[5,23 lal]	
	[4,50,12]	[	1,50],12 šú	40,27, 1, 3,53,20 tab		2,32 tab	[42,59 tab]	
	[4,15,31]	[	3,3]4,41 šú	1,30,37,52,55 tab	21,7½,59 lal	3,27,30 tab	[1,55, 8 tab]	
	[3, 0, 15]	[	3]4,26 šú	2,20,48,44,46, 6,40	21, 2,59 lal	3,[27,30 tab]	[2,45,19 tab]	
15.	[2,36,47]	[	3,5[7,39 šú	3,10,44,15,33,20	21, 2,59 lal	2, 4,3[0 tab]	[3]34,[1 tab]	15.
	[2,14,27]	[	1,4[3,12, šú	3,46	21, 2,59 lal	[41,30 tab]	4,[7,44 tab]	
	[1,52,15]	[	5,50,46 šú	3,55, 33, 20	21, 2,59 lal	[41,30 lal]	4,[15,55 tab]	
	[1,46,22]	[	4, 4,24 šú	3,53,47,13,20	21, 2,59 lal	2,[4,30 lal]	[4,12, 45 tab]	
	[2, 3,50]	[	2, 0,34 šú	3,34,12, 2, 13,20		3,41, 20 lal]	[3,27,31 tab]	
20.	[2,52,23]	[	5, 8,11] šú	2,45,13,51,15		[3,41,20 lal]	[2,41,32 tab]	20.
Rev. 1.	[3,12,36]	[	1,55,36 šú]	[1, 55, 2,59,23,53,20		[2,12,48 lal]	[1,52,50 tab]	1.
	[3,34,24]	[	4,21, 12 šú]	1, 4,52, 7,32,46,40		44,16 lal	[1, 4, 8 tab]	
	[3,56,13]	[	24,59 šú]	14,41,15,41,40 tab		44,16 tab	15,26[tab]	
	[4,18, 1]	[	2, 6,57 šú]	19, 1,17,46,40 lal		2,12,48 tab	16,48 lal]	
5.	[4,39,47]	[	3,27,10 šú]	4,21, 0,52,46,40 lal	⟨8,14,32,30⟩	8,12,35,30 tab	3, 36,55 [ʳ]	5.
	[4, 0,32]	[	5,26,37] šú	43,15, 2, 5 tab	21, 2,59 lal	3,27,30 tab	1, 7,4[6 tab]	
	[3,25,34]	[	2, 1], 2 šú	1,33,25,53,58, ...	21, 2,59 lal	2, 4,30 tab	1,56,[33 tab]	
	[3, 3, 15]	[	4]57,44 šú	1,23,36,45,47,13, 20 tab	21, 2,59 lal	41,30 tab	2,4[5,20 tab]	
	[2,40,56]	[	] 2,16,50 šú	3,13,31,40 tab	21, 2,59 lal	41,30 lal	3, 3[8, 53 tab]	
10.	[2,18,38]	[ ]	5,58,12 šú	3,47,14, 4,26,40 tab	21, 2,59 lal	2, 4,30 lal	4,[6, 12 tab]	10.
	[1, 56,53]	[28	4, 1,19 šú	3,55,33,20 tab	7,13,40,30 lal	3,32, 5 lal	[3,59,15 tab]	
	[2,42,37]	[28	1,18,42 šú	3,53,10,22,13,20		3,41,20 lal	[3,49,29 tab]	
	[2,50]	[28	4,28,42 šú	3,29, 11, 6,40 tab		2,19,12 lal	[3,26,52 tab]	
	[2,49, 7]	[28	1,49, 5 šú	2,42,25,50,13,53,20 tab		50,40 lal	[2,41,35 tab]	
15.	[3, 7,30]	[28,	4,32, 4 šú	1,52,14,58,22,46,40 tab		37,52 tab	[1,52,52 tab]	15.
	[3,29,19]	[ ]	1, 2,46 šú	1, 2, 4, 6,31,40 tab		3, 6,24 [tab]	[1, 4,10 tab]	
	[3,51, 8]	[29	3, 11,36 šú	11,56,23,33,53,20		3,34,5[6 tab]	[15,31 tab]	
	[3,49,59]	[29	5,21,38 šú	19,29,26,40 ⟨lal⟩	21, 2,59 lal	3,27,30 tab]	[5, 1 tab]	

B.M. 40094 (81-2-1, 59)

ran the columns together and in which line 5 of the reverse
was damaged; and that he copied what he saw in the correct
line, but shifted one column to the right.

2*

Obv. V.   All readings are very uncertain.
Obv. V, 3.   1, . ta[b]: reading not certain, might even be 1 u[š].
Rev. V, 5.   See note to Rev. line 5.
Rev. V,16.   3,6,24: should be 2,6,24.
Rev. VI, 3.   Reading uncertain.
Rev. VI, 5.   See note to Rev. line 5.

Commentary

I shall first comment on the text column by column, beginning briefly with the ones I found it necessary to compute for the sake of restoring the preserved columns, and then proceed to a few more general remarks. I shall adhere to the terminology of ACT as far as possible.

Column T, the date column, is reconstructed in the following manner. From well-preserved $\varLambda$-values in Column III, I found, via Table 3, the corresponding $\varPhi$-values, which turned out to be $\varPhi_1$-values (i. e., $\varPhi$-values associated with conjunction) and Column $\varPhi$ of the text was thus recaptured. Assuming that these $\varPhi$-values are connectible to those of the ACT System A texts, the date column could then be provisionally restored. Assuming further that the solar longitudes, too, are connectible to those in the ACT corpus, the dates then yielded the solar longitudes given in Column B. These solar longitudes were later confirmed by Column Y (particularly Rev. IV, 11), as well as by columns which depend on length of daylight which, in turn, derives from solar longitude.

The reconstructed dates are then beyond doubt, though they are very early. The hitherto earliest known lunar ephemeris according to System A was ACT No. 1 (from Uruk) for the years S.E. 124–125.

To proceed with the reconstructed columns, Column C gives the length of daylight in large hours and is derived from Column B according to the standard System A scheme given in ACT.[12]

Column G, which played a large rôle in the introductory discussions, is derived from Column $\varPhi$ according to the standard ACT set of rules.[13]

Column J, the correction for solar anomaly, is derived from Column B by the rules discussed above, and Column C' derives from Column C by the relation:

$$C_n{}' = \tfrac{1}{2}(C_{n-1} - C_n),$$

as in ACT.[14]

[12] ACT I, p. 47.
[13] ACT I, p. 60.
[14] ACT I, p. 62.

The first preserved column of our text is Column K, where

$$K_n = G_n + J_n + C_n',$$

i. e., it denotes the length of the month, but for 29^d, with a correction, C', built in to account for the monthly variation in the length of daylight; this is necessitated by the desire to denote the moment of conjunction relative to sunset. Column K is, as usual, abbreviated to three places.

Column II is Column M which gives the moment of conjunction; thus, Obv. II,1 says, that in S.E. –8, month XII, the conjunction of sun and moon happened on the 29th day, 5;29,46^H before sunset (šú, short for *ana šú šamaš*, means *until sunset*). In order to compute the date of conjunction, one must know whether the previous month was full or hollow. This information would have been given by Column P, but our text is not preserved that far; thus I have made no attempt at restoring the dates of the conjunction, since I chose to work only with internal evidence. However, the dates can be quite securely reconstructed from PARKER and DUBBERSTEIN's Chronology,[15] if one wishes.

The hours of conjunction are readily computed from K by the rule that

$$M_n = M_{n-1} - K_n,$$

letting M stand for the hours. K is subtracted because M denotes the hours *before* sunset. M, too, is limited to three places; thus, my restoration of K and M may occasionally be off by one in the last digit.

Thus far our text has followed the pattern of System A lunar texts in ACT. The next columns are found here for the first time in an ephemeris, though Λ was known from procedure texts.

Column III gives Λ, month by month. In analogy with the situation for G, it is convenient to introduce a pure zig-zag function, $\hat{\Lambda}$, which has the same period as Λ and Φ (ultimately the anomalistic month) and which agrees with Λ on its linear stretches.

The parameters for $\hat{\Lambda}$ are

$$M\hat{\Lambda} = 5;3,33,53,33,53,20^H$$
$$m\hat{\Lambda} = -0;46,18,8,53,20^H$$
$$d\hat{\Lambda} = 0;50,10,51,51,6,40^{H/m}$$

with reflexion parameters

[15] RICHARD A. PARKER and WALDO H. DUBBERSTEIN, *Babylonian Chronology 626 B.C. – A.D. 75*. Providence, R.I., 1956.

Table 3.

Φ	$\dot{\Phi}$	Λ	*Interpol.*
2, 13, 20 ↑	2, 13, 20 ↑	3, 55, 33, 20	0
2, 15, 27, 2, 13, 20 ↑	2, 13, 2, 13, 20 ↑	3, 55, 33, 20	1
2, 15, 44, 48, 53, 20 ↑	2, 12, 44, 26, 40 ↑	3, 55, 15, 33, 20	2
2, 16, 2, 35, 33, 20 ↑	2, 12, 26, 40 ↑	3, 54, 40	3
2, 16, 20, 22, 13, 20 ↑	2, 12, 8, 53, 20 ↑	3, 53, 46, 40	4
2, 16, 38, 8, 53, 20 ↑	2, 11, 51, 6, 40 ↑	3, 52, 35, 33, 20	5
2, 16, 55, 55, 33, 20 ↑	2, 11, 33, 20 ↑	3, 51, 6, 40	6
2, 16, 55, 55, 33, 20 ↓	2, 11, 15, 33, 20 ↑	3, 49, 20	7
2, 16, 38, 8, 53, 20 ↓	2, 10, 57, 46, 40 ↑	3, 47, 15, 33, 20	8
2, 16, 20, 22, 13, 20 ↓	2, 10, 40 ↑	3, 44, 53, 20	9
2, 16, 2, 35, 33, 20 ↓	2, 10, 22, 13, 20 ↑	3, 42, 13, 20	10
2, 15, 44, 48, 53, 20 ↓	2, 10, 4, 26, 40 ↑	3, 39, 15, 33, 20	11
2, 15, 27, 2, 13, 20 ↓	2, 9, 46, 40 ↑	3, 36	12
2, 15, 9, 15, 33, 20 ↓	2, 9, 28, 53, 20 ↑	3, 32, 26, 40	13
2, 14, 51, 28, 53, 20 ↓	2, 9, 11, 6, 40 ↑	3, 28, 35, 33, 20	14
2, 14, 33, 42, 13, 20 ↓	2, 8, 53, 20 ↑	3, 24, 26, 40	15
2, 14, 15, 55, 33, 20 ↓	2, 8, 35, 33, 20 ↑	3, 20	16
2, 13, 58, 8, 53, 20 ↓	2, 8, 17, 46, 40 ↑	3, 15, 15, 33, 20	17
2, 13, 40, 22, 13, 20 ↓	2, 8 ↑	3, 10, 13, 20	18
2, 13, 22, 35, 33, 20 ↓	2, 7, 42, 13, 20 ↑	3, 4, 53, 20	18, 8, 45
2, 13, 4, 48, 53, 20 ↓	2, 7, 24, 26, 40 ↑	2, 59, 30, 44, 26, 40	18; 8 45
⋮	⋮	⋮	
2, 4, 11, 28, 53, 20 ↓	1, 58, 31, 6, 40 ↑	18, 12, 57, 46, 40	18; 8, 45
2, 3, 53, 42, 13, 20 ↓	1, 58, 13, 20 ↑	12, 50, 22, 13, 20	17; 8, 45
2, 3, 35, 55, 33, 20 ↓	1, 57, 55, 33, 20 ↑	7, 45, 33, 20	16; 8, 45
2, 3, 18, 8, 53, 20 ↓	1, 57, 58, 8, 53, 20 ↓	2, 58, 31, 6, 40	15; 8, 45
2, 3, 0, 22, 13, 20 ↓	1, 58, 15, 55, 33, 20 ↓	− 1, 30, 44, 26, 40	14; 8, 45
2, 2, 42, 35, 33, 20 ↓	1, 58, 33, 42, 13, 20 ↓	− 5, 42, 13, 20	13
2, 2, 24, 48, 53, 20 ↓	1, 58, 51, 28, 53, 20 ↓	− 9, 33, 20	11
2, 2, 7, 2, 13, 20 ↓	1, 59, 9, 15, 33, 20 ↓	− 12, 48, 53, 20	9
2, 1, 49, 15, 33, 20 ↓	1, 59, 27, 2, 13, 20 ↓	− 15, 28, 53, 20	7
2, 1, 31, 28, 53, 20 ↓	1, 59, 44, 48, 53, 20 ↓	− 17, 33, 20	5
2, 1, 13, 42, 13, 20 ↓	2, 0, 2, 35, 33, 20 ↓	− 19, 2, 13, 20	3
2, 0, 55, 55, 33, 20 ↓	2, 0, 20, 22, 13, 20 ↓	− 19, 55, 33, 20	1
2, 0, 38, 8, 53, 20 ↓	2, 0, 38, 8, 53, 20 ↓	− 20, 13, 20	

$$2M - d = 9;16,56,55,16,40$$
$$2m + d = -0;42,25,25,55,33,20$$

and the period

$$P_{\hat{A}} = P_{A} = P_{\Phi} = \frac{1,44,7}{7,28}.$$

A agrees with $\hat{A}$ for

$$0;12,50,22,13,20 \leqq A \leqq 3;4,53,20.$$

Beyond these limits, A is derived from Φ by the scheme given in Table 3. In this table the arrow after a Φ-value indicates whether it belongs to an ascending or descending branch of the zig-zag function; the last column presents interpolation coefficients referring to the subsequent interval.

Column IV gives the function Y, the correction to A for solar anomaly, which has been discussed above. As said, the Y-values, but for the first four, are erroneously denoted "lal" by a scribe who was probably familiar with the similarly appearing Column J. However, as we shall see, the values in Column $\check{K}$ show clearly that Y is to be taken as positive when not zero.

Transitional values are rare, as I said above. The one in Rev. IV, 11, i. e.

$$Y = 0;7,13,40,30^{H}$$

follows precisely the rules set out in the introduction. It would, by itself, have sufficed as a base for reconstructing the solar longitudes, had I only understood Column Y in time.

Column V, which I call $\tilde{C}'$, is a correction to A for the change in length of daylight, analogous to the correction C' to G.

It is precisely derived from C by the rule

$$\tilde{C}'_{n} = \tfrac{1}{2}(C_{n-12} - C_{n}).^{16}$$

In order to restore the first 12 values of this column, I have provided the solar longitudes and the corresponding values of C in Table 4.

Column VI, the last preserved column of the tablet, of which but little remains, I call $\tilde{K}$. It is in an analogous relation to A as K is to G, for

$$\tilde{K}_{n} = A_{n} + Y_{n} + \tilde{C}'_{n}$$

abbreviated to three places.

---

[16] Cf. ACT No. 200b, Section 3, which gives the change in C for 12 month intervals. If one halves these values, one gets $\tilde{C}'$ under certain conditions.

TABLE 4.

T	B_1	C_1
S.E. -9, XII₂	♈ 21;48,45	3, 7,52,30
-8, I	♉ 19;56,15	3,23,58,30
II	♊ 18; 3,45	3,33, 4,30
III	♋ 16;11,15	3,35,10,30
IV	♌ 14;18,45	3,30, 9,30
V	♍ 12;26,15	3,18,22,30
VI	♎ 12,24	2,58,24
VII	♏ 12;24	2,39, 2,24
VIII	♐ 12;24	2,27,40,40
IX	♑ 12;24	2,24,19,12
X	♒ 12;24	2,28,57,36
XI	♓ 12;24	2,41,36
l.1 = XII	♈ 11;26,15	3, 0,57,30

The few numbers which remain of $\tilde{K}$ suffice to show that the designation of the Y-values as negative, but for the first four, is an error without consequence.

The discovery of the columns $\tilde{C}'$ and $\tilde{K}$ makes me unable to see any justification for $\varLambda$ except that it, or rather $\tilde{K}$, provides a much needed check for Column M. Using the relations of G to $\varLambda$, J to Y, and C to C' and $\tilde{C}'$, it is readily seen that we have, at least ideally,

$$M_{n-12} - \tilde{K}_n = M_n \ (\text{mod } 6^H);$$

to give a specific example from the text:

$$
\begin{aligned}
M_{15} &= 3;57,39 \\
-\ \tilde{K}_{27} &= -1;56,33 \\
\hline
&2;\ 1,\ 6
\end{aligned}
$$

and the text gives:

$$M_{27} = 2;1,2.$$

The slight disagreement was, in part, to be expected from what we found in the above comparison between G and $\varLambda$; the relations between J and Y, and C' and $\tilde{C}'$ are, of course, exact.

Since M is a conglomerate of quite unrelated parts, it has, in modern times, always been a problem to check M-values, and the problem is, of course, aggravated by the very nature of M which preserves an error once introduced, as well as by M's importance. It is, then, not very surprising to learn that the Babylonians had constructed $\tilde{K}$, and its ingredients, as a checking

device, of necessity elaborate, nor is it, then, odd that Λ and the other new functions do not appear elsewhere in the regular, finished ephemerides.

If $\tilde{\mathrm{K}}$ is to serve well as a control on M, it is very desirable that its constituent parts be as independent of their analogues in K as possible. As we have seen, Λ is found directly from Φ and independently of G; so I am confident that we shall eventually find textual evidence for the rules I have given above for deriving Y directly from the solar longitude without J as an intermediary.

Yale University
New Haven, Connecticut, U. S. A.

PLATE I

Obv.

Rev.
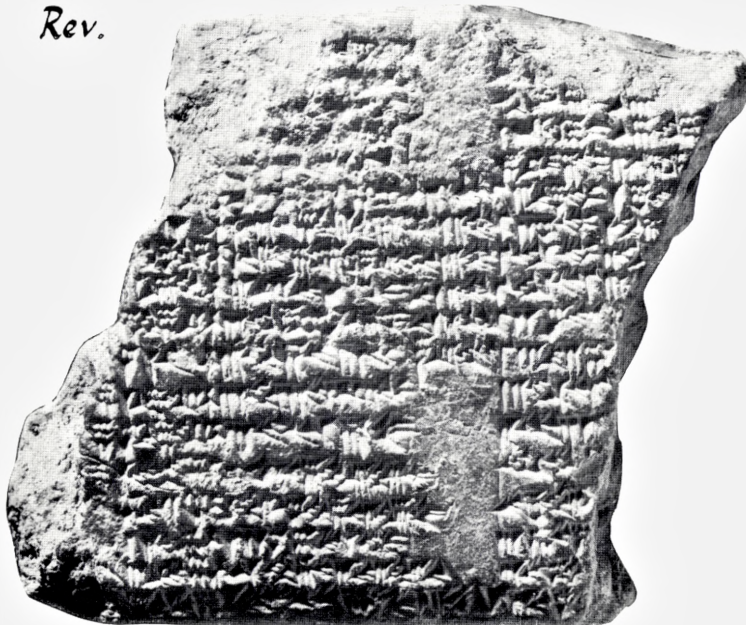
B.M. 40094

C. MØLLER

THE THERMODYNAMICAL POTENTIALS IN THE THEORY OF RELATIVITY AND THEIR STATISTICAL INTERPRETATION

Synopsis

In the theory of relativity the thermodynamical state of a homogeneous isotropic body is determined by five independent variables. In the present paper it is shown that the thermodynamical properties of the body are completely determined by relativistically invariant functions Φ and Ψ of the state variables, which are the appropriate generalizations of the classical free energies of Helmholtz and Gibbs. When the 'potential' Φ (or Ψ) is given, all thermodynamical quantities, such as the four-momentum, entropy etc., can be obtained by partial differentiations of the potentials with respect to the state variables. Finally it is shown that the potentials Φ and Ψ have a simple statistical interpretation in the relativistic generalization of Gibbs' classical statistical mechanics, which allows to calculate the functions Φ and Ψ when the mechanical constitution of the system is known.

1. Introduction and Survey

In classical non-relativistic thermodynamics the thermodynamical potentials —the free energies of HELMHOLTZ and GIBBS — play an important role. When a potential is given as a function of the thermodynamical state variables all state functions can be obtained by partial differentiations of the potential, i.e. the thermodynamical properties of the body in question are completely determined by the potentials. For a homogeneous isotropic body *at rest* and in thermal equilibrium the state is determined by two variables, for instance the volume V^0 and the temperature T^0, and the free energy of HELMHOLTZ is defined by

$$F^0 = H^0 - T^0 S^0, \tag{1.1}$$

where H^0 and S^0 are the energy and the entropy, respectively. When F^0 is known as a function of T^0 and V^0, the entropy and pressure are given by

$$S^0 = -\frac{\partial F^0(T^0, V^0)}{\partial T^0}, \; p^0 = -\frac{\partial F^0(T^0, V^0)}{\partial V^0}, \tag{1.2}$$

and by (1.1) it follows for the energy

$$H^0 = F^0 - T^0 \frac{\partial F^0(T^0, V^0)}{\partial T^0}. \tag{1.3}$$

In a relativistic theory, the relations (1.2) must still be valid in the rest system S^0 of the body, but there is no a priori reason that the same relations should hold in every system of inertia S. The principle of relativity requires only that the corresponding relativistic relations must be covariant and must reduce to (1.2) in the rest system. Nevertheless, PLANCK in his classical paper [1] tried to determine transformation laws for the thermodynamical quantities in such a way that relations of the form (1.2) remain valid in

1*

every system of inertia S. If v is the velocity of the body (or of S^0) with respect to S, we have

$$p = p^0, \quad V = V^0\sqrt{1 - \beta^2}, \quad \beta = v/c. \tag{1.4}$$

The pressure is relativistically invariant, and the same is assumed for the entropy, i.e.

$$S = S^0. \tag{1.5}$$

In order that relations (1.2) be valid also for the transformed quantities, we have then to accept PLANCK's transformation laws for the free energy and temperature in the form

$$F = F^0\sqrt{1 - \beta^2} \tag{1.6}$$

$$T_P = T^0\sqrt{1 - \beta^2}, \tag{1.7}$$

In fact, from (1.2 –7) one easily finds the relations

$$S = -\frac{\partial F(T_P, V)}{\partial T_P}, \quad p = -\frac{\partial F(T_P, V)}{\partial V} \tag{1.8}$$

which have the same form as the equations (1.2) valid in the rest system.

By this argument PLANCK was led to introduce a temperature T_P relative to the arbitrary system of inertia S given by the formula (1.7) and his point of view has been accepted again quite recently in a paper by R. BALESCU [2]. However, in the meantime H. OTT [3] had given strong arguments for introducing a different temperature T_O given by

$$T_O = T^0/\sqrt{1 - \beta^2}. \tag{1.9}$$

In fact, this formula follows uniquely (see (1.35)) if one wants the second law for reversible processes to have the same form

$$dS = \frac{dQ_{\text{rev}}}{T_O} \tag{1.10}$$

as in the rest system, where we have

$$dS^0 = \frac{dQ^0_{\text{rev}}}{T^0}. \tag{1.11}$$

The violent discussions in the literature following Ott's paper have made it clear that the relativity principle alone does not lead to a unique concept of temperature relative to an arbitrary system S, for the transformation law for the temperature will depend on which of the classical thermodynamical relations holding in the rest system, are assumed to retain their form under Lorentz transformations. Beforehand it does not seem quite natural to base the definition of temperature on the requirement of form-invariance of the relations (1.2, 8). Firstly, they refer to the rather special case of a homogeneous isotropic body and it would seem more natural to postulate the form-invariance of the first and the second laws of thermodynamics which are believed to be valid for any thermodynamic system. Secondly, in an arbitrary system of inertia the definition of the state of a homogeneous and isotropic body requires the fixation of five (not two) independent variables, for instance besides T^0 and V^0 the three components of the velocity $\boldsymbol{v}$. This is also the case in the non-relativistic theory, but there the internal thermodynamic properties are entirely separated from the external kinetic properties of the body. This is not so in relativity theory since the inertial mass of the body depends on the internal state. Therefore it is to be expected that the pertinent relativistic generalization of the equations (1.2) will consist of *five* equations which express five thermodynamical quantities as partial derivatives of the relativistic potentials with respect to five suitably chosen independent state variables. These equations must of course reduce to the two equations (1.2) in the rest system S^0.

In section 2 of the present paper we shall see that these expectations are fulfilled when we use the formulation of relativistic thermodynamics which, as was shown in a recent paper [4], is suggested by relativistic statistical mechanics. In the remaining part of the present section we shall give a short account of the relativistic formulation of the first and the second laws obtained in the just quoted paper.

In view of the above mentioned arbitrariness in the general definition of the temperature, it was proposed to abandon the notion of a separate temperature relative to the different systems of inertia. Therefore, when we speak of the temperature of the body we simply mean the proper temperature as measured by a thermometer at rest in the body. In any system of inertia S different from S^0 it appears more adequate to speak of a temperature 4-vector T^i as defined by ARZELIÈS [5]. If V^i is the four-velocity of the body with components

$$V^i = \{\gamma \boldsymbol{v}, \gamma c\}, \qquad \gamma = (1 - \beta^2)^{-\frac{1}{2}} \tag{1.12}$$

the temperature vector is

$$T^i = T^0 V^i / c. \tag{1.13}$$

In the rest system this 4-vector has only the one non-vanishing component T^{04} which is equal to the proper temperature T^0. In an arbitrary system S the fourth component T^4 is equal to the Ott temperature (1.9).

In many thermodynamical considerations it is more convenient to introduce the reciprocal proper temperature

$$\theta = 1/T^0 \tag{1.14}$$

as a measure of the thermal state. Then, if we also introduce a function

$$\Phi^0(\theta^0, V^0) = \theta^0 F^0 \tag{1.15}$$

($-\Phi^0$ is the so-called Planck potential), the relations (1.2) take the form

$$H^0 = \frac{\partial \Phi^0(\theta^0, V^0)}{\partial \theta^0}, \quad p^0 = -\frac{1}{\theta^0} \frac{\partial \Phi^0(\theta^0, V^0)}{\partial V^0}. \tag{1.16}$$

Since θ^0 goes to zero with increasing temperature, Truesdell [6] has coined the word *coldness* for the quantity θ^0. Instead of the temperature vector T^i, it is also convenient to introduce a "coldness vector" θ^i by

$$\theta^i = \theta^0 V^i \tag{1.17}$$

which in the rest system has the components

$$\theta^{0i} = \delta_4^i \, c \theta^0 = \delta_4^i \, c / T^0. \tag{1.18}$$

In an arbitrary system S the fourth component θ^4 is equal to c times the reciprocal of the Planck temperature (1.7). In contrast to the V^i, which satisfies the relation

$$V_i V^i = -c^2, \tag{1.19}$$

the components θ^i of the coldness vector are four independent variables which may replace T^0 and $\boldsymbol{v}$ as state variables. Thus, for a homogeneous isotropic body the thermodynamic state is completely determined by the five variables (θ^i, V^0) or (θ^i, p).

The coldness vector is a time-like 4-vector with the norm

$$\theta(\theta^i) = \sqrt{-\theta_i\theta^i}/c. \tag{1.20}$$

From (1.17–19) it follows that the value of the invariant θ is equal to the coldness,

$$\theta = \theta^0 \tag{1.21}$$

and that

$$V^i = \theta^i/\theta. \tag{1.22}$$

Thus, for given θ^i the coldness and the four-velocity (and so $\boldsymbol{v}$) are determined by (1.21, 22).

Now, as was shown in ref. 4, the appropriate relativistic expressions for the first and second laws of thermodynamics are the following. For an infinitesimal process we have

$$\text{1. law:} \quad dG_i = dI_i + dQ_i \tag{1.23}$$

$$\text{2. law:} \quad dS \geqslant -\theta^i dQ_i. \tag{1.24}$$

In (1.23)

$$dG_i = \{d\boldsymbol{G}, -dH/c\} \tag{1.25}$$

is the change of the four-momentum of the body

$$G_i = \{\boldsymbol{G}, -H/c\}, \tag{1.26}$$

and

$$dQ_i = \{d\boldsymbol{Q}, -dQ/c\} \tag{1.27}$$

is the four-momentum of supplied heat in the process, i.e. dQ is the heat energy and $d\boldsymbol{Q}$ is the momentum conveyed to the body by the heat supply. Finally,

$$dI_i = \{d\boldsymbol{I}, -dA/c\} \tag{1.28}$$

is the 'four-impulse' of the external mechanical forces, i.e. $d\boldsymbol{I}$ is the impulse or the time integral of the total mechanical force acting on the body and dA is the work performed by these forces during the process.

In non-relativistic thermodynamics the first law is expressed by one equation only, the law of conservation of energy. Due to the symmetry between momentum and energy in the theory of relativity, the first law has to be supplemented by three other equations expressing the conservation of momentum. In general neither G_i, dG_i nor dI_i are 4-vectors, but the differences

$$dQ_i = dG_i - dI_i \tag{1.29}$$

are the covariant components of a 4-vector for any process and for an arbitrary thermodynamical system [7] [8] [9]. This important result was obtained first in the case of a fluid in ref. 7. In ref.s 8 and 9 the proof was given for an arbitrary thermodynamical system. For the validity of this theorem it is essential that dI_i by definition includes the impulse and the work of truly 'mechanical' forces only, i.e. the force acting on any infinitesimal part of the body, combined with the rate of work, must form a usual Minkowski four-force.

For a *reversible* process it can further be shown [7] that the four-momentum dQ_i^{rev} of supplied heat is proportional to the four-velocity, i.e.

$$dQ_i^{rev} = \frac{dQ_{rev}^0}{c^2} V_i. \tag{1.30}$$

Since θ^i and dQ_i are 4-vectors the right hand side of (1.24) is an invariant which, on account of (1.18, 27), has the value

$$-\theta^i dQ_i = -\theta^{0i} dQ_i^0 = -\frac{c dQ_4^0}{T^0} = \frac{dQ^0}{T^0}. \tag{1.31}$$

Therefore, by (1.5), the relation (1.24) is equivalent to the relation

$$dS^0 \geqslant \frac{dQ^0}{T^0} \tag{1.32}$$

which is known to be valid in the rest system. Since the equality sign in (1.32) holds for reversible processes only, it follows that also in (1.24) the validity of the equality sign means that the process in question is reversible. For such processes dQ_i^{rev} is given by (1.30), which for $i = 4$ gives

$$dQ_{rev} = dQ_{rev}^0 / \sqrt{1 - \beta^2} \tag{1.33}$$

on account of (1.12, 27). Thus, for a reversible process, (1.24) becomes

$$dS = -\theta^i dQ_i^{rev} = \frac{dQ_{rev}^0}{T^0} = \frac{dQ_{rev}\sqrt{1-\beta^2}}{T^0} \tag{1.34}$$

by means of (1.31, 33). This may also be written in the form (1.10)

$$dS = \frac{dQ_{rev}}{T_0}, \tag{1.35}$$

where T_O is the Ott temperature (1.9). However, it should be noted that (1.24) for an *irreversible* process in general is *not* equivalent to

$$dS > \frac{dQ}{T_O}. \tag{1.35}$$

The latter relation is valid only for very special irreversible processes such as in the case of pure heat conduction.

After this short survey of the general laws of relativistic thermodynamics, we shall in the next section give the appropriate relativistic generalization of the thermodynamical potentials and of the classical relations of the type (1.16). Finally, in the last section the statistical interpretation of the relativistic potentials is given, which will allow us to calculate these quantities when the mechanical constitution of the system is known.

2. Relativistically Invariant Thermodynamical Potentials for Homogeneous Isotropic Bodies

The thermodynamical system considered in this section is a fluid, contained in a vessel of rest volume V^0, which exerts normal pressure only against the walls of the container. In thermal equilibrium the four-momentum of the fluid has the following components in the Lorentz system S [10]:

$$G_i = \{\boldsymbol{G}, -H/c\} = \{(H^0 + p^0 V^0)\gamma \boldsymbol{v}/c^2, -(H^0 + \beta^2 p^0 V^0)\,\gamma/c\} \tag{2.1}$$

where the superscript "0" refers to the rest system S^0 of the fluid. The G_i are not the components of a 4-vector. Nevertheless, $V^i G_i$ is an invariant, for we have in any system S by (1.12) and (2.1)

$$V^i G^i = (H^0 + p^0 V^0)\gamma^2\beta^2 - (H^0 + \beta^2 p^0 V^0)\gamma^2,$$
$$V^i G^i = -H^0. \tag{2.2}$$

Hence, $-V^i G_i$ is equal to the rest energy.

Besides the four-momentum we shall consider two other quantities P_i and E_i which, in contrast to G_i, are 4-vectors. The first one is defined by

$$P_i = H^0 V_i/c^2 \tag{2.3}$$

which would be the four-momentum of the system if it were a free system. Following the terminology of LANDSBERG [11], we shall call P_i the *inclusive* four-momentum. The second 4-vector E_i is defined by

$$E_i = (H^0 + p^0 V^0) \, V_i / c^2. \tag{2.4}$$

A comparison with (2.1) shows that the spatial components E_t are equal to the components of the momentum $\boldsymbol{G}$. The fourth component is of the form

$$E_4 = -E/c \tag{2.5}$$

with

$$E = -cE_4 = (H^0 + p^0 V^0)\gamma = H + p^0 V^0 \gamma (1 - \beta^2)$$

or, on account of (1.4),

$$E = H + pV. \tag{2.6}$$

Hence, E is the quantity usually called enthalpy and therefore E_t will be named four-enthalpy. G_i, E_i, P_i are obviously related by the equations

$$\left. \begin{array}{l} E_i = P_i + p^0 V^0 V_i / c^2 \\[2mm] G_i = E_i + \delta_{i4} pV/c. \end{array} \right\} \tag{2.7}$$

From (2.2–4) we get

$$V^i E_i = -(H^0 + p^0 V^0) = -E^0 \tag{2.8}$$

where E^0 is the enthalpy in the rest system, and

$$V^i P_i = V^i G_i = -H^0. \tag{2.9}$$

Differentation of the second equation (2.7) gives

$$dG_i = dE_i + \delta_{i4} d(pV)/c.$$

Therefore, the first law (1.23) may also be written in the form

$$dE_i = dJ_i + dQ_i \tag{2.10}$$

where

$$dJ_i = dI_i - \delta_{i4} d(pV)/c = \{d\boldsymbol{I}, -[dA + d(pV)]/c\} \tag{2.11}$$

on account of (1.28). In contrast to dI_i, the quantity dJ_i is a 4-vector. This follows at once from (2.10) since both dE_i and dQ_i are 4-vectors. Thus, $\theta^i dJ_i$ is an invariant with the value

$$\theta^i dJ_i = \theta^{0i} dJ_i^0 = c\theta^0 dJ_4^0 = -\theta^0[dA^0 + d(p^0 V^0)]. \tag{2.12}$$

Here we have used (1.18) and (2.11). For a reversible process the work dA^0 in the rest system is

$$dA^0 = -p^0 dV^0. \tag{2.13}$$

Hence

$$\theta^i dJ_i^{\text{rev}} = -\theta^0 V^0 dp^0 = -\theta V^0 dp \tag{2.14}$$

on account of (1.4, 21).

By means of the first and second laws in the forms (2.10) and (1.24) applied to a reversible process we get

$$dS = -\theta^i dQ_i^{\text{rev}} = -\theta^i dE_i + \theta^i dJ_i^{\text{rev}}$$

or, using (2.14),

$$dS = -\theta^i dE_i - \theta V^0 dp. \tag{2.15}$$

On account of the relations (2.7) between E_i, P_i and G_i, this equation may also be written in the alternative forms

$$dS = -\theta^i dP_i + \theta p dV^0 \tag{2.16}$$

and

$$dS = -\theta^i dG_i + \frac{\theta^4 p}{c} dV, \tag{2.17}$$

where

$$\theta^4 = \theta^0 \gamma c = \theta \gamma c \tag{2.18}$$

is the fourth component of the coldness vector. Here we have used (1.4, 12, 19), which imply

$$\theta^i V_i = -\theta c^2. \tag{2.19}$$

Now, we define two invariant state functions Φ and Ψ by

$$\Phi \equiv -\theta^i P_i - S \tag{2.20}$$

$$\Psi \equiv -\theta^i E_i - S. \tag{2.21}$$

Since θ^i is proportional to V^i, (2.9) shows that Φ also may be defined as

$$\Phi = -\theta^i G_i - S. \tag{2.22}$$

On account of (2.7, 18), (1,4), Φ and Ψ are connected by

$$\Psi = \Phi + \theta p V^0. \tag{2.23}$$

By differentiating the expressions (2.20–22) and using the appropriate forms (2.15–17) of dS, one easily finds

$$d\Phi = - P_i d\theta^i - \theta p dV^0 \tag{2.24}$$

$$d\Psi = - E_i d\theta^i + \theta V^0 dp \tag{2.25}$$

$$d\Phi = - G_i d\theta^i - \theta^4 p dV/c. \tag{2.26}$$

For a homogeneous isotropic body of the type considered here the thermal equilibrium states are determined by five independent variables. If we choose (θ^i, V^0) as state variables, every state function appears as a function of these variables. In particular this holds for the quantity Φ. When the function $\Phi(\theta^i, V^0)$ is given, we can calculate five other state functions by differentiations of Φ with respect to the five variables (θ^i, V^0). In fact we get from (2.24) for the inclusive four-momentum and the pressure

$$P_i = - \frac{\partial \Phi(\theta^i, V^0)}{\partial \theta^i}, \quad p = - \frac{1}{\theta} \frac{\partial \Phi(\theta^i, V^0)}{\partial V^0}. \tag{2.27}$$

Then, expressions for the remaining state functions follow from (2.7, 20). For the entropy we get for instance

$$S = - \Phi(\theta^i, V^0) + \theta^i \frac{\partial \Phi(\theta^i, V^0)}{\partial \theta^i}. \tag{2.28}$$

On the other hand, if we choose θ^i and p as state variables we get from (2.25) the following expressions for the four-enthalpy and the rest volume

$$E_i = - \frac{\partial \Psi(\theta^i, p)}{\partial \theta^i}, \quad V^0 = \frac{1}{\theta} \frac{\partial \Psi(\theta^i, p)}{\partial p}. \tag{2.29}$$

Finally, choosing θ^i and V as state variables, (2.26) gives for the four-momentum and the pressure

$$G_i = - \frac{\partial \Phi(\theta^i, V)}{\partial \theta^i}, \quad p = - \frac{c}{\theta^4} \frac{\partial \Phi(\theta^i, V)}{\partial V}. \tag{2.30}$$

A relativistically invariant state function which is a function of tensorial state variables can only depend on invariant combinations of these variables. The only invariant combination of the θ^i is the norm θ defined by (1.20). Thus, since also V^0 is an invariant, the function $\Phi(\theta^i, V^0)$ must be of the form

$$\Phi(\theta^i, V^0) = f(\theta, V^0) , \qquad (2.31)$$

where f is an invariant function characteristic of the material system in question. Similarly, since also p is invariant, we must have

$$\Psi(\theta^i, p) = g(\theta, p) \qquad (2.32)$$

where the function $g(\theta, p)$ is connected with $f(\theta, V^0)$ by he relation

$$g(\theta, p) = f(\theta, V^0) + \theta p V^0 \qquad (2.33)$$

following from (2.23).

Obviously, any state function which only depends on (θ, V^0) or (θ, p) is relativistically invariant, i.e. velocity-independent. From (2.27, 29) and (2.31, 32) we get

$$p = -\frac{1}{\theta} \frac{\partial f(\theta, V^0)}{\partial V^0}, \qquad V^0 = \frac{1}{\theta} \frac{\partial g(\theta, p)}{\partial p}. \qquad (2.34)$$

Thus, p and V^0 are functions of (θ, V^0) and (θ, p), respectively, in accordance with the invariance of these quantities. It is easily seen that also the right hand side of (2.28) is a function of θ and V^0 only, in accordance with the invariance of the entropy. For, by (2.31), (2.28) becomes

$$S = -f(\theta, V^0) + \theta^i \frac{\partial \theta}{\partial \theta^i} \frac{\partial f(\theta, V^0)}{\partial \theta} \qquad (2.35)$$

and, by differentiation of θ in (1.20) with respect to θ^i, we get

$$\left. \begin{aligned} \frac{\partial \theta}{\partial \theta^i} &= -\theta_i/c^2\theta \\[2mm] \theta^i \frac{\partial \theta}{\partial \theta^i} &= -\theta^i\theta_i/\theta c^2 = \theta. \end{aligned} \right\} \qquad (2.36)$$

However, as a function of the variables (θ^i, V), $\Phi(\theta^i, V)$ does not only depend on θ and V, but also on the fourth component θ^4 of the coldness vector. In fact, since

$$V^0 = \gamma V = \frac{V\theta^4}{c\theta}, \tag{2.37}$$

we get from (2.31)

$$\Phi(\theta^i, V) = f\left(\theta, \frac{V\theta^4}{c\theta}\right). \tag{2.38}$$

By differentiating this equation with respect to θ^i (for constant V) and using (2.30) and (2.27) we get back the relations (2.7).

Multiplication of the equations (2.8, 9) by $\theta = \theta^0$ gives

$$\left.\begin{aligned}
\theta^i E_i &= -\theta^0(H^0 + p^0 V^0) \\
\theta^i P_i &= \theta^i G_i = -\theta^0 H^0.
\end{aligned}\right\} \tag{2.39}$$

This discloses the physical meaning of the invariant functions Φ and Ψ defined by (2.20, 21). Obviously we have

$$\Phi = \Phi^0, \tag{2.40}$$

where

$$\Phi^0 = \theta^0 H^0 - S^0 = \theta^0 F^0(\theta^0, V^0) \tag{2.41}$$

is the classical potential (1.15) obtained by multiplying the free energy of HELMHOLTZ by the coldness. Similarly we have

$$\Psi = \Psi^0 \tag{2.42}$$

where

$$\Psi^0 = \theta^0(H^0 + p^0 V^0) - S^0 = \theta^0 G^0 \tag{2.43}$$

and

$$G^0 = F^0 + p^0 V^0 \tag{2.44}$$

is the classical free energy of Gibbs.

Thus, Φ and Ψ are the natural relativistic generalizations of the classical thermodynamic potentials — the free energies of Helmholtz and Gibbs. They have all the properties which, as mentioned in section 1, should be required of relativistic potentials. By the equations (2.27–30), all state functions are expressed in terms of partial derivatives of the potentials with respect to the variables which determine the state. In the rest system, three of the five equations (2.27) simply express the vanishing of the momentum and the two remaining equations are identical with the classical equations (1.16) which are equivalent to (1.2). In contrast to the equations (2.27–30),

which comprise the transformation properties of all thermodynamic state functions under Lorentz transformations, the Planck relations (1.8) are rather trivial transcriptions of the equation (1.2) in the rest system. In excess of (1.2), (1.8) only contains the transformation properties of S, p and V. The function $F(T_P, V)$ does not determine all thermodynamic properties of the system. For instance, there is no equation analogous to (1.3) by which the energy H is determined, not to speak of the components of the momentum $\boldsymbol{G}$. Thus, the free energy $F(T_P,V)$, as defined by (1.6), does not have all the properties of a thermodynamical potential.

From (2.31, 32) and (2.40–44) we get, since $\theta = \theta^0$ and $p = p^0$

$$\left.\begin{aligned}
\Phi^0 &= f(\theta^0, V^0) = \theta^0 F^0(\theta^0, V^0) \\
\Psi^0 &= g(\theta^0, p^0) = \theta^0 G^0(\theta^0, p^0).
\end{aligned}\right\} \quad (2.45)$$

The functions $F^0(\theta^0, V^0)$ and $G^0(\theta^0, p^0)$ can in principle be determined by usual thermodynamical experiments in the laboratory performed on bodies at rest. Then, by (2.45), also the functions $f(\theta^0, V^0)$ and $g(\theta^0, p^0)$ are known functions of the state variables, and by replacing θ^0 by θ and p^0 by p in these functions we get the expressions (2.31, 32) for the relativistic potentials $\Phi(\theta^i, V^0)$, $\Psi(\theta^i, p)$. Also the function $\Phi(\theta^i, V)$ of the variables (θ^i, V) is then determined by (2.38) and, by means of (2.27–30), we can calculate all thermodynamical state functions in an arbitrary system of inertia.

3. Statistical Interpretation of the Relativistic Potentials

Historically, statistical mechanics was developed with the aim to provide a 'rational explanation' of the thermodynamic laws and thereby obtaining a means of calculating the thermodynamical state functions from the knowledge of the mechanical structure of the system in question. In non-relativistic mechanics the statistical methods developed by GIBBS supplied the most general solution of this problem. In the paper quoted in reference [4], a relativistic generalization of Gibbs' classical theory was given which, as we shall see now, supplies an immediate interpretation of the relativistic thermodynamical potentials introduced in section 2.

Consider a system consisting of n particles of proper mass m which, in a certain system of inertia S^0, are acted upon by forces derivable from a timeindependent mechanical potential

$$U_g^0(\boldsymbol{x}_1^0, \ldots \boldsymbol{x}_r^0, \ldots \boldsymbol{x}_n^0, a_l). \quad (3.1)$$

Here, the a_l are invariant parameters describing the configurations of the external systems which may influence our system. U_g^0 will contain the interaction $U^0(\boldsymbol{x}_r^0, a_l)$ of the separate particles with outside systems (for instance the walls of a container) as well as the interaction $W^0(\boldsymbol{x}_1^0, \ldots \boldsymbol{x}_n^0)$ between the particles. Thus, we assume that the forces acting on the particles are derivable from a potential of the form

$$U_g^0 = \sum_{r=1}^{n} U^0(\boldsymbol{x}_r^0, a_l) + W^0(\boldsymbol{x}_1^0, \ldots \boldsymbol{x}_n^0). \tag{3.2}$$

This assumption restricts somewhat the applicability of the theory, for in relativity theory it is generally not possible to describe the interaction between the particles in this simple way. In general the interaction has to be described by an intermediary field which has to be treated as a separate physical system with an infinite number of degrees of freedom. However, for a gas of particles of nucleonic mass, the relation

$$\frac{kT^0}{mc^2} \ll 1, \quad (k = \text{Boltzmann's constant}) \tag{3.3}$$

is very well satisfied, which means that the system may be treated non-relativistically in S^0. In fact, if m is the mass of a nucleon, the proper temperature T^0 would have to be of the order of $10^{13}\ {}^0K$ in order to make the left hand side of (3.3) of order unity and, as far as we know, temperatures of this order of magnitude are reached nowhere in our present universe. A violation of the condition (3.3) will occur only for electrons under very special circumstances. Excluding these rare cases from our consideration, it has a good meaning to describe the interaction in S^0 by a potential of the form (3.2). As regards the mutual interaction of the particles the treatment is then only approximate (although in practically all cases an extremely good approximation), but for a system of non-interacting particles, where $W^0 = 0$, the detailed treatment given in reference [4] is exact.

In the following development, the potential U^0 will be regarded as an invariant scalar which means that we, in any Lorentz system S, introduce a function $U_g(x^i, \ldots, x^i)$ of the space-time coordinates of the particles defined by

$$U_g(x_1^i, \ldots x_r^i, \ldots x_n^i, a) = U_g^0(\boldsymbol{x}_1^0, \ldots \boldsymbol{x}_r^0, \ldots \boldsymbol{x}_n^0, a), \tag{3.4}$$

where $x_r^i = \{x_r, ct_r\}$ and $\boldsymbol{x}_r^0$ are connected by the Lorentz transformation leading from S^0 to S. Thus, U_g is obtained from U_g^0 by eliminating the

arguments x_r^0 in the latter function by means of the Lorentz transformation. If we put all the time-coordinates equal to t in this function,

$$t_1 = t_2 = \ldots . = t_n = t, \tag{3.5}$$

we arrive at a definite function of the space-coordinates x_r and the time variable t:

$$U_g(x_1, \ldots x_r, \ldots x_n, t, a). \tag{3.6}$$

This function will of course depend on the external parameters (a), but it will obviously also depend on the parameters of the Lorentz transformation, in particular on the relative velocity v of S^0 and S. Thus, for a special Lorentz transformation, where

$$x_r^0 = \gamma(x_r - vt_r), \; y_r^0 = y_r, \; z_r^0 = z_r, \tag{3.7}$$

the function (3.6) is

$$U_g(\ldots, x_r, y_r, z_r, \ldots, t, a) = U_g^0(\ldots, \gamma(x_r - vt), y_r, z_r, \ldots, a). \tag{3.8}$$

Now let us assume that our system (the gas of n particles) is in a state of thermodynamical equilibrium which in a Lorentz system S is described by the state variables (θ^i, a). In this situation we do not have a precise knowledge of the *mechanical* state, which is defined by the $6n$ 'coordinates'

$$(\xi_\mu) = (p_1, x_1, \ldots, p_r, x_r, \ldots p_n, x_n) \tag{3.9}$$

of the points in the phase space $\Sigma(S)$ of the system in S. According to the developments in reference [4], the situation in question is statistically described by the following 'canonical' probability density $\mathfrak{P}(\xi_\mu)$ in $\Sigma(S)$:

$$\left. \begin{aligned} \mathfrak{P}(\xi) &= \exp\{(\Phi + \theta^i P_i^g(\xi, a))/k\} \\ P_i^g &= \sum_{r=1}^{n} p_i^r + U_g(x_1, \ldots, x_r, \ldots x_n, t, a) V_i/c^2 \end{aligned} \right\} \tag{3.10}$$

(cf. Eqs. (4; 7.1, 2) in section 7 of reference [4]). In (3.10), $p_i^r = \{p_r, -E_r/c\}$ is the 'bare' four-momentum of the r'th particle, V_i is the four-velocity of S^0 relative to S, and the quantity Φ is defined by

$$\int \cdots \int \mathfrak{P}(\xi)d\xi = 1,$$

$$d\xi = \prod_{\mu=1}^{6n} d\xi\mu, \tag{3.11}$$

or

$$\exp\{-\Phi(\theta^i,a)/k\} = \int \cdots \int \exp\{\theta^i P_i^g(\xi,a)/k\} d\xi. \tag{3.12}$$

A comparison of (2.22) with (4; 5.38) in reference [4] shows that the statistical quantity Φ in (3.10) may be identified with the relativistic thermodynamic potential introduced in section 2 of the present paper.

In the 'rest' system S^0, (3.10) reduces to the canonical distribution of GIBBS

$$\mathfrak{P}^0 = \exp\{(\Phi^0 - \theta^0 \mathfrak{H}_g^0)/k\}, \tag{3.13}$$

where

$$\Phi^0 = \Phi,$$

and

$$\mathfrak{H}_g^0 = \sum_{r=1}^{n} E_r^0 + U_g^0 \tag{3.14}$$

is the Hamiltonian in S^0. Further, in S^0 the equation (3.12) becomes

$$\exp\{-\Phi^0(\theta^0,a)/k\} = \int \cdots \int \exp\{-\theta^0 \mathfrak{H}_g^0/k\} d\xi^0, \tag{3.15}$$

which in the usual way gives us $\Phi^0(\theta^0,a)$ as a function of (θ^0,a).

In section 7 of reference [4] we have calculated the functions Φ and Φ^0 in (3.12, 15). According to (4; 7,53, 54, 33, 35, 41) we have

$$\Phi(\theta^i,a) = f(\theta,a), \qquad \Phi^0(\theta^0,a) = f(\theta^0,a), \tag{3.16}$$

where $f(\theta,a)$ is a function of the norm θ and (a), defined by

$$f(\theta,a) = f_p(\theta) + f_q(\theta,a), \tag{3.17}$$

$$\exp\{-f_p(\theta)/k\} = \int \cdots \int \exp\{-\theta \sum_r E_r^0/k\} d\boldsymbol{p}_1^0 \ldots d\boldsymbol{p}_n^0$$

$$= \left[\int \exp\{-\theta E^0/k\} d\boldsymbol{p}^0\right]^n = \left[\frac{2\pi^2 m^2 ck}{i\theta} H_2^{(1)}(imc^2\theta/k)\right]^n, \tag{3.18}$$

$$\exp\{-f_q(\theta,a)/k\} = \int \cdot \cdot \int \exp\{-\theta U_g^0(\boldsymbol{x}_1^0, \dots \boldsymbol{x}_n^0, a)/k\} \boldsymbol{dx}_1^0 \dots \boldsymbol{dx}_n^0. \quad (3.19)$$

For non-interacting particles the latter expression reduces to the n'th power of the expression (4; 7.41). In the case considered here, where (3.3) holds, the argument in the Hankel function in (3.18) is very large and we can substitute this function by its asymptotical expansion. Then (3.18) becomes

$$\exp\{-f_p(\theta)/k\} = \frac{2\pi mk}{\theta} \exp\{-nmc^2\theta/k\} \quad (3.20)$$

in accordance with the corresponding formula in non-relativistic statistical mechanics. From (4; 7.56, 57) we get

$$P_i \equiv -\frac{\partial \Phi(\theta^i, a)}{\partial \theta^i} = \frac{\langle \mathfrak{H}_g^0 \rangle^0}{c^2} V_i \quad (3.21)$$

which is the statistical expression for the inclusive four-momentum of the system defined by (2.3).

We shall now in particular consider the case where the interaction between the particles and the walls of a container are the only external forces on the particles. Then, $U^0(\boldsymbol{x}_r^0, a)$ is zero inside the container and increases rapidly to a very high value when the particles approach the walls. Let us for simplicity assume that the container has the form of a cylinder with the axis lying in the direction of the x^0-axis of the system S^0 and with the endwalls placed at $x^0 = 0$ and $x^0 = l^0$, respectively. If the latter wall is a movable piston we may change the volume V^0 by moving the piston i.e. by changing l^0, for we have

$$V^0 = F^0 l^0 \quad (3.22)$$

where F^0 is the (constant) area of the endwalls. With this arrangement the only way in which the system (the gas) can be influenced *mechanically* by the external world is by changing the position of the piston. Thus, in this case there is only one external parameter a for which we can choose l^0 or V^0 and

$$f_q(\theta,a) = f_q(\theta,l^0) = f_q(\theta,V^0) \quad (3.23)$$

is a function of θ and l^0 or V^0. For non-interacting particles, where $W^0 = 0$ and $U^0(\boldsymbol{x}_r^0, a)$ has the property mentioned above, we get from (3.19)

$$\exp\{-f_q/k\} = (F^0 l^0)^n = V^{0n}$$

$$f_q = -kn\,lu(F^0 l^0) = kn\,lu\,V^0.$$

Thus, for an ideal gas f_q is a function of l^0 or V^0 only, but for interacting particles f_q (and f) will in general depend on both θ and V^0. Therefore, in our case, (3.16) gives

$$\Phi(\theta^i, V^0) = f(\theta, V^0), \qquad \Phi^0(\theta^0, V^0) = f(\theta^0, V^0) \tag{3.24}$$

and the equations (3.21) become identical with four of the thermodynamical equations (2.27). Further, if we identify the mean value of the force p per unit area exerted by the piston on the fluid with the thermodynamic pressure p, we get from (4; 7.15)

$$\left.\begin{aligned}
p = \langle p \rangle = -\frac{1}{\theta}\frac{\partial \Phi(\theta^i, V^0)}{\partial V^0} = -\frac{1}{\theta}\frac{\partial f(\theta, V^0)}{\partial V^0}, \\[2mm]
p^0 = \langle p^0 \rangle^0 = -\frac{1}{\theta^0}\frac{\partial f(\theta^0, V^0)}{\partial V^0} = -\frac{1}{\theta^0}\frac{\partial \Phi^0(\theta^0, V^0)}{\partial V^0},
\end{aligned}\right\} \tag{3.25}$$

in accordance with the last equations (2.27) and (1.16). This identification is justified, since the ratio of the fluctuation to the mean value of the piston force is proportional to $n^{-1/2}$ and therefore generally speaking extremely small for a ponderable amount of matter, where n is of the order of Avogadro's number. In the rest system the equations (3.21) reduce to the single equation

$$\langle \mathfrak{H}_g^0 \rangle^0 = \frac{\partial f(\theta^0, V^0)}{\partial \theta^0} = \frac{\partial \Phi^0(\theta^0, V^0)}{\partial \theta^0}. \tag{3.26}$$

The statistical mean value equations (3.21, 25, 26) are in complete agreement with the thermodynamic equations (2.27) and (1.16).

Thus, relativistic statistical mechanics provides an immediate interpretation of the thermodynamic potential Φ and the relations (2.27) and, by means of (3.12) (with $a = V^0$), we are now also able to *calculate* $\Phi = f(\theta, V^0)$ when the mechanical potential U_g is given. However, in accordance with the remarks at the end of section 2, it is not necessary to perform the calculation of Φ in the general system S for, by (3.16–19), the function f is already completely determined by the equation (3.15) holding in the rest system S^0.

Now we turn to the question of the statistical mechanical interpretation of the relativistic potential $\Psi(\theta^i, p)$ introduced in (2.21). Just as in the case

of Φ it is sufficient to give an interpretation of the function $\Psi^0(\theta^0, p^0)$ in the rest system. In the preceding considerations it was found that $\Phi(\theta^i, V^0)$ appears as an essential quantity in the canonical distribution (3.10) corresponding to a situation where the thermodynical variables θ^i and V^0 have well-defined values. In S^0 this means that the piston is fixed in a definite position at $x^0 = l^0$ and that the gas has been brought in thermal contact with a heat reservoir of coldness θ^0. *Thermodynamically*, fixed values of θ^0 and V^0 correspond to definite values of H^0 and p^0 for the energy and the pressure as given by the equations of state, for instance in the form (1.16). Therefore, we can eliminate V^0 and define the state by (θ^0, p^0) instead of by (θ^0, V^0) and the potential Ψ^0 is then given by the relation (2.23), i.e.

$$\Psi^0 = \Phi^0 + \theta^0 p^0 V^0 . \tag{3.27}$$

However, in the statistical mechanical description, fixed values of θ^0 and V^0 do *not* correspond to exactly defined values for the energy and the pressure and the thermodynamical equations of state are valid only for the *mean values* of the energy and the external force. As often emphasized by NIELS BOHR [12], this circumstance constitutes an instructive example of complementarity in classical physics. Energy and pressure are complementary to temperature and volume, respectively, in much the same way as momentum and position of a particle in quantum mechanics. It is true that, for systems of ponderable size where n is very large, the complementary character of the mentioned quantities is usually not apparent, but in principle, and in special cases also in praxis, the recognition of this complementarity is of importance for the understanding of the properties of thermodynamical systems.

As in quantum mechanics, the complementarity of the mentioned thermodynamical quantities is due to the fact that the experimental arrangements which allow the fixation of definite values for the quantities in question are mutually exclusive. For instance, in order to give definite values to the coldness θ^0 and the volume V^0 we have, as already mentioned, to bring the gas in thermal contact with a large heat reservoir for a sufficiently long time during which the piston is fastened in a fixed position. When thermal equilibrium is reached, any previous knowledge of the energy and the piston force will be lost, and our knowledge of the mechanical state of the system after this procedure is adequately described by the canonical distribution (3.13, 15) with $a = V^0$, according to which the thermodynamical relations (1.16) are valid for the *mean values* of the energy and pressure only.

On the other hand, if we want to assure definite values for the coldness θ^0 and the *pressure* p^0, we have to *unfasten* the piston and subject it to a constant external force

$$K_p^0 = F^0 p^0 \tag{3.28}$$

instead of keeping it in a fixed position. After thermal equilibrium is reached, this situation is again adequately described by a canonical distribution (3.13, 15) but now applied to the system $(g+p)$ consisting of the gas plus the piston. The latter can be treated as a particle of macroscopical mass M which can move freely along the x^0-axis. Thus, if n is the number of degrees of freedom of the gas, the corresponding number for the system $(g+p)$ is $n+1$, and the coordinate l^0 of the piston and the volume V^0 given by (3.22) do not have exactly defined values in this situation. The constant external force (3.28) is derivable from a potential U_p^0:

$$K_p^0 = -\frac{\partial U_p^0(l^0, p^0)}{\partial l^0}$$

with

$$U_p^0(l^0, p^0) = K_p^0 l^0 = p^0 F^0 l^0 = p^0 V^0 \equiv U_p^0(V^0, p^0), \tag{3.29}$$

and as external parameter a for the system $(g+p)$ we may choose the pressure p^0.

If we use V^0 instead of l^0 as 'generalized' coordinate of the piston, its (non-relativistic) kinetic energy is

$$T_p^0 = M\dot{V}^{02}/2F^{02} = \quad , \quad \dot{V}^0 = \frac{dV^0}{dt^0}. \tag{3.30}$$

The corresponding canonical momentum is

$$p_p^0 = \frac{dT_p^0}{d\dot{V}^0} = M\dot{V}^0/F^{02}. \tag{3.31}$$

Now, the mechanical potential of the system gas + piston is

$$U_{(g+p)}^0 = U_g^0(\boldsymbol{x}_1^0, \ldots \boldsymbol{x}_u^0, V^0) + U_p^0(V^0, p^0) \tag{3.32}$$

and its Hamiltonian (disregarding the rest energy of the piston)

$$\mathfrak{H}_{(g+p)}^0 = \mathfrak{H}_g^0 + p^0 V^0 + F^{02} p_p^{02}/2M. \tag{3.33}$$

Thus, the probability density (3.13) of the system $(g+p)$ is

$$\mathfrak{P}^0_{(g+p)} = \exp\{(\Phi^0_{(g+p)} - \theta^0\mathfrak{H}^0_{(g+p)})/k\}. \tag{3.34}$$

It is a function of the phase-coordinates (ξ^0) of the gas and the canonical variables p^0_p and V^0 of the piston, and $\Phi^0_{(y+p)})$ is determined by the equation

$$\int \cdots \int \mathfrak{P}^0_{(g+p)} d\xi^0 dp^0_p dV^0 = 1. \tag{3.35}$$

We may now calculate the mean values of quantities referring to the gas and the piston. According to the equipartition theorem, the mean value of the kinetic energy of the piston is kT^0 and the velocity of the piston will be of the order $v_p \sim (kT^0/M)^{1/2}$. For M of the order of a gram, v_p is therefore extremely small which means that the piston will practically always be found at rest in spite of its being unfastened. By integration of (3.34) over p^0_p from $-\infty$ to $+\infty$ we get the probability density $\mathfrak{P}^*(\xi^0, V^0)$ of finding the gas at a point (ξ^0) in its phase space and with a volume V^0, irrespective of the momentum of the piston. Obviously $\mathfrak{P}^*$ is of the form

$$\mathfrak{P}^* = \exp\{(\Psi^0 - \theta^0\mathfrak{H}^*)/k\}, \tag{3.36}$$

where

$$\mathfrak{H}^* = \mathfrak{H}^0_g(\xi^0, V^0) + p^0 V^0 \tag{3.37}$$

and Ψ^0 is a function of θ^0 and p^0 given by

$$\int \cdots \int \mathfrak{P}^* d\xi^0 dV^0 = \int\int \exp\{(\Psi^0 - \theta^0\mathfrak{H}^*(\xi^0, V^0, p^0))/k\} d\xi^0 dV^0 = 1. \tag{3.38}$$

Further integration of $\mathfrak{P}^*$ over (ξ^0) gives us the probability density $W(V^0)$ for the gas having the volume V^0. By means of (3.36, 37) and (3.15) (with $a = V^0$), we get

$$W(V^0) = \exp\{(\Psi^0 - \Phi(\theta^0, V^0) - \theta^0 p^0 V^0)/k\}, \tag{3.39}$$

$$\int_0^\infty W(V^0) dV^0 = \int_0^\infty \exp\{\Psi^0(\theta^0, p^0) - \Phi(\theta^0, V^0) - \theta^0 p^0 V^0)/k\} dV^0 = 1. \tag{3.40}$$

The latter equation may also be written

$$\exp\{-\Psi^0/k\} = \int_0^\infty \exp\{-(\Phi(\theta^0, V^0) + \theta^0 p^0 V^0)/k\} dV^0, \tag{3.41}$$

which allows to calculate $\Psi^0(\theta^0, p^0)$ when the function $\Phi^0(\theta^0, V^0)$ in (3.24) is known. The most probable value $\bar{V}^0$ of V^0 is determined by the equation

i.e.

$$
\left.\begin{array}{c}
\dfrac{dW(V^0)}{dV^0} = -W(V^0)\left(\dfrac{\partial \Phi(\theta^0, V^0)}{\partial V^0} + \theta^0 p^0\right)/k = 0, \\[4mm]
\dfrac{\partial \Phi(\theta^0, \bar{V}^0)}{\partial \bar{V}^0} + \theta^0 p^0 = 0.
\end{array}\right\} \quad (3.42)
$$

By partial differentiation of (3.40) with respect to θ^0, we get in the usual way

or

$$
\left.\begin{array}{c}
\displaystyle\int_0^\infty \left(\dfrac{\partial \Psi^0(\theta^0, p^0)}{\partial \theta^0} - \dfrac{\partial \Phi(\theta^0, V^0)}{\partial \theta^0} - p^0 V^0\right) W(V^0) dV^0 = 0 \\[4mm]
\dfrac{\partial \Psi^0(\theta^0, p^0)}{\partial \theta^0} = \left\langle \dfrac{\partial \Phi(\theta^0, V^0)}{\partial \theta^0}\right\rangle^0 + p^0 \langle V^0 \rangle^0.
\end{array}\right\} \quad (3.43)
$$

Further, by differentiations of (3.40) with respect to p^0,

$$
\langle V^0 \rangle^0 = \frac{1}{\theta^0} \frac{\partial \Psi^0(\theta^0, p^0)}{\partial p^0}, \tag{3.44}
$$

$$
\sigma^2\{V^0\} \equiv \langle (V^0 - \langle V^0 \rangle^0)^2 \rangle^0 = -\frac{k}{\theta^{02}} \frac{\partial^2 \Psi^0(\theta^0, p^0)}{\partial p^{02}} = -\frac{k}{\theta^0} \frac{\partial \langle V^0 \rangle^0}{\partial p^0}, \tag{3.45}
$$

where $\sigma^2\{V^0\}$ is the square of the fluctuation of the volume around its mean value $\langle V^0 \rangle^0$. Since both $\langle V^0 \rangle^0$ and $\sigma^2\{V^0\}$ are proportional to n, the ratio R of the fluctuation to the mean value of V^0 is proportional to $n^{-1/2}$:

$$
R(\theta^0, p^0) = \frac{\sigma\{V^0\}}{\langle V^0 \rangle^0} = O(n^{-1/2}). \tag{3.46}
$$

Apart from very special cases where $\dfrac{\partial \langle V^0 \rangle^0}{\partial p^0}$ is exceptionally large (like at transitions from one phase of the gas to another), the fluctuation of V^0 is completely negligible for a ponderable amount of gas where n is of the order of Avogadro's number. Therefore, in such cases $\langle V^0 \rangle^0$ may be identified with the thermodynamical variable V^0, and the relation (3.44) between

volume, coldness, and pressure must be identical with the relation (3.25). Moreover, the most probable volume $\bar{V}^0$ given by (3.42) must be equal to the mean value in this case, i.e.

$$\bar{V}^0 = \langle V^0 \rangle^0, \tag{3.47}$$

in accordance with the result of a comparison of (3.42) with (3.25). This means that the function (3.39) (for fixed θ^0 and p^0) must have a very steep maximum at $V = \bar{V}^0 = \langle V^0 \rangle^0$ with a mean breadth equal to $R(\theta^0, p^0)$. Thus the integral in (3.40) becomes equal to the maximum value $W(\bar{V}^0)$ times R, and we get from (3.40)

$$R(\theta^0, p^0) \exp\{(\Psi^0(\theta^0, p^0) - \Phi(\theta^0, \bar{V}^0) - \theta^0 p^0 \bar{V}^0)/k\}. = 1 \tag{3.48}$$

or

$$\Psi^0(\theta^0, p^0) = \Phi^0(\theta^0, \bar{V}^0) + \theta^0 p^0 \bar{V}^0 - k\ln R. \tag{3.49}$$

Since Ψ^0, Φ^0 and $\bar{V}^0$ are proportional to n while $\ln R$ only contains the logarithm of n, we may neglect the last term in (3.49) in the case of large n where (3.47) holds.

Hence

$$\Psi^0(\theta^0, p^0) = \Phi^0(\theta^0, \langle V^0 \rangle^0) + \theta^0 p^0 \langle V^0 \rangle^0. \tag{3.50}$$

A comparison of this equation with the thermodynamical relation (3.27) shows that the statistical quantity Ψ^0 entering in (3.36) may be identified with the thermodynamical potential $\Psi^0(\theta^0, p^0)$.

The quantity $\mathfrak{H}^*$ defined by (3.37) is equal to the energy of the gas plus the potential energy (3.29) of the piston in the external field. By partial differentiation of (3.38) with respect to θ^0 we get for the mean value of H^*

$$\langle \mathfrak{H}^* \rangle = \frac{\partial \Psi^0(\theta^0, p^0)}{\partial \theta^0} = \langle \frac{\partial \Phi^0(\theta^0, V^0)}{\partial \theta^0} \rangle^0 + p^0 \langle V^0 \rangle^0 \tag{3.51}$$

on account of (3.43). According to (3.26), $\dfrac{\partial \Phi^0(\theta^0, V^0)}{\partial \theta^0}$ is the mean value of the energy $\mathfrak{H}^0_g$ of the gas in a canonical ensemble with a fixed value V^0 of the volume. Hence, $\langle \dfrac{\partial \Phi^0(\theta^0, V^0)}{\partial V^0} \rangle^0$ is the mean value of H^0_g in the ensemble with varying V^0 described by (3.34). This is in accordance with the relation obtained by taking the mean value of the equation (3.37) over the ensemble (3.34)

$$\langle \mathfrak{H}^* \rangle^0 = \langle \mathfrak{H}_g^0 \rangle^0 + p^0 \langle V^0 \rangle^0. \tag{3.52}$$

The equations (3.51, 52) are exact for all n. However, for large n, where the function $W(V^0)$ has a steep maximum and (3.47) holds, (3.51) becomes

$$\langle \mathfrak{H}^* \rangle^0 = \frac{\partial \Phi^0(\theta^0, \bar{V}^0)}{\partial \theta^0} + p^0 \bar{V}^0. \tag{3.53}$$

A comparison with the first equation (1.16) shows that the first term on the right hand side of (3.53) must be identified with the thermodynamical energy H^0 of the gas and, taking account of (2.8), we come to the conclusion that $\langle \mathfrak{H}^* \rangle^0$ in (3.51, 53) must be the statistical analogue of the thermodynamical enthalpy E^0 of the gas in the rest system. The (exact) mean value equations (3.44, 51) are obviously the statistical analogues of the thermodynamical relations (2.29) which, in the rest system S^0, reduce to the two equations

$$V^0 = \frac{1}{\theta^0} \frac{\partial \Psi^0(\theta^0, p^0)}{\partial p^0}, \quad E^0 = \frac{\partial \Psi^0(\theta^0, p^0)}{\partial \theta^0}. \tag{3.54}$$

Thus, the statistical quantity Ψ^0 given by (3.38) or (3.40) has all the properties of the thermodynamical potential Ψ^0. It is closely connected with the Φ^0-function for the system gas + piston (if we disregard the rest energy of the piston). From the definitions (3.38, 35) of Ψ^0 and $\Phi^0_{(g+p)}$ one easily finds

$$\Phi^0_{(g+p)} = \Psi^0 - k \ln \frac{\sqrt{2\pi M k / \theta^0}}{F^0}. \tag{3.55}$$

Since Φ^0 and Ψ^0 are proportional to n, we may neglect the last term on the right side of this equation for a ponderable amount of gas. Thus, for large n,

$$\Phi^0_{(g+p)}(\theta^0, p^0) = \Psi^0(\theta^0, p^0). \tag{3.55}$$

In an arbitrary system S, the corresponding potential $\Psi(\theta^i, p)$ is obtained from $\Psi^0(\theta^0, p^0)$ by replacing θ^0 and p^0 by the norm θ and p, respectively. These considerations lead to the following physical interpretation of the four-enthalpy E_i in an arbitrary system S. *The quantities E_i, as defined by (2.4) or (2.29), are equal to the components of the inclusive four-momentum of the system $(g+p)$ minus MV_i where M is the proper mass of the piston.*

The Niels Bohr Institute
and NORDITA

References

1. M. PLANCK, Berl. Ber. p 542 (1907); Ann. d. Phys. **76**, 1 (1908).
2. R. BALESCU, Relativistic Statistical Mechanics. Solvay colloquium, May 1968.
3. H. OTT Zs. f. Phys. **175** 70 (1963).
4. C. MØLLER, Mat. Fys. Medd. Dan. Vid. Selsk. **36**, 16 (1968).
5. H. ARZELIÈS, Nuovo Cimento **35**, 792 (1965).
6. C. TRUESDELL, Six Lectures on Modern Natural Philosophy (Springer, New York 1966) p. 72.
7. C. MØLLER, Mat. Fys. Medd. Dan. Vid. Selsk. **36**, 1 (1967).
8. I. BREVIK, Mat. Fys. Medd. Dan. Vid. Selsk. **36**, 3 (1967).
9. L. SÖDERHOLM, Nuovo Cimento, 57 B, 173 (1968).
10. See f. inst. reference 7 or any textbook on relativity.
11. P. P. LANDSBERG, Proc. Phys. Soc. **89**, 1007 (1966).
12. N. BOHR, Faraday Lecture, 1930, published in the Journal of the Chemical Society, 1932.

H. HØJGAARD JENSEN AND P. HEDEBOL NIELSEN

PARTICLE ASPECTS
OF PHONONS

Synopsis

The possibility of introducing dynamical variables for a single phonon is investigated. A space time description of localized phonons leads to position and direction variables. Lattice translations, point group transformations and local rotations are used to define variables analogous to momentum, angular momentum, parity and spin of an ordinary particle.

1. Introduction

A system with $3N$ degrees of freedom which can perform harmonic vibrations may be treated quantum mechanically in two formally different ways. In the first case it is described as $3N$ distinguishable oscillators, preferably the normal vibrations of the system. In the second case the excitations of the system are treated as a gas of indistinguishable Bose-particles, phonons.

The purpose of the present note is to investigate how far it is possible to carry the latter description. In particular we shall try to introduce dynamical variables of a single phonon analogous to the variables of ordinary particles like spatial coordinate, momentum, orbital angular momentum and spin angular momentum.

An analysis of the so called pseudomomentum of a phonon has been carried through by Süssmann[1] [2]. The concept of phonon spin is discussed by Vonsovskii and Svirskii[3] and by Levine[4] in the continuum limit for an isotropic and a cubic material respectively. In the present note which extends previous work[5], these and other concepts are treated, starting from an atomistic description of the vibrating system.

2. Space-time Description of Phonons

Consider a crystal with N atoms. Phonons are introduced on the basis of the harmonic approximation in which the crystal is described by the Hamiltonian

$$H = \tfrac{1}{2}(p_r T_{rs} p_s + u_r V_{rs} u_s) \tag{1}$$

(summation over indices occurring twice being understood).

Here the summation indices r and s run over all $3N$ degrees of freedom, i. e. they label both the equilibrium positions of the atoms and the cartesian

components of the momenta p and displacements u. The matrix T is diagonal ($T_{rs} = (1/m_r)\delta_{rs}$, where m_r is the mass related to the r'th degree of freedom) but the formalism which we are going to describe is valid also for the more general case of non-diagonal T. The potential energy is assumed to be positive definite*; V is a symmetric matrix**.

For convenience we introduce mass-adjusted canonically conjugate variables

$$\pi_r = (T^{1/2})_{rs}p_s \qquad v_r = (T^{-1/2})_{rs}u_s \tag{2}$$

where $T^{1/2}$ is the real, symmetric, positive definite square root of the matrix T. In our case $(T^{1/2})_{rs} = (1/\sqrt{m_r})\delta_{rs}$.

In terms of the new variables the Hamiltonian becomes

$$H = \tfrac{1}{2}(\pi_r\pi_r + v_r D_{rs}v_s) \tag{3}$$

where

$$D = T^{1/2}VT^{1/2} \tag{4}$$

is the so called dynamical matrix of the system. It is a symmetric, positive definite and real $3N \times 3N$ matrix.

From the assumed properties of the matrix D it follows that there exists one and only one symmetrical, positive definite and real matrix M which fulfils the relation

$$M^4 = D. \tag{5}$$

This matrix has a reciprocal M^{-1} because it is positive definite.

The actual calculation of functions of hermitian matrices, e. g. $D^{1/4}$, is most conveniently done in the following way: The dynamical matrix D is diagonalized. The diagonal elements are replaced by their function values, e. g. by their positive fourth roots, and finally the matrix is transformed to the original representation. In ref.[5] this is described in more detail using the infinite linear chain with nearest neighbour interaction as an example***.

A mathematical treatment of functions of matrices is given in several textbooks, e.g. A. I. MAL'CEV[6].

By means of M we introduce $3N$ creation and $3N$ destruction operators $b_r^\dagger$ and b_r through the definitions

---

* If needed, this may be enforced by adding, e. g., a small fictitious term proportional to $u_r u_r$ and letting the proportionality constant go to zero in the final results.

** The most general case, with H containing terms of the type $p_r G_{rs}u_s$ as in the presence of magnetic forces or Coriolis forces, is considered in Appendix I.

*** We take the opportunity to correct an error in ref.[5]; the right side of eq. 4.11 should be multiplied by 4.

$$v_s = \sqrt{\frac{\hbar}{2}} (M^{-1})_{sr}(b_r + b_r^\dagger) \tag{6}$$

$$\pi_s = \frac{1}{i}\sqrt{\frac{\hbar}{2}} M_{sr}(b_r - b_r^\dagger) \tag{7}$$

with the inverse relations

$$b_r = \frac{1}{\sqrt{2\hbar}}(M_{rs}v_s + i(M^{-1})_{rs}\pi_s) \tag{8}$$

$$b_r^\dagger = \frac{1}{\sqrt{2\hbar}}(M_{rs}v_s - i(M^{-1})_{rs}\pi_s). \tag{9}$$

From (8) and (9) together with the canonical commutation relations for π_r and v_r it follows that the b and $b^\dagger$ operators obey the commutation relations characterizing destruction and creation operators for Bose-particles

$$\left.\begin{aligned}[b_r, b_s^\dagger] &\equiv b_r b_s^\dagger - b_s^\dagger b_r = \delta_{rs}\\ [b_r, b_s] &= [b_r^\dagger, b_s^\dagger] = 0.\end{aligned}\right\} \tag{10}$$

When we introduce (6) and (7) in (3) we obtain the Hamiltonian in terms of the creation and destruction operators

$$H = \frac{\hbar}{2}(M^2)_{rr} + \hbar b_r^\dagger (M^2)_{rs}b_s. \tag{11}$$

Thus H is written as the sum of a zero point energy

$$E_0 = \frac{\hbar}{2} \text{ trace } (M^2) \tag{12}$$

and an excitation Hamiltonian, the form of which is characteristic for a system of non-interacting bosons.

The boson operators b_r and $b_r^\dagger$ defined by (6) and (7) are said to destroy and create a localized phonon at the atom and at the coordinate axis denoted by r. If the system given by the Hamiltonian (3) is large, then the excitation energy of the localized phonons is to a large extent localized in the neighbourhood of the atom corresponding to the index r (appendix II).

The form of eq. (11) makes it natural to consider the matrix $\hbar M^2 = \hbar\sqrt{D}$ as the Hamiltonian matrix for a single phonon. Henceforth it will be denoted by h

$$h_{rs} = \hbar(M^2)_{rs} = \hbar(\sqrt{D})_{rs}. \tag{13}$$

Having defined b and $b^\dagger$ operators and the one-particle Hamiltonian we can proceed in principle as in the case of an ordinary boson gas. The ground state of the system (including the time dependent phase factor $\exp(-(i/\hbar)E_0 t)$) is denoted $|0\rangle$ and obeys the equations $b_r|0\rangle = 0$ for all r. From this state a complete set of states is obtained by successive application of the creation operators. In particular the state $b_s^\dagger|0\rangle$ will be said to contain one phonon with the position and direction given by s. It is an eigenfunction with the eigenvalue s of the dynamical variable

$$\hat{r} = \sum_r r b_r^\dagger b_r \tag{14}$$

which may be called the position-direction operator of the phonon.

The most general one-phonon state is

$$|\psi\rangle = \sum_r \psi_r(t) b_r^\dagger |0\rangle \tag{15}$$

where $\psi_r(t)$ will be called the Schrödinger function of the phonon in the r-representation. $|\psi_r(t)|^2$ is the probability that when exactly one phonon is present it has the position and direction r. From (14), (11) and (13) together with the general Schrödinger equation

$$i\hbar \frac{\partial}{\partial t}|\psi\rangle = H|\psi\rangle \tag{16}$$

we find that $\psi_r(t)$ obeys the one-phonon Schrödinger equation

$$i\hbar \frac{d\psi_r}{dt} = h_{rs}\psi_s. \tag{17}$$

The analogy with the non relativistic quantum theory for ordinary particles is nearly complete. The main difference is that the position variable of the phonon in this formalism can take on only discrete values, i. e. the equilibrium positions of the vibrating particles. Therefore (17) is a difference equation in r instead of a differential equation.

Similarly we can discuss states with more than one phonon.

The procedure outlined above is to some extent arbitrary. Starting from canonically conjugate coordinates and momenta many linear transformations lead to Boson operators. In fact it can be shown that the most general transformation of the form

$$
\left.\begin{aligned}
u_r &= \sqrt{\frac{\hbar}{2}}(A_{rs}b_s + A_{rs}^* b_s^\dagger) \\[2mm]
p_r &= \frac{1}{i}\sqrt{\frac{\hbar}{2}}(B_{rs}b_s - B_{rs}^* b_s^\dagger)
\end{aligned}\right\} \tag{18}
$$

which leads to operators obeying the commutation relations (10) is such that (in matrix notation)

$$
\left.\begin{aligned}
A &= S^{-1}W \\
B &= S(1 + iC)W
\end{aligned}\right\} \tag{19}
$$

where S and C are real and symmetric matrices, while W is a unitary matrix. (The matrix A must have a reciprocal matrix in order to ensure that (18) can be reversed).

However, in order to have a reasonable particle concept, the total number of particles, $\hat{n} = b_r^\dagger b_r$, must be a constant of motion under movements described by the unperturbed Hamiltonian (1).

If we impose this condition on the transformation and use the Hamiltonian (1) with positive definite T and V we find that the matrix C in (19) must vanish, while the matrix S must obey the relation

$$
S^2 T S^2 = V \tag{20}
$$

by which the positive definite, real, symmetric matrix S^2 is uniquely determined. It now readily follows from (18) that all acceptable phonon variables are connected by transformations of the type $b_r' = U_{rs}b_s$, where U_{rs} is a unitary matrix.

Among the acceptable sets of phonon variables we have chosen a particular one (defined by (8) and (9)) as describing spatially localized phonons. In certain simple cases, notably when all masses are equal and all diagonal elements of the dynamical matrix are equal, the choice is justified by the fact that the excitation energy becomes spatially localized to the highest degree possible. In the general case this is not necessarily so, but the transformation leading to maximum localization of energy cannot then be described in terms of simple functions of the matrices T and V. Such a functional relationship is important for the following discussions; in all cases we therefore define localized phonons by means of (8) and (9). With equal right we might have chosen other transformations which coincide with (8) and (9) in case the matrices T and V commute. We could, e. g., have reversed the rôles of T and V in the procedure leading from the Hamiltonian (1) to the localized phonons given by (8) and (9), or—most symmetrical with respect to kinetic and potential energy—we could have chosen a symmetrical $A(= S^{-1})$ in (18). The actual choice agrees most closely with standard methods and concepts described in the literature.

In Appendix II the localization of excitation energy is treated in more detail.

3. Transformations and Dynamical Variables

The most important dynamical variables of a system are those (like momentum and angular momentum) which are connected with coordinate transformations or symmetry operations. We consider transformations of the particle variables u_r and p_r of the form

$$u'_r = L_{rs} u_s$$
$$p'_r = L_{rs} p_s \qquad\qquad (21)$$

where the transformation matrix L is real and orthogonal

$$\tilde{L} = L^{-1}. \qquad\qquad (22)$$

These transformations include translations and rotations of the displacement pattern of the system. Special cases are treated in the next paragraph.

Introducing (21) in the Hamiltonian (1) we obtain new matrices T' and V' defining the kinetic and potential energy:

$$T' = LTL^{-1} \qquad V' = LVL^{-1}. \qquad\qquad (23)$$

They are again real, symmetric and positive definite matrices; consequently transformed matrices D', M' and h' together with transformed creation and destruction operators $b_r^{\dagger'}$ and b'_r can be defined as before. All matrices like D, M and h are seen to transform according to the rule (23) whereas vectors like v, π, $b^\dagger$ and b transform like u and p; in particular

$$b'_r = L_{rs} b_s$$
$$b_r^{\dagger'} = L_{rs} b_s^\dagger. \qquad\qquad (24)$$

The ground state is unchanged under this transformation and the phonon number operator is unchanged.

The transformation (24) can be written as a contact transformation; in fact, we can always find a hermitian operator

$$\hat{O} = b_r^\dagger O_{rs} b_s \qquad\qquad (25)$$

where

$$O_{rs}^* = O_{sr} \qquad\qquad (26)$$

such that (24) becomes

$$b'_r = \exp(i\hat{O}) \, b_r \exp(-i\hat{O})$$
$$b_r^{\dagger'} = \exp(i\hat{O}) \, b_r^\dagger \exp(-i\hat{O}). \qquad\qquad (27)$$

Each transformation like (21) thus motivates the introduction of a dynamical variable $\hat{O}$. From (25) we see that $\hat{O}$ commutes with the phonon number operator and thus $\hat{O}$ can be said to describe a property of the single phonon. If the Hamiltonian (1) is form invariant under the transformation (21) the Hamiltonian matrix h commutes with L and thus $h' = h$. From this it follows that the operator $\exp(i\hat{O})$ commutes with the Hamiltonian operator. In this case it is therefore a constant of motion.

The actual calculation of $\hat{O}$ can be performed according to the following procedure (for the proof see appendix III).

a) Find a complete orthonormal set of eigenvectors B_r^α of the matrix L, i. e. solve

$$L_{rs}B_s^\alpha = \lambda_\alpha B_r^\alpha. \tag{28}$$

Since L is unitary, any eigenvalue λ_α has modulus 1.

b) For each eigenvector determine a real number l_α so that

$$\lambda_\alpha = \exp(il_\alpha). \tag{29}$$

c) The matrix O_{rs} may then be chosen as

$$O_{rs} = \sum_\alpha l_\alpha B_r^{\alpha*} B_s^\alpha (= i(\ln(L))_{rs}). \tag{30}$$

d) Introducing (30) into (25) we find

$$\hat{O} = \sum_\alpha l_\alpha b_\alpha^\dagger b_\alpha \tag{31}$$

where

$$\left. \begin{array}{l} b_\alpha \stackrel{\text{def}}{=} \sum_r B_r^\alpha b_r \\[2mm] b_\alpha^\dagger \stackrel{\text{def}}{=} \sum_r B_r^{\alpha*} b_r^\dagger \end{array} \right\} \tag{32}$$

constitute a new set of phonon destruction and creation operators.

The state $b_\alpha^\dagger |0\rangle$ is a one phonon eigenstate of the operator $\hat{O}$ with the eigenvalue l_α.

It is seen that the scheme described is completely analogous to the usual transformation theory in the quantum mechanics of particles.

The operator $\hat{O}$ is not uniquely defined by the rules given so far. In fact it is evident from the definition of l_α that $\exp(i\hat{O})$ is not changed when we add arbitrary integer multiples of 2π to the numbers l_α in (30). In each single case the definition can be made unique by a suitable convention (e. g. a continuity convention for continuous groups or limitation of wavevectors to the first Brillouin zone in case of the lattice translation group).

It might be considered more straighforward to introduce dynamical variables by writing the transformations of displacements and momenta (21) as contact transformations,

$$\exp(i\hat{F})u_r\exp(-i\hat{F}) \; = \; L_{rs}u_s$$
$$\exp(i\hat{F})p_r\exp(-i\hat{F}) \; = \; L_{rs}p_s. \tag{33}$$

In general, however, an operator $\hat{F}$ satisfying (33) will not be a one-phonon operator, i. e. when expressed in terms of the phonon variables b and $b^\dagger$, it will contain terms of the form $b_r b_s$ and $b_r^\dagger b_s^\dagger$. Thus it does not commute with the phonon number operator, in contrast to $\hat{O}$. In particular, $\hat{F}$ and also $\exp(i\hat{F})$ may change the ground state into a superposition of the ground state and states with phonons present. For these reasons, in the general case $\hat{F}$ cannot be said to describe a property of a single phonon.

More specifically we can find under what conditions the operator $\hat{F}$ can be a one-phonon operator. We try a solution to (33) of the form

$$\hat{F} \; = \; b_r^\dagger F_{rs}b_s. \tag{34}$$

Expressing u's and p's in terms of b's and $b^\dagger$'s by means of (2), (6) and (7) and using eq. (III, 1) (see Appendix III) we find that a solution of the type (34) exists if and only if the matrix L commutes with the matrix $T^{-1/2}M^2T^{-1/2}$. If, in particular, L commutes with both the potential and kinetic energy matrices, V and T, the equations determining $\hat{O}$ and $\hat{F}$ become identical, so that $\hat{F}$ can be chosen equal to $\hat{O}$.

In the general case explicit solutions to (33) may be written down, but they are usually not of much interest. We only mention that if the matrix O_{rs} is antisymmetric, the following expression satisfies (33):

$$\hat{F} \; = \; \frac{i}{\hbar}u_r O_{rs}p_s. \tag{35}$$

This may be proved by means of eq. (III,1) (Appendix III).

4. Application to Phonons in Crystals

To each atom in a crystal belong a displacement vector $\boldsymbol{u}$ and a momentum vector $\boldsymbol{p}$. Introducing phonon variables we get for each atom a three component creation and a three component destruction operator which transform as vectors under rotation. The equilibrium positions of the atoms will be described as a lattice with a basis. If there are N lattice points with v atoms in the basis we have altogether $3Nv$ creation operators forming Nv vectors. An atom will be labelled by the lattice vector $\boldsymbol{r}$ and the basis vector $\boldsymbol{c}$ of its equilibrium position which is $\boldsymbol{r} + \boldsymbol{c}$. The phonon operators are denoted $\boldsymbol{b}_{rc}$ and $\boldsymbol{b}_{rc}^\dagger$ or in components b_{rc}^α and $b_{rc}^{\alpha\dagger}$, where α labels three cartesian coordinate

axes with unit vectors $\boldsymbol{e}_\alpha$. Following eq. (14) we can then define dynamical variables

$$\hat{\boldsymbol{r}} = \sum_{rc} \boldsymbol{r}(\boldsymbol{b}_{rc}^\dagger \cdot \boldsymbol{b}_{rc})$$

$$\hat{\boldsymbol{c}} = \sum_{rc} \boldsymbol{c}(\boldsymbol{b}_{rc}^\dagger \cdot \boldsymbol{b}_{rc}) \qquad\qquad (36)$$

$$\hat{\boldsymbol{e}} = \sum_{rc\alpha} \boldsymbol{e}_\alpha b_{rc}^{\alpha\dagger} b_{rc}^\alpha.$$

In the one-phonon case they constitute a complete commuting set of dynamical variables with eigenstates $b_{r'c'}^{\alpha'\dagger}|0\rangle$ and corresponding eigenvalues $\boldsymbol{r}'$, $\boldsymbol{c}'$, and $\boldsymbol{e}_{\alpha'}$. They may be called the lattice position operator, the basis position operator and the polarisation direction operator respectively.

The transformations of the type (21) which can be applied to phonons in crystals include permutations of the field vectors among the sites of the crystal and changes of the directions of the field vectors. Of greatest interest are those which can be described as simple spatial operations. This is the case with the following transformations:

a) The cyclic translational group of the crystal lattice applied to the field vectors. This is applicable to all ideal crystals. It affects $\hat{\boldsymbol{r}}$ but not $\hat{\boldsymbol{c}}$ and $\hat{\boldsymbol{e}}$.

b) Proper and improper rotations of the field vectors without permutation among sites. They are applicable to all crystals. They affect $\hat{\boldsymbol{e}}$ but not $\hat{\boldsymbol{r}}$ and $\hat{\boldsymbol{c}}$.

c) If the lattice of a crystal is mapped into itself by a certain point group transformation like rotation, reflection or inversion (possibly made cyclic by suitable boundary conventions), this transformation can be applied to the field vectors without changing their direction or basis vector. It affects $\hat{\boldsymbol{r}}$ but not $\hat{\boldsymbol{c}}$ and $\hat{\boldsymbol{e}}$.

d) If the set of equilibrium sites in the basis of a crystal is mapped into itself by a certain symmetry operation this can be applied to the field vectors without changing their direction or lattice vector. It affects $\hat{\boldsymbol{c}}$ but not $\hat{\boldsymbol{r}}$ and $\hat{\boldsymbol{e}}$.

We shall study the cases a), b) and examples among c) and d). We will show that these cases lead to the introduction of dynamical variables analogous to momentum, angular momentum and parity, and to the splitting of the latter two into orbital and intrinsic parts (like orbital and spin angular momentum)*.

* Space group transformations, like e. g. screw translations, which are not combinations of the cases a) to d) will not be considered in detail. They lead to operators which are not analogous to simple operators of ordinary particles.
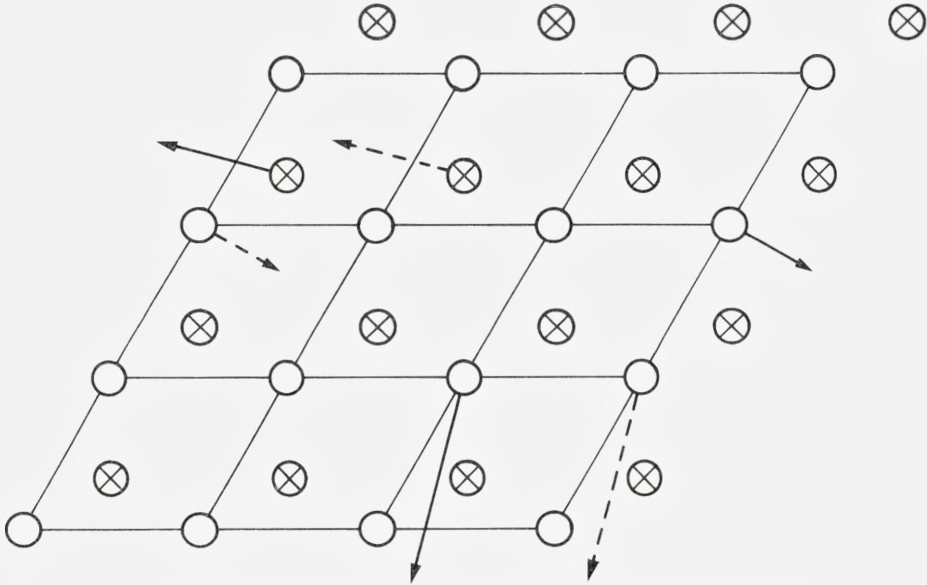
Fig. 1. A cyclic transformation in a finite net. Fully drawn arrows and dashed ones are field vectors before and after the transformation.

We want to emphasize that none of these transformations imply movement of the crystal as a whole. What is, e. g., translated or rotated by the transformations (21) is not the atoms but the patterns of displacements, i. e. the sound field. It is of course also possible to study translation and rotation of the crystal as a whole. This leads to the introduction of the proper momentum and angular momentum operators of the crystal. They are not phonon operators of the type considered here, i. e. they are not of the form (31) (compare [1] and [5]).

5. Translation and Pseudomomentum

A thorough discussion of the concept of pseudomomentum has been given by Süssmann[1] [2]. We include a short treatment of this concept in order to see how it fits into the framework presented above.

The transformation group considered is the cyclic shifting of the sound field vectors by integer multiples of the primitive translation vectors of the lattice a_1, a_2, and a_3 (fig. 1). Let the crystal have the form of a parallelepiped with sides $N_1 a_1$, $N_2 a_2$ and $N_3 a_3$, so that it contains $N = N_1 N_2 N_3$ unit cells.

The wavevector lattice of the crystal has three primitive translation vectors $\boldsymbol{g}_i$ defined by

$$\boldsymbol{g}_i \cdot \boldsymbol{a}_j = 2\pi\delta_{ij}. \tag{37}$$

The transformations in question are obtained by repeated application of the three commuting primitive translations

$$\left.\begin{aligned}
\boldsymbol{b}'_{rc} &= \boldsymbol{b}_{(r-a_i)c} & \text{for } \boldsymbol{r} - \boldsymbol{a}_i \text{ inside the crystal} \\
\boldsymbol{b}'_{rc} &= \boldsymbol{b}_{(r+(N_i-1)a_i)c} & \text{for } \boldsymbol{r} - \boldsymbol{a}_i \text{ outside the crystal} \\
(i &= 1, 2, 3).
\end{aligned}\right\} \tag{38}$$

We now proceed as described in section 3. The three transformation matrices corresponding to (38) have the well known set of simultaneous $3N\nu$-component eigenvectors (α labels three cartesian components).

$$B_{rc\alpha}^{qc'\alpha'} = \frac{1}{\sqrt{N}}\exp(-i\boldsymbol{q}\cdot\boldsymbol{r})\delta_{cc'}\delta_{\alpha\alpha'}. \tag{39}$$

Here the wave vector $\boldsymbol{q}$ can take the values

$$\boldsymbol{q} = \sum_{i=1}^{3} \boldsymbol{g}_i p_i/N_i \tag{40}$$

where p_i is an integer which can take on N_i different values, usually chosen so that the possible $\boldsymbol{q}$-vectors are those contained in the first Brillouin zone of the lattice.

The eigenvalues belonging to (39) of the transformation (38) are $\exp(i\boldsymbol{q}\cdot\boldsymbol{a}_i)$. They are already written in the form required by (29), so we can immediately write down expressions like (31) for the three operators $\hat{O}_i$ which generate the transformations (38). The result is

$$\hat{O}_i = \sum_{qc}(\boldsymbol{q}\cdot\boldsymbol{a}_i)(\boldsymbol{b}_{qc}^{\dagger}\cdot\boldsymbol{b}_{qc}) \tag{41}$$

where the new destruction and creation operators are defined by

$$\left.\begin{aligned}
\boldsymbol{b}_{qc} &= \frac{1}{\sqrt{N}}\sum_r \exp(-i\boldsymbol{q}\cdot\boldsymbol{r})\boldsymbol{b}_{rc} \\
\boldsymbol{b}_{qc}^{\dagger} &= \frac{1}{\sqrt{N}}\sum_r \exp(i\boldsymbol{q}\cdot\boldsymbol{r})\boldsymbol{b}_{rc}^{\dagger}.
\end{aligned}\right\} \tag{42}$$

Considering the analogy between equation (41) and the definition of momentum proper in terms of operators generating continous translations of matter, it is now natural to define the vector operator

$$\hbar \hat{\boldsymbol{q}} = \sum_{qc} \hbar \boldsymbol{q}(\boldsymbol{b}_{qc}^{\dagger} \cdot \boldsymbol{b}_{qc}) \tag{43}$$

and to call it the pseudomomentum operator. The state $b_{qc}^{\alpha\dagger} |0\rangle$ is said to contain one phonon with cell position $\boldsymbol{c}$, polarisation $\boldsymbol{e}_{\alpha}$ and pseudomomentum $\hbar \boldsymbol{q}$. All possible values of the lattice position operator $\hat{\boldsymbol{r}}$ have the same probability in such a state, compare (42).

For further details, including a discussion of conservation laws, the reader is referred to [1], [2] and [5].

6. Local Rotation and Spin

Next we want to consider a common rotation of all field vectors around the equilibrium position of the atoms to which they belong (compare fig. 2). We could of course equally well consider an opposite rotation of the coordinate system $\boldsymbol{e}_x$, $\boldsymbol{e}_y$ and $\boldsymbol{e}_z$ used to describe the field vector components.

The rotation in question belongs to the continuous group of vector rotations and is well known. Let us first consider a rotation with angle θ around the z-axis $\boldsymbol{e}_z$. The transformation of the $\boldsymbol{b}$-vectors is then (we leave out the reference to the atoms ($\boldsymbol{r}$ and $\boldsymbol{c}$) the numbering of which is not changed)

$$b^{\alpha'} = L_{\alpha\beta} b^{\beta} \tag{44}$$

where

$$\{L_{\alpha\beta}\} = \begin{Bmatrix} \cos\theta & -\sin\theta & 0 \\ \sin\theta & \cos\theta & 0 \\ 0 & 0 & 1 \end{Bmatrix}. \tag{45}$$

Eigenvectors of this matrix and the corresponding eigenvalues are

$$\left. \begin{aligned} \{B_{\alpha}^{+1}\} &= \frac{1}{\sqrt{2}} \begin{Bmatrix} 1 \\ -i \\ 0 \end{Bmatrix}; \quad \{B_{\alpha}^{0}\} = \begin{Bmatrix} 0 \\ 0 \\ 1 \end{Bmatrix}; \quad \{B_{\alpha}^{-1}\} = \frac{1}{\sqrt{2}} \begin{Bmatrix} 1 \\ i \\ 0 \end{Bmatrix} \\ \lambda_1 &= \exp(i\theta) \qquad\quad \lambda_2 = 1 \qquad\qquad \lambda_3 = \exp(-i\theta) \\ l_1 &= \theta \qquad\qquad\quad\; l_2 = 0 \qquad\qquad\; l_3 = -\theta \end{aligned} \right\} \tag{46}$$
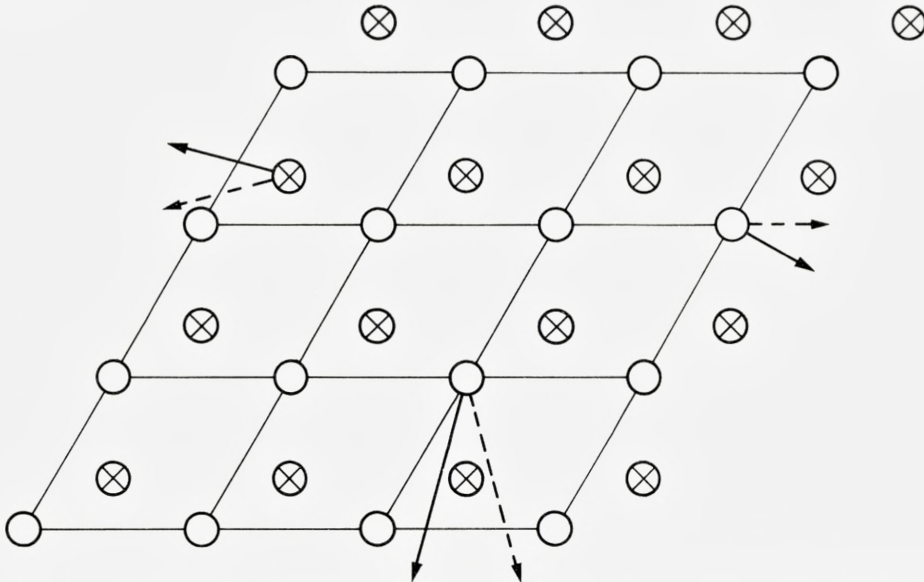
Fig. 2. Local rotation. The fully drawn and the dashed arrows are field vectors before and after the rotation.

Again proceeding as described in section 3 we find from (32) the new basic creation and destruction operators, the latter are:

$$\left\{\begin{array}{c} b^{+1} \\ b^0 \\ b^{-1} \end{array}\right\} = \left\{\begin{array}{c} \frac{1}{\sqrt{2}}(b^x - ib^y) \\ b^z \\ \frac{1}{\sqrt{2}}(b^x + ib^y) \end{array}\right\}. \tag{47}$$

From (46), (47) and (31) the $\hat{O}$-operator for this transformation is found to be

$$\hat{O} = \theta((b^{+1})^\dagger b^{+1} - (b^{-1})^\dagger b^{-1}) = -i\theta(\boldsymbol{b}^\dagger \times \boldsymbol{b})_z. \tag{48}$$

Combining this with the results for rotations around the two other axes we are led to define the axial vector operator

$$\hat{\boldsymbol{S}} = \frac{\hbar}{i} \sum_{rc} \boldsymbol{b}_{rc}^\dagger \times \boldsymbol{b}_{rc} \tag{49}$$

(we again introduce explicitly the summation over the atoms ($\boldsymbol{r}$ and $\boldsymbol{c}$)).

Comparing with the theory of rotations for ordinary particles it is natural to identify $\hat{\boldsymbol{S}}$ with an angular momentum, and because it is independent of the origin chosen for the position coordinates of the phonons, it should be called a spin angular momentum.

As the transformation generated by $\hat{\boldsymbol{S}}$ is a continuous rotation it is to be expected that $\hat{\boldsymbol{S}}$ fulfils the usual commutation relations for angular momentum. A straightforward calculation confirms this, particularly it is found that all one-phonon states are eigenfunctions of

$$\hat{\boldsymbol{S}}^2 = \hat{S}_x^2 + \hat{S}_y^2 + \hat{S}_z^2$$

with the eigenvalue $2\hbar^2$. The one-phonon eigenfunctions of $\hat{S}_z$ are (leaving out $\boldsymbol{r}$ and $\boldsymbol{c}$)

$$(b^{+1})^\dagger \,|\, 0\rangle = \frac{1}{\sqrt{2}}(b^{x\,\dagger} + ib^{y\,\dagger}) \,|\, 0\rangle, \quad \text{eigenvalue } +\hbar,$$

$$(b^0)^\dagger \,|\, 0\rangle = b^{z\,\dagger} \,|\, 0\rangle, \qquad\qquad\qquad \text{eigenvalue } 0,$$

$$(b^{-1})^\dagger \,|\, 0\rangle = \frac{1}{\sqrt{2}}(b^{x\,\dagger} - ib^{y\,\dagger}) \,|\, 0\rangle, \quad \text{eigenvalue } -\hbar.$$

The phonon must consequently be said to be a spin one particle in conformity with its vectorial character. The state $(b_{rc}^{+1})^\dagger \,|\, 0\rangle$ is said to contain one phonon with $\hat{S}_z = \hbar$ at the position $\boldsymbol{r} + \boldsymbol{c}$.

The $\hat{F}$ operators (compare eq. (33)) generating local rotations of the displacements and momenta are well known from the quantum mechanics of ordinary particles. They are the components of the vector operator

$$\hat{\boldsymbol{F}} = \frac{\theta}{\hbar} \sum_{rc} (\boldsymbol{u}_{rc} \times \boldsymbol{p}_{rc}). \tag{50}$$

This is obtained from (35) or directly verified by using the commutation relations for the displacements and momenta. The operator $\hat{\boldsymbol{F}}$ divided by $\theta/\hbar$ is immediately recognized as a part of the angular momentum proper of the total system. When specialized to the continuum limit, it is identical with the spin-operator derived in ref. [3] by means of Noether's theorem. However, in ref. [3] only the isotropic case is treated. The operators $\hat{O}$ (48) and $\hat{F}_z$ (50) are identical if both the kinetic and potential energy are invariant under local rotations. In the anisotropic case $\hat{\boldsymbol{F}}$ (50) is not a one-phonon operator, and the term phonon spin operator should be reserved for the quantity (49).
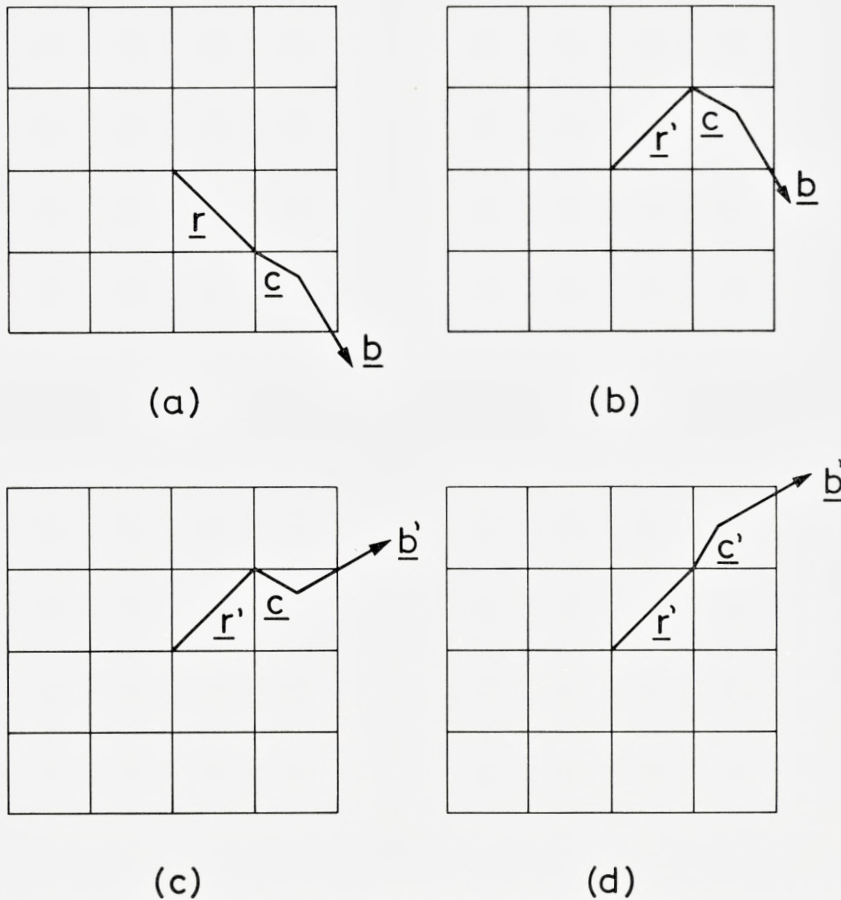
Fig. 3. A 90° rotation decomposed into successive rotations of the lattice vector r, the field vector b and the basis vector c.

7. Point Group Rotation and Pseudo Angular Momentum

Let us consider a crystal, the atomic equilibrium positions of which form a structure with an n-fold axis of symmetry through a lattice point, the axis is called the z-axis.

We transform the excitation pattern of the crystal by rotating it through an angle $2\pi/n$ around the z-axis. This transformation can be split into three commuting operations of the types c), b) and d) of section 4 (compare fig. 3)*.

* We only consider an infinite crystal. In order to give meaning to the transformation for a finite crystal we would have to choose a special form of the crystal and a special axis or to impose suitable cyclic boundary conditions on the transformation.

The second operation on fig. 3, which is possible for an arbitrary angle, has already been treated and has led to the introduction of the spin operator (49). The first operation and the third one are cyclic transformations very similar to the transformations which led to the concept of pseudomomentum. They permute in a cyclic way the field vectors belonging to n equivalent positions and first we need only consider the n $\boldsymbol{b}$-vectors belonging to such a "star" of equivalent points. These points are labelled by the angle θ (modulo 2π) between, say, the xz-plane and the normal from the point to the z-axis. For a definite "star" θ takes values with intervals $2\pi/n$.

The transformation in question is then

$$\boldsymbol{b}_\theta' = \boldsymbol{b}_{\theta-2\pi/n} \tag{51}$$

with the convention that

$$\boldsymbol{b}_\theta = \boldsymbol{b}_{\theta+2\pi}.$$

A complete set of eigenvectors B_θ^m and eigenvalues λ^m of the transformation (51) is (for one "star" and one direction of the field vectors)

$$B_\theta^m = \frac{1}{\sqrt{n}} e^{-im\theta} \tag{52}$$

$$\lambda^m = e^{i2\pi m/n} \tag{53}$$

where m is an integer which can take on n consecutive values. Following the scheme of section 3 we find that the $\hat{O}$-operator in question is

$$\hat{O} = \frac{2\pi}{n} \sum_m m\boldsymbol{b}_m^\dagger \cdot \boldsymbol{b}_m \tag{54}$$

where

$$\boldsymbol{b}_m = \frac{1}{\sqrt{n}} \sum_\theta \boldsymbol{b}_\theta \, e^{-im\theta}. \tag{55}$$

As $2\pi/n$ in (54) is the angle of rotation and as the analogous rotation operator for an ordinary particle is $1/\hbar$ times the product of the angle of rotation and the component along the axis of rotation of the orbital angular momentum operator it is natural to call the operator $\hbar \sum_m m\boldsymbol{b}_m^\dagger \cdot \boldsymbol{b}_m$ the z-component of a "pseudo orbital angular momentum". The full expression for this operator becomes

$$\hat{L}_z = \hbar \sum_{ms} m\boldsymbol{b}_{ms}^\dagger \cdot \boldsymbol{b}_{ms} \tag{56}$$

where the summation index s runs over all distinct "stars" of n equivalent sites.

The resemblance of the pseudo orbital angular momentum to the pseudo-momentum is now evident: each "star" corresponds to a one-dimensional cyclic crystal with n lattice sites.

The full rotation shown on fig. 3 is generated by an operator

$$\exp\left(\frac{i}{\hbar}\frac{2\pi}{n}\hat{J}_z\right) = \exp\left(\frac{i}{\hbar}\frac{2\pi}{n}\hat{L}_z\right)\exp\left(\frac{i}{\hbar}\frac{2\pi}{n}\hat{S}_z\right). \tag{57}$$

The operator $\hat{J}_z$ may be defined so that the three operators $\hat{J}_z$, $\hat{L}_z$ and $\hat{S}_z$ commute and thus have simultaneous eigenfunctions. If their eigenvalues are denoted by $\hbar m_j$, $\hbar m_l$ and $\hbar m_s$ respectively, we can only conclude from (57) that

$$m_j = m_l + m_s \text{ modulo } n. \tag{58}$$

A convenient choice of m_j would be such that it is limited to the same range of values as m_l.

If, e. g., we consider the case $n = 4$, the twelve independent one-phonon eigenstates of $\hat{S}_z$, $\hat{L}_z$ and $\hat{J}_z$ of a single star can be classified by means of the following quantum numbers.

m_s	-1	0	1	-1	0	1	-1	0	1	-1	0	1	
m_l	-1	-1	-1	0	0	0	1	1	1	2	2,	2	(59)
m_j	2	-1	0	-1	0	1	0	1	2	1	2	-1	

It is tempting to try to use $\hbar\hat{\boldsymbol{r}}\times\hat{\boldsymbol{q}}$ (or rather $\frac{1}{2}\hbar(\hat{\boldsymbol{r}}\times\hat{\boldsymbol{q}} + h.c.)$) as a "pseudo orbital angular momentum" but the operator does not generate rotations, not even in the limit of an infinite crystal (compare fig. 4). This is seen in the following way:

The operator $\hat{\boldsymbol{r}}$ is found to generate translations in the q-space just as $\hat{\boldsymbol{q}}$ generates translations in the r-space. In the limit of an infinite crystal $\hat{\boldsymbol{q}}$ has a continuum of eigenvalues and in this limit $\hat{\boldsymbol{r}}$ and $\hbar\hat{\boldsymbol{q}}$ resemble (in the q-representation) the usual position and momentum operators (in momentum representation) except for the fact that the eigenvalues of $\hat{\boldsymbol{q}}$ are limited to, say, the Brillouin zone. Denoting a vector in q-space by $\boldsymbol{Q}$ it is therefore possible to make the identification

$$\hat{\boldsymbol{r}} = i\frac{\partial}{\partial\boldsymbol{Q}}.$$

In order to stay within the space of functions which are periodic in the q-space the operator $\hat{\boldsymbol{q}}$ must be identified by a periodic function of $\boldsymbol{Q}$ and not just by $\boldsymbol{Q}$. This explains why $\hbar\hat{\boldsymbol{r}}\times\hat{\boldsymbol{q}}$ does not generate rotations except within a sphere which does not touch the Brillouin zone boundary and which has its centre at $\boldsymbol{Q} = 0$. The difficulties of $\hbar\hat{\boldsymbol{r}}\times\hat{\boldsymbol{q}}$ are connected with the fact that the spherical harmonics are not orthogonal functions in the Brillouin zone.

2*
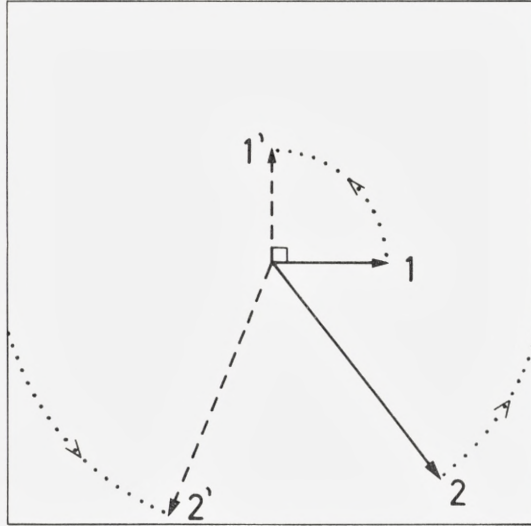
Fig. 4. The fully drawn arrows and the dashed ones show two wave vectors in the Brillouin zone before and after a 90° "rotation" generated by $h\hat{r} \times \hat{q}$. Only the wave vector which does not touch the zone boundary during the "rotation" is really rotated.
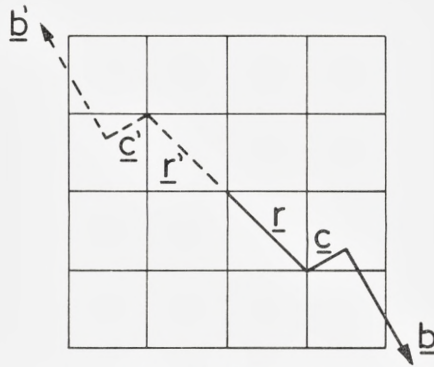
Fig. 5. Inversion of the excitation pattern.

8. Inversion and Parity

For a crystal whose atomic sites form a pattern with inversion symmetry, we can consider the following transformation of the excitation vectors (compare fig. 5).

$$b'_{rc} = -b_{-r-c}. \qquad (60)$$

This can be split into an inversion without changing the direction of the vectors and a local inversion $\boldsymbol{b} \to -\boldsymbol{b}$. The latter leads to the definition of the *intrinsic parity* which clearly has the eigenvalue -1 for a single phonon. The full intrinsic parity operator is the trivial operator $(-1)^{\hat{n}}$, where $\hat{n}$ is the particle number operator.

The rest of the transformation (60), i. e.

$$\boldsymbol{b}'_{rc} = \boldsymbol{b}_{-r-c}, \tag{61}$$

leads to the definition of the concept of *extrinsic parity*. It is generated by a unitary operator with the eigenvalues $+1$ and -1 for states which are symmetric and antisymmetric respectively under the inversion (61). Of course one could introduce an $\hat{O}$-type operator in this case too in complete analogy with the case of rotation. It does not seem to be useful, however, so we shall not write it down explicitly.

If the crystal—not only the pattern of atomic sites—has inversion symmetry around $\boldsymbol{r} = 0$ the total parity is conserved. The intrinsic parity, however, is not conserved when uneven anharmonic terms are present in the Hamiltonian.

Appendix I

The usual harmonic Hamiltonian may be generalized so as to contain "mixed products" i. e. terms of the form $p_r G_{rs} u_s$. For simplicity only the following Hamiltonian will be treated (in this appendix bold face types as $\boldsymbol{u}$ stand for a $1 \times 3N$ column matrix)

$$
\left.\begin{aligned}
H &= \tfrac{1}{2}(\tilde{\boldsymbol{p}} - \tilde{\boldsymbol{u}}\tilde{A})(\boldsymbol{p} - A\boldsymbol{u}) + \tfrac{1}{2}\tilde{\boldsymbol{u}}D\boldsymbol{u} \\
A &= A^* = -\tilde{A} \qquad D = D^* = \tilde{D} \\
&\text{$3N$ degrees of freedom,} \\
&\text{D is a positive definite matrix.}
\end{aligned}\right\} \quad (\mathrm{I},\,1)
$$

The term $A\boldsymbol{u}$ may be the result of a homogeneous magnetic field around every single particle or a Coriolis field.

This Hamiltonian will be shown to describe a set of one dimensional harmonic oscillators just as the usual harmonic Hamiltonian. In order to show this the Heisenberg picture will be used.

The equations of motion are now

$$
\left.\begin{aligned}
\dot{\boldsymbol{u}} &= \boldsymbol{p} - A\boldsymbol{u} \\
\dot{\boldsymbol{p}} &= -(D - A^2)\boldsymbol{u} - A\boldsymbol{p}.
\end{aligned}\right\} \quad (\mathrm{I},\,2)
$$

This is a system of linear first order differential equations with constant coefficients. In order to show that these equations have a complete set of harmonic solutions new variables are introduced

$$
\left.\begin{aligned}
\boldsymbol{r} &= \boldsymbol{u} & \boldsymbol{u} &= \boldsymbol{r} \\
\boldsymbol{s} &= D^{-1/2}(\boldsymbol{p} + A\boldsymbol{u}) & \boldsymbol{p} &= D^{1/2}\boldsymbol{s} - A\boldsymbol{r}
\end{aligned}\right\} \quad (\mathrm{I},\,3)
$$

$$
\begin{Bmatrix} \dot{\boldsymbol{r}} \\ \dot{\boldsymbol{s}} \end{Bmatrix} = \begin{Bmatrix} -2A & D^{1/2} \\ -D^{1/2} & 0 \end{Bmatrix} \begin{Bmatrix} \boldsymbol{r} \\ \boldsymbol{s} \end{Bmatrix} = \Xi \begin{Bmatrix} \boldsymbol{r} \\ \boldsymbol{s} \end{Bmatrix}. \qquad (\mathrm{I},\,4)
$$

The Hamiltonian may be expressed by $\boldsymbol{r}$ and $\boldsymbol{s}$ in the following ways

$$H = \tfrac{1}{2}(\tilde{\boldsymbol{r}}, \tilde{\boldsymbol{s}})\, \tilde{\Xi}\Xi \begin{Bmatrix} \boldsymbol{r} \\ \boldsymbol{s} \end{Bmatrix} = \tfrac{1}{2}(\tilde{\boldsymbol{r}}, \tilde{\boldsymbol{s}}) \begin{Bmatrix} \dot{\boldsymbol{r}} \\ \dot{\boldsymbol{s}} \end{Bmatrix}. \tag{I, 5}$$

The matrix $i\Xi$ is a $6N \times 6N$ dimensional and hermitian matrix and can consequently be diagonalized by a unitary matrix

$$\Xi\Gamma = i\Gamma\Omega \qquad \Gamma^{\dagger}\Gamma = \Gamma\Gamma^{\dagger} = 1$$
$$\Omega = \text{a diagonal matrix, } \Omega = \Omega^*. \left.\phantom{\begin{matrix}a\\a\end{matrix}}\right\} \tag{I, 6}$$

The matrix $D^{1/2}$ has no eigenvalue equal zero and eq. (I, 4) shows therefore that Ξ has no eigenvalue equal zero. It is also immediately seen that if $(\xi_{\nu}, i\omega_{\nu})$ are corresponding eigenvectors and eigenvalues of Ξ, then $(\xi_{\nu}^*, -i\omega_{\nu})$ are also corresponding eigenvectors and eigenvalues of Ξ. It is therefore possible to choose Γ and Ω in the following way

$$\Gamma = \begin{Bmatrix} E & E^* \\ F & F^* \end{Bmatrix} \qquad \Omega = \begin{Bmatrix} \omega & 0 \\ 0 & -\omega \end{Bmatrix} \tag{I, 7}$$

ω is a $3N \times 3N$, positive definite and diagonal matrix.

In order to separate the Hamiltonian we introduce new variables $\boldsymbol{f}$ and $\boldsymbol{f}^{\dagger}$

$$\begin{Bmatrix} \boldsymbol{r} \\ \boldsymbol{s} \end{Bmatrix} = \Gamma \begin{Bmatrix} \boldsymbol{f}^{\dagger} \\ \boldsymbol{f} \end{Bmatrix}. \tag{I, 8}$$

The operators $(\boldsymbol{f}^{\dagger})_{\alpha}$ and $(\boldsymbol{f})_{\alpha}$ are hermitian conjugate operators because $(\boldsymbol{r})_{\beta}$ and $(\boldsymbol{s})_{\beta}$ are hermitian operators.

If $\boldsymbol{u}$ and $\boldsymbol{p}$ are replaced by $\boldsymbol{f}^{\dagger}$ and $\boldsymbol{f}$ then the Hamiltonian (I, 5) will be

$$H = \tfrac{1}{2}\left(\tilde{\boldsymbol{f}}^{\dagger}\omega^2\boldsymbol{f} + \tilde{\boldsymbol{f}}^{\dagger}\omega^2\boldsymbol{f}\right). \tag{I, 9}$$

In order to show that H really is separated into one-dimensional systems, it is necessary to study the commutation relations of $\boldsymbol{f}$ and $\boldsymbol{f}^{\dagger}$. After some lengthy calculations the following result is found

$$[(\boldsymbol{f}^{\dagger})_{\alpha}, (\boldsymbol{f}^{\dagger})_{\beta}] = [(\boldsymbol{f})_{\alpha}, (\boldsymbol{f})_{\beta}] = 0$$
$$[(\boldsymbol{f})_{\alpha}, (\boldsymbol{f}^{\dagger})_{\beta}] = \hbar(\omega^{-1})_{\alpha\beta}. \left.\phantom{\begin{matrix}a\\a\end{matrix}}\right\} \tag{I, 10}$$

Now destruction operators of phonons in stationary states can immediately be constructed

$$b_\alpha = \sqrt{\frac{\omega_\alpha}{\hbar}} (f)_\alpha$$

$$H = \hbar \sum_\alpha \omega_\alpha (b_\alpha^\dagger b_\alpha + \tfrac{1}{2})$$

$$[b_\alpha, b_\beta] = 0 \qquad [b_\alpha, b_\beta^\dagger] = \delta_{\alpha\beta}.$$

$$(I, 11)$$

In cases where the matrices A and D of the Hamiltonian (I, 1) commute it is possible to choose destruction operators for localized phonons of the form (8) where

$$M = (D - A^2)^{1/4} \qquad\qquad (I, 12)$$

can be used (note that $-A^2$ has no negative eigenvalues). In the general case it does not appear very useful to introduce localized phonons, at least not localized with respect to direction.

The whole question of phonons and magnetic fields is not an important one because the most essential result of a magnetic field will be a change of the electronic structure, i. e. a change of the dynamical matrix D. The reason for this is that the charge-mass ratio is much larger for the electrons than for the nuclei. It may, however, be of some importance to realize that a homogeneous magnetic field itself is not an anharmonic force.

Appendix II

The most reasonable way to study how phonons are localized is to study how the corresponding excitation energy is localized. This means that the matrix elements of $p_r p_s$ and $u_r u_s$ must be studied. In the usual case where the matrix T (1) of the kinetic energy is a diagonal matrix, π_r and v_r (2) can evidently be used instead of p_r and u_r and this will be done here.

If $|A\rangle$ is a normalized state vector containing a definite number of localized phonons (8) (9), i. e. if $|A\rangle$ is an eigenvector of all operators $b_r^\dagger b_r$, then a short calculation gives these results:

$$\langle A | \pi_r \pi_s | A \rangle = \hbar \sum_t M_{rt} M_{ts} (\langle A | b_t^\dagger b_t | A \rangle + \tfrac{1}{2}) \qquad (II, 1)$$

$$\langle A | v_r v_s | A \rangle = \hbar \sum_t (M^{-1})_{rt} (M^{-1})_{ts} (\langle A | b_t^\dagger b_t | A \rangle + \tfrac{1}{2}) \qquad (II, 2)$$

$$\langle A | H | A \rangle = \hbar \sum_t (M^2)_{tt} (\langle A | b_t^\dagger b_t | A \rangle + \tfrac{1}{2}) \qquad (II, 3)$$

$$\langle A | H | A \rangle = \sum_t \langle A | \pi_t \pi_t | A \rangle = \sum_{st} \langle A | v_s D_{st} v_t | A \rangle. \qquad (II, 4)$$

It is seen that the energy of $|A\rangle$ is, as expected, divided into two equal parts, a potential energy part and a kinetic energy part.

The excitation energy of a phonon created by $b_u^\dagger$ from the state $|A\rangle$ is now determined by the increment in the matrix elements (II, 1) and (II, 2) when $b_u^\dagger b_u$ is increased by one. In particular, that part of the kinetic exciation energy which belongs to the r'th degree of freedom is (from II, 1)

$$\delta E_{\text{kin}, r} = \delta \tfrac{1}{2} \langle A \,|\, \pi_r^2 \,|\, A\rangle = \tfrac{1}{2}\hbar (M_{ru})^2 \qquad (\text{II}, 5)$$

Thus the kinetic excitation energy of the phonon created by $b_u^\dagger$ would be strictly localized if and only if M were a diagonal matrix; but then $D = M^4$ would be a diagonal matrix too, and this is clearly not true. The kinetic energy connected with "localized" phonons is therefore not strictly localized, but if M_{rs} is small when the atoms to which r and s belong are rather far apart then it is quite reasonable to call the phonon localized. As a matter of fact in the case of sufficiently large systems D_{rs} will usually be small when the atoms to which r and s belong are sufficiently far apart, and this feature will, more or less, be preserved for functions of D, e. g. $M = D^{1/4}$ (reasons for this will be given later).

Another way to study the localization of "localized phonons" would be to study the transitions between different states of localized phonons. This will lead to the study of the matrix elements of the Hamiltonian H or according to eq. (II, 3) the matrix elements of M^2.

From the preceding considerations it is seen that the localization of "localized phonons" is connected with functions of D. We shall not give any real proof but only sketch how one may investigate to what extent it follows that if D_{rs} is small when the distance between r and s is large enough then the same is, more or less, true for functions of D. We shall limit ourselves to the case where

$$D_{rs} = 0 \text{ when distance } (r,s) > d. \qquad (\text{II}, 6)$$

It follows immediately that

$$(D^n)_{rs} = 0 \text{ when distance } (r,s) > n \times d, \; n = 1, 2, 3, \ldots \qquad (\text{II}, 7)$$

Polynomials of D will therefore have the wanted property.

If the eigenvalues of D are such that a function $f(x)$ may be approximated by a polynomial of x for x equal to any of the eigenvalues of D, then $f(D)$ may be approximated by the same polynomial in D instead of x. This is most easily seen in a representation where D is a diagonal matrix. Approxima-

tion by polynomials gives now an explanation of the said property of functions of D.

Instead of giving examples using the approximation by polynomials only a few numerical results will be given. For some simple models of crystals it has been calculated how much of the kinetic excitation energy of a localized phonon belongs to the same degree of freedom as the phonon; this means (see II, 5) that $(M_{rr})^2/(M^2)_{rr}$ has been calculated. The examples are:

1) A harmonic, infinite, one-dimensional and diatomic crystal with nearest neighbour interaction. The masses are m_1 and m_2, and the phonon is localized at the atom with mass m_1. Except for $m_1/m_2 = 1$ numerical integration is necessary.

m_1/m_2	0.1	0.5	1	2	10
$(M_{11})^2/(M^2)_{11}$	0.978	0.938	0.914	0.892	0.865

It is seen that a phonon is better localized at a light atom than at a heavy atom, but the kinetic energy part of the excitation energy is in all cases quite well localized.

2) A harmonic, infinite, two-dimensional and hexagonal crystal with one atom in the basis and nearest neighbour interaction.

Numerical calculations have shown that

$$(M_{rr})^2/(M^2)_{rr} \approx 0.97.$$

3) This is a Debye model with a "spherical" Brillouin zone and only one sound velocity. The model is not very realistic but particularly in one and three dimensions many calculations are easily performed.

	1-dim.	2-dim.	3-dim.
$(M_{rr})^2/(M^2)_{rr}$	8/9	24/25	48/49

Although the interaction range of a Debye model is long it is found that the kinetic excitation energy of a localized phonon is well localized. Note that the degree of localization increases with the number of dimensions.

Appendix III

Below is shown that the operator $\hat{O}$ (31) generates the transformation (27) of the destruction operators b_r.

First we define by induction an operator $[A, B]^{(n)}$ for all integers $n \geqslant 0$ (A and B are usual operators)

$$[A, B]^{(0)} = B \qquad [A, B]^{(1)} = AB - BA$$
$$[A, B]^{(n+1)} = [A, [A, B]^{(n)}]^{(1)}.$$

We have now the following identity*

$$\exp(A)B \exp(-A) = \sum_{n=0}^{\infty} \frac{1}{n!}[A, B]^{(n)} \quad (= \exp([A, B])). \qquad \text{(III, 1)}$$

Here the last expression is to be understood in a purely formal way.

A proof of the identity is easily constructed using the formula

$$[A, B]^{(n)} = \sum_{\nu=0}^{n} (-1)^{n+\nu} \binom{n}{\nu} A^\nu B A^{n-\nu} \qquad \text{(III, 2)}$$

which is found by induction.

Using the commutation relations (10) for b_α and $b_\alpha^\dagger$ (32) it is found by induction that

$$[b_\alpha^\dagger b_\alpha, b_\beta]^{(n)} = (-1)^n b_\alpha \delta_{\alpha\beta} \qquad n > 0.$$

The transformation of b_α is now immediately accessible

$$\exp(i\hat{O})b_\alpha \exp(-i\hat{O}) = \exp(-il_\alpha)b_\alpha = \lambda_\alpha^* b_\alpha.$$

The transformation of b_r is consequently

$$\exp(i\hat{O})b_r \exp(-i\hat{O}) = \sum_\alpha B_r^{\alpha*} \lambda_\alpha^* b_\alpha = \sum_{\alpha st} L_{rs} B_s^{\alpha*} B_t^\alpha b_t = \sum_s L_{rs} b_s \qquad \text{q. e. d.}$$

* See F. Hausdorff (7). A more recent treatment is given by Wilhelm Magnus et al. (8).

H. C. Ørsted Institute, Physics Laboratory I,
  University of Copenhagen, Denmark.

References

(1) GEORG SÜSSMANN, Zeitschrift für Naturforschung **11a**, 1–11 (1956).

(2) GEORG SÜSSMANN, Zeitschrift für Naturforschung **13a**, 1–6 (1958).

(3) S. V. VONSOVSKII and M. S. SVIRSKII, Soviet Physics. – Solid State **3**, 1568 (1962). (Translated from Fizika Tverdogo Tela **3**, 2160 (1961)).

(4) A. D. LEVINE, Il Nuovo Cimento **26**, 190 (1962).

(5) H. HØJGAARD JENSEN, Aarhus Summer School Lectures, 1963: Phonons and Phonon Interactions, edited by Thor A. Bak, W. A. Benjamin, New York 1964.

(6) A. I. MAL'CEV, Foundations of Linear Algebra, (translated from the Russian), W. H. Freeman and Co., San Fransisco 1963.

(7) F. HAUSDORFF, Berichte über die Verhandlungen der Königlich Sächsischen Gesellschaft der Wissenschaften zu Leipzig, Mathematisch-Physische Klasse, **58**, 19–48 (1906).

(8) WILHELM MAGNUS, ABRAHAM KARRASS and DONALD SOLITAR, Combinatorial Group Theory: Presentations of Groups in Terms of Generators and Relations, Interscience Publisher, New York 1966.

CHRISTIAN BERG

CORPS CONVEXES ET
POTENTIELS SPHÉRIQUES

TABLE DES MATIÈRES

Synopsis

On étudie une théorie du potentiel sur la sphère unité dans l'espace euclidien de q dimensions. Les fonctions propres de l'opérateur de Laplace-Beltrami pour la valeur propre $1-q$ jouent le rôle de fonctions harmoniques. Plusieurs théorèmes de la théorie classique du potentiel ont leurs analogues dans cette théorie, par exemple le théorème de représentation de Riesz, disant ici qu'une fonction sousharmonique s'écrit uniquement comme somme d'un potentiel sphérique d'une mesure positive et d'une fonction harmonique.

La fonction d'appui d'un corps convexe est sousharmonique sur la sphère unité, et on trouve que sa partie potentielle est le potentiel de la première mesure de surface du corps, et que sa partie harmonique est déterminée par le point de Steiner du corps. On aboutit à retrouver le théorème classique disant qu'un corps convexe est déterminé à une translation près par sa première mesure de surface, et ce qui est plus intéressant, on obtient une caractérisation des mesures qui peuvent être la première mesure de surface d'un corps convexe.

Introduction

Il y a 30 ans, que A. D. Aleksandrov [1] et indépendamment W. Fenchel et B. Jessen [7] ont introduit les mesures de surface d'un corps convexe. Depuis ce temps là L. Schwartz a créé la théorie des distributions, et il nous semble naturel d'en faire usage aux problèmes linéaires des corps convexes.

Un problème intéressant, posé dans [1], [7], est la caractérisation des mesures positives sur la sphère unité Ω_q dans $\mathbf{R}^q$, qui peuvent être la mesure de surface p-ième $\mu_p(K)$ d'un corps convexe K dans $\mathbf{R}^q$. La mesure $\mu_p(K)$ est par définition la mesure de surface mixte $\mu(K, \cdots, K, E_q, \cdots, E_q)$, où le corps K est pris p fois, et la boule unité E_q de $\mathbf{R}^q$ est prise $q - 1 - p$ fois. Pour la définition voir [7] p. 21.

Le cas $p = q - 1$ est résolu complètement dans [2], [7], tandis que la réponse pour $p = 1, \cdots, q - 2$ est inconnue. Contrairement à la réponse du cas $p = q - 1$, où tous les mesures positives, satisfaisant à des conditions trivialement nécessaires, peuvent paraître comme mesures $\mu_{q-1}(K)$, c'est connu depuis longtemps que la classe des mesures $\mu_1(K)$ est beaucoup plus restrictive. Un des buts du présent travail est de donner une condition nécessaire et suffisante, pour qu'une mesure positive soit la première mesure de surface $\mu_1(K)$ d'un corps convexe K. Une condition suffisante mais non nécessaire est donnée par A. V. Pogorelov [16]. Pendant la rédaction finale du présent travail nous avons fait la connaisance de deux travaux de W. J. Firey [8], [9], dont le dernier contient essentiellement la même caractérisation comme la nôtre, mais obtenue dans une manière complètement différente.

La mesure $\mu_1(K)$ dépend linéairement du corps convexe K dans $\mathbf{R}^q$, ou ce qui est équivalent, linéairement de la fonction d'appui h_K de K:

$$h_{K+L} = h_K + h_L, \quad \mu_1(K+L) = \mu_1(K) + \mu_1(L),$$

$$h_{\lambda L} = \lambda h_L, \qquad \mu_1(\lambda K) = \lambda \mu_1(K),$$

pour des corps convexes K, L et $\lambda \geqq 0$.

1*

Ce fait indique, qu'on pourrait espérer de trouver un opérateur diffé-rentielle D_q^* sur la sphère unité Ω_q tel que

$$D_q^* h_K = \mu_1(K), \tag{1}$$

au sens de distribution pour tout corps convexe K. Nous allons démontrer, qu'en effet c'est le cas, et que

$$D_q^* = \frac{1}{q-1} \Delta_q^* + 1, \tag{2}$$

où Δ_q^* est l'opérateur de Laplace-Beltrami sur la sphère unité Ω_q. Dans le cas où K est suffisamment différentiable, la formule (1) s'écrit pour $\xi \in \Omega_q$

$$\sum_{i=1}^{q} \frac{\partial^2 h_K}{\partial x_i^2}(\xi) = \{\Delta_q^* + (q-1)\} h_K(\xi) = R_1(\xi) + \cdots + R_{q-1}(\xi), \tag{3}$$

où $R_1(\xi), \cdots, R_{q-1}(\xi)$ sont les rayons de courbure principaux au point frontière $\operatorname{grad} h_K(\xi)$ de K. La formule (3) est classique, et remonte à E. B. Christoffel pour l'espace ordinaire de trois dimensions.

Il est bien naturel de chercher la formule inverse de (1), c'est-à-dire trouver une fonction de Green g_q de l'opérateur D_q^*. Nous sommes arrivés à démontrer l'existence d'une telle fonction – dans tout le suivant appelée le noyau sphérique – et à calculer g_q explicitement, à cause d'une formule de récursion simple entre g_{q+2} et g_q. En vertu de l'invariance de D_q^* par rapport au groupe $O(q)$ des rotations, le noyau sphérique

$$g_q : \Omega_q \times \Omega_q \to \mathbf{R} \cup \{-\infty\}$$

ne dépend que du produit scalaire $\xi \cdot \eta$ des vecteurs $\xi, \eta \in \Omega_q$, et par consé-quent g_q est considéré comme fonction sur l'intervalle $[-1, 1]$. Alors la for-mule inverse de (1) peut s'écrire pour $\xi \in \Omega_q$

$$h_K(\xi) = \frac{1}{\|\omega_{q-1}\|} \int_{\Omega_q} g_q(\xi \cdot \eta) d\mu_1(K)(\eta) + \mathscr{S}(K) \cdot \xi, \tag{4}$$

où

$$\mathscr{S}(K) = \frac{q}{\|\omega_q\|} \int_{\Omega_q} \eta h_K(\eta) d\omega_q(\eta), \tag{5}$$

valable pour tout corps convexe K dans $\mathbf{R}^q$. Ici ω_q désigne la mesure de sur-face ordinaire sur Ω_q de masse totale $\|\omega_q\|$. Le point $\mathscr{S}(K)$ de $\mathbf{R}^q$ est appelé

le point de Steiner [18]. Pendant les dernières années $\mathscr{S}(K)$ a joué un rôle dans des diverses travaux, surtout par G. C. Shephard (cf. B. Grünbaum [10] p. 307).

Les formules (1) et (4) ressemblent au théorème de représentation de F. Riesz dans la théorie du potentiel classique, et en effet ils représentent un cas particulier d'un théorème complètement analogue à celui-là. Nous allons développer une «théorie du potentiel sphérique» qui admet ce «théorème de Riesz». Chez nous g_q va jouer le rôle de r^{-q+2}, et D_q^* le rôle du laplacien. Beaucoup de résultats classiques possèdent des analogues dans cette théorie, citons par exemple le théorème dû à G. C. Evans et à F. Vasilesco (cf. [6] p. 49).

Dans le chapitre 1 nous allons réunir la notation et au convenance du lecteur donner quelques définitions et théorèmes, qui seront souvent utilisés. Dans le chapitre 2 nous allons utiliser la théorie des distributions sur la sphère unité Ω_q, et notre outil le plus important sera le développement d'une distribution en série de fonctions sphériques. Une espèce de produit de convolution entre des fonctions sur l'intervalle $[-1, 1]$ et des distributions sur la sphère unité Ω_q nous permet de faire une régularisation des distributions. Dans le chapitre 3 nous allons démontrer l'existence du noyau sphérique g_q, et donner quelques propriétés de g_q, indispensables dans le chapitre 4, qui est consacré à la théorie du potentiel sphérique. Finalement dans le chapitre 5 nous retournons aux corps convexes et prouvons entre autres choses les formules (1) et (4), et la caractérisation promise.

Le présent travail a été commencé sur l'invitation de M. B. Jessen. Au cours de son élaboration, de fructueuses conversations avec lui m'ont bien souvent mis sur la voie. Qu'il veuille trouver ici l'expression de ma profonde reconnaissance.

Chapitre 1

CORPS CONVEXES. NOTATION ET RÉSUMÉ

Dans la suite nous allons considérer l'espace euclidien de q dimensions, noté $\mathbf{R}^q$, et nous nous bornerons aux cas $q \geqq 2$.

Deux ensembles vont jouer un rôle dominant:

$$E_q = \{x \in \mathbf{R}^q | \|x\| \leqq 1\}, \text{ la boule unité,}$$

et

$$\Omega_q = \{x \in \mathbf{R}^q | \|x\| = 1\}, \text{ la sphère unité.}$$

Quant à la théorie de la mesure, nous allons nous servir de la termino-logie du traité de N. Bourbaki [4]. On désigne par $\mathcal{M}(\Omega_q)$ (resp. $\mathcal{M}_+(\Omega_q)$) l'espace des mesures de Radon (resp. mesures de Radon positives) sur Ω_q. L'espace $\mathcal{M}(\Omega_q)$ est le dual de $\mathcal{C}(\Omega_q)$, qui est l'espace de Banach des fonc-tions continues $f:\Omega_q \to \mathbf{R}$, muni de la norme de la convergence uniforme

$$\|f\| = \max\{|f(\xi)| \mid \xi \in \Omega_q\}.$$

Dans la suite $\mathcal{M}(\Omega_q)$ est toujours muni de la topologie vague. La mesure de surface ordinaire sur Ω_q est notée ω_q. Elle est invariante par rapport au groupe $O(q)$ des rotations dans $\mathbf{R}^q$, et elle a la masse totale

$$\|\omega_q\| = \frac{2\pi^{\frac{1}{2}q}}{\Gamma(\frac{1}{2}q)}.$$

D'ailleurs elle est uniquement déterminée par ces deux conditions.

Pour une $\mu \in \mathcal{M}_+(\Omega_q)$ et un $p \in [1, \infty]$ l'espace $\mathcal{L}^p(\Omega_q, \mu)$ a le sens or-dinaire. Nous écrivons brièvement $\mathcal{L}^p(\Omega_q)$ pour $\mathcal{L}^p(\Omega_q, \omega_q)$, et nous con-sidérons toujours $\mathcal{L}^1(\Omega_q)$ comme un sous-espace de $\mathcal{M}(\Omega_q)$, en vertu du plongement canonique, qui à une fonction $f \in \mathcal{L}^1(\Omega_q)$ attache la mesure

$$\varphi \mapsto \int_{\Omega_q} f(\xi)\varphi(\xi)d\omega_q(\xi).$$

Un corps convexe K dans $\mathbf{R}^q$ sera un ensemble convexe compact non vide de $\mathbf{R}^q$. L'ensemble $\mathcal{C}_q$ des corps convexes dans $\mathbf{R}^q$ est muni d'une structure algébrique

$$K + L = \{x + y \mid x \in K, y \in L\} \in \mathcal{C}_q, \text{ pour } K, L \in \mathcal{C}_q,$$

$$\lambda K = \{\lambda x \mid x \in K\} \in \mathcal{C}_q, \text{ pour } K \in \mathcal{C}_q, \ \lambda \geqq 0,$$

et muni d'une structure topologique, définie par la distance de Hausdorff

$$D(K, L) = \inf\{\varepsilon > 0 \mid K \subseteq L + \varepsilon E_q, L \subseteq K + \varepsilon E_q\}.$$

Les deux opérations algébriques sont continues comme des applications $\mathcal{C}_q \times \mathcal{C}_q \to \mathcal{C}_q$ et $[0, \infty[\times \mathcal{C}_q \to \mathcal{C}_q$. De plus $\mathcal{C}_q$ est un espace localement compact et complet. D'après H. Minkowski on sait que les polyèdres et les corps convexes lisses forment deux ensembles partout denses dans $\mathcal{C}_q$.

Précisons le mot lisse. Un corps convexe lisse $K \in \mathcal{C}_q$ sera pour nous un corps convexe de dimension q (i.e. d'intérieur non vide), dont la fron-

tière ∂K est une variété différentiable de dimension $q - 1$; pour tout $\xi \in \Omega_q$ l'hyperplan d'appui de K de normale extérieure ξ rencontre K en un seul point $\Phi_K(\xi)$, et l'application Φ_K sera un difféomorphisme $\Omega_q \to \partial K$.

Tout corps convexe $K \in \mathscr{C}_q$ a un volume $V_q(K)$. D'après H. Minkowski il existe une application $V_q\colon \mathscr{C}_q^q \to \mathbf{R}$, qui à q corps convexes $K_1, \cdots, K_q$ attache un nombre $V_q(K_1, \cdots, K_q)$, appelé le volume mixte de $K_1, \cdots, K_q$. L'application V_q est multilinéaire et symétrique, et si tous les corps convexes $K_1, \cdots, K_q$ sont égaux à K, on a $V_q(K, \cdots, K) = V_q(K)$. D'ailleurs il n'est pas difficile de voir que ces trois propriétés déterminent l'application V_q uniquement. Concernant le volume mixte voir [3] p. 38.

Pour tout $K \in \mathscr{C}_q$ on introduit la fonction d'appui $h_K\colon \mathbf{R}^q \to \mathbf{R}$, donnée par la formule

$$h_K(x) = \sup_{y \in K} (x \cdot y),$$

où $x \cdot y$ désigne le produit scalaire de x et y. Toute fonction d'appui h_K vérifie

(a) $\quad h_K(x + y) \leq h_K(x) + h_K(y)$

et

(b) $\quad h_K(\lambda x) = \lambda h_K(x), \qquad$ si $\lambda \geq 0$,

ce qui montre que h_K est convexe, et par conséquent continue. Inversement, toute fonction $\mathbf{R}^q \to \mathbf{R}$ satisfaisant aux conditions (a) et (b) est la fonction d'appui d'un corps convexe et d'un seul.

Grâce à la condition (b), on ne perd pas de l'information en considérant la fonction d'appui seulement sur Ω_q, c'est-à-dire comme élément de l'espace de Banach $\mathscr{C}(\Omega_q)$. Il est bien connu que l'application $\mathscr{C}_q \to \mathscr{C}(\Omega_q)$, donnée par $K \mapsto h_K$, possède les propriétés suivantes:

(i) $\quad K \subseteq L$ si et seulement si $h_K \leq h_L$, pour $K, L \in \mathscr{C}_q$.

(ii) $\quad h_{K+L} = h_K + h_L, \; h_{\lambda K} = \lambda h_K \qquad$, pour $K, L \in \mathscr{C}_q, \lambda \geq 0$.

(iii) $\quad D(K, L) = \|h_K - h_L\| \qquad$, pour $K, L \in \mathscr{C}_q$.

(iv) $\quad h_{\mathrm{conv}(K \cup L)} = \max(h_K, h_L) \qquad$, pour $K, L \in \mathscr{C}_q$.

On en déduit que l'ensemble des fonctions d'appui forme un cône convexe réticulé $\mathscr{H}$ dans $\mathscr{C}(\Omega_q)$, et que $\mathscr{H} - \mathscr{H}$ est un espace de Riesz, qui de plus contient les fonctions constantes et sépare les points de Ω_q. D'après le théorème de Weierstrass-Stone, $\mathscr{H} - \mathscr{H}$ est partout dense dans $\mathscr{C}(\Omega_q)$, c'est-à-dire $\mathscr{H}$ est un cône convexe total de $\mathscr{C}(\Omega_q)$. Cette observation est

très utile, et peut servir à l'introduction des mesures de surface mixtes de $q - 1$ corps convexes dans $\mathbf{R}^q$. Pour nous il suffit de connaître la première mesure de surface $\mu_1(K)$ d'un corps convexe K, définie comme la mesure de surface mixte $\mu(K, E_q, \cdots, E_q)$ de K, et de E_q prise $q - 2$ fois. Cette mesure est caractérisée de la manière suivante:

PROPOSITION 1.1. *Soit $K \in \mathscr{C}_q$. Il existe une mesure positive $\mu_1(K)$ sur Ω_q et une seule telle que, pour tout corps convexe $L \in \mathscr{C}_q$*

$$V_q(L, K, \underbrace{E_q, \cdots, E_q}_{q-2}) = \frac{1}{q} \int_{\Omega_q} h_L(\xi) d\mu_1(K)(\xi).$$

Démonstration: L'unicité résulte de la totalité du cône convexe $\mathscr{H}$ des fonctions d'appui. Pour voir l'existence nous considérons l'application $\mathscr{H} \to \mathbf{R}$, donnée par

$$h_L \mapsto q V_q(L, K, E_q, \cdots, E_q).$$

Elle est linéaire et croissante à cause des propriétés du volume mixte. Cela entraîne que le prolongement par linéarité au sous-espace $\mathscr{H} - \mathscr{H}$ est une forme linéaire positive. Un prolongement par continuité donne la mesure désirée. /

Dans la proposition suivante nous allons résumer les propriétés de la mesure $\mu_1(K)$. Elles se déduisent facilement de ce qui est connu sur le volume mixte (cf. [7] §§ 5, 6).

PROPOSITION 1.2. (i) *La mesure $\mu_1(K)$ est indépendante de translations de K, c'est-à-dire $\mu_1(K + a) = \mu_1(K)$ pour $a \in \mathbf{R}^q$.*

(ii) *La mesure $\mu_1(K)$ admet 0 pour barycentre, c'est-à-dire*

$$\int_{\Omega_q} \xi d\mu_1(K)(\xi) = 0$$

(iii) *L'application $\mu_1 \colon \mathscr{C}_q \to \mathscr{M}_+(\Omega_q)$ est linéaire et continue.*

(iv) *Si K est un corps convexe lisse, la mesure $\mu_1(K)$ possède une densité par rapport à la mesure ω_q, plus précisément*

$$\mu_1(K) = \frac{R_1(\xi) + \cdots + R_{q-1}(\xi)}{q - 1} \omega_q,$$

où $R_1(\xi), \cdots, R_{q-1}(\xi)$ sont les rayons de courbure principaux au point frontière grad $h_K(\xi)$ *de K, où la normale extérieure est ξ.*

De plus pour un corps convexe lisse K, d'après [3] p. 62, on a

$$\Delta_q h_K(\xi) = \sum_{i=1}^{q} \frac{\partial^2 h_K}{\partial x_i^2}(\xi) = R_1(\xi) + \cdots + R_{q-1}(\xi),$$

donc
$$\Delta_q h_K = (q-1)\mu_1(K), \tag{1}$$

où nous avons identifié la mesure et sa densité par rapport à ω_q.

Chapitre 2

SUR LE DÉVELOPPEMENT D'UNE DISTRIBUTION EN SÉRIE DE FONCTIONS SPHÉRIQUES

§ 1. *La théorie des distributions sur Ω_q*

La sphère unité Ω_q est une variété différentiable de dimension $q-1$, possédant une base dénombrable d'ensembles ouverts. Selon [17] on peut introduire les espace vectoriels topologiques fondamentaux de la théorie des distributions, traditionellement notés $\mathscr{D}, \mathscr{D}', \mathscr{E}, \mathscr{E}'$, sur une telle variété. La compacité de Ω_q entraîne que $\mathscr{D} = \mathscr{E}$ et $\mathscr{D}' = \mathscr{E}'$. L'espace vectoriel topologique $\mathscr{D} = \mathscr{D}(\Omega_q)$ est l'ensemble $C^\infty(\Omega_q)$ des fonctions indéfiniment dérivables $\Omega_q \to \mathbf{R}$ muni d'une topologie convenable. Pour la définition de cette topologie et ses propriétés voir [17] § 9; mentionnons seulement que $\mathscr{D}(\Omega_q)$ est un espace de Fréchet.

L'espace dual topologique $\mathscr{D}'(\Omega_q)$ forme l'espace des distributions sur Ω_q. On le munit de la topologie faible de la dualité.

Dans la théorie des distributions de $\mathbf{R}^q$, on utilise fréquemment le produit de convolution, quand il s'agit d'approximer une fonction par une fonction indéfiniment dérivable. On pourrait croire, qu'on allait perdre ce procédé d'approximation ici, parce qu'il est lié à la structure de groupe de $\mathbf{R}^q$. Il y a cependant dans ce cas simple un procédé, qui ressemble au produit de convolution, et qui nous donne des résultats ressemblants à ceux du cas classique $\mathbf{R}^q$.

Soit $(\psi_\varepsilon)_{\varepsilon \in]0,1[}$ une unité approchée dans l'algebre de Banach $\mathscr{L}^1(\mathbf{R}^q)$ telle que

(i) $\psi_\varepsilon \in C^\infty(\mathbf{R}^q)$,

(ii) $\psi_\varepsilon \geq 0$, $\operatorname{supp} \psi_\varepsilon \subseteq \{x \in \mathbf{R}^q \mid \|x\| \leq \varepsilon\}$,

(iii) $\psi_\varepsilon(x) = \psi_\varepsilon(y)$, si $\|x\| = \|y\|$,

(iv) $\int_{\mathbf{R}^q} \psi_\varepsilon(x)dx = 1$.

On définit $\chi_\varepsilon : \Omega_q \times \Omega_q \to \mathbf{R}$ par

$$\chi_\varepsilon(\xi,\eta) = \|\omega_{q-1}\| \int_0^\infty \psi_\varepsilon(\xi - r\eta)r^{q-1}dr.$$

En effet il suffiit de faire l'intégration sur l'intervalle $[0,2]$, parce que si $r \geq 2$ et $\xi, \eta \in \Omega_q$, on a

$$\|\xi - r\eta\| \geq |r - 1| \geq 1.$$

Ceci montre que $\chi_\varepsilon \in C^\infty(\Omega_q \times \Omega_q)$. De plus on a

$$\|\xi - r\eta\|^2 = 1 + r^2 - 2r(\xi \cdot \eta),$$

donc $\chi_\varepsilon(\xi,\eta)$ ne dépend que de $\xi \cdot \eta$. Si $\xi \cdot \eta = t$, nous écrivons

$$\varphi_\varepsilon(t) = \varphi_\varepsilon(\xi \cdot \eta) = \chi_\varepsilon(\xi,\eta) = \|\omega_{q-1}\| \int_0^\infty \psi_\varepsilon(\xi - r\eta)r^{q-1}dr. \tag{1}$$

DÉFINITION: *La famille* $(\varphi_\varepsilon)_{\varepsilon \in]0,1[}$ *est appelée une unité approchée de* Ω_q, *provenue de l'unité approchée* $(\psi_\varepsilon)_{\varepsilon \in]0,1[}$ *de* $\mathscr{L}^1(\mathbf{R}^q)$ *par la formule* (1).

PROPOSITION 2.1. *L'unité approchée* $(\varphi_\varepsilon)_{\varepsilon \in]0,1[}$ *de* Ω_q *possède les propriétés suivantes*:

(i) *Pour tout* $\xi \in \Omega_q$ *la fonction* $\eta \to \varphi_\varepsilon(\xi \cdot \eta)$ *de* Ω_q *dans* $\mathbf{R}$ *est indéfiniment dérivable. De même* $\varphi_\varepsilon : [-1,1] \to \mathbf{R}$ *est indéfiniment dérivable.*

(ii) $\varphi_\varepsilon \geq 0$, $\text{supp } \varphi_\varepsilon \subseteq [(1-\varepsilon^2)^{\frac{1}{2}}, 1]$.

(iii)   *Pour tout* $\xi \in \Omega_q$ *on a*

$$\int_{\Omega_q} \varphi_\varepsilon(\xi \cdot \eta)d\omega_q(\eta) = \|\omega_{q-1}\|,$$

donc

(iv) $\int_{-1}^1 \varphi_\varepsilon(t)(1-t^2)^{\frac{1}{2}(q-3)} dt = 1$.

Démonstration: Remarquons à (ii) que si $\varphi_\varepsilon(\xi \cdot \eta) > 0$, il existe un $r > 0$ tel que $\|\xi - r\eta\| < \varepsilon$, d'où

$$1 + r^2 - 2r(\xi \cdot \eta) < \varepsilon^2.$$

Cela entraîne d'une part que $\xi \cdot \eta \geq 0$, d'autre part que $1 - (\xi \cdot \eta)^2 < \varepsilon^2$, parce que $1 + r^2 - 2r(\xi \cdot \eta)$ a la valeur minimale $1 - (\xi \cdot \eta)^2$. En tout on a $\xi \cdot \eta > (1-\varepsilon^2)^{\frac{1}{2}}$.

La vérification de (iii) est facile:

$$\int_{\Omega_q} \varphi_\varepsilon(\xi \cdot \eta) d\omega_q(\eta) = \|\omega_{q-1}\| \int_{\Omega_q} \left(\int_0^\infty \psi_\varepsilon(\xi - r\eta) r^{q-1} dr \right) d\omega_q(\eta) =$$

$$\|\omega_{q-1}\| \int_{\mathbf{R}^q} \psi_\varepsilon(\xi - x) dx = \|\omega_{q-1}\| \int_{\mathbf{R}^q} \psi_\varepsilon(x) dx = \|\omega_{q-1}\|,$$

et (iv) est une conséquence immédiate de (iii). /

DÉFINITION: *Soit $(\varphi_\varepsilon)_{\varepsilon \in]0,1[}$ une unité approchée de Ω_q comme donnée ci-dessus. Pour $F \in \mathscr{L}^1(\Omega_q)$, $\mu \in \mathscr{M}(\Omega_q)$, $T \in \mathscr{D}'(\Omega_q)$, nous posons pour $\xi \in \Omega_q$*

$$\varphi_\varepsilon * F(\xi) = \frac{1}{\|\omega_{q-1}\|} \int_{\Omega_q} \varphi_\varepsilon(\xi \cdot \eta) F(\eta) d\omega_q(\eta),$$

$$\varphi_\varepsilon * \mu(\xi) = \frac{1}{\|\omega_{q-1}\|} \int_{\Omega_q} \varphi_\varepsilon(\xi \cdot \eta) d\mu(\eta),$$

$$\varphi_\varepsilon * T(\xi) = \frac{1}{\|\omega_{q-1}\|} \underset{\eta}{T}(\varphi_\varepsilon(\xi \cdot \eta)).$$

Alors $\varphi_\varepsilon * X$ est une fonction $\Omega_q \to \mathbf{R}$ appelée le produit de convolution de φ_ε et X, ou la régularisée de X.

Le principe de la régularisation dit que $\varphi_\varepsilon * X$ est indéfiniment dérivable et une bonne approximation à X.

Précisions ce principe par la proposition suivante.

PROPOSITION 2.2. *Soit E un des espaces $\mathscr{D}(\Omega_q)$, $\mathscr{C}(\Omega_q)$, $\mathscr{L}^1(\Omega_q)$. Alors, pour toute $F \in E$, on a $\varphi_\varepsilon * F \in C^\infty(\Omega_q) \subseteq E$ et $\lim_{\varepsilon \to 0} \varphi_\varepsilon * F = F$ dans l'espace E.*

Démonstration: Si $F \in \mathscr{L}^1(\Omega_q)$ on déduit que $\varphi_\varepsilon * F \in C^\infty(\Omega_q)$ à l'aide d'un théorème sur la dérivation sous le signe d'intégration.

(i) *Soit $E = \mathscr{D}(\Omega_q)$.* La démonstration ne se déroule pas, comme on pourrait le croire, par analogie avec la proposition correspondante de $\mathbf{R}^q$. La cause en est qu'on ne peut pas changer les rôles de φ_ε et F comme dans le produit de convolution ordinaire. On se débrouille de la manière suivante. Prolongeons F à toute $\mathbf{R}^q$ en posant

$$F(0) = 0, \quad \text{et} \quad F(x) = F\left(\frac{x}{\|x\|}\right), \text{ si } x \neq 0.$$

Alors $F \in C^\infty(\mathbf{R}^q \setminus \{0\})$. Soit $(\psi_\varepsilon)_{\varepsilon \in]0,1[}$ l'unité approchée de $\mathscr{L}^1(\mathbf{R}^q)$ de laquelle $(\varphi_\varepsilon)_{\varepsilon \in]0,1[}$ provient. Pour le produit de convolution ordinaire

$$\psi_\varepsilon * F(x) = \int\limits_{\mathbf{R}^q} F(y)\psi_\varepsilon(x - y)dy = \int\limits_{\mathbf{R}^q} \psi_\varepsilon(y)F(x - y)dy$$

nous savons que $\psi_\varepsilon * F \in C^\infty(\mathbf{R}^q)$ et $\lim\limits_{\varepsilon \to 0} \psi_\varepsilon * F = F$ dans l'espace $\mathscr{E}(\mathbf{R}^q \setminus \{0\})$, i. e. chacune des dérivées partielles de $\psi_\varepsilon * F$ converge vers la dérivée partielle correspondante de F, uniformément sur tout compact de $\mathbf{R}^q \setminus \{0\}$. Cela entraîne $\lim\limits_{\varepsilon \to 0} \psi_\varepsilon * F = F$ dans l'espace $\mathscr{D}(\Omega_q)$. Calculons maintenant $\psi_\varepsilon * F(\xi)$ pour un $\xi \in \Omega_q$:

$$\psi_\varepsilon * F(\xi) = \int\limits_{\mathbf{R}^q} F(y)\psi_\varepsilon(\xi - y)dy = \int\limits_{\Omega_q}\left(\int\limits_0^\infty F(r\eta)\psi_\varepsilon(\xi - r\eta)r^{q-1}dr\right)d\omega_q(\eta)$$

$$= \frac{1}{\|\omega_{q-1}\|}\int\limits_{\Omega_q} F(\eta)\varphi_\varepsilon(\xi \cdot \eta)d\omega_q(\eta) = \varphi_\varepsilon * F(\xi),$$

d'après la formule (1).

(ii) *Soit* $E = \mathscr{C}(\Omega_q)$. En vertu de la formule

$$|F(\xi) - \varphi_\varepsilon * F(\xi)| \leq \frac{1}{\|\omega_{q-1}\|}\int\limits_{\Omega_q} \varphi_\varepsilon(\xi \cdot \eta)|F(\xi) - F(\eta)|d\omega_q(\eta),$$

nous concluons à l'aide de la continuité uniforme de F que $\varphi_\varepsilon * F(\xi) \to F(\xi)$, uniformément sur Ω_q pour $\varepsilon \to 0$.

Par conséquent nous avons aussi $\lim\limits_{\varepsilon \to 0} \varphi_\varepsilon * F = F$ dans $\mathscr{L}^1(\Omega_q)$.

(iii) *Soit* $E = \mathscr{L}^1(\Omega_q)$. Grâce au théorème de Fubini, on a pour tout $\varepsilon \in]0,1[$

$$\|\varphi_\varepsilon * F\|_1 \leq \|F\|_1.$$

Pour $\delta > 0$ donné on choisit $G \in \mathscr{C}(\Omega_q)$ telle que $\|F - G\|_1 < \frac{1}{3}\delta$. Donc

$$\|F - \varphi_\varepsilon * F\|_1 \leq \frac{2}{3}\delta + \|G - \varphi_\varepsilon * G\|_1 < \delta,$$

dès que ε est suffisamment petit. /

De cette proposition résulte que $\mathscr{D}(\Omega_q)$ est partout dense dans $\mathscr{C}(\Omega_q)$, ce qui nous permet de considérer les mesures $\mathscr{M}(\Omega_q)$ comme un sous-espace

des distributions $\mathscr{D}'(\Omega_q)$. Par conséquent on a les plongements $\mathscr{L}^1(\Omega_q)$ $\subseteq \mathscr{M}(\Omega_q) \subseteq \mathscr{D}'(\Omega_q)$. Une fonction $f \in \mathscr{L}^1(\Omega_q)$ s'identifie avec la distribution

$$\varphi \;\longmapsto\; \int_{\Omega_q} f(\xi)\varphi(\xi)d\omega_q(\xi).$$

On remarque que les trois définitions de la régularisée sont compatibles avec ces plongements.

Une distribution $T \in \mathscr{D}'(\Omega_q)$ est dite positive, si pour toute $\varphi \in \mathscr{D}(\Omega_q)$, $\varphi \geqq 0$, on a $T(\varphi) \geqq 0$.

PROPOSITION 2.3. *Après le plongement* $\mathscr{M}(\Omega_q) \subseteq \mathscr{D}'(\Omega_q)$ *il y a identité entre les mesures positives* $\mathscr{M}_+(\Omega_q)$ *et les distributions positives* $\mathscr{D}'_+(\Omega_q)$.

Démonstration: Trivialement $\mathscr{M}_+(\Omega_q) \subseteq \mathscr{D}_+(\Omega_q)$. Inversement, soient T une distribution positive, $\varphi \in \mathscr{D}(\Omega_q)$. Puisque

$$- \|\varphi\| \;\leqq\; \varphi \;\leqq\; \|\varphi\|,$$

on a

$$- \|\varphi\|T(1) \;\leqq\; T(\varphi) \;\leqq\; \|\varphi\|T(1),$$

donc

$$|T(\varphi)| \;\leqq\; \|\varphi\|T(1).$$

Il en découle que T est continue sur $\mathscr{D}(\Omega_q)$ muni de la topologie induite par celle de $\mathscr{C}(\Omega_q)$. Alors T se prolonge uniquement par continuité en une mesure sur Ω_q, encore notée T, et T est une mesure positive, car si $\varphi \in \mathscr{C}(\Omega_q)$, $\varphi \geqq 0$, on a

$$\varphi_\varepsilon * \varphi \in \mathscr{D}(\Omega_q), \qquad \varphi_\varepsilon * \varphi \geqq 0,$$

donc

$$T(\varphi_\varepsilon * \varphi) \;\geqq\; 0.$$

Faisons $\varepsilon \to 0$, d'après la proposition 2.2 $\varphi_\varepsilon * \varphi \to \varphi$ dans l'espace $\mathscr{C}(\Omega_q)$, d'où

$$T(\varphi_\varepsilon * \varphi) \;\to\; T(\varphi),$$

et par suite

$$T(\varphi) \;\geqq\; 0. \;/$$

Nous allons utiliser le produit tensoriel de distributions. Pour les détails voir [17] théorèmes 9, 10; citons seulement la proposition suivante.

PROPOSITION 2.4. *Soient* $S, T \in \mathscr{D}'(\Omega_q)$, $\varphi \in C^\infty(\Omega_q \times \Omega_q)$. *Les applications* $\xi \longmapsto T(\varphi(\xi,\eta))$ *et* $\eta \longmapsto S(\varphi(\xi,\eta))$ *sont indéfiniment dérivables sur* Ω_q. *De plus*

$$S_\xi(T_\eta(\varphi(\xi,\eta))) = T_\eta(S_\xi(\varphi(\xi,\eta))). \tag{2}$$

Cette formule détermine une distribution sur $\Omega_q \times \Omega_q$, appelée le produit tensoriel de S et T, et elle est notée $S \times T$.

Voici un autre exemple du principe de la régularisation :

PROPOSITION 2.5. *Soit $T \in \mathscr{D}'(\Omega_q)$. Alors $\varphi_\varepsilon * T \in C^\infty(\Omega_q)$, et $\lim_{\varepsilon \to 0} \varphi_\varepsilon * T = T$ dans $\mathscr{D}'(\Omega_q)$, i.e. faiblement au sens des distributions.*

Démonstration : La proposition 2.4 montre que $\varphi_\varepsilon * T \in C^\infty(\Omega_q)$. La fonction $\xi \to 1$ est une distribution, et une application de la formule (2) au produit tensoriel $1 \times T$ et à la fonction $(\xi,\eta) \mapsto \varphi_\varepsilon(\xi \cdot \eta)\varphi(\xi)$, où $\varphi \in \mathscr{D}(\Omega_q)$, donne

$$\int_{\Omega_q} T_\eta(\varphi_\varepsilon(\xi \cdot \eta)\varphi(\xi))d\omega_q(\xi) = T_\eta\Big(\int_{\Omega_q} \varphi_\varepsilon(\xi \cdot \eta)\varphi(\xi)d\omega_q(\xi)\Big),$$

d'où

$$\int_{\Omega_q} \varphi(\xi)\varphi_\varepsilon * T(\xi)d\omega_q(\xi) = T_\eta(\varphi_\varepsilon * \varphi(\eta)).$$

Si nous interprétons $\varphi_\varepsilon * T$ comme distribution, nous venons de voir que

$$\varphi_\varepsilon * T(\varphi) = T(\varphi_\varepsilon * \varphi).$$

Si $\varepsilon \to 0$, il résulte de la proposition 2.2 que

$$\varphi_\varepsilon * T(\varphi) \to T(\varphi),$$

valable pour toute $\varphi \in \mathscr{D}(\Omega_q)$. |

§ 2. L'opérateur $\varDelta_q^*$ de Laplace-Beltrami sur Ω_q

Dans le suivant $\varDelta_q^*$ désigne l'opérateur de Laplace-Beltrami sur Ω_q (cf. [11] p. 387), et $\varDelta_q$ désigne le laplacien ordinaire dans q variables. Résumons quelques faits, nécessaires pour ce qui suit.

PROPOSITION 2.6. *Si $x \in \mathbf{R}^q \setminus \{0\}$, on pose $x = r\xi$, où $r = \|x\| \in]0, \infty[$ et $\xi = x/\|x\| \in \Omega_q$. Alors on a*

$$\varDelta_q = \frac{\partial^2}{\partial r^2} + \frac{q-1}{r}\frac{\partial}{\partial r} + \frac{1}{r^2}\varDelta_q^*. \tag{3}$$

Si $a \in \Omega_q$, on pose $\Omega_{q-1} = \{\eta \in \Omega_q \mid a \cdot \eta = 0\}$, *et on obtient la description paramétrique suivante de $\Omega_q \setminus \{a, -a\}$:*

$$\xi = ta + (1 - t^2)^{\frac{1}{2}}\eta, \quad o\grave{u} \quad t \in \,]-1,1[, \eta \in \Omega_{q-1}.$$

Alors on a (si $q \geq 3$)

$$\Delta_q^* = (1 - t^2)\frac{\partial^2}{\partial t^2} - (q-1)t\frac{\partial}{\partial t} + \frac{1}{1-t^2}\Delta_{q-1}^*. \tag{4}$$

Pour toutes $\varphi,\psi \in C^2(\Omega_q)$, on a

$$\int_{\Omega_q} \varphi(\xi)\Delta_q^*\psi(\xi)d\omega_q(\xi) = \int_{\Omega_q} \Delta_q^*\varphi(\xi)\psi(\xi)d\omega_q(\xi). \tag{5}$$

Pour tout $A \in O(q)$ et toute $\varphi \in C^2(\Omega_q)$, on a

$$\Delta_q^*(\varphi \circ A) = (\Delta_q^*\varphi) \circ A. \tag{6}$$

Démonstration: Les formules (3), (4) résultent de l'expression dans des coordonnées locales de Δ_q^* (cf. [15] p. 38), et (5), (6) sont des cas particuliers d'un théorème général sur les variétés de Riemann (cf. [11] p. 387). Nous allons obtenir (5) comme corrollaire du théorème 4.3. /

Soit h_K la fonction d'appui d'un corps convexe lisse K. Puisque pour $r > 0$, $\xi \in \Omega_q$,

$$h_K(r\xi) = rh_K(\xi),$$

la formule (3) donne

$$\Delta_q h_K(r\xi) = \frac{q-1}{r}h_K(\xi) + \frac{1}{r}\Delta_q^* h_K(\xi).$$

Si $r = 1$, on a

$$\Delta_q h_K(\xi) = \{\Delta_q^* + (q-1)\}h_K(\xi), \quad \text{pour} \quad \xi \in \Omega_q. \tag{7}$$

D'après (1) chapitre 1 nous avons

$$\left\{\frac{1}{q-1}\Delta_q^* + 1\right\}h_K = \mu_1(K). \tag{8}$$

Pour des raisons de commodité nous posons

$$D_q^* = \frac{1}{q-1}\Delta_q^* + 1, \tag{9}$$

donc, pour tout corps convexe lisse K, on a

$$D_q^* h_K = \mu_1(K). \tag{10}$$

L'opérateur $\varDelta_q^*$ est une application linéaire continue $\mathscr{D}(\Omega_q) \to \mathscr{D}(\Omega_q)$. La continuité résulte des faits que $\varDelta_q^*$ applique un ensemble borné de $\mathscr{D}(\Omega_q)$ sur un ensemble borné, et que $\mathscr{D}(\Omega_q)$ est un espace de Fréchet et par conséquent bornologique. L'application ${}^t\varDelta_q^*$, transposée de $\varDelta_q^*$, est alors une application linéaire continue $\mathscr{D}'(\Omega_q) \to \mathscr{D}'(\Omega_q)$, donnée par

$$ {}^t\varDelta_q^* T(\psi) = T(\varDelta_q^*\psi), \quad \text{pour des } T \in \mathscr{D}'(\Omega_q), \psi \in \mathscr{D}(\Omega_q). $$

Pour une $\varphi \in \mathscr{D}(\Omega_q)$ considérée comme distribution, on a pour toute $\psi \in \mathscr{D}(\Omega_q)$

$$ {}^t\varDelta_q^*\varphi(\psi) = \varphi(\varDelta_q^*\psi) = \int_{\Omega_q} \varphi(\xi)\varDelta_q^*\psi(\xi)d\omega_q(\xi) = \int_{\Omega_q} \varDelta_q^*\varphi(\xi)\psi(\xi)d\omega_q(\xi) = \varDelta_q^*\varphi(\psi). $$

Donc, l'application ${}^t\varDelta_q^*$ est une extension de $\varDelta_q^*$ de $\mathscr{D}(\Omega_q)$ à $\mathscr{D}'(\Omega_q)$. Dorénavant nous considérons toujours l'opérateur de Laplace-Beltrami $\varDelta_q^*$ comme un opérateur dans l'espace $\mathscr{D}'(\Omega_q)$. Ces observations sont valables aussi pour l'opérateur $D_q^* = \dfrac{1}{q-1}\varDelta_q^* + 1$. Remarquons de plus que (5), (6) subsistent encore, si $\varDelta_q^*$ est remplacé par D_q^*.

§3. Le produit de convolution

La fonction régularisée $\varphi_\varepsilon * X$ de § 1 est un produit de convolution. Dans ce paragraphe nous allons considérer des produits de convolution $F * G$ plus généraux. Sur l'intervalle $[-1,1]$ nous considérons la mesure $(1-t^2)^{\frac{1}{2}(q-3)}dt$, $q \geq 2$, qui donne les espaces

$$ \mathscr{L}^p([-1,1],(1-t^2)^{\frac{1}{2}(q-3)}dt) = \mathscr{L}^p([-1,1],q) $$

pour $p \in [1, \infty]$. Nous posons $\bar{\mathbf{R}} = \mathbf{R} \cup \{-\infty,\infty\}$.

PROPOSITION 2.7. *Soit $f: [-1,1] \to \bar{\mathbf{R}}$ une fonction borélienne appartenant à $\mathscr{L}^1([-1,1],q)$, et soit ξ un point de Ω_q. Alors la fonction $f(\xi\cdot): \Omega_q \to \bar{\mathbf{R}}$ donnée par $\eta \mapsto f(\xi\cdot\eta)$ est borélienne et appartient à $\mathscr{L}^1(\Omega_q)$. De plus*

$$ \frac{1}{\|\omega_{q-1}\|} \int_{\Omega_q} f(\xi\cdot\eta)d\omega_q(\eta) = \int_{-1}^{1} f(t)(1-t^2)^{\frac{1}{2}(q-3)}\,dt, $$

et l'application $\Omega_q \to \mathscr{L}^1(\Omega_q)$ donnée par $\xi \mapsto f(\xi\cdot)$ est continue.

Démonstration: L'application $\eta \mapsto f(\xi\cdot\eta)$ est trivialement borélienne. Alors

$$\frac{1}{\|\omega_{q-1}\|}\int_{\Omega_q}|f(\xi\cdot\eta)|d\omega_q(\eta) = \int_{-1}^{1}|f(t)|(1-t^2)^{\frac{1}{2}(q-3)}\,dt < \infty,$$

d'où $f(\xi\cdot\,)\in\mathscr{L}^1(\Omega_q)$, et on voit que la formule donnée est valable. La continuité de l'application $\xi\mapsto f(\xi\cdot\,)$ se déduit ainsi: Soit $\varepsilon > 0$. On choisit une $g\in\mathscr{C}([0,1])$ telle que

$$\|\omega_{q-1}\|\int_{-1}^{1}|f(t)-g(t)|(1-t^2)^{\frac{1}{2}(q-3)}\,dt < \tfrac{1}{3}\varepsilon.$$

Alors

$$\|f(\xi\cdot\,)-f(\zeta\cdot\,)\|_1 < \tfrac{2}{3}\varepsilon + \|g(\xi\cdot\,)-g(\zeta\cdot)\|_1 < \varepsilon,$$

dès que ζ est suffisamment voisin à ξ, en vertu de la continuité uniforme de g. $/$

DÉFINITION DU PRODUIT DE CONVOLUTION. *Soient f une fonction borélienne de $\mathscr{L}^1([-1,1],q)$, $\mu\in\mathscr{M}(\Omega_q)$. Nous posons*

$$f*\mu(\xi) = \frac{1}{\|\omega_{q-1}\|}\int_{\Omega_q}f(\xi\cdot\eta)d\mu(\eta).$$

Si $F\in\mathscr{L}^1(\Omega_q)$ nous avons identifié F et la mesure $Fd\omega_q$, et nous écrivons simplement $f*F$ au lieu de $f*Fd\omega_q$, i.e.

$$f*F(\xi) = \frac{1}{\|\omega_{q-1}\|}\int_{\Omega_q}f(\xi\cdot\eta)F(\eta)d\omega_q(\eta).$$

Soient $\varphi\in C^\infty([-1,1])$, $T\in\mathscr{D}'(\Omega_q)$; nous posons

$$\varphi*T(\xi) = \frac{1}{\|\omega_{q-1}\|}\,T_\eta(\varphi(\xi\cdot\eta)).$$

PROPOSITION 2.8. *Par la notation ci-dessus $f*\mu$ est définie ω_q-presque partout et appartient à $\mathscr{L}^1(\Omega_q)$, et $\varphi*T$ appartient à $C^\infty(\Omega_q)$.*

Démonstration: L'application $(\xi,\eta)\mapsto f(\xi\cdot\eta)$ est trivialement borélienne. Grâce au théorème de Fubini on a

$$\int\limits_{\Omega_q \times \Omega_q} |f(\xi \cdot \eta)| d\omega_q \times |\mu|(\xi,\eta) = \int\limits_{\Omega_q} \left(\int\limits_{\Omega_q} |f(\xi \cdot \eta)| d\omega_q(\xi) \right) d|\mu|(\eta)$$

$$= \|\omega_{q-1}\| \int\limits_{\Omega_q} \left(\int\limits_{-1}^{1} |f(t)| (1-t^2)^{\frac{1}{2}(q-3)} \, dt \right) d|\mu|(\eta) = \|\omega_{q-1}\| \, \|\mu\| \int\limits_{-}^{1} |f(t)| (1-t^2)^{\frac{1}{2}(q-3)} \, dt < \infty,$$

d'où $f(\xi \cdot \eta) \in \mathcal{L}^1(\Omega_q \times \Omega_q, \omega_q \times |\mu|)$, ce qui entraîne l'assertion. Que $\varphi * T \in C^\infty(\Omega_q)$, résulte de la proposition 2.4. /

PROPOSITION 2.9. *Soient f une fonction borélienne de $\mathcal{L}^1([-1,1],q)$, $F \in \mathcal{L}^\infty(\Omega_q)$. Alors $f * F$ est partout définie, et elle est continue.*

Démonstration: Pour tout $\xi \in \Omega_q$ on a

$$\frac{1}{\|\omega_{q-1}\|} \int\limits_{\Omega_q} |f(\xi \cdot \eta) F(\eta)| d\omega_q(\eta) \leq \|F\|_\infty \int\limits_{-1}^{1} |f(t)|(1-t^2)^{\frac{1}{2}(q-3)} \, dt < \infty,$$

et par conséquent $f * F$ est partout définie. La continuité résulte de la proposition 2.7, parce que

$$|f * F(\xi) - f * F(\zeta)| \leq \frac{\|F\|_\infty}{\|\omega_{q-1}\|} \|f(\xi \cdot \,) - f(\zeta \cdot \,)\|_1. /$$

Qu'on remarque que la proposition subsiste encore, si f est une fonction borélienne de $\mathcal{L}^\alpha([-1,1],q)$, et $F \in \mathcal{L}^\beta(\Omega_q)$, où $1 \leq \alpha, \beta \leq \infty$; $\alpha^{-1} + \beta^{-1} = 1$.

§4. Développements en séries de polynômes de Legendre dans q dimensions, et de fonctions sphériques

Un exposé court et élégant de la théorie des fonctions sphériques et des polynômes de Legendre dans q dimensions se trouve dans [15]. Nous allons en utiliser la notation et les théorèmes.

Une fonction sphérique d'ordre n dans q dimensions est par définition un polynôme homogène harmonique de degré n à q variables $x_1, \cdots, x_q$. On la considère comme fonction sur Ω_q. L'ensemble des fonctions sphériques d'ordre n et la fonction $\xi \mapsto 0$ forment un espace vectoriel de dimension finie de fonctions $\Omega_q \to \mathbf{R}$. Il est noté H_n, et sa dimension est notée $N(q,n)$ (cf. [15] p. 2–4). Les espaces H_n, $n = 0,1,\cdots$, sont orthogonaux entre eux dans l'espace de Hilbert $\mathcal{L}^2(\Omega_q)$, et leur somme hilbertienne est égale à

$\mathscr{L}^2(\Omega_q)$. Si S_i, $i = 1, \cdots, N(q,n)$ forment une base orthonormale de H_n, la fonction

$$F_n(\xi, \eta) = \sum_{i=1}^{N(q,n)} S_i(\xi)S_i(\eta)$$

ne dépend pas de la base choisie; elle est appelée le noyau réproductif de l'espace H_n. Son importance est la suivante: Si $f \in \mathscr{L}^2(\Omega_q)$, et si f_n est la projection de f sur H_n, alors $f = \sum_{n=0}^{\infty} f_n$ dans l'espace $\mathscr{L}^2(\Omega_q)$, et f_n se calcule

$$f_n(\xi) = \int_{\Omega_q} F_n(\xi, \eta)f(\eta)d\omega_q(\eta).$$

La série $\sum_{n=0}^{\infty} f_n$ est appelée le développement de f en série de fonctions sphériques. Avant d'étendre ce développement aux distributions, il nous faut connaître le noyau réproductif F_n.

Les polynômes de Legendre dans q dimensions seront notés $p_n(q,t)$; ils sont des polynômes de degré $n = 0, 1, \cdots$ dans le variable t caractérisés par les conditions

$$\int_{-1}^{1} p_n(q,t)p_m(q,t)(1 - t^2)^{\frac{1}{2}(q-3)} \, dt = 0 \quad \text{si} \quad n \neq m,$$

$$p_n(q,1) = 1 \quad \text{pour} \quad n = 0, 1, \cdots. \tag{11}$$

De plus on a (cf. [15] p. 15)

$$\int_{-1}^{1} p_n^2(q,t)(1 - t^2)^{\frac{1}{2}(q-3)} \, dt = \frac{\|\omega_q\|}{\|\omega_{q-1}\| N(q,n)}. \tag{12}$$

Ils sont aussi appelés les polynômes ultrasphériques. Si $q = 3$ on obtient les polynômes classiques de Legendre, et on sait que $p_n(2,t) = \cos(n \operatorname{Arc-cos} t)$ pour $t \in [-1,1]$ sont les polynômes de Čebyčev.

De la formule (11) on tire

$$p_0(q,t) = 1, \quad p_1(q,t) = t,$$

$$p_2(q,t) = \frac{q}{q-1} t^2 - \frac{1}{q-1}, \quad p_3(q,t) = \frac{q+2}{q-1} t^3 - \frac{3}{q-1} t. \tag{13}$$

D'après (11), (12) le système

$$\left(\frac{\|\omega_{q-1}\| N(q,n)}{\|\omega_q\|} \right)^{\frac{1}{2}} p_n(q,t), \quad n = 0, 1, \cdots,$$

est une base orthonormale dans l'espace de Hilbert $\mathscr{L}^2([-1,1],q)$.

2*

$\grave{A}$ *une fonction* $f \in \mathscr{L}^1([-1,1], q)$ *on attache la série*

$$f \sim \sum_{n=0}^{\infty} \frac{\|\omega_{q-1}\| N(q,n)}{\|\omega_q\|} a_n p_n(q,t), \tag{14}$$

où

$$a_n = \int_{-1}^{1} f(t) p_n(q,t)(1-t^2)^{\frac{1}{2}(q-3)} dt,$$

appelée le développement de f en série de polynómes de Legendre dans q dimensions.

Le noyau réproductif F_n a une liaison étroite avec $p_n(q,t)$. Puisqu'il est très important, nous citons ce résultat.

THÉORÈME 2.10. (*Le théorème d'addition de G. Herglotz.*) *Le noyau réproductif* F_n *de l'espace* H_n *des fonctions sphériques d'ordre n est donné par*

$$F_n(\xi, \eta) = \frac{N(q,n)}{\|\omega_q\|} p_n(q, \xi \cdot \eta).$$

Pour la démonstration voir [15] p. 9. Il est important de remarquer qu'il en découle:

Pour un $\eta \in \Omega_q$ fixé, l'application $\xi \longmapsto p_n(q, \xi \cdot \eta)$ est une fonction sphérique d'ordre n.

Citons aussi:

THÉORÈME 2.11. (*P. Funk, E. Hecke.*) *Soient f une fonction borélienne de* $\mathscr{L}^1([-1,1], q)$ *et* $S \in H_n$. *Alors*

$$\int_{\Omega_q} f(\xi \cdot \eta) S(\eta) d\omega_q(\eta) = \lambda S(\xi),$$

où

$$\lambda = \|\omega_{q-1}\| \int_{-1}^{1} f(t) p_n(q,t)(1-t^2)^{\frac{1}{2}(q-3)} dt.$$

Le théorème est démontré dans [15] p. 18, mais sous la condition f continue. Cependant, une revue de la démonstration montre qu'on utilise essentiellement les conditions ci-dessus, et la proposition 2.7.

$\grave{A}$ *une* $F \in \mathscr{L}^1(\Omega_q)$ *on attache la série*

$$F \sim \sum_{n=0}^{\infty} S_n, \tag{15}$$

où

$$S_n(\xi) = \frac{N(q,n)}{\|\omega_q\|} \int_{\Omega_q} p_n(q, \xi \cdot \eta) F(\eta) d\omega_q(\eta) = \frac{\|\omega_{q-1}\| N(q,n)}{\|\omega_q\|} p_n(q, \ ) * F(\xi),$$

et à une distribution $T \in \mathcal{D}'(\Omega_q)$ on attache la série

$$T \sim \sum_{n=0}^{\infty} S_n, \tag{16}$$

où

$$S_n(\xi) = \frac{N(q,n)}{\|\omega_q\|} T_\eta(p_n(q, \xi \cdot \eta)) = \frac{\|\omega_{q-1}\| N(q,n)}{\|\omega_q\|} p_n(q, \ ) * T(\xi).$$

Les séries sont appelées les développements en séries de fonctions sphériques.

D'après 2.10 S_n est zéro ou une fonction sphérique d'ordre n. Les deux définitions sont compatibles avec le plongement $\mathcal{L}^1(\Omega_q) \subseteq \mathcal{D}'(\Omega_q)$.

Le théorème suivant montre que le produit de convolution est important en relation avec les développements.

THÉORÈME 2.12. (i) *Soit f une fonction borélienne de $\mathcal{L}^1([-1,1], q)$, et posons $F(\xi) = f(a \cdot \xi)$ pour un $a \in \Omega_q$. (Donc $F \in \mathcal{L}^1(\Omega_q)$.) Pour les développements*

$$f \sim \sum_{n=0}^{\infty} \frac{\|\omega_{q-1}\| N(q,n)}{\|\omega_q\|} a_n p_n(q,t) \quad et \quad F \sim \sum_{n=0}^{\infty} S_n,$$

on a

$$S_n(\xi) = \frac{\|\omega_{q-1}\| N(q,n)}{\|\omega_q\|} a_n p_n(q, a \cdot \xi).$$

(ii) *Soient $\varphi \in C^{\infty}([-1,1])$ et $T \in \mathcal{D}'(\Omega_q)$ avec les développements*

$$\varphi \sim \sum_{n=0}^{\infty} \frac{\|\omega_{q-1}\| N(q,n)}{\|\omega_q\|} a_n p_n(q,t) \quad et \quad T \sim \sum_{n=0}^{\infty} S_n.$$

Alors $\varphi * T$ a le développement

$$\varphi * T \sim \sum_{n=0}^{\infty} a_n S_n.$$

(iii) *Soient f une fonction borélienne de $\mathcal{L}^1([-1,1], q)$ et $\mu \in \mathcal{M}(\Omega_q)$ avec les développements*

$$f \sim \sum_{n=0}^{\infty} \frac{\|\omega_{q-1}\| N(q,n)}{\|\omega_q\|} a_n p_n(q,t) \quad et \quad \mu \sim \sum_{n=0}^{\infty} S_n.$$

Alors $f * \mu$ a le développement

$$f * \mu \sim \sum_{n=0}^{\infty} a_n S_n.$$

Démonstration: (i) Nous avons

$$S_n(\xi) = \frac{N(q,n)}{\|\omega_q\|} \int_{\Omega_q} p_n(q, \xi \cdot \eta) f(a \cdot \eta) d\omega_q(\eta)$$

$$= p_n(q, a \cdot \xi) \frac{\|\omega_{q-1}\| N(q,n)}{\|\omega_q\|} \int_{-1}^{1} f(t) p_n(q,t) (1 - t^2)^{\frac{1}{2}(q-3)} dt$$

$$= \frac{\|\omega_{q-1}\| N(q,n)}{\|\omega_q\|} a_n p_n(q, a \cdot \xi).$$

Nous nous sommes servis du fait que pour un ξ fixe, l'application $\eta \longmapsto p_n(q, \xi \cdot \eta)$ est une fonction sphérique, et ensuite nous avons utilisé le théorème 2.11.

(ii) La valeur en $\xi \in \Omega_q$ du terme n-ième du développement de $\varphi * T$ est

$$\frac{N(q,n)}{\|\omega_q\|} \int_{\Omega_q} p_n(q, \xi \cdot \eta) \varphi * T(\eta) d\omega_q(\eta) = \frac{N(q,n)}{\|\omega_q\| \|\omega_{q-1}\|} \int_{\Omega_q} p_n(q, \xi \cdot \eta) \underset{\sigma}{T} (\varphi(\eta \cdot \sigma)) d\omega_q(\eta)$$

$$= \frac{N(q,n)}{\|\omega_q\| \|\omega_{q-1}\|} \underset{\sigma}{T} \left\{ \int_{\Omega_q} \varphi(\eta \cdot \sigma) p_n(q, \xi \cdot \eta) d\omega_q(\eta) \right\}$$

$$= \frac{N(q,n)}{\|\omega_q\| \|\omega_{q-1}\|} \underset{\sigma}{T} \{ \|\omega_{q-1}\| a_n p_n(q, \xi \cdot \sigma) \} = a_n S_n(\xi),$$

en vertu de la proposition 2.4 et le théorème 2.11.

(iii) La démonstration de (iii) est égale à celle de (ii), excepté que le «théorème de Fubini» 2.4 est remplacé par le théorème de Fubini proprement dit.

COROLLAIRE 2.13. (i) *Si deux distributions* T_1, $T_2 \in \mathscr{D}'(\Omega_q)$ *ont le même développement en série de fonctions sphériques, on a* $T_1 = T_2$.

(ii) *Si deux fonctions boréliennes* f_1, f_2 *de* $\mathscr{L}^1([-1,1], q)$ *ont le même*

développement en série de polynômes de Legendre dans q dimensions, on a $f_1 = f_2$ dans $\mathscr{L}^1([-1,1], q)$, donc $f_1 = f_2$ presque partout.

Démonstration: (i) Dans ce cas la distribution $T = T_1 - T_2$ a le développement $\sum_{n=0}^{\infty} 0$. Soit $(\varphi_\varepsilon)_{\varepsilon \in \,]0,1[}$ une unité approchée de Ω_q, alors $\varphi_\varepsilon * T \in C^\infty(\Omega_q)$, et d'après le théorème précédent $\varphi_\varepsilon * T$ a également le développement $\sum_{n=0}^{\infty} 0$. Cependant, nous savons qu'une fonction de $\mathscr{L}^2(\Omega_q)$ est 0 presque partout si son développement est $\sum_{n=0}^{\infty} 0$. Par conséquent $\varphi_\varepsilon * T = 0$, ce qui entraîne $T = 0$, parce que $\lim_{\varepsilon \to 0} \varphi_\varepsilon * T = T$ dans $\mathscr{D}'(\Omega_q)$.

(ii) Choisissons $a \in \Omega_q$, et posons $F(\xi) = f(a \cdot \xi)$, où $f = f_1 - f_2$. D'après le théorème précédent F a le développement $\sum_{n=0}^{\infty} 0$, donc d'après (i) $F = 0$ ω_q-presque partout, ce qui entraîne $f_1 = f_2$ dans $\mathscr{L}^1([-1,1], q)$. |

Soit S_n une fonction sphérique d'ordre n dans q dimensions. Alors pour $\lambda > 0$, $\xi \in \Omega_q$ on a

$$S_n(\lambda \xi) = \lambda^n S_n(\xi).$$

De plus on sait que $\Delta_q S_n = 0$. D'après 2.6 formule (3) il résulte que

$$\Delta_q^* S_n(\xi) = -n(n+q-2)S_n(\xi), \quad D_q^* S_n(\xi) = -\frac{(n-1)(n+q-1)}{q-1}S_n(\xi). \quad (17)$$

En particulier

$$D_{\eta}^* p_n(q, \xi \cdot \eta) = -\frac{(n-1)(n+q-1)}{q-1}p_n(q, \xi \cdot \eta). \quad (18)$$

THÉORÈME 2.14. *Soit $T \in \mathscr{D}'(\Omega_q)$ avec le développement $T \sim \sum_{n=0}^{\infty} S_n$ en série de fonctions sphériques. Alors la distribution $D_q^* T$ a le développement*

$$D_q^* T \sim \sum_{n=0}^{\infty} -\frac{(n-1)(n+q-1)}{q-1}S_n.$$

Démonstration: On calcule

$$\frac{N(q,n)}{\|\omega_q\|} \underbrace{D_q^* T}_{\eta}(p_n(q, \xi \cdot \eta)) = \frac{N(q,n)}{\|\omega_q\|} \underset{\eta}{T}(D_{\eta}^* p_n(q, \xi \cdot \eta))$$

$$= -\frac{(n-1)(n+q-1)}{q-1}\frac{N(q,n)}{\|\omega_q\|}\underset{\eta}{T}(p_n(q, \xi \cdot \eta)),$$

ce qui montre l'assertion. |

Puisque

$$\frac{(n-1)(n+q-1)}{q-1} = 0$$

équivaut à $n = 1$ lorsque $n \geq 0$, on conclut:

COROLLAIRE 2.15. *Le noyau de l'opérateur* $D_q^*\colon \mathscr{D}'(\Omega_q) \to \mathscr{D}'(\Omega_q)$ *est* H_1,*i.e. l'ensemble des fonctions* $\{\xi \mapsto a \cdot \xi \,|\, a \in \mathbf{R}^q\}$.

Chapitre 3
LE NOYAU SPHÉRIQUE g_q

§ 1. L'existence du noyau sphérique g_q

Soit $K \in \mathscr{C}_q$ un corps convexe lisse. D'après (10) chapitre 2, nous savons que pour un $\xi \in \Omega_q$

$$D_q^* h_K(\xi) = \frac{R_1 + \cdots + R_{q-1}}{q-1}(\xi). \tag{1}$$

Nous cherchons une fonction borélienne g_q de $\mathscr{L}^1([-1,1],q)$ telle que

$$g_q * \frac{R_1 + \cdots + R_{q-1}}{q-1} = h_K. \tag{2}$$

Supposons qu'elle existe, et posons

$$h_K \sim \sum_{n=0}^{\infty} S_n,$$

$$g_q \sim \sum_{n=0}^{\infty} \frac{\|\omega_{q-1}\| N(q,n)}{\|\omega_q\|} a_n p_n(q,t).$$

Selon (1) et le théorème 2.14 nous avons

$$\frac{R_1 + \cdots + R_{q-1}}{q-1} \sim S_0 - \sum_{n=2}^{\infty} \frac{(n-1)(n+q-1)}{q-1} S_n,$$

et par conséquent en vertu du théorème 2.12

$$g_q * \frac{R_1 + \cdots + R_{q-1}}{q-1} \sim a_0 S_0 - \sum_{n=2}^{\infty} \frac{(n-1)(n+q-1)}{q-1} a_n S_n.$$

Pour la réalisation de (2) il faut avoir

$$a_0 = 1, \quad a_n = -\frac{q-1}{(n-1)(n+q-1)} \quad \text{si} \quad n \geqq 2, \quad \text{et} \quad S_1 = 0,$$

tandis que a_1 puisse être arbitraire. La condition $S_1 = 0$ dit exactement

$$\frac{q}{\|\omega_q\|} \int_{\Omega_q} \xi \cdot \eta \, h_K(\eta) \, d\omega_q(\eta) = 0$$

pour tout $\xi \in \Omega_q$, donc le point de Steiner $\mathscr{S}(K)$ de K doit remplir l'équation

$$\mathscr{S}(K) = \frac{q}{\|\omega_q\|} \int_{\Omega_q} \eta \, h_K(\eta) \, d\omega_q(\eta) = 0.$$

On peut toujours obtenir $\mathscr{S}(K) = 0$ par une translation convenable de K. Si on choisit $a_1 = 0$, on est conduit au développement suivant de g_q:

$$g_q \sim \frac{\|\omega_{q-1}\|}{\|\omega_q\|} \left(1 - \sum_{n=2}^{\infty} \frac{(q-1)N(q,n)}{(n-1)(n+q-1)} p_n(q,t) \right). \tag{3}$$

Par avance on ne peut pas savoir si le développement (3) provient d'une fonction $g_q \in \mathscr{L}^1([-1,1],q)$. Qu'en effet c'est le cas, va être démontré dans le théorème 3.3. Si nous présumons ce résultat, nous avons la proposition provisoire:

PROPOSITION 3.1. *Soit $K \in \mathscr{C}_q$ un corps convexe lisse tel que $\mathscr{S}(K) = 0$. Alors*

$$h_K(\xi) = g_q * \frac{R_1 + \cdots + R_{q-1}}{q-1}(\xi) = \frac{1}{\|\omega_{q-1}\|} \int_{\Omega_q} g_q(\xi \cdot \eta) \frac{R_1 + \cdots + R_{q-1}}{q-1}(\eta) \, d\omega_q(\eta).$$

Démonstration: Nous savons que h_K et $g_q * \dfrac{R_1 + \cdots + R_{q-1}}{q-1}$ ont le même développement en série de fonctions sphériques, et par conséquent ils sont égaux ω_q-presque partout (2.13). De plus tous les deux sont des fonctions continues, la dernière selon 2.9; donc l'identité est démontrée. /

Retournons au développement (3), et déterminons quand il provient d'une fonction g_q de $\mathscr{L}^2([-1,1],q)$. Puisque la base orthonormale utilisée est

$$\left(\frac{\|\omega_{q-1}\| N(q,n)}{\|\omega_q\|}\right)^{\frac{1}{2}} p_n(q,t), \qquad n = 0,1,\cdots,$$

les coefficients du développement sont

$$\left(\frac{\|\omega_{q-1}\|}{\|\omega_q\|}\right)^{\frac{1}{2}}\left(1,0,\cdots,\frac{-(q-1)N(q,n)^{\frac{1}{2}}}{(n-1)(n+q-1)},\cdots\right),$$

et leur somme carrée est

$$\frac{\|\omega_{q-1}\|}{\|\omega_q\|}\left(1 + (q-1)^2 \sum_{n=2}^{\infty}\frac{N(q,n)}{(n-1)^2(n+q-1)^2}\right). \tag{4}$$

D'après [15] p. 4 on a

$$\lim_{n\to\infty}\frac{N(q,n)}{n^{q-2}} = \frac{2}{(q-2)!},$$

donc (4) est convergente précisément pour $4 - q + 2 > 1$, i.e. pour $q = 2,3,4$.

PROPOSITION 3.2. *Pour les dimensions* $q = 2,3,4$ *on peut trouver une fonction* g_q *de* $\mathscr{L}^2([-1,1],q)$, *qui possède le développement* (3). *Ceci ne subsiste pas pour les dimensions plus grandes.*

Le théorème suivant montre explicitement qu'il existe pour tous les dimensions $q \geqq 2$ une fonction (et une seule) g_q de $\mathscr{L}^1([-1,1],q)$ avec le développement désiré (3).

THÉORÈME 3.3. *Soient* $g_q: \,]-1,1[\,\to \mathbf{R}$, $q \geqq 2$, *une suite de fonctions définies par*

$$g_2(t) = \frac{1}{\pi}(\pi - \text{Arccos}\,t)(1 - t^2)^{\frac{1}{2}} - \frac{1}{2\pi}t,$$

$$g_3(t) = 1 + t\log(1-t) + (\tfrac{4}{3} - \log 2)t,$$

et ensuite par la formule de récursion $(q \geqq 2)$

$$g_{q+2}(t) = \frac{q+1}{(q-1)^2}tg_q'(t) + \frac{q+1}{q-1}g_q(t) + \frac{q+1}{q+2}\frac{\|\omega_{q+1}\|}{\|\omega_{q+2}\|}t. \tag{5}$$

Il est possible de prolonger g_q *à l'intervalle* $[-1,1]$, *parce que* g_q *a des valeurs limites aux points* ± 1. *Plus précisément on a:*

(i) *La valeur limite* $\lim\limits_{t \to -1} g_q(t)$ *existe et est finie pour* $q \geqq 2$.

(ii) *La valeur limite* $\lim\limits_{t \to 1} g_q(t)$ *est égale à* $-\infty$ *pour* $q \geqq 3$, *tandis que* $\lim\limits_{t \to 1} g_2(t) = -1/2\pi$. *De plus on a*

$$\lim_{t \to 1}(1 - t)^{\frac{1}{2}(q-3) + \varepsilon} g_q(t) = 0,$$

pour tout $\varepsilon > 0$ *si* $q \geqq 3$.

Les fonctions g_q *possèdent les propriétés suivantes*:

(iii) *La fonction* $g_q \colon [-1, 1] \to \mathbf{R} \cup \{-\infty\}$ *est semi-continue supérieurement pour* $q \geqq 3$, *et la fonction* $g_2 \colon [-1, 1] \to \mathbf{R}$ *est continue. On a de plus* $g_q \in C^\infty(]-1, 1[)$ *pour* $q \geqq 2$.

(iv) *La fonction* $g_q(t)(1 - t^2)^{\frac{1}{2}(q-3)}$ *est intégrable sur* $[-1, 1]$, *donc* $g_q \in \mathscr{L}^1([-1, 1], q)$ *pour* $q \geqq 2$. *Pour* $q \geqq 3$ *un peu plus est valable, puisqu'en effet* $g_q(t)(1 - t^2)^{\frac{1}{2}(q-4)}$ *est intégrable sur* $[-1, 1]$.

(v) *Le développement de* g_q *en série de polynômes de Legendre dans* q *dimensions est celui désiré ci-dessus* (3).

Démonstration:

(a) *Le théorème est vrai pour* g_2.

En effet g_2 est bien définie et continue sur l'intervalle $[-1, 1]$ par la formule donnée, et $g_2(-1) = -g_2(1) = 1/2\pi$. Trivialement g_2 est indéfiniment dérivable dans $]-1, 1[$, alors il nous manque seulement le point -1. Dans l'intervalle $[-1, 0]$ on a

$$g_2(t) = \frac{1}{\pi}(1 - t^2)^{\frac{1}{2}} \operatorname{Arcsin}(1 - t^2)^{\frac{1}{2}} - \frac{1}{2\pi}t.$$

Considérons la série entière de $u\operatorname{Arcsin} u$, valable pour $u \in]-1, 1[$

$$u\operatorname{Arcsin} u = \sum_{p=0}^{\infty} \binom{-\frac{1}{2}}{p} \frac{(-1)^p}{2p + 1} u^{2p+2}.$$

Le rayon de convergence est 1. Il en découle que

$$t \longmapsto \sum_{p=0}^{\infty} \binom{-\frac{1}{2}}{p} \frac{(-1)^p}{2p + 1}(1 - t^2)^{p+1}$$

définit une fonction holomorphe dans l'ouvert

$$\{t \in \mathbf{C} \mid |1 - t^2| < 1\},$$

qui est borné d'un lemniscate aux points focaux -1 et 1. Ceci montre que g_2 peut se prolonger à une fonction holomorphe dans la partie gauche du lemniscate. Par conséquent $g_2 \in C^{\infty}([-1,1[)$, et g_2 et toutes ses dérivées possèdent une valeur limite finie, quand t tend vers -1.

Dans l'intervalle $[0,1]$ on a

$$g_2(t) = (1 - t^2)^{\frac{1}{2}} - \frac{1}{\pi}(1 - t^2)^{\frac{1}{2}} \operatorname{Arcsin}(1 - t^2)^{\frac{1}{2}} - \frac{1}{2\pi}t.$$

Du raisonnement ci-dessus il résulte que $(1 - t^2)^{\frac{1}{2}} \operatorname{Arcsin}(1 - t^2)^{\frac{1}{2}}$ peut se prolonger à une fonction holomorphe dans la partie droite du lemniscate. De plus on voit facilement qu'on a, en posant $\varphi(t) = (1 - t^2)^{\frac{1}{2}}$,

$$\lim_{t \to 1} \varphi^{(n)}(t) = -\infty \quad \text{pour} \quad n \geqq 1,$$

ce qui entraîne

$$\lim_{t \to 1} g_2^{(n)}(t) = -\infty \quad \text{pour} \quad n \geqq 1.$$

On sait que la fonction

$$g_2(t)(1 - t^2)^{-\frac{1}{2}} = \frac{1}{\pi}(\pi - \operatorname{Arccos} t) - \frac{t}{2\pi}(1 - t^2)^{-\frac{1}{2}}$$

est intégrable sur $[-1,1]$.

Il nous reste de trouver le développement de g_2 en série de polynômes de Legendre dans deux dimensions. Le développement est donné par

$$g_2 \sim \frac{\|\omega_1\|}{\|\omega_2\|} \sum_{n=0}^{\infty} N(2,n) a_n p_n(2,t),$$

où

$$a_n = \int_{-1}^{1} p_n(2,t) g_2(t)(1 - t^2)^{-\frac{1}{2}} dt.$$

Si on pose $t = \cos\theta$ pour $\theta \in [0,\pi]$, les calculs sont faciles parce que $p_n(2, \cos\theta) = \cos(n\theta)$, et on trouve

$$a_0 = 1, a_1 = 0 \quad \text{et} \quad a_n = \frac{-1}{(n-1)(n+1)} \quad \text{pour} \quad n \geq 2,$$

donc

$$g_2 \sim \frac{\|\omega_1\|}{\|\omega_2\|}\left(1 - \sum_{n=2}^{\infty} \frac{N(2,n)}{(n-1)(n+1)} p_n(2,t)\right),$$

ce qui montre le théorème pour $q = 2$. D'ailleurs $\|\omega_1\| / \|\omega_2\| = 1/\pi$, et $N(2,n) = 2$ pour $n \geqq 2$.

Dans ce qui suit nous allons utiliser la représentation suivante:

Pour $n \geqq 1$ on a

$$g_2^{(n)} = \frac{(1 - t^2)^{-\frac{1}{2}}(\pi - \text{Arccos } t)P_n(t) + Q_{n-1}(t)}{(1 - t^2)^{n-1}}, \tag{6}$$

où P_n et Q_{n-1} sont des polynômes de degré resp. $\leq n$ et $\leq n - 1$. En outre $P_n(1) \neq 0$.

Ceci s'obtient par récurrence sur n. Pour $n = 1$ on a

$$g_2'(t) = (1 - t^2)^{-\frac{1}{2}}(\pi - \text{Arccos } t)\left(-\frac{1}{\pi}t\right) + \frac{1}{2\pi},$$

ce qui montre l'assertion avec $P_1(t) = -t/\pi$ et $Q_0(t) = 1/2\pi$. Supposons que l'assertion soit vrai pour un n; il en résulte que

$$g_2^{(n+1)}(t) = \frac{(1 - t^2)^{-\frac{1}{2}}(\pi - \text{Arccos } t)P_{n+1}(t) + Q_n(t)}{(1 - t^2)^n},$$

où nous avons posé

$$P_{n+1}(t) = (2n - 1)tP_n(t) + (1 - t^2)P_n'(t),$$
$$Q_n(t) = P_n(t) + (1 - t^2)Q_{n-1}'(t) + 2(n - 1)tQ_{n-1}(t).$$

Par conséquent $P_{n+1}(1) = (2n - 1)P_n(1) \neq 0$, et l'assertion est démontrée.

(b) *Le théorème est vrai pour g_3.*

L'expression qui définit g_3 peut être utilisée dans l'intervalle $]-\infty, 1[$, et y représente une fonction indéfiniment dérivable, donc

$$\lim_{t \to -1} g_3^{(n)}(t) \text{ existe et est finie pour tout } n \geqq 0.$$

Il est évident que

$$g_3(t) \to -\infty, \qquad (1-t)^\varepsilon g_3(t) \to 0 \quad \text{pour tout } \varepsilon > 0$$

quand $t \to 1$. De plus on a

$$g_3'(t) = \log(1 - t) - \frac{t}{1 - t} + \tfrac{4}{3} - \log 2 \to -\infty,$$

$$g_3^{(n)}(t) = -\frac{(n - 2)!\,(n - t)}{(1 - t)^n} \to -\infty \quad \text{pour} \quad n \geqq 2, \tag{7}$$

quand $t \to 1$.

Il est facile à voir que $g_3(t)(1-t^2)^{-\frac{1}{2}}$ est intégrable sur $[-1,1]$.

Le calcul du développement de g_3 en série de polynômes de Legendre ordinaires est facilité par la formule de O. Rodrigues (cf. [15] p. 17)

$$p_n(3,t) = \frac{(-1)^n}{2^n n!}\left(\frac{d}{dt}\right)^n \{(1-t^2)^n\}.$$

Le développement de g_3 est donné par

$$g_3 \sim \frac{\|\omega_2\|}{\|\omega_3\|} \sum_{n=0}^{\infty} N(3,n)a_n p_n(3,t),$$

où $\dfrac{\|\omega_2\|}{\|\omega_3\|} = \frac{1}{2}$ et $N(3,n) = 2n+1$, et où

$$a_n = \int_{-1}^{1} g_3(t)p_n(3,t)dt = \frac{(-1)^n}{2^n n!}\int_{-1}^{1} g_3(t)\left(\frac{d}{dt}\right)^n\{(1-t^2)^n\}dt.$$

Nous allons utiliser l'intégration par parties n fois. Les termes

$$\left[g_3^{(j)}(t)\left(\frac{d}{dt}\right)^{n-j-1}\{(1-t^2)^n\}\right]_{t=-1}^{t=1} \quad \text{pour} \quad j = 0,1,\cdots,n-1$$

sont tous 0 d'après (7), car

$$\left(\frac{d}{dt}\right)^{n-j-1}\{(1-t^2)^n\}$$

est égal à $(1-t^2)^{j+1}$ multiplié par un polynôme en t. Par conséquent on a

$$a_n = \frac{1}{2^n n!}\int_{-1}^{1} g_3^{(n)}(1-t^2)^n\, dt,$$

et un calcul facile découvre que

$$a_0 = 1, a_1 = 0 \quad \text{et} \quad a_n = \frac{-2}{(n-1)(n+2)} \quad \text{pour } n \geq 2,$$

donc g_3 possède le développement désiré (3) pour $q = 3$.

(c) *Le théorème est vrai pour g_q, $q \geq 4$.*

La formule de récursion (5) entraîne pour $t \in\,]-1,1[$

$$g_q(t) = a_q t + \sum_{n=0}^{\frac{1}{2}(q-\alpha(q))} b_{q,n}\, t^n g_{\alpha(q)}^{(n)}(t) \quad \text{pour} \quad q > \alpha(q), \tag{8}$$

où $\alpha(q)$ doit être 2 si q est pair, et 3 si q est impair. Dans (8) on a $a_q \in \mathbf{R}$ et $b_{q,n} > 0$ pour $n = 0, 1, \cdots, \frac{1}{2}(q - \alpha(q))$. D'après ce que nous avons démontré sur $g_2^{(n)}(t)$ et $g_3^{(n)}(t)$, on voit facilement en vertu de (8) que les assertions (i), (ii), (iii) du théorème sont vrais pour $q \geqq 4$, sauf peut-être la relation

$$\lim_{t \to 1}(1-t)^{\frac{1}{2}(q-3)+\varepsilon} g_q(t) = 0 \quad \text{pour} \quad \varepsilon > 0, q \geqq 4. \tag{9}$$

Si q est pair, il suffit selon (8) et l'identité $\lim_{t \to 1} g_2(t) = -1/2\pi$ de montrer que

$$\lim_{t \to 1}(1-t)^{\frac{1}{2}(q-3)+\varepsilon} g_2^{(n)}(t) = 0 \quad \text{pour} \quad \varepsilon > 0 \quad \text{et} \quad n = 1, \cdots, \tfrac{1}{2}(q-2).$$

Utilisant (6), nous voyons que

$$(1-t)^{\frac{1}{2}(q-3)+\varepsilon} g_2^{(n)}(t) = (1-t)^{\frac{1}{2}(q-2n-1)+\varepsilon} \frac{(1-t^2)^{-\frac{1}{2}}(\pi - \operatorname{Arccos} t)P_n(t) + Q_{n-1}(t)}{(1+t)^{n-1}},$$

ce qui tend vers 0 quand $t \to 1$, parce que $n \leqq \frac{1}{2}(q-2)$.

Si q est impair (donc $q \geqq 5$) il suffit selon (8) de montrer que

$$\lim_{t \to 1}(1-t)^{\frac{1}{2}(q-3)+\varepsilon} g_3^{(n)}(t) = 0 \quad \text{pour} \quad \varepsilon > 0 \quad \text{et} \quad n = 0, 1, \cdots, \tfrac{1}{2}(q-3).$$

Ceci est une conséquence immédiate de (7).

Choisissons $\varepsilon \in \,]0, \tfrac{1}{2}[$. Pour $q \geqq 4$ nous écrivons

$$g_q(t)(1-t^2)^{\frac{1}{2}(q-4)} = \frac{g_q(t)(1-t^2)^{\frac{1}{2}(q-3)+\varepsilon}}{(1-t^2)^{\frac{1}{2}+\varepsilon}},$$

et d'après (9) le numérateur est une fonction continue sur l'intervalle $[-1, 1]$. Comme $(1-t^2)^{-\frac{1}{2}-\varepsilon}$ est intégrable sur $[-1, 1]$, on conclut que (iv) est valable.

Il nous reste seulement de démontrer que g_q a le développement (3) pour $q \geqq 4$. Cela va être démontré par récurrence sur q à l'aide de la formule de récursion (5). Nous aurons besoin de plusieures formules entre les polynômes de Legendre de différents degrés et dimensions. Les voici:

(α) $(q-1)p'_n(q,t) = n(n+q-2)p_{n-1}(q+2,t)$.

(β) $(n+q-2)(1-t^2)p_{n-1}(q+2,t) = (q-1)p_{n-1}(q,t) - (q-1)tp_n(q,t)$.

(γ) $np_{n-1}(q+2,t) = (n+q-1)tp_n(q+2,t) - (q-1)p_{n+1}(q,t)$.

(δ) $(2n+q)tp_{n+1}(q,t) = (n+q-1)p_{n+2}(q,t) + (n+1)p_n(q,t)$.

Ces formules sont des cas particuliers des formules analogues pour les polynômes de Gegenbauer $C_n^v(t)$, puisque

$$p_n(q,t) = \binom{n+q-3}{n}^{-1} C_n^{\frac{1}{2}(q-2)}(t) \quad \text{(cf. [15] p. 33)}.$$

On trouve ces formules analogues dans [14] p. 282 sous les numéros (4), (10), (3) et (8) dans le même ordre comme ci-dessus. Nous allons en déduire:

LEMME 3.4. *La formule suivante est valable:*

$$(q-1)p_n(q+2,t) - (1-t^2)(p_n(q+2,t) + tp'_n(q+2,t))$$

$$= \frac{q-1}{2n+q}((n+q-1)p_n(q,t) + (n+1)p_{n+2}(q,t)).$$

Démonstration: D'après (α) et (β) on a

$$(1-t^2)p'_n(q+2,t) = np_{n-1}(q+2,t) - ntp_n(q+2,t).$$

Si on multiplie ceci par t et additionne $(1-t^2)p_n(q+2,t)$, on a

$$(1-t^2)(p_n(q+2,t) + tp'_n(q+2,t))$$
$$= (n+1)(1-t^2)p_n(q+2,t) + ntp_{n-1}(q+2,t) - np_n(q+2,t).$$

Donc le membre gauche G de la formule désirée est égal à

$$G = (n+q-1)p_n(q+2,t) - ntp_{n-1}(q+2,t) - (n+1)(1-t^2)p_n(q+2,t).$$

En vertu de (γ) on a

$$-ntp_{n-1}(q+2,t) = (q-1)tp_{n+1}(q,t) - (n+q-1)t^2p_n(q+2,t).$$

Si on substitue ceci dans l'expression de G, on obtient

$$G = (q-2)(1-t^2)p_n(q+2,t) + (q-1)tp_{n+1}(q,t).$$

D'après (β) avec n remplacé par $n+1$ on voit que

$$(n + q - 1)G = (q - 2)(q - 1)p_n(q,t) + (n + 1)(q - 1)tp_{n+1}(q,t),$$

et en appliquant (δ) sur le terme dernier, on trouve

$$(2n + q)(n + q - 1)G = (n + q - 1)(n + 1)(q - 1)p_{n+2}(q,t)$$
$$+ (q - 1)(n + q - 1)^2 p_n(q,t),$$

ce qui montre le lemme. /

Supposons que g_q possède le développement (3), c'est-à-dire

$$a_n(q) = \int_{-1}^{1} g_q(t)p_n(q,t)(1 - t^2)^{\frac{1}{2}(q-3)}\, dt = \begin{cases} -\dfrac{q-1}{(n-1)(n+q-1)} & \text{si } n \neq 1, \\ 0 & \text{si } n = 1. \end{cases} \quad (10)$$

Nous allons démontrer

$$a_n(q+2) = \int_{-1}^{1} g_{q+2}(t)p_n(q+2,t)(1 - t^2)^{\frac{1}{2}(q-1)}\, dt = \begin{cases} -\dfrac{q+1}{(n-1)(n+q+1)} & \text{si } n \neq 1, \\ 0 & \text{si } n = 1. \end{cases} \quad (11)$$

D'après la formule de récursion (5) $a_n(q+2)$ est la somme des expressions A_n, B_n et C_n, où

$$A_n = \frac{q+1}{(q-1)^2} \int_{-1}^{1} g_q'(t)p_n(q+2,t)\,t(1 - t^2)^{\frac{1}{2}(q-1)}\, dt.$$

$$B_n = \frac{q+1}{q-1} \int_{-1}^{1} g_q(t)p_n(q+2,t)(1 - t^2)^{\frac{1}{2}(q-1)}\, dt.$$

$$C_n = \frac{q+1}{q+2}\frac{\|\omega_{q+1}\|}{\|\omega_{q+2}\|} \int_{-1}^{1} tp_n(q+2,t)(1 - t^2)^{\frac{1}{2}(q-1)}\, dt = \begin{cases} 0 & \text{si } n \neq 1, \\ \dfrac{q+1}{(q+2)^2} & \text{si } n = 1. \end{cases}$$

Ce dernier est tiré des formules (11), (12) et (13) du chapitre 2.

Soit $n = 0$. L'intégration par parties dans A_0 donne

$$A_0 = -\frac{q+1}{(q-1)^2} \int_{-1}^{1} g_q(t)(1 - qt^2)(1 - t^2)^{\frac{1}{2}(q-3)}\, dt,$$

puisque

$$[g_q(t)(1-t^2)^{\frac{1}{2}(q-1)}]_{t=-1}^{t=1} = 0. \tag{12}$$

D'après (13) chapitre 2, et (10) on a

$$A_0 = \frac{q+1}{q-1} \int_{-1}^{1} g_q(t)p_2(q,t)(1-t^2)^{\frac{1}{2}(q-3)}\, dt = -1.$$

De la même manière on obtient

$$B_0 = \frac{q+1}{q} \int_{-1}^{1} g_q(t)(p_0(q,t) - p_2(q,t))(1-t^2)^{\frac{1}{2}(q-3)}\, dt = 2,$$

donc $a_0(q+2) = A_0 + B_0 + C_0 = 1$.

   Soit $n = 1$. Des calculs analogues et faciles montrent que $a_1(q+2) = 0$.
   Soit $n \geqq 2$. L'intégration par parties dans A_n montre d'après (12) que

$$A_n = -\frac{q+1}{(q-1)^2} \int_{-1}^{1} g_q(t)(1-t^2)^{\frac{1}{2}(q-3)}\{q(1-t^2)p_n(q+2,t)$$

$$+ t(1-t^2)p'_n(q+2,t) - (q-1)p_n(q+2,t)\}\,dt,$$

d'où

$$A_n + B_n = \frac{q+1}{(q-1)^2} \int_{-1}^{1} g_q(t)(1-t^2)^{\frac{1}{2}(q-3)} D_n(t)\,dt,$$

où nous avons posé

$$D_n(t) = (q-1)p_n(q+2,t) - (1-t^2)(p_n(q+2,t) + t p'_n(q+2,t)).$$

D'après le lemme 3.4 on sait que

$$D_n(t) = \frac{q-1}{2n+q}((n+q-1)p_n(q,t) + (n+1)p_{n+2}(q,t)),$$

d'où

$$A_n + B_n = \frac{q+1}{(q-1)(2n+q)}((n+q-1)a_n(q) + (n+1)a_{n+2}(q)).$$

Si on utilise (10), on trouve

$$A_n + B_n = -\frac{q+1}{(n-1)(n+q+1)},$$

et comme $n \geqq 2$ entraîne $C_n = 0$, il en résulte que

$$a_n(q+2) = -\frac{q+1}{(n-1)(n+q+1)},$$

et le théorème 3.3 est complètement démontré. /

La fonction g_q est le noyau de Green de l'opérateur D_q^*, et elle est appelée le noyau sphérique dans q dimensions.

De la formule de récursion (5) nous pouvons tirer une expression directe de g_q. Si q est pair, on trouve

$$g_q(t) = \frac{(q-1)\|\omega_{q-1}\|}{\|\omega_q\|}\left\{(\pi - \operatorname{Arccos} t)(1-t^2)^{\frac{1}{2}}\sum_{k=0}^{\frac{1}{2}(q-2)} a_k(1-t^2)^{-k} + t\sum_{k=1}^{\frac{1}{2}(q-4)} b_k(1-t^2)^{-k} + c_q t\right\},$$

et si q est impair, on trouve

$$g_q(t) = \frac{(q-1)\|\omega_{q-1}\|}{\|\omega_q\|}\left\{1 + t\log(1-t) + (q-3)\sum_{k=1}^{\frac{1}{2}(q-3)} d_k(1-t)^{-k} + e_q t\right\}.$$

Évidemment on peut établir des formules de récursions entre les coefficients paraîssants. Nous préférons de donner les formules explicites pour g_q dans les cas $q = 2, 3, 4, 5, 6$:

$$g_2(t) = \frac{1}{\pi}\left\{(\pi - \operatorname{Arccos} t)(1-t^2)^{\frac{1}{2}} - \tfrac{1}{2}t\right\}.$$

$$g_3(t) = 1 + t\log(1-t) + (\tfrac{4}{3} - \log 2)t.$$

$$g_4(t) = \frac{3}{\pi}\left\{(\pi - \operatorname{Arccos} t)(1-2t^2)(1-t^2)^{-\frac{1}{2}} + \tfrac{1}{2}t\right\}.$$

$$g_5(t) = 3(1 + t\log(1-t)) - (1-t)^{-1} + (\tfrac{28}{5} - 3\log 2)t.$$

$$g_6(t) = \frac{5}{3\pi}\left\{(\pi - \operatorname{Arccos} t)(8t^4 - 12t^2 + 3)(1-t^2)^{-\frac{3}{2}} - t(1-t^2)^{-1} + \tfrac{16}{3}t\right\}.$$

§ 2. Quelques propriétés du noyau sphérique g_q

PROPOSITION 3.5. Le noyau sphérique g_q remplit:

(i) Pour tout $a \in \Omega_q$ on a au sens des distributions

$$D_{q}^{*}\{g_q(a \cdot \xi)\} = \|\omega_{q-1}\|\delta_a - \frac{q\|\omega_{q-1}\|}{\|\omega_q\|}a \cdot \xi, \qquad (13)$$

3*

où δ_a désigne la mesure de Dirac au point a, i.e. la mesure de masse 1 concentrée dans a.

(ii) Dans l'intervalle $]-1,1[$ le noyau g_q satisfait à l'équation différentielle

$$(1-t^2)g_q''(t) - (q-1)tg_q'(t) + (q-1)g_q(t) = -\frac{q(q-1)\|\omega_{q-1}\|}{\|\omega_q\|}t. \quad (14)$$

Démonstration: (i) D'après 2.7 on sait que $g_q(a \cdot) \in \mathcal{L}^1(\Omega_q)$, et selon les théorèmes 2.12 et 3.3 son développement est donné par

$$g_q(a \cdot \xi) \sim \frac{\|\omega_{q-1}\|}{\|\omega_q\|}\left(1 - \sum_{n=2}^{\infty}\frac{(q-1)N(q,n)}{(n-1)(n+q-1)}p_n(q, a \cdot \xi)\right).$$

Par conséquent on a

$$D_q^*\{g_q(a \cdot \xi)\} \sim \frac{\|\omega_{q-1}\|}{\|\omega_q\|}\left(1 + \sum_{n=2}^{\infty}N(q,n)p_n(q, a \cdot \xi)\right).$$

La mesure de Dirac δ_a possède le développement

$$\delta_a \sim \frac{1}{\|\omega_q\|}\sum_{n=0}^{\infty}N(q,n)p_n(q, a \cdot \xi),$$

donc

$$D_q^*\{g_q(a \cdot \xi)\} \text{ et } \|\omega_{q-1}\|\delta_a - \frac{q\|\omega_{q-1}\|}{\|\omega_q\|}a \cdot \xi$$

ont le même développement, ce qui entraîne le résultat en vertu de 2.13.

(ii) Par restriction à l'ouvert $\Omega_q\backslash\{a\}$, on déduit de (13) l'équation de distribution suivante

$$\left(\Delta_q^* + (q-1)\right)g_q(a \cdot \xi) = -\frac{q(q-1)\|\omega_{q-1}\|}{\|\omega_q\|}a \cdot \xi, \quad (15)$$

car δ_a induit la distribution 0 sur $\Omega_q\backslash\{a\}$. Cependant la fonction $\xi \mapsto g_q(a \cdot \xi)$ est indéfiniment dérivable sur $\Omega_q\backslash\{a\}$, donc (15) est une équation ordinaire entre des fonctions. Posons

$$\xi = ta + (1-t^2)^{\frac{1}{2}}\eta, \quad \text{où } t \in]-1,1[\quad \text{et} \quad \eta \in \Omega_{q-1} = \{\eta \in \Omega_q \,|\, a \cdot \eta = 0\}.$$

Alors $g_q(a \cdot \xi) = g_q(t)$ ne dépend pas de η, et (14) résulte de (4) de la proposition 2.6. ∕

LEMME 3.6. *L'équation différentielle homogène sur l'intervalle $]-1,1[$*

$$\frac{d^2}{dt^2} - \frac{q-1}{1-t^2} t \frac{d}{dt} + \frac{q-1}{1-t^2} = 0, \quad q = 2, 3, \cdots, \tag{16}$$

a deux solutions indépendantes t et $\varphi_q(t)$ telles que $\varphi_2(t) = (1-t^2)^{\frac{1}{2}}$, tandis que pour $q \geq 3$, on ait $\varphi_q(t) \to \infty$ quand $t \to \pm 1$.

Démonstration: Dans le cas $q = 2$ on voit immédiatement que t et $\varphi_2(t) = (1-t^2)^{\frac{1}{2}}$ sont deux solutions indépendantes de (16). Dans le cas $q \geq 3$ on sait que t et

$$\varphi_q(t) = t \int\limits_{t_0}^{t} u^{-2}(1-u^2)^{\frac{1}{2}(1-q)} \, du,$$

où $t_0 \in \,]0, 1[$, sont deux solutions indépendantes de (16) sur $]0, 1[$. Si on développe la fonction qu'on intègre en série entière, on trouve

$$\varphi_q(t) = -1 + k(t_0) t + \sum_{n=1}^{\infty} \binom{\frac{1}{2}(1-q)}{n} \frac{(-1)^n}{2n-1} t^{2n}, \tag{17}$$

où $k(t_0)$ est une constante dépendante de t_0. La série entière est convergente pour $|t| < 1$, donc la formule (17) donne une solution de (16) sur tout l'intervalle $]-1, 1[$. Puisque

$$\binom{\frac{1}{2}(1-q)}{n} \frac{(-1)^n}{2n-1} = \frac{(\frac{1}{2}(q-3)+1) \cdots (\frac{1}{2}(q-3)+n)}{n!(2n-1)} \geq \frac{1}{2n-1},$$

on voit que $\varphi_q(t) \to \infty$ quand $t \to \pm 1$. /

À l'aide des solutions t et $\varphi_q(t)$ de (16) on sait trouver une formule explicite pour la solution g_q de (14). On trouve

$$g_q(t) = -\frac{q(q-1)\|\omega_{q-1}\|}{\|\omega_q\|} t \int\limits_{\alpha_q}^{t} \left(s^{-2}(1-s^2)^{\frac{1}{2}(1-q)} \int\limits_{-1}^{s} u^2(1-u^2)^{\frac{1}{2}(q-3)} \, du \right) ds.$$

Les limites inférieures -1 et α_q des intégrales sont fixées par les demandes que g_q soit régulière au point -1 et que

$$\int\limits_{-1}^{1} t g_q(t)(1-t^2)^{\frac{1}{2}(q-3)} \, dt = 0.$$

Dans la théorie du potentiel sphérique nous aurons besoin de quelques lemmes sur g_q.

LEMME 3.7. *Soient* $\breve{g}_q(t) = g_q(-t)$ *et* $h_q(t) = g_q(t) + \breve{g}_q(t)$ *pour* $t \in [-1, 1]$. *Alors* $h_q(t)/t$ *est une fonction décroissante sur* $]0, 1[$ *pour* $q \geqq 2$.

Démonstration: Comme g_q satisfait à l'équation différentielle (14), on voit que $\breve{g}_q$ satisfait à

$$(1 - t^2)(\breve{g}_q)''(t) - (q-1)t(\breve{g}_q)'(t) + (q-1)\breve{g}_q(t) = \frac{q(q-1)\|\omega_{q-1}\|}{\|\omega_q\|}t,$$

et par l'addition à (14), on obtient

$$(1 - t^2)h_q''(t) - (q-1)th_q'(t) + (q-1)h_q(t) = 0 \quad \text{pour} \quad t \in]-1, 1[,$$

d'où

$$(1 - t^2)h_q''(t) = (q-1)t^2\left(\frac{h_q(t)}{t}\right)' \quad \text{pour} \quad t \in]0, 1[.$$

Il en découle:

> Pour que $h_q'(t)$ soit décroissante sur $]0, 1[$, il faut et il suffit que $h_q(t)/t$ soit décroissante sur $]0, 1[$. $\left.\phantom{\begin{array}{c}a\\b\end{array}}\right\}$ (18)

Dans la même manière comme ci-dessus la formule de récursion (5) donne la formule suivante pour h_q:

$$h_{q+2}(t) = \frac{q+1}{(q-1)^2}th_q'(t) + \frac{q+1}{q-1}h_q(t) \quad \text{pour} \quad t \in]-1, 1[,$$

d'où

$$\frac{h_{q+2}(t)}{t} = \frac{q+1}{(q-1)^2}h_q'(t) + \frac{q+1}{q-1}\frac{h_q(t)}{t} \quad \text{pour} \quad t \in]0, 1[. \qquad (19)$$

Le lemme résulte maintenant par récurrence sur q. On trouve

$$\frac{h_2(t)}{t} = \frac{(1 - t^2)^{\frac{1}{2}}}{t} \quad \text{et} \quad \frac{h_3(t)}{t} = \frac{2}{t} + \log\frac{1-t}{1+t},$$

qui sont décroissantes sur $]0, 1[$. D'après (18), (19) il est évident que la décroissance de $h_q(t)/t$ sur $]0, 1[$ entraîne celle de $h_{q+2}(t)/t$ sur $]0, 1[$. /

LEMME 3.8. *Le noyau sphérique* g_q *vérifie*

$$\lim_{t \to 1} \frac{g_q(t)}{g_q(2t^2 - 1)} = \begin{cases} 1 & \text{si} \quad q = 2. \\ 2^{q-3} & \text{si} \quad q \geqq 3. \end{cases}$$

Démonstration: Comme $\lim_{t \to 1} g_2(t) = -1/2\pi$, l'assertion est évidente pour $q = 2$. Par contre, le lemme n'est pas évident pour $q \geqq 3$ parce que $g_q(t) \to -\infty$ quand $t \to 1$.

Si q est pair, $q \geq 4$, on a d'après (6)

$$\lim_{t \to 1} (1 - t^2)^{\frac{1}{2}(q-3)} g_2^{(n)}(t) = \begin{cases} 0 & \text{si } 0 \leq n \leq \frac{1}{2}(q-4), \\ \pi P_n(1) & \text{si } n = \frac{1}{2}(q-2), \end{cases}$$

et

$$\lim_{t \to 1} (1 - t^2)^{\frac{1}{2}(q-3)} g_2^{(n)}(2t^2 - 1) = \begin{cases} 0 & \text{si } 0 \leq n \leq \frac{1}{2}(q-4), \\ \pi P_n(1) 2^{3-q} & \text{si } n = \frac{1}{2}(q-2). \end{cases}$$

En vertu de (8) on trouve

$$\lim_{t \to 1} \frac{g_q(t)}{g_q(2t^2 - 1)} = \frac{\pi P_n(1)}{\pi P_n(1) 2^{3-q}} = 2^{q-3}.$$

Si $q = 3$ le lemme résulte d'un calcul simple.

Si q est impair, $q \geq 5$, on a d'après (7)

$$\lim_{t \to 1} (1 - t)^{\frac{1}{2}(q-3)} g_3^{(n)}(t) = \begin{cases} 0 & \text{si } 0 \leq n \leq \frac{1}{2}(q-5), \\ -(\frac{1}{2}q - \frac{5}{2})! & \text{si } n = \frac{1}{2}(q-3), \end{cases}$$

et

$$\lim_{t \to 1} (1 - t)^{\frac{1}{2}(q-3)} g_3^{(n)}(2t^2 - 1) = \begin{cases} 0 & \text{si } 0 \leq n \leq \frac{1}{2}(q-5), \\ -(\frac{1}{2}q - \frac{5}{2})! 2^{3-q} & \text{si } n = \frac{1}{2}(q-3). \end{cases}$$

Par conséquent on a d'après (8)

$$\lim_{t \to 1} \frac{g_q(t)}{g_q(2t^2 - 1)} = \frac{-(\frac{1}{2}q - \frac{5}{2})!}{-(\frac{1}{2}q - \frac{5}{2})! 2^{3-q}} = 2^{q-3}. \;\;|$$

COROLLAIRE 3.9. *Soit $q \geq 2$. Il existe deux constantes positives A_q et B_q, et un $t_q \in \,]0,1[$ tels que*

$$g_q(t) + A_q \geq B_q g_q(s) \qquad (20)$$

pour

$$\{(t,s) \in [-1,1]^2 \,|\, (t \leq t_q) \vee (t > t_q \wedge s \geq 2t^2 - 1)\}.$$

Démonstration: Naturellement le corollaire dit seulement quelque chose d'intérêt quand $q \geq 3$, parce que g_2 est continue sur l'intervalle $[-1, 1]$.

Soit $q \geq 3$. Nous savons que $g_q^{(n)}(t) \to -\infty$, si $n \geq 0$, quand $t \to 1$, et par conséquent $g_q(t)$ est négative et décroissante, dès que t est suffisamment voisin à 1. Soit B_q une constante telle que $B_q > 2^{q-3}$. D'après le lemme 3.8 il existe un $t_q \in \,]0,1[$ tel que:

(α) g_q est décroissante et négative sur l'intervalle $[2t_q^2 - 1, 1]$.

(β)   Pour $t \in [t_q, 1]$, on ait $\dfrac{g_q(t)}{g_q(2t^2 - 1)} < B_q$.

Comme g_q est semi-continue supérieurement sur $[-1, 1]$ il existe un $M > 0$ tel que

$$g_q(t) \leqq M \qquad \text{pour} \ \ t \in [-1, 1], \tag{21}$$

et comme g_q est continue sur $[-1, t_q]$ il existe un $A_q > 0$ tel que

$$g_q(t) + A_q \geqq MB_q \qquad \text{pour} \ \ t \in [-1, t_q]. \tag{22}$$

Nous allons démontrer que

$$g_q(t) + A_q \geqq B_q g_q(s),$$

pour toutes (t, s) dans l'ensemble indiqué.

L'assertion est vrai pour $t = s = 1$ parce que $g_q(1) = -\infty$.

Si $t \in \,]t_q, 1[$ et $s \geqq 2t^2 - 1$, on a d'après (α) et (β)

$$g_q(2t^2 - 1) < 0 \quad \text{et} \quad g_q(t) > B_q g_q(2t^2 - 1) \geqq B_q g_q(s),$$

et par conséquent

$$g_q(t) + A_q > g_q(t) > B_q g_q(s).$$

Enfin, si $t \in [-1, t_q]$ et $s \in [-1, 1]$, on a

$$B_q g_q(s) \leqq B_q M \leqq g_q(t) + A_q,$$

en vertu de (21) et (22). /

Chapitre 4
LA THÉORIE DU POTENTIEL SPHÉRIQUE

§ 1. *Fonctions harmoniques dans Ω_q*

Par fonctions harmoniques dans une variété de Riemann on entend le plus souvent les solutions f de l'équation de Laplace $\Delta^* f = 0$, où Δ^* est l'opérateur de Laplace-Beltrami. Ce que nous allons appeler les fonctions harmoniques dans Ω_q, seront les solutions f de l'équation

$$\{\Delta_q^* + (q - 1)\} f = 0,$$

autrement dit, les solutions f de l'équation $D_q^* f = 0$.

Il est possible de caractériser les fonctions harmoniques par des propriétés de moyenne. Nous préférons de commencer de cette manière.

Pour $a \in \Omega_q$ et $\varrho \in \,]0, \tfrac{1}{2}\pi[$ on pose

$$C(a,\varrho) = \{\xi \in \Omega_q \mid a \cdot \xi \geqq \cos\varrho\}, \quad S(a,\varrho) = \{\xi \in \Omega_q \mid a \cdot \xi = \cos\varrho\},$$

et on appelle $C(a,\varrho)$ et $S(a,\varrho)$ le disque sphérique et le cercle sphérique de centre a et de rayon sphérique ϱ. Le disque sphérique $C(a,\varrho)$ porte la mesure ω_q, et a la masse totale

$$m(\varrho) = \omega_q(C(a,\varrho)) = \|\omega_{q-1}\| \int\limits_{\cos\varrho}^{1} (1-t^2)^{\frac{1}{2}(q-3)} dt. \tag{1}$$

Le cercle sphérique $S(a,\varrho)$ est une sphère de dimension $q-2$, de centre $a\cos\varrho$ et de rayon $\sin\varrho$. Il porte la mesure de surface σ_ϱ donnée par

$$d\sigma_\varrho(\eta) = \sin^{q-2}\varrho \, d\omega_{q-1}\begin{pmatrix} \eta \\ \overline{\sin\varrho} \end{pmatrix}. \tag{2}$$

Elle a la masse totale $\|\omega_{q-1}\| \sin^{q-2}\varrho$.

Soient ω un ouvert de Ω_q, et $f\colon \omega \to \mathbf{R}$ une fonction continue, et soit $C(a,\varrho) \subseteq \omega$ pour un $\varrho \in \,]0, \tfrac{1}{2}\pi[$. Noterons $\mathscr{M}_f^\varrho(a)$ la moyenne de f sur le cercle sphérique $S(a,\varrho)$, i.e.

$$\mathscr{M}_f^\varrho(a) = (\|\omega_{q-1}\|\sin^{q-2}\varrho)^{-1} \int\limits_{S(a,\varrho)} f(\xi) d\sigma_\varrho(\xi), \tag{3}$$

et poserons

$$\mathscr{A}_f^\varrho(a) = \frac{1}{\|\omega_{q-1}\|} \int\limits_{C(a,\varrho)} f(\xi) d\omega_q(\xi). \tag{4}$$

Donc $\|\omega_{q-1}\| m(\varrho)^{-1} \mathscr{A}_f^\varrho(a)$ est la moyenne de f dans le disque sphérique $C(a,\varrho)$. Les expressions (3) et (4) gardent leurs sens, si f est seulement semi-continue dans ω. On voit que

$$\mathscr{M}_f^\varrho(a) = \frac{1}{\|\omega_{q-1}\|} \int\limits_{a\cdot\eta=0} f(a\cos\varrho + \eta\sin\varrho) d\omega_{q-1}(\eta), \tag{5}$$

et que

$$\mathscr{A}_f^\varrho(a) = \int\limits_{\cos\varrho}^{1} (1-t^2)^{\frac{1}{2}(q-3)} \mathscr{M}_f^{\operatorname{Arccos}t}(a) dt = \int\limits_{0}^{\varrho} \sin^{q-2}u \, \mathscr{M}_f^u(a) du. \tag{6}$$

Dans les applications il est important d'observer qu'on peut considérer la moyenne $\mathscr{M}_f^\varrho(a)$ comme une moyenne sur le groupe $O(q,a)$, le sous-groupe des rotations de $O(q)$ qui laissent a fixe.

Soit μ la mesure de Haar normalisée sur le groupe compact $O(q,a)$, et soit ξ un point de $S(a,\varrho)$. L'application $\mathscr{C}(S(a,\varrho)) \to \mathbf{R}$, donnée par

$$\varphi \longmapsto \int_{O(q,a)} \varphi(A\xi)\,d\mu(A),$$

est une mesure positive sur $S(a,\varrho)$. Cette mesure est invariante par rapport au groupe $O(q,a)$, et a la masse totale 1. Donc, elle satisfait aux conditions, qui caractérisent la mesure de surface normalisée $\varphi \longmapsto \mathscr{M}_\varphi^\varrho(a)$ de $S(a,\varrho)$, et nous avons démontré le lemme suivant:

LEMME 4.1. *Quels que soient* $a \in \Omega_q$, $\varrho \in \,]0,\tfrac{1}{2}\pi[$, $\xi \in S(a,\varrho)$, *pour toute* $\varphi \in \mathscr{C}(S(a,\varrho))$ *on ait*

$$\int_{O(q,a)} \varphi(A\xi)\,d\mu(A) = \mathscr{M}_\varphi^\varrho(a).$$

Évidemment ce lemme est valable non seulement pour les fonctions continues, mais aussi par exemple pour les fonctions semi-continues.

Soient $f \in \mathscr{C}(\Omega_q)$ et $\varrho \in \,]0,\tfrac{1}{2}\pi[$. On désigne par $\mathscr{M}_f^\varrho$ la fonction $a \longmapsto \mathscr{M}_f^\varrho(a)$ de Ω_q dans $\mathbf{R}$. Elle est continue. Par $f \longmapsto \mathscr{M}_f^\varrho$ on définit un opérateur linéaire continu dans $\mathscr{C}(\Omega_q)$. Plus tard nous aurons besoin de savoir qu'il est symétrique; c'est-à-dire qu'on a:

LEMME 4.2. *Soient* $f,g \in \mathscr{C}(\Omega_q)$ *et* $\varrho \in \,]0,\tfrac{1}{2}\pi[$, *alors*

$$\int_{\Omega_q} \mathscr{M}_f^\varrho(\xi)g(\xi)\,d\omega_q(\xi) = \int_{\Omega_q} f(\xi)\mathscr{M}_g^\varrho(\xi)\,d\omega_q(\xi).$$

Démonstration: Remarquons d'abord que si $f \in \mathscr{C}(\Omega_q)$, $a \in \Omega_q$, l'application

$$\varrho \longmapsto \mathscr{A}_f^\varrho(a) = \frac{1}{\|\omega_{q-1}\|}\int_{C(a,\varrho)} f(\xi)\,d\omega_q(\xi)$$

est dérivable avec la dérivée continue

$$\sin^{q-2}\varrho\,\mathscr{M}_f^\varrho(a).$$

Ensuite posons

$$K_\varrho = \{(\xi,\eta) \in \Omega_q^2 \mid \xi\cdot\eta \geq \cos\varrho\}.$$

Grâce au théorème de Fubini pour la fonction

$$(\xi, \eta) \longmapsto 1_{K_\varrho}(\xi, \eta) f(\xi) g(\eta)$$

de $\Omega_q \times \Omega_q$ dans **R**, on obtient

$$\int_{\Omega_q} \left(f(\xi) \int_{C(\xi, \varrho)} g(\eta) \, d\omega_q(\eta) \right) d\omega_q(\xi) = \int_{\Omega_\eta} \left(g(\eta) \int_{C(\eta, \varrho)} f(\xi) \, d\omega_q(\xi) \right) d\omega_q(\eta).$$

Selon l'observation ci-dessus on peut dériver cette équation sous le signe d'intégration par rapport à ϱ, donc

$$\int_{\Omega_\eta} f(\xi) \sin^{q-2} \varrho \, \mathcal{M}_g^\varrho(\xi) \, d\omega_q(\xi) = \int_{\Omega_\eta} g(\eta) \sin^{q-2} \varrho \, \mathcal{M}_f^\varrho(\eta) \, d\omega_q(\eta),$$

ce qui prouve le lemme. /

On voit sans difficultés que le lemme 4.2 est encore valable pour des fonctions semi-continues.

Il est important pour la théorie du potentiel sphérique d'avoir un théorème qui montre que $D_q^* f(a)$ est déterminé par les moyennes $\mathcal{M}_f^\varrho(a)$. Voici un résultat très précis.

THÉORÈME 4.3. *Soient* ω *un ouvert de* Ω_q, $f \in C^2(\omega)$. *Pour tout point* $a \in \omega$, *on a*

$$D_q^* f(a) = \lim_{\varrho \to 0} \frac{2\cos\varrho}{\sin^2\varrho} (\mathcal{M}_f^\varrho(a) - \cos\varrho f(a)),$$

uniformément dans a *sur tout compact* $\varkappa$ *de* ω.

Démonstration: Nous prolongeons f par homogénéité positive au cône ouvert $K_\omega = \{\lambda\xi \mid \lambda > 0, \xi \in \omega\}$ de base ω et de sommet 0, i.e. nous définissons

$$\tilde{f} : K_\omega \to \mathbf{R} \quad \text{par} \quad \tilde{f}(\lambda\xi) = \lambda f(\xi).$$

Alors $\tilde{f} \in C^2(K_\omega)$.

Soit $\varkappa$ un compact de ω. Il existe un $\varrho_0 \in \,]0, \tfrac{1}{2}\pi[$ tel que pour $\varrho \leq \varrho_0$, $a \in \varkappa$, on ait $C(a, \varrho) \subseteq \omega$. Posons

$$\varLambda = \{(a, \eta) \in \Omega_q^2 \mid a \in \varkappa, \, a \cdot \eta = 0\}.$$

Grâce à la formule de Taylor, pour $(a, \eta) \in \varLambda$, $\varrho \leq \varrho_0$, on a

$$\left. \begin{aligned} & f(a\cos\varrho + \eta\sin\varrho) - \tilde{f}(a\cos\varrho) = \\ & d\tilde{f}(a\cos\varrho; \eta\sin\varrho) + \tfrac{1}{2} d^2\tilde{f}(a\cos\varrho; \eta\sin\varrho) + \tfrac{1}{2}\sin^2\varrho\,\alpha(a, \eta, \varrho), \end{aligned} \right\} \quad (7)$$

où $\alpha(a,\eta,\varrho) \to 0$ quand $\varrho \to 0$, uniformément pour $(a,\eta) \in \Lambda$. Fixons $a \in \varkappa$, et introduisons une base orthonormale $\varepsilon_1, \cdots, \varepsilon_q$ de $\mathbf{R}^q$ telle que $a = \varepsilon_q$. Si le point $x \in K_\omega$ possède les coordonnées $x_1, \cdots, x_q$ dans cette base, nous écrivons

$$\tilde{f}(x) = \overset{\scriptscriptstyle\wedge}{f}(x_1, \cdots, x_q).$$

Alors

$$d\tilde{f}(a\cos\varrho; \eta\sin\varrho) = \sin\varrho \sum_{i=1}^{q-1} \frac{\partial \tilde{f}}{\partial x_i}(a\cos\varrho)(\eta \cdot \varepsilon_i),$$

et

$$d^2\tilde{f}(a\cos\varrho; \eta\sin\varrho) = \sin^2\varrho \sum_{i,j=1}^{q-1} \frac{\partial^2 \tilde{f}}{\partial x_i \partial x_j}(a\cos\varrho)(\eta \cdot \varepsilon_i)(\eta \cdot \varepsilon_j).$$

Pour $i = 1, \cdots, q-1$ on a

$$\frac{1}{\|\omega_{q-1}\|} \int_{\eta \cdot a = 0} (\eta \cdot \varepsilon_i) \, d\omega_{q-1}(\eta) = 0, \quad \frac{1}{\|\omega_{q-1}\|} \int_{\eta \cdot a = 0} (\eta \cdot \varepsilon_i)(\eta \cdot \varepsilon_j) \, d\omega_{q-1}(\eta) = \frac{\delta_{ij}}{q-1},$$

donc, en formant la moyenne sur $\eta \cdot a = 0$ dans (7), on obtient

$$\mathscr{M}_f^\varrho(a) - \tilde{f}(a\cos\varrho) = \frac{\sin^2\varrho}{2(q-1)} \sum_{i=1}^{q-1} \frac{\partial^2 \tilde{f}}{\partial x_i^2}(a\cos\varrho) + \tfrac{1}{2}\sin^2\varrho\beta(a,\varrho), \qquad (8)$$

où nous avons posé

$$\beta(a,\varrho) = \frac{1}{\|\omega_{q-1}\|} \int_{\eta \cdot a = 0} \alpha(a,\eta,\varrho) \, d\omega_{q-1}(\eta). \qquad (9)$$

On voit que $\beta(a,\varrho) \to 0$ quand $\varrho \to 0$, uniformément pour $a \in \varkappa$.

La droite $\{\lambda a \mid \lambda \in \mathbf{R}\}$ est décrite par $\{(0, \cdots, 0, x_q) \mid x_q \in \mathbf{R}\}$, et puisque

$$\tilde{f}(0, \cdots, 0, x_q) = x_q f(a)$$

pour $x_q > 0$, on conclut que

$$\frac{\partial^2 \tilde{f}}{\partial x_q^2}(a\cos\varrho) = \frac{\partial^2 \tilde{f}}{\partial x_q^2}(0, \cdots, 0, \cos\varrho) = 0.$$

Par conséquent (8) s'écrit

$$\mathscr{M}_f^\varrho(a) - \cos\varrho f(a) = \frac{\sin^2\varrho}{2(q-1)} \Delta_q \tilde{f}(a\cos\varrho) + \tfrac{1}{2}\sin^2\varrho\beta(a,\varrho). \qquad (10)$$

D'après (3) de la proposition 2.6 on a

$$\Delta_q \tilde{f}(a \cos \varrho) = \frac{q-1}{\cos \varrho} f(a) + \frac{1}{\cos \varrho} \Delta_q^* f(a),$$

et par suite

$$\frac{2}{\sin^2 \varrho} (\mathscr{M}_f^\varrho(a) - \cos \varrho f(a)) = \frac{1}{\cos \varrho} \left(f(a) + \frac{1}{q-1} \Delta_q^* f(a) \right) + \beta(a, \varrho), \quad (11)$$

d'où

$$D_q^* f(a) = \frac{2 \cos \varrho}{\sin^2 \varrho} (\mathscr{M}_f^\varrho(a) - \cos \varrho f(a)) - \cos \varrho \beta(a, \varrho), \quad (12)$$

ce qui entraîne le théorème. /

Remarquons que le lemme 4.2 et le théorème 4.3 entraînent (5) de la proposition 2.6 avec Δ_q^* remplacé par D_q^*, et par conséquent aussi (5) lui-même.

DÉFINITION : *On dit qu'une fonction $f : \omega \to \mathbf{R}$ définie dans un ouvert ω de Ω_q est harmonique dans ω, si elle est continue, et si elle vérifie les conditions équivalentes :*

(i) *Pour tout $C(a, \varrho) \subseteq \omega$ où $\varrho \in]0, \frac{1}{2}\pi[$ on a*
$$\mathscr{M}_f^\varrho(a) = \cos \varrho f(a).$$

(ii) *Pour tout $C(a, \varrho) \subseteq \omega$ où $\varrho \in]0, \frac{1}{2}\pi[$ on a*
$$\mathscr{A}_f^\varrho(a) = \frac{\sin^{q-1}}{q-1} f(a).$$

Que (i) entraîne (ii) résulte de la formule (6). Inversement si (ii) est remplit, et si $a \in \omega$ est fixe, on conclut que

$$\int_0^\varrho \sin^{q-2} u \mathscr{M}_f^u(a) \, du = \frac{\sin^{q-1} \varrho}{q-1} f(a)$$

pour $\varrho \in]0, \varrho_0[$, où $\varrho_0 = \sup \{ \varrho \in]0, \frac{1}{2}\pi[\mid C(a, \varrho) \subseteq \omega \}$, ce qui par dérivation entraîne (i).

PROPOSITION 4.4. *Soit f une fonction harmonique dans l'ouvert $\omega \subseteq \Omega_q$. Alors f est indéfiniment dérivable dans ω et $D_q^* f(a) = 0$ pour tout $a \in \omega$.*

La démonstration de l'énoncé $f \in C^\infty(\omega)$ se fait exactement comme dans la théorie classique, à l'aide de l'unité approchée $(\varphi_\varepsilon)_{\varepsilon \in]0, 1[}$ de Ω_q. En vertu du théorème 4.3 il est évident que $D_q^* f(a) = 0$ pour tout $a \in \omega$.

La théorie des fonctions harmoniques s'achève par la proposition inverse :

PROPOSITION 4.5. *Soit ω un ouvert de Ω_q, et soit $f \in C^2(\omega)$ une fonction telle que $D_q^* f(a) = 0$ pour tout $a \in \omega$. Alors f est harmonique dans ω.*

Démonstration: Soit $a \in \omega$ et posons

$$\varrho_0 = \sup\{\varrho \in]0, \tfrac{1}{2}\pi[\mid C(a, \varrho) \subseteq \omega\}.$$

Soit $\varphi : \mathring{C}(a, \varrho_0) \to \mathbf{R}$ la fonction définie dans l'intérieur de $C(a, \varrho_0)$ par (cf. le lemme 4.1)

$$\varphi(\xi) = \int\limits_{O(q, a)} f(A\xi) d\mu(A) = \begin{cases} \mathcal{M}_f^\varrho(a), & \text{si } \xi \neq a, \varrho = \text{Arccos}(a \cdot \xi). \\ f(a), & \text{si } \xi = a. \end{cases}$$

La fonction φ est de la classe C^2 dans l'ouvert $\mathring{C}(a, \varrho_0)$, et en vertu de (6) de la proposition 2.6 on a

$$D_q^* \varphi(\xi) = \int\limits_{O(q, a)} D_q^*(f \circ A)(\xi) d\mu(A) = \int\limits_{O(q, a)} D_q^* f(A\xi) d\mu(A) = 0. \tag{13}$$

En outre φ ne dépend que de $t = a \cdot \xi$, c'est-à-dire φ est constante sur les cercles sphériques $S(a, \varrho)$ où $\varrho < \varrho_0$.

(a) *Soit $q = 2$.* Nous paramétrisons $\mathring{C}(a, \varrho_0)$ par $(\cos\varrho, \sin\varrho)$, $\varrho \in]-\varrho_0, \varrho_0[$, et considérons φ comme fonction de ϱ. D'après (13) on a alors

$$\varphi''(\varrho) + \varphi(\varrho) = 0, \quad \varrho \in]-\varrho_0, \varrho_0[, \tag{14}$$

et puisque $\varphi(\varrho) = \varphi(-\varrho)$ et $\varphi(0) = f(a)$, on obtient

$$\varphi(\varrho) = f(a)\cos\varrho. \tag{15}$$

(b) *Soit $q \geq 3$.* Utilisons la représentation paramétrique de $\mathring{C}(a, \varrho_0) \backslash \{a\}$:

$$\xi = ta + (1 - t^2)^{\frac{1}{2}}\eta \quad \text{où} \quad t \in]\cos\varrho_0, 1[, \quad \eta \cdot a = 0.$$

Alors d'après (13), et (4) de la proposition 2.6 on a

$$(1 - t^2)\frac{d^2\varphi}{dt^2} - (q - 1)t\frac{d\varphi}{dt} + (q - 1)\varphi(t) = 0, \quad t \in]\cos\varrho_0, 1[,$$

parce que φ ne dépend pas de η. Selon le lemme 3.6 il existe deux constantes $k_1, k_2 \in \mathbf{R}$ telles que

$$\varphi(t) = k_1 t + k_2 \varphi_q(t), \quad t \in \,]\cos \varrho_0, 1[\,.$$

Quand $t \to 1$ on a $\varphi(t) \to f(a)$, tandis que $\varphi_q(t) \to \infty$. Il en découle que $k_2 = 0$, et que

$$\varphi(t) = f(a)t, \quad t \in \,]\cos \varrho_0, 1[\,. \tag{16}$$

Les formules (15) et (16) s'expriment

$$\mathscr{M}_f^\varrho(a) = \cos \varrho f(a), \quad \varrho \in \,]0, \varrho_0[\,,$$

ce qui démontre la proposition. /

Soit ω un ouvert de Ω_q. On désigne par K_ω le cône ouvert de base ω et de sommet 0, i.e.

$$K_\omega = \{\lambda \xi \mid \lambda > 0, \xi \in \omega\}.$$

Une fonction $f : \omega \to \mathbf{R}$ se prolonge par homogénéité positive à la fonction $\tilde{f} : K_\omega \to \mathbf{R}$ donnée par

$$\tilde{f}(\lambda \xi) = \lambda f(\xi).$$

Alors on a $f \in C^p(\omega)$ si et seulement si $\tilde{f} \in C^p(K_\omega)$ pour $p = 0, 1, \cdots, \infty$, et si $f \in C^2(\omega)$ on sait que

$$\Delta_q \tilde{f}(r\xi) = \frac{q-1}{r} D_q^* f(\xi) \quad \text{pour} \quad r > 0, \xi \in \omega.$$

Donc

$$D_q^* f \begin{Bmatrix} \geq \\ = \\ \leq \end{Bmatrix} 0 \text{ dans } \omega, \text{ si et seulement si } \Delta_q \tilde{f} \begin{Bmatrix} \geq \\ = \\ \leq \end{Bmatrix} 0 \text{ dans } K_\omega. \tag{17}$$

Résumons les résultats précédents dans le théorème suivant:

THÉORÈME 4.6. *Soient ω un ouvert de Ω_q, $f \in C^\infty(\omega)$. Les propriétés suivantes sont équivalentes à l'harmonicité de f dans ω:*

(i) *Pour tout $C(a, \varrho) \subseteq \omega$ où $\varrho \in \,]0, \frac{1}{2}\pi[$ on a*
$$\mathscr{M}_f^\varrho(a) = \cos \varrho f(a).$$

(ii) *Pour tout $C(a, \varrho) \subseteq \omega$ où $\varrho \in \,]0, \frac{1}{2}\pi[$ on a*
$$\mathscr{A}_f^\varrho(a) = \frac{\sin^{q-1}\varrho}{q-1} f(a).$$

(iii) *Pour tout $a \in \omega$ on a $D_q^* f(a) = 0$.*

(iv) *La fonction prolongée $\tilde{f}$ est harmonique au sens classique dans K_ω.*

D'après le corollaire 2.15 les fonctions harmoniques dans tout Ω_q sont les fonctions $H_1 = \{a \cdot \xi \mid a \in \mathbf{R}^q\}$. Dans un ouvert différent de Ω_q il y a par contre plus de fonctions harmoniques que celles-ci. Par exemple dans $\Omega_q \setminus \{a, -a\}$ on a la fonction harmonique $\xi \mapsto \varphi_q(a \cdot \xi)$, où φ_q est la solution du lemme 3.6.

Remarquons que les fonctions harmoniques dans un ouvert connexe ω différent de Ω_q satisfont aux axiomes de M. Brelot [5] comme démontré par R. M. Hervé [13]. Par conséquent on pourrait compléter la précédente par plusieurs théorèmes, par exemple par le principe du maximum.

§ 2. *Fonctions sousharmoniques dans Ω_q*

DÉFINITION: *Soit ω un ouvert de Ω_q. On dit qu'une fonction $f : \omega \to \mathbf{R} \cup \{-\infty\}$ est sousharmonique dans ω, si elle vérifie les conditions suivantes:*

(i)   *La fonction f est semi-continue supérieurement.*

(ii)   *La fonction f est localement ω_q-intégrable.*

(iii)   *Pour tout $C(a,\varrho) \subseteq \omega$ où $\varrho \in \,]0, \tfrac{1}{2}\pi[$ on a*
$$\cos \varrho f(a) \leq \mathscr{M}_f^{\varrho}(a).$$

On dit qu'une fonction $f : \omega \to \mathbf{R} \cup \{\infty\}$ est *surharmonique* dans ω, si $-f$ est sousharmonique dans ω. Donc, une fonction $f : \omega \to \mathbf{R} \cup \{\pm\infty\}$ est harmonique dans ω, si et seulement si f est à la fois sousharmonique et surharmonique dans ω.

Si f est sousharmonique il résulte de (6) qu'on a pour tout $C(a,\varrho) \subseteq \omega$ où $\varrho \in \,]0, \tfrac{1}{2}\pi[$
$$\frac{\sin^{q-1}\varrho}{q-1} f(a) \leq \mathscr{A}_f^{\varrho}(a). \tag{18}$$

Si on supprime la condition (ii), on appelle f sousharmonique au sens large, et on montre – exactement comme chez M. Brelot [6] p. 22 – qu'une fonction sousharmonique au sens large est ou bien localement ω_q-intégrable ou bien identique à $-\infty$ dans chaque composante connexe de ω.

PROPOSITION 4.7. *Soit ω un ouvert de Ω_q, et soit f une fonction sousharmonique dans ω. Alors pour tout $a \in \omega$ on a*
$$\lim_{\varrho \to 0} \frac{q-1}{\sin^{q-1}\varrho} \mathscr{A}_f^{\varrho}(a) = f(a).$$

Démonstration: Soient $a \in \omega$, $\varrho \in]0, \frac{1}{2}\pi[$. Nous savons que

$$\frac{m(\varrho)}{\|\omega_{q-1}\|} = \int_{\cos\varrho}^{1} (1 - t^2)^{\frac{1}{2}(q-3)} \, dt, \qquad \frac{\sin^{q-1}\varrho}{q-1} = \int_{\cos\varrho}^{1} t(1 - t^2)^{\frac{1}{2}(q-3)} \, dt,$$

et par conséquent

$$\frac{m(\varrho)\cos\varrho}{\|\omega_{q-1}\|} \leqq \frac{\sin^{q-1}\varrho}{q-1} \leqq \frac{m(\varrho)}{\|\omega_{q-1}\|},$$

donc

$$1 \leqq \frac{(q-1)m(\varrho)}{\|\omega_{q-1}\|\sin^{q-1}\varrho} \leqq \frac{1}{\cos\varrho}.$$

Soit $k > f(a) \geqq 0$. Choisissons un $\delta < 1$ tel que $k\delta > f(a)$. Puisque f est semicontinue supérieurement, il existe un $\varrho_0 \in]0, \frac{1}{2}\pi[$ tel que $C(a, \varrho_0) \subseteq \omega$ et $f(\xi) < k\delta$ pour tout $\xi \in C(a, \varrho_0)$. Donc

$$\frac{\|\omega_{q-1}\|}{m(\varrho)} \mathscr{A}_f^\varrho(a) \leqq k\delta$$

pour tout $\varrho \leqq \varrho_0$, et par conséquent d'après (18)

$$f(a) \leqq \frac{q-1}{\sin^{q-1}\varrho} \mathscr{A}_f^\varrho(a) \leqq \frac{(q-1)m(\varrho)}{\|\omega_{q-1}\|\sin^{q-1}\varrho} k\delta \leqq \frac{k\delta}{\cos\varrho} \leqq k,$$

dès que $\varrho \leqq \varrho_0$ et $\cos\varrho \geqq \delta$. Puisque $k > f(a)$ était arbitraire, la proposition est prouvée. Si $f(a) < 0$ on procède pareillement. /

COROLLAIRE 4.8. *Soient f et g deux fonctions sousharmoniques dans un ouvert ω de Ω_q. Si f et g sont égaux ω_q-presque partout dans ω, ils sont identiques dans ω.*

Ce corollaire sera très important dans la suite.

Nous allons démontrer un théorème sur les fonctions sousharmoniques correspondant au théorème 4.6 (pour la notation cf. ce théorème).

THÉORÈME 4.9. *Soit ω un ouvert de Ω_q, et soit $f \in C^2(\omega)$. Les conditions suivantes sont équivalentes*:

(i)   *La fonction f est sousharmonique dans ω.*

(ii) *Pour tout $a \in \omega$ on a $D_q^* f(a) \geqq 0$.*

(iii) *La fonction $\tilde{f}$ est sousharmonique au sens classique dans K_ω.*

Démonstration: De (17) on voit que (ii) est équivalent à (iii), et c'est une conséquence immédiate du théorème 4.3 que (i) entraîne (ii). Il n'est pas si facile de démontrer que (ii) entraîne (i). L'assertion est un cas particulier de la théorie générale, développée par R. M. Hervé [13], pour les solutions d'une équation $\Phi f + c f \geqq 0$, où Φ est un opérateur différentiel du second ordre, de type elliptique, et où c est une constante. L'idée de la démonstration est d'utiliser le principe du maximum de E. Hopf, qui est valable quand $c \leqq 0$. Dans le cas $c > 0$ (comme ici) il faut procéder autrement, soit par un lemme de D. Gilbarg et J. Serrin (cf. [13] § 34).

Cependant, dans notre cas simple, une démonstration élémentaire se fait. Nous aurons besoin du principe du maximum pour les fonctions positivement homogènes et sousharmoniques dans $\mathbf{R}^q$.

LEMME 4.10. *Dans l'hyperplan* $x_q = 1$ *de* $\mathbf{R}^q$ *on considère pour* $k > 0$ *la boule*

$$B_k = \left\{ x \in \mathbf{R}^q \mid x_q = 1, \sum_{i=1}^{q-1} x_i^2 \leqq k^2 \right\},$$

qui est la base du cône $C_k = \{ \lambda x \mid \lambda \geqq 0, \ x \in B_k \}$. *Soit* $F : C_k \to \mathbf{R}$ *une fonction continue et positivement homogène. On suppose de plus* $F \in C^2(\mathring{C}_k)$ *et* $\varDelta_q F(x) \geqq 0$ *pour tout* $x \in \mathring{C}_k$. *Si* $F \leqq 0$ *sur la frontière du cône, alors* $F \leqq 0$ *dans* C_k.

Démonstration: Soit $(u_1, \cdots, u_{q-1}, 1) \in B_k$. Nous posons

$$f(u_1, \cdots, u_{q-1}) = F(u_1, \cdots, u_{q-1}, 1),$$

alors f est une fonction continue dans B_k, et $f \in C^2(\mathring{B}_k)$.

Il suffit de montrer $f \leqq 0$ dans B_k. Si $x \in \mathring{C}_k$ alors $x_q > 0$, et grâce à l'homogénéité de F on a

$$x_q f \left(\frac{x_1}{x_q}, \cdots, \frac{x_{q-1}}{x_q} \right) = F(x_1, \cdots, x_q). \tag{19}$$

Un calcul facile montre

$$\varDelta_q F(x_1, \cdots, x_q) = \sum_{i=1}^{q-1} \left(\frac{1}{x_q} + \frac{x_i^2}{x_q^3} \right) \frac{\partial^2 f}{\partial u_i^2} \left(\frac{x_1}{x_q}, \cdots, \frac{x_{q-1}}{x_q} \right) + \sum_{\substack{i,j=1 \\ i \neq j}}^{q-1} \frac{x_i x_j}{x_q^3} \frac{\partial^2 f}{\partial u_i \partial u_j} \left(\frac{x_1}{x_q}, \cdots, \frac{x_{q-1}}{x_q} \right), \tag{20}$$

et si $x_q = 1$, $u_i = x_i$ pour $i = 1, \cdots, q-1$, la formule (20) se réduit à

$$\varDelta_q F(x_1, \cdots, x_{q-1}, 1) = \sum_{i=1}^{q-1} (1 + u_i^2) \frac{\partial^2 f}{\partial u_i^2} (u_1, \cdots, u_{q-1}) + \sum_{\substack{i,j=1 \\ i \neq j}}^{q-1} u_i u_j \frac{\partial^2 f}{\partial u_i \partial u_j} (u_1, \cdots, u_{q-1}). \tag{21}$$

Nous sommes conduits à considérer l'opérateur différentiel L du second ordre dans $\mathring{B}_k$, donné par

$$L = \sum_{i,\,j\,=\,1}^{q-1} a_{ij} \frac{\partial^2}{\partial u_i\,\partial u_j}, \quad \text{où} \quad a_{ij} = \begin{cases} 1 + u_i^2 & \text{si} \quad i = j. \\ u_i u_j & \text{si} \quad i \neq j. \end{cases}$$

L'opérateur L est de type elliptique, et nous savons que $Lf \geq 0$ dans $\mathring{B}_k$. Le principe du maximum de E. Hopf (cf. [12] p. 86) valable pour f, entraîne l'impossibilité d'un maximum sans constance au voisinage, et puisque $f \leq 0$ sur la frontière de B_k, il en résulte que $f \leq 0$ dans B_k. |

Retournons à la démonstration du fait que (ii) entraîne (i) du théorème 4.9.

Soient $a \in \omega$, $C(a, \varrho_0) \subseteq \omega$. Nous allons démontrer que

$$\cos \varrho_0 f(a) \leq \mathscr{M}_f^{\varrho_0}(a).$$

Soit $\varphi : C(a, \varrho_0) \to \mathbf{R}$ la fonction définie par

$$\varphi(\xi) = \int_{O(q,a)} f(A\xi)\,d\mu(A) = \begin{cases} \mathscr{M}_f^{\varrho}(a) & \text{si} \quad \xi \neq a, \quad \varrho = \text{Arccos}(a \cdot \xi). \\ f(a) & \text{si} \quad \xi = a. \end{cases}$$

On voit que φ est continue dans $C(a, \varrho_0)$, de la classe C^2 dans $\mathring{C}(a, \varrho_0)$, et que $D_q^*\varphi \geq 0$ dans $\mathring{C}(a, \varrho_0)$ (cf. la proposition 4.5).

Soit $\psi : C(a, \varrho_0) \to \mathbf{R}$ définie par

$$\psi(\xi) = \varphi(\xi) - \frac{a \cdot \xi}{\cos \varrho_0} \mathscr{M}_f^{\varrho_0}(a).$$

Alors ψ est continue dans $C(a, \varrho_0)$ et $\psi \in C^2(\mathring{C}(a, \varrho_0))$. De plus on a $\psi = 0$ sur la frontière de $C(a, \varrho_0)$, et $D_q^*\psi = D_q^*\varphi \geq 0$ dans $\mathring{C}(a, \varrho_0)$, parce que $a \cdot \xi$ est harmonique dans $\mathring{C}(a, \varrho_0)$.

Soit $\tilde{\psi} : K_{C(a,\varrho_0)} \to \mathbf{R}$ la fonction définie dans le cône

$$K_{C(a,\varrho_0)} = \{\lambda \xi \,|\, \lambda \geq 0, \xi \in C(a, \varrho_0)\}$$

par $\tilde{\psi}(\lambda \xi) = \lambda \psi(\xi)$. D'après (17) la fonction $\tilde{\psi}$ satisfait aux conditions du lemme 4.10 – $\tilde{\psi}$ est même nulle sur la frontière du cône – et on y conclut

$$\varphi(\xi) \leq \frac{a \cdot \xi}{\cos \varrho_0} \mathscr{M}_f^{\varrho_0}(a) \quad \text{pour tout } \xi \in C(a, \varrho_0).$$

Posant $\xi = a$, on obtient l'inégalité désirée

$$\cos \varrho_0 f(a) \leq \mathscr{M}_f^{\varrho_0}(a). \,|$$

(Si on pose $\cos\varrho = a \cdot \xi$, on obtient

$$\frac{\mathscr{M}_f^0(a)}{\cos\varrho} \leqq \frac{\mathscr{M}_f^0(a)}{\cos\varrho_0} \quad \text{pour} \quad \varrho \in \,]0, \varrho_0[,$$

i.e. l'application

$$\varrho \longmapsto \frac{\mathscr{M}_f^0(a)}{\cos\varrho}$$

est croissante. Il n'est pas difficile d'étendre ce résultat à toute fonction sousharmonique.)

Remarque: Le théorème 4.9 reste valable pour toute fonction $f: \omega \to \mathbf{R} \cup \{-\infty\}$ semi-continue supérieurement et localement ω_q-intégrable, si on exprime la condition (ii) en disant que $D_q^* f$ est une distribution positive.

Nous n'entrons pas dans la démonstration, parce que nous n'utiliserons pas cette extension du théorème 4.9 dans la suite.

§3. *Potentiels sphériques*

DÉFINITION: *Étant donnée une mesure positive μ sur Ω_q, on appelle potentiel sphérique de μ la fonction $S^\mu = g_q * \mu : \Omega_q \to \mathbf{R} \cup \{-\infty\}$. Pour tout $\xi \in \Omega_q$ on a*

$$S^\mu(\xi) = \frac{1}{\|\omega_{q-1}\|} \int_{\Omega_q} g_q(\xi \cdot \eta)\, d\mu(\eta).$$

En vertu des propriétés de g_q on a pour toute mesure positive $\mu \in \mathscr{M}_+(\Omega_q)$:

(i) *Le potentiel sphérique S^μ est semi-continu supérieurement. Dans deux dimensions ($q = 2$) il est même continu.*

(ii) *Le potentiel sphérique S^μ est indéfiniment dérivable dans le complémentaire du support de μ.*

(iii) *Le potentiel sphérique S^μ est ω_q-intégrable, i.e. $S^\mu \in \mathscr{L}^1(\Omega_q)$. (Cf. la proposition 2.8.)*

Nous allons démontrer un théorème sur la continuité d'un potentiel sphérique. Il est analogue au théorème dû à G. C. Evans et F. Vasilesco (cf. [6] p. 49) valable pour les potentiels classiques. Notre outil sera le corollaire 3.9, qui nous permet de démontrer le lemme suivant.

LEMME 4.11. *Soient μ une mesure positive sur Ω_q, $\varkappa$ un compact de Ω_q contenant le support de μ. Pour un $\xi \in \Omega_q$ on choisit un $\eta \in \varkappa$ tel que*

$$\text{Arccos}(\xi \cdot \eta) = \inf_{\sigma \in \varkappa} \text{Arccos}(\xi \cdot \sigma).$$

Alors

$$S^\mu(\xi) + A_q \frac{\|\mu\|}{\|\omega_{q-1}\|} \geqq B_q S^\mu(\eta).$$

Démonstration: Soit $\sigma \in \varkappa$. Alors

$$\text{Arccos}(\eta \cdot \sigma) \leqq \text{Arccos}(\eta \cdot \xi) + \text{Arccos}(\xi \cdot \sigma) \leqq 2\text{Arccos}(\xi \cdot \sigma).$$

Si $\text{Arccos}(\xi \cdot \sigma) \in [0, \frac{1}{2}\pi]$ alors $t = \xi \cdot \sigma \in [0, 1]$ et

$$s = \eta \cdot \sigma \geqq \cos(2\text{Arccos}(\xi \cdot \sigma)) = 2t^2 - 1.$$

Donc, d'après 3.9

$$g_q(\xi \cdot \sigma) + A_q \geqq B_q g_q(\eta \cdot \sigma). \tag{22}$$

Si $\text{Arccos}(\xi \cdot \sigma) \in]\frac{1}{2}\pi, \pi]$ alors $t = \xi \cdot \sigma \in [-1, 0[$, donc $t = \xi \cdot \sigma < t_q$ (t_q du corollaire 3.9), et par conséquent (22) subsiste encore. Puisque (22) est valable pour tout $\sigma \in \varkappa$, on obtient

$$\int_\varkappa g_q(\xi \cdot \sigma) \, d\mu(\sigma) + A_q \|\mu\| \geqq B_q \int_\varkappa g_q(\eta \cdot \sigma) \, d\mu(\sigma),$$

d'où

$$S^\mu(\xi) + A_q \frac{\|\mu\|}{\|\omega_{q-1}\|} \geqq B_q S^\mu(\eta). \; \vert$$

THÉORÈME 4.12. *Soient μ une mesure positive sur Ω_q, $\varkappa = \text{supp}(\mu)$ son support compact. Soit $P \colon \varkappa \to \mathbf{R} \cup \{-\infty\}$ la restriction de S^μ à $\varkappa$.*

Si P est continue en un point $\xi_0 \in \varkappa$, alors S^μ est continue en ξ_0.

Le théorème est sans intérêt pour $q = 2$, parce que tout potentiel sphérique sur Ω_2 est continu.

Démonstration: Soit $q \geqq 3$, et soit P continue en $\xi_0 \in \varkappa$. Implicitement $P(\xi_0) = S^\mu(\xi_0)$ est fini, c'est-à-dire $g_q(\xi_0 \cdot)$ est μ-intégrable. On en déduit que

$$\{\xi_0\} \text{ est } \mu\text{-négligeable},$$

car il existe une constante k telle que $g_q + k \leqq 0$ sur $[-1, 1]$, d'où

$$g_q(\xi_0 \cdot \eta) + k \leqq -n 1_{\{\xi_0\}}(\eta) \quad \text{pour tout } n \in \mathbf{N},$$

parce que $g_q(1) = -\infty$. Par conséquent on a

$$\int\limits_{\Omega_q} g_q(\xi_0 \cdot \eta)\,d\mu(\eta) + k\,\|\mu\| \leqq -n\mu(\{\xi_0\}) \quad \text{pour tout } n \in \mathbf{N},$$

ce qui entraîne $\mu(\{\xi_0\}) = 0$.

Soit B un disque sphérique ouvert quelconque de centre ξ_0, alors on a

$$\int\limits_B g_q(\xi_0 \cdot \eta)\,d\mu(\eta) \to 0 \quad \text{et} \quad \int\limits_B d\mu(\eta) \to 0, \tag{23}$$

quand le rayon sphérique de B tend vers zéro.

Soient μ_B et μ_{CB} les mesures induites par μ sur B et sur $CB = \Omega_q \setminus B$. Alors (23) s'exprime

$$S^{\mu_B}(\xi_0) \to 0 \quad \text{et} \quad \|\mu_B\| \to 0, \tag{24}$$

quand le rayon sphérique de B tend vers zéro.

Soit $\varepsilon > 0$, et choisissons B suffisamment petit pour que

$$|S^{\mu_B}(\xi_0)| < \varepsilon \quad \text{et} \quad \|\mu_B\| < \varepsilon. \tag{25}$$

Le potentiel sphérique $S^{\mu_{CB}}$ est continu dans B. Puisque

$$S^\mu = S^{\mu_B} + S^{\mu_{CB}},$$

l'hypothèse entraîne la continuité en ξ_0 de la restriction de S^{μ_B} à $\varkappa$, donc il existe un $\varrho_0 \in {]0, \tfrac{1}{2}\pi[}$ tel que

$$|S^{\mu_B}(\xi)| < 2\varepsilon \quad \text{pour tout} \quad \xi \in C(\xi_0, \varrho_0) \cap \varkappa. \tag{26}$$

À tout $\xi \in \Omega_q$ on choisit $\eta \in \varkappa$ tel que

$$\mathrm{Arccos}(\xi \cdot \eta) = \inf_{\sigma \in \varkappa} \mathrm{Arccos}(\xi \cdot \sigma).$$

Alors $\xi \in C(\xi_0, \tfrac{1}{2}\varrho_0)$ entraîne $\eta \in C(\xi_0, \varrho_0)$, et par conséquent on trouve d'après 4.11

$$S^{\mu_B}(\xi) \geqq B_q S^{\mu_B}(\eta) - A_q \frac{\|\mu_B\|}{\|\omega_{q-1}\|} \geqq -\varepsilon\left(2B_q + \frac{A_q}{\|\omega_{q-1}\|}\right). \tag{27}$$

Puisque S^{μ_B} est semi-continue supérieurement en ξ_0, il existe un $\varrho_1 \in {]0, \tfrac{1}{2}\pi[}$ tel que

$$S^{\mu_B}(\xi) < S^{\mu_B}(\xi_0) + \varepsilon < 2\varepsilon \quad \text{pour tout} \quad \xi \in C(\xi_0, \varrho_1). \tag{28}$$

En somme nous avons démontré:

Quel que soit $\varepsilon > 0$, il existe un disque sphérique ouvert B de centre ξ_0, et un $\varrho_0 \in \,]0, \tfrac{1}{2}\pi[$ tels que $\xi \in C(\xi_0, \varrho_0)$ entraîne $|S^{\mu_B}(\xi)| < \tfrac{1}{3}\varepsilon$.

Par suite pour $\xi \in C(\xi_0, \varrho_0)$ on a

$$|S^{\mu}(\xi) - S^{\mu}(\xi_0)| \leqq |S^{\mu_{CB}}(\xi) - S^{\mu_{CB}}(\xi_0)| + |S^{\mu_B}(\xi)| + |S^{\mu_B}(\xi_0)| < \varepsilon,$$

si

$$|S^{\mu_{CB}}(\xi) - S^{\mu_{CB}}(\xi_0)| < \tfrac{1}{3}\varepsilon,$$

ce qui est remplit dans un voisinage de ξ_0. La continuité de S^{μ} en ξ_0 est démontrée. /

COROLLAIRE 4.13. *Soient $a \in \Omega_q$, $\varrho \in \,]0, \tfrac{1}{2}\pi[$ et σ_ϱ la mesure de surface ordinaire sur le cercle sphérique $S(a, \varrho)$. Alors le potentiel sphérique S^{σ_ϱ} est continu sur Ω_q.*

Démonstration: Nous supposons $q \geqq 3$. La mesure σ_ϱ est invariante par rapport au groupe $O(q, a)$ (cf. le lemme 4.1), ce qui montre la constance de S^{σ_ϱ} sur $S(a, \varrho)$. Cette constante est finie parce que

$$g_q(t)(1 - t^2)^{\frac{1}{2}(q-4)}$$

est intégrable sur $[-1, 1]$ d'après 3.3. La restriction de S^{σ_ϱ} à $S(a, \varrho)$ est par conséquent continue en tout point de $S(a, \varrho)$, ce qui entraîne la continuité de S^{σ_ϱ}. /

Le noyau sphérique $\eta \longmapsto g_q(\xi \cdot \eta)$ est surharmonique dans l'ouvert $\{\eta \in \Omega_q \,|\, \xi \cdot \eta > 0\}$ et sousharmonique dans l'ouvert $\{\eta \in \Omega_q \,|\, \xi \cdot \eta < 0\}$ en vertu de 3.5 et de 4.9.

Le noyau classique $y \longmapsto - \|x - y\|^{2-q}$ est sousharmonique dans tout l'espace $\mathbf{R}^q$.

À cause de cette différence un potentiel sphérique n'est pas nécessairement sousharmonique, mais nous allons démontrer que cette défaut disparaît, si on considère seulement des mesures positives admettant 0 pour barycentre.

LEMME 4.14. *Pour tout $\varrho \in \,]0, \tfrac{1}{2}\pi[$ il existe une constante réelle k_ϱ telle que pour tout $a, \xi \in \Omega_q$, on ait*

$$\mathscr{M}^o_{g_q(\xi \cdot)}(a) - \cos \varrho \, g_q(\xi \cdot a) \geqq k_\varrho \, \xi \cdot a.$$

Démonstration: (a) *Soit $q = 2$*. Écrivons $a = e^{i\alpha}$ et $\xi = e^{i\varphi}$ où $\alpha, \varphi \in [0, 2\pi[$. Alors $a \cdot \xi = \cos(\alpha - \varphi)$. Le membre gauche de l'inégalité cherchée est

$$\tfrac{1}{2}g_2(\cos(\alpha - \varphi + \varrho)) + \tfrac{1}{2}g_2(\cos(\alpha - \varphi - \varrho)) - \cos\varrho\, g_2(\cos(\alpha - \varphi)),$$

et en utilisant la formule

$$g_2(\cos\theta) = \frac{1}{\pi}((\pi - \theta)\sin\theta - \tfrac{1}{2}\cos\theta)$$

on le réduit sans peine à

$$-\frac{\varrho\sin\varrho}{\pi}\cos(\alpha - \varphi),$$

ce qui démontre l'inégalité, étant une égalité avec

$$k_\varrho = -\frac{\varrho\sin\varrho}{\pi}.$$

(b) *Soit* $q \geqq 3$. Pour des $a \in \Omega_q$ et $\varrho \in \,]0,\tfrac{1}{2}\pi[$ fixes, nous considérons la fonction de Ω_q dans **R** donnée par

$$\xi \longmapsto \mathscr{M}^\varrho_{g_q(\xi\,\cdot\,)}(a).$$

Elle ne dépend que de $a\cdot\xi$. Puisqu'on a

$$\mathscr{M}^\varrho_{g_q(\xi\,\cdot\,)}(a) = \frac{\sin^{2-q}\varrho}{\|\omega_{q-1}\|}\int_{S(a,\varrho)} g_q(\xi\cdot\eta)\,d\sigma_\varrho(\eta) = \sin^{2-q}\varrho\, S^{\sigma_\varrho}(\xi),$$

on conclut que la fonction considérée est continue dans Ω_q, indéfiniment dérivable dans $\Omega_q\setminus S(a,\varrho)$, et là satisfaisant à

$$D^*_\xi\{\mathscr{M}^\varrho_{g_q(\xi\,\cdot\,)}(a)\} = \frac{\sin^{2-q}\varrho}{\|\omega_{q-1}\|}\int_{S(a,\varrho)} D^*_\xi\{g_q(\xi\cdot\eta)\}\,d\sigma_\varrho(\eta)$$

$$= \frac{-q\sin^{2-q}\varrho}{\|\omega_q\|}\int_{S(a,\varrho)} (\xi\cdot\eta)\,d\sigma_\varrho(\eta) = \frac{-q\|\omega_{q-1}\|\cos\varrho}{\|\omega_q\|}a\cdot\xi$$

en vertu de 3.5.

Par conséquent, si nous posons $s = \cos\varrho$, $t = a\cdot\xi$ et considérons la fonction $f_s : [-1,1] \to$ **R** donnée par

$$f_s(t) = \mathscr{M}^\varrho_{g_q(\xi\,\cdot\,)}(a),$$

nous savons que f_s est une fonction continue dans $[-1,1]$, indéfiniment dérivable dans $]-1,s[$ et $]s,1[$, et là satisfaisant à

$$(1 - t^2) f_s''(t) - (q - 1) t f_s'(t) + (q - 1) f_s(t) = \frac{- q(q - 1) \|\omega_{q-1}\| s}{\|\omega_q\|} t. \quad (29)$$

D'après 3.7 on sait que $-s \check{g}_q(t)$ et $s g_q(t)$ sont des solutions de (29) dans $]-1, 1[$, donc tous les solutions de (29) sont données d'une part comme

$$- s \check{g}_q(t) + c_1 t + c_2 \varphi_q(t), \quad c_1, c_2 \in \mathbf{R}, \quad (30)$$

d'autre part comme

$$s g_q(t) + d_1 t + d_2 \varphi_q(t), \quad d_1, d_2 \in \mathbf{R}, \quad (31)$$

où φ_q est la solution du lemme 3.6. Par conséquent il existe des constantes $c_1, c_2, d_1, d_2, \in \mathbf{R}$ telles que

$$f_s(t) = - s \check{g}_q(t) + c_1 t + c_2 \varphi_q(t) \qquad \text{pour} \quad t \in]s, 1[, \quad (32)$$

$$f_s(t) = s g_q(t) + d_1 t + d_2 \varphi_q(t) \qquad \text{pour} \quad t \in]-1, s[. \quad (33)$$

Faisant $t \to 1$ dans (32) et $t \to -1$ dans (33), nous concluons $c_2 = d_2 = 0$ d'après les propriétés de f_s, g_q et φ_q. Faisant $t \to s$, nous obtenons

$$f_s(s) = - s \check{g}_q(s) + c_1 s = s g_q(s) + d_1 s,$$

donc

$$c_1 - d_1 = g_q(s) + \check{g}_q(s) = h_q(s)$$

avec la notation de 3.7, et il en résulte que

$$f_s(t) - s g_q(t) = \begin{cases} d_1 t + t h_q(s) - s h_q(t) & \text{pour} \quad s \leqq t \leqq 1, \\ d_1 t & \text{pour} \quad -1 \leqq t \leqq s, \end{cases} \quad (34)$$

où

$$d_1 = \frac{f_s(s)}{s} - g_q(s) = \frac{1}{s} \frac{\|\omega_{q-2}\|}{\|\omega_{q-1}\|} \int_{-1}^{1} g_q(s^2 + (1 - s^2)\theta)(1 - \theta^2)^{\frac{1}{2}(q - 4)} \, d\theta - g_q(s).$$

La formule (34) montre le lemme avec $k_\varrho = d_1$, $s = \cos\varrho$ et $t = a \cdot \xi$, parce que $0 \leqq s \leqq t$ entraîne $t h_q(s) - s h_q(t) \geqq 0$ en vertu du lemme 3.7. /

THÉORÈME 4.15. *Soit μ une mesure positive sur Ω_q admettant 0 pour barycentre. Alors on a:*

(i) *Le potentiel sphérique S^μ de μ est sousharmonique dans Ω_q, harmonique dans le complémentaire du support de μ.*

(ii) *Au sens de distribution on a $D_q^* S^\mu = \mu$.*

Démonstration: (i) Pour établir la sousharmonicité de S^μ il reste à montrer la condition (iii) de la définition. Soient $a \in \Omega_q$, $\varrho \in]0, \frac{1}{2}\pi[$. Grâce au théorème de Fubini on a

$$\mathcal{M}^\varrho_{S^\mu}(a) = \frac{1}{\|\omega_{q-1}\|} \int\limits_{\Omega_q} \mathcal{M}^\varrho_{g_\eta(\xi \cdot)}(a)\, d\mu(\xi),$$

et par suite

$$\mathcal{M}^\varrho_{S^\mu}(a) - \cos\varrho\, S^\mu(a) = \frac{1}{\|\omega_{q-1}\|} \int\limits_{\Omega_\eta} \left\{ \mathcal{M}^\varrho_{g_\eta(\xi \cdot)}(a) - \cos\varrho\, g_q(\xi \cdot a) \right\} d\mu(\xi)$$

$$\geqq \frac{k_\varrho}{\|\omega_{q-1}\|} \int\limits_{\Omega_\eta} a \cdot \xi\, d\mu(\xi) = 0,$$

à cause du lemme 4.14. Nous avons déja observé que

$$S^\mu \in C^\infty(\Omega_q \setminus \mathrm{supp}(\mu)),$$

et si $\xi \in \Omega_q \setminus \mathrm{supp}(\mu)$ on trouve

$$D^*_q S^\mu(\xi) = \frac{1}{\|\omega_{q-1}\|} \int\limits_{\mathrm{supp}\,(\mu)} D^*_\xi \{ g_q(\xi \cdot \eta) \}\, d\mu(\eta) = \frac{-q}{\|\omega_q\|} \int\limits_{\mathrm{supp}\,(\mu)} \xi \cdot \eta\, d\mu(\eta) = 0,$$

ce qui par 4.6 entraîne l'harmonicité de S^μ dans le complémentaire du support de μ.

(ii) Soit $\mu \sim \sum_{n=0}^\infty S_n$ le développement de μ en série de fonctions sphériques. Le barycentre de μ est 0 si et seulement si $S_1 = 0$. D'après 2.12, 2.14 on sait que $D^*_q S^\mu = D^*_q (g_q * \mu)$ a le développement $S_0 + \sum_{n=2}^\infty S_n$, égal à celui de μ, donc $\mu = D^*_q S^\mu$. /

La proposition suivante est une généralisation du théorème 4.9.

PROPOSITION 4.16. *Soit* $T \in \mathscr{D}'(\Omega_q)$ *une distribution sur* Ω_q. *Les conditions suivantes sont équivalentes*:

(i) *La distribution* $D^*_q T$ *est positive.*

(ii) *La distribution* T *est une fonction sousharmonique.*

Démonstration: Nous montrons d'abord que (i) entraîne (ii). D'après 2.3 on sait que $D^*_q T$ est une mesure positive, posons $\mu = D^*_q T$. Soit $T \sim \sum_{n=0}^\infty S_n$ le développement de la distribution T en série de fonctions sphériques. Alors μ a le développement

$$\mu \sim \sum_{n=0}^{\infty} - \frac{(n-1)(n+q-1)}{q-1} S_n.$$

Dans ce développement le terme avec $n = 1$ est égal à 0, donc μ admet 0 pour barycentre. Par conséquent le potentiel sphérique S^μ de μ est sousharmonique dans Ω_q, et comme S_1 est harmonique, $S^\mu + S_1$ est de même sousharmonique dans Ω_q. Puisque $S^\mu + S_1$ a le même développement comme T, on sait que T est égal à la distribution définie par $S^\mu + S_1$, i.e. T est une fonction sousharmonique dans Ω_q.

Ensuite, soit T une fonction sousharmonique dans Ω_q. Nous allons démontrer que $D_q^* T \geqq 0$. Si T est de la classe C^2, l'assertion est déja prouvée (4.9). Dans le cas général nous nous servirons du procédé de la régularisation du chapitre 2. Soit $(\varphi_\varepsilon)_{\varepsilon \in \,]0,\,1[}$ une unité approchée de Ω_q, alors nous avons pour tout $a \in \Omega_q$, $\varrho \in \,]0, \tfrac{1}{2}\pi[$

$$\mathscr{M}_{\varphi_\varepsilon * T}^o(a) = \varphi_\varepsilon * \mathscr{M}_T^o(a), \tag{35}$$

car, grâce au théorème de Fubini on a

$$\mathscr{M}_{\varphi_\varepsilon * T}^o(a) = \frac{\sin^{2-q}\varrho}{\|\omega_{q-1}\|^2} \int_{\Omega_q} \left(T(\eta) \int_{S(a,\varrho)} \varphi_\varepsilon(\xi \cdot \eta)\, d\sigma_\varrho(\xi) \right) d\omega_q(\eta)$$

$$= \frac{\sin^{2-q}\varrho}{\|\omega_{q-1}\|^2} \int_{\Omega_q} \left(T(\eta) \int_{S(\eta,\varrho)} \varphi_\varepsilon(a \cdot \zeta)\, d\sigma_\varrho(\zeta) \right) d\omega_q(\eta) = \frac{1}{\|\omega_{q-1}\|} \int_{\Omega_q} T(\eta) \mathscr{M}_{\varphi_\varepsilon(a \,\cdot\,)}^o(\eta)\, d\omega_q(\eta),$$

et à l'aide du lemme 4.2 on conclut

$$\mathscr{M}_{\varphi_\varepsilon * T}^o(a) = \frac{1}{\|\omega_{q-1}\|} \int_{\Omega_q} \mathscr{M}_T^o(\eta)\, \varphi_\varepsilon(a \cdot \eta)\, d\omega_q(\eta) = \varphi_\varepsilon * \mathscr{M}_T^o(a).$$

La formule (35) entraîne la sousharmonicité dans Ω_q de la régularisée $\varphi_\varepsilon * T$, parce que

$$\mathscr{M}_{\varphi_\varepsilon * T}^o(a) = \frac{1}{\|\omega_{q-1}\|} \int_{\Omega_q} \varphi_\varepsilon(a \cdot \eta)\, \mathscr{M}_T^o(\eta)\, d\omega_q(\eta)$$

$$\geqq \frac{1}{\|\omega_{q-1}\|} \int_{\Omega_q} \varphi_\varepsilon(a \cdot \eta) \cos\varrho\, T(\eta)\, d\omega_q(\eta) = \cos\varrho\, \varphi_\varepsilon * T(a).$$

Comme $\varphi_\varepsilon * T \in C^\infty(\Omega_q)$ nous savons que $D_q^*(\varphi_\varepsilon * T) \geqq 0$, et en faisant $\varepsilon \to 0$, nous obtenons que $D_q^* T \geqq 0$. /

Voici le théorème analogue au théorème de représentation de F. Riesz dans la théorie du potentiel classique.

THÉORÈME 4.17. *Quel que soit la fonction sousharmonique f dans Ω_q, il existe une représentation de f et une seule comme*

$$f(\xi) = S^\mu(\xi) + h(\xi), \qquad \xi \in \Omega_q,$$

où S^μ est le potentiel sphérique d'une mesure positive μ admettant 0 pour barycentre, et h est une fonction harmonique dans Ω_q.

La mesure μ est appelée la mesure associée à f, et on a $\mu = D_q^* f$ au sens de distribution.

La fonction h est appelée la fonction harmonique associée à f, et on a $h(\xi) = \mathscr{S}(f) \cdot \xi$, où $\mathscr{S}(f)$ est le point de $\mathbf{R}^q$ déterminé par l'intégrale vectorielle

$$\mathscr{S}(f) = \frac{q}{\|\omega_q\|} \int_{\Omega_\eta}^{\bullet} \eta f(\eta) \, d\omega_q(\eta).$$

On en conclut que f est le potentiel sphérique d'une mesure positive admettant 0 pour barycentre si et seulement si $\mathscr{S}(f) = 0$, et que f est harmonique si et seulement si la mesure associée est la mesure nulle.

Démonstration: Soit $f = S^\mu + h$ une représentation avec les propriétés désirées. D'après 4.6 et 4.15 on a donc

$$D_q^* f = D_q^* S^\mu + D_q^* h = \mu,$$

ce qui montre l'unicité de la représentation.

L'existence s'établit ainsi: D'après 4.16 on sait que $\mu = D_q^* f$ est une mesure positive admettant 0 pour barycentre. Soit $f \sim \sum_{n=0}^\infty S_n$ le développement de f en série de fonctions sphériques. Alors on a

$$S_1(\xi) = \frac{N(q, 1)}{\|\omega_q\|} \int_{\Omega_\eta}^{\bullet} p_1(q, \xi \cdot \eta) f(\eta) \, d\omega_q(\eta) = \mathscr{S}(f) \cdot \xi,$$

où nous avons posé

$$\mathscr{S}(f) = \frac{q}{\|\omega_q\|} \int_{\Omega_\eta}^{\bullet} \eta f(\eta) \, d\omega_q(\eta).$$

La fonction $S_1(\xi)$ est harmonique, et on voit que f et $S^\mu + S_1$ possèdent le même développement en série de fonctions sphériques. Donc f et $S^\mu + S_1$ sont égaux ω_q-presque partout, et tous les deux sont des fonctions sousharmoniques. En vertu du corollaire 4.8 on conclut que f est identique à $S^\mu + S_1$. /

COROLLAIRE 4.18. *Les applications* $f \mapsto D_q^* f$ *et* $\mu \mapsto S^\mu$ *établissent une correspondance biunivoque entre les fonctions sousharmoniques* f *satisfaisant à* $\mathscr{S}(f) = 0$, *et les mesures positives* μ *de barycentre à l'origine.*

Chapitre 5
CORPS CONVEXES ET POTENTIELS SPHÉRIQUES

Nous allons expliquer la liaison entre la théorie du potentiel sphérique et la théorie des corps convexes.

THÉORÈME 5.1. *La fonction d'appui* h_K *d'un corps convexe quelconque* $K \in \mathscr{C}_q$ *est une fonction sousharmonique dans* Ω_q.

La mesure associée à h_K *est égale à la première mesure de surface de* K, *i.e.*

$$D_q^* h_K = \mu_1(K) \quad \text{ou} \quad \{\Delta_q^* + (q-1)\} h_K = (q-1)\mu_1(K) \tag{1}$$

au sens des distributions.

La fonction harmonique associée à h_K *est la fonction* $\xi \mapsto \mathscr{S}(K) \cdot \xi$ *où* $\mathscr{S}(K) = \mathscr{S}(h_K)$ *est le point de Steiner de* K *donné par*

$$\mathscr{S}(K) = \frac{q}{\|\omega_q\|} \int_{\Omega_q} \eta \, h_K(\eta) \, d\omega_q(\eta). \tag{2}$$

Nous avons la représentation suivante:

$$h_K(\xi) = \frac{1}{\|\omega_{q-1}\|} \int_{\Omega_q} g_q(\xi \cdot \eta) \, d\mu_1(K)(\eta) + \mathscr{S}(K) \cdot \xi, \quad \text{pour} \ \xi \in \Omega_q. \tag{3}$$

Démonstration: Soient $a \in \Omega_q$, $\varrho \in \,]0, \tfrac{1}{2}\pi[$ et soit

$$\eta \in \Omega_{q-1}, \ \text{où} \ \Omega_{q-1} = \{\xi \in \Omega_q \,|\, a \cdot \xi = 0\}.$$

La convexité et l'homogénéité positive de h_K montrent que

$$\cos \varrho \, h_K(a) \leqq \tfrac{1}{2} h_K(a\cos\varrho + \eta\sin\varrho) + \tfrac{1}{2} h_K(a\cos\varrho - \eta\sin\varrho).$$

Formant la moyenne en η sur Ω_{q-1}, on obtient

$$\cos\varrho\, h_K(a) \leqq \tfrac{1}{2}\mathscr{M}^{o}_{h_K}(a) + \tfrac{1}{2}\mathscr{M}^{o}_{h_K}(a) = \mathscr{M}^{o}_{h_K}(a),$$

donc h_K est soushamonique dans Ω_q.

Si $K \in \mathscr{C}_q$ est un corps convexe lisse, nous savons d'après (10) chapitre 2 que la mesure associée à h_K est égale à $\mu_1(K)$.

Soit $K \in \mathscr{C}_q$ un corps convexe quelconque. Il existe une suite $K_n \in \mathscr{C}_q$ de corps convexes lisses telle que $K_n \to K$ dans $\mathscr{C}_q$, donc $h_{K_n} \to h_K$ dans $\mathscr{C}(\Omega_q)$. Il en découle que $h_{K_n} \to h_K$ faiblement au sens des distributions (i.e. dans $\mathscr{D}'(\Omega_q)$), et par conséquent $D_q^* h_{K_n} \to D_q^* h_K$ dans $\mathscr{D}'(\Omega_q)$. D'après 1.2 on sait que $\mu_1(K_n) \to \mu_1(K)$ dans $\mathscr{M}(\Omega_q)$, et en particulier $\mu_1(K_n) \to \mu_1(K)$ dans $\mathscr{D}'(\Omega_q)$. Puisque $D_q^* h_{K_n} = \mu_1(K_n)$, il en découle que $D_q^* h_K = \mu_1(K)$ au sens des distributions.

Le théorème de représentation 4.17 finit la démonstration. |

THÉORÈME 5.2. *Deux corps convexes $K, L \in \mathscr{C}_q$ ont la même première mesure de surface, si et seulement si l'un résulte de l'autre par une translation.*

Ce théorème – d'ailleurs bien connu – est une conséquence immédiate du théorème 5.1 combiné avec les observations du chapitre 1. Le théorème remonte à E. B. Christoffel pour des corps convexes lisses dans l'espace de trois dimensions. De plus il est un cas particulier d'un théorème dû à A. D. Aleksandrov [2], et à W. Fenchel et B. Jessen [7].

Remarquons que nous n'avons pas supposé la dimension de K et L au moins 2, comme fait dans [7]. Cependant, cette extension n'est pas profonde.

THÉORÈME 5.3. *Pour qu'une mesure positive μ sur la sphère unité Ω_q soit la première mesure de surface d'un corps convexe, il faut et il suffit qu'elle satisfasse aux conditions suivantes:*

(i) *La mesure μ admet 0 pour barycentre.*

(ii) *Le potentiel sphérique S^μ de μ est une fonction d'appui sur Ω_q.*

Démonstration: Les conditions sont nécessaires; la condition (i) en vertu de 1.2 et la condition (ii) en vertu de 5.1.

Pour montrer qu'elles sont suffisantes, remarquons que S^μ, étant une fonction d'appui, détermine un corps convexe K et un seul tel que $h_K = S^\mu$. La première mesure de surface $\mu_1(K)$ de K est alors

$$\mu_1(K) = D_q^* h_K = D_q^* S^\mu = \mu$$

en vertu de 5.1 et 4.15. |

On voit facilement qu'il y a identité entre les fonctions d'appui sur Ω_2 et les fonctions sousharmoniques dans Ω_2. La condition (ii) est par conséquent vide quand $q = 2$.

D'après les théorèmes 5.2 et 5.3 l'application μ_1 établit une correspondance biunivoque entre l'ensemble $\mathscr{C}'_q$ des corps convexes dont le point de Steiner est à l'origine et l'ensemble $\mathscr{P}$ des mesures positives sur Ω_q satisfaisant à (i) et (ii). Cette correspondance est additive et positivement homogène, et de plus on a:

THÉORÈME 5.4. *L'application $\mu_1 : \mathscr{C}'_q \to \mathscr{P}$ est un homéomorphisme, et $\mathscr{P}$ est un cône convexe fermé de $\mathscr{M}_+(\Omega_q)$.*

Démonstration: Puisque μ_1 est continue et positivement homogène, il suffit de démontrer que l'ensemble

$$\mathscr{A} = \{K \in \mathscr{C}'_q \mid \|\mu_1(K)\| = 1\}$$

est compact.

On voit immédiatement que $\mathscr{A}$ est fermé dans $\mathscr{C}_q$.

Pour tout $K \in \mathscr{A}$ et tout point $a \in K$, le segment $[0,a]$ est contenu dans K parce que $0 = \mathscr{S}(K) \in K$. Alors

$$\|\mu_1([0, a])\| \leq \|\mu_1(K)\| = 1$$

Comme

$$\|\mu_1([0, a])\| = \frac{\|\omega_{q-1}\|}{q-1} \|a\|,$$

on voit que $\|a\|$ et par conséquent $\mathscr{A}$ est borné. Le théorème de sélection de Blaschke fournit la compacité de $\mathscr{A}$. /

Soient $K \in \mathscr{C}_q$ un corps convexe, $\mu_p(K)$, $p = 1, \cdots, q-1$, ses mesures de surface. Les mesures $\mu_1(K)$ et $\mu_{q-1}(K)$ sont caractérisées par leurs potentiels sphériques, étant resp. des fonctions d'appui et des fonctions sousharmoniques. Nous croyons qu'il serait fertile de chercher la caractérisation des mesures $\mu_p(K)$, $p = 2, \cdots, q-2$, par leurs potentiels sphériques $S^{\mu_p(K)}$.

Bibliographie

[1] ALEKSANDROV, A. D. – Zur Theorie der gemischten Volumina von konvexen Körpern I, II. (En russe, résumé en allemand.) *Mat. Sbornik N. S.*, 2, 1937, pp. 947–972, 1205–1238.

[2] ALEKSANDROV, A. D. – Zur Theorie der gemischten Volumina von konvexen Körpern III. (En russe, résumé en allemand.) *Mat. Sbornik N. S.*, 3, 1938, pp. 27–46.

[3] BONNESEN, T. et FENCHEL, W. – *Theorie der konvexen Körper*. Springer, Berlin 1934.

[4] BOURBAKI, N. – *Intégration, chap. 1–4*. Hermann, Paris 1965.

[5] BRELOT, M. – *Axiomatique des fonctions harmoniques*. Les presses de l'université de Montréal. 1966.

[6] BRELOT, M. – *Éléments de la théorie classique du potentiel*. Les cours de Sorbonne. Paris 1965.

[7] FENCHEL, W. et JESSEN, B. – Mengenfunktionen und konvexe Körper. *Det Kgl. Danske Videnskabernes Selskab. Mat.-fys. Meddelelser XVI*, 3, 1938.

[8] FIREY, W. J. – The determination of convex bodies from their mean radius of curvature functions. *Mathematika* 14, 1967, pp. 1–13.

[9] FIREY, W. J. – Christoffel's problem for general convex bodies. *Mathematika* 15, 1968, pp. 7–21.

[10] GRÜNBAUM, B. – *Convex polytopes*. J. Wiley. New York 1967.

[11] HELGASON, S. – *Differential geometry and symmetric spaces*. Academic Press. New York 1962.

[12] HELLWIG, G. – *Partielle Differentialgleichungen*. Teubner. Stuttgart 1960.

[13] HERVÉ, R. M. – Recherches axiomatiques sur la théorie des fonctions surharmoniques et du potentiel. *Ann. Inst. Fourier, Grenoble*, 12, 1962, pp. 415–571.

[14] LENSE, J. – *Kugelfunktionen*. Akademische Verlagsgesellschaft. Leipzig 1950.

[15] MÜLLER, C. – Spherical harmonics. *Lecture notes in mathematics 17*. Springer. New York 1966.

[16] POGORELOV, A. V. – On the question of the existence of a convex surface with a given sum of the principal radii of curvature. *Uspehi Mat. Nauk*, 8, 1953, pp. 127–130. (En russe.)

[17] RHAM, G. de – *Variétés différentiables*. Hermann. Paris 1955.

[18] STEINER, J. – Von dem Krümmungsschwerpunkte ebener Curven. *J. Reine Angew. Math.*, 21, 1840, pp. 33–63, 101–133.

P. O. TJØM and B. ELBEK

A STUDY OF ENERGY LEVELS IN ODD-MASS ERBIUM NUCLEI BY MEANS OF (d,p) AND (d,t) REACTIONS

CONTENTS

Synopsis

The energy levels of ^{161}Er, ^{163}Er, ^{165}Er, ^{167}Er, ^{169}Er and ^{171}Er have been investigated by means of (d,p) and (d,t) reactions on the stable erbium isotopes. The deuteron energy was 12.1 MeV and the charged reaction products were analyzed in a magnetic spectrograph at 60°, 90°, and 125°. A total of 16 different Nilsson orbitals or components thereof were identified on the basis of the intensity patterns for the rotational states, the absolute cross sections, and the rate of intensity change with angle. For the majority of the orbitals, the observations are in reasonable agreement with the theoretical predictions based on the single-particle functions in a deformed potential. A few of the observed intensities do, however, deviate considerably from the theoretical intensities. Among the reasons for such deviations are the crossing of energy levels from different oscillator shells and couplings to other single-particle states or collective vibrations, but for a number of cases no obvious explanation has yet been found.

1. Introduction

The present study of the energy levels in the odd erbium isotopes by means of neutron stripping and pick-up reactions is a continuation of earlier investigations of the energy levels in odd gadolinium[1] and ytterbium[2] nuclei.

The main motivation for this type of experiments is the possibility it offers for a systematic localization of a large number of neutron single-particle states. At the same time, the amplitudes of certain components of the wave functions are obtained from the observed single-particle transfer cross sections. The interpretation of the cross sections is based on relatively few assumptions about the nuclear reaction mechanism and has been tested in a large number of cases.

A complex structure of the wave function of the excited nuclear states often complicates the analysis of the transfer reaction data and, although there has been little reason to doubt the single-nucleon nature of the (d,p) and (d,t) reaction studies, there are also in the present work several examples of observations, which cannot be accounted for in a satisfactory manner.

Among the phenomena which limit the applicability of the single-nucleon description is the particle coupling to the various collective vibrational modes. Examples of such couplings have been discussed in earlier papers[1, 2], especially in connection with the gamma vibrational states. The even erbium nuclei have low-lying vibrations, which are connected with the ground states by large $E2$ matrix elements. These and other collective states in the even nuclei have been studied by means of the (d,d') reaction[3], actually on the basis of the charged particle spectra of which the proton and triton parts are analyzed here. The well-developed gamma vibrational states in the erbium nuclei offer a possibility for the study of the particle-vibration coupling in deformed nuclei. Most of the cases investigated up to now have been characterized by relatively weak collective states, and it is an interesting problem whether the large single-particle amplitudes in the vibrational states[1, 2] in the odd nuclei are also observed when the vibrations are strongly collective.

1*

Probably, the Coriolis coupling between rotational bands differing one unit in the angular momentum projection, K, is the most important and well understood phenomenon, which gives rise to intermixing of the one-particle wave functions. The Coriolis coupling is obviously responsible for a large fraction of the observed departures from the simple theoretical intensity distributions for the one-nucleon transfer reactions. However, only in a few cases has the material available been subject to a detailed analysis of such effects.

The coupling between single-particle states with $N = 4$ and $N = 6$ was found to be of major importance for several spectra of the gadolinium nuclei. The single-particle states in question also occur as relatively low-lying levels in the erbium nuclei and thus permit a further study of this type of coupling.

The experimental methods are closely the same as those used before[1, 2]. The beam of 12.1 MeV deuterons was obtained from the Niels Bohr Institute's tandem accelerator, and the charged reaction products were analyzed in a high-resolution magnetic spectrograph with photographic plate recording. The targets for the investigations were $\sim 40 \ \mu g/cm^2$ layers of the relevant isotope directly deposited on $\sim 40 \ \mu g/cm^2$ carbon foils in the electromagnetic isotope separator at the University of Aarhus.

The absolute spectroscopic factors obtained from the (d, p) and (d, t) cross sections depend in a critical manner on the nuclear optical parameters used for the reaction calculations by means of the distorted wave Born approximation (DWBA) method. It has been the general philosophy followed in the earlier investigations first to select a set of reasonable potentials and, then, to use these potentials throughout. In this way, no optimum adjustment to angular distribution data is obtained, but, on the other hand, the important comparison of spectroscopic factors for the different nuclei is facilitated. Moreover, the limitations of the fixed potentials are not easily realized, as there is a lack of detailed angular distribution data. Unfortunately, the deuteron potential selected originally[2] was somewhat shallow compared to the standard potential of PEREY[4]; nevertheless, it gave satisfactory results for the (d, t) angular distributions with minor adjustments of the triton parameters[5]. Also the (d, p) angular distributions were satisfactory, although little experimental material was available for comparison[6, 7]. When the same parameters were used for the Er nuclei, the calculated angular distributions for the (d, t) reactions were essentially unchanged, but the (d, p) distributions—especially for even l-values— showed pronounced oscillations, which have not been observed experimentally in the few cases investigated. No (d, p) distribution for even l has been measured in Er, but

Table 1. The DWBA single-particle cross sections $\sigma_l(90°)$ for (d,t) and (d,p) reactions.

	$\sigma_0(90°)$	$\sigma_2(90°)$	$\sigma_4(90°)$	$\sigma_1(90°)$	$\sigma_3(90°)$	$\sigma_5(90°)$	$\sigma_0(90°)$	$\sigma_2(90°)$	$\sigma_4(90°)$	$\sigma_6(90°)$
Reaction	$N = 4$ $\mu b/sr$	$N = 4$ $\mu b/sr$	$N = 4$ $\mu b/sr$	$N = 5$ $\mu b/sr$	$N = 5$ $\mu b/sr$	$N = 5$ $\mu b/sr$	$N = 6$ $\mu b/sr$	$N = 6$ $\mu b/sr$	$N = 6$ $\mu b/sr$	$N = 6$ $\mu b/sr$
(d,t) $Q = -2$ MeV	214	120	23.4	251	88.4	13.7	372	222	58.5	6.4
(d,p) $Q = 3$ MeV				500	195	26.5	580	365	102	15.5

The optical model parameters used for the calculation are those listed in Table 1 of ref. 1, which also defines the DWBA cross section $\sigma_l(\theta)$.

it seems unlikely that the experimental distributions should show oscillations as pronounced as those calculated. Somewhat arbitrarily, a smooth curve was drawn to reproduce the main trends in the calculated distributions. This procedure found some justification in the fact that a calculation based on the standard deuteron parameters considerably reduces the oscillations without significant changes in the absolute cross sections. Obviously, this point needs clarification; however, in order to be consistent with earlier spectroscopic factor calculations, the above-mentioned averaging procedure was used. The DWBA single-particle cross sections $\sigma_l(\theta)$ (defined as in ref.[1]) for the reference Q-values $+3$ MeV for (d,p) and -2 MeV for (d,t) are listed in Table 1.

2. Results and Discussion

In Figs. 1–10 a spectrum is shown for each of the ten different transfer reactions possible with the stable targets ^{162}Er, ^{164}Er, ^{166}Er, ^{168}Er, and ^{170}Er. The level energies obtained as averages of the determinations at three different angles are listed in Tables 2–7, which also contain the measured differential cross sections and the suggested Nilsson assignments for some of the levels. The basis for these assignments will be discussed in detail in the following sections.

2.1. Q-values

The identification of the ground-state group did not cause any problems, except in the case of ^{167}Er where the ground-state group was weak. The ground-state Q-values were therefore based on an excitation energy of
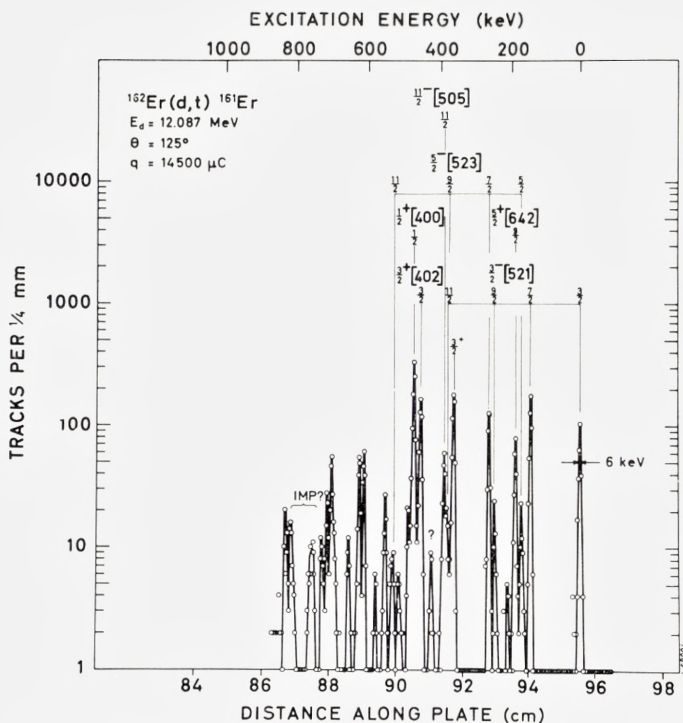
Fig. 1. Triton spectrum for the reaction ^{162}Er$(d,t)^{161}$Er $\theta = 125°$.

79 keV for the well-known 9/2 7/2 + [633] state. The final Q-values, correc-
ted for small effects from partial magnetic saturation of the spectrograph
iron, are given in Table 8, which also lists the neutron separation energies
derived from the Q-values.

2.2. General Features of the Spectra

The (d,t) spectra were scanned from the ground state to the position
of the elastic deuteron group. In the heaviest isotopes, this corresponds to a
region of excitation of about 2 MeV, in the lightest to about 800 keV. The
energy resolution in the (d,t) spectra was about 6 keV, which in most cases
was sufficient to ensure well-separated groups. The (d,p) spectra were scan-
ned up to 2 MeV of excitation. Because of the high proton energy (15 MeV)
and the lower spectrograph dispersion at the smaller radii of curvature at
which the proton spectra were recorded, the energy resolution was only
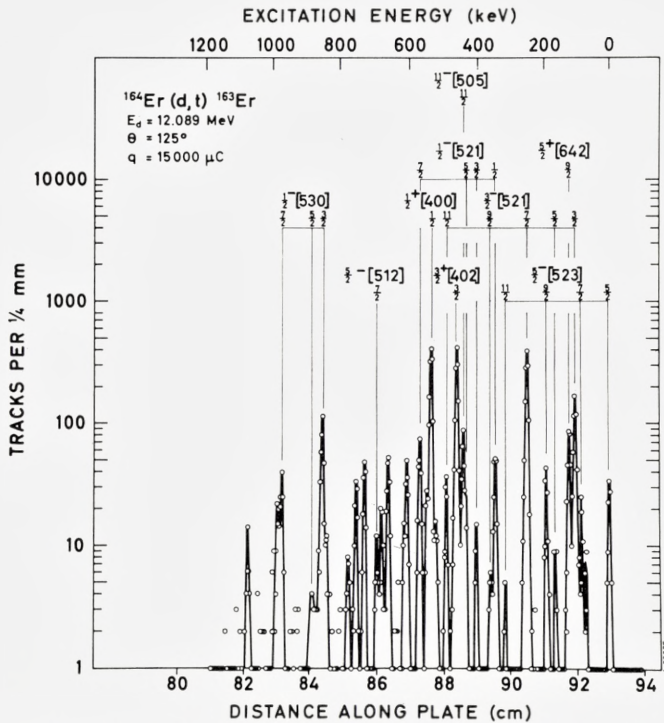
Fig. 2. Triton spectrum for the reaction ^{164}Er$(d,t)^{163}$Er $\theta = 125°$.

about 12 keV. At higher energy of excitation, this was insufficient to ensure complete separation of the proton groups.

The density of levels populated by the transfer reactions shows a moderate increase with excitation energy. Especially for the lighter isotopes, the number of levels populated by the (d,p) reaction is quite large in the region above 1 MeV of excitation. In the same region, the intensities tend to be more evenly distributed, so that the spectra lack easily recognizable patterns (compare, e.g. Fig. 3 and Fig. 10).

The level schemes Figs. 12–17 show that, in general, it has been possible to make rather definite assignments for most of the levels below 1 MeV although, in the lighter isotopes, also some of the lower levels remain unassigned. Already here it should, however, be stressed that the assignments only imply that a sizable fraction of the total single-particle strength of a given Nilsson orbital is found at the positions indicated.

In the earlier investigation of the gadolinium isotopes, it was shown

TABLE 2. Levels populated in ^{161}Er.

Energy average (d,t) keV	Assignment	$d\sigma/d\Omega(d,t)$ $\mu b/sr$		
		60°	90°	125°
0	3/2 3/2 − [521]		55	32
144	7/2 3/2 − [521]	45	77	59
172	5/2 5/2 − [523]	6	9	8
189	9/2 5/2 + [642]?	26	34	28
212		5	5	∼ 2
250	9/2 3/2 − [521]	2	7	7
268	(7/2 5/2 − [523])	26	50	50
369	3/2 3/2 + [402]*	36	79	70
388	{ 11/2 3/2 − [521] } { 9/2 5/2 − [523] }	2	5	6
396	11/2 11/2 − [505]	5	20	23
463	3/2 3/2 + [402]*	40	85	64
481	1/2 1/2 + [400]	73	143	118
495		8	10	7
522		4	4	3
540	11/2 5/2 − [523]		3	5
563		4	13	10
588				2
621		10	21	23
635		16	27	22
665		3	4	4
704		4	10	4
712		12	23	20
724		5	10	10
738		4	8	5
842		5	7	5

* Splitting of intensity probably caused by interaction with 3/2 + [651].

that most of the strength expected on the basis of the Nilsson model was present. A similar analysis for the erbium isotopes confirms this statement especially as far as the hole states are concerned. The strength of the particle states is somewhat less than expected, the total (d,p) cross sections to levels below 2 MeV of excitation being about 75 % of the theoretical value. It is not clear whether this reflects discrepancies in the theoretical cross sections used for the comparison or whether some of the strength has been pushed to higher energies.

TABLE 3. Levels populated in ¹⁶³Er.

Energy average		Assignment	$d\sigma/d\Omega(d,p)$ $\mu b/sr$			$d\sigma/d\Omega(d,t)$ $\mu b/sr$		
(d,p) keV	(d,t) keV		60°	90°	125°	60°	90°	125°
0	0	5/2 5/2 − [523]	18	11		14	20	11
~ 67	~ 69	7/2 5/2 + [642]?		~ 1	~ 2	~ 4		~ 2
82	84	7/2 5/2 − [523]	28	19	6	8		7
102	104	3/2 3/2 − [521]	71	34	8	87	101	60
119	121	9/2 5/2 + [642]	32	25	13	36	53	33
~ 159	164	5/2 3/2 − [521]		~ 1		2		2
188	190	9/2 5/2 − [523]	19	19	10	7	18	14
247	250	7/2 3/2 − [521]	185	153	94	120	198	145
	320	11/2 5/2 − [523]				~ 1	~ 1	~ 1
344	344	1/2 1/2 − [521]	232	103	45	40	47	22
	359	9/2 3/2 − [521]				3	5	2
404	405	3/2 1/2 − [521]	26	23	10	11	11	4
439		5/2 1/2 − [521]		38	21			
	444	11/2 11/2 − [505]				15	39	33
461	463	3/2 3/2 + [402]	~ 50	33	16	108	172	147
495	495	11/2 3/2 − [521]	6	6	9	2	7	13
	525						3	7
541	541	1/2 1/2 + [400]	79	35	16	126	207	156
	553					6	13	8
570	573	7/2 1/2 − [521]	84	64	29	16	34	26
609	610	5/2 5/2 − [512]	10	7	5	9	15	17
	619					2	5	4
636		9/2 1/2 − [521]	10	8	6			
	664					14	26	20
	683					9	11	7
699	698	7/2 5/2 − [512]	256	156	69	3	5	3
	735					7	17	17
757	759		14	6	2	12	18	12
779	781		12	11	6	3	5	3
~ 805		9/2 5/2 − [512]	~ 1	~ 2	~ 1			
827			13	10	10			
841	842		27	28	10	5	4	4
854	856	3/2 1/2 − [530]	42	21	7	33	63	37
872	877	5/2 1/2 − [530]	7	8	4	2	4	~ 1
	973	7/2 1/2 − [530]				8	16	13
979			21	16	12			
	987					4	10	8
1029			6	3	2			
1055			12	5	4			
1074	1075	1/2 1/2 − [510]	8	5	~ 1		4	4

TABLE 3 (continued).

Energy average		Assignment	$d\sigma/d\Omega(d,p)$ $\mu b/sr$			$d\sigma/d\Omega(d,t)$ $\mu b/sr$		
(d,p) keV	(d,t) keV		60°	90°	125°	60°	90°	125°
1098		3/2 1/2 − [510]	246	143	59			
1164			11	15	8			
1183		5/2 1/2 − [510]	59	44	26			
1204			11	7	4			
1245		7/2 1/2 − [510]	44	19	7			
1277			40	24	12			
1316			35	31	6			
1344			88	79	33			
1395		9/2 1/2 − [510]	10	5	2			
1433			68	40	17			
1485			87	52	20			
1529			80	40	19			
1562			76	45	24			
1635			40	22	7			
1671			45	19	13			
1686			44	37	18			
1717			28	12	7			
1759			80	41	21			
1784			33	25	11			
1803			46	23	10			
1817			37	21	14			
1856			34	18	7			
1871			27	12	6			
1900			34	18	12			
1920			49	30	13			
1938			89	49	19			
1959			58	29	11			
1971			24	22	8			
1984			20	13	4			
2019			75	40	24			
2031			76	38	16			
2051			73	51	26			
2077			140	102	58			
2096			30	27	13			
2113			67	36	19			
2135			57	37	20			
2148			43	34	17			
2165			45	29	22			
2183			54	34	20			
2200			36	22	8			
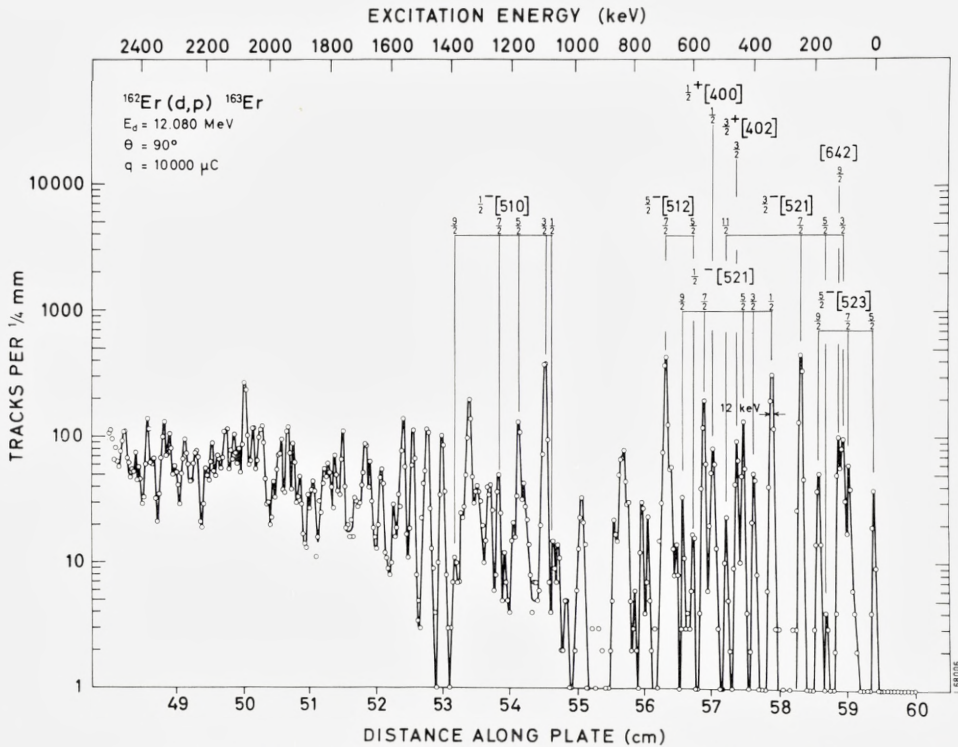
Fig. 3. Proton spectrum for the reaction $^{162}\mathrm{Er}(d,p)^{163}\mathrm{Er}\ \theta = 90°$.

2.3. Detailed Interpretation of the Spectra

The methods of interpretation closely follow those used for gadolinium and ytterbium. The discussion below is arranged according to the Nilsson assignments for the different bands identified. As remarked earlier, an $IK\pi[Nn_z\Lambda]$ assignment indicates only that the Nilsson orbital in question contributes an essential fraction of the wave function. In a number of cases, it has been possible to identify some of the couplings responsible for the splitting of the single-particle intensity among several bands. These cases are discussed under the heading of that single-particle level which receives most of the intensity.

2.3.1. The 3/2-[521] Orbital

The $3/2 - [521]$ orbital was known previously[8, 9] in the isotopes from $^{161}\mathrm{Er}$ to $^{167}\mathrm{Er}$. The present assignments are in agreement with the earlier

Table 4. Levels populated in ^{165}Er.

Energy average		Assignment	$d\sigma/d\Omega(d,p)$ $\mu b/sr$			$d\sigma/d\Omega(d,t)$ $\mu b/sr$		
(d,p) keV	(d,t) keV		60°	90°	125°	60°	90°	125°
0	0	5/2 5/2 − [523]	9	6		30	34	17
	48	5/2 5/2 + [642]				8	3	2
76	76	7/2 5/2 − [523]		7	3	11	16	9
99	98	9/2 5/2 + [642]		21	8	53	71	37
176	176	9/2 5/2 − [523]	13	11	5	15	33	27
240	242	3/2 3/2 − [521]	80	57	44	159	233	124
298	297	1/2 1/2 − [521]	256	121	48	92	92	39
356	355	3/2 1/2 − [521]	8	13	6	12	9	5
373	372	7/2 3/2 − [521]	198	122	44	164	217	136
∼ 382	∼ 384	5/2 1/2 − [521]		27	21	∼ 13	∼ 21	∼ 13
470	469	9/2 3/2 − [521]		4	2	2	∼ 5	5
	507	1/2 1/2 + [660]				114	∼ 168	102
514		7/2 1/2 − [521]	89	60	27			
533	534	3/2 3/2 + [402]	43	27	14	169	∼ 305	
	547					∼ 17	∼ 57	∼ 36
575	575	7/2 5/2 − [512]	288	175	83	∼ 10	∼ 18	13
593	591	11/2 11/2 − [505]		42	17	∼ 18	∼ 33	∼ 27
608	601		26	18	5	∼ 10	∼ 23	∼ 9
	652						3	6
684		9/2 5/2 − [512]		7	3			
700			9	5	3			
728	724		∼ 29	24	9	5		5
746	742	1/2 1/2 + [400]	∼ 13	7	5	114	190	139
761	760			6	3	15	40	24
820	817	11/2 5/2 − [512]		7	2	30	58	32
846				4	4			
	863					14	17	6
873				10	5			
896			6	8	5			
925		1/2 1/2 − [510]		∼ 2	∼ 1			
961		3/2 1/2 − [510]	205	119	46			
	972					9	14	13
1024		5/2 1/2 − [510]	74	48	28			
	1039	3/2 1/2 − [530]				65	96	56
1043			70	42	10			
	1063	5/2 1/2 − [530]				4	8	5
1073			9	11	2			
1110		7/2 1/2 − [510]	30	31	10			
	1107					8	9	6
	1139					9	15	9

(continued)

TABLE 4 (continued).

| Energy average | | Assignment | $d\sigma/d\Omega(d,p)$ $\mu b/sr$ | | | $d\sigma/d\Omega(d,t)$ $\mu b/sr$ | | |
(d,p) keV	(d,t) keV		60°	90°	125°	60°	90°	125°
1145			6	4	6			
	1172	7/2 1/2 − [530]				6	17	14
1177			14	5	6			
1198			5	3	5			
1233			4	7	6			
	1276					18	28	24
1285			114	82	36			
1378			14	14	9			
	1383					10	13	12
1413			65	35	14			
1474		3/2 3/2 − [512]	99	49	22			
1490				14	5			
1539		5/2 3/2 − [512]	123	82	44			
1564			44	21	7			
1612			39	∼ 28	7			
1631		7/2 3/2 − [512]	56	∼ 28	13			
1656			79	63	26			
1728			77	44	9			
1761			112	51	22			
1780			66	45	16			
1805			83	45	21			
1819			102	63	25			
1851			56	23	14			
1889			65	35	20			
1901			90	53	22			
1940			173	78	47			
1951				38	33			
1968			176	86	39			
2004			33	22	7			
2018				23	11			
2033			107	45	11			
2047				35	24			
2057			75	30	23			

ones. In ^{169}Er, there is a pattern similar to that observed for the $3/2 - [521]$ orbital in the other nuclei with a band-head energy of 713 keV. The $3/2 -$, $7/2$, and $9/2 -$ members of the band are observed in all the erbium isotopes except ^{171}Er, where the (d,p) spectra do not allow any identification of the $3/2 - [521]$ band, which here occurs as a hole excitation. In addition, the

Table 5. Levels populated in ¹⁶⁷Er.

Energy average		Assignment	$d\sigma/d\Omega(d,p)$ $\mu b/sr$			$d\sigma/d\Omega(d,t)$ $\mu b/sr$		
(d,p) keV	(d,t) keV		60°	90°	125°	60°	90°	125°
0	0	7/2 7/2 + [633]	~ 1		~ 0.3	~ 2	~ 1	~ 0.6
79	79	9/2 7/2 + [633]	19	9	8	41	57	22
176	177	11/2 7/2 + [633]	~ 3		~ 1	~ 1	~ 2	~ 1
208	208	1/2 1/2 − [521]	292	149	51	265	201	72
262	264	3/2 1/2 − [521]	5	10	4	9	5	3
280	281	5/2 1/2 − [521]	63	38	18	32	34	16
295	295	13/2 7/2 + [633]	27	42	34	37	71	50
347	345	5/2 5/2 − [512]	13		3	2	1	~ 0.5
413	414	7/2 1/2 − [521]	125	84	37	60	65	37
430	431	7/2 5/2 − [512]	304	260	112	66	82	41
	~ 438	9/2 1/2 − [521]						~ 8
535	534	9/2 5/2 − [512]	15	11	8	9	13	7
573	573	5/2 +, γ-vib	20	6	2	4	5	2
598			9	3	1			
644	643	11/2 1/2 − [521]	6	7	5	~ 1	5	6
665	668	{ 11/2 5/2 − [512] } { 5/2 5/2 − [523] }	11	10	11	31	38	22
711	711	9/2 +, γ-vib	7	7	2	5	7	3
750	753	3/2 3/2 − [521]	42	34	11	195	200	90
802	802	3/2 1/2 − [510]	255	~136	67	31	31	17
	812	5/2 5/2 + [642]?				26	31	14
	843	9/2 5/2 − [523]				14	38	35
854		5/2 1/2 − [510]	73	~ 80	33			
894	895	7/2 3/2 − [521]	70	~ 77	23	150	200	110
	911	13/2 +, γ-vib				~ 6	~ 6	~ 1
	933	9/2 5/2 + [642]				42	60	34
941	943	7/2 1/2 − [510]	20	27	13	10	13	9
	967	11/2 5/2 − [523]				~ 1	3	2
	1002	9/2 3/2 − [521]				~ 2	4	3
1049	1052	11/2 11/2 − [505]	5			15	55	46
1084	1086	3/2 3/2 + [402]	21	15	9	242	345	215
	1109	13/2 5/2 + [642]				13	25	36
1132	1135	1/2 1/2 + [400]	46	39	18	269	384	224
1173			84	77	36			
	1190							26
	1205					8	21	24
	1222							12
1247			11	11	4			
1280			27	26	19			
	1302					44	6	7

(continued)

TABLE 5 (continued).

Energy average		Assignment	$d\sigma/d\Omega(d,p)$ $\mu b/sr$			$d\sigma/d\Omega(d,t)$ $\mu b/sr$		
(d, p) keV	(d, t) keV		60°	90°	125°	60°	90°	125°
1332			2	3	2			
	1352					3	5	2
	1377	3/2 1/2 − [530]				62	75	47
1384		3/2 3/2 − [512]	123	67	28			
1408			5	10	5			
	1426					36	61	52
1440		5/2 3/2 − [512]	156	121	65			
	1525					~ 10	~ 9	9
1526		7/2 3/2 − [512]	70	74	45			
	1536					~ 13	~ 18	10
	1545					~ 12	~ 27	17
1548			76	49	17			
	1558						~ 26	~ 16
	1590					2	2	3
1596			88	53	29			
	1625					32	36	28
1629		9/2 3/2 − [512]	32	14	5			
	1638					6	11	6
1645			27	15	14			
	1657*					39	51	29
1684			126	71	30			
1718			268	178	80			
1747			202	126	60			
	1748					6	5	10
1779			15	13	7			
1800			15	15	6			
	1812					5	4	4
1815			34	24	13			
1842			30	28	15			
	1853					5	4	9
1865			222	122	60			
	1893					17	28	33
1912			194	98	48			
	1940					5	10	4

* Several weak groups from 1657 keV to 1892 keV.

TABLE 6. Levels populated in ^{169}Er.

Energy average		Assignment	$d\sigma/d\Omega(d,p)$ $\mu b/sr$			$d\sigma/d\Omega(d,t)$ $\mu b/sr$		
(d,p) keV	(d,t) keV		60°	90°	125°	60°	90°	125°
0	0	1/2 1/2 − [521]	273	158	49	783	397	188
65	66	3/2 1/2 − [521]	~ 22	~ 16			~ 24	~ 17
74	74	5/2 1/2 − [521]	~ 50	~ 36	~ 22		~ 62	~ 37
90	91	5/2 5/2 − [512]	14	10	3	11	6	
176	176	7/2 5/2 − [512]	333	280	104	293	229	131
225	224	7/2 1/2 − [521]	116	96	37	212	167	95
	243	9/2 1/2 − [521]				9	11	25
285	284	9/2 5/2 − [512]	10	9	6	5	7	5
317	318	9/2 7/2 + [633]	12	16	5	67	54	31
415	414	11/2 5/2 − [512]	9	6	8	4	10	13
474	474	11/2 1/2 − [521]	7	7	8	7	11	23
527	527	13/2 7/2 + [633]	21	32	20	50	72	76
565		1/2 1/2 − [510]	~ 2	3				
599	599	3/2 1/2 − [510]	325	151		52	35	19
654	653	5/2 1/2 − [510]	115	83	38	30	25	11
714	713	3/2 3/2 − [521]	96		14	270	165	87
739	739	7/2 1/2 − [510]	36	29	21	9	7	
769	768	5/2 3/2 − [521]?		2	1	4	6	
822		7/2 7/2 − [514]	33	41	22			
844	850	7/2 3/2 − [521]	35	44	23	154	132	97
930	927	9/2 7/2 − [514]	42	41	36	11	16	15
	940	7/2 5/2 − [523]				36	41	33
	~ 947	9/2 3/2 − [521]				9	~ 5	
	991					7	8	3
1051		11/2 7/2 − [514]	6	~ 3	3			
	1052	9/2 5/2 − [523]				33	30	23
	1076	11/2 3/2 − [521]				20	29	23
1082		3/2 3/2 − [512]	134	74	35			
	1096					7	7	
	1116					14	12	8
1119			25		7			
1141	1142	5/2 3/2 − [512]	208	167	80	11	10	7
1187	1186	11/2 5/2 − [523]	~ 5		~ 2	5	12	13
	1215					6	10	13
1230	1229	7/2 3/2 − [512]	101	71	47	26	25	22
	1239					16	19	10
	1274					7	6	5
1341		9/2 3/2 − [512]	7	~ 7	9			
	1360					42	54	38
1364			8	~ 7	4			

(continued)

Table 6 (continued).

Energy average		Assignment	$d\sigma/d\Omega(d,p)$ $\mu b/sr$			$d\sigma/d\Omega(d,t)$ $\mu b/sr$		
(d,p) keV	(d,t) keV		60°	90°	125°	60°	90°	125°
1388			276	205	72			
	1394	11/2 11/2 − [505]				12	50	74
1415			72	63	29			
	1415						13	11
1457			18	12	6			
	1457					25	46	15
	1471					38	38	23
	1484					106	104	61
1488				362	119			
	1526ᵃ	3/2 3/2 + [402]				188	229	183
1535			74	67	39			
1554			145	95	38			
	1564					41	49	35
1570			163	64	25			
	1601					15	24	16
1608			106	69	34			
1622			66	52	28			
	1623					34		29
	1644	1/2 1/2 + [400]				151	199	140
1650			113	67	31			
	1677					107	109	95
1681				16	10			
1699				38	21			
	1702					36	31	34
1715				66	35			
	1718					9	31	34
1727				104	46			
1755			156	141	72			
1776			34	20	27			
	1790					33	43	39
1823			39	23	14			
	1825						7	11
1844			24	18	10			
	1857					50	69	74
1867			83	63	30			
	1886					10	9	
1899			31	26	12			
	1904					7	8	
1913			66	58	30			
	1924					52	24	19

TABLE 6 (continued).

Energy average (d,p) keV	(d,t) keV	Assignment	dσ/dΩ(d,p) μb/sr 60°	90°	125°	dσ/dΩ(d,t) μb/sr 60°	90°	125°
1929[b]			107	83	46			
	1958					9	10	
	1974					13	13	
	1994					6	8	
	2018					24	60	42
	2031						18	18
2053			147	120	46			
	2057						21	16
2092			32	17	12			
2123[c]			44	27	18			
2184			67	42	26			
2204			142	98	48			
2228			33	29	11			
2255			74	69	25			
2272			44	26	17			
2295			38	33	14			
2336			122	71	36			
2382				351	149			
2420				39	20			
2440				65	35			

a Unresolved groups from 1526 keV to 1564 keV.
b Unresolved groups from 1929 keV to 2053 keV.
c Unresolved groups from 2123 keV to 2184 keV.

11/2 − member is observed in ¹⁶¹Er, ¹⁶³Er, and ¹⁶⁹Er. The 5/2 − member of the band is not predicted to be populated with an observable intensity. A weak group at the expected energy is observed in the ¹⁶³Er and ¹⁶⁹Er spectra, and may be caused by the Coriolis coupling between the 3/2 − [521] and the 5/2 − [523] orbitals.

In ¹⁶⁹Er, the 3/2 − [521] orbital is found a little lower than was the case in ¹⁶⁷Er. This lowering, which is unexpected in view of the usual rapid change in excitation energy with the neutron number, might be caused by admixtures of the gamma vibration based on the 1/2 − [521] ground state.

The absolute cross sections and relative values of $C_{j,l}^2$ obtained from the (d,t) reaction are given in Table 10. The intensities are considerably higher than the theoretical predictions, especially for the 3/2 − state in ¹⁶⁵Er (probably double, cf. Sec. 2.3.2) and the 7/2 − state in ¹⁶³Er. There are many

TABLE 7. Levels populated in ^{171}Er.

Energy (d, p)	Assignment	$d\sigma/d\Omega(d,p)$ $\mu b/sr$		
		60°	90°	125°
keV				
0	5/2 5/2 − [512]	22	10	3
76	7/2 5/2 − [512]	311	204	102
176	9/2 5/2 − [512]	∼ 7		∼ 9
195	1/2 1/2 − [521]	155	∼ 66	21
∼ 253	3/2 1/2 − [521]			∼ 9
276	5/2 1/2 − [521]	48	29	24
304	11/2 5/2 − [512]	8	7	
378	9/2 9/2 + [624]	2	8	
420	7/2 1/2 − [521]	75	49	35
455	9/2 1/2 − [521]	10	7	6
531	7/2 7/2 − [514]	49	38	26
616	13/2 9/2 + [624]	28	32	30
645	9/2 7/2 − [514]	54	44	36
674	11/2 1/2 − [521]	5	4	3
706	1/2 1/2 − [510]	11	12	7
745	3/2 1/2 − [510]	552	287	143
795	5/2 1/2 − [510]	215	149	94
880	7/2 1/2 − [510]	105	70	50
906	3/2 3/2 − [512]	208	95	47
972	5/2 3/2 − [512]	211	161	114
1061	7/2 3/2 − [512]	100	71	55
1106	11/2 1/2 − [510]	6	4	12
1171	9/2 3/2 − [512]	10	9	9
1224		136	82	37
1261		53	32	15
1304		36	14	10
1376			314	150
1405			440	246
1435			24	31
1471		313	152	105
1508		165	102	67
1535		62	49	32
1570		138	94	51
1616		407	289	169
1647		46	41	20
1682		38	27	18
1722		64	52	35
1764		39	25	19
1795		236	170	97
1823		38		21

TABLE 7 (continued).

Energy (d,p)	Assignment	$d\sigma/d\Omega(d,p)\ \mu b/sr$		
		60°	90°	125°
keV				
1857		28	22	14
1925		119	112	46
1985			44	23
2093			70	40
2138			71	41
2172			48	27
2195			87	41
2265			187	80
2285			72	44
2308			44	23
2335			96	56
2361			350	204
2385			125	80

TABLE 8. Q-values and neutron separation energies for Er nuclei.

	$Q(d,t)$ $A \rightarrow A-1$ keV	$Q(d,p)$ $A-1 \rightarrow A$ keV	$S_n(d,t)$ keV	$S_n(d,p)$ keV
162	-2952 ± 10		9215 ± 10	
163		4682 ± 10		6907 ± 10
164	-2593 ± 10		8851 ± 10	
165		4431 ± 10		6657 ± 10
166	-2218 ± 10		8476 ± 10	
167		4214 ± 10		6439 ± 10
168	-1523 ± 10		7781 ± 10	
169		3781 ± 10		6006 ± 10
170	-1010 ± 10		7268 ± 10	
171		3458 ± 10		5683 ± 10

indications that these deviations are caused by Coriolis coupling to the several near-lying negative parity bands, but a quantitative explanation of the intensities must await a complete theoretical analysis based on the information now available on excitation energies and coupling matrix elements.
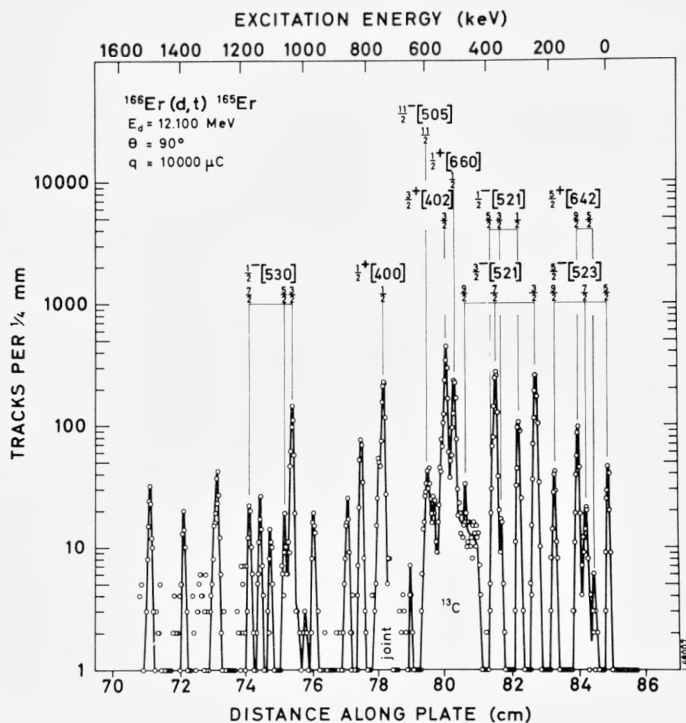
Fig. 4. Triton spectrum for the reaction $^{166}Er(d,t)^{165}Er \, \theta = 90°$. In this and the following figures, groups ascribed to reactions on target impurities are indicated by the symbol of the target impurity. Thus, the broad group marked ^{13}C is due to the $^{13}C(d,t)^{12}C$ reaction.

2.3.2. The 5/2 + [642] Orbital

This orbital is the ground state in ^{161}Dy and should therefore be expected to appear as a low-lying state in ^{161}Er where, however, it has been impossible to identify the band with certainty. It is suggested that the strong state at 189 keV is the 9/2 + member of the band. The 13/2 + state can then be concealed in the strong groups around 369 keV to 396 keV or, more likely, in the too strong 7/2 5/2 − [523] group at 268 keV.

In ^{163}Er, the angular intensity variation for the strong group at 121 keV is consistent with a 9/2 5/2 + [642] assignment, although the cross section is somewhat large. The 22 keV 5/2 + level suggested by radioactivity studies[10] would fit into the band for an inertial parameter $A = 6$ keV. The weak group at 67 keV might be the 7/2 + state, and the 13/2 + state would then be expected near the strong 250 keV (7/2 3/2 − [521]) group, but it is not observed.

Fig. 5. Proton spectrum for the reaction ^{164}Er$(d,p)^{165}$Er $\theta = 90°$.

The $5/2 + [642]$ band poses problems also in ^{165}Er. A weak group is observed at 48 keV, which earlier was assigned as $5/2$ $5/2 + [642]^{10)}$. The only possible place for the $9/2 +$ group is 98 keV, and one could then suspect that the $13/2 +$ group is hidden in the $3/2$ $3/2 - [521]$ group at 242 keV, which is too intense. If this were the case, the band is distorted to a considerable extent.

The (d, t) spectra for ^{167}Er show two strong groups at 933 keV and 1109 keV with large $125°$ yields, which indicates high l-values. These groups might correspond to the $9/2 +$ and $13/2 +$ states of the $5/2 + [642]$ band. In view of the high excitation energies, the assignments are of course not very certain and are mentioned only because of the importance of observing the $3/2 + [651]$ (Sec. 2.3.3) and $5/2 + [642]$ orbitals in one nucleus.

Fig. 6. Triton spectrum for the reaction ^{168}Er$(d,t)^{167}$Er $\theta = 125°$.

2.3.3. The 3/2 + [651] Orbital

The (d,t) spectrum of ^{161}Er contains three strong groups at 369 keV, 463 keV, and 481 keV, of which the two first have identical angular intensity variations which are different from that of the third group. In the present interpretation, the two lowest groups are associated with the $3/2 + [402]$ orbital (Sec. 2.3.6) which could interact strongly with the $3/2 + [651]$ orbital because of the crossing of these two states in the Nilsson diagrams and thus give rise to a splitting of the large 3/2 $3/2 + [402]$ cross section. This phenomenon was observed earlier in ^{155}Gd[1]. The exact condition for the occurrence of a violent interaction between such crossing levels is not clear, but it could be strongly dependent on deformation[21]. It is remarkable that it is not observed for the $3/2 +$ levels in any of the other Er nuclei.

It has been suggested[11] that the $K = 3/2 +$ gamma-vibrational band in ^{167}Er starts at 532 keV. Coulomb excitation[12] shows levels at 532 keV, 575 keV, and 642 keV. These levels are also observed in the (d,d') spectra[13]. In the (d,p) and (d,t) spectra, the 532 keV group cannot be resolved from

Fig. 7. Proton spectrum for the reaction ^{166}Er$(d,p)^{167}$Er $\theta = 60°$.

the $9/2$ $5/2 - [512]$ group, the intensity of which, however, shows that the $3/2 +$ contribution is low. This excludes any large admixture of the $3/2$ $3/2 + [402]$ state into the gamma vibration (Sec. 2.3.6). A group in both the (d, p) and (d, t) spectra corresponds to the 575 keV level. The 643 keV level coincides with the $11/2$ $1/2 - [521]$ state, but levels at 711 keV and 911 keV could correspond to the $9/2$ and $13/2$ states in a $K = 3/2$ band. These groups are rather weak. One explanation for the (d, t) intensities to the vibrational band is an admixture of the $3/2 + [651]$ wave function. The observed intensities are approximately 10% of the theoretical prediction for a pure $3/2 + [651]$ state. In judging this number, one should remember that the intensities observed for high l-transitions usually are somewhat larger than the calculated ones. The intensity of the $3/2 + [651]$ component in the K-2 gamma vibration has theoretically[20] been estimated to 7%. Probably there

Fig. 8. Triton spectrum for the reaction ^{170}Er$(d,t)^{169}$Er $\theta = 90°$.

are other single-particle admixtures in the gamma vibration in ^{167}Er, as evidenced by the (d,p) population which hardly can be ascribed to the $3/2 + [651]$ hole state. Apart from the cases discussed above, it has not been possible to identify the $3/2 + [651]$ orbital in the Er isotopes. As in the Gd isotopes, the nonappearance of this orbital might be associated with its strong Coriolis coupling to the $5/2 + [642]$ orbital.

2.3.4. The 1/2 + [660] Orbital

The (d,t) cross section for the $1/2$ $1/2 + [400]$ state in ^{165}Er is approximately 25 % less than in ^{163}Er and ^{167}Er. A possible reason for this reduction in intensity is the coupling between the $1/2 + [660]$ and the $1/2 + [400]$ orbitals. The same phenomenon has been discussed for ^{159}Gd[1]). In order to find all triton groups in ^{165}Er with an $l = 0$ component, a measurement of the (d,t) spectra at $5°$ was performed. At this angle, the yields for all other l-values are low. In this way, the 742 keV group which is discussed below (Sec. 2.3.6) and the 507 keV group are singled out as belonging to $1/2 +$

TABLE 9. Inertial parameters and decoupling parameters.
Numbers in brackets are decoupling parameters for $K = 1/2$ bands.

Nilsson Orbital	171	169	167	165	163	161
3/2 − [521]		11.2	11.8	10.8	12.1	12.0
5/2 + [642]			7.3			
3/2 + [651]			8.5			
1/2 − [530]				10.2 (0.53)	8.9 (0.53)	
5/2 − [523]		12.4	11.0	11.0	11.9	13.6
7/2 + [633]		8.7	8.8			
1/2 − [521]	12.2 (0.68)	11.7 (0.85)	10.9 (0.72)	12.3 (0.56)	13.2 (0.41)	
5/2 − [512]	11.0	12.1	11.8	12.2	12.6	
7/2 − [514]	12.6	12.0				
9/2 + [624]	9.8					
1/2 − [510]	11.1 (0.10)	11.6 (0.067)	11.4 (0.087)	12.5 (−0.01)	12.9 (−0.32)	
3/2 − [512]	12.9	12.2	11.6	13.0		

TABLE 10. (d, t) population of the $3/2 − [521]$ band.

Spin	$d\sigma/d\Omega$, $\theta = 90°$, $Q = -2$ MeV						Relative values of $C_{j,l}^2$					
	Theory	¹⁶¹Er	¹⁶³Er	¹⁶⁵Er	¹⁶⁷Er	¹⁶⁹Er	Theory	¹⁶¹Er	¹⁶³Er	¹⁶⁵Er	¹⁶⁷Er	¹⁶⁹Er
3/2	157	135	180	334	202**	139	0.10	0.10	0.10	0.23	0.19	0.23
5/2	0	–	~ 2*	–	–	5	~ 0	–	~ 0.003	–	–	~ 0.03
7/2	281	207	395	340	269	121	0.53	0.42	0.61	0.66	0.71	0.58
9/2	21	21	12	~ 9	6	5	0.25	0.27	0.12	0.11	0.10	0.16
11/2	9	17***	16	–	–	–	0.11	0.22	0.16	–	–	–

    * From 60° yield.
  ** Assumes that 7/2 5/2 − [523] state contributes with 43 $\mu b/sr$.
*** Contains also the 9/2 5/2 − [523] state.

TABLE 11. (d, t) population of the $11/2 − [505]$ band.

Spin	$d\sigma/d\Omega$, $\theta = 90°$, $Q = -2$ MeV					
	Theory	¹⁶¹Er	¹⁶³Er	¹⁶⁵Er	¹⁶⁷Er	¹⁶⁹Er
11/2	82	71	95*	~ 62	84	66

  * Contains also the 5/2 1/2 − [521] state.
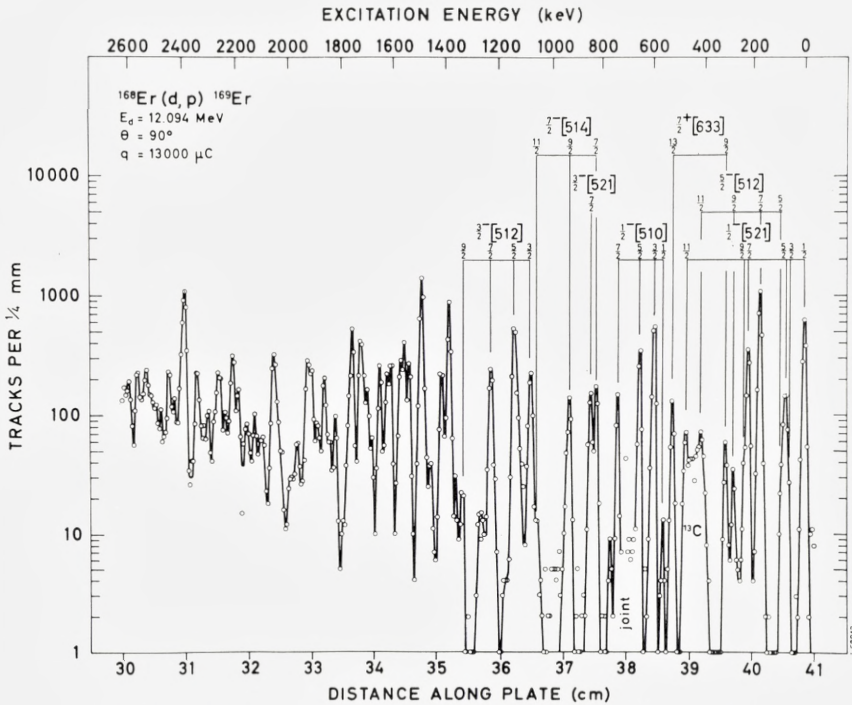
Fig. 9. Proton spectrum for the reaction ^{168}Er$(d,p)^{169}$Er $\theta = 90°$.

levels. The 507 keV level has already been assigned as 1/2 + from decay studies[10] and is probably associated with the 1/2 1/2 + [660] state. If this interpretation is correct, the intensity corresponds to a 38 % admixture of the 1/2 1/2 + [400] state. It is not possible to identify with certainty other states of the 1/2 + [660] band.

2.3.5. The 11/2-[505] Orbital

In the gadolinium isotopes, the 11/2 – [505] orbital was observed between the 3/2 – [521] and 3/2 + [402] orbitals, and it is therefore expected to be observed also in the (d, t) spectra of erbium. A unique identification of the 11/2 – [505] orbital is, however, rather difficult, because only the 11/2 – member of the band is populated. On the basis of the angular dependence, a possible 11/2 11/2 – [505] state has been located in all the erbium nuclei from ^{161}Er to ^{169}Er, but, in some cases, several groups with $l = 5$ angular dependence and reasonable intensity are present. The group with the lowest energy is then preferred.
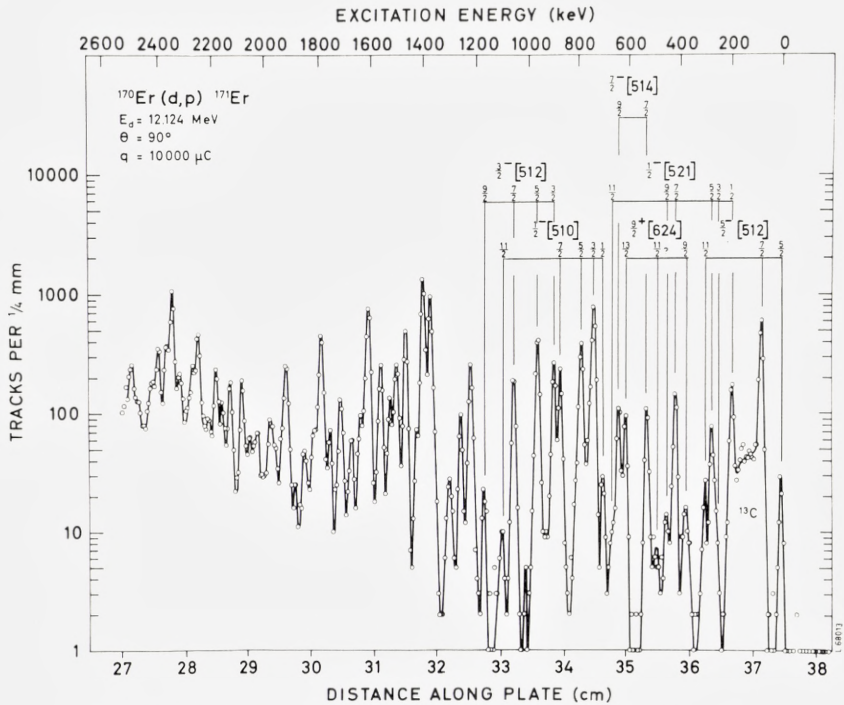
Fig. 10. Proton spectrum for the reaction $^{170}Er(d,p)^{171}Er$ $\theta = 90°$.

2.3.6. The 3/2 + [402] and the 1/2 + [400] Orbitals

The $3/2 + [402]$ and the $1/2 + 400]$ orbitals are expected to give rise to intense groups in the (d,t) spectra. Two strong groups were observed in the gadolinium spectra[1] and were ascribed to the $3/2\ 3/2 + [402]$ and the $1/2\ 1/2 + [400]$ states. In the erbium spectra similar groups are observed, and it is again reasonable to associate them with the two $N = 4$ states which originate in the $d_{3/2}$ and $s_{1/2}$ shell-model states. As in the gadolinium case, there are rather large fluctuations in intensities and problems with the assignment of the associated rotational bands, which make the distinction between the $3/2 + [402]$ and $1/2 + [400]$ orbitals difficult.

The (d,t) spectra recorded at $5°$ for ^{165}Er and ^{167}Er show that the upper level has $l = 0$, and this has been assumed to be the case for the other nuclei as well. Some additional support for the assignments was obtained from the angular intensity variations and the absolute cross sections.

The absolute cross sections, reduced to $Q = -2$ MeV, are given in Table 12 for the $N = 4$ orbitals and indicate an increased filling of the $3/2\ 3/2 + [402]$
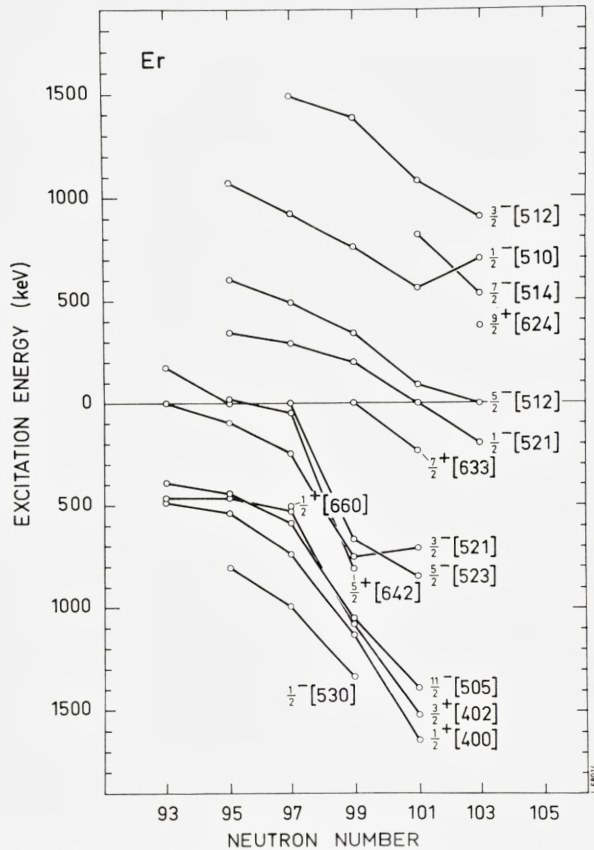
Fig. 11. Energies of the band heads for the Nilsson states observed. Points at negative energies indicate hole states.

state from ^{161}Er to ^{167}Er and a dilution of the state in ^{169}Er. The 1/2 1/2 + [400] group discloses the same general behaviour and, in addition, a somewhat reduced intensity in ^{165}Er (Sec. 2.3.4).

It has not been possible to identify the rotational bands built on the 1/2 + [400] and 3/2 + [402] states, although several of the rotational states are predicted to be populated quite strongly. The same situation prevailed in the Gd isotopes.

2.3.7. The 3/2-[532] Orbital

In spite of the relatively large (d,t) cross sections expected, no definite identification has been made of groups belonging to the 3/2 − [532] band.
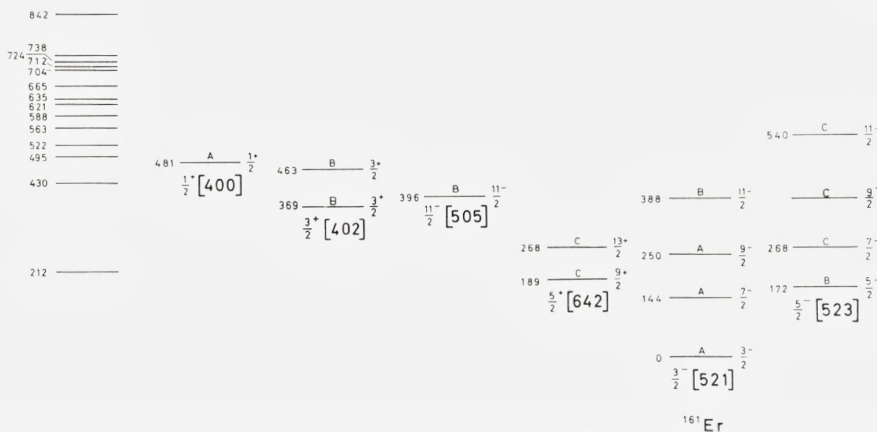
Fig. 12. Level scheme for ¹⁶¹Er. Nilsson states to the left are hole excitations, those to the right are particle excitations. The letter A indicates that all the available data suggest the assignment, B an assignment consistent with the observations, but where lack of resolution or intensity prevents a definite assignment. Finally, C indicates that a group was observed at the position expected, e.g., for a rotational level but with an intensity considerably different from theoretically predicted intensity.

In ¹⁶³Er, there are several (d, t) groups between 600 keV and 800 keV of excitation, which might belong to this band, but no obvious rotational structure can be found. In ¹⁶⁵Er, there are unidentified groups around 1200 keV above the 1/2 − [530] band. In the Gd nuclei[1], this energy region was free of strong lines, and it is conceivable that their presence in the heavier Er nuclei indicates that the 3/2 − [532] band has crossed the 1/2 − [530] band.

2.3.8. The 1/2–[530] Orbital

The strong (d, t) group at 856 keV in ¹⁶³Er has an angular variation which indicates a low angular momentum transfer, and as the intensity is close to the prediction for the 3/2 1/2 − [530] state, this identification is made, which is also supported by the analogy to the Gd nuclei where the band has been observed before[1]. The groups at 877 keV and 973 keV are probably due to the 5/2 − and 7/2 − members of the rotational band. Their intensities are about 60 % of the theoretical predictions. The decoupling parameter is then $a = 0.53$ and the inertial parameter $A = 8.9$ keV, which is consistent with the findings in the Gd nuclei.

A similar band in ¹⁶⁵Er can be based on the strong (d, t) group at 1039 keV as the 3/2 1/2 − [530] group. Possible 5/2 − and 7/2 − groups are found at 1063 keV and 1172 keV. This band will have the same decoupling para-
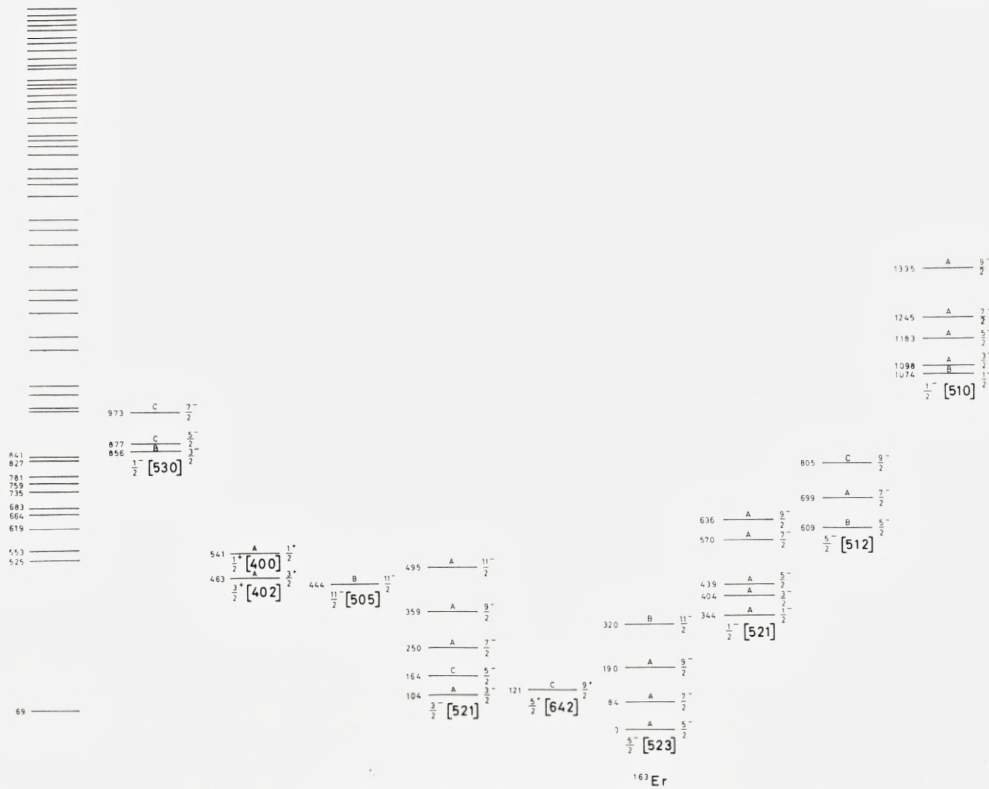
Fig. 13. Level scheme for ^{163}Er.

meter as in ^{163}Er, but $A = 10.2$ keV. Other choices for the $5/2-$ and $7/2-$
groups are, however, possible.

In ^{167}Er, the $3/2 \, 1/2 - [530]$ state is probably the one at 1377 keV ($l = 1$?),
but the associated rotational band is by no means obvious in the (d, t)
spectra. The intensity of the $3/2-$ group is $57\,^0/_0$ of the theoretical intensity;
this indicates a beginning breakdown of the $1/2 - [530]$ state, which seems
to be complete in ^{169}Er where the state has not been located at all. It is in-
teresting to note that the suggested $3/2 \, 1/2 - [530]$ state in ^{167}Er is strongly
populated in the (d, d') reaction[13], which would indicate admixtures of an
octupole vibration.

TABLE 12. (d,t) population of the $N = 4$ states.

Level	$d\sigma/d\Omega$, $\theta = 90°$, $Q = -2$ MeV					
	Theory	^{161}Er	^{163}Er	^{165}Er	^{167}Er	^{169}Er
3/2 3/2 + [402]	612	366	450	567	600	346
1/2 1/2 + [400]	780	630	602	440	650	337

TABLE 13. (d,t) population of the $5/2 - [523]$ band.

Spin	$d\sigma/d\Omega$, $\theta = 90°$, $Q = -2$ MeV					Relative values of $C^2_{j,l}$				
	Theory	^{163}Er	^{165}Er	^{167}Er	^{169}Er	Theory	^{163}Er	^{165}Er	^{167}Er	^{169}Er
5/2	39	31	39	43	41***	0.07	0.11	0.11	0.10	0.11
7/2	41	~ 20*	19	43**	41	0.08	0.07	0.06	0.10	0.11
9/2	65	34	43	48	30	0.79	0.78	0.83	0.73	0.54
11/2	5	~ 2	–	4	12	0.06	0.05	–	0.06	0.23

    * Estimated from 60° and 125° yields.
    ** Assumes that the unresolved 7/2 state has the same intensity as the 5/2 member of
the band.
    *** Assumes that the unresolved 5/2 state has the same intensity as the 7/2 member of
the band.

TABLE 14. (d,t) population of the $7/2 + [633]$ band.

Spin	$d\sigma/d\Omega$, $\theta = 90°$, $Q = -2$ MeV			Relative values of $C^2_{j,l}$		
	Theory	^{167}Er	^{169}Er	Theory	^{167}Er	^{169}Er
7/2	0.4	~ 1	–	0.001	0.002	–
9/2	25	43	37	0.07	0.08	0.07
11/2	0.6	~ 1	–	0.02	0.02	–
13/2	35	59	50	0.92	0.91	0.93

TABLE 15. (d,p) population of the $5/2 - [523]$ band.

Spin	$d\sigma/d\Omega$, $\theta = 90°$, $Q = 3$ MeV			Relative values of $C^2_{j,l}$		
	Theory	^{163}Er	^{165}Er	Theory	^{163}Er	^{165}Er
5/2	44	17	9	0.07	0.07	0.07
7/2	45	29	10	0.08	0.11	0.07
9/2	63	29	16	0.79	0.82	0.86
11/2	5	–	–	0.06	–	–
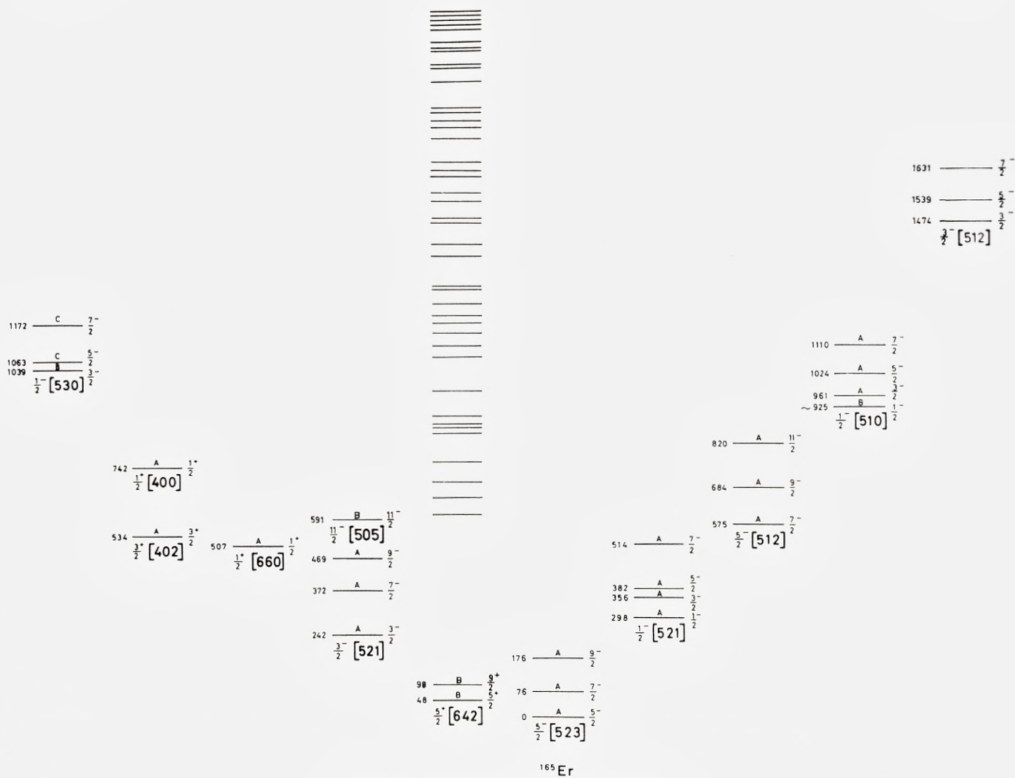
Fig. 14. Level scheme for ^{165}Er.

2.3.9. The 5/2–[523] Orbital

The level at 172 keV in ^{161}Er is assigned as 5/2 5/2 – [523], in agreement with decay studies[16] which also place a 9/2 – state at 344.7 keV. This level is definitely not observed in the (d, t) spectra, in disagreement with the theoretical predictions for the 9/2 5/2 – [523] state. Therefore, the most reasonable band based on the (d, t) data is one where the band head is still placed at 172 keV, but where the 7/2 –group is a part of the strong group at 268 keV, and the 9/2 – group coincides with the 11/2 – state in the ground-state band at 388 keV. The 11/2 – member of the band could then be the group observed at 540 keV, or part thereof.

The 5/2 – [523] orbital forms the ground states in ^{163}Er and ^{165}Er, where all the members of the rotational band are observed, except the 11/2 – state in ^{165}Er which is obscured by the strong 1/2 1/2 – [521] group at 298 keV.
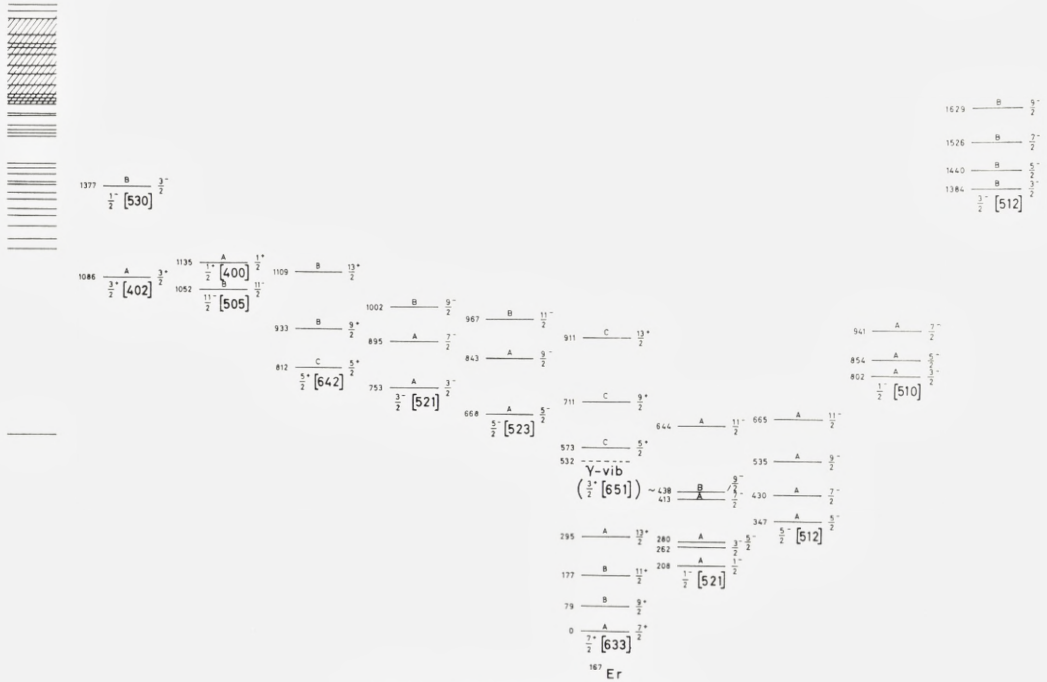
Fig. 15. Level scheme for ^{167}Er.

In ^{167}Er, a 5/2 5/2 – [523] level at 667.9 keV has been proposed earlier by Koch[14]. The (d, t) spectra show groups at 668 keV, 735 keV (coincides with the 3/2 3/2 – [521] state), 843 keV, and 967 keV, which could be the 5/2, (7/2), 9/2, and 11/2 states of this band. The intensities for the unobscured peaks are in good agreement with the theory.

In ^{169}Er, the 5/2 – [523] orbital is expected to be a component of the gamma vibration with $K = 5/2$ built on the 1/2 – [521] ground state. In the region between 900 keV and 1350 keV, there are approximately 13 weak lines in the (d, t) spectra, of which only a few have strong counterparts in the (d, p) spectra. The 5/2 – [523] band is expected in this region. The assignments for this band made from the ^{169}Ho decay[15] are 5/2 – at 850 keV and 7/2 – at 920 keV. If these assignments are accepted, the 5/2 – group is concealed in the 7/2 3/2 – [521] group and there is no 9/2 – group in the (d, t) spectra, which group is predicted to be as strong as the 5/2 – and 7/2 – groups. If the 7/2 – state is moved to 940 keV (which might be compatible with the decay data if the two final states for decay are shifted to
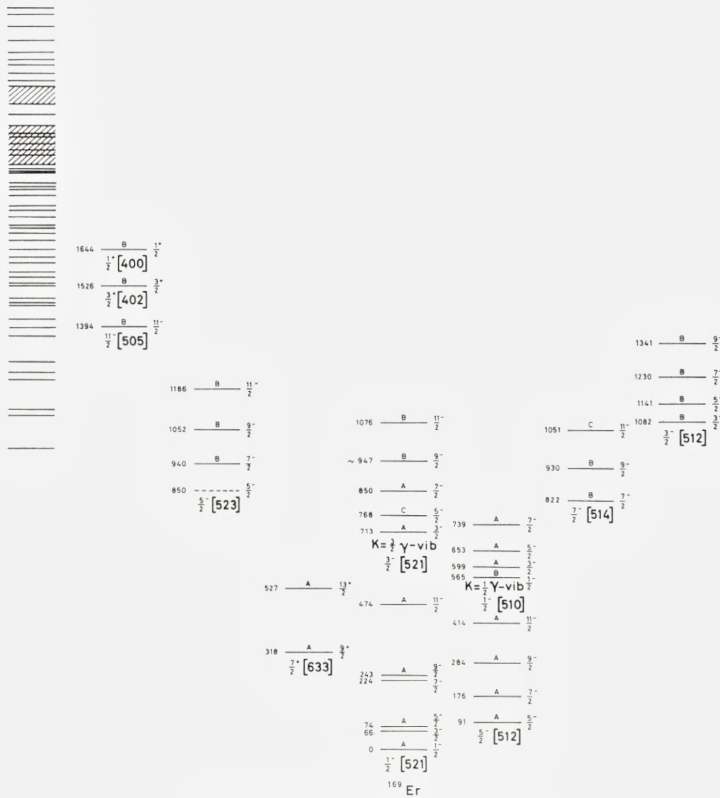
Fig. 16. Level scheme for ^{169}Er.

existing states approximately 20 keV higher), a 9/2 − group can be post-
ulated at 1052 keV, where a (d, t) group is seen. The 11/2 − state can then
be at 1186 keV. These assignments are given in Table 6.

2.3.10. The 7/2 + [633] Orbital

The states of the 7/2 + [633] ground-state band in ^{167}Er are observed up
to the 13/2 + state. The (d, p) intensities are in reasonable agreement with
the theory, whereas the (d, t) intensities for the 9/2 + and 13/2 + states are
around 1.8 times the theoretical estimates. The partial filling of the ground-
state level due to pairing can be estimated to reduce the cross sections by
factors of U^2 and $V^2 \sim 0.5$ for the (d, p) and (d, t) reactions, respectively.
The observed cross sections are thus considerably larger than expected and
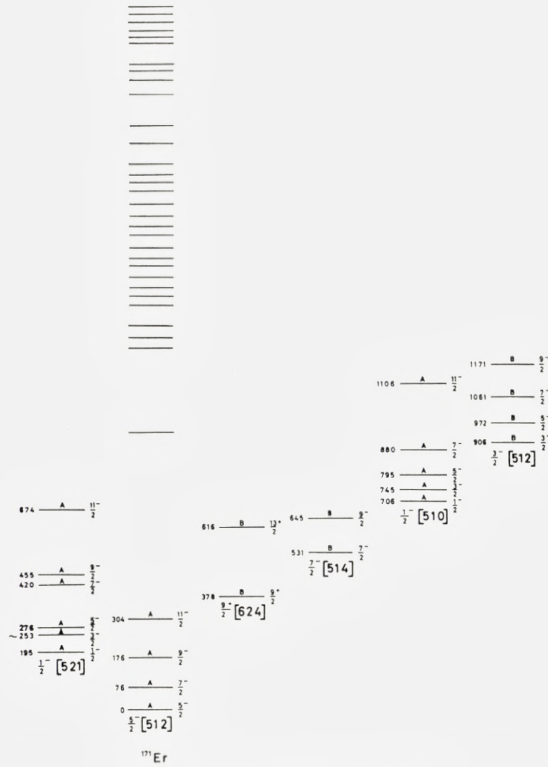
Fig. 17. Level scheme for ¹⁷¹Er.

indicate a significant increase in single-particle strength. The strong Coriolis coupling between the $N = 6$ states might again be responsible for this effect.

In ¹⁶⁹Er, the $7/2 + [633]$ band is placed with the $9/2 +$ state at 318 keV and the $13/2 +$ state at 527 keV. The $7/2 +$ group can then be expected to coincide with the $7/2$ $1/2 - [521]$ group. The (d, p) intensities are approximately 0.8 times and the (d, t) intensities approximately 1.5 times the theoretical values.

It has not been possible to identify the band with any degree of certainty in the other nuclei.

2.3.11. The 1/2–[521] Orbital

This orbital has been identified in a large number of cases and is known in all the erbium nuclei[9]. The present results are in agreement with the previous assignments.

TABLE 16. (d,p) population of the $7/2 + [633]$ band.

Spin	$d\sigma/d\Omega,\ \theta = 90°,\ Q = 3$ MeV			Relative values of $C^2_{j,l}$		
	Theory	^{167}Er	^{169}Er	Theory	^{167}Er	^{169}Er
7/2	~ 0.5	~ 0.5	–	0.001	~ 0.001	–
9/2	21	14	17	0.07	0.04	0.07
11/2	0.7	–	–	0.02	–	–
13/2	42	57	32	0.92	0.96	0.93

TABLE 17. (d,p) population of the $1/2 - [521]$ band.

Spin	$d\sigma/d\Omega,\ \theta = 90°,\ Q = 3$ MeV						Relative values of $C^2_{j,l}$					
	Theory	^{163}Er	^{165}Er	^{167}Er	^{169}Er	^{171}Er	Theory	^{163}Er	^{165}Er	^{167}Er	^{169}Er	^{171}Er
1/2	377	164	181	213	214	73	0.25	0.17	0.21	0.20	0.20	0.15
3/2	38	37	19	14	~ 20	18*	0.02	0.04	0.02	0.01	0.02	0.03
5/2	107	50	39	52	~ 46	31	0.18	0.14	0.12	0.12	0.11	0.16
7/2	136	94	82	110	116	49	0.23	0.25	0.25	0.26	0.27	0.25
9/2	21	11	12**	16**	17**	7	0.27	0.22	0.26	0.27	0.29	0.27
11/2	4	9	~ 6	8	7	4	0.05	0.18	0.13	0.14	0.12	0.15

  * From 125° yield.
  ** Assumes an intensity ratio 1:7 for the spin 7/2 and 9/2 members.

From Table 17 it is seen that the relative values of $C^2_{j,l}$ are in good agreement with the predicted values. The (d,t) and (d,p) cross sections for the states of the $1/2 - [521]$ band show in a qualitative way the increased filling of the orbital from ^{167}Er to ^{171}Er, but the behaviour is less regular than that observed in the ytterbium isotopes[2] where the $1/2 - [521]$ orbital showed all the characteristics of a pure single-particle state. Both cases differ from the gadolinium results, where large fluctuations in the cross sections were observed, probably as a result of the coupling to the gamma-vibrational states. The same couplings are possibly responsible for the slightly smaller $1/2 - [521]$ intensity in ^{163}Er and ^{165}Er than in ^{167}Er and for the reduction of the decoupling parameters (cf. Table 9).

2.3.12. The 5/2–[512] Orbital

The $5/2 - [512]$ orbital is characterized by a strong population of the $7/2 -$ member of the band. It is the ground state in ^{171}Er[8] where all the members of the band are observed. In ^{169}Er and ^{167}Er, the band is expected as a low-lying particle excitation. The 176 keV group in ^{169}Er and the

430 keV group in ^{167}Er have the expected angular intensity variation. The 430 keV level has also been assigned to the 7/2 5/2−[512] state from the ^{166}Er(n,γ)^{167}Er work[14]. The corresponding 5/2−, 9/2−, and 11/2− states are all identified in the (d,p) spectra of ^{167}Er and ^{169}Er.

The theoretical cross sections and the reduced (d,p) cross sections are compared in Table 18. The 7/2− state has a lower cross section than predicted, whereas the weakly populated 5/2−, 9/2−, and 11/2− states are two to three times stronger than predicted.

In ^{165}Er, the strong 575 keV (d,p) group is assigned as 7/2 5/2−[512], which assignment is supported by an $l = 3$ angular dependence. The intensity, however, corresponds to only 48% of the expected cross section. The 5/2− state is obscured, but the groups at 684 keV and 820 keV could be associated with the 9/2− and 11/2− levels, respectively.

In ^{163}Er, the levels at 609 keV, 699 keV, and 805 keV are possible candidates for the 5/2−, 7/2−, and 9/2− states of the 5/2−[512] band. The angular dependence agrees with the 7/2− assignment for the 699 keV level, but the intensity is only 44% of that expected.

A reduction in intensity of the 7/2 5/2−[512] group in the lighter gadolinium nuclei is parallel to the one observed here.

2.3.13. The 7/2-[514] Orbital

This orbital is expected to appear at an excitation energy below 1 MeV for the heaviest erbium nuclei, in analogy to the assignments in ytterbium nuclei[2].

In ^{171}Er, the band has been placed at 531 keV (7/2−) and 645 keV (9/2−), but the reasons for the assignment are not compelling. The (d,p) groups selected occur in the expected energy region and have reasonable intensities and angular distributions.

There are three peaks in the (d,p) spectra of ^{169}Er with energies 822 keV, 930 keV, and 1051 keV, which can be associated with rotational members of the 7/2−[514] band. The observed intensities of the 7/2− and 9/2− states are approximately equal, whereas the theory predicts a ratio of ∼2 between the intensities of the 9/2− and 7/2− states. An alternative explanation for the states considered here would be an assignment to the 9/2+[624] band, which is expected in the same region of energy.

2.3.14. The 9/2 + [624] Orbital

This orbital should occur as a particle excitation in the erbium nuclei. The pattern predicted consists of a weak 9/2+ group and a somewhat stronger 13/2+ group. In ^{171}Er, the band has been placed at 378 keV (9/2+)

TABLE 18. (d,p) population of the $5/2-[512]$ band.

Spin	$d\sigma/d\Omega$, $\theta = 90°$, $Q = 3$ MeV						Relative values of $C_{j,l}^2$					
	Theory	^{163}Er	^{165}Er	^{167}Er	^{169}Er	^{171}Er	Theory	^{163}Er	^{165}Er	^{167}Er	^{169}Er	^{171}Er
5/2	6	9	–	13*	13	12	0.01	0.04	–	0.03	0.03	0.04
7/2	463	204	220	317	332	228	0.79	0.87	0.65	0.61	0.70	0.67
9/2	11	~ 3	8	13	11	~ 7*	0.14	0.09	0.17	0.18	0.17	~ 0.15
11/2	5	–	8	13	7	~ 7	0.06	–	0.17	0.18	0.11	~ 0.15

* From 60° yield.

TABLE 19. (d,p) population of the $1/2-[510]$ band.

Spin	$d\sigma/d\Omega$, $\theta = 90°$, $Q = 3$ MeV						Relative values of $C_{j,l}^2$					
	Theory	^{163}Er	^{165}Er	^{167}Er	^{169}Er	^{171}Er	Theory	^{163}Er	^{165}Er	^{167}Er	^{169}Er	^{171}Er
1/2	13	6	~ 2	–	~ 3	11	0.01	0.01	0.005	–	0.007	0.01
3/2	615	174	140	~157	160	262	0.40	0.38	0.35	0.35	0.35	0.31
5/2	172	50	53	~ 85	86	139	0.29	0.28	0.34	0.48	0.48	0.42
7/2	113	22	47	29	29	64	0.19	0.12	0.30	0.17	0.16	0.19
9/2	6	5	–	–	–	–	0.09	0.21	–	–	–	–
11/2	1	–	–	–	–	3	0.01	–	–	–	–	0.07

and 616 keV ($13/2+$). The upper group has a rather flat angular distribution, and the $9/2+$ level is an unassigned level at the expected energy. The inertial parameter is $A = 10.0$ keV, which can be compared to $A = 10.7$ keV in ^{175}Yb. The assignment must be considered somewhat uncertain, and it has not been possible to identify the orbital in the lighter erbium isotopes.

2.3.15. The 1/2–[510] Orbital

The $1/2-[510]$ orbital has not been identified in the erbium isotopes before. It is characterized by a strong population of the $3/2-$ state and somewhat smaller populations of the $5/2-$ and $7/2-$ states. The other members of the band are weak.

In ^{171}Er, all states from spin $1/2$ to spin $11/2$ in the $1/2-[510]$ band are clearly observed. The $9/2-$ state does, however, coincide with the $5/2$ $3/2-[512]$ state. The intensities are approximately 60% of the theoretical predictions, except for the $11/2-$ state which is three times too strong.

In ^{169}Er, the $1/2-[510]$ orbital is expected to have an excitation energy above 700 keV, but the most reasonable $3/2-$ group is the one at 599 keV, which has an angular dependence in agreement with this assignment. The

TABLE 20. (d,p) population of the $3/2 - [512]$ band.

Spin	$d\sigma/d\Omega$, $\theta = 90°$, $Q = 3$ MeV					Relative values of $C_{j,l}^2$			
	Theory	^{165}Er	^{167}Er	^{169}Er	^{171}Er	Theory	^{167}Er	^{169}Er	^{171}Er
3/2	120	48	63	66	82	0.08	0.08	0.09	0.12
5/2	376	80	115	152	134	0.64	0.39	0.53	0.49
7/2	70	∼ 27	68	63	57	0.12	0.23	0.22	0.21
9/2	11	–	12	6	7	0.15	0.29	0.15	0.18
11/2	1	–	–	–	–	0.01	–	–	–

TABLE 21. Comparison of experimental and theoretical single-particle amplitudes.

Nucleus	$K\pi[Nn_z\Lambda]$	Excitation energy		Decoupling parameter		% amplitude		Main vib. component theory
		exp	theor	a_{exp}	a_{theor}	exp	theor	
^{165}Er	$1/2 - [521]$	298	340	0.56	0.65	50	73	$Q(22) + 5/2 - [523]$ 22 %
^{167}Er	$3/2 + [651]$	325	750			10	7	$Q(22) + 7/2 + [633]$ 88 %
^{167}Er	$1/2 - [510]$	∼ 768	800			30	32	$Q(22) + 5/2 - [512]$ 54 %
^{167}Er	$3/2 - [521]$	753	750			108	79	$Q(22) + 1/2 - [521]$ 15 %
^{169}Er	$5/2 - [523]$	∼ 850	850			83	46	$Q(22) + 1/2 - [521]$ 47 %
^{171}Er	$1/2 - [510]$	706	800	0.10	− 0.17	52	48	$Q(22) + 5/2 - [512]$ 48 %

absolute intensity is less than in ^{171}Er. A lowering of the energy and the intensity is expected if the $1/2 - [510]$ state is a component of the $K = 2$ gamma vibration built on the $5/2 - [512]$ state.

In the lighter erbium isotopes, it is possible to find similar patterns which are ascribed to the $1/2 - [510]$ band. The intensities and the angular dependencies are in agreement with those observed in ^{169}Er.

The theory predicts a negative decoupling parameter $(a = -0.33)$ for the $1/2 - [510]$ band. The decoupling parameters found in the erbium isotopes are all close to zero, in agreement with the expected effect of admixtures of gamma vibration based on the $5/2 - [512]$ state.

2.3.16. The 3/2–[512] Orbital

Relatively strong groups in the (d,p) spectra of ^{171}Er, ^{169}Er, ^{167}Er, and perhaps ^{165}Er form patterns which resemble the one expected for the $3/2 - [512]$ band. The intensities are, however, considerably smaller than the theoretical values, especially for the $5/2 -$ group, which has only about

35 % of the theoretical intensity compared to 50 % to 90 % for the other groups (cf. Table 20). A similar behaviour was observed in the Yb isotopes[2], and there is therefore little doubt about the correctness of the assignments. The reason for the intensity reduction of the 5/2 – group is not clear, but it should be pointed out that none of the lower-lying bands has excessive 5/2 – strength.

3. Conclusions

The band-head energies of the Nilsson states identified in the erbium isotopes are shown in Fig. 11. The level order, with a few exceptions, is identical to the one found in Gd and Yb. Among the exceptions is the position of the 11/2 – [505] hole state, which in Gd always was found below the 3/2 + [402] state, but which in ^{165}Er is located at a higher excitation energy.

Most of the energy levels observed below 1 MeV of excitation have been explained in terms of the Nilsson model, although some of the observed cross sections deviate considerably from the theoretical prediction. Among the most noticeable discrepancies are those for the 3/2 3/2 – [521] and 7/2 3/2 – [521] states discussed in Sec. 2.3.1. As seen from the reduced (d, t) cross sections in Table 10, a spectroscopic factor for the 3/2 – state, defined as the ratio of the observed cross section to the calculated cross section, varies from 0.86 to 2.18 within a few mass numbers. A ratio of 1.0 would be expected for a pure hole state. The corresponding spectroscopic factors obtained from the (d, p) cross sections are of the order of 0.5, which is rather large for a hole state. Obviously, the description in terms of a pure Nilsson state is inadequate, but is not easy to find, e.g., sufficient $j = 3/2$ cross sections in the neighbouring bands to account for the observations.

A few of the Nilsson states expected in the region of low excitation have not been definitely observed. This is the case for the 3/2 + [651] state which has never been observed as a pure state, but which apparently is responsible for the irregular energy spacings and intensities in the 5/2 + [642] bands and also for the splitting of the 3/2 + [402] intensity observed in ^{161}Er. The 3/2 – [532] state offers another example of a state with a great tendency to fractionation and which, consequently, was not definitely observed in the Er nuclei. In this case, the responsible couplings have not been identified.

The energy spectra above 1 MeV of excitation are complex, and only for a few of the stronger groups it has been possible to make a single-particle assignment. Because of the Q-value dependence of the (d, t) cross section,

the higher parts of the excitation spectrum can be studied only by the (d, p) reaction. Therefore, only states with large particle excitation components are accessible. Unfortunately, the energy resolution in the (d, p) spectra has not been sufficient for a more complete study of the regions of higher excitation energy. It is evident that strong couplings are active in spreading the intensity among several levels. The summed cross section is almost the same for all nuclei, but the level density is slightly decreasing with neutron number. This phenomenon is probably related to a decrease in collective strength, which is apparent from the inelastic deuteron scattering results[3].

Several even-parity states are expected as particle states in the region above 1 MeV of excitation, among which the $1/2 + [651]$ and the $1/2 + [640]$ states have large cross sections. The first of these was observed at ~ 1700 keV in the heavier Gd nuclei and should be present in the Er nuclei as well. In [171]Er, there are several groups present around 1500 keV, which might belong to the $1/2 + [651]$ band, but it has not been possible to identify a band structure. It should be remarked that strong even-parity states[17] have been localized in the Yb nuclei by studies of isobaric analogue resonances. Some of these were erroneously ascribed to negative parity states before[2].

In spite of the difficulties mentioned above, it is evident that the Nilsson model in general gives an amazingly accurate description of the low-lying energy levels in the Er nuclei. The level sequence is accurately reproduced and, in most cases, the components of the wave function obtained from the experiments are in good agreement with the theory.

A further improvement in the description of the states in odd deformed nuclei is obtained by specifically taking into account the particle-vibration interactions[19, 20]. The experimental spectra show several effects of such interactions, but only in a few cases sufficient information is available to allow a closer comparison between theory and experiment. Table 21 summarizes the theoretical single-particle amplitudes for a number of cases, in which the coupling to the gamma vibrations has been considered theoretically[20]. The corresponding experimental amplitudes have been obtained as the average ratios of the experimental and the calculated cross sections, as listed in Tables 10–20. The qualitative agreement between theory and experiment underlines the importance of this type of interaction for the low-energy spectra of odd nuclei.

The present work is meant to be a survey, and it has not been attempted to analyze the material in detail. A more complete test of the ideas underlying the description of the energy levels in deformed nuclei would be greatly facilitated by improved experimental data. Among the most obvious im-

provements is a better energy resolution, especially in the (d,p) spectra. The present techniques can be improved to ensure this. Better methods for l- and j-assignments would be invaluable. Frequently, the angular distribution studies performed up to now did not permit any unique assignments, but might be of increased value if they were combined with the parity information obtained from isobaric analogue resonance studies. Other interesting possibilities are connected with the study of excitation functions. A recent investigation[18] makes some promise that high and low angular momenta could be distinguished in this manner. An enhancement of the intensity of the high angular momentum groups could also be obtained by the use of the $(^3He,\alpha)$ pick-up reaction.

Acknowledgements

The Niels Bohr Institute   *Physics Institute*
University of Copenhagen   *University of Oslo*

References

1) P. O. Tjøm and B. Elbek, Mat. Fys. Medd. Dan. Vid. Selsk. **36** (1967) no. 8.
2) D. G. Burke, B. Zeidman, B. Elbek, B. Herskind and M. C. Olesen, Mat. Fys. Medd. Dan. Vid. Selsk. **35** (1966) no. 2.
3) P. O. Tjøm and B. Elbek, Nuclear Physics **A 107** (1968) 385.
4) C. M. Perey and F. G. Perey, Phys. Rev. **132** (1963) 755.
5) M. Jaskola, K. Nybø, P. O. Tjøm and B. Elbek, Nuclear Physics **A 96** (1967) 52.
6) R. H. Siemssen and J. R. Erskine, Phys. Rev. **146** (1966) 911.
7) M. Jaskola and K. Nybø, private communication (1966).
8) Nuclear Data Sheets, National Academy of Science, Washington.
9) C. W. Reich and M. E. Bunker, unpublished.
10) B. Harmatz, T. H. Handley and J. W. Mihelich, Phys. Rev. **128** (1962) 1186.
11) L. K. Peker, Izv. Akad. Nauk. SSSR, Ser. Fis. **28** (1964) 289.
12) A. Tveter and B. Herskind, to be published in Nuclear Physics.
13) F. Sterba, P. O. Tjøm and B. Elbek, to be published.
14) H. R. Koch, Z. f. Phys. **187** (1965) 450.
15) L. Funke, H. Graber, K. H. Kaun and H. Sodan, Deutsche Akademie der Wissenschaften zu Berlin, Z. f. K. – Ph. **A 23**.
16) A. Abdumalikov, A. Abdurazakov and K. Gromov, Izv. Akad. Nauk. SSSR, Ser. Fis. **28** (1964) 257.
17) Y-т Liu and S. Whineray, to be published.
18) W. R. Hering and M. Dort, private communication.
19) D. R. Bès and Cho Yu-chung, Nuclear Physics **86** (1966) 581.
20) V. G. Soloviev and P. Vogel, Nuclear Physics **A 92** (1967) 449.
21) B. L. Andersen, Nuclear Physics **A 112** (1968) 443.

BØRGE BAK, JENS JØRGEN LED AND
ERIK JONAS PEDERSEN

REVERSIBLE CHEMICAL CHANGES OF POLYPEPTIDES IN CF₃COOH AS SEEN BY NUCLEAR MAGNETIC RESONANCE SPECTRA

CONTENTS

Synopsis

Nuclear magnetic resonance spectra of glucagon, $C_{153}H_{225}O_{49}N_{43}S$ (29 amino acid residues) mol. wt. 3482.8, of porcine insulin, $C_{256}H_{381}O_{76}N_{65}S_6$ (51 residues) mol. wt. 5776.6, of bovine insulin, $C_{254}H_{377}O_{75}N_{65}S_6$ (51 residues) mol. wt. 5733.6, of bovine A-chain tetra-S-sulfonate, $C_{97}H_{151}O_{46}N_{25}S_8$ (21 res.) mol. wt. 2659.9 and of bovine B-chain di-S-sulfonate, $C_{157}H_{232}O_{47}N_{40}S_4$ (30 res.) mol. wt. 3560.0, all dissolved in CF_3COOH, show that the primary alcohol groups of all serine residues convert to $-CH_2OCOCF_3$ in 3–4 h at 30° while the secondary alcohol groups of all threonine residues convert to $>CHOCOCF_3$ in 1–2 days. Biologically active glucagon can be recovered in high yield from the heptatrifluoroacetylated derivative. Also, the $COCF_3$ groups of this compound can be replaced by $COCH_3$ groups.

I. Introduction

Classical chemical studies of polypeptide composition and chemical properties may be supplemented effeciently by the use of accumulated nuclear magnetic resonance (NMR) spectra. This implies, of course, extreme magnetic field stability and homogeneity besides chemical stability of the sample. From a spectroscopic point of view (vide infra) the preferable polypeptide solvent is CF_3COOH. However, we have found that polypeptides containing serine and threonine residues undergo chemical changes in this solvent, their primary and secondary alcohol groups becoming trifluoroacetylated in 1–2 days at 30°. Strictly reproducable spectral work is, therefore, only possible after the elapse of this time. After spectral recording and removal of the solvent biologically active polypeptide can be recovered by hydrolysis as demonstrated for glucagon.

II. Experimental Procedure

^{19}F magnetic resonance (FMR) spectra were recorded at 94.1 MHz, proton magnetic resonance spectra (^{1}HMR) at 100 and 220 MHz, all on Varian instruments. The polypeptide molarity was about 0.02. Internal standards were $CFCl_2CF_2Cl$ (central peak of F triplet) for ^{19}F and $(CH_3)_4Si$ for ^{1}H.

The FMR spectra were single recordings because the low-field spin-satellite from $^{13}CF_3COOH$ (1 $^0/_0$ natural abundance) was so close to and, in some cases, inseparable from the ^{19}F resonances of the trifluoroacetylated polypeptides that accumulation of spectra was no advantage. Recording of the equally intense high-field spin-satellite signal before and after each FMR spectrum served as a means of correcting for the intensity contribution of the low-field satellite to the spectrum which was integrated manually (planimeter). Spectral base-line ambiguity etc. introduced an estimated error of 10 $^0/_0$ in I_{tot} (Table I).

1*

TABLE I. Integrated total intensities of ^{19}F magnetic resonance spectra from trifluoroacetylated polypeptides. Single recordings at 30°.

The integrals are expressed as number of COCF$_3$ groups per mole of substance. Q is the initial quantity of polypeptides in units of 10^{-3} mmole dissolved in 600 μl of CF$_3$COOH. N_S and N_t are the known numbers of serine, resp. threonine OH groups per molecule of substance. h = hours.

	Q	1h	2h	5h	23h	71h	$N_S + N_t$	N_S	N_t
Porcine insulin	8.72	1.09	2.39	3.99	5.61		5	3	2
Bovine insulin	8.66	1.29	2.64	3.92	4.75		4	3	1
Bovine insulin A chain S-sulfonate	8.65	~ 0	1.10	1.82	2.58		2	2	0
Bovine insulin B chain S-sulfonate	8.43	~ 0	0.58	1.43	2.66		2	1	1
Porcine glucagon	5.73	0.76	2.69	4.07	6.90	7.68	7	4	3
Bovine glucagon	5.37	~ 0	3.06	4.15	7.22	7.38	7	4	3

As to ^{1}HMR spectra, usually 50 were accumulated when working at 100 MHz. The temperature at the sample site was 30°. The spectra taken at 220 MHz were single recordings, the temperature at the sample site being 10–15°.

The quality of the insulins and the bovine insuline A and B chains was as described earlier[1]. Two times recrystallized porcine and bovine glucagon were given to us by the NOVO RESEARCH INSTITUTE. The glucagons were dried to constant weight *in vacuo* at room temperature. For a sample it was checked that no further loss of weight occurred at 100°.

III. ^{19}FMR Spectra at 94.1 MHz

The glucagon molecule is especially rich in serine (4) and threonine (3) residues. Porcine and bovine glucagon were included in this investigation to follow their trifluoroacetylation, but also to put their alleged chemical identity[2] to spectroscopic tests. Comparison of spectra 1 and 3 (or 2 and 4) shows the expected slight dependance of chemical shifts on concentration (Table II). Within the limits of error spectra 1 and 2 and 3 and 4 are identical, one positive test of porcine and bovine glucagon identity. The FMR spectrum of hepta-trifluoroacetylated glucagon appears as 7 separate peaks (fig. 1), 4 of which are fully developed in 3–4 h (marked 'f'), the remaining 3 appearing much slower ('s'). Serine and threonine amino acids react with similar relative rates, but much slower on an absolute scale. The 'f' signals are, therefore, probably FMR signals from – CH$_2$OCOCF$_3$ groups. This assignment is verified by noting that in spectra 5, 6, 7, and 8 (Table II) 3, 3, 2, and 1 'fast' signals are recorded corresponding to the authentic

Table II. Chemical shifts in ^{19}FMR spectra of trifluoroacetylated porcine glucagon (spec. 1 and 3), bovine glucagon (spec. 2 and 4), porcine insulin (spec. 5), bovine insulin (spec. 6), of bovine A-chain S-sulphonate (spec. 7), and of bovine B-chain S-sulphonate measured in cps relative to internal $CFCl_2CF_2Cl$. Q as in Table I. Single recordings at 30°.

Spectrum number	Q								
1	5.73	266.6^f		278.6^f	280.4^f	*287^f	310.6^s	312.2^s	329^s
2	5.37	265.6^f		278.2^f	280.4^f	*287^f	310.7^s	313.1^s	329^s
3	14.3	268.0^f		*281^f	*281^f	288.6^f	312.4^s	314.4^s	330^s
4	14.3	268.2^f		*281^f	*281^f	289.1^f	312.2^s	315.2^s	330^s
5	8.72	268.4^s	272.1^f		275.4^f	287.6^{f+s}			
6	8.66	270.0^f	276.1^f		*284.2^f	287.8^s			
7	8.65	265.0^f	274.2^f						
8	8.43					*287^s	289.3^f		

f: resonance fully developed in 3–4 h.
s: resonance fully developed in 1–2 days.
* interference with ^{19}F resonance in $^{13}CF_3COOH$ (1 % natural abundance).

occurrance of 3, 3, 2, and 1 serine residues in the respective insulins and 'chains'. In all five cases the final total intensity of the FMR spectrum, I_{tot}, was close to $N_s + N_t$, the total number of serine and threonine residues per molecule. Since the discrepancy is systematically > 0 it may be evidence of a so far unidentified chemical reaction, but in view of the experimental uncertainty (10 %) of our intensity measurements we shall refrain from any interpretation of the difference which in no case amounts to 1 $COCF_3$ group
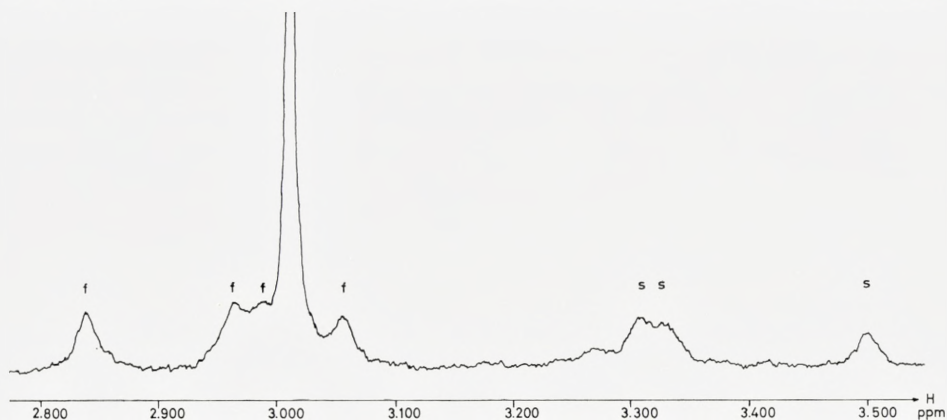
Fig. 1. 10 accumulated FMR spectra of hepta-trifluoroacetylated glucagon in CF_3COOH. f = 'fast' $-CH_2OCOCF_3$ resonance, s = 'slow' $>CHOCOCF_3$ resonance. The strong line at 3.01 ppm/ internal $CFCl_2CF_2Cl$ is the $^{13}CF_3COOH$ low-field spin satellite.

per molecule. Of whatever nature the possible change is, it is reversible by hydrolysis just as the trifluoroacetylation (vide infra).

In a physically denatured polypeptide the main determining factor for the chemical shift of a specific 'serine' or 'threonine' $COCF_3$ group is the chemical nature of the adjoining amino acid residues. The fact that identical FMR spectra are obtained from hepta-trifluoroacetylated porcine and bovine glucagon is a first sign of their chemical identity. The occurrance of 7 separate peaks (fig. 1) verifies the chemical sequence determination[2] inasfar as no serine or threonine residue is placed in identical chemical surroundings. The same conclusion applies to the insulins in agreement with Sanger's formulae[3].

IV. ¹HMR Spectra at 100 and 220 MHz

A complete analysis of the ¹HMR spectrum of glucagon is being published[4]. In the analysis, integrated intensities of a series of separate spectral bands were used as demonstrated earlier[1,5] for the insulins. Thus, a specific spectral band consists of superimposed single protons resonances (p.r.) from a known number of protons in known positions in the molecule.

As a result of progressing trifluoroacetylation the polypeptide ¹HMR spectra should be time-dependant. With glucagon as an example this is illustrated in fig. 2. Due to the reaction

$$XCH_\beta OH + CF_3 COOH \rightarrow XCH_\beta OCOCF_3 + H_2O$$
$$|\qquad\qquad\qquad\qquad\qquad |$$
$$-HNCHCO-\qquad\qquad -HNCHCO-$$

$$X = H_\beta \text{ for serine} \qquad X = CH_3 \text{ for threonine}$$
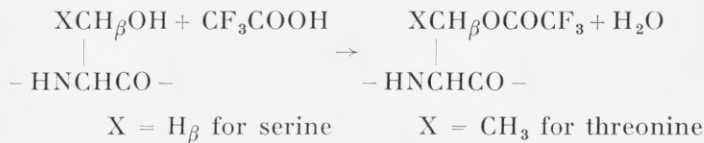
the 8 p.r. of the 8 H_β in the four glucagon serine residues and the 3 p.r. of the 3 H_β in the three threonine residues should undergo downfield chemical shifts. From the analysis of the complete spectrum it follows that the spectral intensity between A and D (fig. 2) corresponds to 42 p.r. per molecule. Since the rapidly disappearing 'shoulder' between C and D corresponds to *ca.* 6 p.r. whereas the slowly occurring band between A and B represents *ca.* 2.5 p.r., one interpretation is obvious. This was fully confirmed by studies at 220 MHz (fig. 3). Here, the area between C and D corresponds to 10.5 p.r. for a newly prepared sample. After a week (practical reasons preventing observation after 2 days) this area had shrunk to *ca.* 3.5 p.r. so that *ca.* 7 p.r. have moved. Between A and B there are practically no signals at
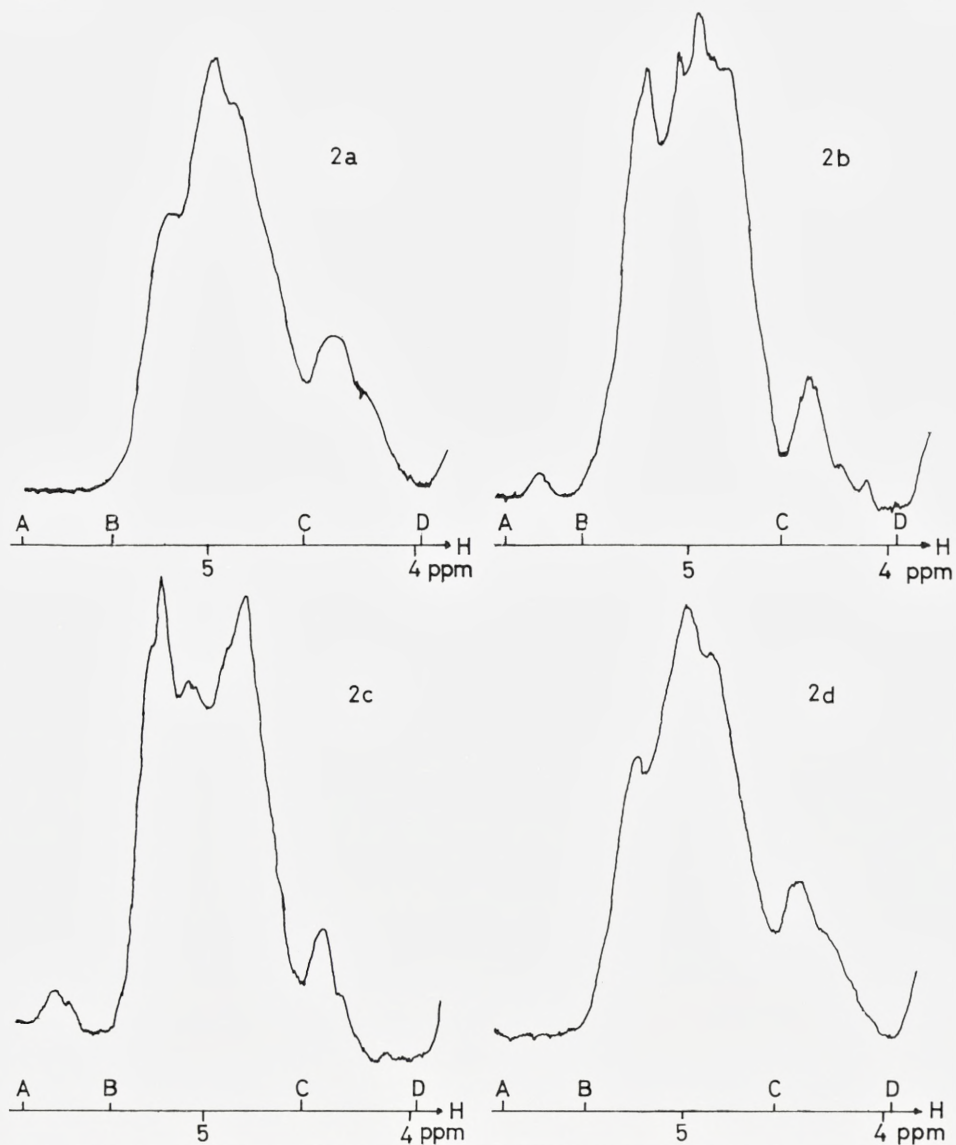
Fig. 2. Section of glucagon ¹HMR spectrum at 100 MHz. 2a: fifty accumulated spectra recorded 1–3 h after preparation of the solution in CF₃COOH. 2b: fifty accumulated spectra recorded 3–5 h after preparation. 2c: after 2 days. 2d: after hydrolysis (see text) and recording 1–3 h after dissolving in CF₃COOH again.
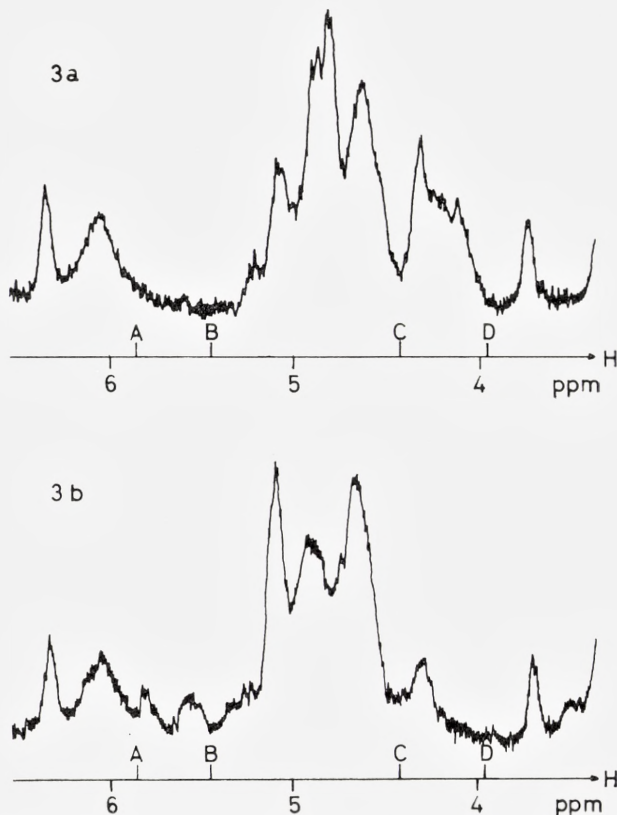
Fig. 3. Section of glucagon ¹HMR at 220 MHz. 3a: single recording immediately after prepara-
tion of the solution. 3b: single recording 1 week (see text) after preparation.

the beginning, but after a week two distinct signals had appeared between
5.66 and 5.90 ppm/TMS with a total intensity corresponding to *ca.* 3.5 p.r.
These signals were positively identified as originating from threonine H_β-
protons. By spin-coupling they produce CH_3 resonance doublets at *ca.* 1.50
ppm/TMS. One at a time these doublets became singlets by irradiating the
glucagon sample at 5.668, 5.827, and 5.882 ppm downfield from TMS.
Serine residues are unable to produce this effect(no CH_3 groups).

Porcine and bovine glucagon identity was checked spectroscopically by
demonstrating the identity of their ¹HMR spectra at 100 MHz. To test the
sensitivity the 0.02 m glucagon solution was afterwards made 0.02 m with
respect to leucine, one of the amino acids occurring as residue. The expected
spectral intensity changes were observed. The identity and the sensitivity
checks were, of course, carried out after chemical 'maturing' for 2 days.

V. Hydrolysis and Acetolysis of Trifluoroacetylated Glucagon

Upon hydrolysis one of the spectral bands of glucagon adopts its original shape (fig. 2). This is true for the entire spectrum, but the changes are far less in most other parts of the spectrum. Hydrolysis of 0.01 mmole of heptatrifluoroacetylated glucagon was carried out by removing the solvent CF_3COOH *in vacuo*, adding $1/_2$ ml of water and 10 μl of CF_3COOH, shaking for 24 h, and finally distilling off water *in vacuo* at room temperature. The remaining glucagon was dissolved in CF_3COOH and its FMR spectrum was immediately recorded. It showed a trace of signals at the location of the 'threonine' $COCF_3$ resonances and a somewhat larger, diffuse band at the location of the 'serine' $COCF_3$ resonances, all amounting to *ca.* 1 $COCF_3$ group per molecule. Part of this is due to trifluoroacetylation starting afresh when glucagon is dissolved in CF_3COOH. Another part is due to incomplete hydrolysis as seen by the occurrance of 'threonine' $COCF_3$ signals.

Once the glucagon derivative

$$(\text{glucagon} - 7 \text{ H}) (COCF_3)_7$$

is available other derivatives become accessible. We have prepared what appeared to be

$$(\text{glucagon} - 7 \text{ H}) (COCH_3)_3^{thr} (COCH_3)_2^{ser} (COCF_3)_2^{ser}$$
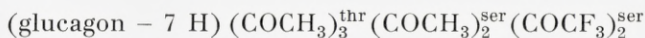
(ser = serine, thr = threonine). 40 mg hepta-trifluoroacetylated glucagon was dissolved in 250 μl of CF_3COOH, 250 μl of CH_3COOH, and 20 μl of water which catalyzes the exchange of $COCF_3$ with $COCH_3$. After 48 h, 100 μl of $(CH_3CO)_2O$ was added, the quantity necessary to remove water chemically. After another 24 h the sample was evaporated to dryness *in vacuo*. 2 ml portions of di-butylether were repeatedly added and distilled-off in order to remove traces of CH_3COOH which would falsify the next spectrum. The remanence was dissolved in CF_3COOH and its ^{1}HMR spectrum was recorded. It showed a large, extra signal at the usual location of $COCH_3$ resonances with an intensity corresponding to 14–16 p.r. per molecule. At 4 h after the preparation of the solution the FMR spectrum was recorded. Practically no 'threonine' signals were seen, but a diffuse 'serine' signal corresponding to ca. 2 $COCF_3$ groups was recorded, all as expressed in the formula above. There can be little doubt that complete acetylation and, in general, a c y l a t i o n is possible.

Unlike the $COCF_3$ groups the $COCH_3$ groups cannot be removed hydrolytically in slightly acid medium. After removal of the solvent of the sample

above, it was shaken for 24 h with dilute NaOH at pH = 11. Water was distilled-off and replaced by CF_3COOH which was immediately distilled-off in order to remove CH_3COOH formed by the hydrolysis. The residue was slightly trifluoroacetylated glucagon as seen by the [1]HMR spectrum of its solution in CF_3COOH.

VI. Biological Activity of Recovered Polypeptides

By immunological determination carried out at the NOVO THERA-PEUTIC LABORATORY the amount of glucagon-like substance was found to be 45–55 %. A more specific biological activity determination[6] showed 55 % activity (fidelity limits 48–62 %).

As mentioned above the average composition of our glucagon sample recovered by hydrolysis of the hepta-trifluoroacetylated derivative, was (glucagon – 1 H)$COCF_3$. If one $COCF_3$ group per molecule impairs biological activity the maximum activity of the sample above would be $100(6/7)^7$ = 35 %. If, on the other hand, the introduction of $COCF_3$ groups in a polypeptide is of no or little consequence for its biological activity an established loss of activity must be due to a (so far not identified) chemical change not reversed by hydrolysis.

VII. Conclusions

The slowly occurring FMR signals and the corresponding changes in the [1]HMR spectra show that polypeptides dissolved in CF_3COOH undergo chemical changes. The demonstrated trifluoroacetylation of all hydroxy groups in serine and threonine residues is thought to be typical.

After hydrolysis of hepta-trifluoroacetylated glucagon 'genuine' glucagon of ca. 50 % biological activity is obtained. As mentioned in an earlier publication[1] the same seems true for insulin. Therefore, although CF_3COOH is a powerful chemical agent it may only cause chemical changes of minor biological importance.

The use of CF_3COOH in preparative and analytical polypeptide studies taking advantage of NMR techniques can be justified like this: 1° Its ability to dissolve at least a majority of polypeptides and many proteins. 2° The CF_3COOH p.r. is well separated from the polypeptide [1]HMR spectra in contrast to H_2O, HDO, H_3O^+ etc. with p.r. occurring in the middle of the spectrum if aqueous medium is applied. 3° CF_3COOH is a very strong acid provoking maximum protonation of the solute. Without this (for instance by studies in aqueous media) solubility differences would necessitate work

at widely different acidities with accompanying changes of chemical shifts of the numerous protons in slow or fast exchange with the solvent proton(s).

The finding of a solvent supplementing CF_3COOH would be of great value. $(CD_3)_2SO$ is under observation, but the isotopic purity of the commercially available compound is less satisfactory (although $> 98\%$) for work applying accumulated spectra.

The easy access to trifluoroacetylated polypeptides here demonstrated opens routes to numerous derivatives differing in molecular weight, isoelectric point, polarity, total electric charge etc. Since biologically activite polypeptides can be retrieved promising perspectives for, for example, the separation of naturally occurring mixtures of polypeptides by way of their derivatives are obvious.

Note Added In Proof

Recent, not yet completed studies at 220 MHz and $25°$ ($\neq 10-15°$ as employed above) show that whereas the free amino acid tryptophane dissolved in CF_3COOH is stable for at least 48 h, ^{1}HMR signals from the aromatic protons of the tryptophane residue of glucagon start fading discernably after 3 h. After 24 h the easily recognizable signal from H(2) of the tryptophane residue has disappeared. At present the nature of the corresponding chemical change is unknown. Also, it may or may not be reversible during the hydrolysis of 'hepta-trifluoroacetylated glucagon'. This type of change does, of course, not occur for polypeptides such as the insulins with no tryptophane residues.

References

1. B. BAK, E. J. PEDERSEN, and F. SUNDBY, J. Biol. Chem. **242**, 2637 (1967).
2. O. K. BEHRENS and W. W. BROMER, Vitamins and Hormons **16**, 263 (1958) and Private communication.
3. F. SANGER, Biochem. J. **44**, 126 (1947); ibid. **45**, 563 (1949).
4. B. BAK, J. J. Led, and E. J. PEDERSEN, J. Mol. Spectry. (to be published).
5. B. BAK, C. DAMBMANN, F. NICOLAISEN, E. J. PEDERSEN, and N. S. BHACCA. J. Mol. Spectry. **26**, 78 (1968).
6. F. TARDING, P. NIELSEN, B. KEISER-NIELSEN, and AA. V. NIELSEN, Diabetologia **5** (1969) (in the press).

RUNE JOHNSON

ON PHONONS
IN SIMPLE METALS
I

Synopsis

The dynamical matrix for simple metals is derived in a local ion-electron potential approximation. In order to get a consistent expression for the dynamical matrix in the weak potential limit it is shown to be necessary to include effects from the lattice potential on the electron response-function. The lowest order corrections to the free particle expression are calculated for zero temperature in the R.P.A.-approximation of the polarization operator.

I. Introduction

The improved experimental technique for determining phonon dispersion curves in crystals has made it possible to investigate them in great detail. The experiments have also revealed many interesting features of these curves, particularly in metals [1], [2], which (at low temperatures) are believed mostly to be effects from the conduction electrons. A proper understanding of these effects may, therefore, give valuable information about the microscopic processes in these crystals.

The theoretical situation, however, is not so encouraging. The origin of of the major difficulty seems to be the splitting of the electrons into two physically quite different groups of either core electrons or conduction electrons, which already makes the electron problem difficult to treat in any kind of approximation. And since the energy associated with a lattice wave is a very tiny quantity (in the electron energy scale), the prospect of getting an accurate estimate of it is very uncertain. For instance, an extension to the lattice dynamics of commonly used theoretical techniques [3] for calculating the electron band structure in the perfect lattice becomes very complicated. For that reason it seems to be inevitable that when doing phonon calculations, we have to rely on the construction of models at the very start, which generally is a very delicate problem indeed. An outstanding exception from this rule, however, is the so called simple metals [4]. In these metals the core electrons form closed shells around the nuclei and the radii of these shells are so small that the nuclei plus the closed shells can be treated in this problem as rigid point particles– the ions. The only dynamically important electrons in the problem are then the conduction electrons. This simplification has, however, to be paid for in terms of a complicated interaction between the ions and the electrons [5]. Still, it is possible in simple cases accurately to replace this complicated interaction by a suitable chosen local potential [6], [7]. Although a purely formal device, this potential can be constructed to reproduce the essential properties of the conduction bands.

1*

In section II we briefly discuss the dynamical matrix for normal metals with simple lattices in this model, i.e. we assume that the ion-electron inter-action is given by a local potential $v_e(\mathbf{r}) = v_e(-\mathbf{r})$. A more complete discussion of this model can be found in [8], [9]. The response-function for the electrons is expanded in section III and the most important terms in the dynamical matrix are discussed for the case where the effective periodic potential in the lattice is weak. In IV the R. P. A. – or Hartree – approximation of the polari-zation operator is discussed and the first corrections to the Lindhard free par-ticle expression are derived. The paper is concluded in section V with a brief discussion of the characteristic functions for these corrections.

II. The Dynamical Matrix

The Hamiltonian for the metal consists of three parts. First we have a purely ionic part for point ions with mass M and charge Ze interacting via a potential $Ze^2 V_i(\mathbf{r})$.

$$H_i = \sum_R \frac{P_R^2}{2M} + Z^2 e^2 \sum_{R,R'}{}' V_i(\mathbf{R} + \mathbf{u}(R,t) - \mathbf{R}' - \mathbf{u}(R',t)) \tag{1}$$

where R and $\mathbf{R}$ denote the R-th ion with the mean position at the lattice point $\mathbf{R}$ and $\mathbf{u}(R,t)$ is the instantaneous position relative to this lattice point. $\sum'$ means exclusion of the term $R = R'$ in the sum.

The second part in the Hamiltonian is a purely electronic part ($\hbar = 1$)

$$H_e = \int \frac{d\mathbf{r}}{2m} \triangledown \psi^+(\mathbf{r},t) \triangledown \psi(\mathbf{r},t) + \frac{e^2}{2} \int \psi^+(\mathbf{r}'t)\psi^+(\mathbf{r},t) v(|\mathbf{r} - \mathbf{r}'|) \cdot \\ \cdot \psi(\mathbf{r},t)\psi(\mathbf{r}'t)\, d\mathbf{r}\, d\mathbf{r}' \left. \right\} \tag{2}$$

where $\psi(\mathbf{r}, t)$ is the field operator for the dynamically important electrons and $e^2 v(|\mathbf{r} - \mathbf{r}'|)$ is their interaction, typically equal to $|\mathbf{r} - \mathbf{r}'|^{-1}.e^2$

Finally we have the interaction between the electrons and ions given by

$$H_{ie} = -Ze^2 \sum_R \int d\mathbf{r}\, v_e(\mathbf{R} + \mathbf{u}(R,t) - \mathbf{r}) \varrho(\mathbf{r},t) \tag{3}$$

in this approximation. ($\varrho(\mathbf{r},t) = \psi^+(\mathbf{r},t)\psi(\mathbf{r},t)$).

The total Hamiltonian is the sum of the three parts

$$H = H_i + H_e + H_{ie}. \tag{4}$$

Standard methods [9] give the following equation of motion for the R-th ion.

$$
\begin{aligned}
M\ddot{u}(R,t) = & -\Big\{Z^2e^2 \sum_{R'}{}' T_i(\boldsymbol{R}-\boldsymbol{R}') - Ze^2\!\int d\boldsymbol{r}\, T_e(\boldsymbol{R}-\boldsymbol{r})\varrho(\boldsymbol{r},t)\Big\}\, \boldsymbol{u}(R,t) + \\
& + Z^2e^2 \sum_{R'}{}' T_i(\boldsymbol{R}-\boldsymbol{R}')\,\boldsymbol{u}(R',t) + Ze^2\!\int d\boldsymbol{r}\, t_e(\boldsymbol{R}-\boldsymbol{r})\varrho(\boldsymbol{r},t)
\end{aligned}
\tag{5}
$$

where in terms depending explicitly on the ionic displacements we only kept terms linear in $\boldsymbol{u}$.

In Eq. (5) means

$$
T_i(\boldsymbol{r}) = \triangledown\,\triangledown\, V_i(\boldsymbol{r});\; t_e(\boldsymbol{r}) = \triangledown\, v_e(\boldsymbol{r});\; T_e(\boldsymbol{r}) = \triangledown\,\triangledown\, v_e(\boldsymbol{r}).
$$

In order to get a consistent equation for the harmonic motion we have to find the electron density operator $\varrho(\boldsymbol{r},t)$ up to terms linear in the displacements $\boldsymbol{u}(R,t)$ also. This is formally easily done with use of response techniques [10], [11]. When the ions are moving the term H_{ie} in the Hamiltonian causes an external time-depending perturbation on the electron system

$$
\begin{aligned}
\delta U(\boldsymbol{r},t) = & -Ze^2 \sum_R \{v_e(\boldsymbol{R}+\boldsymbol{u}(R,t)-\boldsymbol{r}) - v_e(\boldsymbol{R}-\boldsymbol{r})\} = \\
= & \; Ze^2 \sum_R t_e(\boldsymbol{r}-\boldsymbol{R})\cdot\boldsymbol{u}(R,t)
\end{aligned}
\tag{6}
$$

to terms linear in $\boldsymbol{u}(R,t)$.

This perturbation gives to linear terms in $\boldsymbol{u}$ a response in $\varrho(\boldsymbol{r},t)$

$$
\begin{aligned}
\delta\varrho(\boldsymbol{r},t) = \varrho(\boldsymbol{r},t) - \varrho_0(\boldsymbol{r},t) = & -iZe^2 \sum_R\!\int d\boldsymbol{r}'\,dt'\,[\varrho_0(\boldsymbol{r},t),\varrho_0(\boldsymbol{r}',t')]\cdot \\
& \cdot t_e(\boldsymbol{r}'-\boldsymbol{R})\cdot\boldsymbol{u}(R,t')
\end{aligned}
\tag{7}
$$

where $\varrho_0(\boldsymbol{r},t)$ is the density operator in the case all $\boldsymbol{u}(R,t) = 0$, i.e. in the ideal lattice.

By multiplying Eq. (5) from the right with $\boldsymbol{u}(R_0,t_0)$ and forming the statistical average, we arrive at the following equation

$$
\begin{aligned}
M\frac{d^2}{dt^2}\, & \langle \boldsymbol{u}(R,t)\,\boldsymbol{u}(R_0,t_0)\rangle = \\
= & -\Big\{Z^2e^2 \sum_{R'}{}' T_i(\boldsymbol{R}-\boldsymbol{R}') - Ze^2\!\int d\boldsymbol{r}\, T_e(\boldsymbol{R}-\boldsymbol{r})\langle\varrho_0(\boldsymbol{r})\rangle\Big\} \\
& \langle \boldsymbol{u}(R,t)\,\boldsymbol{u}(R_0,t_0)\rangle + Z^2e^2 \sum_{R'}{}' T_i(\boldsymbol{R}-\boldsymbol{R}')\langle\boldsymbol{u}(R',t)\,\boldsymbol{u}(R_0,t_0)\rangle + \\
& + Z^2e^4 \sum_{R'}\!\int d\boldsymbol{r}\,d\boldsymbol{r}'\,dt'\, t_e(\boldsymbol{R}-\boldsymbol{r})\, h(\boldsymbol{r},t;\boldsymbol{r}',t')\, t_e(\boldsymbol{r}'-\boldsymbol{R}')\Big\}\cdot \\
& \cdot \langle\boldsymbol{u}(R',t')\,\boldsymbol{u}(R_0,t_0)\rangle
\end{aligned}
\tag{8}
$$

to terms linear in $\boldsymbol{u}$. In Eq. (8) we have used the fact that

$$\int l_e(\boldsymbol{R} - \boldsymbol{r}) \langle \varrho_0(\boldsymbol{r}) \rangle \, d\boldsymbol{r} = 0$$

from the lattice symmetry. In Eq. (8) we have also introduced the linear response function in the ideal lattice

$$\left.\begin{aligned} h(\boldsymbol{r}, t; \boldsymbol{r}', t') &= -i \langle [\varrho_0(\boldsymbol{r}, t), \varrho_0(\boldsymbol{r}', t')] \rangle \, \theta(t - t') \\ \left(\theta(x) = \begin{matrix} 1 \, ; \, x > 0 \\ 0 \, ; \, x < 0 \end{matrix}\right). \end{aligned}\right\} \quad (9)$$

Since $h(\boldsymbol{r}, t, \boldsymbol{r}', t')$ is a quantity determined in the ideal lattice it is a function only of the time difference $t - t$ and has the full symmetry of the lattice in its spatial indices. In particular this means that

$$h(\boldsymbol{r} + \boldsymbol{R}, \boldsymbol{r}' + \boldsymbol{R}) = h(\boldsymbol{r}, \boldsymbol{r}'). \quad (10)$$

Before leaving this point we want to stress one property of the electron system which is important in practical applications. Since the change in the electron density is generally governed by Eq. (7), we get in particular for an infinitely slow uniform translation of all ions a (small) distance $\boldsymbol{u}$

$$\left.\begin{aligned} \langle \varrho(\boldsymbol{r}) \rangle - \langle \varrho_0(\boldsymbol{r}) \rangle &= -\boldsymbol{u} \cdot \nabla \langle \varrho_0(\boldsymbol{r}) \rangle = \\ &= \sum_R Z e^2 \int d\boldsymbol{r}' \, dt' \, h(\boldsymbol{r}, t; \boldsymbol{r}', t') \cdot l_e(\boldsymbol{r}' - \boldsymbol{R}) \cdot \boldsymbol{u} \end{aligned}\right\} \quad (11)$$

which implies

$$\nabla \langle \varrho_0 \rangle = -Z e^2 \sum_R \int d\boldsymbol{r}' \, dt' \, h(\boldsymbol{r}, t; \boldsymbol{r}', t') \, l_e(\boldsymbol{r}' - \boldsymbol{R}). \quad (12)$$

By the aid of this expression the second term on the R.H.S. in Eq. (8) can be transformed to

$$\left.\begin{aligned} \int d\boldsymbol{r} \, T_e(\boldsymbol{R} - \boldsymbol{r}) \langle \varrho_0(\boldsymbol{r}) \rangle &= -e^2 \sum_{R'} \int l_e(\boldsymbol{R} - \boldsymbol{r}) \, h(\boldsymbol{r}, t; \boldsymbol{r}', t') \cdot \\ &\quad \cdot l_e(\boldsymbol{r}' - \boldsymbol{R}') \, d\boldsymbol{r} \, d\boldsymbol{r}' \, dt'. \end{aligned}\right\} \quad (13)$$

In case $\langle \varrho_0(\boldsymbol{r}) \rangle$ is independent of $\boldsymbol{r}$, its gradient is equal zero, which means completely vanishing of this term. TOYA has demonstrated [12] that this is a quite reasonable approximation in the simpler alkali metals. An inclusion of the effect from the periodic electron distribution gives only minor corrections in these cases [13]. In a more general simple metal, however, there is no hope

of expecting that it is so. When estimating this effect it is, then, important to fulfil Eq. (13) in order to get sensible results.

By Fourier transforming Eq. (8) and by using the property of $\langle \boldsymbol{u}(R,t\ \boldsymbol{u}(R_0, t_0)\rangle$ to be a function of $t - t$ and $\boldsymbol{R} - \boldsymbol{R}$ only one obtains the equation

$$[\omega^2 I - \omega_p^2 D(\boldsymbol{q}, \omega)] \langle \boldsymbol{u}(\boldsymbol{q},\omega)\, \boldsymbol{u}(\boldsymbol{q},\omega)\rangle \;=\; 0 \tag{14}$$

where $D(\boldsymbol{q},\omega)$ is the dimensionless dynamical matrix. It is naturally split into two parts.

$$D(\boldsymbol{q}, \omega) \;=\; D_I(\boldsymbol{q},\omega) + D_E(\boldsymbol{q}, \omega) \tag{15}$$

where D_I stands for the part due to the direct ion-ion interaction and is independent of ω, since we assumed an instantaneous ion-ion interaction.

$$\left.\begin{aligned}
D_I(\boldsymbol{q}) \;&=\; -\frac{1}{4\pi N}\sum_{R'}{}'\{T_i(\boldsymbol{R}-\boldsymbol{R}')\,e^{-i\boldsymbol{q}(\boldsymbol{R}-\boldsymbol{R}')} - T_i(\boldsymbol{R}-\boldsymbol{R}')\} \;=\\
&=\; \frac{1}{4\pi}\sum_K\{V_i(\boldsymbol{K}+\boldsymbol{q})(\boldsymbol{K}+\boldsymbol{q})(\boldsymbol{K}+\boldsymbol{q}) - V_i(\boldsymbol{K})\boldsymbol{K}\boldsymbol{K}\}
\end{aligned}\right\} \tag{16}$$

with $\boldsymbol{K}$ a vector in the reciprocal lattice. The term $V_i(\boldsymbol{K})\boldsymbol{K}\boldsymbol{K}$ with $\boldsymbol{K} = 0$ in Eq. (16) is so far not defined, but we can think of it as the limit $q \to 0$ of $V_i(\boldsymbol{q})\boldsymbol{q}\boldsymbol{q}$. We shall later see that it is exactly cancelled by a corresponding term in $D_E(\boldsymbol{q},\omega)$. In Eq. (16) N is the ion density and $\omega_p^2 = \dfrac{4\pi Z^2 e^2 N}{M}$ is the classical plasma frequency for the ions. With the ion-ion interaction known, this part of the dynamical matrix is readily calculated and no particular attention is paid to it in the following.

Similarly the electronic part of $D(\boldsymbol{q},\omega)$ is written

$$\left.\begin{aligned}
D_E(\boldsymbol{q},\omega) \;=\; -\frac{1}{4\pi N}\sum_{R'}\int d\boldsymbol{r}\,d\boldsymbol{r}'\{&e^{-i\boldsymbol{q}(\boldsymbol{R}-\boldsymbol{R}')}\,t_e(\boldsymbol{R}-\boldsymbol{r})\,h(\boldsymbol{r},\boldsymbol{r}',\omega)\,t_e(\boldsymbol{r}'-\boldsymbol{R}')-\\
&- t_e(\boldsymbol{R}-\boldsymbol{r})\,h(\boldsymbol{r},\boldsymbol{r}',0)\,t_e(\boldsymbol{r}'-\boldsymbol{R}')\}
\end{aligned}\right\} \tag{17}$$

where $h(\boldsymbol{r},\boldsymbol{r}',\omega)$ is the Fourier transform in time of the response function h.

For subsequent use we introduce the function

$$\Phi(\boldsymbol{r},\boldsymbol{r}',t) \;=\; \langle[\varrho_0(\boldsymbol{r},t),\varrho_0(\boldsymbol{r}',0)]\rangle \;=\; \int\frac{d\omega}{2\pi}\,\Phi(\boldsymbol{r},\boldsymbol{r}',\omega)e^{-i\omega t}. \tag{18}$$

It is readily seen that $\Phi(\boldsymbol{r},\boldsymbol{r}',\omega)$ is real, odd in ω and symmetric in its spatial indices. From the spectral representation of the stepfunction

$$\theta(t) = i \int \frac{d\omega}{2\pi} \frac{e^{-i\omega t}}{\omega + i\delta} \quad (\delta = 0^+) \tag{19}$$

and the formal identity

$$\frac{1}{\omega + i\delta} = P\frac{1}{\omega} - i\pi\delta(\omega), \tag{20}$$

where P means the Cauhy principal value, the function $\Phi(\boldsymbol{r},\boldsymbol{r}',\omega)$ enables us to write the response-function $h(\boldsymbol{r},\boldsymbol{r}',\omega)$ in the following form

$$h(\boldsymbol{r},\boldsymbol{r}',\omega) = P \int \frac{d\omega'}{2\pi} \frac{\Phi(\boldsymbol{r},\boldsymbol{r}',\omega)}{\omega - \omega'} - \frac{i}{2} \Phi(\boldsymbol{r},\boldsymbol{r}',\omega). \tag{21}$$

For real ω we have in Eq. (21) $h(\boldsymbol{r},\boldsymbol{r}',\omega)$ written in a real part even in ω and an imaginary part odd in ω.

When dealing with the strongly screening electron system it is in practice convenient to introduce another response-function H instead of h. This can be done by defining the effective potential δU_{eff} acting on the electron system

$$\delta U_{\text{eff}} = \delta U + e^2 v \delta \langle \varrho \rangle \tag{22}$$

and by defining H from

$$\delta \langle \varrho \rangle = H \delta U_{\text{eff}} = h \delta U, \tag{23}$$

which implies

$$h = H\{I - e^2 v H\}^{-1}. \tag{24}$$

So defined, $H(\boldsymbol{r},\boldsymbol{r}',\omega)$ is related to the local polarizability of the electron system and the dielectric operator of the system (with the ions fixed at their lattice sites) is given by

$$\varepsilon(\boldsymbol{r},\boldsymbol{r}',\omega) = I - e^2 v H(\boldsymbol{r},\boldsymbol{r}',\omega). \tag{25}$$

The properties of h found earlier and the symmetry of v give to H the following features

$$\begin{aligned} \text{Re}\, H(\omega) &= \text{Re}\, H(-\omega) \\ \text{Im}\, H(\omega) &= -\text{Im}\, H(-\omega) \\ H(\boldsymbol{r},\boldsymbol{r}') &= H(\boldsymbol{r}',\boldsymbol{r}) = H(\boldsymbol{r}+\boldsymbol{R},\boldsymbol{r}'+\boldsymbol{R}). \end{aligned} \tag{26}$$

In order to preserve the symmetric form of $D_E(\boldsymbol{q},\omega)$ in Eq. (17), we shall make a small adjustment in Eq. (24). By writing

$$v = Q \cdot Q \tag{27}$$

and

$$\varkappa = -QHQ \tag{28}$$

(the minus sign is only for convenience) Eq. (24) is transformed to

$$h = -Q^{-1} \frac{\varkappa}{1 + e^2 \varkappa} Q^{-1} \tag{29}$$

$D_E(\boldsymbol{q},\omega)$ can now be written in the symmetric form

$$
\begin{aligned}
D_E(\boldsymbol{q}, \omega) &= -\frac{1}{4\pi} \sum_{\boldsymbol{K}, \boldsymbol{K}'} \Bigg\{ \frac{v_e(\boldsymbol{K}+\boldsymbol{q})(\boldsymbol{K}+\boldsymbol{q})}{\sqrt{v(\boldsymbol{K}+\boldsymbol{q})}} \cdot \\
&\cdot \langle \boldsymbol{K}+\boldsymbol{q} \, | \, \frac{e^2\varkappa(\omega)}{1 + e^2\varkappa(\omega)} \, | \, \boldsymbol{K}'+\boldsymbol{q} \rangle \, \frac{v_e(\boldsymbol{K}'+\boldsymbol{q})(\boldsymbol{K}'+\boldsymbol{q})}{\sqrt{v(\boldsymbol{K}'+\boldsymbol{q})}} - \\
&- \frac{v_e(\boldsymbol{K})\boldsymbol{K}}{\sqrt{v(\boldsymbol{K})}} \langle \boldsymbol{K} \, | \, \frac{e^2\varkappa(0)}{1 + e^2\varkappa(0)} \, | \boldsymbol{K}' \rangle \, \frac{v_e(\boldsymbol{K}')\boldsymbol{K}'}{\sqrt{v(\boldsymbol{K}')}} \Bigg\}
\end{aligned} \tag{30}
$$

where again we may define the terms containing $\boldsymbol{q} = 0$; $\boldsymbol{K}$ and/or $\boldsymbol{K}' = 0$ by a limiting procedure. We have in Eq. (30) used Eq. (10), which tells us that h (and $\varkappa$) has the following form in Fourier space

$$h(\boldsymbol{r},\boldsymbol{r}') = \sum_{\boldsymbol{K}, \boldsymbol{K}'} \int \frac{d\boldsymbol{q}}{(2\pi)^3} \langle \boldsymbol{K}+\boldsymbol{q} | h | \boldsymbol{K}'+\boldsymbol{q} \rangle \, e^{i\,(\boldsymbol{K}+\boldsymbol{q})\boldsymbol{r} - i\,(\boldsymbol{K}'+\boldsymbol{q})\boldsymbol{r}'} \tag{31}$$

where the integration is only over the first Brillouin zone.

In metals we expect the element $\langle \boldsymbol{q}|H(0)|\boldsymbol{q}\rangle$ to be finite when $\boldsymbol{q}$ tends toward zero. This gives a singularity of order $\frac{1}{q^2}$ in the element $\langle \boldsymbol{q}|\varkappa(0)|\boldsymbol{q}\rangle$ and of order $\frac{1}{q}$ in the elements $\langle \boldsymbol{K}+\boldsymbol{q}|\varkappa(0)|\boldsymbol{q}\rangle$ $(\boldsymbol{K}\neq 0)$, all other elements staying finite. Clearly this is a manifestation of the complete screening of a static, macroscopic long wave external perturbation we have in a metal. The singularity of order $\frac{1}{q^2}$ in $\langle \boldsymbol{q}|\varkappa(0)|\boldsymbol{q}\rangle$ is seen to give one eigenvalue h_0 of the matrix $\varkappa(0)$ of order $\frac{1}{q^2}$ and the corresponding eigenfunction $\psi_0 \xrightarrow[q\to 0]{} e^{iqr}$. This result implies that all terms in the second sum in Eq. (30) with $\boldsymbol{K} = 0$, $\boldsymbol{K}' \neq 0$ or vice versa are equal to zero, since all other factors stay finite when q tends toward zero. The term with both $\boldsymbol{K}$ and $\boldsymbol{K}'$ equal to zero, however, gives $\lim\limits_{q\to 0} \langle \boldsymbol{q}| \frac{e^2\varkappa(0)}{1 + e^2\varkappa(0)} |\boldsymbol{q}\rangle = 1$ and since all potentials (including V_i) have

Fourier-transforms tending to $\dfrac{4\pi}{q^2}$ for small q, we get from this term a con-
tribution to D_E equal 1 which exactly cancels the corresponding contribution
to D_I in Eq. (16).

If we try to find non-trivial solutions to Eq. (14) as it stands, we observe
two disturbing difficulties not present in a Born- von Kármán treatment of
this problem. Primarily, we have the dynamical matrix in Eq. (14) not
Hermitian and it also depends on the eigenvalue we are trying to find in the
equation. Our solutions are no longer the three real roots in a cubic algebraic
equation. We know, however, that in actual cases there are three solutions
to Eq. (14) which we associate with the phonon vibrations. Now, the obvious
way of obtaining only three solutions to Eq. (14) is to completely neglect the
ω-dependency in $D_E(\boldsymbol{q},\omega)$ and thus to discard all possible other solutions to
it. But putting $\omega = 0$ in $D(\boldsymbol{q},\omega)$ means adopting the adiabatic approximation
and this seems, thus, to be the natural starting point when dealing with the
phonon problem (low ω case). Since $D(\boldsymbol{q},0)$ is real, this means that the peaks
in the correlation function $\langle \boldsymbol{u}(\omega)\, \boldsymbol{u}(\omega)\rangle$ in that case become δ-functions and,
consequently, are quite non-physical. We may, however, improve upon the
adiabatic solution by treating corrections to it as a kind of perturbation in
the low ω case. To lowest order this correction means including an imaginary
part (linear in the adiabatic ω) in the dynamical matrix, thus introducing a
finite lifetime of the excitations or a width of the peaks (even in the harmonic
approximation). One part of our problem is, accordingly, to investigate to
what extent this procedure is practical to follow, i.e. to show that the non-
adiabatic corrections are small.

There is also another difficulty in Eq. (30) not present in the simplest
Born- von Kármán treatment. We have even in $D_E(\boldsymbol{q},0)$ in Eq. (30) to deal
with a double sum in the reciprocal space. This means in particular that
we cannot in general find a local effective ion-ion interaction to use in a Born-
von Kármán calculation.

III. Expansion of the Response-Function

In connection with Eq. (13) we mentioned that – even in simple metals –
we are not generally allowed to neglect the effect from the periodic part of
the undisturbed electron density $\langle \varrho_0(\boldsymbol{r})\rangle$. This implies that $\varkappa(\boldsymbol{r},\boldsymbol{r}')$ is not
generally a function of $\boldsymbol{r} - \boldsymbol{r}'$ only. The problem of calculating $D_E(\boldsymbol{q})$ becomes
then much more difficult. Experimental and theoretical results indicate [14],

[15], however, that in some cases of interest the matrix $\varkappa$ is quite close to being diagonal in a plane wave representation. In such cases an expansion of the matrix h seems to be feasible and the problem is to find out which terms in the expansion are of most importance in $D_E(\boldsymbol{q})$.

By writing

$$\varkappa = A + B, \tag{32}$$

where A is the part of the matrix diagonal in a Fourier representation and B is the supposed small purely non-diagonal part, we get formally

$$\frac{e^2\varkappa}{1 + e^2\varkappa} = I - \sum_{n=0}^{\infty} \frac{1}{1 + e^2A} \left(- e^2 B \frac{1}{1 + e^2A} \right)^n. \tag{33}$$

In order to judge which terms in this expansion are of most importance in $D_E(\boldsymbol{q})$, we need some kind of expansion parameter in our problem and then to collect all terms of a certain order in this parameter. A natural choice of this parameter seems to be to consider the periodic part of $\langle \varrho_0(\boldsymbol{r}) \rangle$ as small (say, of first order) compared to the mean (uniform) value of $\langle \varrho_0(\boldsymbol{r}) \rangle = NZ$. This means that the periodic potential in the ideal lattice acting on the electron system is small (of the same order) compared to the kinetic energy of the electrons. For all important Fourier components $V(\boldsymbol{K})$ of this potential we then must have

$$V(\boldsymbol{K}) \ll E_F \approx \frac{k_F^2}{2m} \tag{34}$$

(E_F is the Fermi energy of the electron system). But from Eq. (12) we find that this means

$$Ze^2 N v_e(\boldsymbol{K}) \ll E_F. \tag{35}$$

This inequality implies that the function $v_e(\boldsymbol{k})$ decreases more rapidly for increasing $k \leq$ any K than the function $v(\boldsymbol{k})$, since for metals of interest $\left(\text{with } v(r) \sim \frac{1}{r} \right)$ we have $Ze^2 N v(\boldsymbol{K})$ of the same order as E_F for the first (and most important) reciprocal vectors $\boldsymbol{K}$. For a small q we can from these observations find the most important terms in the series in Eq. (33), when it is used in Eq. (30).

In case $n = 0$ only the diagonal part A enters. When combined with the unit matrix the contribution to $D_E(\boldsymbol{q})$ from the term $\boldsymbol{K} = 0$ is very large and gives mainly a cancellation of the corresponding term in $D_I(\boldsymbol{q})$ in Eq. (16). The remaining part of this contribution is, however, very important and is

in a certain model of the metal entirely responsible for the sound velocity (BOHM and STAVER [16]). Their value for this rest is $\approx \dfrac{E_F}{Ze^2 N} \cdot q^2$. For terms with $\boldsymbol{K} \neq 0$ in the diagonal part we get corrections to this value of order $\left(\dfrac{V(\boldsymbol{K})}{E_F}\right)^2$ compared to 1. Thus, this is the order of the corrections we can expect from the non-uniform electron distribution in the perfect crystal.

From the term with $n = 1$ in Eq. (33) and with B containing a factor $\dfrac{V(\boldsymbol{K})}{E_F}$ we get clearly contributions to $D_E(\boldsymbol{q})$ of this order from elements with either $\boldsymbol{K}$ or $\boldsymbol{K}'$ equal to zero. All other terms (both $\boldsymbol{K}$ and $\boldsymbol{K}' \neq 0$) are a factor $\dfrac{V(\boldsymbol{K})}{E_F}$ smaller.

Similarly, we find contributions to $D_E(\boldsymbol{q})$ of this order in the term with $n = 2$ in Eq. (33) in case both $\boldsymbol{K}$ and $\boldsymbol{K}'$ are equal 0. All other terms in the sum are at least a factor $\dfrac{V(\boldsymbol{K})}{E_F}$ smaller. So is also the case for all contributions from terms with $n \geqslant 3$.

Consequently, in order to take a consistent step beyond the approximation of BOHM-STAVER (and TOYA) regarding the electron distribution in the crystal we have to include all terms of the same order discussed above (at least for small q). This means that for small q we have at least to consider the first "row" and "column" in the matrix $\langle \boldsymbol{K} + \boldsymbol{q} | B | \boldsymbol{K}' + \boldsymbol{q} \rangle$ (corresponding to either $\boldsymbol{K}$ or $\boldsymbol{K}' = 0$). So much about the small q case. But what happens when $\boldsymbol{q}$ increases and approaches any zone boundary? This is a more difficult question to answer. However, the crucial point in the arguments above is the behaviour of the function $v_e(\boldsymbol{k})$. For $\boldsymbol{k}$ equal to any of the important reciprocal lattice vectors we have assumed the value of this function to be so small that the ratio

$$\frac{Ze^2 N v_e(\boldsymbol{k})}{E_F} \approx \frac{Ze^2 N v_e(\boldsymbol{k})}{E_F(1 + e^2 A(\boldsymbol{k}))} \approx \frac{V(\boldsymbol{K})}{E_F}$$

is a suitable expansion parameter. But for $\boldsymbol{k}$ tending to zero the expression $\dfrac{Ze^2 N v_e(\boldsymbol{k})}{E_F(1 + e^2 A(\boldsymbol{k}))}$ tends to order 1. Of importance is then for what value of $\boldsymbol{k}$ this change of order takes place. If it happens for a $\boldsymbol{k}$ well inside the first zone the arguments above hold for any $\boldsymbol{q}$ in the first zone. Although this is – so far – an unsettled point, we shall in the following as a proviso assume

that this is the case and consequently assume that the terms kept in $D_E(\boldsymbol{q})$ for small q contain uniformly in the whole zone all terms of importance. That means we are extrapolating the condition in Eq. (35) to the more general

$$Ze^2 N v_e(\boldsymbol{K} + \boldsymbol{q}) \ll E_F \qquad (36)$$

($\boldsymbol{K} \neq 0$ and any $\boldsymbol{q}$ in the first zone).

Then, the tentative form of $D_E(\boldsymbol{q})$ becomes as follows

$$
D_E(\boldsymbol{q}) = -\frac{1}{4\pi}\left\{ \sum_{\boldsymbol{K}} \frac{v_e^2(\boldsymbol{K}+\boldsymbol{q})(\boldsymbol{K}+\boldsymbol{q})(\boldsymbol{K}+\boldsymbol{q})}{v(\boldsymbol{K}+\boldsymbol{q})}\frac{e^2 A(\boldsymbol{K}+\boldsymbol{q})}{1+e^2 A(\boldsymbol{K}+\boldsymbol{q})} - \right.
$$
$$
- \sum_{\boldsymbol{K}}{}' \frac{v_e^2(\boldsymbol{K})\boldsymbol{K}\boldsymbol{K}}{v(\boldsymbol{K})}\frac{e^2 A(\boldsymbol{K})}{1+e^2 A(\boldsymbol{K})} +
$$
$$
+ \sum_{\boldsymbol{K}}{}' \frac{v_e(\boldsymbol{K}+\boldsymbol{q})v_e(\boldsymbol{q})}{[v(\boldsymbol{K}+\boldsymbol{q})v(\boldsymbol{q})]^{1/2}}\frac{\boldsymbol{q}(\boldsymbol{K}+\boldsymbol{q})+(\boldsymbol{K}+\boldsymbol{q})\boldsymbol{q}}{1+e^2 A(\boldsymbol{K}+\boldsymbol{q})}\frac{e^2\langle\boldsymbol{K}+\boldsymbol{q}|B|\boldsymbol{q}\rangle}{1+e^2 A(\boldsymbol{q})} -
$$
$$
\left. - \sum_{\boldsymbol{K}}{}' \frac{v_e^2(\boldsymbol{q})\boldsymbol{q}\boldsymbol{q}}{v(\boldsymbol{q})}\frac{e^4|\langle\boldsymbol{K}+\boldsymbol{q}|B|\boldsymbol{q}\rangle|^2}{[1+e^2 A(\boldsymbol{q})]^2[1+e^2 A(\boldsymbol{K}+\boldsymbol{q})]}\right\} = D_{E0} + D_{E1} + D_{E2} \qquad (37)
$$

where we have suppressed the ω-dependency. In Eq. (37) we have also discarded the term $\boldsymbol{K} = 0$ (indicated by $\sum'$) in the second sum due to the cancellation from D_I discussed earlier. The symmetry of the matrix B is also used and an obvious notation for the diagonal elements is introduced. We observe that in Eq. (37) the contribution to $D_E(\boldsymbol{q})$ from the static electron distribution $\langle\varrho_0\rangle$ (the second sum) contains only the diagonal part of $\varkappa$. We further note in Eq. (37) that the periodic property in the reciprocal lattice of the complete $D_E(\boldsymbol{q})$ in Eq. (30) is lost when doing this small q approximation. In order to reensure this property one needs consider the complete matrix B in the contribution from the $n = 1$ part (the third sum in Eq. (37)) and at least an extension of the last sum in Eq. (37) (contributions from $n = 2$) by replacing $\boldsymbol{q}$ with $\boldsymbol{K}' + \boldsymbol{q}$ and do the sum over $\boldsymbol{K}'$. If we make these extensions in Eq. (37), we have, however, to adjust the contribution from $\langle\varrho_0\rangle$ in order to satisfy Eq. (13).

IV. Approximation of the Polarizability Matrix

In Eq. (23) we introduced the irreducible polarization operator for the electron system in the ideal lattice. In order to make an explicit calculation we have to know this quantity. However, no closed form for it is known even

in the fairly simple model of the metal we have adopted here. Consequently, we have to rely on more or less realistic approximations. The simplest non-trivial approximation we can adopt is the R. P. A. or Hartre approximation [17], [18], [9], which is the first term in an expansion [19]. In that case we have (ω real)

$$H(\mathbf{r}, \mathbf{r}', \omega) = \sum_{i,j} \varphi_i(\mathbf{r}) \varphi_i^*(\mathbf{r}') \varphi_j(\mathbf{r}') \varphi_j^*(\mathbf{r}) \cdot \left| \frac{f(E_i) - f(E_j)}{E_i - E_j + \omega + i\delta} \right| \quad\quad\right\} \quad (38)$$

$$(\delta = 0^+)$$

where $f(E_i) = \{1 + e^{\beta(E_i - \mu)}\}^{-1} \left(\beta = \dfrac{1}{k_B T}\right)$ is the Fermi factor and $\varphi_i(\mathbf{r})$ is the wavefunction for the single particle electron state with energy E_i. It satisfies an equation

$$\left\{ -\frac{\varDelta}{2m} - V(\mathbf{r}) \right\} \varphi_i(\mathbf{r}) = E_i \varphi_i(\mathbf{r}). \quad (39)$$

Although this seems to be a rather crude approximation, since not even exchange effects between the electrons are properly considered, its effect in Eq. (25) can be substantially improved by a proper choice of the potential $v(\mathbf{r})$. So it is possible in this way to cover the commonly used approximate inclusions of exchange and correlation effects [12], [13], [20], [21] and [22]. $V(\mathbf{r})$ is in Eq. (39) the effective one-electron potential in the ideal lattice and has to be consistently chosen. It has the full symmetry of the lattice and can be written

$$V(\mathbf{r}) = \sum_{\mathbf{K}}' V(\mathbf{K}) e^{i\mathbf{K} \cdot \mathbf{r}} \quad \text{with} \quad V(\mathbf{K}) = V(-\mathbf{K}) \quad (40)$$

in the cases considered here.

We have in Eq. (40) ignored the uniform part, since it has no dynamical effect and can be subtracted in Eq. (39). With $\langle \varrho_0(\mathbf{r}) \rangle$ supposed to be almost uniform, we are led to make a perturbation expansion of E_i and φ_i in eigenfunctions $e^{i\mathbf{k} \cdot \mathbf{r}} = \langle \mathbf{r} | \mathbf{k} \rangle$ to the free electron operator $H_0 = -\dfrac{\varDelta}{2m}$. In an extended zone scheme we get (neglecting spin)

$$\varphi(\mathbf{k}, \mathbf{r}) = \frac{1}{N(\mathbf{k})^{1/2}} \{1 + \sum_{\mathbf{K}}' c(\mathbf{k}, \mathbf{K}) e^{i\mathbf{K} \cdot \mathbf{r}}\} e^{i\mathbf{k} \cdot \mathbf{r}} \quad (41)$$

with [23] and [19]

$$c(\boldsymbol{k},\boldsymbol{K}) = \sum_{n=1}^{\infty} \langle \boldsymbol{K} + \boldsymbol{k} | \left\{ \frac{|\boldsymbol{k}\rangle\langle\boldsymbol{k}| - 1}{E(\boldsymbol{k}) - H_0} V \right\}^n | \boldsymbol{k} \rangle \tag{42}$$

and

$$E(\boldsymbol{k}) = \varepsilon(k) - \sum_{n=1}^{\infty} \langle \boldsymbol{k} | V \left\{ \frac{|\boldsymbol{k}\rangle\langle\boldsymbol{k}| - 1}{E(\boldsymbol{k}) - H_0} V \right\}^n | \boldsymbol{k} \rangle$$

$$\left(\varepsilon(k) = \frac{k^2}{2m} \right). \tag{43}$$

In Eq. (41), $N(\boldsymbol{k})$ is the normalization factor and with $\varphi(\boldsymbol{k},\boldsymbol{r})$ normalized in a unit cube, we get

$$N(\boldsymbol{k}) = 1 + \sum_{\boldsymbol{K}}' |c(\boldsymbol{k},\boldsymbol{K})|^2. \tag{44}$$

The reason why we have used this Wigner-Brillouin expansion in this case rather than a Rayleigh-Schrödinger expansion is because in the latter we get singularities for states close to the Bragg planes.

The zero order terms in these expansions give the usual LINDHARD [17] expression for $\varkappa_0$. It is of interest to find corrections to low order in V to this function. In order to do this we have to study quantities as

$$\langle \boldsymbol{K} + \boldsymbol{q} | M(\boldsymbol{k},\boldsymbol{k}') | \boldsymbol{K}' + \boldsymbol{q} \rangle = \langle \varphi(\boldsymbol{k}) | e^{-i(\boldsymbol{K} + \boldsymbol{q})\boldsymbol{r}} | \varphi(\boldsymbol{k}') \rangle \cdot$$

$$\cdot \langle \varphi(\boldsymbol{k}') | e^{i(\boldsymbol{K}' + \boldsymbol{q})\boldsymbol{r}} | \varphi(\boldsymbol{k}) \rangle. \tag{45}$$

To zero order in V, with $\varphi(\boldsymbol{k})$ and $\varphi(\boldsymbol{k}')$ equal plane waves, these quantities obey a simple momentum conservation rule and are equal to $\delta_{\boldsymbol{k}'}^{\boldsymbol{K} + \boldsymbol{k} + \boldsymbol{q}} \delta_{\boldsymbol{K}'}^{\boldsymbol{K}}$. In other words, all non-zero elements of M_0 are equal to one and then assume the biggest possible value, due to the simple dynamical properties of a free electron when acted upon by an external plane wave. For more general states $|\varphi(\boldsymbol{k})\rangle$, $|\varphi(\boldsymbol{k}')\rangle$, however, we get a more complicated conservation rule and the non-zero elements are no longer constants. With the state $|\varphi(\boldsymbol{k})\rangle = |\boldsymbol{k}\rangle + \sum_{\boldsymbol{K}}' \delta(\boldsymbol{k},\boldsymbol{K})|\boldsymbol{K} + \boldsymbol{k}\rangle$, where $\delta(\boldsymbol{k},\boldsymbol{K})$ is of order V, it is seen that to first order in V this effect sets in only in case $\boldsymbol{K} \neq \boldsymbol{K}'$ in Eq. (45). The first order correction to the Lindhard matrix $\varkappa_0$ is consequently purely non-diagonal, while the first correction to the diagonal elements is of higher order in V. But from the discussion of the approximate dynamical matrix in Eq. (37) it is obvious that what we consistently need there is just the part of B linear in V. Furthermore, it is clear that the only place in Eq. (37) in which we have to consider the first correction to the diagonal elements is in the important term with $\boldsymbol{K} = 0$ in the first sum, i.e. in the term containing $\dfrac{e^2 A(\boldsymbol{q})}{1 + e^2 A(\boldsymbol{q})}$. We

shall in the following include the correction of this term in the second order part D_{E2} in Eq. (37) and thus by D_{E0} mean the expression where $\varkappa_0$ is used throughout.

In the following we concentrate on the real part of H and get, by using the expansion in Eq. (42), the following expression for the non-diagonal element.

$$
\begin{aligned}
\langle \boldsymbol{q}|H(\omega)|\boldsymbol{K}+\boldsymbol{q}\rangle &= 2P \sum_{\boldsymbol{k},\boldsymbol{k}'} \frac{f(E(\boldsymbol{k})) - f(E(\boldsymbol{k}'))}{E(\boldsymbol{k}) - E(\boldsymbol{k}') + \omega} \cdot \\
&\cdot \frac{1}{N(\boldsymbol{k})N(\boldsymbol{k}')} \{[c^*(\boldsymbol{k}',\boldsymbol{K}) + c(\boldsymbol{k},-\boldsymbol{K})]\delta_{\boldsymbol{k}'}^{\boldsymbol{k}+\boldsymbol{q}} + [c(\boldsymbol{k}',-\boldsymbol{K}) + c^*(\boldsymbol{k},\boldsymbol{K})] \cdot \\
&\qquad\qquad\qquad \cdot \delta_{\boldsymbol{k}'}^{\boldsymbol{k}+\boldsymbol{K}+\boldsymbol{q}}\}
\end{aligned}
\tag{46}
$$

where the factor 2 is from the trace over the spin states. We have in Eq. (46) only kept terms that can possibly give lowest order contributions at least in cases where $\boldsymbol{q}$ is not close to a Bragg plane $2\boldsymbol{K}' \cdot \boldsymbol{q} + \boldsymbol{K}'^2 = 0$ with $\boldsymbol{K}'$ parallel to $\boldsymbol{K}$. This restriction on $\boldsymbol{q}$ appears, because we have in Eq. (46) neglected terms of the second and third degrees in the $c(\boldsymbol{k},\boldsymbol{K})$:s. These neglected terms can, however, be of order 1 for states $\boldsymbol{k}$ and $\boldsymbol{k}'$ in narrow intervals of thickness $\frac{mV(\boldsymbol{K})}{K}$ around Bragg planes and the sum over these states may then give contributions of order $V(\boldsymbol{K})$ in case $f(E(\boldsymbol{k})) \neq 0$ and $f(E(\boldsymbol{k}')) = 0$ (or vice versa) in these regions. Therefore, the restriction is of importance only in cases where the Fermi surface is intersected by any Bragg plane. But even in these cases, we are going to neglect the restrictions and consider the expression in Eq. (46) as generally valid for all values on $\boldsymbol{q}$, since the corrections for $\boldsymbol{q}$ within a narrow region close to the Bragg planes discussed can be expected to be quite small. Effects of this kind are obviously to be expected, since the matrix H has a zone-structure in the periodic lattice and a representation of this zone-structure in the extended scheme leads to "rounding off" effects at the Bragg planes, which give a smooth function in the reduced scheme, when the pieces are brought together.

From Eq. (47) we get the desired part of the matrix B linear in $V(\boldsymbol{K})$

$$
\begin{aligned}
e^2\langle \boldsymbol{q}|B(\omega)|\boldsymbol{K}+\boldsymbol{q}\rangle &\backsimeq e^2\langle \boldsymbol{q}|\varkappa_1(\omega)|\boldsymbol{K}+\boldsymbol{q}\rangle = \frac{k_0}{\pi^2 a_0}[v(\boldsymbol{q})v(\boldsymbol{K}+\boldsymbol{q})]^{1/2}\frac{V(\boldsymbol{K})}{\varepsilon_0} \cdot u_1(\boldsymbol{K},\boldsymbol{q},\omega) \\
&\left(\frac{k_0}{\pi^2 a_0} = \frac{Ze^2 N}{\frac{2}{3}\varepsilon_0}\right)
\end{aligned}
\tag{47}
$$

where a_0 is the first Bohr radius in hydrogen and $\varepsilon_0 = \dfrac{k_0^2}{2m}$ is the free electron Fermi energy at $T = 0$. In Eq. (47) u_1 is the characteristic first order function of order 1, which is given in the appendix in zero T case.

From the expansion in Eq. (42) we also get the following expression for the diagonal element of H

$$
\begin{aligned}
\langle \boldsymbol{q}|H(\omega)|\boldsymbol{q}\rangle &= 2P \sum_{\boldsymbol{k},\,\boldsymbol{k}'} \frac{f(E(\boldsymbol{k})) - f(E(\boldsymbol{k}'))}{E(\boldsymbol{k}) - E(\boldsymbol{k}') + \omega} \cdot \\
&\cdot \left\{ \delta_{\boldsymbol{k}'}^{\boldsymbol{k}+\boldsymbol{q}} - \sum_{\boldsymbol{K}}' \frac{\delta_{\boldsymbol{k}'}^{\boldsymbol{k}+\boldsymbol{q}}}{N(\boldsymbol{k})N(\boldsymbol{k}')} |c(\boldsymbol{k},\boldsymbol{K}) - c(\boldsymbol{k}',\boldsymbol{K})|^2 + \right. \\
&\left. + \sum_{\boldsymbol{K}}' \frac{\delta_{\boldsymbol{k}'}^{\boldsymbol{k}+\boldsymbol{K}+\boldsymbol{q}}}{N(\boldsymbol{k})N(\boldsymbol{k}')} |c(\boldsymbol{k},\boldsymbol{K}) + c^*(\boldsymbol{k}',-\boldsymbol{K})|^2 \right\}.
\end{aligned}
\tag{48}
$$

Again this expression contains all effects of the desired order except possibly when $\boldsymbol{q}$ is close to a Bragg plane.

In Eq. (48) the first $\delta_{\boldsymbol{k}'}^{\boldsymbol{k}+\boldsymbol{q}}$ gives in the free electron case the Lindhard formula. It is, therefore, convenient to subtract this part and get the necessary corrections explicitly. We write

$$
\begin{aligned}
2P \sum_{\boldsymbol{k},\,\boldsymbol{k}'} \frac{f(E(\boldsymbol{k})) - f(E(\boldsymbol{k}'))}{E(\boldsymbol{k}) - E(\boldsymbol{k}') + \omega} \delta_{\boldsymbol{k}'}^{\boldsymbol{k}+\boldsymbol{q}} &= 2P \sum_{\boldsymbol{k},\,\boldsymbol{k}'} \left\{ \frac{f(k) - f(k')}{\varepsilon(k) - \varepsilon(k') + \omega} + \right. \\
+ [f(k) - f(k')] &\left[\frac{1}{E(\boldsymbol{k}) - E(\boldsymbol{k}') + \omega} - \frac{1}{\varepsilon(k) - \varepsilon(k') + \omega} \right] + \\
&\left. + \frac{g(\boldsymbol{k}) - g(\boldsymbol{k}')}{E(\boldsymbol{k}) - E(\boldsymbol{k}') + \omega} \right\} \delta_{\boldsymbol{k}'}^{\boldsymbol{k}+\boldsymbol{q}}
\end{aligned}
\tag{49}
$$

where $f(k) = f(\varepsilon(k)) = \{1 + e^{\beta(\varepsilon(k) - \mu_0)}\}^{-1}$ and $g(\boldsymbol{k}) = f(E(\boldsymbol{k})) - f(k)$. The first term in the curly bracket on the R.H.S. in Eq. (49) gives obviously the Lindhard formula and the remaining parts are corrections to this value due to corrections of the energies in the denominator (but with still the free electron Fermi factors) and the corrections of the Fermi factors respectively.

The element $\langle \boldsymbol{q}|\varkappa|\boldsymbol{q}\rangle$ can now to second order in $V(\boldsymbol{K})$ be written (with the restrictions on $\boldsymbol{q}$ mentioned in connection with Ep. (48))

$$
\begin{aligned}
e^2 \langle \boldsymbol{q}|\varkappa(\omega)|\boldsymbol{q}\rangle &= \frac{k_0}{\pi^2 a_0} v(q) \left\{ u_0(q,\omega) + \sum_{\boldsymbol{K}}' \left(\frac{V(\boldsymbol{K})}{\varepsilon_0} \right)^2 u_2(\boldsymbol{K},\boldsymbol{q},\omega) \right\} = \\
&= e^2 \langle q|\varkappa_0|q\rangle + e^2 \langle \boldsymbol{q}|\varkappa_2|\boldsymbol{q}\rangle
\end{aligned}
\tag{50}
$$

where the dimensionless function $u_2(\boldsymbol{K},\boldsymbol{q},\omega)$ is the characteristic function for the correction to the Lindhard formula that is characterized by $u_0(q,\omega)$. In the appendix we have determined the function u_2 in the zero T case.

It now only remains to relate consistently the potential $V(\boldsymbol{r})$ to the inter-action $v_e(\boldsymbol{r})$. This is easily done, since in the tentative dynamical matrix in Eq. (37) we shall put in the zero order matrix $\varkappa_0$ in the terms containing the static electron distribution $\langle\varrho_0\rangle$ (the second sum). From Eq. (22) this immediately gives with $\delta U(\boldsymbol{K}) = - Ze^2Nv_e(\boldsymbol{K})$ and $\delta U_{\text{eff}}(\boldsymbol{K}) = - V(\boldsymbol{K})$

$$V(\boldsymbol{K}) = \frac{Ze^2Nv_e(\boldsymbol{K})}{1 + e^2\varkappa_0(\boldsymbol{K})}. \tag{51}$$

The simple form of Eq. (51) is naturally only valid for the form of $D_E(\boldsymbol{q})$ given in Eq. (37). If we alter this form, for instance by including terms in order to preserve the periodic property of $D_E(\boldsymbol{q})$ in the reciprocal lattice, we have to alter Eq. (51) as well.

V. Discussion

In this section we shall briefly discuss the functions u_1 and u_2 obtained in the appendix in the zero T limit. For simplicity we only consider the adia-batic expressions in the two cases, which – as we indicated in the appendix – is quite sufficient to do in connection with phonons.

The symmetry of the dielectric matrix gives the following general structure for u_1

$$u_1(\boldsymbol{K},\boldsymbol{q}) = w_1(\boldsymbol{K},\boldsymbol{q}) + w_1(\boldsymbol{K}, - (\boldsymbol{K} + \boldsymbol{q})) \tag{52}$$

Since $\boldsymbol{K}$ is an axis of symmetry in u_1, it follows from Eq. (52) that u_1 has the following symmetry plane

$$2\boldsymbol{K}\cdot\boldsymbol{q} + K^2 = 0. \tag{53}$$

It is therefore sufficient to investigate the function u_1 for $\boldsymbol{K}$ and $\boldsymbol{q}$ in a half-plane. In this plane the intersection with the plane in Eq. (53) generates a line of symmetry.

It is of particular interest to observe the difference between the two cases $Z_0 > 1$ and $Z_0 < 1$. This difference is already emphasized in the definition of the function u_1. The integrals I_{ij} in Eq. (A 13) have two different functional forms depending on whether the functions $R_i(Z_j)$ are negative or positive. And as is seen in Eq. (A 31) all these functions $R_i(Z_j)$ are essentially equal

$K = 2$

$2 k_0 = 2.2545$
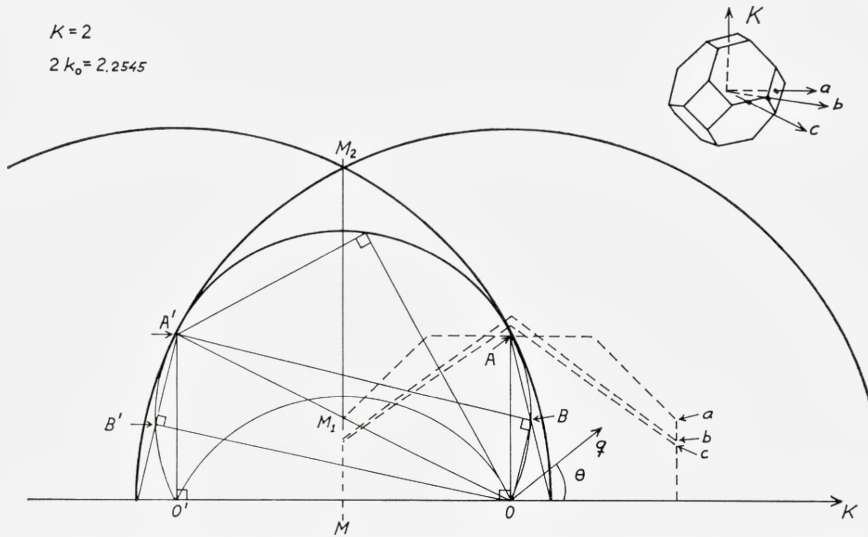
Fig. 1. Figure showing the intersection in the $\mathbf{K} - \mathbf{q}$-plane of the surfaces where u_1 (and u_2) have nonregular behaviour (heavy lines). The dashed figures show the intersection with the zone as indicated in the inset.

in the adiabatic limit. But, for instance, $R_1(Z_0) < 0$ means that the intersection between the singularity planes $2\mathbf{K} \cdot \mathbf{k} - K^2 = 0$ and (for $\omega = 0$) $2\mathbf{k} \cdot \mathbf{q} + q^2 = 0$ in Eq. (A 5) penetrates the Fermi sphere. Accordingly we cannot have $R_1(Z_0)$ negative in case $Z_0 > 1$, since $Z_0 > 1$ means that the plane $2\mathbf{K} \cdot \mathbf{k} - K^2 = 0$ is entirely outside the Fermi sphere. There is consequently an important qualitative difference between metals with a Fermi sphere extending outside the first zone and those with the Fermi sphere completely inside the zone. This is one reason why the polyvalent metals is felt to be much more interesting than, for instance, a metal such as Na.

In order to demonstrate easily the behaviour of the function u_1, some relevant curves have been drawn in Fig. 1 for the case $K = 2$ and $2k_0 = 2.2545$ in $\dfrac{2\pi}{a}$, which is a value appropriate for Al.

$\mathbf{K}$ is here the axis of symmetry and the circles around O and O' are the traces in the $\mathbf{K} - \mathbf{q}$-plane of the "Fermi spheres" (radii $2k_0$) around O and O'. M is the intersection with the plane in Eq. (53). The locus for points making $R_i(Z_j) = 0$ is also shown. This locus is a circle with diameter OA' and centre at M_1 which thus touches the "Fermi spheres" at the points A and A' (note the folded part). The heavy parts of the circles in the figure give the loci for

points where there are infinities in the derivative of u_1. The parts along the "Fermi circles" are to be expected, but it is interesting to note that along the circle around M_1 there are also such points between A and A' and moreover with stronger infinities. The formal reason for these singularities is easily located. Approaching the circle M_1 from the inside means that the functions $R_i(Z_j)$ tend to -0. Then all cyclometric functions approach the values $+\frac{\pi}{2}$ or $-\frac{\pi}{2}$. On the arc between A and A' all functions I_{ij} give a contribution $+\pi$ to the sum in Eq. (A 32). When the factors are considered, a rapid increase is found in the contribution from the sum of I_{ij} there. On the circle the contribution is zero. If, however, the circle is approached from outside, then $R_i(Z_j)$ tends to $+0$ and the integral are given by hyperbolic area functions which themselves go to zero on the circle. These arguments apply for all points on the circle between A and A', since there is no change in sign for the contributions from the cyclometric functions along $A - A'$. This can be seen to be the case, since for any of the integrals the following sum rule applies for the arguments involved in I_{ij}.

$$R_i(Z_j) - (c_i + Z_i Z_j)^2 = -(1 - Z_j^2)(1 - Z_j^2). \tag{54}$$

Eq. (54) demonstrates that on the circle around M_1 where $R_i(Z_j) = 0$, the quantity $(c_i + Z_i Z_j)$ cannot become zero unless Z_i or Z_j equals ± 1. This never happens between A and A': at A (or A'), however, Z_3(or Z_1) equals 1 and there is a change in the sign of I_{30} and I_{32} (or I_{10} and I_{12}). Along $A0$ and $A'0'$, and also along the folded continuation, this edge effect therefore disappears. I_{32} and I_{12} change signs again at B (or B') where $|Z_2| = 1$, but these sign changes cancel, making the function smooth there.

Physically this edge-effect arises from the discontinuity in the expansion coefficients of the electron wave function at the Bragg planes. In the present treatment these discontinuities are infinitely large, since for the integrations, the finite coefficients (in a Wigner Brillouin expansion) have de facto been replaced by the singular coefficients in a Schrödinger expansion. Consequently the form of u_1 used does not give a correct reproduction of the real behaviour of the matrix element $\langle q | \varkappa_1 | K + q \rangle$ for values of q close to this edge. This form of u_1 can only be expected to give the correct behaviour of the true function up to a distance of order $\Delta q = \dfrac{V(K)}{\varepsilon_0} \cdot k_0$ from the edge. The approximation made here yields a function connecting continuously (but with infinite

slope at the edge) points on both sides of this edge. However, even in the real case a rapid variation in the nondiagonal terms of the dielectric matrix can be expected for values of q in that region. It is therefore of interest to find out whether or not this property is observable in the experimental measurements. What makes the situation so interesting is that points on this edge are not in general close to any "ordinary" KOHN point, where the following should apply [24].

$$(\boldsymbol{K} + \boldsymbol{q})^2 - 4k_0^2 = 0. \tag{55}$$

Instead the relationship is of the form [25]

$$(\boldsymbol{K} + \boldsymbol{q})^2 - s^2 4k_0^2 = 0: \quad \text{with} \quad s^2 = \frac{|\boldsymbol{K} \times \boldsymbol{q}|^2}{K^2 q^2}. \tag{56}$$

Although this condition is identical with the condition given by TAYLOR in the limit of vanishing deformation of the Fermi sphere, the reason for the effect is entirely different in this case. In his treatment TAYLOR considers the matrix elements as slowly varying functions and attributes the effect to the shape of the Fermi surface (through the energy of the one-particle states), but here to lowest order the effect is seen to be due to the rapid variation of the matrix element and present even for a spherical Fermi surface.

In Fig. 1 some traces in the $\boldsymbol{K} - \boldsymbol{q}$-plane of the first zone in a f.c.c. lattice have been drawn. It can be seen that the curve $A - A'$ is rather far out from 0, in a region where the influence on the dynamical matrix from elements $\langle \boldsymbol{q} | \varkappa_1 | \boldsymbol{K} + \boldsymbol{q} \rangle$ is expected to be small. In any case it is clear from Fig. 1 that the regions of particular interest are those around A (or A') and also around the intersection M_2, where two singularities are added. It is also of interest to observe the detailed shape of the function u_1 close to the edge along $A - A'$. In Fig. 2 some results of an accurate computation are shown for some values of the angle between $\boldsymbol{K}$ and $\boldsymbol{q}$. In Fig. 3 results are shown of a more extensive computation of u_1 close to A'. The edge-effect is seen to set in for

$$c_1 = \cos \theta > -\frac{K}{2k_0} \approx -0.8871.$$

Around M_2 the function is found to be quite smooth. It is almost impossible to detect the logarithmic infinities in the slope, even in a very detailed computation. However, in both these regions around A' (and A) and M_2 the influence from the neglected terms in Eq. (46) can be expected to give comparatively large "rounding off" effects and the results given here have for that reason to be interpreted with some care.
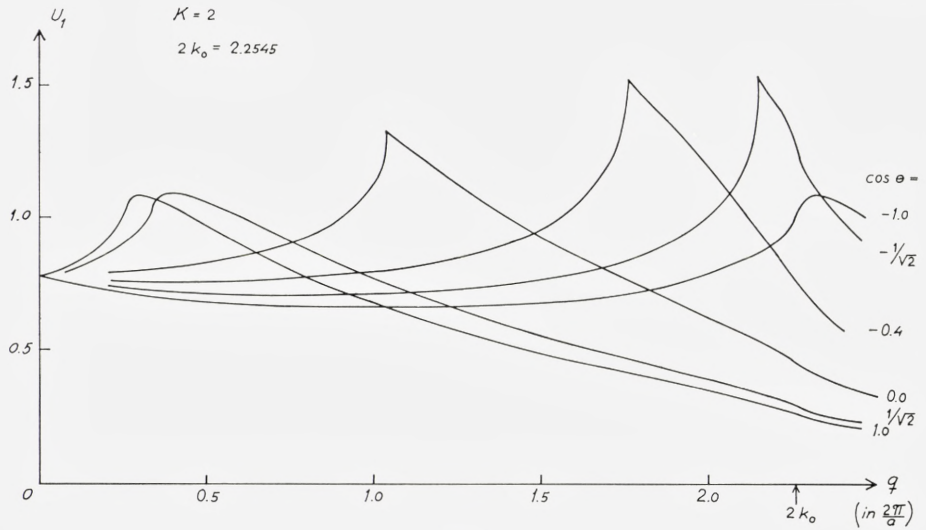
Fig. 2.

Fig. 2, 3 and 4. $u_1(\mathbf{K}, \mathbf{q})$ as a function of q for some K and $\cos \theta = \dfrac{\mathbf{K} \cdot \mathbf{q}}{Kq}$.
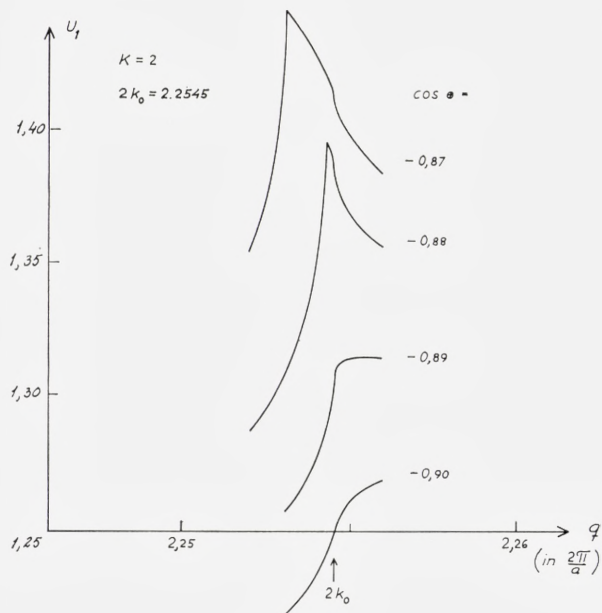
Fig. 3.
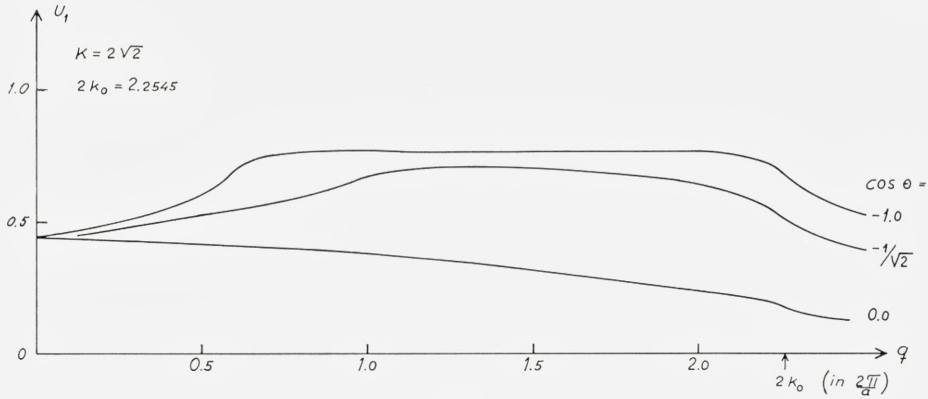
Fig. 4.

In the case $Z_0 > 1$, the function u_1 becomes much less dramatic. In this case the point $0'$ in Fig. 1 lies outside the circle $q = 2k_0$, and $R_i(Z_j) > 0$ for all values of $\boldsymbol{q}$. Hence the edge-effect does not appear in this case and only the logarithmic infinities appear in the slope on the circles $q = 2k_0$ and $|\boldsymbol{K} + \boldsymbol{q}| = 2k_0$. In Fig. 4 the result is shown of a computation for Al in the case $K = 2\sqrt{2}$.

There is a third possibility, namely $Z_0 > 2$: the two circles at 0 and $0'$ in Fig. 1 then lie completely outside each other. This alternative has not been investigated in detail, but nothing of importance is expected to happen in this case either.

In the appendix the function $u_2(\boldsymbol{K}, \boldsymbol{q})$ is split into two parts so that the trivial effect from the change in the Fermi energy is treated separately. We write

$$u_2(\boldsymbol{K}, \boldsymbol{q}) = u_2'(\boldsymbol{K}, \boldsymbol{q}) + u_2''(\boldsymbol{K}, \boldsymbol{q}) \qquad (57)$$

where $u_2''(\boldsymbol{K}, \boldsymbol{q})$ gives the isotropic effect from the decrease in the Fermi energy and is given in Eq. (A 30). The more interesting part $u_2'(\boldsymbol{K}, \boldsymbol{q})$ is in the appendix written as follows

$$u_2'(\boldsymbol{K}, \boldsymbol{q}) = \tfrac{1}{2}\{w_2(\boldsymbol{K}, \boldsymbol{q}) + w_2(-\boldsymbol{K}, \boldsymbol{q})\} \qquad (58)$$

and is also given in Eq. (A 30). Due to the axial symmetry of u_2' around the direction $\boldsymbol{K}$ and its evenness in q it is again only necessary to consider $\boldsymbol{K}$ and $\boldsymbol{q}$ in a plane, and this time only for values of c_1 satisfying $0 \le c_1 \le 1$. Of interest to us here is the behaviour of $u_2(\boldsymbol{K}, \boldsymbol{q})$ for rather small values of q: say for q within a sphere inscribed in the first zone, since it is only for such q:s the corrections from u_2 are expected to be significant. This restriction is important because both the expressions in Eq. (A 30) are singular for q:s outside this sphere. The singularity in u_2'' is obvious at $Z_1 = 1$, which means
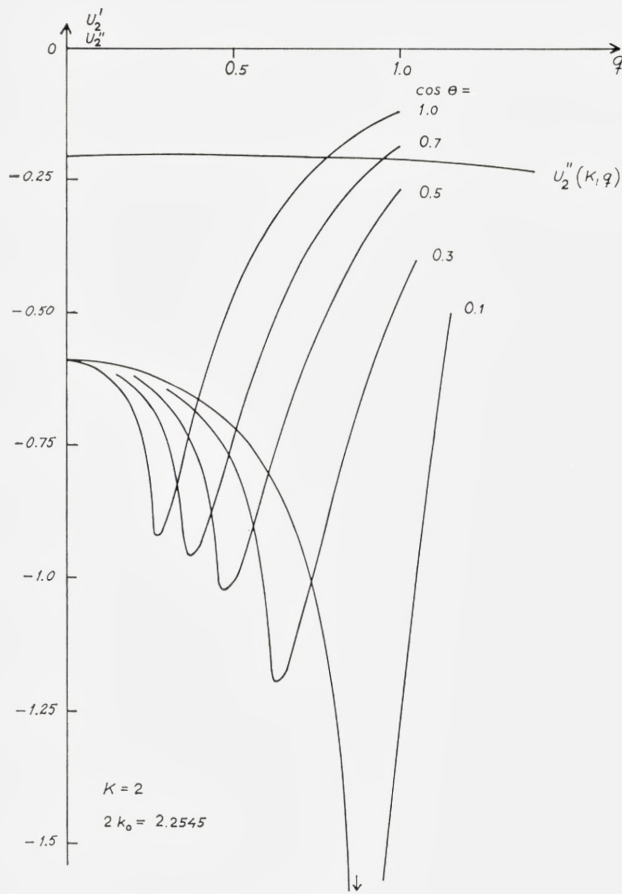
Fig. 5.

Fig. 5 and 6. The second order functions u_2' and u_2'' for some values of K and the angle θ.

when $q = 2k_0$. In u_2 the factor $\dfrac{1}{\sqrt{R_{10}}}$ produces singularities along the arc of the circle at M_1 denoted by $A - A'$ in Fig. 1. This arc also has to be reflected in the line $A - O$ in order to give the total picture in this case. The singularities are naturally quite non-physical, and indicate that the element $\langle q|\varkappa|q\rangle$ cannot be expanded in a power series in $V(K)$ at zero temperature, which might be expected from Lindhard's formula. They have to be removed if the function u_2 is to be defined all over the $K - q$-plane. This removal requires among other things a more careful investigation of the contributions to u_2 from states
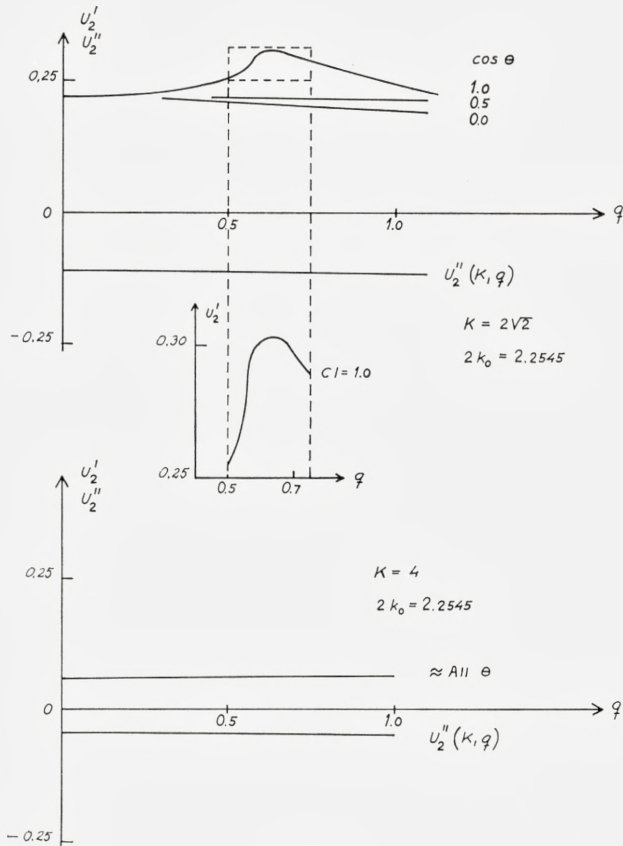
Fig. 6.

close to the zone boundary. At any rate, the expression given would suffice here because the correction is only being considered for small q well inside the first zone.

The qualitative difference between the cases $Z_0 < 1$ and $Z_0 > 1$ is more marked here than in the first order case. In Figs. 5 and 6 some results of a calculation for $K = 2$ and $K = 2\sqrt{2}; 4;$ have been collected, using the value of $2k_0 = 2.2545$.

The significant difference between the two cases is this that for $Z_0 < 1$, $u_2'(\boldsymbol{K}, \boldsymbol{q})$ is comparatively large and negative for the relevant values of $\boldsymbol{q}$ (it becomes positive for larger q) whereas for $Z_0 > 1$, $u_2'(\boldsymbol{K}, \boldsymbol{q})$ is positive. This means that in the $Z_0 < 1$ case there is a comparatively strong reduction of

the dielectric function for small q. The effect from terms with $Z_0 < 1$ is then to increase the frequency of the longitudinal phonons, contrary to what might be expected for the effect from the lattice potential. For $Z_0 < 1$ there are also interesting peaks with infinities in the slope to the left, at points where $|\boldsymbol{K} + \boldsymbol{q}| = 2k_0$. The infinities are here of the same logarithmic kind as those found in the function $u_1(\boldsymbol{K},\boldsymbol{q})$ at these points.

In the case $Z_0 > 1$, however, the function u_2 contains little of interest. For all relevant values of q, $u_2 > 0$, and as in the case of u_1 there is a weak singularity in the slope at $Z_3 = 1$. (Seen in Fig. 6 for $K = 2\sqrt{2}$.) For still larger K the function u_2' becomes practically isotropic for all values of q of interest. This is also seen in Fig. 6 for $K = 4$. There it can also be observed how fast the physically interesting quantity $u_2' + u_2''$ goes to zero. For $K = 2$, this quantity is numerically of the order 1 at $q = 0$. But already for $K = 4$ it has decreased to about 0.01, and for $K = 6$ it has gone down to about 0.002. This rapid convergency even in the function u_2 indicates that no practical problem will arise in the performance of the sum in Eq. (50).

The model developed in this paper has been applied to aluminium by the present author and A Westin. The results of the calculations are collected in: On Phonons in Simple Metals II, AB Atomenergi, Studsvik, Nyköping, Sweden, Report AE-365 (1969).

Appendix

Our problem is to find explicit expressions for the various functions u_i introduced in the text.

For completeness we include also the LINDHARD [17] expression for $u_0(q)$. From Eq. (49) we have ($\boldsymbol{q}$ an arbitrary vector in the following)

$$e^2 \varkappa_0(\boldsymbol{q}, \omega) = - e^2 v(q) 2P \sum_{\boldsymbol{k},\boldsymbol{k}'} \frac{f(k) - f(k')}{\varepsilon(k) - \varepsilon(k') + \omega} \delta_{\boldsymbol{k}'}^{\boldsymbol{k}+\boldsymbol{q}} = \frac{k_0}{\pi^2 a_0} \cdot \\ \cdot v(q) u_0(q, \omega) \qquad \left. \right\} \qquad \text{(A 1)}$$

where

$$u_0(q, \omega) = \frac{1}{2\pi k_0} P \int \frac{f(k) d\boldsymbol{k}}{2\boldsymbol{k} \cdot \boldsymbol{q} + q^2 \pm 2m\omega} \qquad \text{(A 2)}$$

which gives

$$u_0(q, \omega) = \frac{1}{8Z_1} \left\{ (1 - Z_{1\pm}^2) \ln \left| \frac{1 + Z_{1\pm}}{1 - Z_{1\pm}} \right| + 2Z_{1\pm} \right\} \qquad \text{(A 3)}$$

in the zero T case. We have in Eq. (A 3) put $Z_1 = \dfrac{q}{2k_0}$; $Z_{\pm} = Z_1 \pm \dfrac{\omega}{4\varepsilon_0 Z_1}$ and shall add the expression for Z_{1+} and Z_{1-}.

For the first order element we get from Eq. (46) after removing a factor $V(\boldsymbol{K})$ in the coefficients $c(\boldsymbol{k},\boldsymbol{K})$ in Eq. (42) and passing to the limit $V = 0$ in the remaining expression

$$e^2 \langle \boldsymbol{q} | \varkappa_1(\omega) | \boldsymbol{K} + \boldsymbol{q} \rangle = \frac{k_0}{\pi^2 a_0} \frac{V(\boldsymbol{K})}{\varepsilon_0} [v(q) v(\boldsymbol{K} + \boldsymbol{q})]^{1/2} u_1(\boldsymbol{K}, \boldsymbol{q}, \omega) \qquad \text{(A 4)}$$

where

$$u_1(\mathbf{K}, \mathbf{q}, \omega) = -\frac{k_0}{2\pi} P \int f(k)\,d\mathbf{k} \left\{ \frac{1}{2\mathbf{k}\cdot\mathbf{q} + q^2 \pm 2m\omega} \cdot \right.$$

$$\left. \cdot \left[\frac{1}{2\mathbf{K}\cdot\mathbf{k} - K^2} - \frac{1}{2\mathbf{K}(\mathbf{k}+\mathbf{q}) + K^2} \right] - \frac{1}{2\mathbf{k}(\mathbf{K}+\mathbf{q}) + (\mathbf{K}+\mathbf{q})^2 \pm 2m\omega} \cdot \right.$$

$$\left. \cdot \left[\frac{1}{2\mathbf{K}\cdot\mathbf{k} + K^2} - \frac{1}{2\mathbf{K}(\mathbf{k}+\mathbf{q}) + K^2} \right] \right\} \tag{A 5}$$

with the P symbol extended to all singularity planes.

In order to integrate this expression in the zero T limit we choose axes and variables as follows

$$\begin{aligned}
\mathbf{K} &= K(0, 0, 1); \quad \mathbf{q} = q(s_1, 0, c_1) \\
\mathbf{K} + \mathbf{q} &= |\mathbf{K} + \mathbf{q}|(s_3, 0, c_3) \\
\mathbf{k} &= k_0(\varrho\cos\varphi, \varrho\sin\varphi, Z); \quad d\mathbf{k} = k_0^3\,dZ\varrho\,d\varrho\,d\varphi
\end{aligned} \tag{A 6}$$

and are also going to use the following notations

$$\begin{aligned}
Z_0 &= \frac{K}{2k_0}; \quad Z_{1\pm} = Z_1 \pm \frac{\omega}{4\varepsilon_0 Z_1} \quad \text{as earlier} \\
Z_2 &= \frac{\mathbf{K}(\mathbf{K}+\mathbf{q})}{4k_0^2 Z_0} = Z_0 + 2c_1 Z_1 \\
Z_3 &= \frac{|\mathbf{K}+\mathbf{q}|}{2k_0}; \quad Z_{3\pm} = Z_3 \pm \frac{\omega}{4\varepsilon_0 Z_3}.
\end{aligned} \tag{A 7}$$

From (A 6) and (A 7) we get the relationships

$$s_3^2 = \left(\frac{Z_1}{Z_3}\right)^2 s_1^2; \quad c_3 = \frac{Z_0 + c_1 Z_1}{Z_3}. \tag{A 8}$$

After performing some simple integrations, we get for $T = 0$

$$u_1(\mathbf{K}, \mathbf{q}, \omega) = \frac{1}{16Z_0}\left\{ \frac{1}{Z_1 s_1^2}\left[(c_1 Z_0 + Z_{1\pm})\ln\left|\frac{1 + Z_0}{1 - Z_0}\right| \right.\right.$$

$$\left. + P\int_{-1}^{1} dZ \sqrt{R_{1\pm}(Z)}\left(\frac{1}{Z - Z_0} - \frac{1}{Z + Z_2}\right) \right] - \frac{1}{Z_3 s_3^2}\left[(c_3 Z_0 - Z_{3\pm}) \cdot \right.$$

$$\left.\left. \cdot \ln\left|\frac{1 + Z_0}{1 - Z_0}\right| + P\int_{-1}^{1} dZ \sqrt{R_{3\pm}(Z)}\left(\frac{1}{Z + Z_0} - \frac{1}{Z + Z_2}\right) \right] \right\} \tag{A 9}$$

where

$$R_{1\pm}(Z) = Z^2 + 2c_1 Z_{1\pm} Z + Z_{1\pm}^2 - s_1^2$$
$$R_{3\pm}(Z) = Z^2 + 2c_3 Z_{3\pm} Z + Z_{3\pm}^2 - s_3^2. \qquad \Big\} \text{ (A 10)}$$

The integrations in Eq. (A 9) are only over real values of the square-roots which are interpreted in these intervals as follows

$$\sqrt{R_{1\pm}(Z)} = \text{sgn}(c_1 Z + Z_{1\pm})|R_{1\pm}(Z)|^{1/2}$$
$$\sqrt{R_{3\pm}(Z)} = \text{sgn}(c_3 Z + Z_{3\pm})|R_{3\pm}(Z)|^{1/2}. \qquad \Big\} \text{ (A 11)}$$

By writing the integrand

$$\frac{\sqrt{R_{1\pm}(Z)}}{Z - Z_0} = \frac{1}{\sqrt{R_{1\pm}(Z)}(Z - Z_0)}\{R_{1\pm}(Z_0) + R'_{1\pm}(Z_0)(Z - Z_0) +$$
$$+ (Z - Z_0)^2\} \quad \text{where} \quad R'_{1\pm}(Z_0) = \left(\frac{dR_{1\pm}}{dZ}\right)_{Z_0}$$

and similarly for the others, we get after performing the integrations and some reductions.

$$u_1(\boldsymbol{K}, \boldsymbol{q}, \omega) = \frac{1}{16 Z_0 Z_1 s_1^2}\Bigg\{ 2(Z_0 + c_1 Z_1) \ln\left|\frac{1 + Z_{1\pm}}{1 - Z_{1\pm}}\right|$$
$$+ 2(c_1 Z_0 + Z_{1\pm}) \ln\left|\frac{1 + Z_0}{1 - Z_0}\right| - 2c_1 Z_3 \ln\left|\frac{1 + Z_{3\pm}}{1 - Z_{3\pm}}\right| \Bigg\} \text{ (A 12)}$$
$$+ \text{sgn}(R_{1\pm}(Z_0))\sqrt{R_{10}^\pm}(I_{10}^\pm - I_{30}^\pm) - \text{sgn}(R_{1\pm}(-Z_2)) \cdot \sqrt{R_{12}^\pm}(I_{12}^\pm - I_{32}^\pm)\Bigg\}$$

where $I_{ij}^\pm$ means

$$I_{10}^\pm = \sqrt{R_{10}^\pm} P \int_{-1}^{1} \frac{dZ}{(Z - Z_0)\sqrt{R_{1\pm}(Z)}} = \begin{cases} \ln\left|\dfrac{c_1 + Z_0 Z_{1\pm} - \sqrt{R_{10}^\pm}}{c_1 + Z_0 Z_{1\pm} + \sqrt{R_{10}^\pm}}\right| \text{ if } R_{1\pm}(Z_0) > 0 \\[2mm] 2 \,\text{arctg}\left(\dfrac{c_1 + Z_0 Z_{\pm 1}}{\sqrt{R_{10}^\pm}}\right) \text{ if } R_{1\pm}(Z_0) < 0 \end{cases}$$

$$I_{12}^\pm = \sqrt{R_{12}^\pm} P \int_{-1}^{1} \frac{dZ}{(Z + Z_2)\sqrt{R_{1\pm}(Z)}} = \begin{cases} \ln\left|\dfrac{c_1 - Z_2 Z_{1\pm} - \sqrt{R_{12}^\pm}}{c_1 - Z_2 Z_{1\pm} + \sqrt{R_{12}^\pm}}\right| \text{ if } R_{\pm 1}(-Z_2) > 0 \\[2mm] 2 \,\text{arctg}\left(\dfrac{c_1 - Z_2 Z_{1\pm}}{\sqrt{R_{12}^\pm}}\right) \text{ if } R_{1\pm}(-Z_2) < 0 \end{cases} \text{ (A 13)}$$

$$I_{30}^{\pm} = \sqrt{R_{30}^{\pm}} \, P \int_{-1}^{1} \frac{dZ}{(Z + Z_0)\sqrt{R_{1\pm}(Z)}} = \left.\right\} \text{ similar expressions } \left.\right\} \quad (A\,13)$$

$$I_{32}^{\pm} = \sqrt{R_{32}^{\pm}} \, P \int_{-1}^{1} \frac{dZ}{(Z + Z_2)\sqrt{R_{3\pm}(Z)}} =$$

where in Eq. (A 13) $\sqrt{R_{10}^{\pm}} = |R_{1\pm}(Z_0)|^{1/2}$, and similarly for the others. The evaluation of the integrals $I_{ij}^{\pm}$ is a little bit tricky, at least in case $R_{i\pm}(Z_j) < 0$. We have to consider the two distinct cases possible (depending on whether $R_{i\pm}(\pm 1)$ have the same sign or not) with the sign rule in Eq. (A 11) in mind and to keep track of which branch of the cyclometric function we deal with. In Eq. (A 13), however, all angles are in the interval $-\pi \leq I_{ij}^{\pm} \leq \pi$. When doing the reduction in Eq. (A 13) we have also used the following relationships

$$R_{1\pm}(Z_0) = \left(\frac{Z_3}{Z_1}\right)^2 R_{3\pm}(-Z_0) \left.\right\}$$

$$R_{1\pm}(-Z_2) = \left(\frac{Z_3}{Z_1}\right)^2 R_{3\pm}(-Z_2). \quad\quad\quad (A\,14)$$

The corrections to the Lindhard value of the diagonal part of $\varkappa$ had in Eq. (48) and Eq. (49) three different sources. Considering first the contribution from the change in the matrix M in Eq. (45). We get this part after removing a factor $V(\boldsymbol{K})^2$ and passing to the limit $V = 0$ in the remaining expression.

$$e^2 \langle \boldsymbol{q} | \varkappa_2^M | \boldsymbol{q} \rangle = e^2 v(q) \sum_{K}' |V(\boldsymbol{K})|^2 \cdot 2P \sum_{k,\,k'}$$

$$\frac{f(k) - f(k')}{\varepsilon(k) - \varepsilon(k') + \omega} \Biggl\{ \delta_{k'}^{k+q} \left[\frac{1}{\varepsilon(k) - \varepsilon(\boldsymbol{k} + \boldsymbol{K})} - \frac{1}{\varepsilon(k') - \varepsilon(\boldsymbol{k}' + \boldsymbol{K})} \right]^2 - \quad (A\,15)$$

$$- \delta_{k'}^{k+K+q} \left[\frac{1}{\varepsilon(k) - \varepsilon(\boldsymbol{k} + \boldsymbol{K})} + \frac{1}{\varepsilon(k') - \varepsilon(\boldsymbol{k}' - \boldsymbol{K})} \right]^2 \Biggr\}$$

with again the P symbol extended to all singularity planes. This contribution – and as we will see later, the others too – is made up of a sum over all $\boldsymbol{K} \neq 0$. This fact may be used to simplify the calculations by a proper choice of the terms in this sum. Of interest to us is to find the function $u_2(\boldsymbol{K}, \boldsymbol{q})$ having the

same symmetry as the lattice, which means a function even in q in this case. Thus, with

$$e^2 \langle \boldsymbol{q} | \varkappa_2^M | \boldsymbol{q} \rangle = \frac{k_0}{\pi^2 a_0} \sum_{\boldsymbol{K}}{}' \left(\frac{V(\boldsymbol{K})}{\varepsilon_0} \right)^2 v(q) u_2^M(\boldsymbol{K}, \boldsymbol{q}, \omega), \tag{A 16}$$

we write

$$
\left.
\begin{aligned}
& u_2^M(\boldsymbol{K}, \boldsymbol{q}, \omega) = -\frac{k_0^3}{2\pi} P \int \left\{ \frac{f(k) d\boldsymbol{k}}{2\boldsymbol{K} \cdot \boldsymbol{q} + q^2 \pm 2m\omega} \right. \\
& \left. \cdot \left[\left(\frac{1}{2\boldsymbol{K} \cdot \boldsymbol{k} - K^2} \right)^2 + \left(\frac{1}{2\boldsymbol{K}(\boldsymbol{k} + \boldsymbol{q}) + K^2} \right)^2 \right] - \frac{f(k) d\boldsymbol{k}}{2\boldsymbol{k}(\boldsymbol{K} + \boldsymbol{q}) + (\boldsymbol{K} + \boldsymbol{q})^2 \pm 2m\omega} \right. \\
& \left. \cdot \left[\left(\frac{1}{2\boldsymbol{K} \cdot \boldsymbol{k} + K^2} \right)^2 + \left(\frac{1}{2\boldsymbol{K}(\boldsymbol{k} + \boldsymbol{q}) + K^2} \right)^2 \right] \right\} - \frac{1}{4Z_0 Z_1 c_1} u_1(\boldsymbol{K}, \boldsymbol{q}, \omega)
\end{aligned}
\right\} \tag{A 17}
$$

where we have made a substitution $\boldsymbol{K} \to -\boldsymbol{K}$ in appropriate terms. Similar calculations as in the previous case give in the zero T limit

$$
\left.
\begin{aligned}
& u_2^M(\boldsymbol{K}, \boldsymbol{q}, \omega) = \frac{1}{64 Z_0} \left(\left\{ \frac{c_1}{Z_1 s_1^2} \ln \left| \frac{1 + Z_0}{1 - Z_0} \right| - \frac{c_1}{Z_1 s_1^2} \right. \right. \\
& \left. \cdot \ln \left| \frac{1 + Z_2}{1 - Z_2} \right| + \frac{c_3}{Z_3 s_3^2} \ln \left| \frac{1 + Z_0}{1 - Z_0} \right| + \frac{c_3}{Z_3 s_3^2} \ln \left| \frac{1 + Z_2}{1 - Z_2} \right| + \right. \\
& \left. + P \int_{-1}^{1} dZ \frac{\sqrt{R_{1\pm}(Z)}}{Z_1 s_1^2} \left[\frac{1}{(Z - Z_0)^2} + \frac{1}{(Z + Z_2)^2} \right] - P \int_{-1}^{1} dZ \frac{\sqrt{R_{3\pm}(Z)}}{Z_3 s_3^2} \cdot \right. \\
& \left. \cdot \left[\frac{1}{(Z + Z_0)^2} + \frac{1}{(Z + Z_2)^2} \right] \right\} - \frac{1}{4 Z_0 Z_1 c_1} u_1(\boldsymbol{K}, \boldsymbol{q}, \omega)
\end{aligned}
\right\} \tag{A 17}
$$

where we have exposed the integrals, which are singular in case $|Z_0| < 1$ or/and $|Z_2| < 1$, if the integrations are over these Z-values. With

$$\int dZ \frac{\sqrt{R_{1\pm}(Z)}}{(Z - Z_0)^2} = -\frac{\sqrt{R_{1\pm}(Z)}}{(Z - Z_0)} + \int \frac{dZ\, R_{1\pm}'(Z)}{2(Z - Z_0)\sqrt{R_{1\pm}(Z)}} \tag{A 18}$$

and similar expressions for the others, we get from Eqs. (A 7), (A 8), (A 11) and (A 14) a cancellation of the dangerous terms; in fact all integrated parts in Eq. (A 18) and the similar expressions for the others are seen to completely cancel. Performing the remaining integrations, gives

$$
u_2^M(\boldsymbol{K}, \boldsymbol{q}, \omega) = \frac{1}{64 Z_0^2 Z_1^2 s_1^2} \left\{ Z_2 \ln \left| \frac{1 + Z_0}{1 - Z_0} \right| + \right.
$$

$$
\left. + 2 Z_1 \ln \left| \frac{1 + Z_{1\pm}}{1 - Z_{1\pm}} \right| + Z_0 \ln \left| \frac{1 + Z_2}{1 - Z_2} \right| - 2 Z_3 \ln \left| \frac{1 + Z_{3\pm}}{1 - Z_{3\pm}} \right| \right\}
$$

$$
+ \frac{1}{64 Z_0^2} \left\{ \frac{(Z_0 + c_1 Z_{1\pm})}{s_1^2 Z_1 / R_{10}^{\pm}} I_{10}^{\pm} - \frac{(Z_2 - c_1 Z_{1\pm})}{s_1^2 Z_1 / R_{12}^{\pm}} I_{12}^{\pm} \right.
$$

$$
+ \frac{(Z_0 - c_3 Z_{3\pm})}{s_3^2 Z_3 / R_{30}^{\pm}} I_{30}^{\pm} + \frac{(Z_2 - c_3 Z_{3\pm})}{s_3^2 Z_3 / R_{32}^{\pm}} I_{32}^{\pm} \left. \right\} - \frac{1}{4 Z_0 Z_1 c_1} u_1(\boldsymbol{K}, \boldsymbol{q}, \omega) \qquad (A\ 15)
$$

where again we may reduce the expression by use of the relationships given earlier. We leave, however, this to a later stage in this case.

Next we consider the lowest order contribution to $\langle \boldsymbol{q} | \varkappa_2 | \boldsymbol{q} \rangle$ from the correction of the energy denominator in Eq. (49). By a similar procedure as in the previous case, we get

$$
u_2^E(\boldsymbol{K}, \boldsymbol{q}, \omega) = \frac{k_0^3}{2\pi} P \int d\boldsymbol{k} \frac{f(k)}{(2\boldsymbol{k} \cdot \boldsymbol{q} + q^2 \pm 2m\omega)^2} \left\{ \frac{1}{2\boldsymbol{K} \cdot \boldsymbol{k} - K^2} + \right.
$$

$$
\left. + \frac{1}{2\boldsymbol{K}(\boldsymbol{k} + \boldsymbol{q} + K^2)} \right\} \qquad (A\ 20)
$$

where the second order singularity clearly must be interpreted as the limit of two nearby first order singularities, then giving zero contribution when the principal value is taken.

Similar calculations as those already shown give in the zero T limit

$$
u_2^E(\boldsymbol{K}, \boldsymbol{q}, \omega) = \frac{1}{64 Z_0 Z_1^2 s_1^2} \left\{ 2 c_1 \ln \left| \frac{1 + Z_{1\pm}}{1 - Z_{1\pm}} \right| + \right.
$$

$$
+ \ln \left| \frac{1 + Z_0}{1 - Z_0} \right| - \ln \left| \frac{1 + Z_2}{1 - Z_2} \right| + \frac{(c_1 Z_0 + Z_{1\pm})}{/ R_{10}^{\pm}} I_{10}^{\pm} - \frac{(c_1 Z_2 - Z_{1\pm}}{/ R_{12}^{\pm}} I_{12}^{\pm} \left. \right\}. \qquad (A\ 21)
$$

In this case it is practical to use axes with $\boldsymbol{q} = q(0, 0, 1)$ and $\boldsymbol{K} = K(s_1, 0, c_1)$ and, then, to introduce functions $R_0(Z) = Z^2 - 2c_1 Z_0 Z + Z_0^2 - s_1^2$ and $R_2(Z) = Z^2 + 2c_1 Z_2 Z + Z_2^2 - s_1^2$, which lead to integrals as

$$
\int_{-1}^{1} \frac{dZ}{(Z + Z_{1\pm}) / R_0(Z)} = \int_{-1}^{1} \frac{dZ}{(Z - Z_0) / R_{1\pm}(Z)} = \frac{I_{10}^{\pm}}{/ R_{10}^{\pm}}.
$$

Finally we consider the effect from the change in the Fermi factors in Eq. (49).

To lowest order we have

$$g(\boldsymbol{k}) = \frac{\partial f(k)}{\partial \varepsilon} \{E(\boldsymbol{k}) - \varepsilon(k) - (\mu - \mu_0)\} \qquad \text{(A 22)}$$

and then a contribution to u_2

$$u_2^F(\boldsymbol{K}, \boldsymbol{q}, \omega) = \frac{k_0^3}{4m\pi} P \int d\boldsymbol{k} \frac{\dfrac{\partial f(k)}{\partial \varepsilon}}{2\boldsymbol{k} \cdot \boldsymbol{q} + q^2 \pm 2m\omega} \cdot \left\{ \frac{1}{2\boldsymbol{K} \cdot \boldsymbol{k} - K^2} - \frac{\eta(\boldsymbol{K})}{k_0^2} \right\} \qquad \text{(A 23)}$$

where we have written

$$\mu - \mu_0 = \frac{1}{\varepsilon_0} \sum_{\boldsymbol{K}}{}' |V(\boldsymbol{K})|^2 \eta(\boldsymbol{K}). \qquad \text{(A 24)}$$

In the zero T limit is $\dfrac{\partial f(k)}{\partial \varepsilon} = -\delta(\varepsilon - \varepsilon_0) = -\dfrac{m}{k_0}\{\delta(k - k_0) + \delta(k + k_0)\}$.

In that case we get from the condition $\sum_{\boldsymbol{K}} g(\boldsymbol{k}) = 0$ the following expression for $\eta(\boldsymbol{K})$

$$\eta(\boldsymbol{K}) = -\frac{1}{8Z_0} \ln \left| \frac{1 + Z_0}{1 - Z_0} \right|, \qquad \text{(A 25)}$$

which finally gives

$$u_2^F(\boldsymbol{K}, \boldsymbol{q}, \omega) = -\frac{1}{64 Z_0 Z_1} \left\{ \frac{2}{\sqrt{R_{10}^{\pm}}} I_{10}^{\pm} + \ln \left| \frac{1 + Z_0}{1 - Z_0} \right| \cdot \ln \left| \frac{1 + Z_{1\pm}}{1 - Z_{1\pm}} \right| \right\}. \qquad \text{(A 26)}$$

Collecting all contributions gives the following cumbersome expression (where the first two terms cancel when the sum over $\boldsymbol{K}$ is performed)

$$\begin{aligned}
u_2^M + u_2^E + u_2^F = {}&-\frac{1}{32 Z_0^2 Z_1 c_1} \ln \left| \frac{1 + Z_0}{1 - Z_0} \right| - \\
&-\frac{1}{32 Z_0 Z_1^2 c_1} \ln \left| \frac{1 + Z_{1\pm}}{1 - Z_{1\pm}} \right| + \frac{1}{64 Z_0^2 Z_1^2 c_1 \sqrt{R_{10}^{\pm}}} \\
&\frac{[c_1 Z_1 (Z_0 + c_1 Z_{1\pm}) + c_1 Z_0 (c_1 Z_0 + Z_{1\pm}) - 2 s_1^2 c_1 Z_0 Z_1 - R_{1\pm}(Z_0)]}{s_1^2} \cdot \\
&\cdot I_{10}^{\pm} + \frac{[c_1 Z_1 (Z_0 - c_3 Z_{3\pm}) + R_{3\pm}(-Z_0)]}{s_3^2} I_{30}^{\pm} \Biggr\} -
\end{aligned} \qquad \text{(A 27)}$$

$$
-\frac{1}{64Z_0^2 Z_1^2 c_1 \sqrt{R_{12}^\pm}} \left\{ \frac{[c_1 Z_1(Z_2 - c_1 Z_{1\pm}) + c_1 Z_0(c_1 Z_2 - Z_{1\pm}) - R_{1\pm}(-Z_2)]}{s_1^2} \cdot I_{12}^\pm \right.
$$

$$
\left. -\frac{[c_1 Z_1(Z_2 - c_3 Z_{3\pm}) - R_{3\pm}(-Z_2)]}{s_3^2} I_{32}^\pm \right\} + u_2'' \qquad \text{(A 27)}
$$

with $u_2''(\boldsymbol{K}, \boldsymbol{q}, \omega)$ the last part of u_2^F in Eq. (A 26), i.e. the contribution from the change in the Fermi energy caused by the periodic potential.

As mentioned earlier, we are in this case interested in the function $u_2(\boldsymbol{K}, \boldsymbol{q}, \omega)$ which is even in q. For this reason we define the function

$$
u_2 = u_2' + u_2''. \qquad \text{(A 28)}
$$

With u_2'' already of the desired form and with

$$
u_2'(\boldsymbol{K}, \boldsymbol{q}, \omega) = \tfrac{1}{2}\left[u_2^M(\pm c_1) + u_2^E(\pm c_1) + u_2^F(\pm c_1)\right] - u_2''. \qquad \text{(A 29)}
$$

We have here consequently dragged along the ω-dependency of the various functions u_i in order to explicitly show how unimportant (in this case) the non-adiabatic corrections are in the real part of $\varkappa$. The ω-dependency comes in via quantities like $Z_{1\pm} = Z_1 \pm \dfrac{\omega}{4\varepsilon_0 Z_1}$. In the phonon case $Z_{1\pm}$ is thus almost identical with Z_1 except when Z_1 is very small. In this limit $\dfrac{\omega}{4\varepsilon_0 Z_1}$ tends to a constant $\dfrac{c}{v_0}$ = (sound velocity/Fermi velocity at zero T for the free electrons) $\approx 10^{-3}$. In almost all practical calculations it is, therefore, quite safe to neglect the non-adiabatic corrections completely in the real part of $\varkappa$. And in the adiabatic limit the expression containing the integrals $I_{ij}^\pm$ in Eq. (A 27) becomes surprisingly simple. We get in that case

$$
u_2'(\boldsymbol{K}, \boldsymbol{q}, 0) = -\frac{1}{64Z_0^2 Z_1^2} \left\{ \frac{(Z_3^2 - 1)}{c_1 \sqrt{R_{10}}} [I_{10} - I_{12} - I_{30} + I_{32}] \right\}_{\pm c_1}
$$

$$
u_2''(\boldsymbol{K}, \boldsymbol{q}, 0) = -\frac{1}{32 Z_0 Z_1} \cdot \ln\left|\frac{1 + Z_0}{1 - Z_0}\right| \cdot \ln\left|\frac{1 + Z_1}{1 - Z_1}\right| \qquad \text{(A 30)}
$$

where we shall add the two expressions with $\pm c_1$. In the adiabatic limit we have

$$
R_{1\pm}(Z_0) = R_1(Z_0) = R_1(-Z_2) = (Z_3^2 - s_1^2);
$$

$$
R_{3\pm}(-Z_0) = R_3(-Z_0) = R_3(-Z_2) = (Z_1^2 - s_3^2) = \left(\frac{Z_1}{Z_3}\right)^2 (Z_3^2 - s_1^2). \qquad \text{(A 31)}
$$

The expression for $u_1(\boldsymbol{K}, \boldsymbol{q}, \omega)$ in Eq. (A 12) becomes also somewhat simpler in the adiabatic limit. We get from Eq:s (A 12) and (A 31)

$$u_1(\boldsymbol{K}, \boldsymbol{q}, 0) = \frac{1}{8 Z_0 Z_1 s_1^2} \left\{ 2(Z_0 + c_1 Z_1) \cdot \ln\left|\frac{1 + Z_1}{1 - Z_1}\right| + \right.$$

$$+ 2(c_1 Z_0 + Z_1) \cdot \ln\left|\frac{1 + Z_0}{1 - Z_0}\right| - 2 c_1 Z_3 \cdot \ln\left|\frac{1 + Z_3}{1 - Z_3}\right| + \qquad \left. \right\} \qquad \text{(A 32)}$$

$$+ \operatorname{sgn}(R_{10}) \sqrt{R_{10}} \left[I_{10} - I_{12} - I_{30} + I_{32} \right] \left. \right\}$$

where in Eq:s (A 30) and (A 32)

$$\sqrt{R_{10}} = |R_{10}|^{1/2}.$$

There is one point worth noticing in connection with the performance of the integrations above. The expressions found for u_1 and u_2 are both singular in case $Z_0 = 1$ and this value for Z_0 is consequently not allowed. We can physically understand this situation by remembering that $Z_0 = 1$ means that the free electron Fermi sphere is just touching a Bragg plane. The principal value calculation close to this plane then breaks down, since this calculation assumes an (essentially continuous) distribution of occupied states on both sides of the plane. In order safely to obtain such a distribution, we must require that Z_0 is sufficiently different from 1, which in physical terms means that we require for any $k = 2 k_0 Z_0 = \dfrac{K}{2}$

$$|\varepsilon(k) - \varepsilon_0| > |V(\boldsymbol{K})|.$$

This condition is no serious restriction in actual cases.

NORDITA, Copenhagen, Denmark
and
AB Atomenergi, Studsvik, Nyköping, Sweden

References

[1] B. N. Brockhouse, T. Arase, G. Caglioti, K. R. Rao and A. D. B. Woods, Phys. Rev. **128**, 1099 (1962).
   A. P. Miiller and B. N. Brockhouse, Phys. Rev. Letters, **20**, 798 (1968).

[2] R. Stedman, Measurements on Phonons in Aluminium and Lead with a Neutron Crystal Spectrometer, Acta Universitatis Upsaliensis 109, Uppsala (1968).

[3] F. S. Ham and B. Segall, Phys. Rev. **124**, 1786 (1961).

[4] W. A. Harrison, Pseudopotentials in the Theory of Metals (New York, 1966).

[5] C. Herring, Phys. Rev. **57**, 1169 (1940).

[6] J. C. Phillips and L. Kleinman, Phys. Rev. **116**, 287 (1959).

[7] M. H. Cohen and V. Heine, Phys. Rev. **122**, 1821 (1961).

[8] A. Sjölander and R. Johnson, in Inelastic Scattering of Neutrons, Vol. 1 (International Atomic Energy Agency, Vienna, 1965), p. 61.

[9] G. Baym, Annals of Physics, **14**, 1 (1961).

[10] H. B. Callen and T. A. Welton, Phys. Rev. **83**, 34 (1951).

[11] R. Kubo, J. Phys. Soc. Japan **12**, 570 (1957).

[12] T. Toya, J. Res. Inst. for Catalys., Sapporo, **6**, 161 (1958); **6**, 183 (1958); **7**, 60 (1959).

[13] L. J. Sham, Proc. Roy. Soc. **283 A**, 33 (1965).

[14] A. V. Gold, Phil. Trans. Roy. Soc. **A 251**, 85 (1958).

[15] B. Segall, Phys. Rev. **124**, 1797 (1961).

[16] D. Bohm and T. Staver, Phys. Rev. **84**, 836 (1952).

[17] J. Lindhard, Mat. Fys. Medd., Dan. Vid. Selsk., **28**, No 8 (1954).

[18] P. C. Martin and J. Schwinger, Phys. Rev. **115**, 1342, (1959).

[19] N. H. March, W. H. Young and S. Sampanthar, The Many-Body Problem in Quantum Mechanics, Cambridge (1967).

[20] J. Hubbard, Proc. Roy. Soc. **243 A**, 336 (1958).

[21] S. H. Vosko, R. Taylor and G. H. Keech, Can. J. Phys. **43**, 1187 (1965).

[22] N. W. Ashcroft, J. Phys. C, **1**, 232 (1968).

[23] N. M. Hugenholtz, in Lectures on Theoretical Physics, vol. II. Intersience Publishers Inc. New York (1960).

[24] W. Kohn, Phys. Rev. Letters **2**, 393 (1959).

[25] P. L. Taylor, Phys. Rev. **131**, 1995 (1963).

RUNE JOHNSON

AN EXAMINATION OF
SOME STRUCTURE IN THE PHONON
DISPERSION CURVES FOR
ALUMINIUM

Synopsis

Some observed structure in the phonon dispersion curves in the [111]-direction in Al is compared with theoretical calculations in a local potential approximation of the interaction between the ions and the conduction electrons. A previously derived expression for the lowest order non-diagonal part of the R.P.A. dielectric matrix is shown to account for most of the structure. The same approximation of the imaginary part of the dielectric matrix is also shown to satisfactorily reproduce the observed phonon damping in the longitudinal mode.

The accuracy of the neutron spectroscopy is by now so high that it is possible to obtain very detailed phonon dispersion curves. It has then been shown that in many metals there are rather complicated strucures in these curves that may contain much information about the microscopic situation in the crystal [1], [2], [3], [4]. A closer analysis of this structure seems for that reason to be well worth while and in this short note we report some results of a comparison between some recent accurate experimental results (at $80°K$) [4] and a theoretical model previously used in phonon calculations [5], [6]. As an example we will here concentrate on only one symmetry direction and this only for small q (the phonon momentum), where the analysis is relatively simple. A more complete account of the subject will be given elsewhere.

The phonon frequencies $\omega_i(\boldsymbol{q})$ are in the harmonic approximation given of the three lowest eigenvalues to the dynamical matrix

$$\omega_i^2(\boldsymbol{q}) \cdot \boldsymbol{e}_i = \omega_p^2 D(\boldsymbol{q}, \omega) \cdot \boldsymbol{e}_i \tag{1}$$

where $\boldsymbol{e}_i$ is the phonon polarisation vector and $\omega_p(\simeq 18.91 \cdot 10^{13} \ r/s$ in Al at $80°K$) is the plasma frequency for the ions. In a metal the matrix D is naturally split into an ionic part D_i and an electronic part D_e, where in the local potential approximation of the unscreened ion-electron interaction the part D_e has the following form in a simple lattice

$$D_e(\boldsymbol{q}, \omega) = -\frac{1}{4\pi} \left\{ \sum_{\boldsymbol{K}', \boldsymbol{K}''} \frac{v_e(\boldsymbol{K}' + \boldsymbol{q}) v_e(\boldsymbol{K}'' + \boldsymbol{q})(\boldsymbol{K}' + \boldsymbol{q})(\boldsymbol{K}'' + \boldsymbol{q})}{[v(\boldsymbol{K}' + \boldsymbol{q}) v(\boldsymbol{K}'' + \boldsymbol{q})]^{1/2}} \cdot \right.$$
$$\left. \cdot \langle \boldsymbol{K}' + \boldsymbol{q}| \frac{e^2 \varkappa(\omega)}{1 + e^2 \varkappa(\omega)} |\boldsymbol{K}'' + \boldsymbol{q}\rangle \text{-similar terms with } q = \omega = 0 \right\} \tag{2}$$

where $\boldsymbol{K}$ is a vector in the reciprocal lattice $v_e(\boldsymbol{k})$, $v(\boldsymbol{k})$ are the Fourier transforms of the ion-electron and electron-electron interactions (per unit charge square) and $1 + e^2 \varkappa(\omega)$ is the symmetrized dielectric matrix for the conduction electrons with the elements in Eq. (2) in a plane wave representation. It is the structure in the q-dependence of these elements that is reflected

1*

in the dispersion curves. For a uniform conduction electron system the dielectric matrix is diagonal in the plane wave representation and in the R.P.A.-approximation its elements are given by the Lindhard formula. The structure in $D_e (= D_{e0}$ in that case) is then the structure pointed out by Kohn [7]. Inclusion of effects on the electron system from the periodic lattice potential gives a more general dielectric matrix containing also non-diagonal elements in the plane wave representation. In the R.P.A. approximation of $\varkappa$ calculations indicate [6] that its diagonal elements ($\boldsymbol{K}' = \boldsymbol{K}''$) are in the actual case (nearly free electrons) quite accurately given by the Lindhard formula whereas the non-diagonal elements ($\boldsymbol{K}' \neq \boldsymbol{K}''$), although much smaller than the diagonal elements, are considerable. With $\varkappa = \varkappa_0 + \varkappa_1$, where $\varkappa_0$ is the Lindhard matrix and $\varkappa_1$ is the important, purely non-diagonal correction to it, we can expand D_e in Eq. (2) and get to first order in $\varkappa_1$

$$D_e = D_{e0} + D_{e1} \tag{3}$$

where we expect D_{e1} to be responsible for much of the structure in the dispersion curves [5], [6]. This opinion is supported by some of the experimental results in that the same observed peak has different signs in different branches in the same direction. For the elements of $\varkappa_1$ the following lowest order expression was derived in [5]

$$e^2 \langle \boldsymbol{K}' + \boldsymbol{q} | \varkappa_1 | \boldsymbol{K}'' + \boldsymbol{q} \rangle = [v(\boldsymbol{K}' + \boldsymbol{q}) v(\boldsymbol{K}'' + \boldsymbol{q})]^{1/2} \frac{k_0}{\pi^2 a_0} \frac{V(\boldsymbol{K})}{\varepsilon_0} u_1(\boldsymbol{K}, \boldsymbol{K}' + \boldsymbol{q}) \left. \right\} \tag{4}$$

$$(\boldsymbol{K}' \neq \boldsymbol{K}'')$$

where $\boldsymbol{K} = \boldsymbol{K}'' - \boldsymbol{K}'$, $\varepsilon_0 = \dfrac{k_0^2}{2m}$ ($\simeq 0.867$ Ry in Al) is the Fermi energy for the free electrons at $T = 0$ and $V(\boldsymbol{K})$ is the Fourier coefficient of the effective lattice potential for the electrons. $u_1(\boldsymbol{K}, \boldsymbol{q}')$ (where $\boldsymbol{q}' = \boldsymbol{K}' + \boldsymbol{q}$) is the first order function that was discussed in [5], [6] in the zero T and adiabatic ($\omega = 0$) limit.

$$
\begin{aligned}
u_1(\boldsymbol{K}, \boldsymbol{q}) = \frac{1}{8 Z_0 Z_1 s_1^2} &\Big\{ 2(Z_0 + c_1 Z_1) \ln \left| \frac{1 + Z_1}{1 - Z_1} \right| + \\
+ 2(c_1 Z_0 + Z_1) \ln &\left| \frac{1 + Z_0}{1 - Z_0} \right| - 2 c_1 Z_3 \ln \left| \frac{1 + Z_3}{1 - Z_3} \right| + \\
+ \operatorname{sgn}(R) \sqrt{R} \big[I(- Z_0, Z_1, c_1) &- I(Z_1, Z_2, c_1) - \\
- I(Z_0, Z_3, c_3) &+ I(Z_2, Z_3, c_3) \big] \Big\}
\end{aligned} \tag{5}
$$

where

$$Z_0 = \frac{|K|}{2k_0}; \quad Z_1 = \frac{|q|}{2k_0}; \quad Z_2 = Z_0 + 2c_1 Z_1$$

$$Z_3 = \frac{|K+q|}{2k_0}; \quad c_1 = \frac{K \cdot q}{|K||q|}; \quad s_1^2 = 1 - c_1^2$$

$$c_3 = \frac{Z_0 + c_1 Z_1}{Z_3}$$

and

$$I(a,b,c) = \begin{cases} \ln \left| \dfrac{c - ab - \sqrt{R(a,b,c)}}{c - ab + \sqrt{R(a,b,c)}} \right| & \text{if } R(a,b,c) > 0 \\[4mm] 2 \arctan \dfrac{c - ab}{\sqrt{R(a,b,c)}} & \text{if } R(a,b,c) < 0 \end{cases}$$

with

$$R(a,b,c) = a^2 + b^2 - 2abc - 1 + c^2; \quad \sqrt{R(a,b,c)} = |R(a,b,c)|^{1/2}$$

and

$$R = R(-Z_0, Z_1, c_1)$$

Since the origin of u_1 is the first order effect from the lattice potential on the one-electron wave-functions but with still free particle one-electron energies it has a rather simple structure. It is axially symmetric about K and has a mirror plane in $2K \cdot q' + K^2 = 0$. Its derivative $\nabla_q u_1$ is logarithmically singular on the "Fermi spheres" $|q'| = 2k_0$ and $|K + q'| = 2k_0$. More important in our case is, however, that for $|K| < 2k_0$, $\nabla_q u_1$ is also singular on the shell where $(K + q')^2 - 4k^2 \sin^2 \theta = 0$ (θ is the angle between K and q'), if $-K^2 \leqslant K \cdot q' \leqslant 0$. This singularity is stronger (of power $-1/2$) which is the reason why the effects from these terms are observable at all in spite of the small expansion parameter $\dfrac{V(K)}{\varepsilon_0}$ (a few per cent) in Eq. (4).

The geometry in the reciprocal space with an elementary cell laid in for an actual case is shown in Fig. 1, where $|K'| = \sqrt{3}$, $|K''| = 2$ and $|K| = |K'' - K'| = \sqrt{3}$. K is in Fig. 1 the axis of symmetry in u_1 and the traces in the half-plane of the "Fermi spheres" around $0'$ and $0''$ are indicated. The trace of the shell with $(K + q')^2 - 4k_0 \cdot \sin^2 \theta = 0$ where $\nabla_q u_1$ is singular is also shown. It is a circle with radius k_0 and its centre at M on the mirror plane. The three points of intersection with this shell for an actual q in the [111] (or equivalent) direction are denoted by 1, 3 and 4 (a point 2 appears when $|K'| = |K''| = \sqrt{3}$ and $K = 2$). Two Kohn points in D_{e0} for
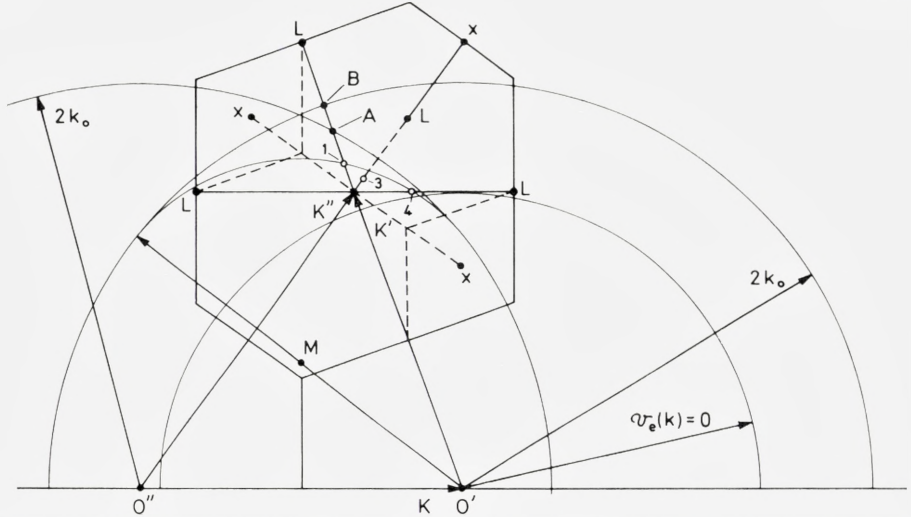
Fig. 1. The geometry in the reciprocal space showing a half-plane through the symmetry axis K in case $|K'| = \sqrt{3}$, $|K''| = 2$ and $|K| = \sqrt{3}$. Full lines are in the plane and dashed lines are out of the plane. The small open circles are some intersections with the shell $(K + q')^2 - 4k_0^2$ $\sin^2\theta = 0$ for a q in the [111] (or equivalent) direction. The dots A and B are the intersections with the "Fermi spheres" responsible for the Kohn anomalies in D_{e0} from these vectors (B from $K' = 1, 1, 1$ and A from $K' = 2, 0, 0$ or equivalent). For the explanation of the circle $v_e(k) = 0$, see the text.

this direction associated with the actual reciprocal lattice vectors are also denoted by A (one of three degenerate points) and B (non-degenerate). These four plus two points are the only critical points appearing in D_{e1} and D_{e0} for a q in the interval we are considering here. Some characteristics of the indicated critical points are collected in Table I.

In Fig. 2 we have collected results of a calculation of the contribution to the derivative $\dfrac{dD_e}{dq}$ from terms of interest. Curve a in 111L and the curve

TABLE 1.

| Point	q_x	Typical K'	Typical K''	$|K|$	Number of critical terms in D_e
1	0.119	1, 1, 1	2, 0, 0	$\sqrt{3}$	2×3
2	0.157	1, 1, 1	-1, 1, 1	2	2×3
3	0.164	1, 1, -1	2, 0, 0	$\sqrt{3}$	2×6
4	0.216	1, -1, -1	2, 0, 0	$\sqrt{3}$	2×3
A	0.231	2, 0, 0			3
B	0.302	1, 1, 1			1
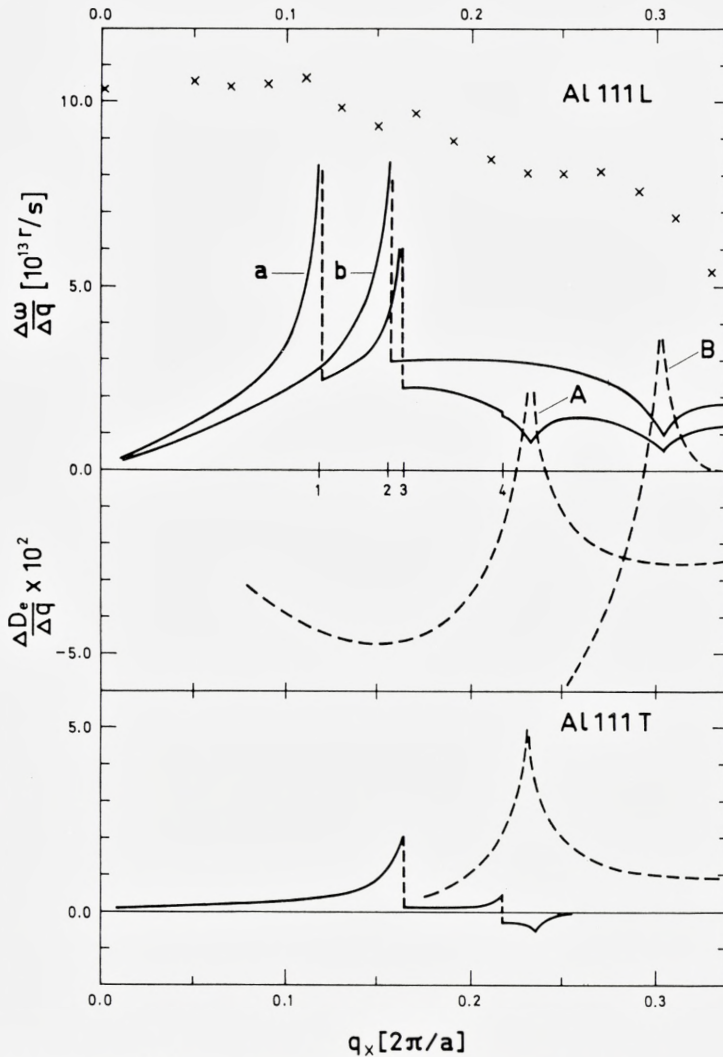
Fig. 2. Contributions to $\dfrac{\Delta D_e}{\Delta q}$ from the terms discussed in the text. Curve a in 111L and the curve in full line in 111T give the contributions from non-diagonal terms in $\varkappa$ with $|\mathbf{K}'| = \sqrt{3}$, $|\mathbf{K}''| = 2$ (or vice versa) and $|\mathbf{K}| = \sqrt{3}$ whereas curve b shows the contribution from terms with $|\mathbf{K}'| = |\mathbf{K}''| = \sqrt{3}$ and $|\mathbf{K}| = 2$. The contributions from terms of interest in D_{e0} are also shown (dashed). In the figure are also the experimental $\dfrac{\Delta \omega}{\Delta q}$ shown in the longitudinal mode (marked as x) with the value for $q = 0$ from G. N. KAMM and G. A. ALERS, J. Appl. Phys. **35**, 327 (1964).

in full line 111T show the effects from the terms in D_{e1} of the type shown in Fig. 1 (i.e. $|\boldsymbol{K}'| = \sqrt{3}$, $|\boldsymbol{K}''| = 2$ or vice versa and $|\boldsymbol{K}| = \sqrt{3}$) and curve b in 111L shows the effects from terms with $|\boldsymbol{K}'| = |\boldsymbol{K}''| = \sqrt{3}$ and $|\boldsymbol{K}| = 2$. The latter terms give no particular effects in the transverse mode in the actual q-interval. In these calculations we have used the adiabatic and zero T function u_1 given in Eq. (5) and values on $V(\sqrt{3})$ and $V(2)$ given by ASHCROFT [8] (i.e. $V(\sqrt{3}) = -0.0179$ and $V(2) = -0.0562$ Ry), which seem to be the most reliable values available today. We have in Fig. 2 also shown (dashed) the contributions to $\dfrac{dD_{e0}}{dq}$ from terms in D_{e0} of interest (again in the adiabatic and zero T limit). Curve A shows the contribution from terms with $|\boldsymbol{K}'| = 2$, while the curve in 111T contains all vectors $|\boldsymbol{K}'| \leqslant 2$. The curve B, finally, shows the effect in $\dfrac{dD_{e0}}{dq}$ from the single term $\boldsymbol{K}' = (1, 1, 1)$, which explains why it is so oblique.

It is seen in Fig. 2 that the effects from the non-diagonal terms are quite comparable in size to those from D_{e0} although the terms themselves are much smaller. The reason for that is the earlier mentioned stronger singularity in $\nabla_q u_1$. The peak 4 is, however, rather weak in the transverse mode and almost invisible in the longitudinal mode due to a small factor $\boldsymbol{e}_L \cdot (\boldsymbol{K}' + \boldsymbol{q})$ there (can be seen in Fig. 1). We will comment on this exception later on.

In Fig. 2 we also observe a small effect from the logarithmic singularity in $\nabla_q u_1$ on the "Fermi spheres" in Fig. 1. Although small in the shown cases this is a significant effect, since it is present in many terms with for instance a fixed $\boldsymbol{K}'$ and different $\boldsymbol{K}''$. It turns out that in the actual cases the effects to the Kohn anomalies from D_{e0} is drastically reduced by these small but coherent contributions from the non-diagonal terms (can be seen in Fig. 12 in Ref. [6]). In particular the cancellation of the peak A is almost complete in the longitudinal mode, which explains why no visible peak is found there in the experimental $\dfrac{\Delta\omega}{\Delta q}$ shown in Fig. 2. This circumstance excludes the possibility of a simple determination of $v_e^2(2ko)$ by a comparison to the experimental results around the Kohn points.

A more detailed analysis of the experimental results is shown in Fig. 3. We show there the experimental quantity (q in $2\pi/a$)

$$d_{\exp}(q) = \frac{\omega_{\exp}^2(q)}{\omega_p^2 \cdot q^2} \qquad (6)$$
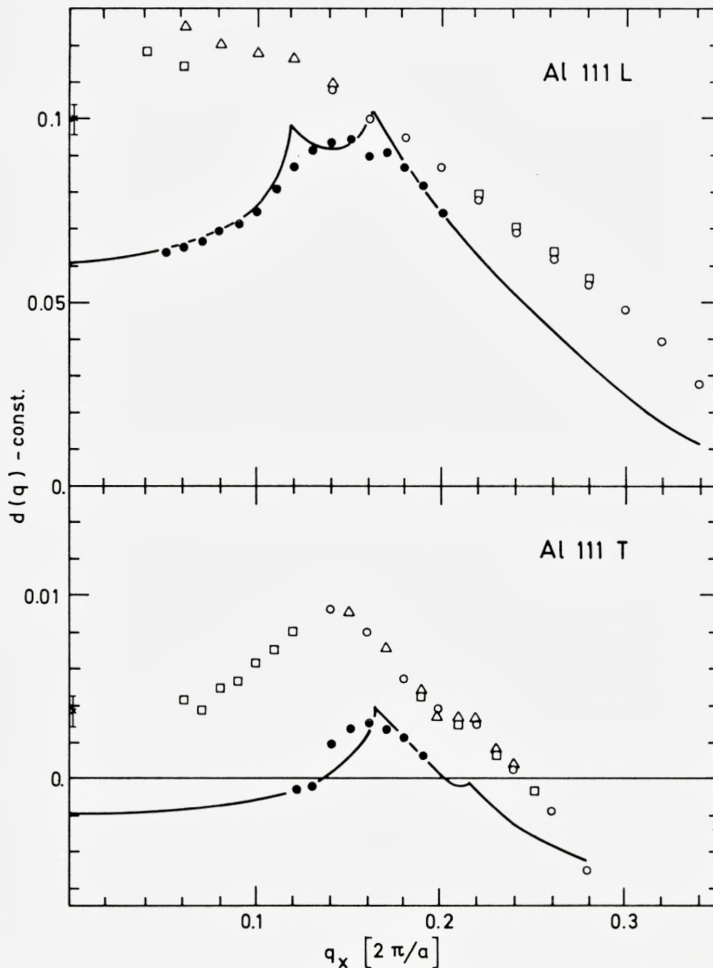
Fig. 3. $d_{exp} - c$ (width $c_L = 0.2$ and $c_T = 0.065$) and $d_{th} - c$ (with $c_L = 0.06$ and $c_T = 0.008$) versus q_x. The geometrical figures □ △ ○ indicate different experimental runs. The spread in the experimental values for different runs gives an idea of the accuracy. Experimental elastic values (with 1.5 per cent error bars) are from the reference in Fig. 2. The dots give theoretical values when the critical part in the analytic u_1 is replaced by a Monte Carlo sum.

which means that we determined (the real part of) the experimental eigenvalues of $D(q)$ by use of Eq. (1). These eigenvalues are in Eq. (6) divided by q^2 in order to get a more stable function in Fig. 3, where $d_{exp}(q)$ − const. (const. = 0.2 in the L-mode, = 0.065 in the T-mode) is plotted. The experimental curves are seen to contain interesting structures not present in D_{e0}. From D_i and D_{e0} in Eq. (1) we expect a d_{exp} which, as a function of q,

starts out rather constant or weakly increasing up to the broad humps just outside the Kohn points in D_{e0} after which the curve would rapidly decrease (can be qualitatively seen in Fig. 6 and Fig. 17 in [6]). However, as is seen in the figure, the experimental curves have quite different shapes. The rapid decrease starts much earlier and when compared to the theoretical curves also given in Fig. 3, the behaviour of the experimental and theoretical curves are seen to be very similar. Although the broad humps from the Kohn points in D_{e0} are visible in d_{exp} (at least in the longitudinal mode) they are much smaller than expected due to the earlier mentioned cancellations. In the theoretical curves shown in Fig. 3 we have calculated the (zero T and adiabatic) contribution to

$$d_{th}(q) = \frac{D_{e1}(q)}{q^2} \quad \left(q \text{ in } \frac{2\pi}{a}\right) \tag{7}$$

(and subtracted a const. $= 0.06$ in the L-mode, $= 0.008$ in the T-mode) where we in D_{e1} included only terms that give an appreciable structure in the actual q-interval (and keep the cubical symmetry of D_{e1}) i.e. the terms with $0 < |\boldsymbol{K'}|, |\boldsymbol{K''}|$ and $|\boldsymbol{K}| \leqslant 2$. A precise comparison between the theoretical and experimental curves in Fig. 3 is for that reason not possible, since we have to add to d_{th} a smooth function (out to the Kohn points in D_{e0}) in order to get the total d_{th}. This smooth function would, however, not alter the structure in the interesting q-interval.

Unfortunately, the experimental errors in the longitudinal mode increase so rapidly for decreasing q that the expected decrease in d_{exp} to the elastic limit [9] is not possible to establish, but in the transverse mode this effect is clearly seen. Anyway, the non-diagonal terms kept in d_{th} in the longitudinal mode here (only 72 out of about 10^4 almost equally important terms) give a surprisingly large contribution. (The situation is similar in the other symmetry directions.) So is for instance at $q = 0$ this contribution about 0.12 compared to the elastic value on $d_{exp} \simeq 0.30$ with interesting implications to the elastic properties.

We have in Fig. 3 also given results (marked by dots) of a calculation where close to the critical point in the analytic u_1 we have replaced the critical contribution to the integral defining u_1 from the occupied electron states around the actual zone-plane by a Monte Carlo sum and in this sum used the correct one-particle energies (up to first order in the periodic potential). Details of this calculation will be given elsewhere.

The effect in the transverse mode from the critical point 4 is of particular

interest. Several experimental runs have established this effect (results of
only two runs are shown in Fig. 3) and we have in fact used this peak when
determining the function $v_e(k)$ used in these calculations. It turned out
that the functions $v_e(k)$ used in earlier calculations [6] gave a (weak but)
negative peak there. This was a consequence of the fact that the earlier
functions had the first zero rather far out (at $k \simeq 1.7$). In order to remove
this defect we had to adjust the first zero in $v_e(k)$ to a somewhat smaller
value on k. This change made them almost identical with one of the functions
used by Vosko et al. [10]. Awaiting a direct experimental determination of
the k-value where $v_e(k)$ is equal zero we have—so far—determined $v_e(k)$
by fitting our function $F(k)$

$$F(k) = \frac{1}{4\pi} \frac{v_e^2(k)k^2}{v(k)} \frac{e^2 \varkappa_0(k)}{1 + e^2 \varkappa_0(k)} \tag{8}$$

at $k = 2.5$ to the value of the corresponding function $F_0(k)$ in [10]. We
think this can be of theoretical interest since their value at this point (they
manipulate their values for smaller k) has a first principle calculation as a
basis. The fit was made by simply adding a constant $\left(= -4\pi \cdot 0.03 \cdot \left(\frac{2\pi}{a}\right)^2 \right)$
to a function $v_e(k)$ used in [6] (potential 3 there). In Fig. 4 we have com-
pared the different functions $F(k)$ in the interval of interest $(1.6 < k < 2.25)$.
The zero in $v_e(k)$ is seen to be shifted from $k \simeq 1.7$ to $k \simeq 1.62$ by the ad-
justment. We have in Fig. 1 drawn the circle around $0'$ where the used
$v_e(k)$ is zero and it is seen there how close the critical point 4 is to this circle.
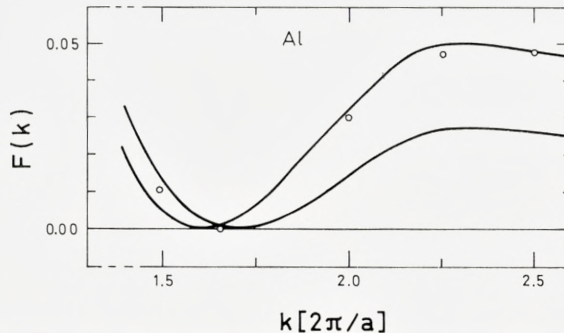
Fig. 4. The function $F(k)$ obtained with the potential $v_e(k)$ used in these calculations (upper
curve at $k = 2.5$) compared to the function with a potential used in an earlier calculation.
The small circles are estimated values from [10].
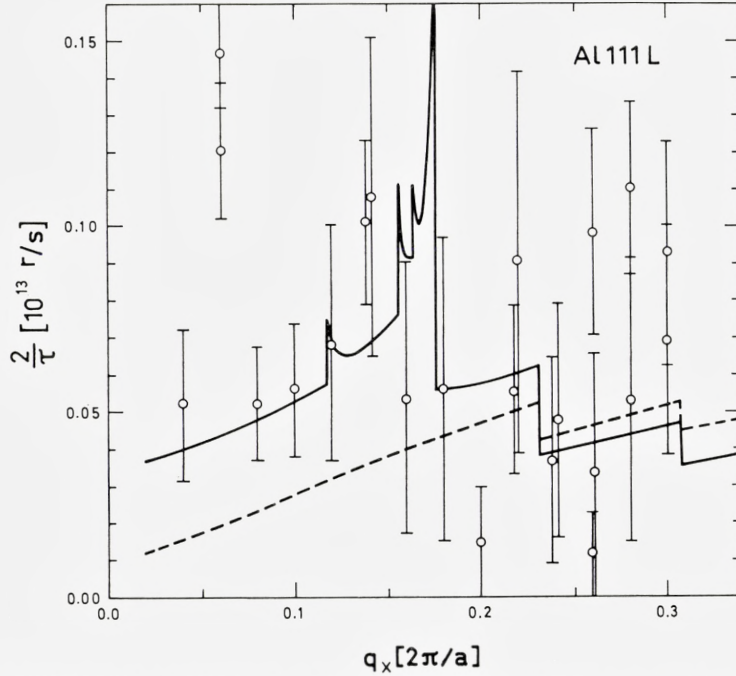
Fig. 5. Experimental and theoretical values for the phonon damping at small q in the 111L branch. In the theoretical curve only the electronic contribution is shown, but the anharmonic contribution is small for these q-values at this temperature (80°K).

Finally, the new measurements have shown that the earlier reported experimental life-times τ at 80°K [11] for the phones in Al are somewhat too short. The new experimental results for small q in the 111L-mode in Al are shown in Fig. 5. The curves show the theoretical results when the function $v_e(k)$ and $V(K)$:s used in the other calculations here are put in the expression given in [12]. In the imaginary part of $\varkappa$ the non-diagonal terms included are again only those with $|K'|,|K''|$ and $|K| \le 2$, but here we have also included the important terms with $|K'|$ or $|K''| = 0$ ($|K| \neq 0$). The terms considered give in this case almost the entire contribution (the corrections from the remaining terms in $Im\varkappa$ are only of order a few per cent). The free electron part (dashed) is here, naturally, almost identical with the results given by Björkman et al. [13]. Considering the large uncertainties in both the experimental and theoretical results the agreement is seen to be remarkable good in this q interval, where the anharmonic contributions to the damping are small [14]. In particular there is some structure in the ob-

served results at the lower q end which we think might have observable effects on the temperature dependency of the resistance These effects on the resistance from the imaginary part of $\varkappa$ would correspond to the effects on the specific heat from the structure in the real part of $\varkappa$ [15].

I want to thank Dr. R. STEDMAN and Professor J. WEYMOUTH for making their experimental results available to me prior to their publication. My special thanks are due to Dr. R. STEDMAN for his patient answers to many questions about the experimental technique and difficulties.

References

[1] A. P. MIILLER and B. N. BROCKHOUSE, Phys. Rev. Letters 20, 798 (1968).

[2] R. STEDMAN and G. NILSSON, Phys. Rev. Letters, 15, 634 (1965).

[3] R. STEDMAN, L. ALMQVIST, G. NILSSON and G. RAUNIO, Phys. Rev. 162, 545 (1967).

[4] R. STEDMAN and J. WEYMOUTH (to be published).

[5] R. JOHNSON, Mat. Fys. Medd., Dan. Vid. Selsk. 37, no. 9 (1970).

[6] R. JOHNSON and A. WESTIN, On phonons in simple metals II, AB Atomenergi, Stockholm, Sweden, Report AE-365 (1969).

[7] W. KOHN, Phys. Rev. Letters 2, 393 (1959).

[8] N. W. ASHCROFT, Phil. Mag. 8, 2055 (1963).

[9] W. GOTZE, Phys. Rev. 156, 951 (1967).

[10] S. H. VOSKO, R. TAYLOR and G. H. KEECH, Can. J. Phys. 43, 1187 (1965).

[11] R. STEDMAN and G. NILSSON, Phys. Rev. 145, 492 (1965).

[12] R. JOHNSON, Electronic contributions to the phonon damping in metals, AB Atomenergi, Stockholm, Sweden, Report AE-328 (1968).

[13] G. BJÖRKMAN, B. I. P. LUNDQVIST and A. SJÖLANDER, Phys. Rev. 159, 551 (1967).

[14] T. HÖGBERG and R. SANDSTRÖM, Physica Status Solidi, 33, 169 (1969).

[15] R. STEDMAN, L. ALMQVIST and G. NILSSON, Phys. Rev. 162, 549 (1967).

I. BREVIK

ELECTROMAGNETIC ENERGY-MOMENTUM TENSOR WITHIN MATERIAL MEDIA

1. MINKOWSKI'S TENSOR

CONTENTS

Synopsis

The electromagnetic energy-momentum tensor inside a material medium is studied, mainly from a phenomenological point of view. The influence from the medium is taken into account by introducing a dielectric constant and a magnetic permeability. In this paper only Minkowski's tensor is studied, since a comparison between the theory and available experiments indicates that this tensor is well suited to describe usual optical phenomena. Other tensor forms will be dealt with in a forthcoming paper. Here deductive formal procedures are employed; in particular, two sets of conditions are given under which Minkowski's tensor is determined uniquely. Further, attention is given to various characteristic effects, such as negative field energy, which are encountered with the use of Minkowski's tensor.

I. Introduction

1. Presentation of the Problem

The electromagnetic energy-momentum tensor in a material medium represents a problem that has given rise to a very long-lasting discussion. Maxwell's field equations may be written in covariant form as

$$\partial_\lambda F_{\mu\nu} + \partial_\mu F_{\nu\lambda} + \partial_\nu F_{\lambda\mu} = 0, \quad \partial_\nu H_{\mu\nu} = \frac{1}{c} j_\mu, \tag{1.1}$$

where the antisymmetric field tensors $F_{\mu\nu}$ and $H_{\mu\nu}$ are defined by (F_{23}, F_{31}, F_{12}) = $\boldsymbol{B}$, (F_{41}, F_{42}, F_{43}) = $i\boldsymbol{E}$, (H_{23}, H_{31}, H_{12}) = $\boldsymbol{H}$ and (H_{41}, H_{42}, H_{43}) = $i\boldsymbol{D}$. The four-vector $j_\mu = (\boldsymbol{j}, ic\varrho)$ is the *external* current density, it does not include polarization or magnetization currents.

By means of the field equations the energy-momentum tensor can easily be constructed if one knows the four-force density in some inertial system. This is the case for an electromagnetic field in vacuum interacting with incoherent matter, the four-current density of which be given by j_μ. In that case the four-force density is given by $f_\mu = (1/c)F_{\mu\nu}j_\nu$ in any reference frame K, since in K^0 – the frame in which the matter under consideration is at rest – the force takes the form $f_\mu^0 = (\varrho^0 \boldsymbol{E}^0, 0)$. Thus $f_\mu = -\partial_\nu S_{\mu\nu}$, where the energy-momentum tensor $S_{\mu\nu}$ is determined by means of (1.1) as

$$S_{\mu\nu} = F_{\mu\alpha} F_{\nu\alpha} - \tfrac{1}{4} \delta_{\mu\nu} F_{\alpha\beta} F_{\alpha\beta} \tag{1.2}$$

since, in this case, $F_{\mu\nu} = H_{\mu\nu}$.

In ponderable bodies, however, it is well known that the force expression is not so easily constructed. If we use (1.1) to form the expression

$$\frac{1}{c} F_{\mu\nu} j_\nu + \tfrac{1}{4}(F_{\alpha\nu}\partial_\mu H_{\alpha\nu} - H_{\alpha\nu}\partial_\mu F_{\alpha\nu}) = -\partial_\nu S_{\mu\nu}^M \tag{1.3}$$

where

$$S_{\mu\nu}^M = F_{\mu\alpha} H_{\nu\alpha} - \tfrac{1}{4} \delta_{\mu\nu} F_{\alpha\beta} H_{\alpha\beta}, \tag{1.4}$$

1*

we see that $S_{\mu\nu}^M$ may be interpreted as an energy-momentum tensor. This is the proposal put forward by H. Minkowski. According to his view, the left hand side of (1.3) is interpreted as the force density within matter.

The expression (1.4) leads to the following interpretation

$$- S_{ik}^M = E_i D_k + H_i B_k - \tfrac{1}{2}\delta_{ik}(\boldsymbol{E}\cdot\boldsymbol{D}+\boldsymbol{H}\cdot\boldsymbol{B}) \tag{1.5a}$$

$$S_{4k}^M = \frac{i}{c}S_k^M = i(\boldsymbol{E}\times\boldsymbol{H})_k, \quad S_{k4}^M = icg_k^M = i(\boldsymbol{D}\times\boldsymbol{B})_k \tag{1.5b}$$

$$- S_{44}^M = W^M = \tfrac{1}{2}(\boldsymbol{E}\cdot\boldsymbol{D}+\boldsymbol{H}\cdot\boldsymbol{B}) \quad (i,k = 1,2,3), \tag{1.5c}$$

where $\boldsymbol{S}^M, \boldsymbol{g}^M, W^M$ denote the energy flux, momentum density and energy density in any frame K.

The connection between the components of the field tensors $F_{\mu\nu}^0$ and $H_{\mu\nu}^0$ in the rest frame K^0 can, in the absence of dispersion, be written as $D_i^0 = \varepsilon_{ik}E_k^0$, $B_i^0 = \mu_{ik}H_k^0$, where ε_{ik} and μ_{ik} are the tensors of dielectric and magnetic permeability. (Dispersion effects are always present, but they are not of essential importance for the present problem and shall therefore simply be omitted.) Now the most important application of the phenomeno-logical theory is in connection with optical phenomena, where ε_{ik} and μ_{ik} are real quantities. In the following we shall always assume ε_{ik} and μ_{ik} to be real. Further, we shall consider only *homogeneous* bodies, such that the gradients of ε_{ik} or μ_{ik} will differ from zero only in the boundary layers. It can readily be verified that in the interior domain of a homogeneous body the second term to the left in (1.3) vanishes, such that

$$\partial_\nu S_{\mu\nu}^M = 0 \tag{1.5d}$$

for optical phenomena ($j_\mu = 0$).

Then define the angular momentum by the quantities

$$M_{\mu\nu} = \int (x_\mu g_\nu - x_\nu g_\mu)dV, \tag{1.6}$$

where $g_\mu = -(i/c)S_{\mu 4}$. When the electromagnetic system is limited in space, it follows from (1.6) that

$$d/dt M_{\mu\nu} = \int (x_\nu f_\mu - x_\mu f_\nu + S_{\nu\mu} - S_{\mu\nu})dV, \tag{1.7}$$

where $f_\mu = -\partial_\nu S_{\mu\nu}$. Now consider a finite radiation field enclosed within a homogeneous body at rest, and insert Minkowski's tensor $S_{\mu\nu}^M$ into (1.7).

If the body is optically anisotropic, we obtain even in the frame K^0 an expression for $d/dt^0 M_{ik}^{M0}$ which is different from zero. If the body is optically isotropic, we find $d/dt^0 M_{ik}^{M0} = 0$ since S_{ik}^{M0} is symmetrical when $\boldsymbol{D}^0 = \varepsilon \boldsymbol{E}^0$, $\boldsymbol{B}^0 = \mu \boldsymbol{H}^0$. In another system of reference, however, we have in general $S_{ik}^M \neq S_{ki}^M$ also for isotropic bodies, and thus $d/dt M_{ik}^M \neq 0$. As a conclusion, we find both for anisotropic and isotropic media that an asymmetric mechanical energy-momentum tensor is necessary to achieve balance of the total (field and mechanical) angular momentum. This circumstance has sometimes been felt to be a real difficulty for Minkowski's theory.

Besides, Minkowski's tensor seems to get into conflict with Planck's principle of inertia of energy, as expressed by the relation $\boldsymbol{S} = c^2 \boldsymbol{g}$.

To overcome the difficulties just mentioned, various other proposals of an electromagnetic energy-momentum tensor have been put forward, the best known of which is due to M. ABRAHAM.

For a general introduction to the subject—and for references to some original papers—we refer to Møller's book.[1]

2. Summary and Survey of the Subsequent Work

To facilitate the reading of some of the detailed expositions in the following, we shall in this section give a survey of what follows, and mention some results.

In this paper, which will be followed by a second one on the subject, we shall limit ourselves to a study of Minkowski's tensor. From the phenomenological point of view we are adopting, this tensor is found to be adequate for the description of the usual electromagnetic phenomena, as for instance the situation where an optical wave travels through transparent matter at rest. Comparison with experiments plays an important role in the investigation. But we stress already now that the experimental results do not exclude other possible forms of the electromagnetic energy-momentum tensor; the essential point is rather that Minkowski's form adapts itself to the experiments in a very *simple* way.

The long-lasting discussion on the subject has given rise to an extensive literature, and it appears that in previous phenomenological treatments mainly two lines of attack have been followed. In the first place one uses a deductive method and constructs the energy-momentum tensor on the basis of commonly accepted quantities, for instance the energy in electrostatic and magnetostatic fields, or the (macroscopic) field Lagrangian. In the second place one examines the consequences of using the various tensor

forms in appropriate physical situations, and compares with results that can be expected on physical grounds. In these two papers we shall deal with topics connected with both methods of approach.

Let us now review the individual sections. Chapter II is devoted to deductive, and mainly formal, procedures. We start in section 3 by considering a variational method which is applicable to the case of static fields, and which in general leads to the force density and stress tensor when the energy density is known. For the latter density in the electrostatic case, we use the common expression $\frac{1}{2} \boldsymbol{E} \cdot \boldsymbol{D}$. Minkowski's tensor is different from other tensor forms proposed even in the case of an electrostatic field in an anisotropic medium, and some contradictory results have appeared in the literature by the use of this method. We show how Minkowski's tensor is one of the legitimate alternatives that result from the formalism, and illustrate the considerations by an example that involves detectable torques on an anisotropic dielectric sphere. An important point is that we shall have the opportunity to make an explicit statement of a crucial assumption which must be imposed if the formalism shall yield Minkowski's tensor. This is the assumption that each volume element experiences a torque density equal to $\boldsymbol{D} \times \boldsymbol{E}$, even if the force on the element is zero.

In section 4 we use this assumption (the "dipole model") as one of the initial conditions in a formal uniqueness proof of the energy-momentum tensor. The dipole model corresponds to a certain requirement on the non-diagonal components of the energy-momentum tensor, and to a vanishing ordinary force density in charge-free homogeneous regions. We require that all components of the four-force density shall vanish, and that the tensor shall be a bilinear form in the field quantities. With these initial conditions, we are led to Minkowski's tensor as the unique result.

Section 5 is devoted to a formal procedure along similar lines as in section 4, but with different initial conditions. In this case relativistic considerations are also involved. We require the energy-momentum tensor to be a bilinear form which is divergence-free and an explicit function of the field quantities $\boldsymbol{E}, \boldsymbol{D}, \boldsymbol{H}, \boldsymbol{B}$ in any inertial frame (but not an explicit function of the four-velocity of the medium). Both anisotropic and isotropic homogeneous media are included in the description. We find that the above-mentioned conditions, in addition to the fact that ε_{ik} and μ_{ik} are symmetric quantities, determine Minkowski's tensor uniquely. In the procedure we use ideas from the corresponding proof for the vacuum-field case, presented by V. Fock.

In order to understand the underlying physical mechanism of wave propagation, it seems desirable as well to examine simple physical situations. In chapter III we undertake this task and construct the electromagnetic energy-momentum tensor in K^0 from semi-phenomenological arguments in the following way: The stress tensor and energy density are taken to be the sum of the two parts corresponding to the electrostatic and magnetostatic cases. Further, we use the fact that the fourth component of the four-force vanishes when an electromagnetic wave travels through a non-absorptive medium. From the continuity equation for energy we can then find the Poynting vector $S = c(E \times H)$ and hence the electromagnetic momentum density $g = (1/c)(E \times H)$ from Planck's principle of inertia of energy, which is assumed to be valid also for the electromagnetic field in matter. The stress and momentum components determined so far lead to a force density whose effect *may* be to excite a small mechanical momentum of the constituent particles (dipoles). By comparing with a radiation pressure experiment due to R. V. Jones and J. C. S. Richards we find that this suggestion is in fact supported. Corresponding to the mechanical momentum there is a small transport of mechanical energy which, however, together with the rest energy itself, is included in the mechanical part of the total energy-momentum tensor. The conclusion is that Minkowski's tensor gives an adequate description of the propagating wave.

In section 7, some attention is given to the microscopical method of approach. Some difficulties for the acceptance of Minkowski's tensor, which have arisen from microscopical considerations, are discussed. It is stressed that the ambiguity inherent in the formalism is not removed upon transition to the microscopical theory.

In chapter IV we consider methods and specific effects connected with relativity, and limit ourselves to the case of isotropic media. We start in section 8 with a Lagrangian method which involves the use of Noether's theorem, such that the canonical energy-momentum tensor is obtained by a symmetry transformation. Minkowski's tensor is closely connected with the canonical tensor, although the canonical procedure does not rule out other tensor forms. In section 9 we analyse the well-known criterion due to von Laue and Møller on the transformation property of the velocity of the energy in a light wave. By comparing with the Fizeau experiment involving the velocity of light in moving media it is argued that the transformation criterion ought to be fulfilled for an electromagnetic energy-momentum tensor which shall describe the whole light wave. It is a satisfactory feature of Minkowski's tensor that it actually fulfils this criterion. A related experiment

reported recently, involving the propagation of light through media in an accelerated reference frame, is also considered.

Section 10 deals with a property which has caused difficulties for the acceptance of Minkowski's tensor, namely the appearance of negative electromagnetic energy in certain cases. We find this to be a direct consequence of the state of covariance of the phenomenological theory: One chooses covariant quantities to be compatible with a scheme one has established on physical grounds in some inertial system. Since certain mechanical quantities are counted together with the field quantities, one obtains—when covariance is imposed—a total four-momentum which is space-like. Therefore, by means of (proper) Lorentz transformations, one can find inertial systems where the total field energy is negative. Closely related to these features is the behaviour of the Čerenkov radiation in the inertial system where the radiating particle is at rest: The energy flow vanishes, while the momentum flow is different from zero and corresponds to a force on the particle.

In section 11 we employ an infinitesimal Lorentz transformation as a symmetry transformation in Noether's theorem and show how the formalism readily adjusts itself to angular momentum quantities which are equivalent to those obtained from Minkowski's tensor. The division of the total field angular momentum into coordinate dependent and coordinate independent parts is discussed.

In the last section we introduce the centre of mass of the field in a relativistic manner. It is found that the various centres obtained in different inertial frames do not in general coincide when considered simultaneously in one frame. By considering in the rest frame K^0 the centres of mass obtained by varying the direction and magnitude of the medium velocity v, we find that they are located on a circular disk lying perpendicular to the inner angular momentum vector in K^0 with centre at the centre of mass in K^0.

II. A Variational Method. Uniqueness from two Sets of Conditions

3. A Variational Method in the Case of Static Fields

In this chapter we shall follow a rather formal kind of approach. Our main task is to give two different sets of conditions under which Minkowski's tensor is uniquely determined. In the first place, however, we shall in the present section deal with a derivation of the stress tensor and force density when the electrostatic or magnetostatic field energy in K^0 is known. The

calculation will be carried through in the electrostatic case. The method is of interest in itself in so far as Minkowski's tensor is different from the other tensor forms that have been proposed even in the electrostatic case for anisotropic media, and the method has been treated to some extent in the literature[2,3,4,5], but the results do not always agree and we shall go into some details. We shall show how Minkowski's tensor is one of the admissible tensors that result from the formalism, and in particular we shall show the underlying assumptions explicitly. This latter result is of interest in relation to the statement of conditions in the next section.

Then consider an electrostatic field in a medium characterized by material constants η_{ik}, where $E_i = \eta_{ik}D_k$.[1] We assume η_{ik} to have remained unchanged at each point during the (infinitely slow) formation of the field. Then we can integrate the work exerted in building up the field, and obtain in the usual way the free energy

$$\mathscr{F} = \tfrac{1}{2} \int \boldsymbol{E} \cdot \boldsymbol{D} dV. \tag{3.1}$$

Now let each volume element dV undergo an arbitrary virtual displacement $\boldsymbol{s}$ so slowly that the process can be taken as reversible. Then we can equate the change of free energy to the mechanical work during the displacement. This "energy method" has been somewhat criticised by some authors (see Smith-White's paper[6] with further references), but there should be little doubt that the method is applicable under the above conditions.

From (3.1) we have

$$\delta\mathscr{F} = \int \boldsymbol{E} \cdot \delta\boldsymbol{D} dV + \tfrac{1}{2} \int D_i D_k \delta\eta_{ik} dV. \tag{3.2}$$

The variations of the integrand are taken at fixed points in space. Letting the electric charge density be denoted by ϱ, we obtain by a partial integration

$$\int \boldsymbol{E} \cdot \delta\boldsymbol{D} dV = -\int \triangledown \Phi \cdot \delta\boldsymbol{D} dV = -\int_{\text{cond.}} \Phi \delta\boldsymbol{D} \cdot \boldsymbol{n} dS + \int \Phi \delta\varrho dV, \tag{3.3}$$

where the surface integration is taken over the fixed, charged conductors that are supposed to produce the field. On each conductor Φ is a constant, and as the total charge on a conductor does not change under the displacement, the surface term must vanish. Then

---

[1] In this section we omit the superscript zero on quantities taken in K°.

$$\frac{d\mathscr{F}}{dt} = \int \left(\Phi \frac{\partial \varrho}{\partial t} + \tfrac{1}{2} D_i D_k \frac{\partial \eta_{ik}}{\partial t} \right) dV. \tag{3.4}$$

Applying the continuity equation $\triangledown \cdot (\varrho \boldsymbol{u}) + \partial \varrho / \partial t = 0$ $(\boldsymbol{u} = d\boldsymbol{s}/dt)$, we have

$$
\left.
\begin{aligned}
\frac{d\mathscr{F}}{dt} &= - \int_{\text{cond.}} \Phi \varrho \boldsymbol{u} \cdot \boldsymbol{n} dS + \int \left(\triangledown \Phi \cdot \varrho \boldsymbol{u} + \tfrac{1}{2} D_i D_k \frac{\partial \eta_{ik}}{\partial t} \right) dV = \\
&= \int \left(- \varrho \boldsymbol{E} \cdot \boldsymbol{u} + \tfrac{1}{2} D_i D_k \frac{\partial \eta_{ik}}{\partial t} \right) dV.
\end{aligned}
\right\} \tag{3.5}
$$

It remains to put $\partial \eta_{ik}/\partial t$ in a form which involves the velocity $\boldsymbol{u}$ explicitly. We therefore write

$$\frac{\partial \eta_{ik}}{\partial t} = \frac{d\eta_{ik}}{dt} - \triangledown \eta_{ik} \cdot \boldsymbol{u}, \tag{3.6}$$

where the last term corresponds to the fact that, at a given point $\boldsymbol{r}$, there appears matter which was originally at the point $\boldsymbol{r} - \boldsymbol{s}$. The first term to the right in (3.6) corresponds to the change during the displacement of the element, and arises from two effects. Firstly, η_{ik} may change on account of the components of strain in the body. For small deformations one can make a linear expansion

$$d\eta_{ik}/dt = \gamma_{lm}^{ik} ds_{lm}/dt, \tag{3.7}$$

where $s_{lm} = \tfrac{1}{2} (\partial_m s_l + \partial_l s_m)$ is the symmetrical strain tensor. By symmetry arguments the number of the coefficients γ_{lm}^{ik} can be reduced so that only two of them remain in the case where the body originally is isotropic but under small displacements changes its dielectric properties and becomes anisotropic[7]. If the body is a fluid, so that all shearing strains $s_{lm} (l \neq m)$ vanish, then only one of the γ_{lm}^{ik} remains and corresponds to the electrostriction term $\tfrac{1}{2} \triangledown (E^2 \varrho_m \partial \varepsilon / \partial \varrho_m)$ (where ϱ_m is the mass density) in the final expression for the force density. However, we shall neglect these strain effects; they have no interest of principle for our problem. One sees also by an integration over the total system that the contribution to the total force from the electrostriction term vanishes.

Secondly, there will be a contribution to $d\eta_{ik}/dt$ because the crystallographic axes corresponding to a volume element dV rotate by an angle $\varphi = (\varphi_1, \varphi_2, \varphi_3)$ relative to the fixed coordinate system. This effect can be evaluated by transforming η_{ik} as a tensor under the infinitesimal rotation $-\varphi$ of the coordinate axes. Thus we find

$$\tfrac{1}{2}\int D_i D_k \frac{d\eta_{ik}}{dt} dV = -\int (\boldsymbol{D} \times \boldsymbol{E}) \frac{d\varphi}{dt} dV. \tag{3.8}$$

So far we have not specified the variations; the angle φ may vary from element to element. But in order to collect the contributions to the free energy variation, we shall need the relation between φ and $\boldsymbol{s}$, and shall from now on assume the variation to consist of a pure rotation of each element about the origin. Hence $\boldsymbol{s} = \varphi \times \boldsymbol{r}$ and $\varphi = \tfrac{1}{2} \triangledown \times \boldsymbol{s}$. When the medium is thus rotated as a rigid body, we see that possible strain effects are not accounted for; however, as mentioned above, these effects are ignored. To make this kind of variation possible, we assume that the fixed, charged conductors are placed in the vacuum outside the dielectric.

Eq. (3.8) now takes the form

$$\left. \begin{aligned} \tfrac{1}{2}\int D_i D_k \frac{d\eta_{ik}}{dt} dV &= -\tfrac{1}{2}\int (\boldsymbol{D} \times \boldsymbol{E}) \cdot (\triangledown \times \boldsymbol{u}) dV = \\ &= -\tfrac{1}{2} \int_{\text{cond.}} (E_i \boldsymbol{D} \cdot \boldsymbol{n} - D_i \boldsymbol{E} \cdot \boldsymbol{n}) u_i dS + \tfrac{1}{2} \int \partial_k (ED_k - E_k \boldsymbol{D}) \cdot \boldsymbol{u} dV, \end{aligned} \right\} \tag{3.9}$$

where the surface integral vanishes.

From (3.5), (3.6) and (3.9) we get

$$\frac{d\mathscr{F}}{dt} = \int [-\varrho \boldsymbol{E} - \tfrac{1}{2} D_i D_k \triangledown \eta_{ik} + \tfrac{1}{2} \partial_k (ED_k - E_k \boldsymbol{D})] \cdot \boldsymbol{u} dV. \tag{3.10}$$

Equating $-d\mathscr{F}/dt$ to the mechanical work $\int \boldsymbol{f} \cdot \boldsymbol{u} dV$ exerted by the volume forces $\boldsymbol{f}$, we obtain

$$\boldsymbol{f} = \varrho \boldsymbol{E} + \tfrac{1}{2} D_i D_k \triangledown \eta_{ik} - \tfrac{1}{2} \partial_k (ED_k - E_k \boldsymbol{D}). \tag{3.11}$$

By Maxwell's equations this means $f_i = -\partial_k S_{ik}^A$, where the tensor S_{ik}^A is defined by[1]

$$S_{ik}^A = -\tfrac{1}{2}(E_i D_k + E_k D_i) + \tfrac{1}{2} \delta_{ik} \boldsymbol{E} \cdot \boldsymbol{D}. \tag{3.12}$$

The interpretation of (3.11) as a force density and (3.12) as a stress tensor is the result found by LORENTZ[2], POCKELS[3] and LANDAU and LIFSHITZ[4]. But there exists an effect not yet considered. There may be a torque present in a volume element also when the force on it is zero, and this torque will perform work during the displacement. Denoting the corre-

---

[1] Actually, S_{ik}^A is equal to Abraham's tensor in the electrostatic case.

sponding torque density by τ, the additional amount to the total work done is $\int \tau \cdot \varphi dV$. This is the case if the difference $\boldsymbol{P} = \boldsymbol{D} - \boldsymbol{E}$ is due to a distribution of electric dipoles in the medium with the density $\boldsymbol{P}$; we may then write $\tau = \boldsymbol{P} \times \boldsymbol{E} = \boldsymbol{D} \times \boldsymbol{E}$, and

$$\int \tau \cdot \frac{d\varphi}{dt} dV = \frac{1}{2} \int (\boldsymbol{D} \times \boldsymbol{E}) \cdot (\nabla \times \boldsymbol{u}) dV = \frac{1}{2} \int \partial_k (E_k \boldsymbol{D} - \boldsymbol{E} D_k) \cdot \boldsymbol{u} dV. \qquad (3.13)$$

Equating $- d\mathscr{F}/dt$ to the total mechanical work done per unit time, we obtain from (3.10) and (3.13)

$$\left. \begin{aligned} \int \left[\varrho \boldsymbol{E} + \tfrac{1}{2} D_i D_k \nabla \eta_{ik} + \tfrac{1}{2} \partial_k (E_k \boldsymbol{D} - \boldsymbol{E} D_k) \right] \cdot \boldsymbol{u} dV = \\ = \int \left[\boldsymbol{f} + \tfrac{1}{2} \partial_k (E_k \boldsymbol{D} - \boldsymbol{E} D_k) \right] \cdot \boldsymbol{u} dV. \end{aligned} \right\} \quad (3.14)$$

Hence

$$\boldsymbol{f} = \boldsymbol{f}^M = \varrho \boldsymbol{E} + \tfrac{1}{2} D_i D_k \nabla \eta_{ik}, \; f_i^M = - \partial_k S_{ik}^M, \qquad (3.15)$$

i. e. Minkowski's force. Of course the deduction leading to (3.15) is not a proof of the correctness of $\boldsymbol{f}^M$. Its validity is based upon the assumption about the distribution of electric dipoles that leads to (3.13), although it should be noted that this assumption seems to be most natural. As a check we can put $\varrho = \nabla \eta_{ik} = 0$ in (3.15), then it follows that $\boldsymbol{f} = 0$, as expected.

Minkowski's force density was obtained by E. DURAND in his book[5].

An example

Let us elucidate the preceding considerations by the following example, considered also by MARX and GYÖRGYI[8]. Let a dielectric sphere be located in a homogeneous electrostatic field, for instance between two condenser plates. Assume that the external field is $\boldsymbol{E}^0 = (E_1^0, E_2^0, 0)$, and choose the principal axes of the sphere to coincide with the coordinate axes so that $\varepsilon_{ik} = (\varepsilon_1, \varepsilon_2, \varepsilon_3)$. The field in the vacuum outside the sphere is

$$\boldsymbol{E}^{\mathrm{vac}} = \boldsymbol{E}^0 - \frac{1}{4\pi} \nabla \left(\frac{\boldsymbol{p} \cdot \boldsymbol{n}}{r^2} \right), \qquad (3.16)$$

the induced field being a dipole field. One has $\boldsymbol{p} = 3V[(\varepsilon_1 - 1) E_1^0/(\varepsilon_1 + 2), (\varepsilon_2 - 1) E_2^0/(\varepsilon_2 + 2), 0]$, where V is the volume of the sphere. Within the sphere $\boldsymbol{E} = [3E_1^0/(\varepsilon_1 + 2), 3E_2^0/(\varepsilon_2 + 2), 0]$.

The components of the body torque $\boldsymbol{N}$ are determined by the angular momentum balance

$$N_l = -d/dt M_{ik} - \sum_c N_l^{(c)}, \tag{3.17}$$

which we imagine to be taken at an instant just after that the external devices, which might be necessary to keep the system fixed, have been removed. In (3.17) $N_l^{(c)}$ is the l'th component of the torque acting on conductor c, and i, k, l is a cyclic combination of indices. By making use of (1.6) and the conservation laws $f_i = -\partial_\nu S_{i\nu}$, we find

$$\left. \begin{aligned} N_l = \int\limits_{\substack{\text{internal}\\\text{body}}} (x_i f_k - x_k f_i + S_{ik} - S_{ki}) \, dV + \int\limits_{\substack{\text{body}\\\text{surface}}} [\boldsymbol{r} \times (\boldsymbol{S}_n - \boldsymbol{S}_n^{\text{vac}})]_l \, dS + \\ + \sum_c \int\limits_{(c)} [\boldsymbol{r} \times \boldsymbol{S}_n^{\text{vac}}]_l \, dS - \sum_c N_l^{(c)}. \end{aligned} \right\} \tag{3.18}$$

Here we have introduced $\boldsymbol{S}_n$ as a vector with components $S_{ni} = S_{ik} n_k$, where the normal vector $\boldsymbol{n}$ points outwards from the body and inwards to a conductor. It is apparent that the two last terms in (3.18) compensate each other, so that we are left with an expression for the body torque which agrees with the expression we would obtain by a direct evaluation of the integral in (1.7), with the opposite sign. This should be expected, sine the torque is a *local* effect.

Now return to the dielectric sphere and insert Minkowski's tensor into (3.18). The only non-vanishing component of the torque is

$$\left. \begin{aligned} N_3^M = \int\limits_{\text{body}} (\boldsymbol{D} \times \boldsymbol{E})_3 \, dV - a^3 \int\limits_{\text{surface}} (\boldsymbol{n} \times \boldsymbol{E})_3 (\boldsymbol{D} \cdot \boldsymbol{n}) \, d\Omega + \\ + a^3 \int\limits_{\text{surface}} (\boldsymbol{n} \times \boldsymbol{E}^{\text{vac}})_3 (\boldsymbol{E}^{\text{vac}} \cdot \boldsymbol{n}) \, d\Omega, \end{aligned} \right\} \tag{3.19}$$

where a is the radius of the sphere and $d\Omega$ the element of solid angle. By using spherical coordinates the two last integrals can be evaluated, so that

$$N_3^M = \int\limits_{\text{body}} (\boldsymbol{D} \times \boldsymbol{E})_3 \, dV - (\boldsymbol{p} \times \boldsymbol{E}^0)_3 + (\boldsymbol{p} \times \boldsymbol{E}^0)_3 = (\boldsymbol{p} \times \boldsymbol{E}^0)_3. \tag{3.20}$$

(Actually, the compensation of the two last integrals in (3.19) can be verified also by a mere inspection of the boundary conditions.) The result (3.20) could be checked by experiment. As a characteristic feature of Minkowski's

tensor, we see that the body surface term in (3.18) vanishes; it is natural to interpret the effect as a volume effect.

As regards the effects considered in this section, the magnetostatic field is analogous to the electrostatic field and requires no special attention.

4. Uniqueness from first Set of Conditions

This section deals with a formal proof. A set of conditions shall be given, from which we shall show that, within a multiplicative factor in the energy density component, Minkowski's tensor must follow uniquely for the electromagnetic (time-dependent) field inside a homogeneous, anisotropic medium at rest[1].

1. Let us first assume that each volume element experiences a torque density $\tau = \boldsymbol{P} \times \boldsymbol{E} = \boldsymbol{D} \times \boldsymbol{E}$ due to the fact that the constituent electric dipoles are not collinear to the field $\boldsymbol{E}$. This we may call the "dipole model", and it was encountered for the first time in connection with eq. (3.13). We may express this requirement in mathematical form by the relation

$$S_{ik} - S_{ki} = E_k D_i - E_i D_k, \tag{4.1}$$

where S_{ik} is the energy-momentum tensor to be determined.

2. Then require the energy-momentum tensor to be divergence-free,

$$\sum_{\beta} \partial_{\beta} S_{\alpha\beta} = 0, \tag{4.2}$$

the torque being described by the asymmetry only. For simplicity, we put $\mu = 1$. The summation convention is avoided in this section.

3. As the third condition, $S_{\alpha\beta}$ is required to be a bilinear form in the field quantities.

The three quantities $\boldsymbol{E}$, $\boldsymbol{D}$ and $\boldsymbol{H}$ characterize the field, and (4.2) is an algebraic consequence of the field equations and the constitutive relations which read $E_i = \eta_i D_i$ when the coordinate axes are chosen so that the tensor η_{ik} is diagonal. We first suppose that the η_i are all different. It is now convenient to eliminate $\boldsymbol{E}$ and treat $\boldsymbol{D}$ and $\boldsymbol{H}$ as the independent variables, and we can rewrite (4.2) in the form

[1] We mention already now that both sets of conditions automatically exclude Abraham's tensor from consideration.

$$\sum_{i,l} \left(\frac{\partial S_{\alpha i}}{\partial D_l} \frac{\partial D_l}{\partial x_i} + \frac{\partial S_{\alpha i}}{\partial H_l} \frac{\partial H_l}{\partial x_i} \right) + \frac{1}{ic} \sum_l \left(\frac{\partial S_{\alpha 4}}{\partial D_l} \frac{\partial D_l}{\partial t} + \frac{\partial S_{\alpha 4}}{\partial H_l} \frac{\partial H_l}{\partial t} \right) = 0, \qquad (4.3)$$

where the summations run from 1 to 3.

The time derivatives can be eliminated by means of the two Maxwell's equations

$$\frac{\partial D_k}{\partial t} = c \sum_{m,l} \delta_{kml} \frac{\partial H_l}{\partial x_m}$$

$$\frac{\partial H_k}{\partial t} = -c \sum_{m,l} \delta_{kml} \frac{\partial E_l}{\partial x_m} = -c \sum_{m,l} \delta_{kml} \eta_l \frac{\partial D_l}{\partial x_m}. \qquad (4.4)$$

Hence

$$\sum_{i,l} \left(\frac{\partial S_{\alpha i}}{\partial D_l} + i \frac{\partial S_{\alpha 4}}{\partial H_k} \delta_{kil} \eta_l \right) \frac{\partial D_l}{\partial x_i} + \sum_{i,l} \left(\frac{\partial S_{\alpha i}}{\partial H_l} - i \frac{\partial S_{\alpha 4}}{\partial D_k} \delta_{kil} \right) \frac{\partial H_l}{\partial x_i} = 0. \qquad (4.5)$$

Here k is supposed to take the value that makes δ_{kil} different from zero. Now having used (4.4) and the constitutive relations, we conclude that (4.5) must be algebraic consequences of the remaining Maxwell's equations, hence (4.5) must be of the form

$$A^{\alpha} \sum_i \partial_i D_i + B^{\alpha} \sum_i \partial_i H_i = 0. \qquad (4.6)$$

Comparing (4.5) with (4.6), we have then $(i = l)$

$$\frac{\partial S_{\alpha 1}}{\partial D_1} = \frac{\partial S_{\alpha 2}}{\partial D_2} = \frac{\partial S_{\alpha 3}}{\partial D_3}. \qquad (4.7)$$

Similarly

$$\frac{\partial S_{\alpha 1}}{\partial H_1} = \frac{\partial S_{\alpha 2}}{\partial H_2} = \frac{\partial S_{\alpha 3}}{\partial H_3}. \qquad (4.8)$$

When $i \neq l$, it follows that

$$\frac{\partial S_{\alpha i}}{\partial D_l} + i \frac{\partial S_{\alpha 4}}{\partial H_k} \delta_{kil} \eta_l = 0 \qquad (4.9)$$

and

$$\frac{\partial S_{\alpha i}}{\partial H_l} - i \frac{\partial S_{\alpha 4}}{\partial D_k} \delta_{kil} = 0. \qquad (4.10)$$

Hence

$$\frac{\partial S_{\alpha i}}{\partial D_l}\eta_i + \frac{\partial S_{\alpha l}}{\partial D_i}\eta_l = 0 \qquad\qquad (4.11)$$

$$\left.\begin{array}{c}(i \neq l)\end{array}\right.$$

$$\frac{\partial S_{\alpha i}}{\partial H_l} + \frac{\partial S_{\alpha l}}{\partial H_i} = 0. \qquad\qquad (4.12)$$

If in (4.9) we interchange l and k and differentiate with respect to H_l, and compare with (4.10) differentiated with respect to D_k, we get

$$\frac{\partial^2 S_{\alpha 4}}{\partial H_l \partial H_l}\eta_k = \frac{\partial^2 S_{\alpha 4}}{\partial D_k \partial D_k} \qquad (l \neq k). \qquad\qquad (4.13)$$

The discussion hitherto has closely followed the uniqueness proof for $S_{\mu\nu}$ given by V. Fock[9] in the case of an electromagnetic field in vacuum.

Now the assumption of bilinearity of the tensor components, together with the above equations, are sufficient to determine S_{44} within a multiplicative constant. For this component must be a linear combination of E^2, D^2, H^2 and $\boldsymbol{E}\cdot\boldsymbol{D}$ since it is a three-dimensional scalar. Terms involving $\boldsymbol{H}\cdot\boldsymbol{D}$ and $\boldsymbol{H}\cdot\boldsymbol{E}$ are excluded since $\boldsymbol{E}, \boldsymbol{D}$ are polar vectors in opposition to $\boldsymbol{H}$, which is an axial vector. These properties are included in the expression

$$S_{44} = \sum_i a_i D_i^2 + bH^2, \qquad\qquad (4.14)$$

where a_i and b may involve the material constants. From (4.13) one then finds $a_i = b\eta_i$. The constant b is not determined; with our customary choice of units $b = -\frac{1}{2}$, i. e. $S_{44} = -\frac{1}{2}(\boldsymbol{E}\cdot\boldsymbol{D}+H^2)$.

Considering now the spatial component S_{ik}, we see that it can contain linear combinations of the terms $E_i E_k, E_i D_k, E_k D_i, D_i D_k$ and $H_i H_k$. From (4.2) with $\alpha = i$ it follows, since the momentum density is a polar vector, that S_{ik} must be invariant under space inversion. Therefore terms like $E_i H_k$ and $D_i H_k$ cannot be present. Moreover, we can have terms with the unit tensor δ_{ik} multiplied with a scalar, the scalar being of a form like the right hand side of (4.14). We then write

$$\begin{aligned} S_{ik} &= c_1 E_i E_k + c_2 E_i D_k + c_3 D_i E_k + c_4 D_i D_k + c_5 H_i H_k - \delta_{ik}\left(\sum_{l=1}^{3} d_l D_l^2 + c_6 H^2\right) = \\ &= (c_1\eta_i\eta_k + c_2\eta_i + c_3\eta_k + c_4)D_i D_k + c_5 H_i H_k - \delta_{ik}\left(\sum_{l=1}^{3} d_l D_l^2 + c_6 H^2\right). \end{aligned} \qquad (4.15)$$

The constants c_l and d_l shall not be restricted to be independent of the material; they shall be permitted to contain symmetric terms such as the sum $\eta_1 + \eta_2 + \eta_3$. From (4.1) we now have $(\eta_i - \eta_k)(c_2 - c_3 + 1) = 0$, which means

$$c_3 = c_2 + 1. \tag{4.16}$$

From (4.7) with $\alpha = 1$,

$$\left.\begin{aligned} 2(c_1\eta_1^2 + c_2\eta_1 + c_3\eta_1 + c_4 - d_1) = \\ = c_1\eta_1\eta_2 + c_2\eta_1 + c_3\eta_2 + c_4 = c_1\eta_1\eta_3 + c_2\eta_1 + c_3\eta_3 + c_4. \end{aligned}\right\} \tag{4.17}$$

From the last equation it follows that

$$c_1\eta_1 + c_3 = 0. \tag{4.18}$$

With $\alpha = 2$ we get

$$\left.\begin{aligned} 2(c_1\eta_2^2 + c_2\eta_2 + c_3\eta_2 + c_4 - d_2) = \\ = c_1\eta_2\eta_1 + c_2\eta_2 + c_3\eta_1 + c_4 = c_1\eta_2\eta_3 + c_2\eta_2 + c_3\eta_3 + c_4. \end{aligned}\right\} \tag{4.19}$$

Hence

$$c_1\eta_2 + c_3 = 0. \tag{4.20}$$

Comparison of (4.20) with (4.18) gives $c_1 = c_3 = 0$. From (4.16) then $c_2 = -1$. Now (4.17) and (4.19), together with the corresponding equation for $\alpha = 3$, yield

$$c_4 = 2d_1 + \eta_1 = 2d_2 + \eta_2 = 2d_3 + \eta_3. \tag{4.21}$$

If we use (4.11) with $\alpha = 1, i = 1, l = 2$, we obtain

$$\eta_2 c_4 = \eta_1(2d_2 + \eta_2), \tag{4.22}$$

which, together with (4.21), is sufficient to determine the constants

$$c_4 = 0, d_1 = -\tfrac{1}{2}\eta_1, d_2 = -\tfrac{1}{2}\eta_2, d_3 = -\tfrac{1}{2}\eta_3. \tag{4.23}$$

We now turn our attention to the terms S_{i4}. As the momentum density is a polar vector, any actual bilinear combination can be written in the form

$$S_{i4} = \sum_{j,\,k} \delta_{ijk} f_j D_j H_k, \tag{4.24}$$

where f_j may contain material constants. Putting $\alpha = 1$ in (4.9), we have

$$\frac{\partial S_{14}}{\partial H_1} = 0, \quad \frac{\partial S_{14}}{\partial H_2} = -iD_3, \quad \frac{\partial S_{14}}{\partial H_3} = iD_2, \tag{4.25}$$

which are compatible with (4.24), when $f_2 = f_3 = i$. Similar arguments for $\alpha = 2,3$ give $f_1 = i$. Therefore

$$S_{i4} = i\sum_{j,k}\delta_{ijk}D_jH_k = i(\boldsymbol{D}\times\boldsymbol{H})_i. \tag{4.26}$$

Then (4.10) gives, when $\alpha = 1$, $i = 1$, $l = 2$, that $c_6 = -\tfrac{1}{2}$. With another combination of indices, or from (4.8) or (4.12), one finds $c_5 = -1$. Inserted into (4.15)

$$S_{ik} = -E_iD_k - H_iH_k + \delta_{ik}\tfrac{1}{2}(\boldsymbol{E}\cdot\boldsymbol{D}+H^2). \tag{4.27}$$

In the same way one finds from (4.9) and (4.10) that the remaining components are

$$S_{4i} = i\sum_{j,k}\delta_{ijk}\eta_jD_jH_k = i(\boldsymbol{E}\times\boldsymbol{H})_i. \tag{4.28}$$

We have thus arrived at Minkowski's tensor.

Note that as a result of the linear combination postulated in (4.15), we obtained to a certain extent the dependence on η_i of the coefficient in front of D_iD_k on the right of this equation. If instead we had put the first term of the last expression equal to the general form $c_{ik}D_iD_k$, the equations (4.1) and (4.7—10) would not have been sufficient to determine the components c_{ik} such as given above, where $c_{ik} = c_1\eta_i\eta_k + c_2\eta_i + c_3\eta_k + c_4$.

The foregoing procedure is based on the assumption of different material constants; the conclusions are valid only when $\eta_i - \eta_k \neq 0$. If, however, two of these constants are equal, but different from the third, we see without difficulty that the present treatment need not be changed. In the deduction of (4.16) for instance, we use first the two unequal η_i and η_k to give $c_3 = c_2 + 1$. The same considerations apply when we construct the equations corresponding to (4.18) and (4.20), giving $c_1 = c_3 = 0$, as before. We arrive again at Minkowski's tensor as the final result.

But if the η_i are all equal, our equations are not sufficient to determine the components $S_{i\alpha}$ uniquely. With a simplified expression for S_{ik} corresponding to (4.15) and the assumption (4.24), we can use (4.7—10) and determine the quantities $S_{i\alpha}$, except for a multiplicative constant. This constant comes in addition to the multiplicative factor appearing in the determination of S_{44}. This is connected with the fact that we cannot take advantage of the dipole model in this case; instead, we may take into account that $S_{\alpha\beta}$ is a tensor under Lorentz transformations. These concepts are taken up in the next section.

5. Uniqueness from Second Set of Conditions

In this section we shall give another formal derivation of Minkowski's tensor, based on somewhat different initial conditions.

Let us first refer to the treatment in Fock's book[9], for a consideration of the problem to determine in general an energy-momentum tensor $S_{\alpha\beta}$ uniquely. He takes explicitly into account that $S_{\alpha\beta}$ be a tensor, and he requires it to be symmetric and to have a vanishing four-divergence. However, to determine $S_{\alpha\beta}$ uniquely (or within a constant multiplying factor, provided that suitable conditions exist at infinity), he finds it essential to lean on the requirement that the energy-momentum tensor should be a function of the state of the system. By "state" is meant the following. If the equations of motion and the field equations are written as first order equations for the unknown functions φ_i, the latter functions are said to characterize the state. Any function of φ_i that does not contain their derivatives and also does not contain the coordinates explicitly, is called a function of the state. With this additional conditions imposed, he claims the energy-momentum tensor to be determined in principle for every physical system.

Now our system is different from those considered by Fock since $S_{\alpha\beta}$ must be permitted to be asymmetric. Therefore we shall carry through the proof in detail.

We recall the three initial conditions which were given in the preceding section. Here we shall release the condition 1 and instead require $S_{\alpha\beta}$ to be a function of the electromagnetic state of the system. Since the field equations contain the field quantities only (and not the four-velocity V_μ of the medium explicitly), it follows that $S_{\alpha\beta}$ also contains only field quantities. This is to be true in *any* inertial frame, and we shall use this property explicitly when we perform Lorentz transformations. We have thus

$$S_{\alpha\beta} = S_{\alpha\beta}(\boldsymbol{E}, \boldsymbol{D}, \boldsymbol{H}, \boldsymbol{B}). \tag{5.1}$$

2. The tensor is still required to be divergence-free

$$\sum_\beta \partial_\beta S_{\alpha\beta} = 0, \tag{5.2}$$

where also in this section the summation convention is avoided.

3. The tensor is still required to be a bilinear form.

The material constants are in general ε_{ik} and μ_{ik}. From geometrical consideration of the fact that in K^0 the magnitude of $\boldsymbol{P}^0$ is proportional to that

2*

of E^0, while the angle between P^0 and E^0 is constant for a given orientation of the field, it follows that ε_{ik} is symmetric. Similar considerations apply to μ_{ik}. Also isotropic media are now included in the description.

The next task is to show that, within a multiplicative constant, the conditions mentioned are sufficient to yield Minkowski's tensor. It is natural to work directly with the field quantities E, D, H, B instead of eliminating some of them by means of the constitutive relations in K^0. Eqs. (5.2) are algebraic consequences of Maxwell's equations

$$\triangledown \times E = -\frac{1}{c}\frac{\partial B}{\partial t}, \quad \triangledown \times H = \frac{1}{c}\frac{\partial D}{\partial t} \tag{5.3}$$

$$\triangledown \cdot D = 0, \ \triangledown \cdot B = 0 \tag{5.4}$$

and the constitutive relations. Eq. (5.1) implies that we have to write the constitutive relations in a form where neither the material constants nor the body velocity is present. The simplest way of eliminating the material constants in K^0 is to write

$$E^0 \cdot \partial_\mu^0 D^0 - D^0 \cdot \partial_\mu^0 E^0 = 0 \tag{5.5}$$

$$H^0 \cdot \partial_\mu^0 B^0 - B^0 \cdot \partial_\mu^0 H^0 = 0, \quad (\mu = 1 - 4) \tag{5.6}$$

so that the constitutive equations involve the first order derivatives of the fields, as do Maxwell's equations. Now (5.5) can be written $\sum(F_{4\beta}^0\partial_\mu^0 H_{4\beta}^0 - H_{4\beta}^0\partial_\mu^0 F_{4\beta}^0) = 0$, which cannot be brought into a covariant form except by introducing the four-velocity V_μ of the medium. Similarly for (5.6). We therefore try to write the constitutive relations in K as a linear combination of the terms $\sum F_{\alpha\beta}\partial_\mu H_{\alpha\beta}$ and $\sum H_{\alpha\beta}\partial_\mu F_{\alpha\beta}$ and readily find that

$$\sum_{\alpha,\beta}(F_{\alpha\beta}\partial_\mu H_{\alpha\beta} - H_{\alpha\beta}\partial_\mu F_{\alpha\beta}) = 0 \tag{5.7}$$

or

$$E \cdot \partial_\mu D - D \cdot \partial_\mu E + H \cdot \partial_\mu B - B \cdot \partial_\mu H = 0 \tag{5.8}$$

represent the simplest form of the constitutive relations with the required properties.

Let us then write (5.2) in the following form, assuming $S_{\alpha\beta}$ to be a function of the state:

$$\sum_{i,l} \left(\frac{\partial S_{\alpha i}}{\partial E_l} \frac{\partial E_l}{\partial x_i} + \frac{\partial S_{\alpha i}}{\partial D_l} \frac{\partial D_l}{\partial x_i} + \frac{\partial S_{\alpha i}}{\partial H_l} \frac{\partial H_l}{\partial x_i} + \frac{\partial S_{\alpha i}}{\partial B_l} \frac{\partial B_l}{\partial x_i} \right) +$$
$$+ \frac{1}{ic} \sum_{l} \left(\frac{\partial S_{\alpha 4}}{\partial E_l} \frac{\partial E_l}{\partial t} + \frac{\partial S_{\alpha 4}}{\partial D_l} \frac{\partial D_l}{\partial t} + \frac{\partial S_{\alpha 4}}{\partial H_l} \frac{\partial H_l}{\partial t} + \frac{\partial S_{\alpha 4}}{\partial B_l} \frac{\partial B_l}{\partial t} \right) = 0, \qquad (5.9)$$

and demand (5.9) to be algebraic consequences of (5.3), (5.4) and (5.8). By means of (5.3) two of the time derivatives can be eliminated, but the derivatives $\dot{E}_l$ and $\dot{H}_l$ cannot be eliminated by means of Maxwell's equations. The actual equation is then (5.8) with $\mu = 4$, and by comparison with (5.9) we obtain the conditions

$$\frac{\partial S_{\alpha 4}}{\partial E_l} = A^\alpha D_l, \qquad \frac{\partial S_{\alpha 4}}{\partial H_l} = A^\alpha B_l. \qquad (5.10)$$

Since $S_{\alpha 4}$ is a bilinear form, the quantity A^α must be independent of the fields. Eq. (5.9) now reads

$$\sum_{i,l} \left(\frac{\partial S_{\alpha i}}{\partial E_l} + iA^\alpha \delta_{kil} H_k + i\delta_{kil} \frac{\partial S_{\alpha 4}}{\partial B_k} \right) \frac{\partial E_l}{\partial x_i} + \sum_{i,l} \left(\frac{\partial S_{\alpha i}}{\partial H_l} - \right.$$
$$\left. - iA^\alpha \delta_{kil} E_k - i\delta_{kil} \frac{\partial S_{\alpha 4}}{\partial D_k} \right) \frac{\partial H_l}{\partial x_i} + \sum_{i,l} \frac{\partial S_{\alpha i}}{\partial D_l} \frac{\partial D_l}{\partial x_i} + \sum_{i,l} \frac{\partial S_{\alpha i}}{\partial B_l} \frac{\partial B_l}{\partial x_i} = 0. \qquad (5.11)$$

This equation must be a linear combination of the remaining equations (5.4) and (5.8) with $\mu = 1, 2, 3$. Only linear forms are permissible because we have assumed the condition (5.1), and inspection of (5.11) then shows that only terms linear in the derivatives are present. Hence (5.11) must be of the form

$$\sum_i C^{\alpha i} (\boldsymbol{D} \cdot \partial_i \boldsymbol{E} + \boldsymbol{B} \cdot \partial_i \boldsymbol{H} - \boldsymbol{E} \cdot \partial_i \boldsymbol{D} - \boldsymbol{H} \cdot \partial_i \boldsymbol{B}) + F^\alpha \triangledown \cdot \boldsymbol{D} + G^\alpha \triangledown \cdot \boldsymbol{B}, \qquad (5.12)$$

where the Lagrangian multipliers $C^{\alpha i}, F^\alpha$ and G^α do not contain differential operators ∂_μ. By equating (5.12) to (5.11) we can look upon this new equation as an identity in the derivatives of the fields with respect to the coordinates, because of the presence of the multipliers. Hence we obtain the relations

$$\frac{\partial S_{\alpha i}}{\partial E_l} + iA^\alpha \delta_{kil} H_k + i\delta_{kil} \frac{\partial S_{\alpha 4}}{\partial B_k} = C^{\alpha i} D_l \qquad (5.13)$$

$$\frac{\partial S_{\alpha i}}{\partial H_l} - iA^\alpha \delta_{kil} E_k - i\delta_{kil}\frac{\partial S_{\alpha 4}}{\partial D_k} = C^{\alpha i} B_l.$$ (5.14)

When $i \neq l$,

$$\frac{\partial S_{\alpha i}}{\partial D_l} = -C^{\alpha i} E_l$$ (5.15)

$$\frac{\partial S_{\alpha i}}{\partial B_l} = -C^{\alpha i} H_l.$$ (5.16)

When $i = l$,

$$\frac{\partial S_{\alpha i}}{\partial D_i} = -C^{\alpha i} E_i + F^\alpha$$ (5.17)

$$\frac{\partial S_{\alpha i}}{\partial B_i} = -C^{\alpha i} H_i + G^\alpha.$$ (5.18)

Then put $\alpha = 4$, and examine which simplifications can be made in these equations from the requirement of bilinearity of $S_{\alpha\beta}$. If we make a rotation of the spatial coordinate axes in K, we know that $\partial_\beta S_{4\beta}$ remains unchanged, and so the expression (5.12) is also unchanged. Hence, since the expression in the parenthesis in (5.12) transforms as a three-dimensional vector, the quantities C^{4i} must transform similarly. But according to the bilinearity of $S_{\alpha\beta}$, C^{4i} must be independent of the fields, therefore $C^{4i} = 0$. By similar arguments we conclude that $F^4 = G^4 = 0$.

The reduced system of equations we have now obtained is easily solved for the components $S_{4\beta}$. By assuming the form

$$S_{4i} = \sum_{j,\,k} \delta_{ijk}(a_1 E_j H_k + a_2 E_j B_k + a_3 D_j H_k + a_4 D_j B_k),$$ (5.19)

we obtain from (5.15) and (5.16) that $a_2 = a_3 = a_4 = 0$. If we fix the remaining constant $a_1 = i$, we obtain

$$S_{4i} = i(\boldsymbol{E} \times \boldsymbol{H})_i.$$ (5.20)

Similarly, by assuming

$$S_{44} = b_1 E^2 + b_2 D^2 + b_3 H^2 + b_4 B^2 + b_5 \boldsymbol{E} \cdot \boldsymbol{D} + b_6 \boldsymbol{H} \cdot \boldsymbol{B},$$ (5.21)

we obtain by virtue of (5.13), (5.14) and (5.10)

$$S_{44} = -\tfrac{1}{2}(\boldsymbol{E} \cdot \boldsymbol{D} + \boldsymbol{H} \cdot \boldsymbol{B}).$$ (5.22)

The discussion hitherto is in principle similar to that leading to the components $S_{4\beta}$ in section 4, although the discussion has been carried through for any K. But in order to find the remaining components, we shall use (5.1) and the tensor property of $S_{\alpha\beta}$. We perform an infinitesimal Lorentz transformation $x'_\mu = x_\mu + \sum \omega_{\mu\nu} x_\nu$, where the antisymmetric $\omega_{\mu\nu}$ is given by $\omega_{ik} = \varphi_l(\text{cycl})$, $\omega_{i4} = iu_i/c$. We obtain

$$\delta \boldsymbol{E} = \boldsymbol{E}' - \boldsymbol{E} = \frac{1}{c}(\boldsymbol{u} \times \boldsymbol{B}) - (\varphi \times \boldsymbol{E})$$

$$\delta \boldsymbol{D} = \frac{1}{c}(\boldsymbol{u} \times \boldsymbol{H}) - (\varphi \times \boldsymbol{D})$$

$$\delta \boldsymbol{H} = -\frac{1}{c}(\boldsymbol{u} \times \boldsymbol{D}) - (\varphi \times \boldsymbol{H}) \qquad\qquad (5.23)$$

$$\delta \boldsymbol{B} = -\frac{1}{c}(\boldsymbol{u} \times \boldsymbol{E}) - (\varphi \times \boldsymbol{B}).$$

When a system in general is described by a set of functions γ_s, the change of these, on account of the present transformation, can be written as

$$\delta \gamma_s = \tfrac{1}{2} \sum_{\mu,\nu} \omega_{\mu\nu} \Psi_s^{\mu\nu}, \qquad\qquad (5.24)$$

where the antisymmetric $\Psi_s^{\mu\nu}$ are functions of γ_s. We follow the method given by Fock[9] (§ 31*) by introducing a set of operators $X^{\mu\nu}$ by the equations

$$X^{\mu\nu}(h) = \sum_s \Psi_s^{\mu\nu} \frac{\partial h}{\partial \gamma_s}, \qquad\qquad (5.25)$$

where h is some function of γ_s. Hence

$$X^{\mu\nu}(\gamma_s) = \Psi_s^{\mu\nu}, \qquad\qquad (5.26)$$

which, inserted into (5.24), gives

$$\delta \gamma_s = \tfrac{1}{2} \sum_{\mu,\nu} \omega_{\mu\nu} X_s^{\mu\nu}(\gamma_s). \qquad\qquad (5.27)$$

The variation δh can also be expressed in terms of these operators; we have

$$\delta h = \sum_s \frac{\partial h}{\partial \gamma_s} \delta \gamma_s = \tfrac{1}{2} \sum_{s,\mu,\nu} \frac{\partial h}{\partial \gamma_s} \omega_{\mu\nu} \Psi_s^{\mu\nu} = \tfrac{1}{2} \sum_{\mu,\nu} \omega_{\mu\nu} X^{\mu\nu}(h). \qquad (5.28)$$

With $h = S_{\alpha\beta}(\gamma_s)$:

$$\delta S_{\alpha\beta} = \tfrac{1}{2} \sum_{\mu, \nu} \omega_{\mu\nu} X^{\mu\nu}(S_{\alpha\beta}). \tag{5.29}$$

This equation is compared with $\delta S_{\alpha\beta}$ obtained from a tensor transformation

$$\delta S_{\alpha\beta} = \sum_{\mu, \nu} \omega_{\mu\nu} (\delta_{\mu\alpha} S_{\nu\beta} + \delta_{\mu\beta} S_{\alpha\nu}), \tag{5.30}$$

and there results

$$X^{\mu\nu}(S_{\alpha\beta}) = \delta_{\mu\alpha} S_{\nu\beta} - \delta_{\nu\alpha} S_{\mu\beta} + \delta_{\mu\beta} S_{\alpha\nu} - \delta_{\nu\beta} S_{\alpha\mu}. \tag{5.31}$$

Finally, from (5.25) and (5.26)

$$X^{\mu\nu}(S_{\alpha\beta}) = \sum_{s} X^{\mu\nu}(\gamma_s) \frac{\partial S_{\alpha\beta}}{\partial \gamma_s}. \tag{5.32}$$

In our case $\delta\gamma_s$ are given by (5.23), and as S_{44} and S_{4i} are already found, we shall see that the present equations are sufficient to determine the remaining components $S_{i\beta}$. It should be noticed that, as γ_s denote the field quantities, eq. (5.1) is essential for the passage from (5.28) to (5.29). Further, it is essential that $S_{\alpha\beta}$ is a tensor for the establishment of (5.30).

Now compare (5.23) with the general (5.27). There results

$$\left. \begin{aligned} X^{ik}(\gamma_s) &= E_k \frac{\partial}{\partial E_i} - E_i \frac{\partial}{\partial E_k} + D_k \frac{\partial}{\partial D_i} - D_i \frac{\partial}{\partial D_k} + \\ &\quad + H_k \frac{\partial}{\partial H_i} - H_i \frac{\partial}{\partial H_k} + B_k \frac{\partial}{\partial B_i} - B_i \frac{\partial}{\partial B_k} \\ X^{4i}(\gamma_s) &= -i \sum_{j,\,k} \delta_{ijk} \left(E_i \frac{\partial}{\partial B_k} - B_j \frac{\partial}{\partial E_k} + D_j \frac{\partial}{\partial H_k} - H_j \frac{\partial}{\partial D_k} \right). \end{aligned} \right\} \tag{5.33}$$

From (5.31) we obtain

$$X^{4i}(S_{44}) = S_{i4} + S_{4i}. \tag{5.34}$$

Calculating from (5.32)

$$X^{4i}(S_{44}) = \sum_{s} \left[X^{4i}(E_s) \frac{\partial S_{44}}{\partial E_s} + X^{4i}(D_s) \frac{\partial S_{44}}{\partial D_s} + X^{4i}(H_s) \frac{\partial S_{44}}{\partial H_s} + X^{4i}(B_s) \frac{\partial S_{44}}{\partial B_s} \right]$$

and using (5.33) and (5.22), we get

$$X^{4i}(S_{44}) = i(\boldsymbol{D} \times \boldsymbol{B} + \boldsymbol{E} \times \boldsymbol{H})_i. \tag{5.35}$$

From (5.35), (5.34) and (5.20) then

$$S_{i4} = i(\boldsymbol{D} \times \boldsymbol{B})_i. \tag{5.36}$$

From (5.31) we have for the spatial components

$$S_{ik} = X^{4i}(S_{4k}) + \delta_{ik} S_{44}. \tag{5.37}$$

From (5.32), (5.33) and (5.20)

$$X^{4i}(S_{4k}) = \sum_s X^{4i}(\gamma_s)\frac{\partial S_{4k}}{\partial \gamma_s} = -E_i D_k - H_i B_k + \delta_{ik}(\boldsymbol{E}\cdot\boldsymbol{D} + \boldsymbol{H}\cdot\boldsymbol{B}), \tag{5.38}$$

and from (5.37) then

$$S_{ik} = -E_i D_k - H_i B_k + \tfrac{1}{2}\delta_{ik}(\boldsymbol{E}\cdot\boldsymbol{D} + \boldsymbol{H}\cdot\boldsymbol{B}). \tag{5.39}$$

The adjustment of the constant a_1 in (5.19) has thus led to Minkowski's expression for all components. It follows that the two sets of assumptions from the preceding section and the present section must be equivalent.

III. Derivation of Minkowski's Tensor by a Semi-Empirical Method

6. Consideration of a Plane Wave Travelling through Matter at Rest

This chapter forms the central part of our work. By using the phenomenological theory and leaning on experiments, we shall construct the electromagnetic energy-momentum tensor in the simple optical situation where a plane light wave travels through a dielectric body at rest. We emphasize that we do not intend to give a *formal* derivation of Minkowski's tensor; we use simple, formal arguments to illustrate what *may* happen, and then take the lacking information from experiments.

Isotropic matter

One might first think of the possibility to use microscopical considerations as a guide to construct an expression for the force density f_μ directly in terms of the macroscopical fields. Some attempts have been made in this direction[10, 11]. We shall study the microscopical line of approach to some extent in the next section, but mention already now that there are some difficulties of principle with a construction of the force density in this way. The macroscopical force can be written as the average over appropriate

regions in space and time of the microscopical force acting on the external charges and currents, as well as on the matter itself. But since the force is of the second order in the field quantities, we cannot simply find it in terms of products of the macroscopical fields when the microscopical fields are correlated in an unknown way.

Further, the macroscopic variational method which is applicable in electrostatic and magnetostatic cases commonly fails when the fields are time varying.

Let us then employ the simple macroscopic method followed, for instance, by LANDAU and LIFSHITZ[4]. It is usually so that the stress tensor and energy density may be taken as the sum of the parts corresponding to the electrostatic and magnetostatic cases. This is a reasonable construction at frequencies much lower than the eigenfrequencies of the molecular or electronic vibrations which lead to the electric or magnetic polarization of the matter. Then the linear relations between E, D and H, B are still valid, when the fields are not too strong. But the latter relations are valid also in the optical regions where the dielectric permeability is approximately frequency independent in virtue of the electronic polarization, but where the contribution from the slower molecular vibrations is absent. In this optical region we can therefore approximately put the magnetic permeability equal to 1. We assume that the above-mentioned construction of the stress tensor and energy density is valid also in this case, so that these quantities are given by (1.5a) and (1.5c).

As in the former treatment in section 3, we ignore electrostriction and magnetostriction effects.

We then have to determine the remaining components of the energy-momentum tensor $S_{\mu\nu}$. First, we use the experimentally known fact that an electromagnetic wave approximately does not lead to heat production in an insulator through which it moves. This corresponds to the fact that the wave is scattered elastically on the particles constituting the matter. So we must practically have $f_4 = 0$. By means of the field equations we can form the expression

$$\nabla \cdot c(E \times H) + \frac{\partial}{\partial t} \frac{1}{2}(E \cdot D + H \cdot B) = 0, \qquad (6.1)$$

which is consistent with the continuity equation for electromagnetic energy when the energy flux equals

$$S = c(E \times H). \qquad (6.2)$$

It is of course true that (6.1) does not unambiguously determine the energy flux to be given by (6.2); for instance, $\boldsymbol{S}$ could in addition contain a term of the form of a curl. But such possibilities are of no interest for our problem.

To determine the momentum components S_{k4}, we make use of the relation $\boldsymbol{S} = c^2\boldsymbol{g}$, whence

$$\boldsymbol{g} = \frac{1}{c}(\boldsymbol{E} \times \boldsymbol{H}). \tag{6.3}$$

The components that we have found up till now constitute a tensor which we shall call[1] $S_{\mu\nu}^A$, with a corresponding force density $\boldsymbol{f}^A$. Our next task is to examine the consequences of this force. Let us therefore consider the simple situation where a plane wave with $\boldsymbol{E} = E_0\boldsymbol{e}_2 \sin(kx - \omega t)$ travels along the x-axis in an isotropic body. We have $k = n\omega/c$, where $n = \sqrt{\varepsilon\mu}$ is the refractive index of the medium. It appears that $f_\mu^A = \delta_{\mu 1}[(n^2 - 1)/c]$ $(\partial/\partial t)(\boldsymbol{E} \times \boldsymbol{H})_1$, so that there is set up a fluctuating force in the x-direction. This force is rather small; we see that f_1^A is of the order $(1/c)(n^2 - 1)(\dot{\boldsymbol{E}} \times \boldsymbol{H})_1$ $= (1/c\mu)(n^2 - 1)(\varepsilon - 1)^{-1}(\dot{\boldsymbol{P}} \times \boldsymbol{B})_1 \approx (1/c)(\dot{\boldsymbol{P}} \times \boldsymbol{B})_1$, which on a microscopical scale (per dipole) corresponds to the magnetic part of the Lorentz force: $(e/c)(\boldsymbol{u} \times \boldsymbol{h})_1$, where $\boldsymbol{h}$ is the microscopical magnetic field and e, $\boldsymbol{u}$ the electric charge and particle velocity, respectively. Now we see that the ratio $u_2/c \ll 1$. In fact, if we accept a simple model with electronic polarization, one dipole per atom, e equal to the electron charge, and put h equal to the macroscopical field strength $B \approx E$ which is set equal to 10 volt/cm, we obtain with optical frequencies $\beta = u/c \approx 10^{-10}$, where $u = |\boldsymbol{u}|$. Such a rough estimation is sufficient to show that quantities proportional to β^2 can be taken to vanish. For instance, since the force on the dipoles in the x-direction is of the order of β times the force on the dipoles in the y-direction, we have also a particle velocity in the x-direction which is $u_1 \approx \beta u_2$. The work performed by f_1^A per unit time is then $f_1^A u_1 \approx \beta^2 \times$ (work performed by f_2^A per unit time) ≈ 0. This is consistent with the result above which also has experimental support: $f_4^A = 0$.

Let us now introduce a mechanical energy-momentum tensor $U_{\mu\nu}$ such that

$$-\partial_\nu S_{\mu\nu}^A = f_\mu^A = \partial_\nu U_{\mu\nu}. \tag{6.4}$$

In writing this equation, we have already assumed that gravity effects are absent. For instance, if the medium is a fluid then, in the absence of fields,

---

[1] $S_{\mu\nu}^A$ is equal to Abraham's tensor.

the diagonal components of the stress tensor are equal to the pressure, and the divergence of U_{ik} yields the gravitational force density. But since these effects are of no principal interest here, we shall omit them; hence we interpret the tensor $(S_{\mu\nu}^A + U_{\mu\nu})$ to describe a closed system.

With the plane wave considered the only interesting component of U_{ik} is U_{11}, the effect from the wave on the other components of U_{ik} is zero. The force f_1^A can be thought to act in two ways. (1) It may cause each dipole to fluctuate about a fixed position, the same position as the dipole occupies when the fields are absent. (We ignore thermal motions, which are of no interest here.) On an average, no momentum is then transferred to the dipoles; instead, a kind of small stress is set up. (2) But the effect may also be that a momentum in the x-direction actually results. Since ∂_1 can be replaced by $-(n/c)(\partial/\partial t)$, we obtain from (6.4), with $U_{14} = icg_1^{\text{mech}}$,

$$\frac{\partial}{\partial t}\left(-\frac{n}{c}U_{11} + g_1^{\text{mech}}\right) = f_1^A. \tag{6.5}$$

From this point of view the main effect of f_1^A is to produce a mechanical momentum, so we shall assume the contribution to U_{11} from mechanical stresses to be vanishingly small. Furthermore, the component U_{11} contains also a part $\varrho_m u_1^2$ corresponding to the kinetic energy of the motion in the x-direction, but the quotient $\varrho_m u_1^2/(cg_1^{\text{mech}}) = u_1/c \ll 1$, so that this kinetic part can be neglected. Hence, ignoring the first term in the parenthesis in (6.5), we obtain by means of (6.3) and (1.5a)

$$g_1^{\text{mech}} = \frac{n^2 - 1}{c}(\boldsymbol{E} \times \boldsymbol{H})_1 + \text{const}, \tag{6.6}$$

where the constant may depend on E_0.

At this point we cannot get any further by theoretical considerations. We shall therefore seek the remaining information from *experiments* in optics. In this paper we shall consider three experiments which are of importance for our problem; these experiments are mutually in agreement and especially two of them seem to yield sufficient information as to which energy-momentum tensor should be taken as the most convenient. The first experiment—which has immediate application in the present situation—is the Jones-Richards experiment to be described below. The two other experiments are related to the propagation of light in moving media, and will be described later in section 9.

Jones and Richards measured the radiation pressure on a metal vane from an electromagnetic wave passing through a dielectric liquid. Their result is most easily explained by attributing a momentum density $(1/c)$ $\boldsymbol{D} \times \boldsymbol{B}$ to the wave. This behaviour is consistent with assuming the alternative (2) above to be correct and putting the integration constant in (6.6) equal to zero. Thus

$$\boldsymbol{g}^{\mathrm{mech}} = \frac{n^2 - 1}{c} \, (\boldsymbol{E} \times \boldsymbol{H}). \tag{6.7}$$

We note that (6.6) cannot be supplemented with some initial condition to give an unambiguous result. SOMMERFELD[12], for example, has examined the behaviour of "die Vorläufer", i. e. the incoming field before the stationary state is achieved. The result is that at first the field frequencies are much higher than the atomic frequencies of the medium. Therefore dispersion effects must occur, in contradiction to the assumptions leading to (6.6).

We then turn our attention to the components $U_{4\nu}$. We found above that $f_1^A u_1$ was practically zero, therefore the mechanical energy density $W^{\mathrm{mech}} = - U_{44}$ must also be practically equal to the rest mass density. (The contribution to the energy on account of the force components lying in the yz-plane is already incorporated in S_{44}^A.) The actual equation of motion is

$$\frac{\partial S_1^{\mathrm{mech}}}{\partial x} + \frac{\partial W^{\mathrm{mech}}}{\partial t} = 0, \tag{6.8}$$

where S_1^{mech} denotes the flow of mechanical energy in the x-direction. According to the principle of inertia of energy we can put $\boldsymbol{S}^{\mathrm{mech}} = c^2 \boldsymbol{g}^{\mathrm{mech}}$, where $\boldsymbol{g}^{\mathrm{mech}}$ is given by (6.7). $\boldsymbol{S}^{\mathrm{mech}}$ corresponds to a very small motion of dipoles; with the simple model above we found that $u_1 \approx 10^{-10}$ cm/s and because of the elastic coupling to the atoms the motion will be even smaller.

The kinetic energy on account of this motion is of course practically zero, but yet a finite energy transport is achieved by the great *rest mass*. As the wave proceeds through the body, new domains of matter are continuously being excited; and when the wave has passed, the dipoles have been displaced by a small amount in the x-direction.

Now, after having interpreted the components of $U_{\mu\nu}$, we introduce the quantities $\Theta_{\mu\nu}$ defined by

$$\Theta_{i\nu} = U_{i\nu}, \; \Theta_{4\nu} = 0, \; (i = 1,2,3; \; \nu = 1 - 4). \tag{6.9}$$

Then

$$- \partial_\nu (S_{\mu\nu}^A + \Theta_{\mu\nu}) = - \partial_\nu S_{\mu\nu}^M = 0, \tag{6.10}$$

where $S_{\mu\nu}^{M}$ is Minkowski's tensor, which accordingly describes the propagation of the total travelling system, both the electromagnetic field and the mechanical excitation caused by the field. The small displacement of matter and the rest energy itself are ignored in this context.

Concerning $\boldsymbol{g}^{\text{mech}}$ given by (6.7) we note that this mechanical quantity is expressed chiefly by electromagnetic ones. This is a characteristic feature of the phenomenological theory, and similar things are also found for instance in the expression for the electrostatic field energy density in an isotropic medium where, besides the pure field part $\frac{1}{2}E^2$, there appears an amount of internal energy in the medium, which is written as $\frac{1}{2}\boldsymbol{E}\cdot\boldsymbol{P} = \frac{1}{2}(\varepsilon-1)E^2$.

The Jones-Richards experiment[13]

We shall now consider the experiment to which we referred above in order to find the result (6.7). In 1951, R. V. JONES[13a] first reported in a short note a measurement of the radiation pressure in various dielectric fluids, and later, in 1954, R. V. JONES and J. C. S. RICHARDS[13b] gave an extensive report of the final experiment. We find that this excellent experiment clearly demonstrates that it is most simple and convenient to ascribe a momentum density $(1/c)(\boldsymbol{D}\times\boldsymbol{B})$ to an optical wave travelling through a refracting fluid. The experimental arrangement was the following: A ray of light passed through a glasswindow into a dielectric liquid and was reflected in the opposite direction by a metal vane immersed in the liquid. (Actually, the authors used two rays of light which were falling asymmetrically on the vane, and the vane was mounted on a torsional suspension.) The ratio between the pressure on the vane when it was immersed in the liquid and the pressure on the vane when it was surrounded by air was measured. This ratio was found to be equal, the external conditions also being equal, to the refractive index of the fluid. Let us apply a simple theoretical argument and first consider the divergence-free Minkowski's tensor with momentum density equal to $g = (1/c)DB = n^2S/c^2$. The symbols are referring to the incoming wave in the liquid. The momentum transferred to a unit surface of the vane per unit time is thus $p_n = (1/c)nS(1+R)$, where R is the reflectivity of the vane. Dividing by the vacuum (air) pressure $p_0 = (1/c)S_0(1+R_0)$ and assuming $S_0 = S$ and $R_0 = R$, we find indeed the simple formula $p_n/p_0 = n$. (See also the analysis by G. ROSENBERG[8].) It is evident that a number of corrections are called for in this formula, owing to the fact that the external conditions in reality are varying with n. For instance, although the intensity

of the radiation source (which is outside the container) is kept constant in the experiment, the intensity S will depend on the refractive index in a way which may be described by means of Fresnel's formulas: The electric field E of the incoming wave in the liquid is related to the electric field E_g of the incoming wave in the glass by $E = 2E_g/(1 + n/n_g)$, where n_g is the refractive index of the glass and μ is put equal to unity. Hence $p_n/p_0 = nS/S_0 = (1 + n_g)^2(1 + n_g/n)^{-2}$ which, in the case of a typical fluid, amounts to a correction of approximately 4% with respect to the simple formula quoted above.

Apart from this correction, JONES and RICHARDS carefully took into account corrections arising from other effects, such as absorption in the liquid, multiple reflections at the vane and the window, and dependence of the reflectivity R on the refractive index of the fluid. Unwanted effects from convective forces in the liquid were eliminated experimentally by means of a chopping technique. After these various secondary effects had been compensated for, the agreement between theory and experiment was found to hold within approximately 1% for all the six various liquids investigated. This agreement is remarkable, in consideration of the small effects involved (the mechanical couple measured was of the order of 10^{-6} dyne cm).

If now in the calculation above we had inserted the expression $g = (1/c) EH$ for the momentum density, we would have got a factor $1/n^2$ different and hence disagreement with the observed data. This does not mean, however, that Minkowski's momentum density is correct and all other alternatives wrong, for the calculation above applies only to the case of a *divergence-free* tensor. The experimental result does not prevent us from using an energy-momentum tensor with a non-vanishing force density such that the effect from the force is to be added to the effect considered above. But for a divergence-free tensor, the experiment supports Minkowski's expression.

Anisotropic matter

This situation is analogous to the preceding one so we shall not go into detailed considerations. We may *choose* the stress tensor to be given by (1.5 a) also in this case, in accordance with the dipole model from section 3. By using the same argument as before, we find that the energy flux and momentum density of the field are given by (6.2) and (6.3). The four-force density f'_μ derived from this preliminary energy-momentum tensor is given by $\boldsymbol{f}' = (1/c)(\partial/\partial t)(\boldsymbol{D} \times \boldsymbol{B} - \boldsymbol{E} \times \boldsymbol{H})$, $f'_4 = 0$, when no charges or currents are present. Then we suppose that this force excites a mechanical momentum

density $(1/c)(\boldsymbol{D} \times \boldsymbol{B} - \boldsymbol{E} \times \boldsymbol{H})$ which travels together with the field. Including this quantity in the energy-momentum tensor, we obtain finally Minkowski's tensor as given by (1.5). That $S_{k4}^M \neq S_{4k}^M$ corresponds to the fact that the small motion of matter particles is not taken into account, while the asymmetry of the spatial components S_{ik}^M is connected with torques.

7. On the Microscopical Method of Approach

Even though we are concerned mainly with the phenomenological theory and in the preceding section employed an intermediate method, we shall here mention some papers where more or less microscopical theories have been developed.

First, we refer to the treatment of Tang and Meixner[14]. This method is not purely microscopical, and the main idea is rather similar to that we presented above. The authors make use of the total energy momentum tensor written in a form given earlier by Kluitenberg and de Groot[15], and examine the excitation of matter set up by a plane electromagnetic wave travelling in a fluid. From the differential conservation equations they obtain an expression for the velocity variations and hence evaluate the total energy-momentum tensor in a form where the oscillating terms are shown explicitly. On a time average the formal results are compatible with the results we earlier obtained. We should perhaps point out, however, that in spite of the formal completeness of the method one should in addition use experimental results to get information about the average velocity of matter in the original rest frame. For instance, in the frame where the constituent particles have no mean motion, one ends up with $S_{\mu\nu}^A$ plus the tensor corresponding to the rest mass properties of the medium as the total one.

Next, we shall take up a question which has led to one of the strongest arguments in favour of a symmetrical tensor: The macroscopical tensor $S_{\mu\nu}$ should be derivable from the corresponding symmetric, microscopical tensor $s_{\mu\nu}$ by averaging over appropriate regions in space-time, and should thus maintain its symmetry property. This argument was originally given by Abraham[16], and his view seems to have been supported by several physicists (i. e. Landau and Lifshitz[4], Pauli[17]).

But it can be seen that averaging procedures do not make difficulties for Minkowski's theory. Consider a limited electromagnetic field within an insulator; by averaging over space-time elements, we obtain for the torque density in component form $- \overline{x_i \partial_\nu s_{k\nu}} + \overline{x_k \partial_\nu s_{i\nu}}$. Comparing with the corresponding torque calculated from the macroscopical tensor, we get

$$- \bar{x}_i \partial_\nu S_{k\nu} + \bar{x}_k \partial_\nu S_{i\nu} + S_{ik} - S_{ki} = - \overline{x_i \partial_\nu s_{k\nu}} + \overline{x_k \partial_\nu s_{i\nu}}. \qquad (7.1)$$

Now introducing the dipole model in charge-free homogeneous regions of the anisotropic body, (7.1) reduces to

$$S_{ik} - S_{ki} = - \overline{x_i \partial_\nu s_{k\nu}} + \overline{x_k \partial_\nu s_{i\nu}}. \qquad (7.2)$$

The right hand side of (7.2) is not necessarily equal to zero, therefore S_{ik} is not equal to S_{ki} in general. This result is what we might have expected; while it is sufficient to regard the macroscopical tensor to be given by the averaged microscopical one in regard to *linear* quantities (forces), this consideration is insufficient in regard to *second order* quantities such as torques. We have $f_i = -\partial_\nu S_{i\nu} = -\partial_\nu \overline{s_{i\nu}}$, but $\overline{s_{i\nu}}$ cannot express that the microscopical forces act at different points within a dipole. However, $S_{\mu\nu}$ must take into account the macroscopical effects arising also from this fact.

The above reasoning is mainly the same as that carried out by Ig. Tamm (see ref. 1, § 75).

Then we shall consider to some extent the recent series of papers by DE GROOT and SUTTORP[18]. These papers represent presumably the most extensive microscopical treatment of the problem that has appeared. The advantage of a purely microscopical method is that one obtains expressions for the *total* energy-momentum tensor, the sum of the electromagnetic and the mechanical part. DE GROOT and SUTTORP give two expressions for the electromagnetic energy-momentum tensor, both of which are different from Minkowski's tensor. They claim that Minkowski's tensor (and also Abraham's tensor) cannot be justified from a microscopical point of view. Their first proposal, obtained by means of statistical arguments, reads in the momentary rest system of matter, if the body is a fluid,

$$S_{ik} = - E_i D_k - H_i B_k + \delta_{ik}(\tfrac{1}{2} E^2 + \tfrac{1}{2} B^2 - \boldsymbol{M} \cdot \boldsymbol{B}) \qquad (7.3\,\mathrm{a})$$

$$S_{4i} = S_{i4} = i(\boldsymbol{E} \times \boldsymbol{H})_i \qquad (7.3\,\mathrm{b})$$

$$S_{44} = - \tfrac{1}{2}(E^2 + B^2), \qquad (7.3\,\mathrm{c})$$

where these terms have been extracted from the expression for the total tensor. But we have to point out that this is not primarily a *derivation* of the electromagnetic tensor, it is a *choice*. There is no a priori reason to take out just these terms and consider them as constituting the electromagnetic tensor, even though it seems to be the simplest choice from a formal point of view. For the macroscopical fields are contained also in the remaining

terms of the total tensor, although they are there mixed up with mechanical quantities. This ambiguity of splitting is inherent in any microscopical theory. DE GROOT and SUTTORP claim that in a macroscopical treatment, in which the material tensor is not determined, the problem is to a large extent undetermined. We agree that there is an ambiguity present in the macroscopical theory—the problem is to some extent a matter of convenience—but we must point out that this ambiguity is not removed upon transition to the microscopical theory.

DE GROOT and SUTTORP also employ thermodynamic methods and give another form for the electromagnetic tensor which includes the whole interaction between field and matter, i. e., it is equal to the total tensor, minus the mechanical tensor in the absence of macroscopical fields. This tensor is interesting since it is closely connected with the result we obtained macroscopically. (The stress tensor obtained in section 3 was based on the free energy (3.1) in the electrostatic case, and this quantity certainly contains the whole interaction between field and matter since it is equal to the work exerted in building up the field.) Actually, this result is compatible with Minkowski's tensor, if one ignores the dependence of the material constants on the density and temperature, as we have done in our investigation, and one employs our former interpretation concerning the moving dipoles in K^0. For in the frame where the matter has no mean motion, their tensor agrees with Minkowski's tensor, except for terms involving gradients of the material constants, and except for the momentum components which are given as $S_{i4} = i(\boldsymbol{E} \times \boldsymbol{H})_i$. If we then go over to the original rest frame K^0 and add the contribution to the momentum from the small motion of the constituent particles in K^0, we obtain Minkowski's tensor. The corresponding contribution to the energy flux is included in the mechanical tensor.

Summing up these remarks, we think that the microscopical theory, involving a derivation of the total energy-momentum tensor, is an interesting and very complete treatment of the problem. Both the macroscopical and the microscopical method imply certain ambiguities, the first one because the mechanical tensor is not determined in this way, the second one because the splitting of the total tensor is not unique. However, if the task is to determine the electromagnetic tensor which is most convenient and therefore ought to be used, we think that the macroscopical method is both effective and by far the simplest method, if one in addition takes into account the experimental results.

Finally, we mention some microscopical treatments in which only the field part of the total energy-momentum tensor has been derived. H. OTT[19]

made an attempt to deduce the macroscopical electromagnetic tensor (assumed to be symmetric) by averaging over the microscopical quantities and imposing the subsidiary condition that, for an optical field, the four-component of force f_4 should be zero. Further, DÄLLENBACH[20] made use of the electron theory to give a covariant derivation of the electromagnetic tensor. He obtained Minkowski's tensor as the result. These different results reflect characteristic ambiguities that are encountered, and we shall not go into further details.

IV. Further Developments, Connected with Relativity Theory

This chapter contains extensions and applications of results that have been obtained up till now. In particular, we shall be interested to demonstrate explicitly the characteristic features that are encountered when Minkowski's tensor is used. Thus we shall consider both specific examples and more deductive procedures which are intimately connected with Minkowski's tensor. These topics have been rather extensively studied in the literature. In this chapter we consider isotropic media only.

8. The Canonical Energy-Momentum Tensor

The Lagrangian and the Hamiltonian formalisms in special relativity are frequently used in order to find the energy-momentum tensor of some system. Let us apply this kind of method to the situation where an isotropic and homogeneous medium, containing a radiation field, is moving with the uniform four-velocity V_μ. We may start from Noether's theorem, which here can be written

$$\frac{\partial}{\partial x_\nu}\left[\left(L\delta_{\mu\nu} - \frac{\partial L}{\partial A_{\alpha,\nu}}A_{\alpha,\mu}\right)\delta x_\mu + \frac{\partial L}{\partial A_{\alpha,\nu}}\delta A_\alpha\right] + \frac{\partial L}{\partial V_\mu}\delta V_\mu = 0. \qquad (8.1)$$

Here A_μ is the electromagnetic four-potential, and $A_{\alpha,\nu} = \partial_\nu A_\alpha$. Further, L is the Lagrangian density, which we choose as

$$L = -\tfrac{1}{4}F_{\mu\nu}H_{\mu\nu} = -\frac{1}{4\mu}F_{\mu\nu}F_{\mu\nu} + \frac{\varkappa}{2\mu}F_\mu F_\mu. \qquad (8.2)$$

$H_{\mu\nu}$ is the tensor defined in section 1; the covariant relation between $H_{\mu\nu}$ and $F_{\mu\nu}$ is

$$\mu H_{\mu\nu} = F_{\mu\nu} + \varkappa(F_\nu V_\mu - F_\mu V_\nu), \tag{8.3}$$

where $\varkappa = (\varepsilon\mu - 1)/c^2, F_\mu = F_{\mu\nu}V_\nu$. It can readily be verified that the variational equations

$$\frac{\partial L}{\partial A_\mu} - \frac{\partial}{\partial x_\nu} \frac{\partial L}{\partial A_{\mu,\nu}} = 0 \tag{8.4}$$

with L inserted from (8.2) lead to Maxwell's equations. In the derivation of (8.1), eqs. (8.4) have been used. For a derivation of Noether's theorem in general see, for instance, the review paper by E. L. Hill[21].

The δ-quantities in (8.1) refer to infinitesimal symmetry transformations of coordinates and dependent variables, i. e. the field equations must be unchanged in form under the transformations. Employing the infinitesimal translation in four-space $x'_\mu = x_\mu + \delta x_\mu, \delta x_\mu = \text{const}$ as a symmetry transformation, we obtain from (8.1), since δA_μ and δV_μ vanish

$$\partial_\nu S^{\text{can}}_{\mu\nu} = 0, \tag{8.5a}$$

where
$$S^{\text{can}}_{\mu\nu} = L\delta_{\mu\nu} - \frac{\partial L}{\partial A_{\alpha,\nu}} A_{\alpha,\mu} \tag{8.5b}$$

is the canonical energy-momentum tensor. By means of (8.2) we then find

$$S^{\text{can}}_{\mu\nu} = H_{\nu\alpha}A_{\alpha,\mu} - \tfrac{1}{4}\delta_{\mu\nu}F_{\alpha\beta}H_{\alpha\beta}. \tag{8.6}$$

This tensor is neither symmetric nor gauge-invariant. In order to eliminate gauge-dependent quantities we may add $H_{\alpha\nu}A_{\mu,\alpha}$ on the right hand side of (8.6), whereby we obtain Minkowski's tensor. The additional term is divergence-free, and does not influence the conserved four-momentum obtained from $S^{\text{can}}_{\mu\nu}$. (When $\varkappa = 0$ the electromagnetic field becomes a *closed* system, and in that case the additional term may be found by means of the well known field theoretical symmetrization procedure, due originally to Belinfante[22] and Rosenfeld[23].)

It is thus apparent that Minkowski's tensor readily adjusts itself to the canonical procedure. We have to emphasize, however, that the foregoing procedure does not determine Minkowski's tensor uniquely. One of the reasons is that the Lagrangian density (8.2) corresponds to a non-closed system and thus we have, from a formal point of view, no initial information as to whether the four-force density vanishes or not. *If* we demand that the force density shall vanish, then Minkowski's tensor is the simplest result

emerging from the formalism. But this tensor is still not determined uniquely, since there is no a priori reason that only the field quantities be present in the electromagnetic tensor. Terms involving the material constants ε and μ and the four-velocity V_μ may be present, and still the tensor may be divergence-free.

We mention that some interest has been given to the problem of how to make use of the phenomenological Lagrangian methods sketched above and then construct the Lagrangian and energy-momentum tensor for the *total* system, matter plus field. We may refer to a paper by SCHMUTZER[24], who as a result claimed Minkowski's tensor to be preferred for the field. It is obvious, however, that the same kind of ambiguity in the formalism is encountered here as in the microscopical theory we remarked upon in section 7: One does not know which division of the total tensor into electromagnetic and mechanical parts should be chosen. One ought to have some information from experiments in simple physical cases in order to make a convenient choice.

Finally we mention that the problem of constructing the total energy-momentum tensor is encountered also in magnetohydrodynamics, a field that seems to have attracted considerable interest during the last years. These works are carried out on a phenomenological level. Now the mechanical energy-momentum tensor for the fluid, in the absence of a field, is symmetric. If Minkowski's tensor is chosen for the field, as is often the case, one then has to add an "interaction" tensor in order to make the total tensor symmetric. See the papers by PICHON[25], PHAM MAU QUAN[26] and RANCOITA[27].

9. Transformation of the Velocity of the Energy in a Light Wave. Two experiments

Consider a plane light wave within an isotropic and homogeneous insulator moving with the uniform four-velocity V_μ in the reference frame K. One defines the so-called ray velocity $\boldsymbol{u}$ as the velocity of propagation of the light energy. It is known that, similarly as in the case of an anisotropic body at rest, one has to distinguish between the ray velocity and the phase velocity. For an electromagnetic field in the vacuum, the ray velocity and phase velocity become in general equal. They are equal also in the presence of an isotropic medium in the special case when the medium is at rest, or, more generally, when the ray is parallel to the direction of the motion of the medium.

It is shown in Møller's book [1] that the ray velocity transforms like the velocity of a material particle. He starts with the following equation for the wave front of a spherical wave in K^0 being emitted from the origin at the time $t^0 = 0$:

$$r^{02} - \frac{c^2}{n^2} t^{02} = 0. \tag{9.1}$$

Further—and that is a crucial point—the corresponding equation for the wave front in K is found by means of the usual *point transformations* of each term in (9.1). That means that the world lines of the propagating wave are assumed to remain invariant in four-space upon a Lorentz transformation. From theoretical considerations there seems to be no cogent reason that nature really should conform to this assumption (it has sometimes been claimed that if a particle travels in the light in one inertial frame it will stay in the light also in another frame, but obviously this can be true only *if* the ray velocity transforms like the particle velocity). However, if we again invoke *experimental* results, such as those obtained in the Fizeau experiment described below, we find that the considered transformation property of the ray velocity actually is verified in simple physical situations. We shall see that this circumstance establishes a simple criterion which an electromagnetic energy-momentum tensor ought to fulfil, in order to be convenient.

Let $S_{\mu\nu}$ be an electromagnetic tensor which shall describe the travelling wave. Since $\boldsymbol{u}$ is defined as the velocity of propagation of the wave energy, we have $u_i = icS_{4i}/S_{44} = S_i/W$. This velocity transforms like a particle velocity if and only if the quantities

$$U_\mu = \left(\frac{\boldsymbol{u}}{\sqrt{1 - u^2/c^2}}, \frac{ic}{\sqrt{1 - u^2/c^2}} \right) \tag{9.2}$$

constitute a four-vector. By performing an infinitesimal Lorentz transformation $x'_\mu = x_\mu + \omega_{\mu\nu}x_\nu$ between two inertial frames K and K', Møller [1] has shown that U_μ transforms like a four-vector between these systems when

$$R_{\mu\nu} \equiv S_{\mu\nu} + \frac{1}{c^2} S_{\mu\alpha} U_\alpha U_\nu \tag{9.3}$$

vanishes in K. Since a finite Lorentz transformation may be composed of infinitesimal transformations, the equation $R_{\mu\nu} = 0$ is a general condition

that $S_{\mu\nu}$ must satisfy in order that $\boldsymbol{u}$ shall have the required transformation property.

It is easily seen that it is sufficient to examine $R^0_{\mu\nu}$ in K^0.

Møller shows that $R^0_{\mu\nu} = 0$ with Minkowski's tensor, when the most general solution of the field equations representing a plane wave in K^0 is inserted. This feature means that Minkowski's tensor gives an adequate description of the velocity of the energy in a light wave in any inertial system.

Similar conclusions have been drawn by several authors. The subject was first treated long ago by Scheye [28]. It was elaborated by von Laue and published in a paper in 1950 [29]. Another treatment was worked out, independently and almost simultaneously, by Møller, and published in his book in 1952 [1]. We may refer also to a paper by Schöpf [30]. It has been shown by Manarini [31] that $\boldsymbol{u}$ given by Minkowski's tensor transforms like a particle velocity also within anisotropic media.

Fizeau's experiment

Assume that the ray travels parallel to the direction of motion of the medium. By using Minkowski's tensor, or simply by transforming the ray velocity $\boldsymbol{u}$, we find in K, to the first order in v/c,

$$u = \frac{c}{n} + v\left(1 - \frac{1}{n^2}\right), \tag{9.4}$$

where the expression in the parenthesis is Fresnel's dragging coefficient.

Fizeau checked the formula (9.4) experimentally. He used a two-beam interferometer with moving water in the beam path. The phase difference between the two beams was measured and was found to be in agreement with the result predicted on the basis of (9.4). Zeeman even verified the dispersion correction term to the formula (9.4). For a more detailed description of the experiment, and for references to the original literature, see § 8 in Møller's book [1].

[*Note added in the proof:* It has recently come to our attention that this kind of experiment has recently been repeated by W. M. Macek, J. R. Schneider, R. M. Salamon, Journ. Appl. Phys. **35**, 2556 (1964). The authors made use of a ring laser in order to measure the phase difference between the waves, thereby improving the sensitivity by several orders of magnitude. The dragging coefficient was measured in both a solid, a gaseous

medium and a liquid, and especially in the two first cases the agreement with the expression $(1 - 1/n^2)$ was found to be good.]

In a paper[14] which we also referred to in section 7, TANG and MEIXNER constructed an expression for the total energy-momentum tensor and also examined the transformation criterion of VON LAUE and MØLLER in connection with a physical interpretation of the various terms in this tensor. Recently, DE GROOT and SUTTORP[18] claimed that TANG and MEIXNER in this paper actually invalidated the transformation criterion. We cannot, however, agree with this statement. At least in the simple situation considered here the mentioned transformation property of the ray velocity u is verified *experimentally*; further, the relation $u = S/W$ ought to be valid for an electromagnetic tensor which shall describe the total light wave.

A Sagnac-type experiment

In a recent paper HEER, LITTLE and BUPP[32] reported an experiment involving the propagation of light through dielectric media in an accelerated system of reference. This is thus a kind of generalization of the Fizeau experiment, which involved inertial systems only. Let us sketch some important features of this new experiment.

The apparatus is a triangular ring laser as shown in Fig. 1. L is a gas laser which gives rise to two travelling electromagnetic waves in the cavity, one circulating clockwise and the other counterclockwise. When the system is at rest the photon frequencies in the two wave modes are equal. Then imagine that the cavity is set into rotation with an angular velocity Ω, such that the direction of Ω is perpendicular to the cavity plane shown in the figure. The photon frequencies of the two beams now become different from each other; the beams interfere to produce beats which are counted at the detector D. This rotation-dependent frequency shift is called the Sagnac effect (see the review paper by POST[33]). If a dielectric medium F is placed in the light path, the effect will depend on the geometry of the medium and on the velocity of light inside it, and will hence be connected with the electromagnetic energy-momentum tensor. This connection can be expressed in mathematical form as follows[34]. The energy density W for one of the modes in the cavity frame is related to the energy density W^0 for this mode in an instanteneous inertial rest frame by

$$W = W^0 + \frac{1}{c} \Omega \cdot [r \times (E \times H)]. \tag{9.5}$$

Only effects to the first order in Ω are investigated, so that the fields in (9.5) may be evaluated for $\Omega = 0$. Within this approximation the integral $H =$
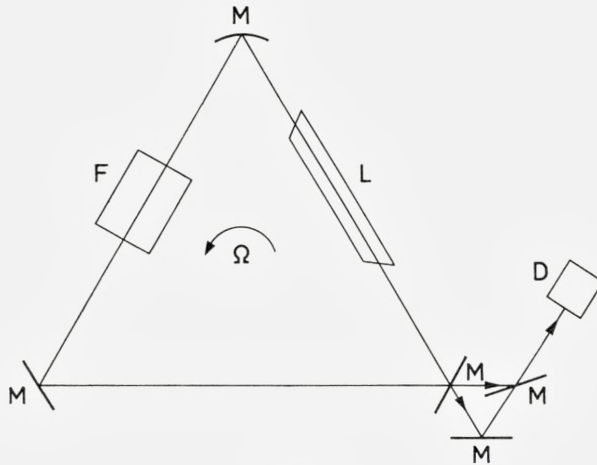
Fig. 1.

$\int W dV$, taken over the volume of the field, is a conserved quantity. Further, the integral of W^0 over the volume is the same for the two modes, so we obtain for the relative frequency shift

$$\Delta \nu / \nu = \Delta H / H =$$
$$= (4/c)[\Omega \cdot \int \mathbf{r} \times (\mathbf{E} \times \mathbf{H}) dV] \left[\int (\mathbf{E} \cdot \mathbf{D} + \mathbf{H} \cdot \mathbf{B}) dV \right]^{-1}. \quad \Bigg\} \quad (9.6)$$

Considering the beam as a plane wave with a small cross section, we obtain from (9.6)

$$\Delta \nu / \nu = (4 \Omega A / c) \left[\int (n + \nu dn/d\nu) dl \right]^{-1}, \quad (9.7)$$

where A is the area enclosed by the light path and dl the line element along the light path. In (9.7) also the correction from the dispersion has been included. The frequency shift $\Delta \nu$ is simply equal to the number of beats counted per unit time.

The material medium F in the beam path was chosen as pairs of quartz plates at anti-parallel Brewster angles. The value of the integral in (9.7) could thus be varied by varying the number of pairs. In order to eliminate the influence from the rotation of the Earth, one had to take the mean of the results obtained by rotating the cavity in the clockwise and in the counterclockwise direction. The agreement between the observed data and the results obtained on the basis of (9.7) was excellent.

As a conclusion, we find that both the JONES-RICHARDS experiment con-
sidered in section 6 and the two experiments considered in this section are
explained on the basis of Minkowski's tensor in a very simple way[1]. And
this is the main reason why we consider Minkowski's tensor to be con-
venient for the description of optical phenomena.

10. Negative Energy. Remarks on the Čerenkov Effect

Negative energy

By making use of Minkowski's tensor we find that the electromagnetic
field energy becomes negative under certain circumstances, and this fact
has caused difficulties for the acceptance of this tensor. We shall show that
such a behaviour is a consequence of the way in which the covariant theory
is constructed.

Consider a plane electromagnetic wave which moves along the x-axis
within an isotropic and homogeneous insulator with index of refraction
denoted by n. If W^0 is the field energy density in the rest frame K^0 of the
body and $v = v_1 = c\beta$ the velocity of K^0 with respect to an inertial frame K,
we find that Minkowski's energy density in K is

$$W^M = \gamma^2(1 + n\beta)(1 + \beta/n)W^0. \tag{10.1}$$

From this expression it follows that $W^M < O$ when $\beta < -(1/n)$.

This feature is, however, connected with the fact that the rest mass
quantities of the medium have been excluded from $S_{\mu\nu}^M$. For the tensor
$\Theta_{\mu\nu}$ introduced in (6.9) has the only non-vanishing component $\Theta_{14}^0 = icg_1^{\text{mech } 0}$
$= i[(n^2 - 1)/n]W^0$ in K^0, which means that in K

$$-\Theta_{44} = \beta\gamma^2[(n^2 - 1)/n]W^0. \tag{10.2}$$

Hence, the contribution to the energy density is negative when β is negative.

For illustration, let us consider the following analogous situation from
mechanics: A material particle with four-momentum $p_\mu = (\boldsymbol{p}, iE/c)$ moves
uniformly along the x-axis and is considered in two frames K and K', where
K' moves with the velocity v with respect to K. Then $E = \gamma(vp' + E')$ and
is of course positive; but by ignoring E', we obtain $E < 0$ when $v < 0$, pro-
vided $p' > 0$. This is the same effect as encountered above. For a material
particle ignoring E' is of course impossible, since we know the relations
between $\boldsymbol{p}, E$ and $\boldsymbol{p}', E'$ from the Lorentz transformation and the principle

---

[1] As we shall see later, the two first of these experiments represent a more critical test than
the last one.

of covariance (cf. § 26 in MØLLER's book [1]), and thus we have only to find that combination $p_\mu = (\boldsymbol{p}, iE/c)$ which makes up a four-vector. But the covariant phenomenological electrodynamics is achieved by *choosing* appropriate four-vectors and tensors which in K^0 are coincident with already established quantities, such as the four-force density. In the picture corresponding to Minkowski's tensor we include the mechanical momentum density $\boldsymbol{g}^{\text{mech }0}$ into the electromagnetic tensor, but not the quantities $\boldsymbol{S}^{\text{mech }0}$ and $W^{\text{mech }0}$. By requiring covariance of this picture, we obtain a space-like, total four-momentum G_μ^M of the field. Therefore, by means of proper Lorentz transformations, we can find inertial frames where the field energy is negative.

The Čerenkov effect

This effect offers an interesting application of Minkowski's theory. We shall suppose that an electron moves along the x-axis with a uniform velocity which in K^0 is larger than c/n, the light velocity in the medium. And we shall consider the process in the inertial frame K where the electron is at rest. In this frame we find that the fields are stationary, and that $\boldsymbol{H} = 0$ [35]. Let us then integrate the differential conservation laws over a volume which contains the electron and which is enclosed by a cylindric surface S of small radius and infinite length such that the axis of the cylinder coincides with the x-axis. As $\boldsymbol{H} = 0$, the energy flow through S vanishes; the field energy does not change, and the work exerted by the electromagnetic force on the electron is zero.

Then examine the momentum balance. Unlike the energy flow the momentum flow is different from zero [35], and the momentum transport through S corresponds to a force on the electron in K. This is again a characteristic consequence of the peculiar construction of Minkowski's momentum density in K^0. The momentum balance in K reads

$$\int S_{ik}^M n_k \, dS = -\int f_i^M dV, \tag{10.3}$$

where the force components on the right hand side are readily obtained in K by transforming Minkowski's force from K^0.

We shall return to this situation in the next paper, in connection with Abraham's tensor.

11. Angular Momentum

We begin with some general remarks in connection with the application of Noether's theorem as given by (8.1). By employing the infinitesimal Lorentz transformation $\delta x_\mu = \omega_{\mu\nu} x_\nu$ as a symmetry transformation in (8.1), we obtain (isotropic media assumed)

$$\frac{\partial M_{\mu\nu\sigma}}{\partial x_\sigma} + \frac{\partial L}{\partial V_\alpha} I_{\nu\mu}^{\alpha\beta} A_\beta = 0, \tag{11.1}$$

where

$$M_{\mu\nu\sigma} = x_\mu S_{\nu\sigma}^{\text{can}} - x_\nu S_{\mu\sigma}^{\text{can}} + \frac{\partial L}{\partial A_{\alpha,\sigma}} I_{\nu\mu}^{\alpha\beta} A_\beta \tag{11.2}$$

and

$$I_{\nu\mu}^{\alpha\beta} = \delta_{\nu\alpha} \delta_{\mu\beta} - \delta_{\nu\beta} \delta_{\mu\alpha}. \tag{11.3}$$

$S_{\mu\nu}^{\text{can}}$ is given by (8.5 b).

If we interpret $M_{\mu\nu\sigma}$ to be connected with the field angular momentum $M_{\mu\nu}$ by

$$M_{\mu\nu} = \frac{1}{ic} \int M_{\mu\nu\,4} \, dV, \tag{11.4}$$

then it can be easily verified that (11.4) is equivalent to $M_{\mu\nu}^M$ obtained from (1.6) with Minkowski's tensor inserted.

From (11.2) we obtain a coordinate-dependent part of angular momentum

$$L_{ik}^M = \int (x_i g_k^{\text{can}} - x_k g_i^{\text{can}}) \, dV = \frac{i}{c} \int \frac{\partial L}{\partial A_{\alpha,4}} (x_i \partial_k - x_k \partial_i) A_\alpha \, dV \tag{11.5}$$

and a coordinate-independent part

$$\Sigma_{ik}^M = \frac{1}{ic} \int \frac{\partial L}{\partial A_{\alpha,4}} I_{ki}^{\alpha\beta} A_\beta \, dV. \tag{11.6}$$

Inserting L from (8.2), we find

$$L_{ik}^M = \frac{1}{c} \int \mathbf{D} \cdot (x_i \partial_k - x_k \partial_i) \mathbf{A} \, dV \tag{11.7}$$

$$\Sigma_{ik}^M = \frac{1}{c} \int (D_i A_k - D_k A_i) \, dV. \tag{11.8}$$

Let us then apply the theory to the physical situation in which a plane, monochromatic wave with wave vector $\boldsymbol{k}$ travels within a homogeneous and isotropic insulator moving with the velocity v in the x-direction. A proper discussion of the expressions (11.7) and (11.8) ought to be made in a quantal treatment, but the following general remarks may be made.

As indicated in (1.7), the quantities M_{ik}^M are in general not conserved. It can be shown in the present case that this non-conservation is due to the part L_{ik}^M, while the contribution from $\sum_{ik}^M$ fluctuates away.

It is known that for an electromagnetic field in the vacuum we can in the Coulomb gauge ($A_4 = 0$) interpret (11.7) as the orbital angular momentum, since this part is independent of the polarization of the photons. Similarly, we obtain for $\varkappa = (n^2 - 1)/c^2 > 0$ that the constant part of L_{ik}^M is polarization independent if we use the gauge in K^0 in which $A_4^0 = 0$. If $k_l = 0$ ($l = 2,3$) or $v = 0$, then all quantities M_{ik}^M, L_{ik}^M and $\sum_{ik}^M$ are conserved. In this case L_{ik}^M is polarization independent and is thus interpreted as orbital angular momentum, while $\sum_{ik}^M$ is interpreted as the spin part.

We can verify that $\sum_{\mu\nu}^M$ is not a tensor, except in the special case $k_l = 0$ when the total angular momentum also is a tensor. In an electromagnetic field in the vacuum $\sum_{\mu\nu}$ is a tensor only when $k_l = 0$; however, when $\varkappa = 0$, $M_{\mu\nu}$ is a tensor.

12. Centre of Mass

Consider in K^0 a bounded radiation field, whose interior domain can be taken as a part of a plane monochromatic wave with wave vector $\boldsymbol{k}^0$. Only in a small boundary layer the fields are assumed not to obey the usual plane wave relations, and this boundary layer is further assumed to contain negligible field energy or momentum.

Then let K^0 move with respect to K with the velocity v along the x-axis, and examine the behaviour of the centre of mass in K with coordinates $\boldsymbol{X}(K)$. Taking into account that the field is bounded and that the total field energy $\mathscr{H}^M$ is conserved, we find

$$\frac{d}{dt}X_i^M(K) = \frac{d}{dt}\left(\frac{1}{\mathscr{H}^M}\int x_i W^M dV\right) = \frac{1}{\mathscr{H}^M}\int S_i^M dV. \tag{12.1}$$

Since the field is homogeneous,

$$d/dt\, X_i^M(K) = S_i^M/W^M = u_i, \tag{12.2}$$

where u_i has been found to transform like the component of a particle velocity. Strictly speaking, Møller's mathematical treatment referred to in section 9 was based on a point transformation, while (12.2) in general refers to different space-time points in two reference frames; however, this does not matter since $\boldsymbol{u}$ is constant along a world line.

We obtain then for the wave under consideration

$$\frac{d}{dt} X_1^M(K) = c\frac{n\beta + k_1^0/k^0}{n + \beta k_1^0/k^0} \tag{12.3a}$$

$$\frac{d}{dt} X_l^M(K) = c\frac{k_l^0/k^0}{\gamma(n + \beta k_1^0/k^0)} \quad (l = 2,3). \tag{12.3b}$$

Here $k^0 = |\boldsymbol{k}^0|$. When $k_1^0 = k^0$, $\beta = -1/n$, K is identical with the rest system K^* of the wave, wherein Poynting's vector and the energy density both vanish in such a way that the quotient (12.3a) also vanishes. If $k_1^0 = k^0$, $\beta < -1/n$, then $S_1^M > 0$, $W^M < 0$, $dX_1^M(K)/dt < 0$.

Investigation of the various mass centres

For a physical system in general, it is known that the different centres of mass we obtain by varying the reference frames K, do not necessarily coincide when considered simultaneously in one frame. We refer to a paper by MøLLER[36], in which it was shown that different positions may occur in the case of a *closed* system possessing angular momentum in its own rest frame (see also ref. 1). Such a closed system is in many ways similar to our radiation field, so that we wish to study this point. To avoid complicated notation, the superscript M shall be omitted in the following.

Since the rest frame K^0 plays a distinguished role we may call the centre of mass $\boldsymbol{X}(K^0)$ in this frame the proper centre of mass. Further, let the space-time coordinates of the *proper* centre of mass in any K be denoted by $X_\mu = (\boldsymbol{X}, X_4)$, so that $\boldsymbol{X}(K^0) \equiv \boldsymbol{X}^0$ in K^0. From the transformation properties of $\boldsymbol{u}$ it is apparent that all possible centres of mass have the same velocity $d\boldsymbol{X}/dt$ in any frame.

Let $m_{\mu\nu}$ represent the four-angular momentum components relative to the proper centre

$$m_{\mu\nu} = \int [(x_\mu - X_\mu)g_\nu - (x_\nu - X_\nu)g_\mu]dV = M_{\mu\nu} - (X_\mu G_\nu - X_\nu G_\mu). \tag{12.4}$$
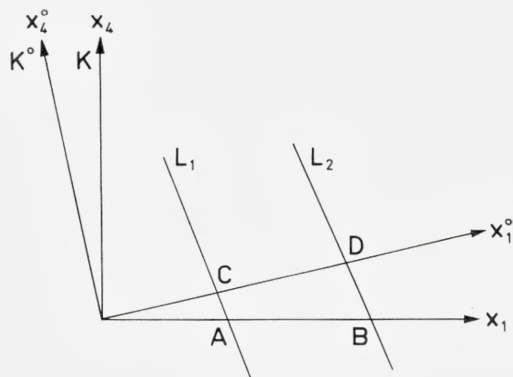
Fig. 2.

By differentiating the expression for $M_{\mu\nu}$ with respect to time along the moving wave elements where $d(g_\mu dV)/dt = 0$, we find that $dM_{\mu\nu}/dt = dx_\mu/dt \cdot G_\nu - dx_\nu/dt G_\mu$. Thus it follows that $dm_{\mu\nu}/dt = 0$ in any frame.

The difference $X_i(K) - X_i$ between simultaneous mass centres is in general related to m_{i4}:

$$m_{i4} = \frac{i}{c}\int (x_i - X_i)WdV = \frac{i}{c}[X_i(K) - X_i]\mathscr{H}. \tag{12.5}$$

Now the quantities $M_{\mu\nu}$ do not constitute a tensor. This follows from the fact that the quantities

$$\partial_\sigma(x_\mu S_{\nu\sigma} - x_\nu S_{\mu\sigma}) = S_{\nu\mu} - S_{\mu\nu} \tag{12.6}$$

in general do not vanish. (The detailed investigation of the tensor property of $M_{\mu\nu}$ goes similarly as the investigation of the four-vector property of G_μ, see § 63 of MØLLER's book [1].) Thus $m_{\mu\nu}$ cannot be obtained in K by a tensor transformation from K^0. This is a fundamental difference from the situation encountered for a closed system.

In order to find the actual coordinate difference we thus have to make an explicit calculation of the integrals in (12.5). In Fig. 2, L_1 and L_2 represent the cut with the $x_1 x_4$-plane of a three-dimensional surface enclosing the field. Since $m_{\mu\nu}$ is a constant of motion, we choose to evaluate it in K at $t = 0$, i. e. along AB. Actually, we have to consider in detail only the first integral ($= M_{i4}$) in (12.5), for the second integral is equal to $-X_i G_4$ and G_4 is a component of a four-vector. We find readily

$$x_1(AB) = \gamma^{-1}x_1^0(AB), x_2(AB) = x_2^0(AB), x_3(AB) = x_3^0(AB), \tag{12.7}$$

and $W(AB)$ is related to the components $S^0_{\mu\nu}(AB)$ by a tensor transformation. Now seek to transform the integral over AB into an integral taken at constant time in K^0, and choose the domain CD for which $t^0 = 0$. This task can readily be accomplished for the internal, *plane* part of the radiation field. To this end we first observe that the world lines determined by S will each intersect AB and CD in two space-time points with coordinates $(x^0_i(AB), t^0(AB))$ and $(x^0_i(CD), 0)$ in K^0, such that

$$
\left.
\begin{aligned}
x^0_1(CD) &= x^0_1(AB) - \frac{ck^0_1}{nk^0}t^0(AB) = x^0_1(AB)\left(1 + \frac{\beta k^0_1}{nk^0}\right) \\[2mm]
x^0_l(CD) &= x^0_l(AB) - \frac{ck^0_l}{nk^0}t^0(AB) = x^0_l(AB) + \frac{k^0_l}{k_0}\frac{\beta x^0_1(CD)}{n + \beta k^0_1/k^0} \quad (l = 2,3) \\[2mm]
t^0(AB) &= -(\beta/c)x^0_1(AB).
\end{aligned}
\right\}
\quad (12.8)
$$

The volume integration in (12.5) shall be performed along the elements dV which follow the wave. Since the x_1-component of the wave velocity in K^0 is equal to $ck^0_1/(nk^0)$, the volume element dV is related to the corresponding element dV^0 taken at constant time in K^0 by

$$
dV^0/dV = \gamma(1 + \beta k^0_1/(nk^0)). \tag{12.9}
$$

Further, we observe that $S^0_{\mu\nu}(AB) = S^0_{\mu\nu}(CD)$ at corresponding world points. For the internal plane wave part we have also

$$
S^0_{ik} = W^0 k^0_i k^0_k/k^{02}, \quad g^0_i = nW^0 k^0_i/(ck^0). \tag{12.10}
$$

When eqs. (12.7–10) are inserted into the expression for M^{int}_{l4}, i. e. the contribution to M_{l4} from the internal field, we obtain

$$
M^{\text{int}}_{l4} = \frac{i\gamma}{c}\frac{1 + n\beta k^0_1/k^0}{1 + \beta k^0_1/(nk^0)}\left[\int_{\text{int}} x^0_l W^0 dV^0 + \frac{v}{n^2}\int_{\text{int}}(x^0_l g^0_1 - x^0_1 g^0_l)dV^0\right], \tag{12.11}
$$

where the integrations are taken along CD, but only over the internal part of the wave.

Now it is apparent that, in addition to (12.11), we have to take into account also the effect from the thin boundary layer, which is responsible for the internal angular momentum of the field. This is in agreement with the fact that in the case of a *closed* system, the coordinate difference which we are seeking is connected with the total angular momentum in the inertial

frame in which the total linear momentum vanishes. To investigate this boundary effect we introduce, purely formally, a tensor $S_{\mu\nu}^S$ which is defined by the following components in K^0:

$$S_{i\nu}^{S0} = S_{i\nu}^0/n^2, \quad S_{4\nu}^{S0} = S_{4\nu}^0. \tag{12.12}$$

Thus the tensor $S_{\mu\nu}^S$ is symmetric and divergence-free, so that $M_{\mu\nu}^S$ is a tensor (cf. (12.6)). We immediately obtain

$$M_{l4}^S = \frac{i\gamma}{c} \int x_l^0 W^0 dV^0 + i\beta\gamma \int (x_l^0 g_1^{S0} - x_1^0 g_l^{S0}) dV^0 \tag{12.13}$$

by a *tensor* transformation, where the integration domain includes the whole field. If we now calculate the internal part $M_{l4}^{S,\,\text{int}}$ by transforming the integrand similarly as we did above, we find

$$M_{l4}^{S,\,\text{int}} = \frac{i\gamma}{c} \int_{\text{int}} x_l^0 W^0 dV^0 + i\beta\gamma \int_{\text{int}} (x_l^0 g_1^{S0} - x_1^0 g_l^{S0}) dV^0. \tag{12.14}$$

Here we have used eqs. (12.7–9) and the relations

$$S_{ik}^{S0} = W^0 k_i^0 k_k^0/(n^2 k^{02}), \quad g_i^{S0} = W^0 k_i^0/(nck^0), \tag{12.15}$$

which are valid for the internal part. By comparing (12.13) and (12.14) it is thus apparent that the total M_{l4}^S is obtained simply by extending the integration domain in (12.14) over the boundary region, such that g_i^{S0} and W^0 refer to the *total* momentum and energy densities in this region. (Actually, the additional term to the first integral in (12.14) is negligible.) Since g_i^{S0} is proportional to g_i^0, the same rule can be used to evaluate M_{l4} from (12.11), and we get

$$M_{l4} = \frac{i\gamma}{c} \frac{1 + n\beta k_1^0/k^0}{1 + \beta k_1^0/(nk^0)} \left(X_l^0 \mathcal{H}^0 + \frac{v}{n^2} M_{l1}^0 \right). \tag{12.16}$$

By means of (12.7), (12.8) and the transformation formula for $\mathcal{H}$ the last term in (12.5) is found as $(i = l)$

$$-\frac{i}{c} X_l \mathcal{H} = -\frac{i\gamma}{c} \frac{1 + n\beta k_1^0/k^0}{1 + \beta k_1^0/(nk^0)} \left[X_l^0 \mathcal{H}^0 + \frac{v}{n^2} (X_l^0 G_1^0 - X_1^0 G_l^0) \right], \tag{12.17}$$

where we have also used the relation $\boldsymbol{G}^0 = n\mathcal{H}^0 \boldsymbol{k}^0/(ck^0)$. The latter relation follows from the fact that the total linear momentum is obtained by inte-

grating over the internal wave part. Then inserting (12.16), (12.17) into (12.5) and taking (12.4) into account, we find

$$m_{l4} = \frac{i\gamma\beta}{n^2} \frac{1 + n\beta k_1^0/k^0}{1 + \beta k_1^0/(nk^0)} m_{l1}^0.$$ (12.18)

This is a boundary effect. Note that it is not necessary that the integral $\int x_i^0 W^0 dV^0$ over the boundary be taken as small in order to obtain (12.18), but when this boundary term is negligible, the expressions (12.17) and (12.11) are equal to each other, apart from a sign.

It can be verified that $X_i^0 G_1^0 - X_1^0 G_i^0$ is equal to L_{l1}^0 given by (11.7), and so m_{l1}^0 in (12.18) may be replaced by Σ_{l1}^0 given by (11.8).

Hitherto we have considered the cases $i = l = 2, 3$. For $i = 1$ we obtain readily by the same method

$$M_{14} = -\frac{i}{c} \frac{1 + n\beta k_1^0/k^0}{1 + \beta k_1^0/(nk^0)} X_1^0 \mathcal{H}^0,$$ (12.19a)

$$m_{14} = M_{14} - \frac{i}{c} X_1 \mathcal{H} = 0.$$ (12.19b)

By means of (12.5), (12.18) and (12.19) we can thus write the coordinate difference as

$$a(K) = X(K) - X = \frac{v \times \Sigma^0}{n^2(1 + \beta \cdot k^0/(nk^0))\mathcal{H}^0},$$ (12.20)

where Σ^0 is a vector with the components $\Sigma_i^0 = \Sigma_{jk}^0$ (i, j, k cyclic). The form (12.20) is obviously independent of the choice of the velocity vector v as lying along the x_1-axis. Since $a(K)$ is perpendicular to v, it will be left unchanged after a transformation from K to K^0.

Now we can calculate Σ^0 from (11.8) and find readily that $\Sigma^0/\mathcal{H}^0 = nk^0/(ck^{02})$. By inserting this relation into (12.20) we get

$$a(K) = \frac{1}{k^0} \frac{\beta \times k^0}{nk^0 + \beta \cdot k^0}.$$ (12.21)

Let us consider in K^0 the positions of the various centres of mass obtained by varying β and k^0 in (12.21). All centres lie in a plane perpendicular to k^0, and if β, k^0 and $\beta \cdot k^0$ are kept constant the end point of the vector $a(K)$ will draw a circle with centre at the proper centre of mass.

The greatest radius of the circle is obtained when $\boldsymbol{k}^0 \cdot \boldsymbol{\beta} = -k^0\beta^2/n$ and is equal to

$$a_{\max} = (\beta/nk^0)(1 - \beta^2/n^2)^{-\frac{1}{2}}. \tag{12.22}$$

An arbitrary angle between β and $\boldsymbol{k}^0$ will in general lead to a centre of mass lying on the disk described by (12.22).

Permitting β to vary, we see that the greatest value of $a_{\max}$ occurs when $\beta = 1$. Further, $a_{\max} \to \infty$ when $k^0 \to 0$.

Instead of relating all centres of mass to the centre of mass in K^0, as seems to be most natural and as we have done in the present section, one may also relate these centres to the centre of mass in K^*, the frame in which the wave is at rest and the medium moving.

References

1. C. Møller, *The Theory of Relativity* (Oxford, 1952).
2. H. A. Lorentz, Encyklop. Math. Wiss. V^{II}, 13 No 23.
3. E. Pockels, Encyklop. Math. Wiss. V^{II}, 16 No 1.
4. L. Landau and E. Lifshitz, *Electrodynamics of Continuous Media* (Pergamon Press, 1960).
5. E. Durand, *Electrostatique et Magnetostatique* (Masson, Paris, 1953).
6. W. B. Smith-White, Phil. Mag. **40**, 466 (1949).
7. J. A. Stratton, *Electromagnetic Theory* (Mc Graw-Hill, 1941).
8. G. Marx and G. Györgyi, Acta Phys. Hung. **3**, 213 (1954).
9. V. Fock, *The Theory of Space, Time and Gravitation* (Pergamon Press, second edition, 1964).
10. G. Marx and G. Györgyi, Ann. d. Phys. **16**, 241 (1955).
11. A. Einstein and J. Laub, Ann. d. Phys. **26**, 541 (1908).
12. A. Sommerfeld, *Vorlesungen über Theoretische Physik*, bd. IV, § 22 (W. Klemm, Wiesbaden, 1950).
13. (a) R. V. Jones, Nature **167**, 439 (1951);
    (b) R. V. Jones and J. C. S. Richards, Proc. Roy. Soc. **221**A, 480 (1954).
14. C. L. Tang and J. Meixner, Phys. Fluids **4**, 148 (1961).
15. G. A. Kluitenberg and S. R. de Groot, Physica **21**, 169 (1955).
16. M. Abraham, Ann. d. Phys. **44**, 537 (1914).
17. W. Pauli, *Theory of Relativity* (Pergamon Press, 1958).
18. S. R. de Groot and L. G. Suttorp, Physica **39**, 28, 41, 61, 77, 84 (1968). Earlier papers in Physica **37**, 284, 297 (1967).
19. H. Ott, Ann. d. Phys. **11**, 33 (1953).
20. W. Dällenbach, Ann. d. Phys. **58**, 523 (1919).
21. E. L. Hill, Rev. Mod. Phys. **23**, 253 (1951).
22. J. Belinfante, Physica **6**, 887 (1939).
23. L. Rosenfeld, Mem. de l'Acad. Roy. de Belgique **18** No 6 (1940).
24. E. Schmutzer, Ann. d. Phys. **20**, 349 (1957).
25. Guy Pichon, Ann. Inst. Henri Poincaré IIA, 21 (1965).
26. Pham Mau Quan, J. Rat. Mech. Anal. **5**, 473 (1956).
27. G. M. Rancoita, Nuovo Cim. Suppl. XI, 183 (1959).
28. A. Scheye, Ann. d. Phys. **30**, 805 (1909).
29. M. von Laue, Z. Physik **128**, 387 (1950).
30. Hans-Georg Schöpf, Z. Physik **148**, 417 (1957).
31. Anna M. Manarini, R. C. Accad. Naz. Lincei **20** No 3, 357 (1956).
32. C. V. Heer, J. A. Little and J. R. Bupp, Ann. Inst. Henri Poincaré VIIIA, 311 (1968).
33. E. J. Post, Rev. Mod. Phys. **39**, 475 (1967).
34. C. V. Heer, Phys. Rev. **134**, A 799 (1964).
35. Ig. Tamm, Journ. of Phys. USSR **1**, 439 (1939).
36. C. Møller, Ann. Inst. Henri Poincaré XI, 251 (1949).

T. GROTDAL, K. NYBØ AND B. ELBEK

A STUDY OF ENERGY LEVELS IN
ODD-MASS DYSPROSIUM NUCLEI
BY MEANS OF
(*d,p*) AND (*d,t*) REACTIONS

CONTENTS

Synopsis

The energy levels of ^{155}Dy, ^{157}Dy, ^{159}Dy, ^{161}Dy, ^{163}Dy, and ^{165}Dy have been investigated by means of (d,p) and (d,t) reactions. The deuteron energy was 12.1 MeV and the charged reaction products were analyzed in a magnetic spectrograph at angles of observation of $60°$, $90°$, and $125°$. A total of 16 Nilsson orbitals or components thereof were identified on the basis of total cross sections and the intensity patterns for the rotational states. Comparison of the experimental cross sections with those predicted on the basis of DWBA calculations and theoretical wave functions allowed an estimate of the single-particle components in the excited states. Some dependence of the neutron level density on the proton number is evident from comparison with the data for the isotopes of Gd and Er.

1. Introduction

The present study of the energy levels in the odd dysprosium isotopes by means of neutron stripping and pick-up reactions is a continuation of earlier investigations of the energy levels in odd gadolinium[1], erbium[2], and ytterbium[3] nuclei.

As in the earlier experiments, the main result of this type of study is the systematic localization of a large number of neutron single-particle states. The relative simplicity of the spectrum analysis permits localization of such states over a considerably wider span of energy than is generally investigated in decay scheme work. Thus, most of the energy levels below 1 MeV of excitation, which are populated in the neutron transfer reactions, can be given a rather definite single-neutron assignment. At higher energies of excitation, only strong single-particle components can be identified, but it should be noted that, also at lower excitation energies, especially in neutron-deficient nuclei, strong couplings of the various modes of excitation give rise to complicated level structures which as yet have been only partially analyzed.

The level structures of several of the dysprosium isotopes have earlier been subject to a number of decay scheme and reaction studies. Thus, ^{159}Dy has been investigated by Borggreen et al.[4] and ^{161}Dy by Funke et al.[5]. The latter authors have also investigated the ^{163}Dy levels, which furthermore have been studied very completely by Schult et al.[6] who used a number of different nuclear reactions including the (d,p) and (d,t) reactions. Finally, the ^{165}Dy levels have been investigated by several groups[7–10]. The results of these former studies have been of great importance for many of the conclusions drawn in the present work. Additional information about ^{161}Dy and ^{163}Dy was obtained from inelastic deuteron scattering spectra recorded separately[11].

The experimental methods used were the same as those in the earlier investigations[1–3]. The beam of 12.1 MeV deuterons was obtained from the Niels Bohr Institute tandem accelerator and the charged reaction products

1*

were analyzed in a broad range magnetic spectrograph with photographic plate recording. The targets for the investigation were ~ 40 $\mu g/cm^2$ layers of the isotopes directly deposited on ~ 40 $\mu g/cm^2$ carbon foils in the electromagnetic isotope separator at the University of Aarhus.

Absolute spectroscopic factors were obtained from the observed cross sections by comparison with the results of distorted wave Born approximation calculations (DWBA). The calculated cross sections for the dysprosium nuclei were actually the averages of those used for gadolinium[1] and erbium[2] and thus suffer from the same deficiencies as discussed before[2]. The DWBA single-particle cross sections $\sigma_l(\theta)$, defined as in ref. 1, were calculated for a (d,p) Q-value of $+3$ MeV and a (d,t) Q-value of -2 MeV. These Q-values are used as reference values to which all experimental cross sections were reduced before comparison with the theoretical cross sections.

2. Results and Discusssion

A spectrum is shown in Figs. 1–10 for each of the ten different transfer reactions possible with the stable targets ^{156}Dy, ^{158}Dy, ^{160}Dy, ^{162}Dy, and ^{164}Dy. The average level energies and the differential cross sections are listed in Tables 1–6, which also contain the suggested Nilsson assignments for some of the levels. The basis for these assignments will be discussed in detail in the following sections.

2.1. Q-values and Neutron Separation Energies

The ground-state group was easily localized in all the spectra and the ground-state Q-values for the (d,p) and (d,t) reactions were therefore obtained in a straightforward manner. The spectrograph calibration was based on the 6.0498 MeV and 8.7864 MeV α-groups from ^{212}Bi and ^{212}Po, respectively. The Q-values are listed in Table 7 together with the corresponding neutron separation energies. Comparison with the 1964 Mass Table[12] reveals considerable deviations especially for the neutron-deficient isotopes. The agreement with the (d,p) Q-values from the Florida group is satisfactory[6, 7].

2.2. General Features of the Spectra

The analysis of the neutron transfer spectra for the dysprosium isotopes was greatly facilitated by the previous analysis of the spectra for the isotopes in the Gd and Er series of isotopes[1, 2]. There is a considerable regularity

TABLE 1. Levels populated in ^{155}Dy.

Energy average (d,t) keV	Assignment	$d\sigma/d\Omega(d,t)$ $\mu b/sr$		
		60°	90°	125°
0	3/2 3/2 − [521]	46	41	25
86	3/2 3/2 + [651] (+ 3/2 + [402])	76	105	67
134	7/2 3/2 − [521]	36	49	34
153	11/2 11/2 − [505]	7	17	16
201		6	5	3
223	9/2 3/2 − [521]	6	13	15
239	3/2 3/2 + [402] (+ 3/2 + [651])	115	170	149
320	1/2 1/2 + [400]	109	166	126
345		13	16	12
381	3/2 1/2 − [530]	46	55	35
422	5/2 1/2 − [530]	6	10	9
445		11	10	9
457		4	4	3
482	7/2 1/2 − [530]	12	20	−

in the change of properties of the various single-particle states and, in most cases, the properties deduced for the Dy nuclei are intermediate of those found for Gd and Er.

Among the more striking regularities is a shift of the energy levels for a given neutron number as the proton number is increased. This is illustrated in Figs. 21—22.

In spite of the strong low-lying collective excitations in the even nuclei, the energy spectra for the odd Dy nuclei are not more complex than those for the odd Gd nuclei.

Some information about the collective levels connected by large matrix elements to the ground states in ^{161}Dy or ^{163}Dy was obtained in a concurrent[11] study of the inelastic deuteron scattering from these nuclei. These data have not yet been finally analyzed, but have nevertheless given supporting evidence for several of the assignments discussed in detail in the following sections.

2.3. Detailed Interpretation of the Spectra

The assignments of the single-neutron orbitals are least ambiguous near the ground states and, consequently, the analysis proceeds from the ground states towards deeper hole states by means of the (d,t) spectra and then from the ground states towards higher particle states by means of the (d,p)

TABLE 2. Levels populated in ^{157}Dy.

Energy average		Assignment	$d\sigma/d\Omega(d,p)$ $\mu b/sr$			$d\sigma/d\Omega(d,t)$ $\mu b/sr$		
(d,p) keV	(d,t) keV		60°	90°	125°	60°	90°	125°
0	0	3/2 3/2 − [521]	86	35	12	56	55	26
59	61	5/2 3/2 − [521]	3	2	1	0.6	0.6	0.4
147	147	7/2 3/2 − [521]	196	96	41	69	96	46
161	161	9/2 +	70	44	17	43	67	34
	187					6	7	4
198	198	11/2 11/2 − [505]	27	10	9	12	30	33
	209					2	9	2
235	235	3/2 3/2 + [651] + 3/2 + [402]	95	74	47	87	153	94
254	257	9/2 3/2 − [521]	19	17	13	5	9	7
306	307	3/2 3/2 + [402] + 3/2 + [651]	43	25	13	86	146	97
339	340	5/2 5/2 − [523]	42	26	14	13	19	14
	350	13/2 +				14	17	7
387	388	1/2 1/2 + [400]	121	44	24	167	283	178
	399	3/2 3/2 − [532]				11	22	8
416	418	7/2 5/2 − [523]	164	99	50	19	30	15
	432					9	17	13
	454	5/2 3/2 − [532]				7	20	12
463	464	1/2 1/2 − [521]	206	102	38	26	34	14
	506					14	24	13
520	517	3/2 1/2 − [521], 9/2 5/2 − [523]	48	36	18	23	40	31
	527	7/2 3/2 − [532]				8	16	11
553	555	5/2 1/2 − [521], 3/2 1/2 − [530]	176	89	38	99	138	68
565	565	5/2 1/2 − [530]	16	23	6	16	16	6
607			32	20	8			
670	673	7/2 1/2 − [521], 7/2 1/2 − [530]	47	32	17	18	27	18
	685					2	4	2
704			2	2	1			
	712					2	3	2
728	731		32	22	12	6	10	10
752	756		18	6	2	7	8	4
768	770		22	18	11	3	6	2
785			4	6	3			
823	828		4	3	1		2	1
863			2	2	2			
881			30	18	5			
901			4	5	2			
934			12	9	4			
965			5	5	2			
985		7/2 5/2 − [512]	70	55	22			

(continued)

TABLE 2 (continued).

Energy average		Assignment	$d\sigma/d\Omega(d,p)$ $\mu b/sr$			$d\sigma/d\Omega(d,t)$ $\mu b/sr$		
(d,p) keV	(d,t) keV		60°	90°	125°	60°	90°	125°
1013			3	4	2			
1049			36	18	8			
1072			16	11	8			
1085			41	21	8			
1101		9/2 5/2 − [512]	7	6	2			
1123			6	3	2			
1145			20	13	6			
1172			29	13	8			
1233[1]			34	22	10			
1245[1]			10	7	3			
1296[2]			112	68	29			
1328			11	7	3			
1346			14	19	3			
1379			77	69	24			
1420			89	56	18			
1452			94	47	23			
1484			59	33	19			
1505			37	15	10			
1524			23	6	7			
1569		3/2 1/2 − [510]	112	58	28			
1602			51	29	16			
1632		5/2 1/2 − [510]	32	17	7			
1653*			117	54	30			
1682			38	18	7			
1701		7/2 1/2 − [510]	55	31	20			
1797			46	19	12			
1836			45	21	15			
1978			39	22	15			
2003			71	39	19			
2157			48	27	14			

[1] Not clearly resolved.

[2] Probably double.

* Several unresolved (d,p) groups from here and up.

spectra. The resulting level schemes for the six nuclei investigated are pre-
sented in Figs. 12–17 whereas Fig. 11 summarizes the energies at which
the main components of the single-particle levels have been observed. The

TABLE 3. Levels populated in ^{159}Dy.

Energy average (d,p) keV	(d,t) keV	Assignment	$d\sigma/d\Omega(d,p)$ $\mu b/sr$ 60°	90°	125°	$d\sigma/d\Omega(d,t)$ $\mu b/sr$ 60°	90°	125°
0	0	3/2 3/2 − [521]	100	39	12	113	91	52
136	137	7/2 3/2 − [521]	146	105	38	132	132	82
176		5/2 5/2 + [642]	4	1.5	3			
206		7/2 5/2 + [642]	10	2	1			
238	239	9/3 3/2 − [521], 9/2 +	70	47	21	59	68	36
309	309	5/2 5/2 − [523]	32	20	9	11	13	7
	352	11/2 11/2 − [505]				15	50	44
362	365	13/2 +, 11/2 3/2 − [521]	51	54	48	18	65	37
394	395	7/2 5/2 − [523]	115	71	30	24	31	21
416	418	3/2 3/2 + [402] (+ 3/2 + [651])	61	43	15	198	290	153
470	471		2	2	2	5		13
504	506	9/2 5/2 − [523]	21	17	9	3	4	7
533	534	1/2 1/2 − [521]	258	140	45	45	36	11
	549	3/2 3/2 + [651] (+ 3/2 + [402])				66	83	62
560	564	1/2 1/2 + [400]	143	68	29	294	399	278
586		3/2 1/2 − [521]	32	19	8			
	607					12	23	11
621		5/2 1/2 − [521]	60	52	16			
	627	3/2 3/2 − [532]				23	13	15
635		(11/2 5/2 − [523])	13	10	9			
688	690	5/2 3/2 − [532]	16	12	5	41	55	37
744	749	7/2 1/2 − [521], 3/2 1/2 − [530]	165	120	45	70	92	28
772	774	7/2 3/2 − [532], 5/2 1/2 − [530]	19	13	3	21	26	6
798	795		64	36	19	58	63	30
825	828	7/2 1/2 − [530]	9	8	3	32	31	8
854	857		3	3	2	12	8	4
983			17	11	6			
1089		7/2 5/2 − [512]	113	86	35			
1150			22	16	6			
1189		9/2 5/2 − [512]	10	9	5			
1213			8	≤ 11	2			
1283			110	≤107	35			
1341			18	13	5			
1391			9	7	6			
1411			26	20	15			
1431			80	41	14			
1473		3/2 1/2 − [510]	132	80	26			
1515			14	14	7			
1535		5/2 1/2 − [510]	27	18	8			

TABLE 3 (continued).

Energy average		Assignment	$d\sigma/d\Omega(d,p)$ $\mu b/sr$			$d\sigma/d\Omega(d,t)$ $\mu b/sr$		
(d,p) keV	(d,t) keV		60°	90°	125°	60°	90°	125°
1558			48	30	13			
1590			35	24	10			
1621		7/2 1/2−[510]	32	21	11			
1643			151	97	31			
1673			26	19	7			
1696			51	34	14			
1727*			52	47	18			
1748			53	33	17			
1786			65	37	15			
1824			54	39	19			
1849			45	32	15			
1891			99	59	21			
1918			43	29	11			
1961			24	18	6			
1989			45	25	24			
2016			63	39	14			

* Several unresolved peaks from here.

identification of the individual quantum states is to a large extent based on a comparison of theoretical and experimental intensities. The data for a number of the more firmly established bands are collected in Tables 9–20.

2.3.1. The 3/2–[521] Orbital

This orbital is characterized by strong 3/2 − and 7/2 − members of the rotational band. The 9/2 − state has approximately 10 % of the 7/2 − strength, whereas the 5/2 − state is very weak and in most cases not observed.

From the angular distributions and the intensity patterns, the ground state in ^{155}Dy, ^{157}Dy, and ^{159}Dy is identified as the 3/2 − [521] orbital.

In ^{155}Dy, the 7/2 − and the 9/2 − states are observed at 134 keV and 223 keV, respectively. The corresponding states in ^{157}Dy are found at 147 keV and 257 keV, and in this nucleus also the 5/2 − state is observed at 61 keV with a cross section of approximately 1 $\mu b/sr$. In ^{159}Dy, the 7/2 − state is observed at 137 keV and the 9/2 − state at 239 keV. The (d,t) cross section for this level is too large, but this can at least partly be explained by

TABLE 4. Levels populated in ^{161}Dy.

Energy average (d,p) keV	Energy average (d,t) keV	Assignment	$d\sigma/d\Omega(d,p)$ $\mu b/sr$ 60°	90°	125°	$d\sigma/d\Omega(d,t)$ $\mu b/sr$ 60°	90°	125°
0	0	5/2 5/2 + [642]	2		3	6	5	2
28	26	5/2 5/2 − [523]	23	20	10	26	23	12
	44	7/2 5/2 + [642]				5	4	2
76	75	3/2 3/2 − [521]	73	29	17	242	183	74
104	101	9/2 + , 7/2 5/2 − [523]	63	49	26	80	84	44
136	132	5/2 3/2 − [521]	9	2	2	9	5	5
197	201	9/2 5/2 − [523]	9	10	7	14	27	18
214	213	7/2 3/2 − [521]	180	124	64	266	217	144
269	268	13/2 +	34	37	30	32	67	48
322	317	9/2 3/2 − [521]	6	2	1	3	6	5
370	368	1/2 1/2 − [521]	258	125	41	98	102	30
421	418	3/2 1/2 − [521]	36	27	7	24	11	7
451	448	5/2 1/2 − [521]	55	48	28	17	35	26
485	486	11/2 11/2 − [505]	7	8	4	27	58	60
512			4	3	2			
553	551	3/2 3/2 + [402] (+ 3/2 + [651])	35	23	14	348	413	214
572	567	7/2 1/2 − [521]	96	66	22	26	19	12
610	608	1/2 1/2 + [400] (+ 1/2 + [660])	58	21	11	278	326	176
634	634	(9/2 1/2 − [521])	24	12	12	8	18	15
682	679	3/2 3/2 + [651] (+ 3/2 + [402])	8	8	9	54	72	56
	717					20	32	13
723			7	9	5			
	730					18	20	11
780	774	1/2 1/2 + [400] (+ 1/2 + [660])	59	27	12	200	260	148
808	801	(11/2 1/2 − [521])	10	9	6	8	14	10
833	827		6	2	3	11	22	11
	850					45	72	49
859	860	3/2 1/2 − [530]	36	39	10	151	148	58
	877	5/2 1/2 − [530]				34	26	16
883		7/2 5/2 − [512]	284	259	115			
928	924		19	38	6	8	7	5
	958	7/2 1/2 − [530]				13	24	17
971	971		8	7	4	11	12	7
995		9/2 5/2 − [512]	10	13	15			
	1007						5	5
	1027					23	27	13
1109			10	10				
	1127					11	19	10
1144	1138		22	18	10	7	12	9

(continued)

TABLE 4 (continued).

Energy average		Assignment	$d\sigma/d\Omega(d,p)$ $\mu b/sr$			$d\sigma/d\Omega(d,t)$ $\mu b/sr$		
(d,p) keV	(d,t) keV		60°	90°	125°	60°	90°	125°
	1155					6	5	6
1170			28	23	21			
	1182						6	6
	1207					11	14	6
1216			5	6	7			
1260			15	12	7			
	1271					8	8	5
	1290					1.5	6	5
1309		3/2 1/2 − [510]	215	152	68			
1363		5/2 1/2 − [510]	55	43	19			
	1379					11	15	8
1384			35	18	11			
	1416	7/2 7/2 + [404]				29	64	45
1422			55	33	21			
	1436					14	19	10
1446		7/2 1/2 − [510]	43	23	22			
	1460					3.5	6	2
1477			56	27	12			
1516			99	48	16			
1535			86	66	32			
1562			12	6	5			
1594*			31	21	10			
1645			47	21	20			
1712			56	38	19			
1825			70	38	23			
1923			80	51	32			
1946			61	38	25			
1977		3/2 3/2 − [512]	205	124	51			
1996			197	102	54			
2039		5/2 3/2 − [512]	321	172	87			
2113		7/2 3/2 − [512]	85	54	40			

* Several unresolved peaks from here.

the occurrence of the 9/2 5/2 + [642] group at the same energy, in accordance with BORGGREEN et al.[4].

The 75 keV level in ^{161}Dy is identified as the band head of the 3/2 − [521] band. The 5/2 −, 7/2 −, and 9/2 − states are then observed at 132 keV, 213 keV, and 317 keV, respectively. Angular distributions and relative cross

TABLE 5. Levels populated in ^{163}Dy.

Energy average		Assignment	$d\sigma/d\Omega(d,p)$ $\mu b/sr$			$d\sigma/d\Omega(d,t)$ $\mu b/sr$		
(d,p) keV	(d,t) keV		60°	90°	125°	60°	90°	125°
0	0	5/2 5/2 − [523]	21	11	6	58	54	25
74	73	7/2 5/2 − [523]	31	18	6	39	43	19
168	167	9/2 5/2 − [523]	17	19	9	32	43	32
	250	5/2 5/2 + [642]				9	4	2
282	281	11/2 5/2 − [523]	4	5	4	7	14	11
	335	9/2 +				91	83	46
350	351	1/2 1/2 − [521]	249	115	42	127	74	29
388		3/2 1/2 − [521]	9	3	1			
(421)	421	3/2 3/2 − [521]	16	8	3	341	221	107
425		5/2 1/2 − [521]	114	57	17			
476	474	5/2 3/2 − [521]	14	8	2	16	14	7
	495	11/2 11/2 − [505]				48	75	67
499		9/2 7/2 + [633]	27	31	24			
517	514	7/2 1/2 − [521], 13/2 +	175	116	53	157	150	84
556	552	7/2 3/2 − [521]	46	28	9	173	152	81
592			9	3	2			
	644	9/2 3/2 − [521]				6	13	13
651			11	8	7			
719	715	13/2 7/2 + [633]	15	20	9	2	8	15
740	736	1/2 1/2 + [660] (+ 1/2 + [400])	16	15	5	123	101	54
	764	11/2 3/2 − [521] (3/2 1/2 + [660])				13	24	27
	780	(5/2 1/2 + [660])				5	10	10
	794					81	55	29
801		7/2 5/2 − [512]	520	306	133			
	820					7	6	2
827			20	12	9			
861	857	3/2 3/2 + [402] (+ 3/2 + [651])	34	21	15	469	526	380
887	883		48	30	16	79	80	48
918	912	9/2 5/2 − [512]	14	9	8	24	28	29
	933					23	23	17
949	945		92	65	29	14	16	12
	989					4	13	20
1058	1057	1/2 1/2 + [400] (+ 1/2 + [660])	83	43	24	556	539	352
1087	1084	(3/2 3/2 + [651] (+ 3/2 + [402]))	6	7	5	40	49	32
1126	1129		15	20	18	50	66	59
1159		(1/2 1/2 − [510])	6	9	10			
1199	1199	3/2 1/2 − [510]	323	180	73	43	44	27
	1252					6	11	6
1262		5/2 1/2 − [510]	99	67	30			

(*continued*)

TABLE 5 (continued).

Energy average		Assignment	$d\sigma/d\Omega(d,p)$ $\mu b/sr$			$d\sigma/d\Omega(d,t)$ $\mu b/sr$		
(d,p) keV	(d,t) keV		60°	90°	125°	60°	90°	125°
	1275	3/2 1/2 − [530]				74	60	30
1284			14	6	6			
	1295					4		3
1342		7/2 1/2 − [510]	40	30	18			
	1359	7/2 1/2 − [530]				9	24	14
	1425	(9/2 1/2 − [530])				13	15	15
1448*			24	12	5			
	1481					6	5	2
1494	1497		14	4	3	12	16	10
	1526					14	19	10
1533			38	18	11			
1549			71	57	30			
	1570					11	11	5
1597			10	9	4			
	1611					8	12	5
1629	1630		26	24	11	20	30	25
1663			22	11	3			
1696	1689		40	20	7	12	9	10
1713	1706		35	19	8	22	38	37
1734			38	31	15			
	1751					31	31	23
1795		3/2 3/2 − [512]	308	169	57			
	1806					3	5	3
1817			114	62	18			
	1840	7/2 7/2 + [404]				35	50	43
1856		5/2 3/2 − [512]	432	232	116			
1936		7/2 3/2 − [512]	169	85	40			
1957			170	79				
1988			258	109	42			
2012			95	42	30			
2067			54	35	10			
2087			37		8			
2114			81		18			
2169			104	32	15			
2317			120	81	38			
2351			72	37	17			

* Several unresolved peaks from here.

TABLE 6. Levels populated in ^{165}Dy.

Energy average (d,p) keV	Assignment	$d\delta/d\Omega(d,p)$ $\mu b/sr$		
		60°	90°	125°
0	7/2 7/2 + [633]	2		
84	9/2 7/2 + [633]	22	14	4
109	1/2 1/2 − [521]	295	164	59
158	3/2 1/2 − [521]	7	15	1
182	5/2 1/2 − [521], 5/2 5/2 − [512]	76	66	22
262	7/2 5/2 − [512]	250	218	110
298	7/2 1/2 − [521]	117	99	54
308	13/2 7/2 + [633]	27	44	23
336	9/2 1/2 − [521]	8	7	5
361	9/2 5/2 − [512]	11	6	5
480	(11/2 5/2 − [521])	8	6	4
518	11/2 1/2 − [521]	8	5	4
535		5	5	2
575		36	12	3
606	3/2 1/2 − [510] + 5/2 − [512] γ-vib	246	143	50
629		39	24	4
658	5/2 1/2 − [510] + 5/2 − [512] γ-vib	48	30	
705		98	67	35
737	7/2 1/2 − [510] + 5/2 − [512] γ-vib	7	10	6
803		4		3
919			4	6
1052		8	7	3
1103		22	10	4
1139		11	8	8
1162		108	85	43
1258	3/2 3/2 − [512]	130	69	25
1283		15	7	5
1312	5/2 3/2 − [512]	156	103	49
1340		172	81	25
1384		272	121	67
1402	7/2 3/2 − [512]	108	53	18
1447		54	16	15
1478		14	9	13
1503		239	120	48
1561		368	174	82
1596		268	172	80
1625		27	11	5
1649		113	71	39
1699		91	62	28
1723		41	42	19

TABLE 6 (continued).

Energy average (d,p) keV	Assignment	$d\sigma/d\Omega(d,p)$ $\mu b/sr$		
		60°	90°	125°
1751		85	59	22
1780		17	12	6
1805		9	8	5
1833		91	64	37
1861		56	41	17
1891		44	20	19
1916		23	18	18
1947		45	34	24
1970		28	22	13
2000		9	9	11
2027*		25	20	10
2097			35	17
2121			16	6
2178			78	37
2208			25	14
2294			35	33
2320			74	33
2371			46	23
2432			62	27
2445			46	26
2459			118	50
2495			98	45

* Several unresolved levels from 2027 keV to 2495 keV.

sections agree well with this assignment, which is also in agreement with the ^{161}Tb measurements[5].

The $3/2-[521]$ band in ^{163}Dy shown in Fig. 16 is in agreement with that proposed by SCHULT et al.[6]. The observed states fit well into the intensity pattern for the different members of the rotational band, although the $7/2-$ state in ^{163}Dy is weak compared to the same state in ^{161}Dy.

The ^{165}Dy nucleus can be reached by the (d,p) reaction only. The $3/2-[521]$ state in ^{165}Dy is a hole excitation and only a small cross section is expected. A band comprising the levels[7-10] 573.6 keV $(3/2-)$, 628.8 keV $(5/2-)$, and 705.9 keV $(7/2-)$ has been associated with the $3/2-[521]$ band or with a γ-vibration built on the $1/2-[521]$ state. Neither of these suggestions does directly explain the rather strong (d,p) groups observed (cf. Table 6).

The $3/2 - [521]$ orbital is the ground state in the three successive nuclei ^{155}Dy, ^{157}Dy, and ^{159}Dy. A similar persistence is found in the isobars ^{155}Gd, ^{157}Gd, and ^{159}Gd and might be explained by changes in deformation with increasing neutron number.

It should also be noted that, according to the Nilsson scheme, one would expect the $11/2 - [505]$ state to be the ground state in nuclei with $N = 91$ for a deformation $\delta \sim 0.3$. SOLOVIEV and VOGEL[13] have made calculations of states close to one-quasiparticle states, taking into account the interaction of quasiparticles with phonons. Their calculations show that the $K = 11/2$ and $9/2$ states are purer one-quasiparticle states (95–99%) than the $K = 1/2$ and $3/2$ states (90–97%). As a consequence, the energies of the low K states are lowered more than the energies of the high K states. The latter are therefore not likely to be ground states if there are near-lying low K orbitals in the Nilsson scheme.

2.3.2. The $1/2 + [660]$, $3/2 + [651]$, and $5/2 + [642]$ Orbitals

The three near-lying orbitals $1/2 + [660]$, $3/2 + [651]$, and $5/2 + [642]$, and partly also $7/2 + [633]$, are expected to give rise to low-lying states in the dysprosium nuclei. These orbitals originate in the $i_{13/2}$ shell-model state and the wave functions of the deformed states have preserved their $i_{13/2}$ character insofar as the coefficients $C_{6, 13/2}$ are all close to unity. In addition, there are small admixtures of the $g_{9/2}$ shell-model state. Consequently, only the $9/2 +$ and $13/2 +$ states of the rotational bands have observable cross sections in the (d,p) and (d,t) reactions.

The localization of states belonging to the orbitals discussed above is complicated by coupling effects of Coriolis and $\Delta N = 2$ type, which quite generally affect the even parity states in the deformed nuclei in this region[14, 15]. The above-mentioned orbitals are coupled by the Coriolis force with matrix elements which, for the $13/2 +$ states, can be as large as $400 \, \text{keV}$. As the expected energy separation of the bands is often much less, the wave functions become completely intermixed. This results in strongly enhanced transfer cross sections for the lowest $9/2 +$ state and the lowest $13/2 +$ state and almost vanishing cross sections for the higher states. Therefore, essentially only one $9/2 +$ and one $13/2 +$ state are observable.

The rotational band structures are greatly affected by the Coriolis coupling, the general effect being a compression of the lowest band and an expansion of the higher bands.

In ^{155}Dy, no $9/2 +$ or $13/2 +$ states have been observed with certainty in this work. In ^{157}Dy, the peak at 161 keV has an angular distribution
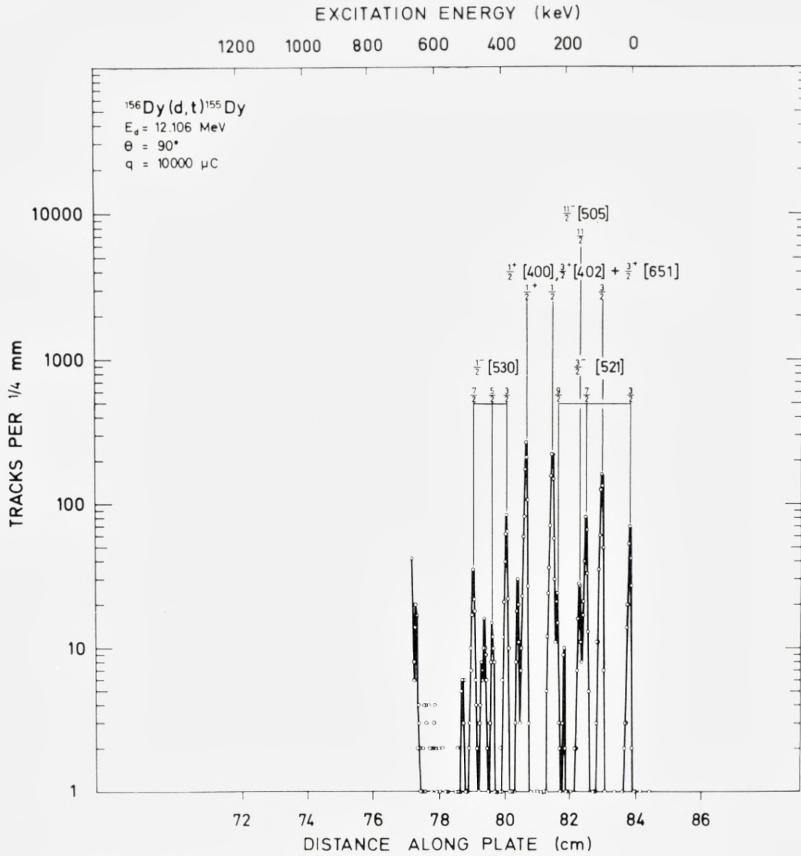
Fig. 1. Triton spectrum for the reaction ^{156}Dy(d,t)^{155}Dy, $\theta = 90°$.

which is consistent with $l = 4$ and has been assigned to the $9/2 +$ state. The peak at 350 keV is tentatively assigned to the $13/2 +$ state although it is weaker than expected.

In ^{159}Dy, the energy of the peak at 239 keV corresponds to the $9/2$ member of the ground-state rotational band. The cross section is, however, more than twice as strong as expected from the intensity pattern of the $3/2 - [521]$ orbital, and it is assumed that the $9/2 +$ state coincides with the $9/2$ $3/2 - [521]$ state. The observed cross section is in reasonable agreement with the expected sum of the two states. The 365 keV group in ^{159}Dy is also double and contains the $11/2$ $3/2 - [521]$ state and the $13/2 +$ state. The cross section of the $11/2 -$ state, as estimated from the $3/2$ $3/2 - [521]$ cross section, should
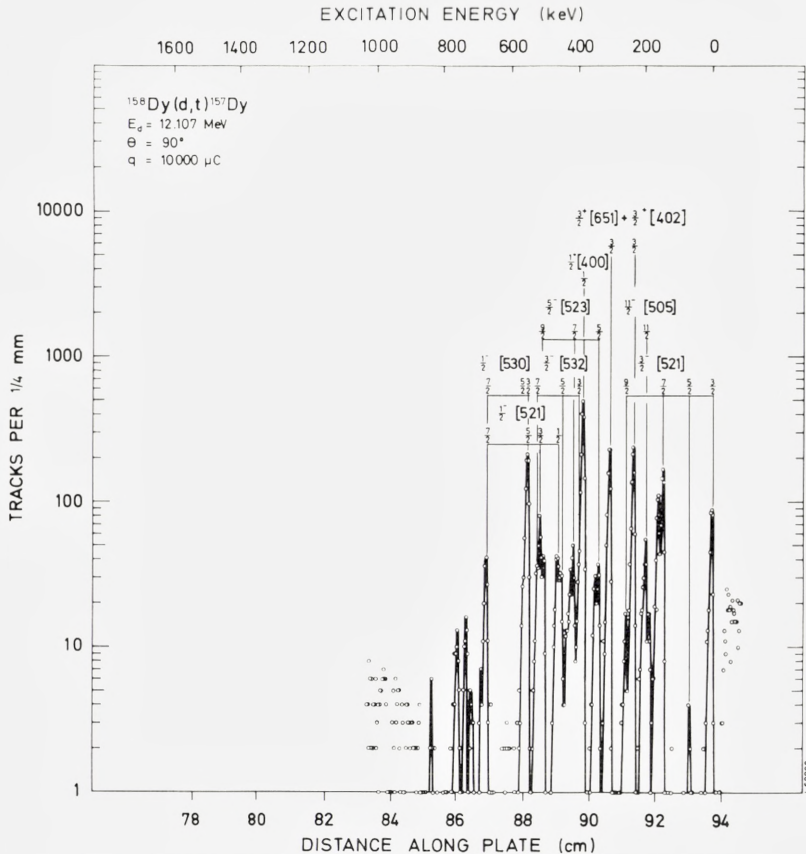
Fig. 2. Triton spectrum for the reaction ^{158}Dy$(d,t)^{157}$Dy, $\theta = 90°$.

not exceed 8 $\mu b/sr$, so the main part of the cross sections is due to the 13/2 +
state. The angular distributions confirm the assignment. The weak levels
at 176 keV and 206 keV are tentatively assigned to the 5/2 + and 7/2 +
members of the rotational band. The band is found to be severely distorted,
but the lower spin states correspond mostly to the 5/2 + [642] orbital.

    In ^{161}Dy, the 5/2 + [642] orbital forms the ground state, and a rotational
band up to and including 13/2 + is observed in the (d,t) spectra with the
exception of the 11/2 + state. The 9/2 + level at 101 keV coincides with the
7/2 5/2 – [523] level, but from comparison with the 7/2 5/2 – [523] state in
the neighbouring nuclei, the 9/2 5/2 + [642] state can be estimated to con-
tribute with approximately 50 % of the observed cross section. The ground-

EXCITATION ENERGY (keV)

3000 2800 2600 2400 2200 2000 1800 1600 1400 1200 1000 800 600 400 200 0
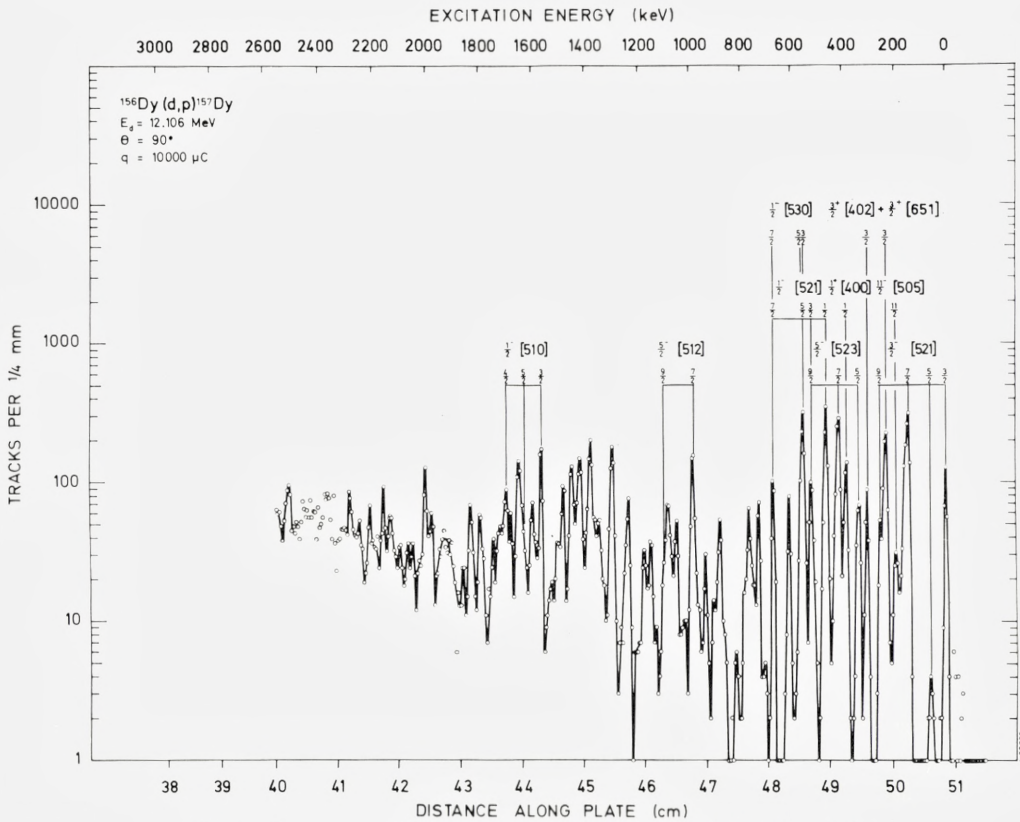
Fig. 3. Proton spectrum for the reaction ^{156}Dy$(d,p)^{157}$Dy, $\theta = 90°$.

state rotational band has a rotational parameter $A = 6.3$ keV. The compression of the rotational band can be ascribed mostly to the Coriolis coupling to the two near-lying orbitals $3/2 + [651]$ and $7/2 + [633]$. The $7/2 + [633]$ orbital is expected as a particle state at approximately 400 keV of excitation energy and the $3/2 + [651]$ orbital is a hole state at approximately 700 keV.

In ^{163}Dy, the $5/2 + [642]$ state is previously known as a hole state. In the present work, the $5/2 +$ state is observed as a weakly populated level at 250 keV. The $9/2 +$ state observed at 335 keV has an angular distribution consistent with $l = 4$. The $13/2 +$ state is expected to have approximately the same strength as the $9/2 +$ state in ^{163}Dy, and it is tentatively assumed that it coincides with the $7/2$ $1/2 - [521]$ state at 514 keV. If we compare the (d,p) and the (d,t) cross sections of the different members of the rotational

2*
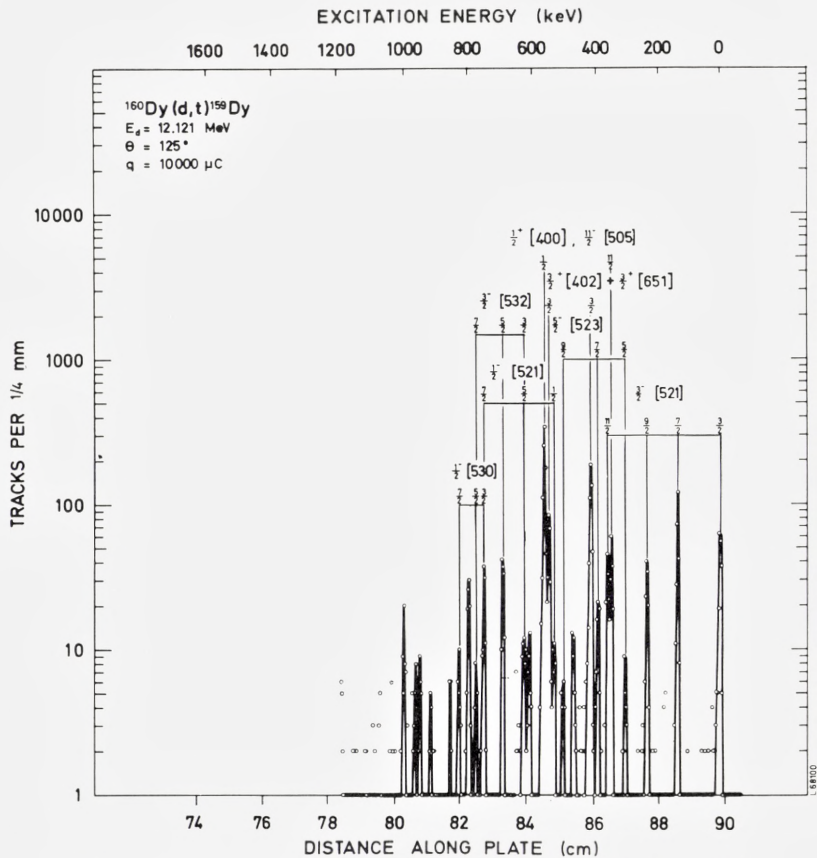
Fig. 4. Triton spectrum for the reaction $^{160}Dy(d,t)^{159}Dy$, $\theta = 125°$.

band which is built on the $1/2 - [521]$ orbital, the (d,t) cross section is found to be 45% of the (d,p) cross section at $90°$ for the $1/2$ $1/2 - [521]$ state, as compared to the peak at 514 keV where the (d,t) cross section is 105% of the (d,p) cross section. It is therefore proposed that the $13/2 +$ group is contained in the group at 514 keV.

Table 10 collects the information on $9/2 +$ and $13/2 +$ states which, according to the discussion above, are ascribed to the lowest of the coupled $N = 6$ states. Some of the assignments are based on insufficient experimental evidence and must therefore be regarded with some caution. The average cross section for the $9/2 +$ states is almost 1.6 times larger than expected for a pure state. The corresponding ratio for the $13/2 +$ states is 2.4. Both

EXCITATION ENERGY (keV)
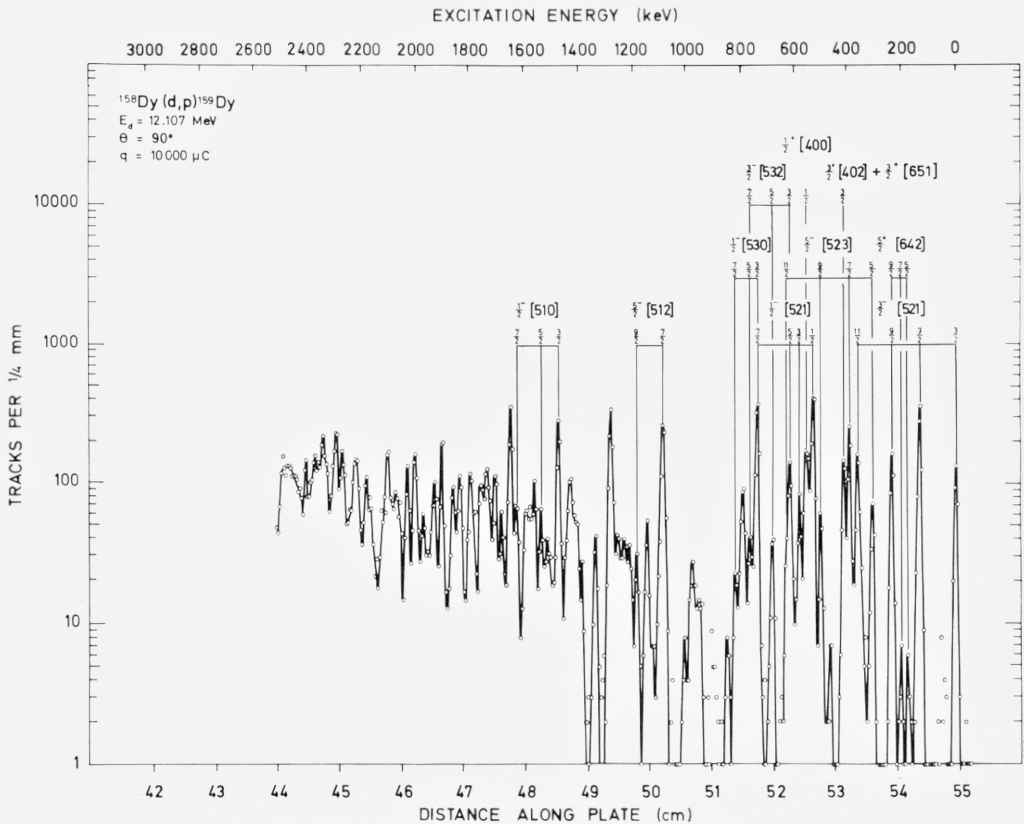
Fig. 5. Proton spectrum for the reaction ^{158}Dy$(d,p)^{159}$Dy, $\theta = 90°$.

values show the influence of the Coriolis coupling effects on the cross section of the high angular momentum states.

Whereas the Coriolis coupling mostly affects the high spin states, the $\Delta N = 2$ coupling is of importance for the low spin states. The dysprosium nuclei present the most complete example observed so far of the coupling of the crossing states $3/2 + [402]$ and $3/2 + [651]$. In addition, some effects of the crossing of the $1/2 + [400]$ and $1/2 + [660]$ can be identified. The $\Delta N = 2$ coupling of the strongly populated $3/2\ 3/2 + [402]$ state to the $3/2\ 3/2 + [651]$ state gives rise to a splitting of the $3/2 +$ strength which relatively easily is located in the spectra. The experimental evidence is discussed below.

In ^{155}Dy, the level at 86 keV has an angular distribution of the (d,t)
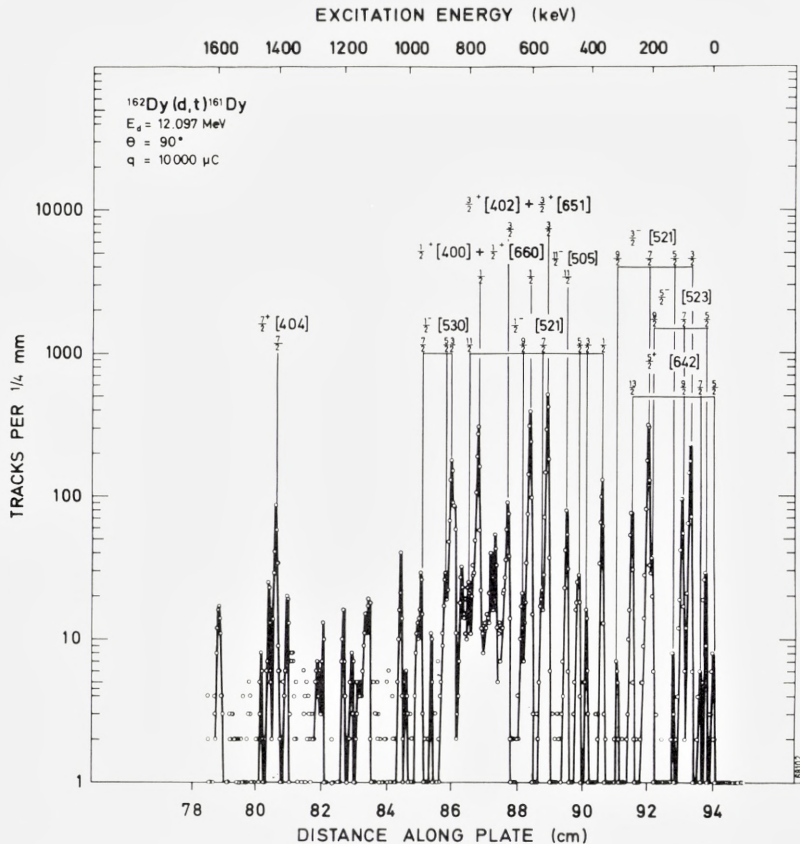
Fig. 6. Triton spectrum for the reaction ^{162}Dy$(d,t)^{161}$Dy, $\theta = 90°$.

cross section which is consistent with $l = 2$, and is also similar to the (d,t) angular distribution of the strong group at 239 keV which represents most of the 3/2 3/2 + [402] strength. The 86 keV level therefore is assigned to the 3/2 + [651] state with admixture of the 3/2 3/2 + [402] state.

In ^{157}Dy, the levels at 235 keV and 307 keV are about equally populated and have very similar angular distributions which are consistent with $l = 2$. The two levels are therefore assigned to the coupling orbitals 3/2 + [651] and 3/2 + [402].

In ^{159}Dy, the 549 keV level has an $l = 2$ angular distribution and is assigned to the 3/2 + [651] (+ 3/2 + [402]) state. The coupling is obviously weaker in this case.

EXCITATION ENERGY (keV)
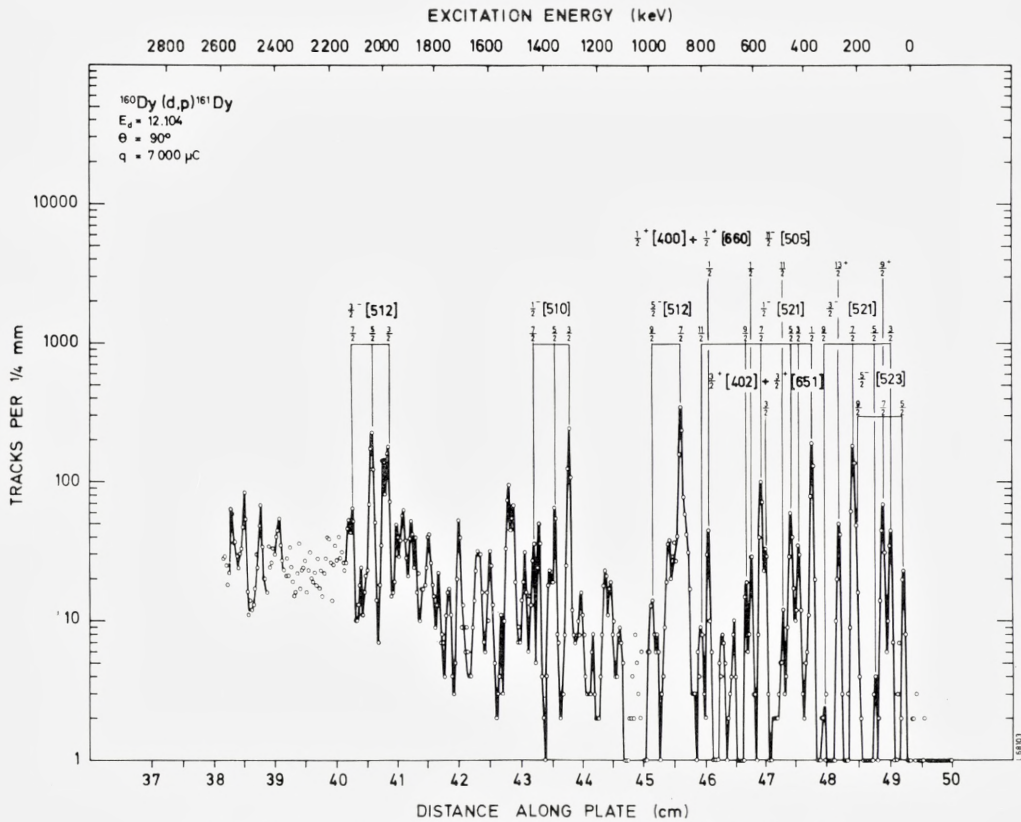
Fig. 7. Proton spectrum for the reaction ^{160}Dy$(d,p)^{161}$Dy, $\theta = 90°$.

In ^{161}Dy, the level at 679 keV has an $l = 2$ angular distribution and a strength which strongly suggests a $3/2 + [651]$ $(+3/2 + [402])$ assignment.

Finally, in ^{163}Dy, the level at 1084 keV is suggested for the same assignment, but the experimental evidence is meager.

In analogy to the case discussed above, the $1/2 + [660]$ orbital couples to the $1/2 + [400]$ orbital, but evidence for this coupling has, however, not been observed in the three lightest nuclei, ^{155}Dy, ^{157}Dy, and ^{159}Dy, investigated in this work.

In ^{161}Dy, the angular distributions of the (d,p) as well as the (d,t) cross sections for the 608 keV level are very similar to those for the 774 keV group. Both of these groups have $l = 0$ angular distributions and are there-
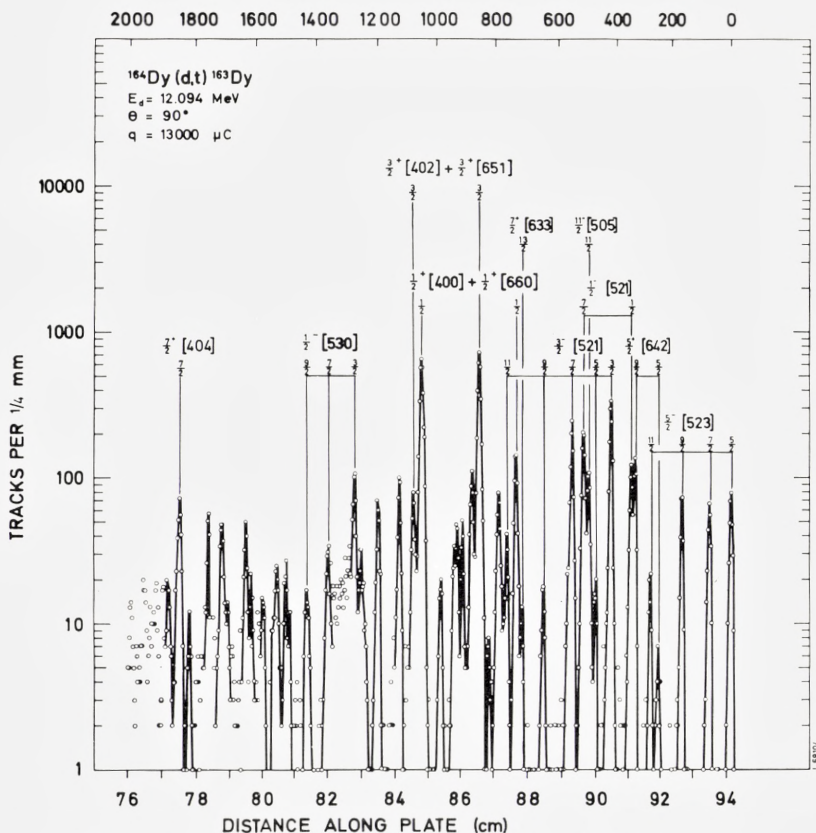
Fig. 8. Triton spectrum for the reaction ^{164}Dy$(d,t)^{163}$Dy, $\theta = 90°$.

fore assigned to the $1/2 + [660] + 1/2 + [400]$ state. Each group represents approximately 50% of the $1/2 + [400]$ strength.

In ^{163}Dy, the group at 736 keV is ascribed to the $1/2 + [660]$ $(+ 1/2 + [400])$ state from the angular distribution of the (d,t) cross section. The 736 keV level is previously proposed[6] to contain also the gamma vibration built on the $5/2 + [642]$ state and the suggested $3/2 +$ and $5/2 +$ members of the rotational band are observed in the (d,t) spectrum. The corresponding low decoupling parameter, $a = 0.5$, seems hard to reconcile with the large fraction ($\sim 80\%$) of the $1/2 + [660]$ state indicated by the fraction present of the $1/2 + [400]$ state.
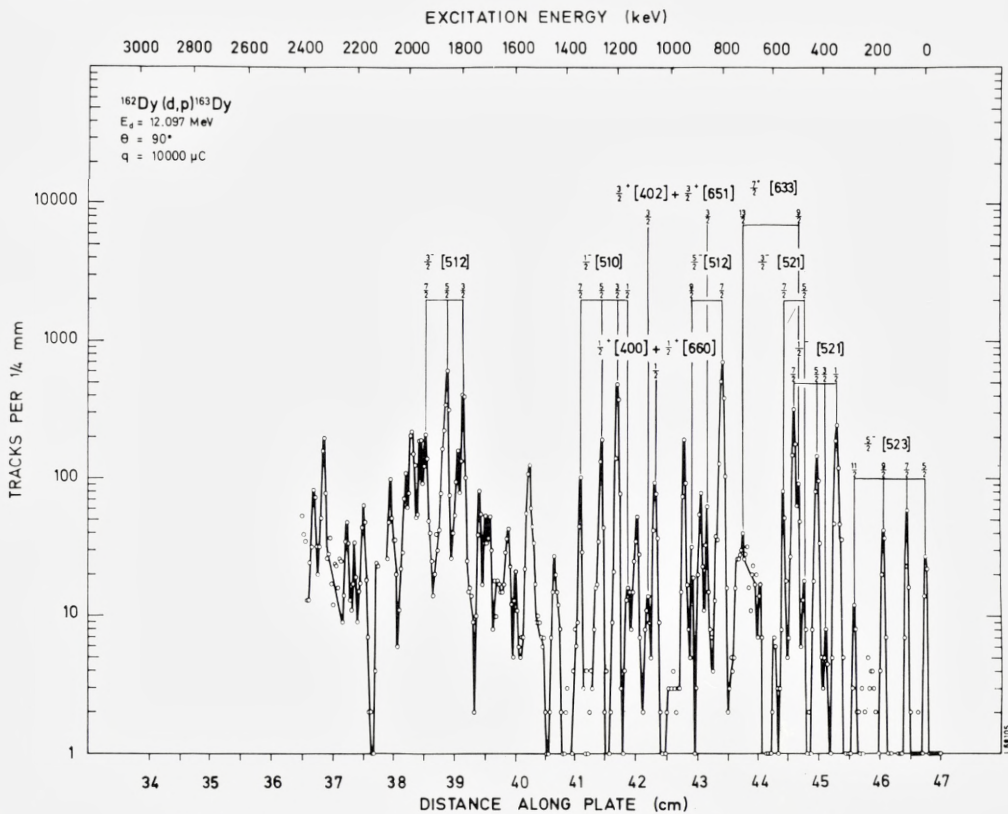
Fig. 9. Proton spectrum for the reaction ^{162}Dy$(d,p)^{163}$Dy, $\theta = 90°$.

2.3.3. The 3/2 + [402] Orbital

This orbital is expected to give rise to strong groups in the (d,t) spectra. As mentioned in sect. 2.3.2, a strong $\Delta N = 2$ coupling to the $3/2 + [651]$ orbital is observed in all of the Dy nuclei investigated, except ^{165}Dy.

The angular distributions of the (d,t) cross sections are very similar for the $3/2 + [402]$ and $1/2 + [400]$ states and it is impossible on this basis to distinguish one from the other. The angular distributions of the (d,p) cross sections are, however, different for the two orbitals, which allows an identification since the spin and parity of one of the states in question are determined in ^{163}Dy (860 keV, 3/2 +) and in ^{161}Dy (551 keV, 3/2 +) from other experiments[6, 18].

In ^{155}Dy, the 239 keV level is ascribed to the $3/2 + [402]$ orbital from
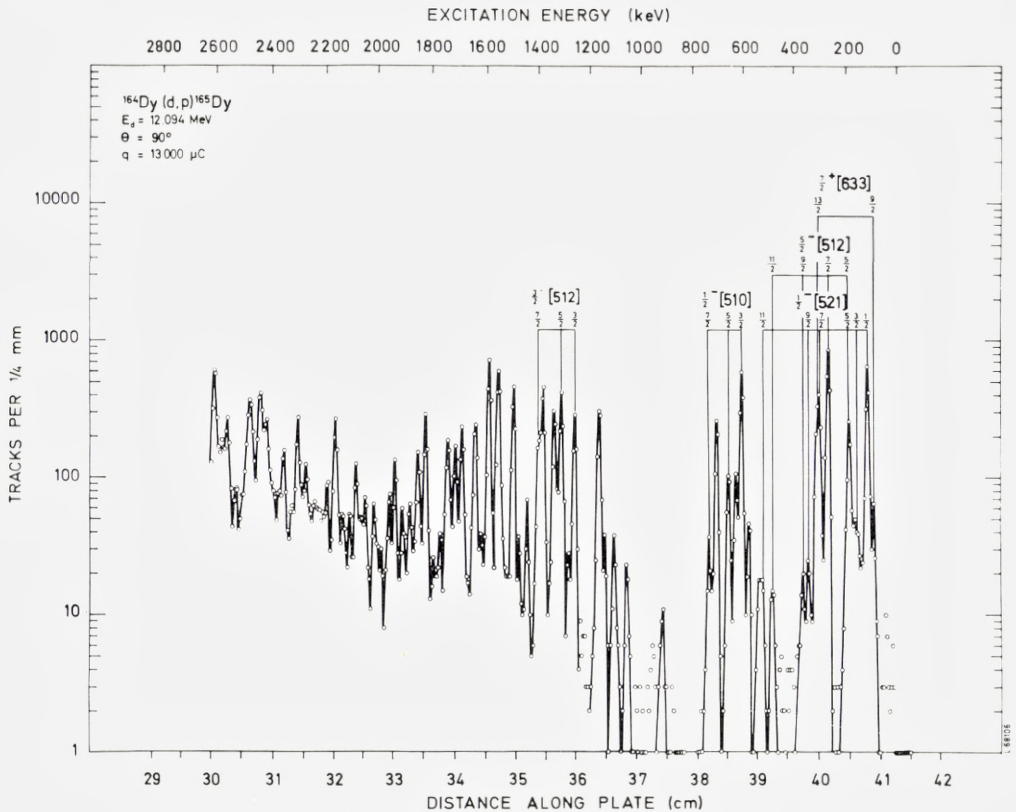
Fig. 10. Proton spectrum for the reaction ^{164}Dy$(d,p)^{165}$Dy, $\theta = 90°$.

the angular distribution and from energy systematics. The strength is split between this level and the 86 keV level.

In ^{157}Dy, the $3/2 + [402] + 3/2 + [651]$ level is observed at 307 keV, and the strength is here almost equally split between this level and the 235 keV level. The levels are identified by the angular distribution of the (d,p) cross sections.

In ^{159}Dy, the 418 keV level is identified as the $3/2 + [402] (+3/2 + [651])$ state from the angular distribution of the (d,p) cross section. The main part of the strength is observed in this level, and the remainder is found in the 549 keV level.

The $\Delta N = 2$ coupling is still weaker in ^{161}Dy, where most of the $3/2 + [402]$ state strength is observed at 551 keV, and in ^{163}Dy where the strength is
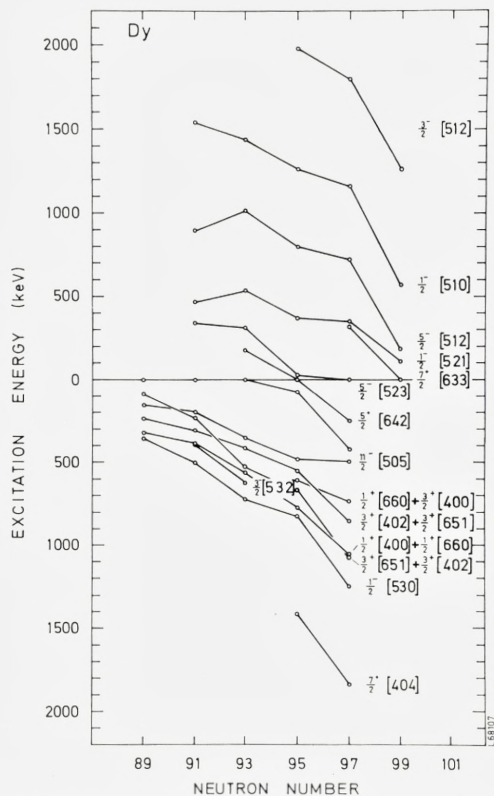
Fig. 11. Energies of the band heads for Nilsson states observed. Points at negative energies indicate hole states.
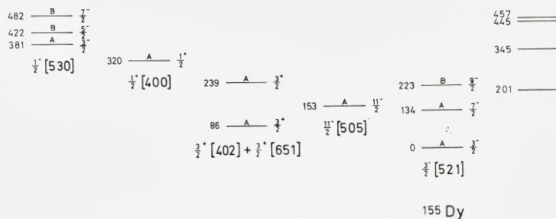
Fig. 12. Level scheme for ^{155}Dy.

TABLE 7. *Q*-values and neutron separation energies for Dy nuclei.

Mass A	$Q(d,t)$ A→A−1 keV	$Q(d,p)$ A−1→A keV	$S_n(d,t)$ keV	$S_n(d,p)$ keV	S_n from mass tables[1] keV
156	−3184 ± 10		9442 ± 10		9890 ± 1010
157		4753 ± 10		6978 ± 10	6830 ± 1010
158	−2804 ± 10		9062 ± 10		8840 ± 1000
159		4600 ± 10		6825 ± 10	6851 ± 34
160	−2323 ± 10		8581 ± 10		8590 ± 30
161	−205 ± 10	4237 ± 10	6463 ± 10	6462 ± 10	6448 ± 12
162	−1944 ± 10	5981 ± 10	8202 ± 10	8206 ± 10	8204 ± 9
163	−27 ± 10	4045 ± 10	6285 ± 10	6270 ± 10	6253 ± 5
164	−1407 ± 10	5441 ± 10	7665 ± 10	7666 ± 10	7656.8 ± 4
165		3496 ± 10		5721 ± 10	5635 ± 10

[1] I. H. E. MATTAUCH et al., Nucl. Phys. 67 (1965) 32.

TABLE 8. Unperturbed energy difference ΔH and $\Delta N = 2$ matrix element V for the $3/2 + [402] + 3/2 + [651]$ and the $1/2 + [400] + 1/2 + [660]$ orbitals in different Dy nuclei.

A	$3/2 + [402] + 3/2 + [651]$		$1/2 + [400] + 1/2 + [660]$	
	ΔH (keV)	V (keV)	ΔH (keV)	V (keV)
155	53	72		
157	1.3	36		
159	−67	56		
161	−86	47	−2.5	83
163	−183	68	240	107

TABLE 9. (d,t) population of the $3/2 − [521]$ band *.

Spin	$d\sigma/d\Omega$, $\theta = 90°$, $Q = −2$ MeV						Relative value of C_{jl}^2					
	Theory	155	157	159	161	163	Theory	155	157	159	161	163
3/2	167	123	106	114	185	197	0.10	0.08	0.10	0.12	0.18	0.22
5/2			1		5	13			∼ 0		0.01	0.04
7/2	297	174	216	173	242	148	0.53	0.32	0.53	0.51	0.68	0.47
9/2	22	52	23	∼ 20	7	13	0.26	0.60	0.37	0.37	0.13	0.27
11/2	10						0.11					

* All cross sections in Tables 9–20 are given in *μb/sr*.

Fig. 13. Level scheme for ^{157}Dy.

observed in the 860 keV level. The splitting of the (d,t) cross sections on the $3/2 + [402] + 3/2 + [651]$ states is shown in Fig. 18, whereas the summed cross section is illustrated in Fig. 19.

The $\Delta N = 2$ coupling of the $1/2 + [660]$ and $1/2 + [400]$ states in ^{159}Gd has earlier been considered in some detail[16]. A derivation of the coupling matrix element V between the $3/2 + [651]$ and $3/2 + [402]$ states is now possible for all the Dy nuclei on the basis of the two components of the $3/2 + [402]$ state identified in each nucleus. If α is the $N = 4$ amplitude in the upper state and β the $N = 4$ amplitude in the lower state, one has for V and the uncoupled energy separation ΔH

$$|V| = \frac{|\alpha/\beta|}{(\alpha/\beta)^2 + 1} \Delta E \tag{1}$$

Fig. 14. Level scheme for ^{159}Dy.

$$\Delta H \;=\; \frac{(\alpha/\beta^2)-1}{(\alpha/\beta)^2+1}\,\Delta E \tag{2}$$

where ΔE is the observed energy separation.

Table 8 lists the values of $|V|$ and ΔH derived from the experimental data. The ΔH values clearly illustrate the crossing of the two states. In ^{157}Dy, the calculated unperturbed states are only a few keV apart. Figure 20 shows the relative unperturbed energies of the $3/2+[402]$ and $3/2+[651]$ states plotted as a function of the nuclear deformation. The theoretical dependence is somewhat steeper than here observed, even when the energy scale of the Nilsson diagram is compressed a factor of two. The coupling matrix element V is of the same order of magnitude as observed for the $1/2+$ states in ^{159}Gd[16]. In judging the constancy of V, it should be remem-
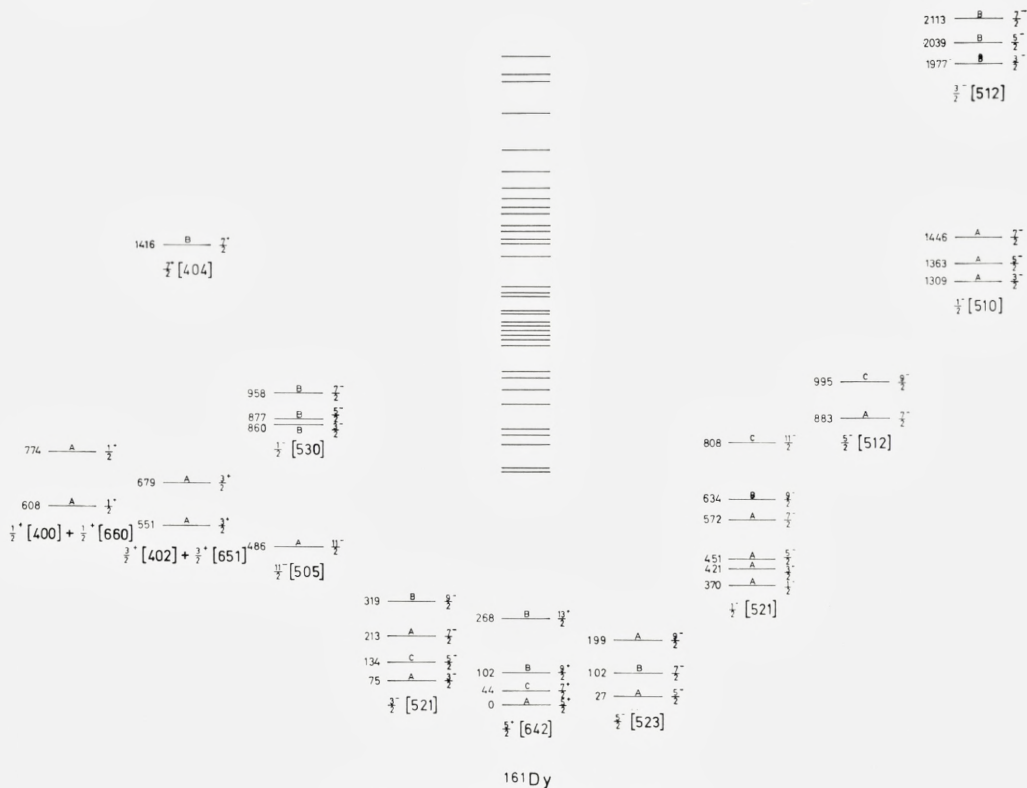
Fig. 15. Level scheme for ^{161}Dy.

bered that the influence of other couplings has been neglected. An estimate of the Coriolis coupling to the $1/2 + [660]$ band shows that the values of V and ΔH might be affected by $\sim 20\,^0/_0$.

2.3.4. The 1/2 + [400] Orbital

From the strength of the cross section, the (d,t) angular distribution and from energy systematics the 320 keV level in ^{155}Dy are ascribed to the $1/2 + [400]$ orbital. Similarly, the levels at 388 keV in ^{157}Dy and at 564 keV in ^{159}Dy are assigned to this orbital on the basis of the (d,p) and (d,t) angular distributions and from the strength of the (d,t) cross section.

In ^{161}Dy, the $1/2 + [400]$ strength is almost equally divided between the levels at 608 keV and 774 keV. These levels have very similar angular
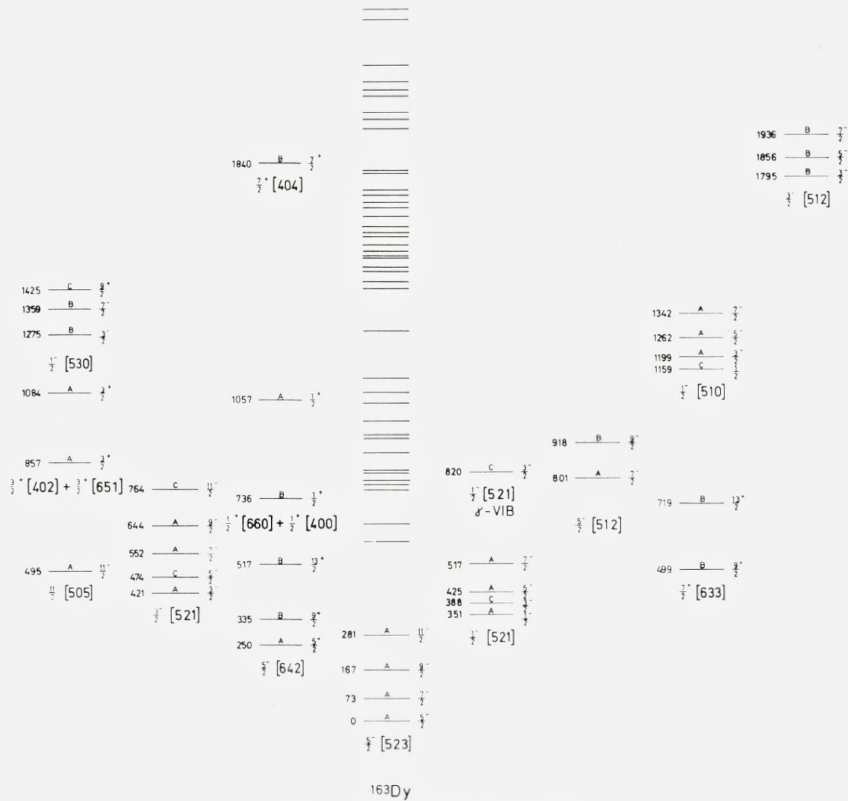
Fig. 16. Level scheme for ¹⁶³Dy.

distributions for the (d,p) as well as for the (d,t) reactions, and the angular distributions are typical for $l = 0$.

The strong peak at 1057 keV in ¹⁶³Dy is ascribed to the $1/2 + [400]$ orbital from the angular distributions of the (d,p) and (d,t) cross sections. The $1/2\ 1/2 + [660]$ state is previously proposed[6] to be at 736 keV. The strength of the 736 keV group suggests that, due to the $\Delta N = 2$ coupling, it contains part of the $1/2 + [400]$ strength.

The matrix element V and the unperturbed energy separation ΔH have also been derived for the coupling of the $1/2 + [660]$ and the $1/2 + [400]$ states in ¹⁶¹Dy and ¹⁶³Dy. The results are given in Table 8.
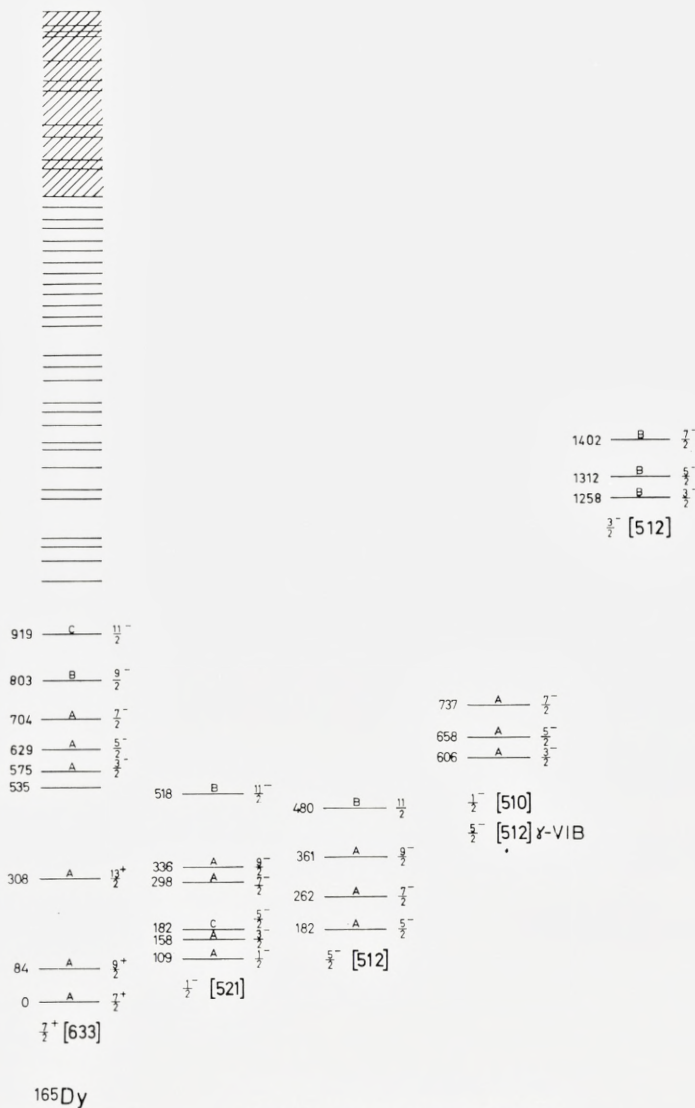
Fig. 17. Level scheme for ^{165}Dy.

2.3.5. The 11/2–[505] Orbital

The $11/2 - [505]$ orbital is found in all Dy nuclei investigated, except ^{165}Dy which could be reached by the (d,p) reaction only. The identification is based mostly on the characteristic angular distributions of the (d,t) cross sections.
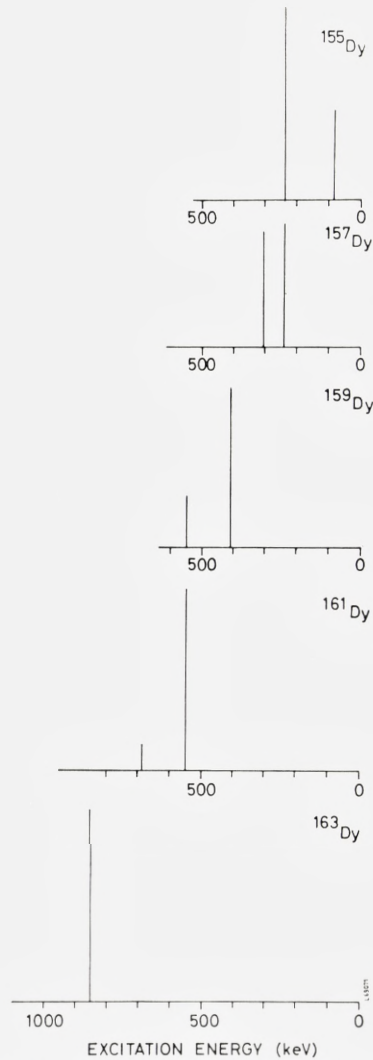
Fig. 18. Relative strength of the $\Delta N = 2$ coupled $3/2 + [651]$ and $3/2 + [402]$ orbitals for different dysprosium nuclei.

In ^{155}Dy, the $11/2 - [505]$ orbital is observed at 153 keV and in ^{157}Dy it is observed at 198 keV.

In ^{159}Dy, the 352 keV level is ascribed to the $11/2 - [505]$ orbital, which is in agreement with data from the ^{160}Dy(^{3}He, α)^{159}Dy reaction[17]. In this nucleus, the $11/2 - [505]$ state is observed as an isomeric state[4].
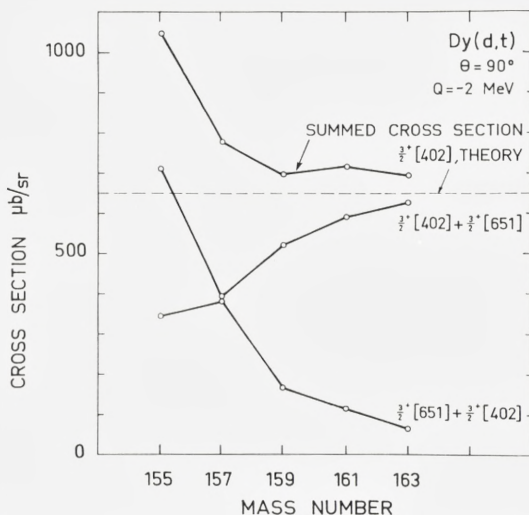
Fig. 19. Summed (d,t) cross sections for the $\Delta N = 2$ coupled $3/2 + [651]$ and $3/2 + [402]$ orbitals.

From the strength and from the angular distribution of the (d,t) cross section, the level at 486 keV in ^{161}Dy and the level at 495 keV in ^{163}Dy are assigned to the $11/2 - [505]$ orbitals in these nuclei.

2.3.6. The 3/2–[532] Orbital

This orbital is observed in ^{157}Dy and in ^{159}Dy. In ^{157}Dy, the observed cross sections differ somewhat from the theoretical cross sections, but this is not unexpected as the couplings possible to $K\pi = 1/2 -$ and $K\pi = 3/2 -$ bands are numerous. The $3/2 -$ level at 399 keV is identified from the angular distribution and from energy systematics. The $5/2 -$ and $7/2 -$ states are observed at 454 keV and 527 keV, respectively.

In ^{159}Dy, the $3/2 -$ state is observed at 627 keV, the $5/2 -$ state at 690 keV, and the $7/2 -$ state at 774 keV. The observed cross sections are in reasonable agreement with theory. The $9/2 -$ triton group cannot be observed because of the presence of scattered deuterons.

2.3.7. The 1/2–[530] Orbital

This orbital is characterized by the strong $3/2 -$ state and is expected at an excitation energy somewhat higher than that of the $1/2$ $1/2 + [400]$ state.

In ^{155}Dy, the $3/2 -$ state is observed at 381 keV and the levels at 422 keV and 482 keV are identified as the $5/2 -$ and $7/2 -$ states. The angular distrib-

3*
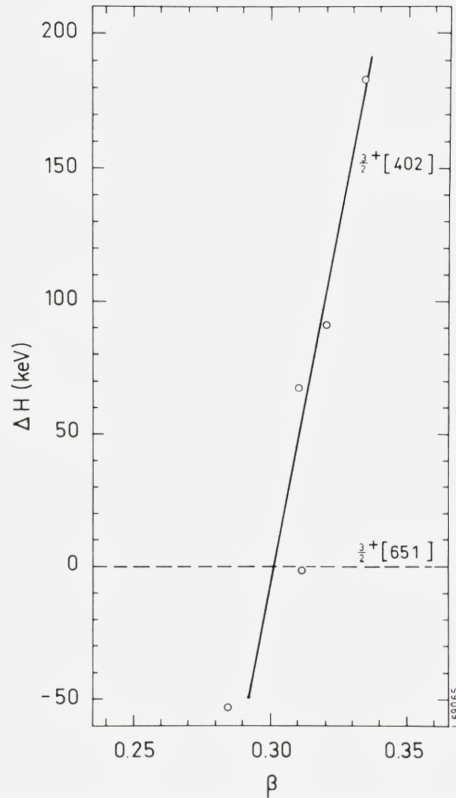
Fig. 20. Relative unperturbed energies of 3/2 + [402] and 3/2 + [651] as a function of the deformation.

utions and the intensity patterns are in reasonable agreement with this assignment.

In ^{157}Dy, the strong group at 555 keV is ascribed to the 3/2 1/2 − [530] state although it is stronger than expected. The only levels with a cross section greater than 5 $\mu b/sr$ are those at 565 keV and 673 keV. The level at 565 keV appears as a tail on the strong level at 555 keV, so the cross section is difficult to determine, but the level at 673 keV is relatively strong and has an angular distribution compatible with $l = 3$. If we assume that the two levels at 565 keV and 673 keV are the 5/2 1/2 − [530] and the 7/2 1/2 − [530] states, respectively, we get the band parameters $A = 8.7$ keV and $a = 0.77$. The decoupling parameter a is greater than in most other cases where the 1/2 − [530] orbital is identified. Another possibility is that the cross section of the 5/2 − state is less than ∼ 5 $\mu b/sr$ and is hidden in the background

TABLE 10. (d,t) population of $N = 6$ states.
$d\sigma/d\Omega$, $\theta = 90°$, $Q = -2\,\mathrm{MeV}$.

Spin	Theory	155	157	159	161	163	165
9/2			152	~ 80	~ 40	71	
13/2			50	~ 100	77	2 ~ 80	

TABLE 11. (d,t) population of the $5/2 - [523]$ band.

Spin	$d\sigma/d\Omega$, $\theta = 90°$, $Q = -2\,\mathrm{MeV}$							Relative values of C_{jl}^2						
	Theory	155	157	159	161	163	165	Theory	155	157	159	161	163	165
5/2	47		53	22	22	38		0.07		0.05	0.16	0.09	0.11	
7/2	48		95	55	43*	31		0.08		0.10	0.41	0.17	0.09	
9/2	55		132**	9	30	33		0.79		0.85	0.43	0.74	0.60	
11/2	4					11		0.06					0.20	
13/2														

* 9/2, 5/2 + [642] not resolved from this level, estimated contribution 51 % from theoretical cross sections.

** Coincides with 3/2 1/2 - [521]. From comparison with the (d,t) cross section of 1/2 1/2 - [521], the 3/2 1/2 - [521] (d,t) cross section is estimated to ~ 12 $\mu b/sr$.

TABLE 12. (d,t) population of the $11/2 - [505]$ band.
$d\sigma/d\Omega$, $\theta = 90°$, $Q = -2$ MeV.

Spin	Theory	155	157	159	161	163	165
11/2	88	62	71	82	79	70	

TABLE 13. (d,t) population of the $N = 4$ states.
$d\sigma/d\Omega$, $\theta = 90°$, $Q = -2$ MeV.

Level	Theory	155	157	159	161	163	165
3/2, 3/2 + [402]*	644	1054	778	694	712	700	
1/2, 1/2 + [400]*	819	786	846	834	947	582	
7/2, 7/2 + [404]	148				245	162	

* The table refers to the summed cross sections. See sects. 2.3.3 and 2.3.4.

which is seen in the spectra around 600 keV of excitation energy. In any case, the $1/2-[530]$ orbital is distorted in the ^{157}Dy nucleus.

In ^{159}Dy, the $3/2$ $1/2-[530]$ state is observed at 749 keV, the identification is based on the strength of the cross section and the angular distribution. The $5/2-$ state probably coincides with the $7/2$ $3/2-[532]$ state at 774 keV, so the cross section cannot be determined accurately. The $7/2-$ state is observed at 828 keV and has a cross section relative to the $3/2-$ state which is compatible with the theoretical cross section pattern.

In ^{161}Dy, the level at 860 keV is assigned as the $3/2$ $1/2-[530]$ state, the $5/2-$ state and the $7/2-$ states are observed at 877 keV and 958 keV, respectively. The angular distributions are reasonable, but the $5/2-$ group is too strong.

In ^{163}Dy, the $1/2-[530]$ orbital is again difficult to establish, but from the strength of the cross section, the angular distribution and the systematics of the excitation energies, the level at 1275 keV is a good candidate for the $3/2$ $1/2-[530]$ state.

The $7/2-$ state is observed at 1359 keV and the level at 1425 keV is tentatively assigned as the $9/2-$ state although it is stronger than expected. None of the assignments made for the $1/2-[530]$ band is entirely satisfactory, and a similar remark applies for the $3/2-[532]$ band which never has been observed without distortions. It seems likely that the Coriolis coupling of these states is responsible for most of the deviations between experimental and theoretical cross section patterns.

2.3.8. The 7/2 + [404] Orbital

The $7/2+[404]$ orbital is characterized by one strong line belonging to the $7/2+$ state. It is observed in ^{161}Dy at 1416 keV and in ^{163}Dy at 1840 keV with angular distributions in agreement with an $l = 4$ assignment. In the lighter dysprosium nuclei, the triton spectra are obscured by scattered deuterons in the region where the $7/2+[404]$ group is expected.

2.3.9. The 5/2–[523] Orbital

The $5/2-[523]$ orbital is a particle state in ^{157}Dy, and the band head is observed at 340 keV. The $7/2-$ state which is observed at 418 keV has an intensity three times larger than expected from theory. Deviations from the intensity patterns have been observed for the $5/2-[523]$ orbital in other cases, and are caused by Coriolis coupling to the near-lying $3/2-[521]$ orbital. The $9/2-$ state coincides with the $3/2$ $1/2-[521]$ state at 517 keV and the cross section cannot be given exactly.

TABLE 14. (d,t) population of the $1/2-[530]$ band.

Spin	$d\sigma/d\Omega$, $\theta = 90°$, $Q = -2$ MeV							Relative values of C_{jl}^2						
	Theory	155	157	159	161	163	165	Theory	155	157	159	161	163	165
1/2	10							0.01						
3/2	339	286	526	238	284	103		0.21	0.52	0.51	0.49	0.68		
5/2	33	52	62	~30*	50			0.06	0.15	0.17	0.23	0.16		
7/2	130	118	122	87	51	45		0.23	0.33	0.32	0.28	0.16		
9/2	30						30	0.35						
11/2	13							0.14						

* Coincides with $7/2$ $3/2-[532]$.

TABLE 15. (d,p) population of the $3/2-[521]$ band.

Spin	$d\sigma/d\Omega$, $\theta = 90°$, $Q = +3$ MeV						Relative values of C_{jl}^2					
	Theory	157	159	161	163	165	Theory	157	159	161	163	165
3/2	103	61	63	42	~10**		0.10	0.17	0.17	0.13	0.14	
5/2	~0	3		3	9			0.01	0.01	0.01	0.13	
7/2	332	157	165	169	33		0.53	0.70	0.72	0.84	0.73	
9/2	18	26	~22*	3			0.26	0.12	0.10	0.02		
11/2	8						0.11					

* Coincides with $9/2$ $5/2+[642]$.
** Coincides with $5/2$ $1/2-[521]$.

TABLE 16. (d,p) population of the $5/2-[523]$ band.

Spin	$d\sigma/d\Omega$, $\theta = 90°$, $Q = +3$ MeV						Relative values of C_{jl}^2					
	Theory	157	159	161	163	165	Theory	157	159	161	163	165
5/2	47	39	30	24	15		0.07	0.07	0.06	0.14	0.05	
7/2	48	150	103	~38*	25		0.08	0.28	0.22	0.22	0.08	
9/2	55	~40**	25	13	25		0.79	0.65	0.47	0.64	0.70	
11/2	4		13		6		0.06		0.25		0.17	
13/2												

* $9/2$, $5/2+[642]$ not resolved from this level.
** Coincides with $3/2$, $1/2-[521]$.

In ^{159}Dy, the $5/2-[523]$ band head is observed at 309 keV, the $7/2-$ and $9/2-$ states at 395 keV and 506 keV, respectively. Also in this nucleus the $7/2-$ state is much stronger than expected. The 635 keV level is tentatively assigned as the $11/2-$ state.

The low-lying state at 26 keV in ^{161}Dy is assigned as the $5/2-[523]$ band head. The $7/2-$ state at 104 keV cannot be separated from the $9/2$ $5/2+[642]$ state in this nucleus, but the summed cross section for the two states seems to indicate that the Coriolis coupling between the $5/2-[523]$ and $3/2-[521]$ orbitals is weaker than in ^{157}Dy and ^{159}Dy.

In ^{163}Dy, the $5/2-[523]$ orbital, the ground state and the rotational states up to the $11/2-$ state are observed. The experimental cross sections are in reasonable agreement with theory and with previous experiments[6].

2.3.10. The 7/2 + [633] Orbital

This orbital is observed in the two heaviest dysprosium nuclei only. All states except the $9/2+$ and $13/2+$ states are expected to be weakly populated.

In ^{163}Dy, $9/2+$ and $13/2+$ assignments are suggested for the 499 keV and 719 keV levels, respectively. The two levels have angular distributions which indicate high angular momenta, and occur in the spectrum at the excitation energy expected. The strength of the $13/2+$ state relative to the $9/2+$ state is, however, less than expected from theory and from comparison with other nuclei where the $7/2+[633]$ orbital is observed. In this connection, the coupling to the $N = 6$ states discussed in sect. 2.3.2 should be kept in mind.

The $7/2+[633]$ orbital forms the ground state in ^{165}Dy[7-10]. Only at $60°$ the ground state is observed with a cross section of ~ 2 μb/sr. The $9/2+$ state at 84 keV and the $13/2+$ state at 308 keV have (d,p) cross sections well in accordance with the theoretical predictions.

2.3.11. The 1/2–[521] Orbital

The $1/2-[521]$ orbital is populated in all the dysprosium nuclei investigated except ^{155}Dy, which can be reached by the (d,t) reaction only. This orbital is characterized by a strong $1/2-$ state. The $5/2-$ and $7/2-$ states have each about half the strength of the $1/2-$ state.

In ^{157}Dy, the $1/2-$ state is observed at 464 keV with an angular distribution which is typical of $l = 1$. The $3/2-$ state coincides with the $9/2$ $5/2-[523]$ state at 520 keV, and the $5/2-$ state is identified at 553 keV from the angular distribution and the strength of the cross section. The strong hole state $3/2$ $1/2-[530]$ is observed at 555 keV and probably con-

TABLE 17. (d,p) population of the 7/2 + [633] band.

Spin	$d\sigma/d\Omega$, $\theta = 90°$, $Q = +3$ MeV							Relative values of C_{jl}^2						
	Theory	155	157	159	161	163	165	Theory	155	157	159	161	163	165
7/2	~ 0							0.001						
9/2	21					≤37*	16	0.07					0.20	0.05
11/2	~ 1							0.02						
13/2	41					22	47	0.92					0.80	0.95

* Probably some contributions from 11/2 11/2 – [505].

TABLE 18. (d,p) population of the 1/2 – [521] band.

Spin	$d\sigma/d\Omega$, $\theta = 90°$, $Q = +3$ MeV						Relative values of C_{jl}^2					
	Theory	157	159	161	163	165	Theory	157	159	161	163	165
1/2	245	151	195	164	143	186	0.25	0.34	0.34	0.37	0.30	0.37
3/2	24	~ 17	25	35	4	17	0.02	0.04	0.04	0.08	0.01	0.04
5/2	114	129	71	61	~ 69**	73	0.18	0.46	0.20	0.21	0.23	0.23
7/2	145	44	155	82	138	106	0.23	0.16	0.42	0.29	0.46	0.33
9/2	19			14		7	0.27			0.05		0.02
11/2	3					4	0.05					0.01

* Coincides with 9/2 5/2 – [523].
** Coincides with 3/2 3/2 – [521].

TABLE 19. (d,p) population of the 5/2 – [512] band.

Spin	$d\sigma/d\Omega$, $\theta = 90°$, $Q = +3$ MeV						Relative values of C_{jl}^2					
	Theory	157	159	161	163	165	Theory	157	159	161	163	165
5/2	6						0.01					
7/2	493	70	100	291	336	236	0.79	0.51	0.50	0.70	0.79	0.69
9/2	10	8	11	14	10	6	0.14	0.49	0.50	0.30	0.21	0.16
11/2	4					6	0.06					0.15

tributes to the (d,p) cross section of the peak at 553 keV, which is too strong according to the theory. On the other hand, the 7/2 – state, which is observed at 670 keV, is weaker than expected.

In ^{159}Dy, the 533 keV level is identified as the 1/2 – state from the angular distribution and the strength of the cross section. The 3/2 – and 5/2 – states are observed at 586 keV and 621 keV, respectively. In this nucleus, the 7/2 – state at 744 keV is stronger than expected. The explanation might also

here be that the (d,p) contribution from the $3/2\ 1/2-[530]$ state cannot be resolved from the $7/2-$ state.

In ^{161}Dy, the $1/2-[521]$ band head is observed at 370 keV with an angular distribution very similar to the previously identified $1/2\ 1/2-[521]$ states. The Q-corrected cross section is also similar to those observed for the corresponding states in ^{157}Dy and ^{159}Dy. The two peaks at 421 keV and 451 keV are identified as belonging to the $3/2-$ state and the $5/2-$ state, respectively, with the $7/2-$ state observed at 572 keV. The peaks at 634 keV and 808 keV are tentatively assumed to belong to the $9/2-$ and $11/2-$ states.

In ^{163}Dy, the $1/2-$ state is placed at 350 keV. The identification of the $1/2-[521]$ band in ^{163}Dy is less straightforward than in the other dysprosium nuclei investigated, and the orbital shows deviations both in the decoupling parameter a and the cross sections of the different members of the rotational band. The $3/2-$ state at 388 keV is very weakly populated. The $5/2-$ state is observed at 425 keV, but part of the strength probably stems from the $3/2\ 3/2-[521]$ state. The $7/2-$ state at 517 keV has a relatively large (d,p) cross section, and also an apparently large (d,t) cross section. The latter may, however, contain contributions from the $13/2+$ state discussed in sect. 2.3.2.

In ^{165}Dy, the $1/2-[521]$ state is a low-lying particle excitation where the band head is observed at 109 keV. The angular distribution fits well into the pattern of the previously observed $1/2\ 1/2-[521]$ states in the dysprosium nuclei. The $3/2-$ state is observed at 158 keV, and the $5/2-$ state at 182 keV. The rather strong peak at 298 keV is ascribed to the $7/2-$ state, and also the $9/2-$ and $11/2-$ states give rise to weak peaks at 336 keV and 518 keV, respectively.

The $1/2-[521]$ orbital has previously been identified at $^{161,\ 163,\ 165}$Dy[5-8] and theoretical calculations of excitation energy, decoupling parameter and purity of the state have been performed for a number of nuclei, including $^{161,\ 163,\ 165}$Dy by SOLOVIEV and VOGEL[13] and BÉS and CHO[19], taking into account the coupling between phonons and quasiparticles. The Coriolis coupling is not considered in these calculations. Especially in ^{163}Dy where the $3/2-[521]$ orbital is close to the $1/2-[521]$ orbital, this interaction is expected to be important.

The experimental values of the decoupling parameter a are collected in Table 21. Apart from the ^{163}Dy case, the variation in a is not more than 15%. This is in contrast to the theoretical values calculated by SOLOVIEV and VOGEL[13], which decrease a factor 2 from ^{165}Dy to ^{159}Dy.

2.3.12. The 5/2–[512] Orbital

The assignments made below are supported by the angular intensity variations, but represent only a fraction of the full theoretical intensity (cf. Table 19). The $5/2-[512]$ band is characterized by a strong $7/2-$ member.

In ^{157}Dy, the level is placed at 985 keV. The $9/2-$ state is tentatively assumed to be the one at 1101 keV.

In ^{159}Dy, the $7/2-$ state and $9/2-$ state are observed at 1089 keV and 1189 keV, respectively. The strong level at 1283 keV could be another choice for the $7/2-$ state, but the angular distribution makes the first assignment preferable.

In ^{161}Dy, the $7/2-$ state is observed at 883 keV. The $9/2-$ state is very likely the one at 995 keV, although the intensity is stronger than expected.

In ^{163}Dy, the level at 801 keV, which is strongly populated by the (d,p) reaction, is proposed to be the $7/2-$ state. The level at 918 keV possibly corresponds to the $9/2-$ state, although the rotational parameter is then larger than found in the other dysprosium nuclei.

In ^{165}Dy, the $5/2-[512]$ orbital is well established by previous work[7–10] as a low-lying particle state. The $7/2-$ state is observed at 262 keV and the $9/2-$ state at 361 keV. The band head coincides with the $5/2 \ 1/2-[521]$ state at 182 keV.

From Table 19, it is seen that the strength of the $7/2 \ 5/2-[512]$ state increases from ^{165}Dy to ^{163}Dy. This is in agreement with the decrease of pair occupation probability, V^2, for the orbital concerned as neutrons are removed. In the lighter dysprosium nuclei, however, the strength decreases drastically, and the $7/2-$ cross section for ^{157}Dy is only 20% of that for ^{163}Dy.

Obviously the strength of the $7/2-$ states is split by some unknown interaction in the lighter dysprosium nuclei, where the excitation energy is comparatively high.

2.3.13. The 1/2–[510] Orbital

This orbital is expected to be a highly excited particle state in the Dy nuclei. The orbital is subject to strong particle-vibration interactions, giving rise to reduced cross sections and decoupling parameters less than the Nilsson value $a = -0.34$. The $3/2-$ state is strong and characteristic of the orbital.

In ^{157}Dy, the 1569 keV level is identified as $3/2-$ from the angular distribution and the cross section. The $5/2-$ and $7/2-$ states are observed at

TABLE 20. (*d,p*) population of the $1/2-[510]$ band.

Spin	$d\sigma/d\Omega$, $\theta = 90°$, $Q = 3$ MeV						Relative values of C_{jl}^2					
	Theory	157	159	161	163	165	Theory	157	159	161	163	165
1/2	9				8		0.01				0.03	
3/2	398	62	84	148	171	138	0.41	0.45	0.57	0.60	0.54	0.70
5/2	183	17	19	42	62	28	0.29	0.19	0.20	0.27	0.30	0.22
7/2	120	32	21	21	27	9	0.19	0.36	0.23	0.13	0.13	0.08
9/2	6						0.09					
11/2	1						0.01					

TABLE 21. Decoupling parameters a for the $1/2-[521]$ orbital.

	^{165}Dy	^{163}Dy	^{161}Dy	^{159}Dy	^{157}Dy
Experiment (this work).........	0.57	0.30	0.48	0.43	0.48
Theory (SOLOVIEV and VOGEL[13])..	0.86	0.60	0.47	0.42	

TABLE 22. Inertial parameters and decoupling parameters.
Number in brackets are decoupling parameters for $K = \frac{1}{2}$ bands.

Nilsson orbital	165	163	161	159	157	155
$3/2-[521]$		10.6	11.5	11.4	12.0	10.9
$5/2-[523]$		10.6	10.9	12.3	11.1	
$5/2+[642]$		5.3	6.3	5.0		
$1/2+[660]$		6.3(0.49)				
$3/2-[532]$				12.6	11.0	
$1/2-[530]$		7.0(−0.04)	7.5(0.55)	7.4(0.05)	8.7(0.77)	8.4(**0.02**)
$1/2-[521]$	10.6(0.57)	10.0(0.30)	11.5(0.48)	12.3(0.43)	12.8(0.48)	
$7/2+[633]$	9.3	9.2				
$5/2-[512]$	11.1	13.0	12.4	11.1	12.9	
$1/2-[510]$	11.2(0.036)	13.2(−0.048)	11.3(0.07)	12.4(−0.04)	11.2(−0.12)	
$1/2+[651]$	9.1(0.03)		7.5(−0.15)			
$3/2-[512]$	12.0	12.2				

1632 keV and 1701 keV, respectively. This assignment gives $A = 11.2$ keV and $a = 0.12$.

In ^{159}Dy, the $3/2-$ state is observed at 1473 keV and the $5/2-$ state at 1535 keV. The 1621 keV level has an angular distribution compatible with $l = 3$, and a $7/2-$ assignment to this level gives the parameters $A = 12.4$ keV and $a = 0.04$.

In ^{161}Dy, the $3/2-$ state is observed at 1309 keV, the $5/2-$ state at 1363 keV and the $7/2-$ state at 1446 keV. The parameters are here $A = 11.4$ keV and $a = 0.049$.

In ^{163}Dy, the $3/2-$ state is observed at 1199 keV with a large cross section. The $5/2-$ and $7/2-$ states are observed at 1262 keV and 1342 keV, respectively, and the weak level at 1159 keV is tentatively assigned to the $1/2-$ state. These assignments correspond to the parameters $A = 12.0$ keV and $a = 0.048$.

In ^{165}Dy, the $3/2$ $1/2-[510]$ state is observed at 606 keV, which is significantly lower than in ^{163}Dy. The reduced cross section for the $3/2-$ state at $90°$ is 138 $\mu b/sr$ as compared to 171 $\mu b/sr$ in ^{163}Dy. These facts indicate a stronger interaction between the $1/2-[510]$ orbital and some vibrational mode than in the lighter dysprosium nuclei.

The theoretical predictions by SOLOVIEV and VOGEL[13] for the $1/2-[510]$ orbital in ^{165}Dy are 32% $1/2-[510]$, 63% gamma vibration based on $5/2-[512]$ and 4% gamma vibration based on $3/2-[512]$. The value of the decoupling parameter from SOLOVIEV and VOGEL's calculation is $a = 0.05$, and from the calculation of BÉS and CHO[19] it is $a = 0.03$. This is in good agreement with the experimental value $a = 0.036$ which results from the identification of the $5/2-$ state at 658 keV and the $7/2-$ state at 737 keV. The inertial parameter is $A = 11.2$ keV.

2.3.14. The 3/2–[512] Orbital

This orbital, which is observed in the three heaviest dysprosium nuclei, has a characteristic pattern consisting of a strong $5/2-$ state and weaker $3/2-$ and $7/2-$ states.

The 1977 keV level in ^{161}Dy is assigned to the $3/2$ $3/2-[512]$ state. The $5/2-$ state is observed at 2039 keV, and the $7/2-$ state is assumed to constitute the main part of an unresolved peak at 2113 keV. Both the angular distributions and the relative cross sections of the rotational band are compatible with the $3/2-[512]$ assignment.

In ^{163}Dy, the $3/2-$, $5/2-$ and $7/2-$ states are observed at 1795 keV, 1856 keV and 1936 keV, respectively. The angular distributions are typical of $l = 1$ and $l = 3$, but the cross section of the $5/2-$ state is smaller than expected.

In ^{165}Dy, the $3/2-$ state is placed at 1258 keV and $5/2-$ and $7/2-$ states at 1312 and 1402 keV, respectively. The assignments are based mainly on the angular distribution. Also in ^{165}Dy, the cross section of the $5/2-$ state relative to the $3/2-$ state and the $7/2-$ state is smaller than expected. Com-

N = 97
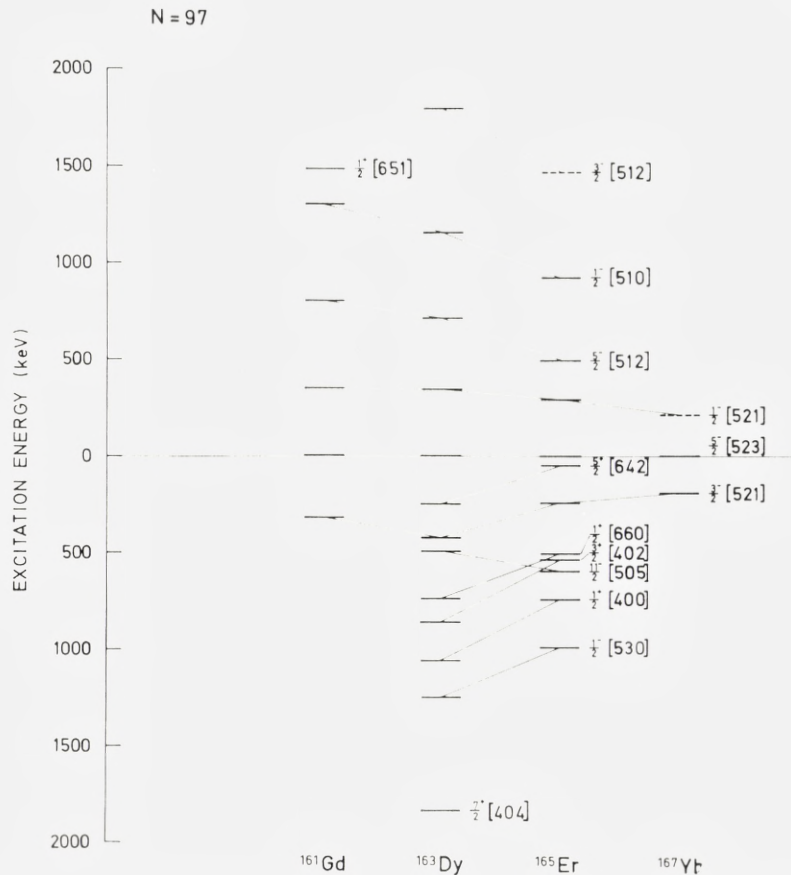
Fig. 21. Z-dependence of the band head energies for the isotones with N = 97.

pared to ^{163}Dy, the relative strengths of the members of the orbital are quite similar in the two nuclei, but the cross sections in ^{165}Dy are less than 50 % of the cross sections in ^{163}Dy.

3. Z-Dependence of Single-Quasiparticle Energies

The number of single quasiparticle states identified in deformed nuclei has increased considerably during the later years. It is therefore possible to compare the single-quasiparticle energies of the same Nilsson state in several nuclei with the same number of neutrons. In all cases, except for
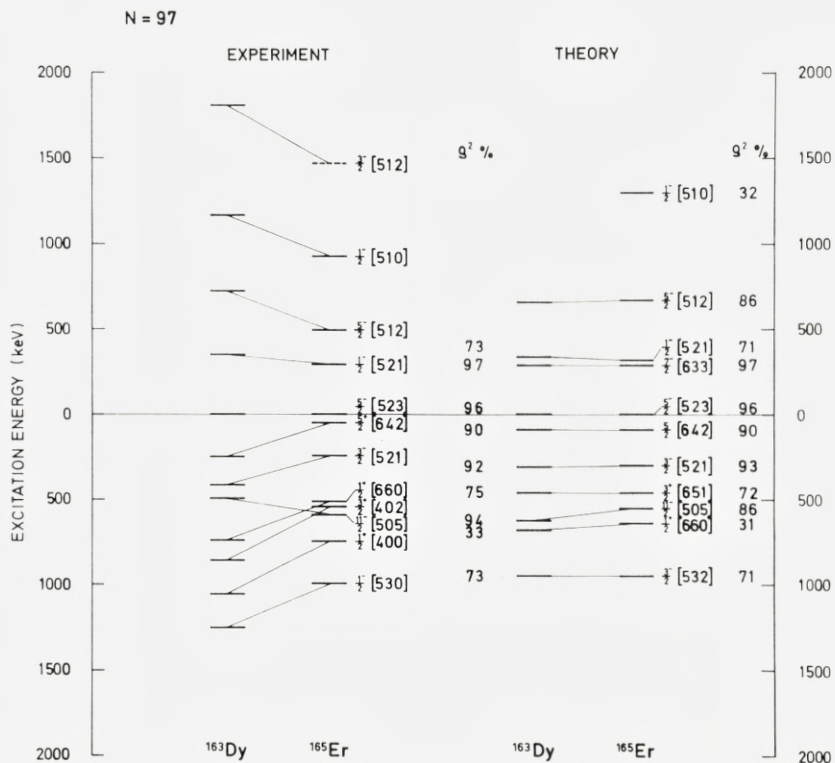
Fig. 22. Theoretical and experimental band head energies for ¹⁶³Dy and ¹⁶⁵Er.

neutron number 89, a systematic change in the band head energies is observed from one isotone to the next.

In Fig. 21, the band head energies of the identified Nilsson states are compared for the $N = 97$ isotones. The data for the gadolinium and erbium nuclei are mainly taken from refs. 1 and 2, the ytterbium data are taken from ref. 3.

The characteristic trend in this and other cases is the general compression or expansion of the band head energies as one goes from one isotone to the next. The few deviations from the pattern often concern orbitals which are affected by strong Coriolis coupling, such as, for instance, the $3/2-[521]$ orbital in ¹⁶¹Gd. Also the $11/2-[505]$ orbital frequently shows an irregular behaviour.

Figure 22 gives a comparison with the theoretical calculations by Soloviev et al.[20], where the interactions between phonons and quasipar-
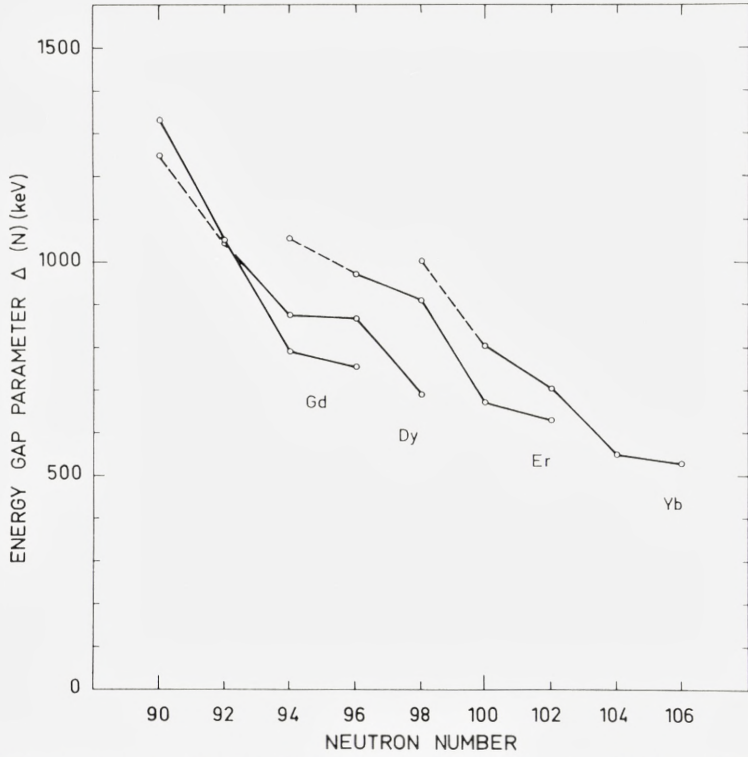
Fig. 23. The energy gap parameter $\Delta(N)$ for different elements as a function of the neutron number.

ticles are taken into account. The calculated energies agree well with the experimental energies for ^{165}Er, but the calculations do not reproduce the expansion in the observed excitation energies in ^{163}Dy.

The observed energies are the quasiparticle energies which, in the pairing formalism, are given by the expression

$$E_j = \sqrt{(\varepsilon_j - \lambda)^2 + \Delta^2} - \Delta, \tag{3}$$

where ε_j is the single-particle energy, λ the chemical potential, and Δ is the energy gap parameter for neutron orbitals.

It is experimentally known that the energy gap parameter Δ varies from element to element. The effect of this variation on the quasiparticle energies can easily be evaluated by Eq. (3) on the assumption of constant $(\varepsilon_j - \lambda)$. The energy gap parameter can be calculated from the neutron separation energies by the formula
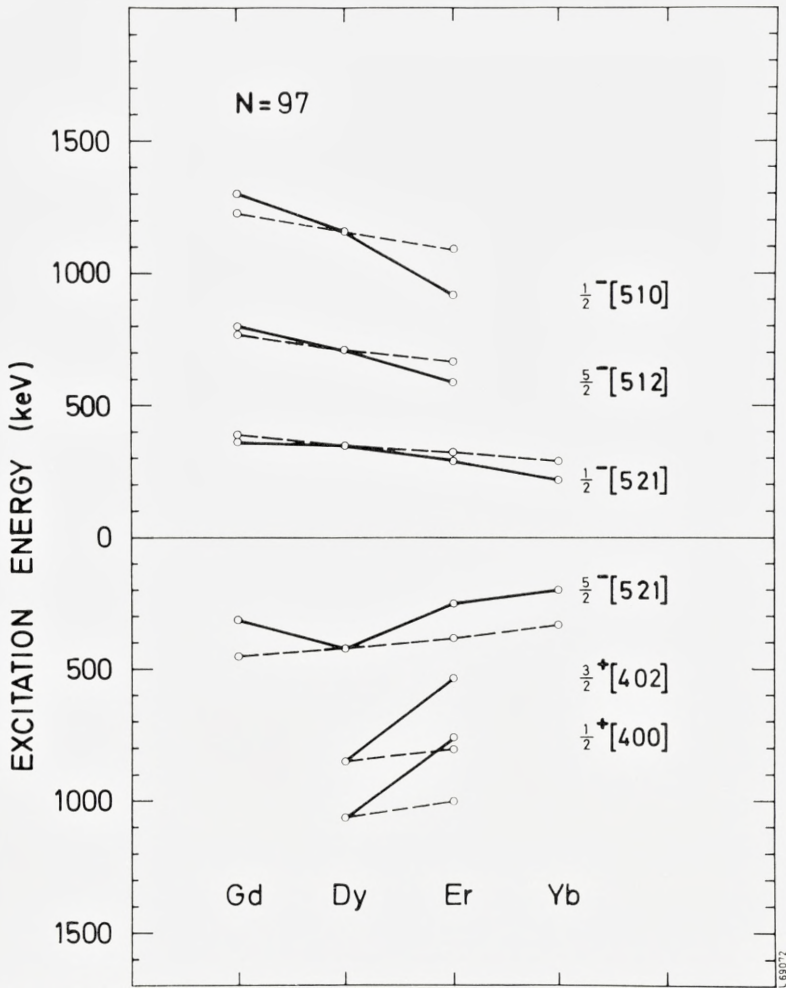
Fig. 24. The effect of Δ on the quasiparticle energies assuming a constant $(\varepsilon - \lambda)$ normalized to the Dy case. The dotted lines show the calculated quasiparticle energies, the full lines the experimental energies.

$$\Delta(N) = 1/2 [S_n(N) - S_n(N-1)], \quad (N \text{ even}) \tag{4}$$

where the experimental neutron separation energies for Gd, Er, and Yb are available[1, 2, 3]. In Fig. 23, the variation of Δ versus the neutron number N is plotted for different elements. The calculated quasiparticle energies for $N = 97$ are shown in Fig. 24, where the observed excitation energies are connected by solid lines, whereas the calculated energies are connected

through dotted lines. The slope of the dotted lines shows the effect of Δ assuming a constant $(\varepsilon_j - \lambda)$ normalized to the Dy case. It is clearly seen that only part of the observed energy shifts can be explained in this way.

The calculations by SOLOVIEV and VOGEL[13] show that the coupling to the gamma vibration affects the single-quasiparticle energies. As the energy and strength of the gamma vibration in the even nuclei, for a fixed neutron number, show some dependence on Z, part of the variation illustrated in Fig. 24 might be ascribed to particle-phonon coupling.

4. Summary

The present work has identified a total of 16 different Nilsson orbitals with their associated rotational bands.

The level order is almost identical to the one found in gadolinium, and again confirms the Nilsson scheme. It is also interesting to see how the inclusion of the phonon-quasiparticle interaction[20] improves the overall agreement (Fig. 22). Some of the remaining discrepancies might have their origin in the Coriolis interaction which is not included in the model.

The Z-dependence of the neutron quasiparticle energies shows a remarkable symmetric pattern with few irregularities. The Z-dependent variation in the level density is more pronounced for the heavier nuclei than in the lighter ones. In the $N = 89$ isotones ^{153}Gd and ^{155}Dy, there is practically no change in the band head energies. If the particle-phonon interaction is included, the quasiparticle energies are compressed compared with the Nilsson scheme. The Z-dependent compression revealed by the data might partly be explained by a difference in the vibration strength from one isotone to another.

Acknowledgements

The Niels Bohr Institute   *Institute of Physics*
University of Copenhagen   *University of Bergen*

References

1) P. O. Tjøm and B. Elbek, Mat. Fys. Medd. Dan. Vid. Selsk. **36**, no. 8 (1967).
2) P. O. Tjøm and B. Elbek, Mat. Fys. Medd. Dan. Vid. Selsk. **37**, no. 7 (1969).
3) D. G. Burke, B. Zeidman, B. Elbek, B. Herskind and M. C. Olesen, Mat. Fys. Medd. Dan. Vid. Selsk. **35**, no. 2 (1966).
4) J. Borggreen and J. P. Gjaldbæk, Nucl. Phys. **A 113** (1968) 659.
5) L. Funke, H. Gruber, K.-H. Kunn, J. Römer and H. Sodan, Nucl. Phys. **84** (1966) 443.
6) O. W. B. Schult et al., Phys. Rev. **154** (1967) 1146.
7) R. K. Sheline and H. T. Motz, Phys. Rev. **136** (1964) B 351.
8) O. W. B. Schult, B. P. Maier and U. Gruber, Z. Phys. **182** (1964) 171.
9) G. Markus, W. Michaelis, H. Schmidt and C. Weitkamp, Z. Phys. **206** (1967) 84.
10) B. C. Dutta, T. V. Egidy, Th. W. Elze and W. Kaiser, Z. Phys. **207** (1967) 153.
11) S. Sjøflot and T. Silnes, private communication.
12) J. H. E. Mattauch, W. Thiele and A. H. Wapstra, Nucl. Phys. **67** (1965) 1.
13) V. G. Soloviev and P. Vogel, Nucl. Phys. **A 92** (1967) 449.
14) J. Borggreen, G. Løvhøiden and J. C. Waddington, Nucl. Phys. **A 131** (1969) 241.
15) M. Jaskola, P. O. Tjøm and B. Elbek, Nucl. Phys. **A 133** (1969) 65.
16) B. L. Andersen, Nucl. Phys. **A 112** (1968) 443.
17) G. Løvhøiden, private communication.
18) L. Funke et al., Nucl. Phys. **55** (1964) 401.
19) D. R. Bés and Cho Yi Chung, Nucl. Phys. **86** (1966) 581.
20) V. G. Soloviev, P. Vogel and G. Jungclaussen, Izv. Akad. Nauk, USSR, Ser. fiz. **31** (1967) 518.

I. BREVIK

ELECTROMAGNETIC ENERGY-MOMENTUM TENSOR WITHIN MATERIAL MEDIA

2. DISCUSSION OF VARIOUS TENSOR FORMS

Synopsis

This paper represents the second part of a study of the electromagnetic energy-momentum tensor within a material medium. Similarly as in the first part, essentially a macroscopical point of view is adopted, and emphasis is laid upon the comparison with experiments, both in the case of static fields and in the case of time-varying fields within bodies at rest and in relativistic motion. For the main part the relative behaviour of Minkowski's and Abraham's tensors is studied, but some attention is also given to the tensors introduced by Einstein and Laub, de Groot and Suttorp, Beck and Marx et al. Deductive procedures are employed, characteristic effects are studied, both within media at rest and in motion, and some attention is given to a critical analysis of earlier treatments. Our main conclusion is that Minkowski's and Abraham's tensors are equivalent in the usual physical cases, while the remaining tensor expressions seem to run into conflict with experimental evidence.

1. Introduction and Summary

In a previous paper[1]—hereafter referred to as I—we discussed the application of Minkowski's energy-momentum tensor in phenomenological electrodynamics. The medium was assumed to be homogeneous, transparent and usually also nondispersive. Since the essential differences between the various competing tensor forms are present also in the most simple media, the above restrictive assumptions were legitimate in relation to the main purpose of the investigation, namely to examine whether Minkowski's tensor is appropriate to use in the most common and simple situations. And the affirmative answer to this question made it just convenient to restrict the treatment so as to incorporate Minkowski's tensor only.

In the present paper we shall consider also other tensor forms, so let us first write down some expressions. The rest inertial frame of the medium shall be denoted by K^0, while the inertial frame in which K^0 moves with the uniform velocity $\boldsymbol{v}$, shall be denoted by K. Minkowski's tensor reads

$$S_{ik}^M = - E_i D_k - H_i B_k + \tfrac{1}{2}\delta_{ik}(\boldsymbol{E}\cdot\boldsymbol{D} + \boldsymbol{H}\cdot\boldsymbol{B}) \tag{1.1a}$$

$$S_{4k}^M = i(\boldsymbol{E}\times\boldsymbol{H})_k,\ \ S_{k4}^M = i(\boldsymbol{D}\times\boldsymbol{B})_k,\ \ S_{44}^M = -\tfrac{1}{2}(\boldsymbol{E}\cdot\boldsymbol{D} + \boldsymbol{H}\cdot\boldsymbol{B}), \tag{1.1b}$$

or, in covariant form,

$$S_{\mu\nu}^M = F_{\mu\alpha}H_{\nu\alpha} - \tfrac{1}{4}\delta_{\mu\nu}F_{\alpha\beta}H_{\alpha\beta} \tag{1.2}$$

(for notation, see I).

Perhaps the main reason why Minkowski's tensor often has been rejected and instead replaced by some other tensor form is the asymmetry of the former, which is present even within isotropic media. The symmetry requirement is met by the following tensor, which we shall call Abraham's tensor,

$$S_{ik}^{A0} = -\tfrac{1}{2}(E_i^0 D_k^0 + E_k^0 D_i^0) - \tfrac{1}{2}(H_i^0 B_k^0 + H_k^0 B_i^0) + \tfrac{1}{2}\delta_{ik}(\boldsymbol{E}^0\cdot\boldsymbol{D}^0 + \boldsymbol{H}^0\cdot\boldsymbol{B}^0) \tag{1.3a}$$

$$S_{k4}^{A0} = S_{4k}^{A0} = i(\boldsymbol{E}^0\times\boldsymbol{H}^0)_k,\ \ S_{44}^{A0} = -\tfrac{1}{2}(\boldsymbol{E}^0\cdot\boldsymbol{D}^0 + \boldsymbol{H}^0\cdot\boldsymbol{B}^0) \tag{1.3b}$$

1*

(here given in K^0), although this symmetrized form of the stress tensor S_{ik}^{A0} for anisotropic media seems to have been given first by H. Hertz[2]. When the body is isotropic, the force density in K reads

$$\boldsymbol{f}^{A0} = \boldsymbol{f}^{M0} + \frac{n^2 - 1}{c^2} \frac{\partial \boldsymbol{S}^{M0}}{\partial t^0}, \quad f_4^{A0} = f_4^{M0}, \tag{1.4}$$

where n is the refractive index. We shall often be concerned with this tensor in the following chapters. Its covariant form can be written as

$$S_{\mu\nu}^A = S_{\mu\nu}^M + \frac{\varkappa}{\mu}\left(F_{\mu\alpha}F_\alpha - \frac{1}{c^2}F_\alpha F_\alpha V_\mu\right)V_\nu, \tag{1.5}$$

where $\varkappa = (\varepsilon\mu - 1)/c^2 = (n^2 - 1)/c^2$, $F_\alpha = F_{\alpha\nu}V_\nu$ and $V_\mu = \gamma(\boldsymbol{v}, ic)$.

Another proposal was put forward by G. Marx and collaborators[3]. They examined a simple radiation field travelling through an isotropic medium, and came to the conclusion that Abraham's tensor, describing the electromagnetic field, must be supplemented with a mechanical tensor to give the symmetrical "radiation" tensor $S_{\mu\nu}^S$ describing the total system: radiation plus connected mechanical field. In K^0 the radiation tensor is given by

$$S_{ik}^{S0} = \frac{1}{n^2}S_{ik}^{A0} = \frac{1}{n^2}S_{ik}^{M0}, \quad S_{4\nu}^{S0} = S_{\nu4}^{S0} = S_{4\nu}^{A0}, \tag{1.6}$$

for all ν between 1 and 4.* The covariant expression can be written

$$S_{\mu\nu}^S = \frac{1}{n^2}S_{\mu\nu}^M + \frac{\varkappa}{\mu n^2}[V_\mu F_{\nu\alpha}F_\alpha + \tfrac{1}{2}V_\mu V_\nu(\varkappa F_\alpha F_\alpha + \tfrac{1}{2}F_{\alpha\beta}F_{\alpha\beta})]. \tag{1.7}$$

A. Einstein and J. Laub[5] have also examined the problem; by means of simple examples they constructed an expression for the force density in K^0 which corresponds to the following components of the energy-momentum tensor

$$S_{ik}^{E0} = -E_i^0 D_k^0 - H_i^0 B_k^0 + \tfrac{1}{2}\delta_{ik}(\boldsymbol{E}^{02} + \boldsymbol{H}^{02}) \tag{1.8a}$$

$$S_{4k}^{E0} = S_{k4}^{E0} = i(\boldsymbol{E}^0 \times \boldsymbol{H}^0)_k. \tag{1.8b}$$

The energy density component was not given.

The last tensors we shall mention here are due to S. R. de Groot and L. G. Suttorp[6]. These authors have examined the problem from a purely

* F. Beck[4] has also introduced a tensor which, however, in the case of a radiation field coincides with Marx's radiation tensor. Therefore we shall not pay any special attention to this form in the following sections.

microscopical point of view, and published recently a series of papers on the subject. (See also I, section 7.) They give two tensor expressions, dependent on whether the total interaction between field and matter is taken into account or not. In the case of an isotropic medium their first proposal reads in K^0

$$S_{ik}^{G0} = -E_i^0 D_k^0 - H_i^0 B_k^0 + \delta_{ik} (\tfrac{1}{2} \boldsymbol{E}^{02} + \tfrac{1}{2} \boldsymbol{B}^{02} - \boldsymbol{M}^0 \cdot \boldsymbol{B}^0) \qquad (1.9\,\mathrm{a})$$

$$S_{4k}^{G0} = S_{k4}^{G0} = i(\boldsymbol{E}^0 \times \boldsymbol{H}^0)_k, \quad S_{44}^{G0} = -\tfrac{1}{2}(\boldsymbol{E}^{02} + \boldsymbol{B}^{02}), \qquad (1.9\,\mathrm{b})$$

where $\boldsymbol{M}^0 = \boldsymbol{B}^0 - \boldsymbol{H}^0$. It is apparent that for $\boldsymbol{M}^0 = 0$, the components (1.8) of the EINSTEIN-LAUB tensor agree with the corresponding components of the DE GROOT-SUTTORP tensor (1.9).

The second tensor expression proposed by DE GROOT and SUTTORP was defined as the difference between the total energy-momentum tensors with and without external electromagnetic fields. This tensor thus corresponds to taking the whole interaction between field and matter into account. By omitting the variations of the material constants with density and temperature, as we mainly do throughout our work, we find that their second field tensor agrees with ABRAHAM's tensor within an isotropic body.

There exist also other proposals that have been put forward, and we shall have the opportunity to comment upon some of them in the detailed considerations later on. Mostly we shall be concerned with the relative merits of ABRAHAM's and MINKOWSKI's tensors, since these tensors, combined with their appropriate interpretations, are found to be both adequate and equivalent in most of the simple physical situations considered.

Further introductions to the subject are given in the books by C. MØLLER[7] and W. PAULI[8], and in the review article by G. MARX[9].

The main task of the subsequent exposition can be conveniently divided into three parts. Firstly, we want to apply some deductive methods in order to see how the various tensors adapt themselves to the formalism. As indicated already in I it must be borne in mind that the power of this kind of method is restricted in the sense that the expressions one obtains are not unique. Secondly, we wish to examine the applicability of the various tensor forms to the description of definite phenomena. The description of the experiments is here a crucial point. Thirdly, we shall spend some effort to comment upon parts of the earlier literature. There has been published a large number of papers on the subject, which are often mutually contradictory and moreover scattered over a number of different journals. We find it therefore of importance to point out some crucial points in the various

derivations as an attempt to find the deeper reason why the results are seemingly incompatible.

Throughout this work we take a phenomenological point of view and refer only occasionally to the simple microscopical treatment in I. This is done for practical reasons, a thorough scrutiny of the microscopical aspects would require a separate treatment. However, we think there is also a reason of principle why it is sensible first to choose the macroscopical line of approach in order to obtain a satisfactory description of the physical phenomena: In the simple cases considered, the results obtained by means of these macroscopic or semi-macroscopic methods are both consistent and moreover fit the observed data in an excellent way. From a pragmatic point of view the macroscopical kind of method is therefore not only a possible kind of approach but in fact the *appropriate* one as a first step, and microscopical methods with their complicated formalism should properly be considered to represent a later stage of the development.

Let us now review the subsequent sections. Section 2 is devoted to an analysis of electrostatic fields. We considor again the variational method which was employed in section 3 of I, and show how MINKOWSKI's and ABRAHAM's tensors emerge from the formalism in an equivalent way. It is found that, as far as a dielectric body is surrounded by a vacuum or an isotropic liquid, no experiment testing electromagnetic forces or torques on the body can decide between these tensors. The two tensors correspond merely to different distributions of forces and torques throughout the body: According to MINKOWSKI the torque is essentially a *volume* effect, described by the tensor asymmetry, while according to ABRAHAM the torque is described completely in terms of the force density. We consider a typical example, in which ABRAHAM's torque naturally comes out as a *surface* effect.

In the remainder of section 2 we discuss to some extent the EINSTEIN-LAUB (or the DE GROOT-SUTTORP) tensor. It is found that also in this case no force or torque experiments on a body surrounded by a vacuum or an isotropic fluid represent a critical test for the tensors in question. However, there is actually one effect which represents a critical test, namely the pressure increase in a dielectric liquid because of the field. In order to apply the theory to this case it is necessary to extend the variational method mentioned earlier (the HELMHOLTZ method) so as to include also the electrostriction effect, although we are otherwise ignoring this effect in our work. S. S. HAKIM and J. B. HIGHAM have tested the pressure increase experimentally, and they found that the HELMHOLTZ force describes the observed data very well. On the contrary, the pressure increase predicted by the EINSTEIN-LAUB

force (which is also called the KELVIN force) was found to be in disagreement with the experiment.

In section 3 we continue the consideration from I, section 6 concerning the propagation of an electromagnetic wave within an isotropic body at rest. By means of the semi-macroscopic method that we are adopting, and by taking the radiation pressure experiment due to R. V. JONES and J. C. S. RICHARDS into account, we find that ABRAHAM's and MINKOWSKI's tensors are equivalent in the following sense: ABRAHAM's force density excites the constituent dipoles of the material and produces a mechanical momentum which travels together with the field. If we count this mechanical momentum together with ABRAHAM's momentum as a field momentum, we obtain MINKOWSKI's tensor. By considering the situation in the frame where the mean motion of the constituent particles vanishes we find that, in the case of an infinite medium, the energy-momentum tensor of the total system can be written as the sum of ABRAHAM's tensor and the mechanical tensor in the absence of fields.

We continue section 3 by discussing an example in which the boundary between two media is involved. Finally we consider alternative tensor forms, and find that the radiation pressure predicted by the radiation tensor is in disagreement with the JONES-RICHARDS experiment.

In section 4 we discuss possibilities for torque experiments, especially when MINKOWSKI's or ABRAHAM's tensors are taken as field tensors. For a stationary optical wave in interaction with a dielectric body we find that the two tensors will always yield the same value for the torque. Thereafter we propose an experiment involving a low-frequency combination of electric and magnetic fields. This experiment should be appropriate for the detection of ABRAHAM's force, which is hidden in the case of optical fields. Finally it is concluded that the case of an optical field travelling through a dielectric body immersed in a dielectric liquid should represent a possible means for a further experimental check of the radiation tensor and the EINSTEIN-LAUB tensor.

Section 5 is devoted to a critical review of some parts of the earlier literature, especially those parts which seem to run into conflict with our own interpretations. We are otherwise commenting upon passages from earlier treatments also in our ordinary exposition of various topics, but there remain interesting arguments which cannot so naturally be dealt with in the ordinary treatment. We think such a critical analysis is desirable in a study of the present problem, since an important part of the task is just to clear up a situation which is confused by mutually contradictory opinions.

For the main part we discuss gedanken experiments which have been put forward to support either MINKOWSKI's or ABRAHAM's tensor, and show how these situations are to be explained with the use of the formerly rejected alternative. In the remaining part of the section we mainly discuss some aspects of the EINSTEIN-LAUB paper.

In the subsequent sections we discuss topics connected with relativity, and, except for the last section, limit the consideration to the case of isotropic media. Section 6 is devoted to a study of the torque acting on a moving body when an electromagnetic wave is travelling within it. We first calculate ABRAHAM's and MINKOWSKI's torque expressions when the body is assumed infinitely extended, and show thereafter that both these expressions are relativistically consistent. In this context we draw into consideration an analogous situation encountered in relativistic mechanics: An elastic body subjected to stresses in its rest system may in other inertial systems require a torque in order to maintain steady motion. A similar situation is found to be present also here in electrodynamics: We require stady motion of matter plus field and find that there must then exist a rate of change of electro-magnetic momentum which is just equal to the previously calculated torque, with the opposite sign.

If the body is *finite*, we find that the most natural division of the total angular momentum into a field part and a mechanical part is obtained with the use of ABRAHAM's tensor for the field.

Section 7 contains a discussion of various relativistic phenomena. We begin by considering the velocity $\boldsymbol{u} = \boldsymbol{S}/W$ of the energy in an optical wave. In section 9 of I we found that $\boldsymbol{u}$ transforms like a particle velocity if MINKOWSKI's tensor is used. We now find that ABRAHAM's tensor cannot fulfil the transformation criterion due to the fact that this tensor does not describe the total travelling wave. We analyse the background for the transformation criterion, and give a rather general form of a tensor that fulfils it. The radiation tensor falls within this category.

Next we consider the relativistic centre of mass of a finite, but practically monochromatic, field. In section 12 of I we found that the various centres obtained with the use of MINKOWSKI's tensor in general do not coincide when considered simultaneously in one frame. Actually, by considering in the rest frame K^0 the centres of mass obtained by varying the direction and magnitude of the medium velocity, we found that they are located on a circular disk lying perpendicular to the inner angular momentum vector in K^0 with centre at the centre of mass in K^0. Now the various centres of mass are found to behave in exactly the same way if the ABRAHAM tensor or the radiation tensor is adopted.

The ČERENKOV effect is thereafter briefly analysed in the inertial frame in which the emitting particle is at rest. From a study of the momentum balance in this situation, I. TAMM has given preference to MINKOWSKI's tensor. We show how the momentum balance appears with the use of ABRAHAM's tensor. Section 7 is closed by some further remarks upon the literature.

In the last section we employ a variational method which implies the application of curvilinear coordinates as a formal remedy. For a closed system this method in general leads to a determination of the energy-momentum tensor, but the method is shown to leave a certain ambiguity here due to the fact that the LAGRANGIAN leading to the electromagnetic field equations corresponds to a non-closed physical system. Section 8 is rather detailed, since this subject has caused some confusion.

Finally we consider again the Sagnac-type experiment due to C. V. HEER, J. A. LITTLE and J. R. BUPP, which was discussed in section 9 of I. We find that this experiment, although it gives an excellent verification of the predictions of macroscopic electrodynamics, does *not* represent a critical test for MINKOWSKI's tensor, such as it was originally claimed. In fact, the experiment is found to be explained equivalently also by ABRAHAM's tensor and the radiation tensor.

The Appendix gives in tabular form a summary of the behaviour of the various examined energy-momentum tensors in some physical situations.

2. Static Fields

We begin with an examination of the various tensors applied to the simplest physical case, namely the static fields. Actually, only electrostatic fields shall be considered since, for the simple case with linear inductive magnetization here considered, the corresponding results in the magneto-static case can be taken over by analogy. In this section we first consider the important point concerning the relative behaviour of MINKOWSKI's and ABRAHAM's tensors, and show how they in general lead to equivalent experimental results. Thereafter we consider various other tensor possibilities. Since all quantities are taken in the rest frame, the superscript zero on them shall simply be omitted.

Minkowski's versus Abraham's tensor

From (1.1a) and (1.3a) it is apparent that MINKOWSKI's and ABRAHAM's tensors are equal in the electrostatic case for isotropic media. We therefore generalize the situation and consider the same physical system as in I,

section 3, namely a dielectric, anisotropic medium containing an electric field which is produced by some external devices. The linear relation $E_i = \eta_{ik} D_k$ is assumed to be valid. By varying the free energy

$$\mathscr{F} = \tfrac{1}{2} \int \boldsymbol{E} \cdot \boldsymbol{D} \, dV \tag{2.1}$$

and equating $-d\mathscr{F}/dt$ to the rate of mechanical work $\int \boldsymbol{f} \cdot \boldsymbol{u} \, dV$ exerted by the volume *forces*, we found in I $\boldsymbol{f} = \boldsymbol{f}^A$, where

$$\boldsymbol{f}^A = \varrho \boldsymbol{E} + \tfrac{1}{2} D_i D_k \nabla \eta_{ik} - \tfrac{1}{2} \partial_k (\boldsymbol{E} D_k - E_k \boldsymbol{D}). \tag{2.2}$$

This corresponds to the stress tensor

$$S_{ik}^A = -\tfrac{1}{2} (E_i D_k + E_k D_i) + \tfrac{1}{2} \delta_{ik} \boldsymbol{E} \cdot \boldsymbol{D}. \tag{2.3}$$

By comparison with (1.3a) it is thus evident that we have obtained ABRAHAM's tensor. However, by invoking the "dipole model" and assuming the existence of a *torque* density $\tau = \boldsymbol{D} \times \boldsymbol{E}$ with a corresponding extra contribution $\int \tau \cdot (d\varphi/dt) dV$ to the rate of mechanical work (φ being the rotational angle), we found instead MINKOWSKI's result

$$\boldsymbol{f}^M = \varrho \boldsymbol{E} + \tfrac{1}{2} D_i D_k \nabla \eta_{ik} \tag{2.4}$$

$$S_{ik}^M = -E_i D_k + \tfrac{1}{2} \delta_{ik} \boldsymbol{E} \cdot \boldsymbol{D}. \tag{2.5}$$

According to this description, the result is dependent explicity on the assumption of an extra torque density.

In order to make a more distinct comparison between the two tensor forms, it is convenient to reformulate the balance equation in terms of the rotational angle φ rather than the velocity $\boldsymbol{u} = d\boldsymbol{s}/dt$. Since $\boldsymbol{f} \cdot \boldsymbol{s} = (\boldsymbol{r} \times \boldsymbol{f}) \cdot \varphi$ we have from (I,3.10,9)

$$\int [\boldsymbol{r} \times (\varrho \boldsymbol{E} + \tfrac{1}{2} D_i D_k \nabla \eta_{ik})] \cdot \varphi dV + \int (\boldsymbol{D} \times \boldsymbol{E}) \cdot \varphi dV$$
$$= \int (\boldsymbol{r} \times \boldsymbol{f}) \cdot \varphi dV + \int \tau \cdot \varphi dV, \tag{2.6}$$

where $\boldsymbol{f}$ and τ are as yet unspecified. As φ is arbitrary, we obtain

$$\boldsymbol{r} \times \boldsymbol{f} + \tau = \boldsymbol{r} \times (\varrho \boldsymbol{E} + \tfrac{1}{2} D_i D_k \nabla \eta_{ik}) + \boldsymbol{D} \times \boldsymbol{E}. \tag{2.7}$$

This relation is fulfilled directly with MINKOWSKI's tensor, and only then. However, let us add the vanishing quantity

$$-\tfrac{1}{2}\int\limits_{\text{cond}} (E_i \boldsymbol{D}\cdot\boldsymbol{n} - \boldsymbol{E}\cdot\boldsymbol{n}D_i)s_i\,dS, \qquad (2.8)$$

taken over the external conductors that produce the field, and let us combine

$$\left.\begin{aligned}\int (\boldsymbol{D}\times\boldsymbol{E})\cdot\varphi dV - \tfrac{1}{2}\int\limits_{\text{cond}} (E_i\boldsymbol{D}\cdot\boldsymbol{n} - \boldsymbol{E}\cdot\boldsymbol{n}D_i)s_i dS \\[2mm] = -\tfrac{1}{2}\int \partial_k(\boldsymbol{E}D_k - E_k\boldsymbol{D})\cdot\boldsymbol{s}dV = -\tfrac{1}{2}\int [\boldsymbol{r}\times\partial_k(\boldsymbol{E}D_k - E_k\boldsymbol{D})]\cdot\varphi dV. \end{aligned}\right\} \quad (2.9)$$

Then (2.6) is equivalent to

$$\left.\begin{aligned}\int [\boldsymbol{r}\times(\varrho\boldsymbol{E} + \tfrac{1}{2}D_iD_k\nabla\eta_{ik} - \tfrac{1}{2}\partial_k(\boldsymbol{E}D_k - E_k\boldsymbol{D}))]\cdot\varphi dV \\[2mm] = \int (\boldsymbol{r}\times\boldsymbol{f})\cdot\varphi dV + \int \tau\cdot\varphi\,dV, \end{aligned}\right\} \quad (2.10)$$

and we obtain now $\boldsymbol{f} = \boldsymbol{f}^A$, $\tau = 0$, i.e. ABRAHAM's tensor. In this case the torque is described in terms of the force density, while in the former case it was described by the asymmetry of the stress tensor. We must conclude that, as far as the dielectric body is surrounded by an isotropic medium (here vacuum), no unambiguous answer can be given for electrostatic systems. And this result is connected with the fact that the total body torque is the same for both tensors in this case: We may put the torque formula into the form

$$N_l = \int (x_i f_k - x_k f_i + S_{ik} - S_{ki})\,dV = -\int\limits_{\text{surface}} (\boldsymbol{r}\times\boldsymbol{S}_n^{\text{vac}})_l\,dS, \qquad (2.11)$$

where $S_{ni} = S_{ik}n_k$. Thus the total torque can be evaluated from the vacuum values of the field, and MINKOWSKI's and ABRAHAM's tensors must yield the same result. Similarly, the total body force can also be put into a form which involves the vacuum field values only; by starting from the balance equation for total momentum we obtain readily for the total body force

$$F_i = -\int\limits_{\text{surface}} S_{ni}^{\text{vac}}\,dS, \qquad (2.12)$$

in accordance with (2.11).

It should be emphasized that in order to obtain MINKOWSKI's tensor in the first procedure above, we had to take into account the existence of extra body torques with the density $\boldsymbol{D}\times\boldsymbol{E}$. In the second procedure, however, the equivalence between MINKOWSKI's and ABRAHAM's tensors was demon-

strated simply by adding the vanishing term (2.8) in the energy balance. The additional assumption concerning the torque $\boldsymbol{D} \times \boldsymbol{E}$ will thus lead to an equivalent description with respect to observable effects for the whole dielectric body, only the distribution of torques and forces within the body will in general be different.

It is clear that the above reasoning will not be changed if we assume that an isotropic, dielectric liquid fills the space between the body and the conductors, since MINKOWSKI's and ABRAHAM's tensors are equal in such a liquid.

The arguments hitherto have dealt with the dielectric system considered as a whole. If several insulators are present between the conductors, then the torque acting on an individual insulator is still independent of which tensor we use. That follows immediately from the fact that we obtain expressions like the last term in eq. (2.11) for each insulator in question.

An example

For the sake of illustration, let us consider again the same physical situation as in I, section 3: A dielectric sphere is located in a homogeneous electrostatic field such that the principal axes of the sphere coincide with the coordinate axes. The external field is given as $\boldsymbol{E}^0 = (E_1^0, E_2^0, E_3^0)$. With the use of MINKOWSKI's tensor, we obtained in I for the single nonvanishing component of the torque

$$N_3^M = \int_{\text{body}} (S_{12}^M - S_{21}^M) \, dV = \int_{\text{body}} (\boldsymbol{D} \times \boldsymbol{E})_3 \, dV = (\boldsymbol{p} \times \boldsymbol{E}^0)_3, \qquad (2.13)$$

where $\boldsymbol{p} = 3V[(\varepsilon_1 - 1)E_1^0/(\varepsilon_1 + 2), (\varepsilon_2 - 1)E_2^0/(\varepsilon_2 + 2), 0], V$ being the volume of the sphere. According to (2.13), it is natural to interpret the effect as a volume effect.

Let us now insert ABRAHAM's tensor into the torque formula (2.11) so as to obtain

$$\left.\begin{aligned}
N_3^A &= \int_{\text{body}} (\boldsymbol{r} \times \boldsymbol{f}^A)_3 \, dV + \int_{\text{surface}} [\boldsymbol{r} \times (\boldsymbol{S}_n^A - \boldsymbol{S}_n^{\text{vac}})]_3 \, dS \\
&= - \int_{\text{surface}} (\boldsymbol{r} \times \boldsymbol{S}_n^{\text{vac}})_3 \, dS = (\boldsymbol{p} \times \boldsymbol{E}^0)_3.
\end{aligned}\right\} \qquad (2.14)$$

The expressions (2.14) and (2.13) are equal, as they should be. But for ABRAHAM's tensor the volume effect vanishes, as is apparent also from the fact that $\boldsymbol{f}^A = 0$ in the homogeneous field in the body. In this case it is natural to interpret the effect as arising from the volume forces in the boundary layer.

Other tensor forms

Let us now examine the various other tensor proposals mentioned in section 1. The radiation tensor due to Marx *et al* is defined for radiation fields within isotropic media only, and shall not be considered here. But there remains the Einstein-Laub tensor (1.8a) and the de Groot-Suttorp tensor (1.9a), which actually are seen to be equal in the electrostatic case. The force density is

$$f^E = \varrho E + (P \cdot \nabla) E, \tag{2.15}$$

which is different from both (2.4) and (2.2). This force is also called the Kelvin force. The difference is expected to be connected with the fact that the force densities (2.2) and (2.4) were obtained from a variational principle based on the free energy in the form (2.1), which includes the interaction energy between field and matter. And this energy is not directly compatible with the energy $_2 \int E^2 dV$ following from (1.9b).

As regards the possibility for an experimental check of the force (2.15) we have first to point out that, as far as the dielectric body is surrounded by a *vacuum*, the total body force and torque obtained from S_{ik}^E must both be equal to those obtained from the two tensors considered earlier. That this is so follows immediately from (2.11) and (2.12); the effects can be calculated directly from the vacuum tensor. We therefore next have to consider the situation where the body is surrounded by an isotropic *liquid*. There exist certainly electrostatic effects for which the influence of a dielectric liquid is essential; we may think of the rising of a liquid between two charged condenser plates partly dipped into the liquid[10], or the force acting on a grounded metal sphere immersed in a liquid and surrounded by an inhomogeneous field.

However, none of these experiments represent critical tests for the validity of either Minkowski's or Einstein's force. This can be seen in a simple way by first noting that the force difference is a gradient term:

$$f^E = \tfrac{1}{2}\nabla(E \cdot P) + \varrho E + \tfrac{1}{2}D_i D_k \nabla \eta_{ik} = \tfrac{1}{2}\nabla(E \cdot P) + f^M. \tag{2.16}$$

Compared to Minkowski's tensor, Einstein's tensor thus gives rise to an extra isotropic pressure

$$p^E - p^M = \tfrac{1}{2} E \cdot P. \tag{2.17}$$

In accordance with (2.11) and (2.12) the total force and the total torque on the solid body are determined by the values of S_n in the liquid just outside the body. We have

$$S_n^E = S_n^M - \tfrac{1}{2} n(E \cdot P), \tag{2.18}$$

but the effect from the last term in (2.18) (acting outwards) is just balanced by the extra pressure (2.17) which the liquid exerts on the solid. Hence MINKOWSKI's and EINSTEIN's tensors give the same values for the body force and torque. This compensation effect is the direct reason why a measurement of the total force on a metal sphere in the liquid represents no critical test: With EINSTEIN's tensor there are additional forces in the boundary layer of the sphere which just counterbalance the additional forces in the liquid tending to press the liquid into regions of higher field.*) If we suppose that the system producing the inhomogeneous electric field (for instance a small, charged metal sphere) is maintained at constant charge when it is surrounded by the dielectric liquid, we find that the total force $F^M = F^E$ on the test sphere will drop in the ratio $1/\varepsilon$ in comparison with the total force in the absence of the liquid, $F^M = (1/\varepsilon) F^{\text{vac}}$.

In the remaining example mentioned above, where two parallel condenser plates are partly immersed in a dielectric liquid, the main reason for the equivalence is simply the compensating forces in the liquid itself: The total electromagnetic force in the liquid between the condenser plates which balances the gravity force at equilibrium is found by integrating the force density over a volume which starts in a domain of the liquid where the field vanishes and ends just above the surface where $\varepsilon = 1$. Thus the effect from the gradient term in (2.16) vanishes, and a measurement of the height of the liquid between the condenser plates cannot serve as a means to determine the validity of either f^E or f^M. This point has been emphasized also by S. S. HAKIM[11].

[As stated above, MINKOWSKI's and EINSTEIN's tensors must be equivalent also with respect to the torque on the body. Actually, this latter kind of equivalence can be seen already by inspection of the expressions (2.5) and (1.8a). For the difference between the tensors is contained entirely in the terms multiplying δ_{ik}, and the torque effect from such a term is found simply by integrating $-\tfrac{1}{2} E \cdot D(r \times n)$ and $-\tfrac{1}{2} E^2(r \times n)$, respectively, where the field variables refer to the fluid, over the body surface. If the body is a sphere, it follows immediately that this torque effect vanishes. Further, the same result also applies if the body does not have a spherical form: In this case we may lay a fictitious spherical surface in the fluid outside the body so that $r \times n = 0$ on the surface, and from the stability of the fluid it follows that the torque exerted on the fictitious surface from the outside must be

---

* We are as usual assuming a rapid but continuous variation of ε across the boundary layers.

equal to the torque acting on the real body surface. In all cases the body torque is determined entirely by the first terms in (1.8a) or (2.5).]

While MINKOWSKI's and EINSTEIN's tensors thus lead to the same expressions for forces and torques, we shall now see that there actually exists another effect which is measurable and which represents a critical test of the two tensors, namely the *pressure* increase in a dielectric non-polar liquid because of the field. Let us then first point out which electromagnetic forces may produce this excess fluid pressure. MINKOWSKI's force density is, in accordance with (2.4),

$$f^M = \varrho \boldsymbol{E} - \tfrac{1}{2} E^2 \nabla \varepsilon, \tag{2.19}$$

and so the only pressure-producing term within the fluid, where $\varrho = 0$, is the term $-\tfrac{1}{2} E^2 \nabla \varepsilon$. This term is of importance in the boundary region between two media. We shall, however, in the following confine ourselves to situations where this term is of no importance, as for instance the situation where a charged condenser is completely immersed in the liquid.*) The condenser is moreover imagined placed horizontally, so that the gravity effect can be ignored.

The next kind of force which may yield an increased pressure effect is the *electrostriction* force. We have hitherto ignored the electrostriction in our work, it has usually no influence upon measurable quantities, but at this point it is indispensable. We then start again from the free energy (2.1) and carry through the variational procedure similarly as in sect. 3 of I, but now with the inclusion of terms showing the dependence of ε on the mass density ϱ_m. For definiteness we shall continue to call the expression (2.19) MIN-KOWSKI's force, while the complete force expression shall be denoted as HELMHOLTZ' force

$$f^H = \varrho \boldsymbol{E} - \tfrac{1}{2} E^2 \nabla \varepsilon + \tfrac{1}{2} \nabla \left(E^2 \varrho_m \frac{d\varepsilon}{d\varrho_m} \right). \tag{2.20}$$

For the simple non-polar liquids here studied we may eliminate the mass density be means of the CLAUSIUS-MOSSOTTI relation $(\varepsilon - 1)/(\varepsilon + 2) = \mathrm{const.}$ ϱ_m, and so (2.20) yields the following expression for the excess pressure, produced by the field:

$$\Delta p^H \equiv p^H - p^0 = \tfrac{1}{6} (\varepsilon - 1)(\varepsilon + 2) E^2, \tag{2.21}$$

* However, even in such a case $\nabla \varepsilon$ will not be exactly equal to zero; ε will increase somewhat in the domain between the condenser plates if the fluid pressure here increases due to some other kind of force. With the simple non-polar liquids and moderate pressure changes that we shall be considering (Δp of the order of one atmosphere), the influence from $\nabla \varepsilon$ on the force is, however, negligible. See refs. 11, 12 or *International Critical Tables*.

where p^0 is the fluid pressure when the field is turned off, thus corresponding to a slightly diminished mass density.

Finally we turn our attention to the EINSTEIN force (2.16). Since MINKOWSKI's force yields no pressure effect in the physical situations we consider, it follows immediately from (2.17) that

$$\Delta p^E \equiv p^E - p^0 = \tfrac{1}{2}(\varepsilon - 1)E^2. \qquad (2.22)$$

It is clear from eqs. (2.21) and (2.22) that an experimental detection of the excess pressure represents a critical test of HELMHOLTZ' and EINSTEIN's force expressions. Now this kind of experiment has actually been performed by S. S. HAKIM and J. B. HIGHAM[12]. They used an ingenious method based on the fact that the excess pressure which the field produces gives rise to a slight compression of the liquid and so increases its refractive index. This increase was determined experimentally by means of a TOEPLER-SCHLIEREN optical technique, i.e. by a measurement of the angular deflection of light rays passing through the liquid. The experimental results were found to be in agreement with the formula (2.21) within limits of accuracy of $\pm 5^0/_0$, while they disagreed completely with the formula (2.22).

The HAKIM-HIGHAM experiment thus yields the important result that the fluid pressure p in the presence of the field can be identified with the HELMHOLTZ pressure p^H. Hence we can draw the conclusion that the validity of the HELMHOLTZ variational method used above, based on the free energy (2.1), is confirmed experimentally. It has sometimes been argued that one has the freedom to define the force density f and the pressure p arbitrarily, also in the electrostatic case, apart from the single restrictive condition that the relation $f = \nabla p$ must be satisfied. We think however that the experiment clearly demonstrates that there is no room for this kind of arbitrariness in the electrostatic case within a dielectric liquid: By an integration of the force density over a volume element one must obtain the total electromagnetic force on that element which is compensated by the external pressure force acting on the surface. Since the excess pressure predicted by HELMHOLTZ' force expression has been verified experimentally, one should not introduce different definitions for pressure and force that would destroy this correspondence.

We also refer to another, theoretical, work[11] by HAKIM in which the HELMHOLTZ force is derived under essentially the same assumptions as those inherent in the usual derivation of the CLAUSIUS-MOSSOTTI equation. Further, HAKIM was able to show that the EINSTEIN force runs into conflict with the CLAUSIUS-MOSSOTTI equation.

Since the electrostatic contribution to the force consists in a gradient term it follows immediately, as indicated above, that the electrostriction will yield no observable effect upon the electromagnetic force or torque acting on a test body. The gradient form implies that there is always a balance between two equally large and oppositely directed forces at the body surface. For this reason HELMHOLTZ' force can usually be replaced by MINKOWSKI's force, as we have done in our work.

It is instructive to give the expression for the *total* stress tensor T_{ik} corresponding to both the liquid and the field:

$$T_{ik} = p^H \delta_{ik} - E_i D_k + \tfrac{1}{2} E^2 \delta_{ik} (\varepsilon - \varrho_m \, d\varepsilon / d\varrho_m) \qquad (2.23a)$$

$$= p^0 \delta_{ik} - E_i D_k + \tfrac{1}{2} \delta_{ik} \boldsymbol{E} \cdot \boldsymbol{D}, \qquad (2.23b)$$

$$\partial_k T_{ik} = 0. \qquad (2.23c)$$

These equations obviously do not apply to the domains in space wherein external bodies have been placed. Note that the validity of eq. (2.23b) is dependent on the fact that we have confined ourselves to systems for which the excess pressure is due entirely to the electrostrictive force. If on the other hand we had considered a situation in which also the term $-\tfrac{1}{2} E^2 \nabla \varepsilon$ in the force had a pressure-producing effect (as for instance the situation where the vertical condenser plates are partly immersed in the liquid), the fluid pressure p^H appearing in (2.23a) would no longer have been determined by the simple equation (2.21).

Now we have considered the pressure as a function of the zero-field pressure p^0 and the squared electric field E^2. It is however possible to regard the pressure as a function of the mass density ϱ_m only, where the latter quantity includes also the contribution from the compressional potential energy set up by the electromagnetic forces. We can write the total free energy density F^{tot} as the sum of a mechanical part F^{mech} and an electromagnetic part $F = \tfrac{1}{2} \boldsymbol{E} \cdot \boldsymbol{D}$:

$$F^{\mathrm{tot}} = F^{\mathrm{mech}}(\varrho_m) + \tfrac{1}{2} \boldsymbol{E} \cdot \boldsymbol{D}, \qquad (2.24)$$

where $\varrho_m = \varrho_m^0 + \Delta\varrho_m$, ϱ_m^0 denoting the zero-field value and $\Delta\varrho_m$ denoting the increase on account of the field. The pressure is then derived according to the familiar formula

$$p = -\frac{\partial(\varrho_m^{-1} F^{\mathrm{mech}})}{\partial \varrho_m^{-1}}. \qquad (2.25)$$

Thus, although the amount of compressional potential energy transferred to the material from the electrostrictive forces is very small, it is nevertheless important to include also the electrostrictive contribution to ϱ_m when deriving the pressure according to (2.25). Otherwise, if the expression (2.25) is calculated simply when the field is switched off, one will obtain the pressure p^0. Obviously it is not the electric field *per se* which is of main importance; we may well assume that the field is absent in calculating (2.25), but then we have to imagine the presence of some other kind of external force which produces the same value of the density at each point.

We now turn to a comparison of the above results with those obtained by DE GROOT *et al.* As mentioned already in section 1, DE GROOT and SUTTORP[6] have introduced also a second form of the electromagnetic energy-momentum tensor, which is assumed to describe the whole interaction between matter and field. This tensor form is in agreement with ABRAHAM's expression when the latter is supplemented with the appropriate electrostrictive and magnetostrictive terms, and when the terms involving the derivatives of the material constants with respect to the temperature are omitted (these temperature-dependent terms being negligible in the case of non-polar media). We then first note the interesting result that the second tensor introduced by DE GROOT and SUTTORP is in accordance with the HELMHOLTZ force in the electrostatic case, and thus is in agreement with our interpretation above. Now, since this tensor is assumed to describe the whole interaction between field and matter, it is constructed as the difference between the total (field plus matter) tensor in the presence of the field, and the total tensor in the absence of the field but at the same value of the density (and the temperature). This last statement is presumably to be understood so that the total mass density ϱ_m (including the contribution from the compressional potential energy) is required to be kept constant, independent of the field, the authors thus implicitly presupposing the existence of some extra kind of force to maintain the compressional energy when the field is switched off. By looking at the theory in this way we find that their mechanical stress tensor can be written as $p^H \delta_{ik}$, the force balance thus reading $\boldsymbol{f}^H = \nabla p^H$, in accordance with our result earlier obtained.

However, in spite of this formal agreement between the results it turns out that the two procedures are essentially different. (Apart from the already cited papers by DE GROOT and SUTTORP, see also similar treatments by MAZUR and DE GROOT[13, 17].) Let us here therefore sketch some important parts of the mathematical formalism. The authors employ the following, rather unusual, balance equation for free energy per unit mass

$$d(\varrho_m^{-1} F^{\text{tot}}) = -p\,d(\varrho_m^{-1}) + \boldsymbol{E} \cdot d(\varrho_m^{-1} \boldsymbol{P}). \tag{2.26}$$

Here we have omitted a temperature-dependent term. We shall not penetrate into the background of this equation, but mention that it is connected with the adoption of $\frac{1}{2}E^2$ as the electrostatic energy density. Eq. (2.26) is integrated at constant ϱ_m to give

$$F^{\text{tot}} = F^{\text{mech}}(\varrho_m) + \tfrac{1}{2}\boldsymbol{E} \cdot \boldsymbol{P}, \tag{2.27}$$

where F^{mech} is the free energy density in the absence of the field, but at the same mass density. The authors then invoke eqs. (2.26) and (2.27) to calculate the pressure

$$p = -\left[\frac{\partial(\varrho_m^{-1} F^{\text{tot}})}{\partial \varrho_m^{-1}}\right]_{(\varrho_m^{-1} \boldsymbol{P})} = p^H + \tfrac{1}{2}\boldsymbol{E} \cdot \boldsymbol{P} - \tfrac{1}{2}E^2 \varrho_m \frac{d\varepsilon}{d\varrho_m}. \tag{2.28}$$

This pressure p is now identified with the EINSTEIN pressure p^E and the expression (2.28) is inserted into the force balance $\boldsymbol{f}^E = \nabla p^E$. The force $\boldsymbol{f}^E$ can be expressed in terms of the field quantities by means of eqs. (2.16) and (2.19), and by comparing with the expression (2.20) for the HELMHOLTZ force one sees that

$$\boldsymbol{f}^E = \boldsymbol{f}^H + \tfrac{1}{2}\nabla\left(\boldsymbol{E} \cdot \boldsymbol{P} - E^2 \varrho_m \frac{d\varepsilon}{d\varrho_m}\right). \tag{2.29}$$

Thus, by using eqs. (2.29) and (2.28) the authors obtain that the force balance $\boldsymbol{f}^E = \nabla p^E$ can alternatively be written $\boldsymbol{f}^H = \nabla p^H$, as previously mentioned. Correspondingly, the identification of the pressure p in eq. (2.28) with the EINSTEIN pressure p^E is in accordance with eq. (2.29).

At this stage it should be clear what in reality distinguishes the method employed by DE GROOT *et al* from the method we have employed earlier in this section. First, the expression (2.27) for the free energy density differs essentially from the expression (2.24) and hence does not correspond to the free energy density $\frac{1}{2}\boldsymbol{E} \cdot \boldsymbol{D}$ for the field. The latter density was used in the variational principle based on eq. (2.1), and it must be equal to the work exerted per unit volume in building up the field. Secondly, a relation of the form (2.28) is incompatible with our earlier interpretation according to which the pressure is a function of the total mass density alone, the field playing only a secondary role in establishing the compressional force. Instead of calculating the pressure as a partial derivative of the type (2.28) whose physical meaning does not appear quite clear to us, we have instead

employed the usual method according to which the pressure gradient and the electromagnetic force emerge from a variational principle wherein respectively the mechanical free energy density F^{mech} and the field free energy density $F = \frac{1}{2}\boldsymbol{E} \cdot \boldsymbol{D}$ are varied. Thus, after variation of the mechanical part, the fluid pressure can be written simply as a partial derivative in the form (2.25), but this quantity is not explicitly dependent on the field. If we instead had inserted the total free energy density F^{tot} into the variational integral we would have obtained the resulting force density equal to zero, in accordance with the fact that the system consisting of matter plus field is a closed system.

The results obtained in this section can be summarized as follows: The variational method based on the energy (2.1) can lead both to MINKOWSKI's and ABRAHAM's tensors, and as far as the dielectric body is surrounded by an isotropic medium (vacuum or liquid), no experiments testing forces or torques can decide between them. These tensors correspond only to different distributions of forces and torques throughout the body. Within an isotropic medium the tensors become equal, and the increased pressure effect predicted in a dielectric liquid (including the electrostriction effect) has been verified experimentally.

The other proposal considered, but forward among others by EINSTEIN and LAUB (as well as DE GROOT and SUTTORP in their first proposal), is different from the above two expressions even in the isotropic case. The extra pressure effect predicted by this tensor does not agree with experiment.

As usual, we have in this section confined ourselves to the macroscopic approach. It seems to be a rather common feature, however, that the *microscopic* treatments that have been given in this field favour the force expression which we have called EINSTEIN's force. Apart form the already cited papers by MAZUR and DE GROOT[13], DE GROOT and SUTTORP[6], we may refer also to a paper by KAUFMAN[14], in which similar conclusions have been drawn. We shall not, however, go into further considerations at this point.

3. Consideration of an Electromagnetic Wave in an Isotropic Body at Rest

We now turn our attention to simple time-varying fields within a dielectric medium at rest. In the first part of the section we rely upon the semi-microscopical arguments from I, section 6 to point out the connection between MINKOWSKI's and ABRAHAM's tensors for a plane wave travelling within an

isotropic and homogeneous body; thereafter the considerations are illustrated by an example where also boundaries are involved. Finally, we examine alternative tensor proposals.

We recall the essential parts of the procedure for constructing the energy-momentum tensor in I: The energy density was taken to be the sum of the electrostatic and magnetostatic energy densities; correspondingly, the stress tensor was constructed as the sum of the electrostatic and magnetostatic stress tensors derived by the usual energy variational method. From the energy density in the form $W = \frac{1}{2}(\boldsymbol{E} \cdot \boldsymbol{D} + \boldsymbol{H} \cdot \boldsymbol{B})$ and from the fact that the four-component of force, f_4, vanishes within the dielectric, we deduced the expression $\boldsymbol{S} = c(\boldsymbol{E} \times \boldsymbol{H})$ for the energy flux. Assuming the relation $\boldsymbol{S} = c^2\boldsymbol{g}$, expressing PLANCK's principle of inertia of energy, to be valid also for the electromagnetic field, we further found the momentum density $\boldsymbol{g} = (1/c)(\boldsymbol{E} \times \boldsymbol{H})$.

In accordance with (1.3) it is apparent that these components form ABRAHAM's tensor. If the remaining part of the total system (the mechanical part) is described by an energy-momentum tensor $U_{\mu\nu}$, the present division of the total system into electromagnetic and mechanical parts may be expressed by the equation

$$- \partial_\nu S^A_{\mu\nu} = f^A_\mu = \partial_\nu U_{\mu\nu}. \tag{3.1}$$

The covariant form of $S^A_{\mu\nu}$ is given in (1.5). ABRAHAM's tensor has been advocated by many authors, and we also agree that it represents a fully adequate description of phenomenological electrodynamics. It must be borne in mind that we are neglecting electrostriction and magnetostriction effects; these effects would lead to additional terms in the tensor components. Actually we find, in the time-dependent case as well as in the static case, that if ABRAHAM's tensor is augmented by the electrostrictive and magneto-strictive terms the resulting expression is just equal to the second tensor expression given by DE GROOT and SUTTORP (apart from terms involving the derivatives of the material constants with respect to temperature).

It must be borne in mind however, that the present problem is to some extent a matter of *convenience*, and the question arises whether there are alternative tensors which can equally well be justified on the basis of (3.1). Our next task is thus to examine the effect induced in the mechanical tensor $U_{\mu\nu}$ on account of the force f^A_μ. According to (1.4) this force has only one nonvanishing component, namely a fluctuating component in the direction of propagation of the plane wave. We take this direction as the x-direction; if the velocity of the constituent dipoles in the x-direction is denoted by u_1,

we found in I that the contributions to the components U_{ik} and U_{44} because of this velocity component are at most of the order $(u_1/c)^2$, which are negligible quantities. On the other hand, the components $U_{14} = U_{41} = icg_1^{\text{mech}} = ic\varrho_m u_1$ are of the first order in u_1/c and may thus be appreciable. By invoking the JONES-RICHARDS experiment[15] we actually determined the induced mechanical momentum density as

$$\boldsymbol{g}^{\text{mech}} = \frac{n^2 - 1}{c} (\boldsymbol{E} \times \boldsymbol{H}) \qquad (3.2)$$

in the case of an optical wave. This mechanical momentum runs always together with the field. Simply by *including* (3.2) in the field momentum density we obtained MINKOWSKI's value $\boldsymbol{g}^M = (1/c)(\boldsymbol{D} \times \boldsymbol{B})$. This is the *total* electromagnetic and mechanical momentum density associated with a propagating optical wave. Further, this interpretation means that the matter is set into a small motion with the velocity u_1 when the field passes through it; the flux of mechanical energy $S_1^{\text{mech}} = -icU_{41} = -icU_{14}$ being present because of this motion must naturally be included in the mechanical tensor. Note that $f_4 = 0$ ($f_1^A u_1$ being negligible), so that $\partial_\nu U_{4\nu} = 0$.

If we suppose that the optical wave travels within an *infinite* medium, so that there are no forces in the boundary layers to cause stresses in the material, the components U_{ik} of the stress tensor are equal to their values at zero field. In more general cases, the components U_{ik} have to describe the elastic stresses which are set up because of the electromagnetic forces at the boundaries.

Further considerations on these topics are contained in I, section 6, but we shall here write down the tensor scheme which pertains to MINKOWSKI's tensor: The field is described by

$$S_{\mu\nu}^M = \begin{pmatrix} S_{ik}^A, & S_{i4}^A + U_{i4} \\ S_{4k}^A, & S_{44}^A \end{pmatrix}, \quad \partial_\nu S_{\mu\nu}^M = 0, \qquad (3.3)$$

and if $T_{\mu\nu}$ is the energy-momentum tensor of the total system the mechanical part is described by

$$T_{\mu\nu} - S_{\mu\nu}^M = \begin{pmatrix} U_{ik}, & 0 \\ U_{4k}, & U_{44} \end{pmatrix}, \qquad (3.4)$$

where $U_{44} = -\varrho_m c^2$. The symmetrical and divergence-free tensor $T_{\mu\nu}$ is thus divided into two asymmetrical but divergence-free tensors describing the electromagnetic and mechanical parts of the system. We emphasize

again that the reason why this kind of division is convenient lies entirely in *experience*. Further, although the division of course does not affect the angular momentum conservation law for the total system, the asymmetry of the partial tensors gives rise to unfamiliar aspects for the angular momenta of the two subsystems.

It is instructive to consider the system not only in the frame K^0—the original rest frame—but also in the frame K' in which the mean velocity of the matter is zero. In this frame all tensor components retain their old values from K^0, except for the components $U'_{4k} = U'_{k4}$ whose average values are zero. Apart from fluctuating terms the above two kinds of splitting then become equivalent: The field is described by the same ABRAHAM tensor as in the frame K^0, and the remaining matter system is described by the tensor $U'_{\mu\nu}$ which, in the case of an *infinite* medium, can be taken to be equal to the energy—momentum tensor at zero field. If the medium is *finite*, the components U'_{ik} must describe also any mechanical stresses that may arise. With the omission of electrostrictive and magnetostrictive terms we thus obtain *in the frame K'* a division of the total energy-momentum tensor into an electromagnetic and a mechanical part in a way which is in agreement with the division that has been proposed by several other authors[6, 16, 17] in the rest frame. The new element of our analysis is essentially that this kind of division is interpreted *not* to run into conflict with MINKOWSKI's tensor, due to the fact that the experiments lead us to distinguish between the original rest frame K^0 and the frame K' in which the mean velocity vanishes.

Further, there is still another aspect which should be emphasized in connection with the comparison between MINKOWSKI's and ABRAHAM's tensors: ABRAHAM's force density is the *real* force acting on a unit volume, i.e. the force on the matter itself as well as on any charges and currents present within the volume. This force is compensated by the mechanical stresses plus the inertial force, in accordance with the relation

$$f_i^A = \partial_k U_{ik} + (\partial/\partial t) g_i^{\text{mech}}. \tag{3.5}$$

MINKOWSKI's force, on the other hand, amounts to counting the inertial force together with the proper force:

$$f_i^M = f_i^A - (\partial/\partial t) g_i^{\text{mech}} = \partial_k U_{ik}, \tag{3.6}$$

and it has thus a less direct physical meaning than ABRAHAM's force. MINKOWSKI's force does not contain any term which corresponds to the magnetic force on the polarization currents, this term is hidden in the field momentum.

The non-appearance of such a magnetic force term has represented an obstacle for the acceptance of MINKOWSKI's tensor, as reflected for instance in EINSTEIN and LAUB's article.[5]

Example involving the boundary between two media

By the above analysis we have come to the important conclusion that the propagation of an electromagnetic wave through matter is conveniently described by MINKOWSKI's tensor in such a way that the rest of the system (the mechanical part) may usually be ignored. In this subsection, however, we shall examine the total momentum and motion of centre of mass for a total system when boundaries are involved; in this case all kinds of momentum and energy flows have to be taken into account.

Imagine a plane wave with $\boldsymbol{E} = E_0 \boldsymbol{e}_y \sin(k_0 x - \omega t)$ that falls in from vacuum towards an isotropic and homogeneous insulator at zero angle of incidence. We take the boundary as the plane $x = 0$, and put for simplicity $\varepsilon = \mu = n$ so that the reflected wave vanishes. We may consider a certain part of the plane wave, say of length l_0 and cross section unity, and examine the consequences of the application of different forms of the momentum expressions. (The length l_0 is then required to be much smaller than the width L of the body over which the field travels.) But it is more convenient simply to consider the field as a wave parcel with length l_0 and cross section unity, where $l_0 \ll L$, so let us look at the system in this way.

The total field energies in vacuum and in the body are equal, $\mathscr{H}_0 = l_0 E_0^2/2 = nl E_0^2/2 = \mathscr{H}$, where l and $\mathscr{H}$ refer to the body. By taking the divergence of ABRAHAM's tensor we obtain

$$\boldsymbol{f}^A = -\tfrac{1}{2}E^2 \nabla \varepsilon - \tfrac{1}{2}H^2 \nabla \mu + \frac{n^2 - 1}{c}\frac{\partial}{\partial t}(\boldsymbol{E} \times \boldsymbol{H}) \tag{3.7}$$

(cf.(1.4)), valid also over the boundary if one assumes a continuous variation of ε and μ. We shall first use this force in a computation of the various momenta. As $E = H$ everywhere, the surface force during the penetration period is $(1 - n)E^2$, and so the total momentum component in the x-direction transferred to the body on account of this force is

$$G^{\text{surf}} = -(n^2 - 1)E_0^2 \int_0^{l_0/c} \sin^2 \omega t \, dt = \frac{1 - n}{c}\mathscr{H}, \tag{3.8}$$

where we have integrated over the penetration period.

According to our earlier results, the effect of the last term in (3.7) is to excite a mechanical momentum in the body:

$$G^{\text{mech}} = \frac{n^2 - 1}{c} \int_0^l EH dx = \frac{n^2 - 1}{nc} \mathscr{H}. \tag{3.9}$$

Finally, the electromagnetic part is

$$G^{\text{el.m.}} = \frac{1}{c} \int_0^l EH dx = \frac{1}{nc} \mathscr{H}. \tag{3.10}$$

Collecting these terms the balance of total momentum can be checked:

$$G^{\text{surf}} + G^{\text{mech}} + G^{\text{el.m.}} = \frac{\mathscr{H}}{c} = G^{\text{vac}}, \tag{3.11}$$

where G^{vac} is the magnitude of the momentum of the incoming field. This simple analysis exhibits the behaviour of the various momentum parts.

If we instead had started from MINKOWSKI's tensor, the last term in (3.7) would have been absent. In this case the momentum component G^{surf} supplied by the forces in the boundary layer, plus the *field* momentum $G^M = G^{\text{el.m.}} + G^{\text{mech}} = n\mathscr{H}/c$, would have added up to give the total momentum $\mathscr{H}/c$.

Let us also examine the centre of mass velocity for the total system. Denoting the coordinates of the centre of mass by $\boldsymbol{X} = (X, 0, 0)$, we have

$$\frac{d}{dt} X^{\text{tot}} = \frac{d}{dt} \left[\frac{1}{\mathscr{H}^{\text{tot}}} \int x W^{\text{tot}} dV \right] = -\frac{ic}{\mathscr{H}^{\text{tot}}} \int \frac{\partial}{\partial x_\nu} (x S_{4\nu}^{\text{tot}}) dV, \tag{3.12}$$

since the contribution to (3.12) from $\nu = 1,2,3$ vanishes when the boundary surface of the integration volume is chosen sufficiently far away. Hence

$$\frac{d}{dt} X^{\text{tot}} = \frac{1}{\mathscr{H}^{\text{tot}}} \int S^{\text{tot}} dV = \frac{c^2 G^{\text{vac}}}{\mathscr{H}^{\text{tot}}} = \frac{\mathscr{H}}{\mathscr{H}^{\text{tot}}} c, \tag{3.13}$$

corresponding to the fact that the parcel travels with the velocity c before it strikes the body. It should be noted that in (3.13) S^{tot} includes also the mechanical energy flux S^{mech} due to the small motion of matter induced by the field.

Since the body has a finite extension L in the x-direction then, during the period when the wave parcel leaves the body, the effect on the body is

equal and opposite to that during the entrance period. Further, the motion of matter described by S^{mech} is considered to be absent when the wave has left, so the body will stay at rest. Since the length of the parcel is small, it can be considered to have remained a time $\tau = Ln/c$ in the body. Let M and ξ denote the total mass and displacement of the body in the x-direction; we then find from (3.8), (3.9) and the relation $M\xi/\tau = G^{surf} + G^{mech}$ that $\xi = (\mathscr{H}/Mc^2)(n-1)L$.

The gedanken experiment above is one of those considered by N. L. Balazs[18]. We cannot agree to his conclusion, however, when he claims the correctness of $S^A_{\mu\nu}$ in contrast with $S^M_{\mu\nu}$ by an analysis of the total momentum and centre of mass. Let us apply his procedure to the above case: The equation of momentum balance is given in the form

$$G^{vac} = G' + M\xi/\tau, \qquad (3.14)$$

where G' is the magnitude of the field momentum in the body which is to be determined. Further, the law of conservation of the centre of mass velocity is written as

$$\mathscr{H}c\tau = \mathscr{H}c\tau/n + Mc^2\xi. \qquad (3.15)$$

From these equations he obtains $G' = \mathscr{H}/(nc)$, which agrees with Abraham's expression only.

But by comparison with our previous treatment it is apparent that the balance equation (3.14) is incomplete. Eq. (3.15) is valid for both tensors, and leads to the expression for ξ found above. But (3.14) implies that the magnitude of the mechanical momentum be given by $M\xi/\tau$, which ,in accordance with (3.15), (3.8) and (3.9), is equal to $G^{surf} + G^{mech}$. This is an assumption which is compatible with Abraham's expression only; we see from (3.14) that $G' = G^{vac} - G^{surf} - G^{mech} = G^{el.m.}$, when the balance equation (3.11) is taken into account.

Finally we should mention that in an examination of an example similar to the one above, E. G. Cullwick[19] has claimed that Abraham's momentum density is satisfactory while Minkowski's momentum density leads to inconsistencies with respect to the momentum balance. His argument is essentially tantamount to saying that, in the situation above, the relations $g^{vac} = g^A$, $g^{vac} \neq g^M$, determine the validity of the Abraham expression. It is however evident that in order to check the momentum balance over the boundary one should integrate the equation $\partial_k S_{ik} + \partial g_i/\partial t = -f_i$ in question over a volume which includes a part of the boundary, and thus one must

consider instead the momentum *flow* described by the components S_{ik}. Moreover, the surface force must also be taken into account. The paper has been criticised also by P. PENFIELD[20, 21].

Other tensor forms

It is convenient to collect the remarks on the alternative tensor forms in this final subsection. First we recall that the DE GROOT-SUTTORP tensor (1.9) must describe essentially another part of the total system than the part which we have made to correspond to the electromagnetic energy—momentum tensor. This follows from a comparison between the energy density (1.9b) and the energy density $W = \frac{1}{2}(\boldsymbol{E}\cdot\boldsymbol{D} + \boldsymbol{H}\cdot\boldsymbol{B})$ on which we have based our derivations (cf. also the HAKIM-HIGHAM experiment mentioned in section 2). Next, the EINSTEIN-LAUB tensor (1.8) is in conformity with the expressions (1.9) when $\mu = 1$. The most interesting alternative in relation to the topics considered in the present section is the radiation tensor (1.6) introduced by MARX and his collaborators; we recall that this tensor was defined for radiation fields only. The essential point in the construction of the radiation tensor can be visualized by an inspection of the equation (3.1): One assumes that the effect of the force $\boldsymbol{f}^A$ is not to create a mechanical *momentum*, described by the components U_{i4}, but rather to form *stresses*, described by the components U_{ik}. Eq. (3.1) can then be written as $\partial_k(S_{ik}^A + U_{ik}) + \partial g_i^A/\partial t = 0$, leading to $U_{ik} = (n^{-2} - 1)S_{ik}^A$, in accordance with (1.6). However, the main reason why we have not constructed the theory in this way is simply the result of the JONES-RICHARDS experiment, to which we have already referred repeatedly. As we pointed out in the rather detailed consideration in I, section 6, it was essential for the validity of the derived formulas that the electromagnetic energy—momentum tensor in question be a *divergence—free* quantity in the interior of the body. Since the radiation tensor just has this property, and since the relation between the momentum flow components is $S_{ik}^S = = (1/n^2)S_{ik}^M$, it follows that the radiation pressure predicted by the radiation tensor is equal to $1/n^2$ times the MINKOWSKI radiation pressure. By a comparison with the observed data we are thus in a position to draw the decisive conclusion that the characteristic assumption inherent in the derivation of the radiation tensor should be rejected. Note that the electrostriction effect will have no influence on this result.

Although it should therefore not be of importance to go into a detailed examination of the use of the radiation tensor in the example considered in the above subsection, let us yet note the following points. The force density

can no longer be written as (3.7), since this expression will violate the law of conservation of momentum. This is so because the last term in (3.7) is no longer associated with a mechanical momentum, and hence the total momentum after the wave has entered the body is $G^{\mathrm{surf}} + G^{\mathrm{el.m.}} \neq G^{\mathrm{vac}}$. In order to fulfil the momentum conservation law the force density must be defined as $f_i^S = - \partial_\nu S_{i\nu}^S$, where the stress components are *not* the sum of the electrostatic and magnetostatic stress components. If we define $S_{i\nu}^S = (1/n^2(x)) S_{i\nu}^M$ also in the spatially dispersive region in the boundary layer, we find that the momentum induced by the surface forces is $(G^S)^{\mathrm{surf}} = (1 - 1/n) \mathcal{H}/c$. The interesting aspect here is that the quantity $(G^S)^{\mathrm{surf}}$ has the opposite *sign* of the quantity G^{surf} calculated earlier in eq. (3.8); while the surface force following from the radiation tensor acts *inwards* to the body the surface force following from ABRAHAM's and MINKOWSKI's tensors acts *outwards* from the body surface. We are not, however, aware of a direct experimental test of this effect (cf. the last part of the next section).

4. Discussion of some Possibilities for Experiments

In this section we examine experimental situations in which time—dependent fields exert torques on dielectric bodies at rest. As usual we first focus our attention on the relative behaviour of MINKOWSKI's and ABRAHAM's tensors. In the first class of experiments considered—the interaction between a stationary radiation field and a dielectric body—the result is that the two tensors lead to the same answers. Thereafter, an example is given of a second type of experiments in which the difference can be measured. Finally, we propose a critical experiment testing the radiation tensor and the EINSTEIN tensor.

Proof of equivalence

As an example of an experiment which traces the angular momentum interaction between an electromagnetic wave and a dielectric body, the old G. BARLOW experiment[22] should first be mentioned. He made a careful measurement of the torque produced by a beam of light in oblique refraction through a glass plate, and obtained good agreement with the theory. We refer also to the famous R. A. BETH experiment[23], in which the existence of angular momentum in a light wave was detected by letting the wave pass through an anisotropic crystal. The latter experiment has more recently been repeated by N. CARRARA[24] with the use of centimetre waves. These ex-

periments consisted in letting a stationary wave interact with the body and then measuring the deflection when equilibrium was established between the electromagnetic torque and the mechanical torque exerted by a torsional suspension. However, we need not go into detailed considerations of these situations in order to test the relative behaviour of MINKOWSKI's and ABRA-HAM's tensors, since we will find the torque $N^A = N^M$, just as we did in the static case. Instead we present a simple argument which shows in general that in a wave-dielectric body situation the two energy-momentum tensors yield the same value for the torque.

Consider then a stationary high-frequency wave interacting with a dielectric body (in general anisotropic). The body is assumed so heavy that no macroscopic motion needs to be taken into account. If the angular momentum of the internal field in the body is denoted by M^i, the torque N can be written as

$$N = - dM^{\text{vac}}/dt - dM^i/dt. \qquad (4.1)$$

It can readily be seen that each of the two terms on the right hand side of this equation is the same for ABRAHAM's or MINKOWSKI's tensor. In both cases the energy flux is given as $c(E \times H)$, therefore the direction and velocity of the travelling field energy is the same, and it follows that the first term on the right of (4.1) is also the same. Further, since we assume that the field is stationary, we can simply put $dM^i/dt = 0$. Hence $N^A = N^M = - dM^{\text{vac}}/dt$: The two energy—momentum tensors are equivalent with respect to torque effects since these effects are determined in terms of the vacuum field.

(Alternatively, we may consider a wave packet in interaction with the body during the time period $t = 0$ to $t = T$, during which the field is assumed to be stationary. Then we can require on physical grounds that N be independent of T at any time t, also in the small transient period when the field leaves the body. We now assume only that dM^i/dt must be equal to some constant during the stationary interaction period, since each component is proportional to the averaged energy density of the incoming wave. When $t > T$, one has $M^i = 0$, but then dM^i/dt can be made arbitrarily large in the transient period when the wave leaves the body, by choosing T large. These features are incompatible with the condition (4.1), hence $dM^i/dt = 0$ in the stationary interaction period.)

Proposal of an experiment

In the preceding we considered an electromagnetic *wave* in interaction with a dielectric system. Now there exists the possibility of combining electric and magnetic fields in a way which, in principle, makes it possible to bring out explicitly the effect arising from ABRAHAM's force. We shall give a proposal similar to one put forward by MARX and GYÖRGYI[3]. A cylindric dielectric shell of isotropic matter with large ε is suspended between the surfaces of a cylindric capacitor so that, in the absence of fields, the shell can oscillate about its axis (z) with a frequency ω_0. The internal surface of the capacitor is then charged to the amount q per unit length, and a homogeneous magnetic field $H_0 e^{-i\omega t}$ is impressed parallel to the z-axis. We suppose that the wavelength which corresponds to the frequency ω is large compared with the dimensions of the system, so that within the internal, massive cylindric conductor, we may write $\nabla \times \boldsymbol{H} = \sigma \boldsymbol{E}/c$, where σ is the conductivity. Taking into account that the penetration depth into the conductor is approximately equal to $\sqrt{c^2/\omega\sigma}$, which is a large quantity when ω is small, and putting $\mu = 1$, we obtain within the internal region of the conductor

$$\boldsymbol{H} = \boldsymbol{H}_0 e^{-i\omega t}, \quad E_\varphi = \frac{i\omega}{2c} r H_0 e^{-i\omega t}. \tag{4.2}$$

Within the dielectric shell $E_r = q/(2\pi\varepsilon r)$, while eqs. (4.2) remain valid also in this domain. Thus

$$f_\varphi^A = -\frac{\varepsilon - 1}{\varepsilon} \frac{\partial}{\partial t}(E_r H_z) = \frac{\varepsilon - 1}{\varepsilon} \frac{q\omega H_0}{2\pi c r} \sin \omega t, \tag{4.3}$$

when we take the real part. Hence the torque component is

$$N_3^A = \int r f_\varphi \, dV = \frac{\varepsilon - 1}{\varepsilon} \frac{q H_0 V}{2\pi c} \omega \sin \omega t \equiv K\omega \sin \omega t, \tag{4.4}$$

where V is the volume of the body. We have ignored the surface forces since these act in the same directions as $-\nabla \varepsilon$ and hence have no influence on the oscillations. The equation of motion can be written as

$$\ddot{\varphi} + \gamma \dot{\varphi} + \omega_0^2 \varphi = \frac{K}{I} \omega \sin \omega t, \tag{4.5}$$

where γ is the damping constant and I the moment of inertia about the z-axis. The largest oscillations occur when $\omega = \omega_0$ and are given by

$$\varphi = -\frac{K}{I\gamma}\cos\omega_0 t. \qquad (4.6)$$

This effect can in principle be measured. With a direct use of MINKOWSKI's tensor one obtains no force that can account for these oscillations, and MINKOWSKI's tensor is thus inappropriate in the present case. (It must be emphasized that the previous derivation of MINKOWSKI's tensor for time-dependent fields in isotropic media applies properly only to the case of *radiation* fields.)

As far as we know, the experiment has not been performed.

We emphasize the essential difference between this situation and those considered in the above subsection: At a given instant, the force component f_φ^A causing the torque does not vanish when integrated over the volume. Further, it is now the total *time oscillations* themselves which are detected and not, as in the previous situation, their effect after integration over a time which is large in comparison with the oscillation period.

Other tensors

Let us consider again the system of a stationary wave field and a dielectric body studied in the first of the subsections above, and first employ the radiation tensor $S_{\mu\nu}^S$. This tensor has been derived for the case of isotropic bodies only, so we shall accordingly assume the body to be isotropic. It is immediately apparent that if the wave comes in from vacuum, interacts with the body and then enters into vacuum again, we can apply just the same argument as before to conclude that the radiation tensor yields the same value for the torque as MINKOWSKI's and ABRAHAM's tensors. But a simple calculation shows that the *direction* and *magnitude* of the surface force will in general be different from what we obtained in the previous cases; it is only the total torque itself that remains unchanged. (For instance, if an appropriately polarised optical wave falls obliquely inwards to the body at BREWSTER's angle of incidence such that the reflected wave vanishes, it can be verified that the surface force acts in a direction parallel to the surface, instead of in a direction outwards along the normal vector, as obtained from MINKOWSKI's or ABRAHAM's tensor.) It has sometimes been claimed that the BARLOW experiment[22] mentioned above, involving a measurement of the torque exerted by a light wave on a glass plate, should actually provide an experimental test of the direction and magnitude of the surface force. But we think that this is not so, although BARLOW himself interprets the effect in a way corresponding to MINKOWSKI's or ABRAHAM's tensor. The only thing

measured is the total torque, which is explained equivalently by all tensors in question.

However, an obvious generalization lies at hand in order to change for instance the BARLOW experiment into a critical experiment with respect to the radiation tensor, namely, to immerse the body into an isotropic dielectric *liquid*. The radiation tensor has a value different from the two other tensors mentioned in the liquid, and so a torque measurement can be crucial. In order to derive the appropriate torque expression it is convenient to write the general formula (cf. (I, 1.7))

$$N_l = \int_{\text{body}} (x_i f_k - x_k f_i + S_{ik} - S_{ki}) \, dV \tag{4.7}$$

in the following compact form:

$$\boldsymbol{N} = - \int_{\text{surface}} (\boldsymbol{r} \times \boldsymbol{S}_n^{\text{liq}}) \, dS - \frac{d}{dt} \int_{\text{body}} (\boldsymbol{r} \times \boldsymbol{g}) \, dV \tag{4.8a}$$

$$= - \int_{\text{surface}} (\boldsymbol{r} \times \boldsymbol{S}_n^{\text{liq}}) \, dS. \tag{4.8b}$$

For an optical wave the last integral in (4.8a) vanishes because the field is assumed to be stationary and the body remains practically at rest, and the surface integrals are taken in the liquid just outside the body. By means of (1.6) and (4.8b) we find the result $\boldsymbol{N}^S = (1/n^2)\boldsymbol{N}^M = (1/n^2)\boldsymbol{N}^A$, where n is the refractive index of the liquid. The surface integral in (4.8b) can be evaluated in the actual experimental situation with one of the tensors inserted, and one can thus check the tensors by a comparison with the observed torque.

As the next point we consider the EINSTEIN-LAUB tensor $S_{\mu\nu}^E$ applied to the same situation. (For optical fields we can put $\mu = 1$, and it is then apparent from (1.8) and (1.9) that the EINSTEIN-LAUB tensor and the DE GROOT-SUTTORP tensor are in agreement.) This tensor is defined also for anisotropic media. We evaluate this case most simply by noting the following relation in the liquid which surrounds the body:

$$\boldsymbol{S}_n^E = \boldsymbol{S}_n^A - \tfrac{1}{2} \boldsymbol{n}(\boldsymbol{E} \cdot \boldsymbol{P}), \tag{4.9}$$

so that (4.8b) yields

$$\boldsymbol{N}^E = \boldsymbol{N}^A + \tfrac{1}{2} \int_{\text{surface}} (\boldsymbol{r} \times \boldsymbol{n}) \boldsymbol{E} \cdot \boldsymbol{P} dS, \tag{4.10}$$

where the surface integral is taken in the liquid. EINSTEIN's tensor thus leads to still another value for the torque, which might be tested experimentally.

The dielectric shell—experiment considered in the second subsection above is not of direct importance for the radiation tensor since this tensor is defined for *radiation* fields only. However, it can readily be seen that both the radiation tensor and EINSTEIN's tensor lead to ABRAHAM's value (4.4) for the torque. To this end we need only examine eq. (4.8a), where now the last term is non-vanishing and where $\boldsymbol{S}_n^{\text{liq}}$ is replaced by $\boldsymbol{S}_n^{\text{vac}}$ in vacuum outside the shell. Since $\boldsymbol{g}^S = \boldsymbol{g}^E = \boldsymbol{g}^A$ it follows that $\boldsymbol{N}^S = \boldsymbol{N}^E = \boldsymbol{N}^A$. (Moreover, the value (4.4) can be checked by inserting the field values (4.2) and the expression for E_r into (4.8a).) This experiment is therefore *not* a critical test of the relative behaviour of the three tensors mentioned. In this case it does not seem either to be an appropriate generalization to immerse the system into a dielectric liquid.

5. Some Remarks on the Literature

Together with the exposition of the various topics we have met up till now—both in I and in the present paper—we have found it desirable to include also some remarks pertinent to essential passages in earlier works on the subject. The literature is however large, and there remain important parts of it that could not naturally be considered or even touched upon in the preceding exposition. We have therefore reserved the present section for a critical review of some earlier (phenomenological) treatments, especially those which seem to be incompatible with the interpretations given above. We think that this avenue is natural to follow, since the present problem is not only a *deductive* task but also a matter of *clarification* of a confused situation. Evidently we cannot give a detailed scrutiny of all the relevant papers of phenomenological nature, but shall rather be concerned with illustrative examples. For a large part we shall be concerned with the analysis of criteria. The present section represents the end of our nonrelativistic treatment; from the next section on we concentrate upon topics connected with relativity.

In the two first subsections we consider two gedanken experiments which have been put forward. The idea behind these gedanken experiments has been that by comparing with results obtained from physical conservation laws, one should be able to decide which energy—momentum tensor is correct. In both the cases we shall consider, MINKOWSKI's tensor has been

claimed to be preferable, as a result of a study of the conservation equations for momentum. We shall show how these experiments can be equivalently described with the use of ABRAHAM's tensor. In the subsequent subsection some aspects of the ČERENKOV effect are considered, and finally we mainly dwell on arguments favouring other tensors than MINKOWSKI's and ABRAHAM's expressions.

Propagation of discontinuities

In two papers A. RUBINOWICZ[25] investigated the situation where electromagnetic discontinuities are propagated through an isotropic body at rest. The conservation equations for energy and momentum are integrated over a domain Σ in four-space bounded by the hyperplanes σ_0, σ_1 and σ_3; σ_0 corresponds to the three-dimensional volume V_0 which at the time t_0 is enclosed within the two-dimensional surface Φ; σ_1 corresponds to the volume V_1 at $t = t_1 > t_0$, and σ_3 is the connecting time-like hypersurface. The surface Φ is considered moving inwards with the velocity $u = c/n$ in the direction of its normal.

Then imagine a two-dimensional surface $\Phi^*(t)$ across which the field is discontinuous:

$$E_1 = E, H_1 = H; \; E_2 = E + \Delta E, H_2 = H + \Delta H. \tag{5.1}$$

Here 1(2) denote the inner (outer) side of Φ^*. For simplicity, we suppose Φ^* also to move together with the field, with the velocity $u = c/n$ in the direction of its normal.

RUBINOWICZ integrates the energy conservation equation over Σ and finds that Φ^* is associated with no source of energy when either of the two energy-momentum tensors is inserted. We therefore turn our attention to the momentum conservation equation written in the following form (our notation), where the time derivative is taken along the moving volume element:

$$\partial_k(S_{ik} - g_i u_k) + \frac{1}{dV}\frac{d}{dt}(g_i dV) = -f_i \tag{5.2}$$

and integrate over Σ:

$$\left(\int_{V_1} - \int_{V_0}\right)g_i \, dV + \int_{t_0}^{t_1} dt \int_{\Phi + \Phi^*} (S_{ik} - g_i u_k) n_k \, dS = -\int_{\Sigma} f_i \, dV dt. \tag{5.3}$$

The contribution from Φ^* to the left hand side of (5.3) can be written in vector form, according to RUBINOWICZ, as

$$\int_{t_0}^{t_1} dt \int_{\Phi^*} [(\boldsymbol{S}_n + \boldsymbol{g}u)_1 + (\boldsymbol{S}_n - \boldsymbol{g}u)_2] dS = \int_{t_0}^{t_1} dt \int_{\Phi^*} \frac{n^2 - p}{n} [\boldsymbol{E} \times \Delta \boldsymbol{H} + \Delta \boldsymbol{E} \times \boldsymbol{H}] dS. \quad (5.4)$$

Here, $\boldsymbol{S}_n$ is a vector with components $S_{ni} = S_{ik}n_k$, and $\boldsymbol{n}$ is taken to point outwards from the integration domains; p is a number, such that $p^M = n^2$, $p^A = 1$. Hence RUBINOWICZ concludes that Φ^* is associated with no source of energy or momentum as far as MINKOWSKI's tensor is employed, in contrast to what is the case with ABRAHAM's tensor, since (5.4) then is non-vanishing. This feature is claimed to favour the former expression.

Let us, however, examine the case $p = 1$. We see that the contribution (5.4) is not yet complete since the effect arising from $\boldsymbol{g}^{\text{mech}}$ has not been incorporated. This effect is connected with the term $(n^2 - 1)/c^2 \partial \boldsymbol{S}/\partial t$ in $\boldsymbol{f}$. Hence, the amount on the left of (5.3) is to be augmented by

$$\left. \begin{array}{c} \dfrac{n^2 - 1}{c^2} \int_{\Sigma} \left[\dfrac{d}{dt}(S_i dV) - \nabla \cdot (S_i \boldsymbol{u}) dV \right] dt \\[4mm] = \dfrac{n^2 - 1}{c^2} \left[\left(\int_{V_1} - \int_{V_0} \right) S_i dV - \int_{t_0}^{t_1} dt \int_{\Phi + \Phi^*} S_i \boldsymbol{u} \cdot \boldsymbol{n} \, dS \right]. \end{array} \right\} \quad (5.5)$$

From (5.5) we see that the contribution from Φ^* equals, in vector form,

$$\frac{n^2 - 1}{c^2} \int_{t_0}^{t_1} dt \int_{\Phi^*} (\boldsymbol{S}_1 - \boldsymbol{S}_2) u \, dS, \quad (5.6)$$

which, together with (5.1) and (5.4), yields MINKOWSKI's result. We see again that the choice between MINKOWSKI's and ABRAHAM's tensors is mainly a matter of interpretation.

Induced motion of a ferromagnetic test body

Let us next examine the gedanken experiment recently considered by COSTA DE BEAUREGARD[26]. The arrangement is rather similar to the one we considered earlier in the second part of section 4: A ferromagnetic shell with mean radius r_0, thickness b and length a is subjected to forces arising from a short current pulse in a rectilinear wire placed along the symmetry axis (z) of the shell. Besides, the wire is charged to a constant charge q per unit length and hence gives rise to the radial electric field $E_r = q/(2\pi r)$,

when ε is put equal to 1. When the current is flowing, a tangential magnetic polarization $\boldsymbol{M} = \boldsymbol{B} - \boldsymbol{H}$ is present, and when the current has decreased to zero, there remains an amount $\Delta\boldsymbol{M} = \Delta\boldsymbol{B}$ in the shell which, together with $\boldsymbol{E}$, gives rise to a linear momentum in the z-direction. Costa de Beauregard integrates the force component $f_3 = -\varrho\partial A_3/c\partial t$ over time and over the volume of the wire, and obtains

$$\int_{\text{wire}} f_3\,dV\,dt = -\frac{1}{c}\,qab\Delta M. \tag{5.7}$$

If we use Minkowski's tensor to calculate the remaining momentum component in the z-direction when the current has left, we find

$$\Delta G_3^M = \frac{1}{c}\Delta\int_{\text{body}} DB\,dV = \frac{1}{c}\int_{\text{body}} E\Delta M\,dV = \frac{1}{c}qab\Delta M. \tag{5.8}$$

A corresponding calculation with Abraham's tensor yields

$$\Delta G_3^A = \frac{1}{c}\Delta\int_{\text{body}} EH\,dV = 0. \tag{5.9}$$

Since (5.7) and (5.8) are obviously in accordance with the balance of total momentum, Costa de Beauregard concludes that Minkowski's expression for the momentum density should be preferred.

Let us, however, continue to consider Abraham's tensor and write the force density in the form

$$\boldsymbol{f}^A = \boldsymbol{f}^M + \frac{\partial}{\partial t}(\boldsymbol{g}^M - \boldsymbol{g}^A). \tag{5.10}$$

Hence, by integration over the total system

$$\left.\begin{array}{c}\left(\displaystyle\int_{\text{wire}} + \int_{\text{body}}\right)f_3^A\,dV\,dt = \displaystyle\int_{\text{wire}} f_3^M\,dV\,dt + \Delta\int_{\text{body}}(g_3^M - g_3^A)\,dV \\[3mm] = \displaystyle\int_{\text{wire}} f_3^M\,dV\,dt + \frac{1}{c}\Delta\int_{\text{body}} DB\,dV = 0,\end{array}\right\} \tag{5.11}$$

in view of (5.7) and (5.8). Eqs. (5.11) and (5.9) show how the momentum balance must be interpreted in terms of Abraham's tensor: Although the electromagnetic field represents a non-closed system, eq. (5.9) shows that

the electromagnetic momentum is *conserved*. (In the case of MINKOWSKI's tensor this was not so, cf. eq. (5.8).) This conservation is carried into effect by the fact that the action from the force on the wire is equal and opposite to the action on the body, in accordance with (5.11). We note in passing that only ABRAHAM's tensor leads to a mechanical *force* on the test body in the z-direction, due to the fact that the surface forces on the body, which are common for the two tensors, are directed in the radial direction. There are also surface forces at the two end surfaces of the body, but these forces compensate each other. With MINKOWSKI's tensor, the presence of electro-magnetic momentum is due to a momentum *flow* into the body.

Following COSTA DE BEAUREGARD we mention that the recent C. GOIL-LOT[27] experiment might be considered as a possible test of the theory. In this experiment a translational motion of a nature similar to the one described above was detected. However, although the qualitative features are similar, COSTA DE BEAUREGARD reports that the GOILLOT effect is far too large to correspond to the effect deduced from the electromagnetic energy-momentum tensors. The effect of the experiment is presumably a spin effect[28]. The inapplicability of the above theory should be expected in this case, since systems exhibiting remanent magnetization are very different from those described by the simple phenomenological theory we are considering.

On the Čerenkov effect

The ČERENKOV effect is a convenient means for a study of the various energy-momentum tensors. We have touched upon this effect before, in connection with relativistic considerations in I, section 10, and we shall take it up again in the relativistic considerations later on in this paper, but here we examine some of its implications when the medium is at rest. In this kind of problem it is most convenient to use MINKOWSKI's tensor, and let us also employ the phenomenological quantum theory (see, for instance, ref. 29 or ref. 30) according to which the four-momentum of the emitted photon is $\hbar k_\mu = \hbar(\boldsymbol{k}, i\omega/c)$. With MINKOWSKI's tensor the balance equations for energy and momentum for the photon plus its radiating electron with momentum $\boldsymbol{p} \to \boldsymbol{p}'$, are

$$c\sqrt{p^2 + m^2 c^2} = \hbar\omega + c\sqrt{p'^2 + m^2 c^2} \tag{5.12a}$$

$$\boldsymbol{p} = \hbar\boldsymbol{k} + \boldsymbol{p}', \tag{5.12b}$$

from which we obtain the well-known expression for the angle θ^M between $\boldsymbol{p}$ and $\boldsymbol{k}$:

$$\cos \theta^M = \frac{c}{mu} + \frac{k\hbar}{2p}\left(1 - \frac{1}{n^2}\right). \qquad (5.13)$$

Here u is the modulus of the velocity of the incoming electron, $\boldsymbol{u} = \boldsymbol{p}/m(u)$.

From the point of view of ABRAHAM's tensor the above argument is only slightly modified: The momentum of the emitted photon in this case is $\hbar\boldsymbol{k}/n^2$, while the force $\boldsymbol{f}^A$ gives rise to a mechanical momentum $(n^2 - 1)$ $\cdot \hbar\boldsymbol{k}/n^2$ which runs together with the field. These two contributions together yield the result $\hbar\boldsymbol{k}$ which was used in (5.12b).

Concerning the literature on this subject we should first of all refer to the clear discussion by G. GYÖRGYI[31]. He shows the equivalence between MINKOWSKI's and ABRAHAM's tensors along similar lines as above. On the other hand, there has recently appeared a paper by J. AGUDÍN[32] on the ČERENKOV effect in which ABRAHAM's tensor, but not MINKOWSKI's tensor, is claimed to be in accordance with EINSTEIN's mass-energy relation. Let us therefore trace out the reason for this result, when we transform the formalism to our notation and simplify the argument, which consists in a study of the conservation equations for total energy, momentum and centre of mass-velocity. Imagine that the initial electron moves along the x-axis with the velocity u and that it emits a photon with mass m' in the direction θ at the time $t = t_1$. After the emission the electron moves with the velocity $u' = p/m(u')$ in the direction φ. The energy balance is written as

$$m(u) = \hbar\omega/c^2 + m(u'). \qquad (5.14a)$$

With ABRAHAM's tensor the magnitude of the momentum of the emitted photon is $\hbar k/n^2 = \hbar\omega/(nc)$, and the balance equation for the x-component of momentum is written as

$$m(u)u = \frac{\hbar\omega}{nc}\cos\theta + G_1^{\text{mech}} + m(u')u'\cos\varphi, \qquad (5.14b)$$

where $\boldsymbol{G}^{\text{mech}}$ is the momentum transferred to the medium.

Finally, AGUDÍN introduces an equation expressing the centre of mass-theorem. During the time period $t = 0$ to $t = t_2$, where $0 < t_1 < t_2$, the centre of mass of the total system is displaced by a distance $m(u)c^2 u t_2/\mathscr{H}^{\text{tot}}$, and the relation given by AGUDÍN is equivalent to writing

$$m(u)ut_2 = m'\left[ut_1 + \left(\frac{c}{n}\cos\theta\right)(t_2 - t_1)\right]$$
$$+ G_1^{\text{mech}}(t_2 - t_1) + m(u')[ut_1 + (u'\cos\varphi)(t_2 - t_1)]. \qquad (5.15)$$

By inserting eqs. (5.14) into (5.15), one finds that the latter relation is fulfilled if $m' = \hbar\omega/c^2$, which is EINSTEIN's mass-energy relation.

Considering MINKOWSKI's tensor, AGUDÍN uses the same set of equations as above with the single difference that the first term on the right hand side of (5.14b) is multiplied by a factor n^2. The new value for m' one now obtains shows an involved geometrical dependence which must be regarded as unphysical. From this he concludes that ABRAHAM's tensor is the one of the two tensors that should be preferred.

Let us now examine the above argument from the point of view of our earlier interpretation. Since G_1^{mech} in (5.15) refers to the small motion of the medium induced by the photon, we must have $G_1^{\mathrm{mech}} = ((n^2 - 1)/nc)\hbar\omega\cos\theta$. This value is in accordance with the value for G_1^{mech} appearing in equation (5.14b), which is constructed on the basis of ABRAHAM's tensor. However, with AGUDÍN's construction of the momentum balance in the case of MINKOWSKI's tensor the right hand side of (5.14b) is changed into $(n\hbar\omega/c)\cos\theta + G_1^{\mathrm{mech}} + m(u')u'\cos\varphi$. Thus the two values of G_1^{mech} become different; in (5.15) G_1^{mech} remains unchanged while in the momentum balance $G_1^{\mathrm{mech}} = 0$. This is the reason for the diverging result. It is instructive to recall that the centre of mass-velocity for an arbitrary (limited) total system is given by $c^2 \boldsymbol{G}^{\mathrm{tot}}/\mathscr{H}^{\mathrm{tot}}$ (cf. eq. (3.13)), which is a constant in view of the conservation equations for *energy* and *momentum*. Applied to the present case this means that the centre of mass-theorem can yield no more information than what is contained in eqs. (5.14) We are evidently free to assign a mass $m' = \hbar\omega/c^2$ to the photon also in the case of MINKOWSKI's tensor.

Finally we note that the ČERENKOV effect provides a convenient opportunity to examine also the radiation tensor (1.6). If we in this case construct the energy and momentum balance similar to (5.12) the only difference is that the term $\hbar\boldsymbol{k}$ in (5.12b) has to be replaced by $\hbar\boldsymbol{k}/n^2$; the radiation tensor is divergence-free and there is no force present to give rise to a mechanical momentum. Thus we find the following expression determining the angle θ^S between $\boldsymbol{p}$ and $\boldsymbol{k}$ in this case:

$$\cos\theta^S = \frac{nc}{u} - \frac{k\hbar}{2p}\left(1 - \frac{1}{n^2}\right). \tag{5.16}$$

Since $k\hbar \ll p$ this equation leads to unphysical values for θ^S. It seems therefore that there are even *formal* difficulties for the application of the radiation tensor to situations where both particles and fields are present.

Final remarks

So far we have limited ourselves to a study of previous treatments advocating the validity of either MINKOWSKI's or ABRAHAM's tensors. In this subsection we discuss briefly, without going into detail, some papers in which diverging tensor expressions have been given preference.

The tensor (1.8) introduced long ago by EINSTEIN and LAUB was encountered already in section 2, in connection with electrostatic phenomena. We recall the important result that the excess pressure effect in a dielectric liquid predicted by this tensor does not fit the HAKIM-HIGHAM experiment. Let us yet write down the complete force expression in the time-varying case:

$$\boldsymbol{f}^E = \varrho\boldsymbol{E} + (\boldsymbol{P}\cdot\triangledown)\boldsymbol{E} + (\boldsymbol{M}\cdot\triangledown)\boldsymbol{H} + \frac{1}{c}(\boldsymbol{j}\times\boldsymbol{H}) + \frac{1}{c}(\dot{\boldsymbol{P}}\times\boldsymbol{H}) + \frac{1}{c}(\boldsymbol{E}\times\dot{\boldsymbol{M}}). \quad (5.17)$$

It should be noted that according to (5.17) the magnetic force density acting on a stationary current distribution, for instance in the interior of a wire, is equal to $(1/c)(\boldsymbol{j}\times\boldsymbol{H})$, instead of the usual $(1/c)(\boldsymbol{j}\times\boldsymbol{B})$ following from ABRAHAM's or MINKOWSKI's tensors. Now, in order to support their force expression, EINSTEIN and LAUB analyse in their paper[5] two examples involving the presence of stationary currents. The second example considered is the following: An infinitely long, rectilinear wire carrying a stationary current $\boldsymbol{J}$ is assumed to prossess a magnetization $\boldsymbol{M}$ in a direction perpendicular to the wire. When no external field is present, it is clear that the electromagnetic force on the wire vanishes. EINSTEIN and LAUB verify by a direct calculation that their tensor leads actually to a vanishing force F_i per unit length in a direction i perpendicular to the wire. We must point out however, that this result is *not* peculiar for the EINSTEIN-LAUB tensor and thereby does not represent any particular support for this tensor. In fact, *any* of the actual tensor expressions will lead to this result, as an immediate consequence of the relations

$$F_i = -\int_{\substack{\text{unit}\\\text{length}}} \partial_k S_{ik}\,dV = -\int S_{ik}^{\text{vac}} n_k\,dS, \quad (5.18)$$

where the value of the last integral goes to zero when the integration surface is taken sufficiently far away from the body.

Concerning the remaining terms in (5.17) we mention that the argument for introducing the term $(1/c)\,(\dot{\boldsymbol{P}}\times\boldsymbol{H})$ was that there must be no distinction in principle between external currents $\boldsymbol{j}$ and polarization currents $\dot{\boldsymbol{P}}$ (cf.

also our remarks in connection with eqs. (3.5) and (3.6)). The magnetic terms in (5.17) were introduced by analogy considerations.

EINSTEIN and LAUB's paper was criticized by R. GANS[33]. He employed the force expression corresponding to MINKOWSKI's tensor, at least for para- and diamagnetic media, and made an explicit calculation of the transversal force on a conductor which carries stationary current and is surrounded by an external magnetic field. Ferromagnetic media were considered separately. In all cases the force was found to vanish when the external field is zero, in accordance with our statement above.

One remark is called for, regarding GANS' claim that the EINSTEIN-LAUB expression comes into conflict with the energy balance. In his argument he uses assumptions that are valid for MINKOWSKI's tensor only, viz. that the energy flux vector is given as $S = c(E \times H)$ also when the velocity of the medium is different from zero. The other tensor expressions will lead to an explicit appearance of the velocity in the energy flux expression.

The use of thermodynamic methods in the present problem represents a special kind of approach. We have already employed such a method in this paper, although in a very simple form, in section 2. In this context we should refer to the work by DE SA[34] and to two papers by KLUITENBERG and DE GROOT[35]. KLUITENBERG and DE GROOT postulate a certain relativistic GIBBS relation and assume the material energy-momentum tensor to be symmetric; they obtain from these assumptions a symmetrical electromagnetic tensor which in the rest system is in accordance with eqs. (1.9), apart from a difference in the energy density component. Further, they claim that the formalism yields ABRAHAM's tensor as an equivalent result, if appropriate new definitions for the hydrostatic pressure and the internal energy are imposed. Concerning this latter statement, however, we must point out that the formalism must always be chosen so as to conform to the observed effects, and the HAKIM-HIGHAM experiment does not seem to leave the room for ambiguities in the definition of pressure in the electrostatic case (cf. section 2).

The papers by G. MARX, G. GYÖRGYI and K. NAGY[3, 36, 37, 38] (with further references) contain a series of arguments of different kinds, and represent together one of the most extensive macroscopic treatments of the problem that has been given. We are considering elements of their papers at various places in our work, for instance in the examination of the radiation tensor. Their main conclusion is that ABRAHAM's tensor is the basic electromagnetic tensor, while the radiation tensor (instead of MINKOWSKI's tensor) is claimed to be the result of a combination with the excited matter induced

by a propagating field. Since in this section we consider fields within matter
at rest, we should mention that the difficulty they claim to exist for MIN-
KOWSKI's tensor in explaining the propagation of the centre of mass for a
limited radiation field within an isotropic dielectric, is cleared up of one
observes that the time derivative of the quantity $(\boldsymbol{S}^M/c^2 - \boldsymbol{g}^M)$, integrated
over the total volume, is equal to zero.

As we have noted, the absence of terms containing polarization and
magnetization entities in MINKOWSKI's force has represented an obstacle for
the acceptance of this expression (cf. also the book by FANO, CHU, ADLER[39]).
In a series of papers published recently[40], P. POINCELOT took the full
consequence of the opposite point of view and proposed the introduction of
all kinds of polarization and magnetization terms in the force on an equal
footing with the free charge and current terms, viz.

$$\boldsymbol{f} = (\varrho - \nabla \cdot \boldsymbol{P})\boldsymbol{E} + \frac{1}{c}(\boldsymbol{j} + \dot{\boldsymbol{P}} + c\nabla \times \boldsymbol{M}) \times \boldsymbol{B} \qquad (5.19a)$$

$$f_4 = \frac{i}{c}\boldsymbol{E} \cdot (\boldsymbol{j} + \dot{\boldsymbol{P}} + c\nabla \times \boldsymbol{M}). \qquad (5.19b)$$

The tensor corresponding to the force (5.19) can be expressed in terms of
$\boldsymbol{E}$ and $\boldsymbol{B}$ in the same form as the electromagnetic tensor in the vacuum-field.
However, although (5.19) cannot be rejected on purely formal grounds, we
cannot find any argument of convenience or experimental evidence that sup-
ports this expression.

6. Angular Momentum in Arbitrary Inertial Systems

In the remaining part of our work we shall be concerned with topics
connected with relativity. To some extent we shall have the opportunity to
return to a study of situations which were considered already in I, chapter
IV, in connection with MINKOWSKI's tensor. From the preceding it should be
clear that in a relativistic theory the latter tensor is convenient to use, in
order to obtain information about the direction and velocity of the pro-
pagating field energy. But it is instructive to consider also the behaviour of
the alternative tensors (especially ABRAHAM's tensor) in arbitrary inertial
systems, since such an anlysis will exhibit characteristic differences between
the tensors. In this section we assume that the medium is homogeneous and
isotropic, and let as usual K denote the inertial system in which the rest
system K^0 moves with the velocity v along the x-axis.

Evaluation of torques within an infinite medium

Let us image a finite radiation field within a large (infinite) dielectric medium. The angular momentum quantities $M_{\mu\nu}$ are in general defined by the integral

$$M_{\mu\nu} = \int (x_\mu g_\nu - x_\nu g_\mu) \, dV, \qquad (6.1)$$

taken over the whole field, in any frame K. Let us further imagine that for each of the electromagnetic tensors in question we insert the appropriate expression for g_μ into the integral in (6.1) and calculate $M_{\mu\nu}$. In this context it should be emphasized that in each case g_μ is considered as a *field* quantity, $M_{\mu\nu}$ thus being considered as a field angular momentum. This definition is the natural one and we have used it throughout, in I as well as in the present paper, although we have repeatedly pointed out that in the MINKOWSKI case the momentum density g_μ^M in reality includes also a mechanical part which is responsible for the asymmetry of MINKOWSKI's tensor. In other words, MINKOWSKI's angular momentum $M_{\mu\nu}^M$ contains in a strict sense also a contribution from the mechanical part of the total system. To call $M_{\mu\nu}^M$ a field angular momentum is obviously just tantamount to calling G_μ^M a field linear momentum. If on the other hand we take the distinction between the two parts of G_μ^M explicitly into account and exclude the mechanical part of g_μ^M from the expression for field angular momentum, we obtain instead ABRAHAM's expression $M_{\mu\nu}^A$, since that part of g_μ^M which pertains to the electromagnetic field is just g_μ^A. The different ways of dividing the total angular momentum into a field part and a mechanical part obviously have no influence upon the conservation of total angular momentum, which is a consequence of the symmetry and the zero divergence of the total energy—momentum tensor. Thus, in each case we obtain the mechanical angular momentum by inserting that part of the total momentum density which is not counted as a field entity.

As regards MINKOWSKI's tensor it seems appropriate to recall from I, section 11 that the quantities $M_{\mu\nu}^M$ are equivalent to the angular momentum quantities one can most simply construct on the basis of NOETHER's theorem. This is in accordance with the general property of MINKOWSKI's tensor that it readily adjusts itself to the LAGRANGIAN procedures. We recall also that $M_{\mu\nu}^M$ is in general not a tensor.

For a comparison between the various tensors it is however not the angular momentum itself which is of primary interest in each case, but rather its time derivative, i.e. essentially the body *torque*. The torque is

defined as $\boldsymbol{N} = -d\boldsymbol{M}/dt$, and we shall in the present subsection start to perform a direct calculation of the torques corresponding to ABRAHAM's and MINKOWSKI's tensors. It will turn out that the two values so obtained in general are different from each other. This difference is what we should expect, since the momentum densities $\boldsymbol{g}^A$ and $\boldsymbol{g}^M$ are themselves essentially different in direction and magnitude.

The last point requires some further explanation. In all electrostatic (or magnetostatic) cases and also in all *high-frequency* electromagnetic cases considered up till now we have found that ABRAHAM's and MINKOWSKI's tensors yield just identical expressions for the torque on a test body immersed either in a vacuum or in a dielectric fluid. The reason for this equality can be understood in a simple way by observing that in those cases the torque could be evaluated as a function of the field stress tensor taken in the domain just *outside* the surface of the body, wherein the equality $S_{ik}^A = S_{ik}^M$ is valid. (Cf. eqs. (2.11) and (4.8b) for the electrostatic and electromagnetic cases, respectively.) In the situations considered in the present section there is however no similar reason why the torque expressions should be the same; we have to lean directly upon the formula (6.1) and evaluate it over the field region within the body. In the MINKOWSKI case the torque can be looked upon as a consequence of the *asymmetry* of the mechanical energy-momentum tensor (this fact having represented as an objection to the acceptance of MINKOWSKI's tensor), while in the ABRAHAM case the torque arises because of the *force* density.

In spite of this difference between the two torque expressions obtained within an infinite medium we shall nevertheless in the next subsection see that the torques are relativistically equivalent from a physical point of view, since both of them are compatible with uniform motion of the physical system in K. In this context we shall draw into consideration the analogous situation encountered in relativistic mechanics of elastic media: An elastic body subjected to stresses in the rest frame will in general require a torque to maintain steady motion in another inertial frame.

Let us now start with ABRAHAM's tensor and perform the calculation. From (6.1) it appears that the torque $\boldsymbol{N}^A = -d\boldsymbol{M}^A/dt$ in K is given by

$$\boldsymbol{N}^A = \int (\boldsymbol{r} \times \boldsymbol{f}^A) dV. \tag{6.2}$$

At first sight it seems that one will meet a difficulty in the evaluation of this integral. This difficulty is connected with the non-invariance in four-space of the world lines corresponding to ABRAHAM's energy flux $\boldsymbol{S}^A$ (cf. the next

section). On the other hand we pointed out in I, section 9 that the ray velocity $\boldsymbol{u}$, which is the velocity of propagation of the wave energy and which may be written as $\boldsymbol{u} = \boldsymbol{S}^M/W^M$, transforms like a particle velocity. From this it follows that the world lines corresponding to MINKOWSKI's energy flux $\boldsymbol{S}^M$ really have the property that they remain invariant in four-space upon a LORENTZ transformation. Now it is clear that in order to obtain a picture of the wave propagation in K one has to transform the *total* wave, i.e. one must include the effect also from the produced mechanical momentum $\boldsymbol{g}^{\text{mech}\,0}$ in K^0. This feature resolves the apparent dilemma in connection with the evaluation of the integral in (6.2): Even though $\boldsymbol{S}^A$ is different from $\boldsymbol{S}^M$ both in direction and magnitude we have to integrate over that part of space where the field is actually present, i.e. across the world lines corresponding to $\boldsymbol{S}^M$.

It is now convenient to assume that the field travels parallel to the xy-plane in such a way that any wave vector $\boldsymbol{k}$ which is contained in the wave, makes an angle ϑ with the x-axis in K. It can readily be verified that the only non-vanishing component in (6.2) is the z-component, the other components fluctuate away. We evaluate the integral in (6.2) over the domain AB, i.e. over the hypersurface $t = 0$ (cf. I, Fig. 2). We obtain

$$N_3^A = \gamma \int\limits_{AB} (x_1^0 f_2^{A^0} - x_2^0 f_1^{A^0} + \beta c t^0 f_2^{A^0})\, dV. \tag{6.3}$$

This integral is to be transformed into an integral taken at constant time in K^0, and similarly as in I, section 12, we choose the domain CD for which $t^0 = 0$. The world lines determined by $\boldsymbol{S}^M$ will each intersect AB and CD in two points with coordinates $(x_i^0(AB),\, t^0(AB))$ and $(x_i^0(CD),\, 0)$ in K^0, such that

$$
\left.
\begin{aligned}
x_1^0(CD) &= x_1^0(AB) - \frac{c}{n} t^0(AB)\cos\vartheta^0 = x_1^0(AB)\left(1 + \frac{\beta}{n}\cos\vartheta^0\right) \\[2mm]
x_2^0(CD) &= x_2^0(AB) - \frac{c}{n} t^0(AB)\sin\vartheta^0 = x_2^0(AB) + \frac{\beta x_1^0(CD)\sin\vartheta^0}{n + \beta\cos\vartheta^0} \\[2mm]
x_3^0(CD) &= x_3^0(AB), \quad t^0(AB) = -\frac{\beta}{c} x_1^0(AB).
\end{aligned}
\right\} \tag{6.4}
$$

The calculation is carried out in a similar way as in section 12 of I, so we abstain from a detailed exposition. The relation between the volume element dV and the element dV^0, taken at constant time in K^0, is given by (I, 12.9). We find

$$N_3^A = \int\limits_{CD} \frac{x_1^0(f_2^{A0}/\gamma^2 + (\beta/n)\sin\vartheta^0 f_1^{A0}) - (1 + (\beta/n)\cos\vartheta^0)x_2^0 f_1^{A0}}{(1 + (\beta/n)\cos\vartheta^0)^2}\,dV^0. \tag{6.5}$$

Since $f^{A0} = [(n^2 - 1)/nc]\partial W^0/\partial t^0$, a representative term in (6.5) can be transformed as follows:

$$\int x_1^0 f_2^{A0}\,dV^0 = \frac{n^2 - 1}{nc}\mathscr{H}^0\sin\vartheta^0\frac{d}{dt^0}\left[\frac{1}{\mathscr{H}^0}\int x_1^0 W^0\,dV^0\right] = \frac{n^2 - 1}{n^2}\mathscr{H}^0\sin\vartheta^0\cos\vartheta^0. \tag{6.6}$$

In the second term we have here used the fact that $d/dt^0[\ ] = (c/n)\cos\vartheta^0$, the centre of mass-velocity in the x^0-direction. By a similar treatment of the other terms in (6.5) we find

$$N_3^A = -\beta^2\frac{n^2 - 1}{n^2}\frac{\sin\vartheta^0\cos\vartheta^0}{(1 + (\beta/n)\cos\vartheta^0)^2}\mathscr{H}^0. \tag{6.7}$$

Thus there results a non-vanishing torque also with the symmetrical ABRA-HAM tensor. So far we have considered only the case where the domains AB and CD are placed at $t = 0$ and $t^0 = 0$ respectively; however, the same result applies also when AB and CD are placed at arbitrary constant times in K and K^0 due to the fact that the force density fluctuates away when integrated over space. So the expression (6.7) is constant in time.

Let us now consider MINKOWSKI's tensor. From (6.1) we find

$$N_3^M = \int (S_{12}^M - S_{21}^M)\,dV. \tag{6.8}$$

Now $S_{21}^M - S_{12}^M = [(n^2 - 1)/n]\beta\gamma W^0\sin\vartheta^0$, and the integration in (6.8) can be carried out in the same way as above. We get

$$N_3^M = -\beta\frac{n^2 - 1}{n}\frac{\sin\vartheta^0}{1 + (\beta/n)\cos\vartheta^0}\mathscr{H}^0. \tag{6.9}$$

We see that the expressions (6.7) and (6.9) in general are different from each other, although they both vanish in the rest frame as they should. It is therefore natural to ask whether it is possible to single out one of these these expressions as preferable. As we shall now see this is not so in the case of an infinite medium, since the torque expressions (6.7) and (6.9) may be looked upon as representing relativistic effects of the same nature as the non-observable effect encountered in ordinary relativistic mechanics of an elastic body possessing stresses in its rest frame.

A relativistic effect

Let us first recall the following situation from mechanics: If an elastic body is subjected to stresses in its rest frame it may in other frames exhibit a momentum component at right angle to the direction of motion. Consequently, the body will require a torque in order to maintain its uniform motion.

We find it desirable to go into some details. Let τ_{ik}^0 be the mechanical stress tensor of the elastic body in K^0. The mechanical torque in K is

$$\boldsymbol{N} = \int (\boldsymbol{r} \times \boldsymbol{f}) \, dV. \tag{6.10}$$

Then make the explicit requirement that the body remain in steady motion in K. This means that we can put $d\boldsymbol{g}/dt = 0$, where $g_i = -i\tau_{i4}/c$ and the time derivative is taken along the volume elements dV which follow the body. Thus, the body experiences a change of angular momentum equal to

$$\frac{d\boldsymbol{M}}{dt} = \int \left(\frac{d\boldsymbol{r}}{dt} \times \boldsymbol{g}\right) dV, \tag{6.11}$$

since also $(d/dt)dV = 0$. Inserting $d\boldsymbol{r}/dt = \boldsymbol{v}$ we obtain

$$\frac{d\boldsymbol{M}}{dt} = \int (\boldsymbol{v} \times \boldsymbol{g}) \, dV = \boldsymbol{v} \times \boldsymbol{G}. \tag{6.12}$$

If the torque (6.10) is equal to the amount (6.12) which the body actually requires in order to preserve stationary motion, then the scheme is consistent, and we have an example of a situation where the existence of a torque is not followed by a rotation. We have to stress the difference between the calculations that led to (6.10) and (6.12): In the first case, the velocity of the body was required to be equal to $\boldsymbol{v}$, and we can imagine that this requirement is fulfilled at a certain time in K just after the Lorentz transformation from K^0 has been performed. But in the latter case, the body velocity was required to be the same at an *arbitrary* instant afterwards, corresponding to the fact that the directions of the world lines of the body were required to be unaltered.

It appears from the text-books (M. von Laue[41], R. Becker[42]) that the equivalence between $\boldsymbol{N}$ and $d\boldsymbol{M}/dt$ has been verified in certain special cases. But the equivalence can also be shown quite generally for an elastic body, by the following simple consideration.

Let us calculate a typical component of the torque in K, say the z-component. We readily find by an insertion into (6.10)

$$N_3 = \int_{AB} [\gamma(x_1^0 + vt^0)f_2^0 - x_2^0\gamma f_1^0]\gamma^{-1}dV^0 = \int_{CD} (\gamma^{-2}x_1^0 f_2^0 - x_2^0 f_1^0)dV^0. \quad (6.13)$$

Using now the fact that $f_i^0 = \partial_k^0 \tau_{ik}^0$, we can write

$$N_3 = \int_{CD} (\gamma^{-2}x_1^0\tau_{2k}^0 - x_2^0\tau_{1k}^0)n_k^0 dS^0 + \beta^2\int_{CD} \tau_{12}^0 dV^0 = \beta^2\int_{CD} \tau_{12}^0 dV^0, \quad (6.14)$$

since the surface integral is performed over a surface outside the body where τ_{ik}^0 vanishes.

Further, by means of the relation $\tau_{24} = i\beta\gamma\tau_{12}^0$ we readily obtain by an insertion into (6.12)

$$\frac{dM_3}{dt} = \beta^2\int_{CD} \tau_{12}^0 dV^0. \quad (6.15)$$

Eqs. (6.14) and (6.15) show the consistency in the case of an elastic body: The body is acted upon by a torque which is equal to the change of momentum required in order to maintain steady motion.

After this digression let us return to the radiation field. The torque on the body is defined as

$$N_l = \int (x_i f_k - x_k f_i + S_{ik} - S_{ki})dV, \quad (6.16)$$

where i,k,l are cyclic. (Actually, the expression (6.16) has been derived indirectly as $N_l = -\,dM_{ik}/dt$; however, the coordinate dependent terms in (6.16) appear similarly as in (6.10), and the two last terms in (6.16) must yield the appropriate torque contribution from the tensor asymmetry, cf. for instance the considerations in section 4 of I.) The expressions for N_l that we need here have been derived in (6.7) and (6.9).

Next, require explicitly steady motion in K. The necessary and sufficient conditions are: (1) The body velocity $\boldsymbol{v} = (v,0,0) = $ constant; (2) $d\boldsymbol{r}/dt = \boldsymbol{u} = \boldsymbol{S}^M/W^M$ along the moving wave elements dV. From these conditions it follows that U_μ is a four-vector and that the world lines remain invariant in four-space. Moreover, it follows that $d\boldsymbol{g}/dt = 0$ along the wave trajectories, since g_i (for any field tensor) is proportional to the energy density W^0, which is a function of the invariant wave phase φ, φ being constant along the

trajectories. Thus, taking the time derivative of the field angular momentum we obtain in the two cases

$$dM_3^A/dt = (\boldsymbol{u} \times \boldsymbol{G}^A)_3, \quad dM_3^M/dt = (\boldsymbol{u} \times \boldsymbol{G}^M)_3. \qquad (6.17)$$

If we here insert the appropriate values for $\boldsymbol{u}$, $\boldsymbol{G}^A$ and $\boldsymbol{G}^M$ we will find the expressions (6.7) and (6.9) respectively, with the opposite sign. If now ABRAHAM's or MINKOWSKI's tensor is taken to describe the field, it follows from the conservation of total angular momentum that the rate of change of the *mechanical* angular momentum is given by the expression (6.17), with the opposite sign. In both cases we therefore find that the scheme is consistent in the same way as it was found to be in the situation considered previously (cf. (6.14) and (6.15)): The body is acted on by a torque which is just equal to the rate of change of mechanical angular momentum being necessary in order to prevent rotation.

At this place we should make a comment on an assertion put forward by VON LAUE in § 19 of his book [41], concerning a verification of the principle of conservation of total angular momentum if MINKOWSKI's tensor is used for the field. This is actually one of the arguments VON LAUE presents in favour of MINKOWSKI's tensor. He first writes the rate of change of field angular momentum similarly as the last of eqs. (6.17), by taking the time derivative along the moving wave elements. Thereafter, and this is the crucial point, the z-component of the torque on the body is claimed to be given by

$$\int (x_1 \partial_k S_{2k}^M - x_2 \partial_k S_{1k}^M)\, dV = \int (S_{12}^M - S_{21}^M)\, dV. \qquad (6.18)$$

Since it can be shown that $(\boldsymbol{u} \times \boldsymbol{g}^M)_3 = S_{21}^M - S_{12}^M$, VON LAUE concludes that the conservation of total angular momentum is verified in the present case.

We cannot find, however, any reason why this torque component should be given by the left hand side of eq. (6.18). Moreover, one cannot find expressions for the rate of change of the field angular momentum and the body torque *independently* of each other, and thereafter check the angular momentum balance. Instead, the torque is found by just *requiring* the angular momentum balance to hold, such that $\boldsymbol{N}$ be given by the relation $\boldsymbol{N} = -\,d\boldsymbol{M}/dt$.

Finite bodies

Hitherto we have restricted ourselves to a consideration of very large (or infinite) dielectric bodies. The case of finite bodies is important, however, since it reveals characteristic features of the angular momentum balance.

Let us therefore consider this case, and for definiteness assume that an optical wave passes through an isotropic and homogeneous glass plate, for instance at BREWSTER's angle of incidence in K^0. The electromagnetic forces are present only in the boundary layers, and we shall assume that an external mechanical surface force $\boldsymbol{F}^{\mathrm{ext}\,0}$ just counterbalances the surface force $\boldsymbol{F}^0$ caused by the field, in such a way that the field is not disturbed. The consequence of the last assumption is that the mechanical angular momentum of the body is conserved in K^0, $\boldsymbol{N}^{A^0} = \boldsymbol{N}^{M^0} = - \boldsymbol{N}^{\mathrm{ext}\,0}$, and that the presence of extra mechanical stresses due to the external forces is avoided.

We now consider the system in the frame K, and adopt ABRAHAM's tensor as the field tensor. From (6.16) it is apparent that the torque is given as $\boldsymbol{r} \times \boldsymbol{f}^A$, integrated over the internal volume, plus $\boldsymbol{r} \times \boldsymbol{F}^A$, integrated over the surfaces. We readily find that the contribution from the first term is zero, and as the electromagnetic surface force $\boldsymbol{F}^A$ transforms similarly as the external force $\boldsymbol{F}^{\mathrm{ext}}$, we can write

$$\boldsymbol{N}^A = - d\boldsymbol{M}^A/dt = - \boldsymbol{N}^{\mathrm{ext}}. \tag{6.19}$$

Thus we obtain the satisfactory explanation that the net torque acting on the body is still zero. If, however, MINKOWSKI's tensor is adopted for the field, the situation is changed. We see that $\boldsymbol{f}^M = 0$ in the interior domain and that $\boldsymbol{F}^M = \boldsymbol{F}^A$ so that the contribution from the forces is the same, but there appears an extra volume effect in the torque because of the asymmetry of the stress tensor S_{ik}^M. According to the theory the body is thus acted upon by a net torque in K, although the motion is uniform and although no account has to be taken of the influence from elastic stresses in K^0. We find this property to be rather inconvenient. It does not mean, however, that MIN-KOWSKI's torque expression should simply be rejected. For we may carry through an analysis of the same kind as in the previous subsection, where now the time derivatives are to be taken along the moving *body* elements, and will find that also now the MINKOWSKI torque is compatible with the requirement of steady motion. The peculiar property of MINKOWSKI's torque is obviously a consequence of the fact that the momentum density $\boldsymbol{g}^{M^0}$ contains both a pure field quantity $\boldsymbol{g}^{A^0}$ and a mechanical quantity $\boldsymbol{g}^{\mathrm{mech}^0}$, cf. also the remarks in the beginning of this section. In conclusion, the study of the case of finite bodies reveals the characteristic effect that the most natural division of the total angular momentum into a field part and a mechanical part is made when one adopts ABRAHAM's expression for the field. On the other hand, in the case of *infinite* bodies we saw in the previous

subsection that no preference could be assigned to either of the two torque expressions.

At this place a remark is in order, in connection with a comparison with the situation where an electromagnetic wave passes through a finite, aniso-tropic body at rest. Such a situation was considered in section 4, and we recall that the equation $N^{A^0} = N^{M^0}$ was found to hold in general. Now our present situation resembles the wave-crystal situation from section 4, since an isotropic body in K^0 becomes anisotropic in K. We may note that the total angular momentum in the vacuum field when the wave has left the body is independent of which energy-momentum tensor is used for the field, since the direction of the wave propagation in either case is determined from S^M. Yet we have found that N^A in general is different from N^M when $\beta \neq 0$.

To point out the difference between these two cases let us once again examine the torque balance (4.1):

$$N = - d/dt M^{\text{vac}} - d/dt M^i, \qquad (6.20)$$

where now the time derivatives are taken along the moving body. In ad-dition to the assumption of the independence of M^{vac} we could, in the case considered in section 4, require on physical grounds that N be independent of the interaction period T (assumed a stationary field during this period), expecially in the small period when the field leaves the medium. The crucial point here is that this latter requirement can no longer be upheld when the body moves. Consequently, dM^i/dt is in general different from zero, i.e. the torque depends in this case also on the internal field. We note that $dM^i/dt \neq 0$ also with Abraham's tensor.

As mentioned above the purpose of assuming $F^0 = - F^{\text{ext}\,0}$ was to obtain a situation in which no complication will arise because of extra mechanical stresses set up in K^0. Let us now briefly consider how the situation is changed if we let the same value of $N^{\text{ext}\,0}$ be obtained by external surface forces which do not compensate the electromagnetic forces at each surface element. In this case there will appear mechanical stresses in K^0, described by the mechanical stress tensor τ_{ik}^0. These may lead to non-vanishing momentum components at right angle to the velocity v in K, and thus be connected with the torque $N_i^{\text{stress}} = - (i/c)\delta_{ijk} \int v_j \tau_{k4} dV$ which follows from the requirement of steady motion. This amount is equal to the resulting torque exerted by the forces, so that we obtain instead of eq. (6.19) the equation

$$N^A + N^{\text{ext}} = N^{\text{stress}}. \qquad (6.21)$$

So far we have considered only ABRAHAM's and MINKOWSKI's tensors. Let us finally for a moment consider the radiation tensor $S_{\mu\nu}^S$, which is symmetric and divergence-free within an isotropic medium. In the situation considered in the first subsection above it follows immediately that $N_3^S = 0$, so that according to the radiation tensor the angular momenta of the field and the body are conserved separately. If the body is finite, the radiation tensor behaves similarly as ABRAHAM's tensor in the sense that the torque in K is determined by the surface forces only. It should however be borne in mind that the radiation tensor yields already in the rest frame a surface force with another direction and magnitude than ABRAHAM's surface force, although the torques are the same (cf. section 4).

7. Further Considerations on Relativity

In this section we continue the investigation of relativistic phenomena. Only effects involving special relativity will be considered. For the main part we shall be concerned with topics that were studied in chapter IV of I in connection with MINKOWSKI's tensor, and shall relate the phenomena to the other tensors. In the following two subsections we study two subjects that are closely related to each other, namely the velocity of the energy in an electromagnetic wave and the behaviour of the relativistic centre of mass.

Transformation of the energy velocity in a light wave

Consider a plane light wave within an isotropic and homogeneous insulator moving with the uniform four-velocity V_μ in the frame K. Similarly as in I, section 9, the ray velocity $\boldsymbol{u}$ is defined as the velocity of propagation of the light energy. The ray velocity is in general different both in magnitude and direction from the phase velocity. We recall that it is shown in MØLLER's book [7] that the ray velocity transforms like the velocity of a material particle, and further that this transformation property is verified experimentally in the FIZEAU experiment, at least to the first order in v/c.

If now an energy-momentum tensor $S_{\mu\nu}$ shall describe the whole travelling wave, it must be possible to relate the ray velocity $\boldsymbol{u}$ to the components of this tensor by the equation $\boldsymbol{u} = \boldsymbol{S}/W$. For such a tensor the quantity $\boldsymbol{S}/W$ must therefore transform like a particle velocity. To investigate whether $S_{\mu\nu}$ behaves in this way is tantamount to examining whether the quantities

$$U_\mu = \left(\frac{\boldsymbol{S}/W}{\sqrt{1 - S^2/(c^2 W^2)}}, \quad \frac{ic}{\sqrt{1 - S^2/(c^2 W^2)}} \right) \tag{7.1}$$

constitute a four-vector. As stated already in I, Møller has shown that the sufficient and necessary condition for U_μ being a four-vector is that

$$R_{\mu\nu} \equiv S_{\mu\nu} + \frac{1}{c^2} S_{\mu\alpha} U_\alpha U_\nu = 0 \qquad (7.2)$$

in some inertial system.

We recall that by inserting Minkowski's tensor one really finds $R_{\mu\nu}^{M_0} = 0$ in the case of a most general plane wave. This circumstance thus provides a further support for our general assertion that Minkowski's tensor describes the whole travelling wave. In particular, if a ray travels parallel to the direction of the medium velocity, one obtains immediately by means of Minkowski's tensor the well known formula, to the first order in v/c,

$$u = \frac{S^M}{W^M} = \frac{c}{n} + v\left(1 - \frac{1}{n^2}\right). \qquad (7.3)$$

This formula was verified in the Fizeau experiment.

After this summary of the results obtained in section 9 of I, we investigate how the situation looks from the point of view of Abraham's tensor. In this case one readily finds that $R_{\mu\nu}^{A_0} \neq 0$ in general, so that the equation (7.2) is not fulfilled and S^A/W^A does not transform like a particle velocity. Correspondingly, the last of eqs. (7.3) is replaced by

$$\frac{S^A}{W^A} = \frac{c}{n} + 2v\left(1 - \frac{1}{n^2}\right), \qquad (7.4)$$

which is essentially different from (7.3). This kind of behaviour is what we should expect: Abraham's tensor leaves out of consideration the influence from the produced mechanical momentum $\boldsymbol{g}^{mech_0}$ in K^0, and thus S^A/W^A cannot be expected to be equal to the ray velocity. The non-compatibility between the transformation criterion and the Abraham tensor evidently does not represent a real difficulty for this tensor.

Let us now follow a more general line of approach and try to find a set of reasonable conditions under which the quantity S/W, obtained from some energy-momentum tensor $S_{\mu\nu}$, actually obeys the transformation criterion. To this end it is advantageous first to recall the essential assumptions inherent in Møller's proof (in § 24 of his book[7]) about the transformation character of the ray velocity $\boldsymbol{u}$: In the first place, the equation for the wave front of an elementary spherical wave in K^0 being emitted from the origin at the time $t^0 = 0$ is written as

$$r^{02} - \frac{c^2}{n^2} t^{02} = 0. \tag{7.5}$$

In the second place, the corresponding equation for the wave front in K is obtained by means of point transformations of each term in (7.5), so that the world lines are assumed to remain invariant in four-space upon a LORENTZ transformation. By means of these conditions MØLLER derives that $\boldsymbol{u}$ transforms like a particle velocity.

Our task is now to transform the above conditions into equivalent conditions imposed on the tensor $S_{\mu\nu}$. In accordance with (7.5) we shall first require that the magnitude of the velocities of propagation of energy and momentum is equal to c/n, as expressed by the equations

$$S_{4k}^0 = -\frac{i}{n} S_{44}^0 e_k^0, \quad S_{ik}^0 = -\frac{i}{n} S_{i4}^0 e_k^0, \tag{7.6}$$

where $\boldsymbol{e}^0$ is the wave normal for the plane wave. Note that these conditions actually mean also that the field is closed, i.e. $\partial_\nu^0 S_{\mu\nu}^0 = 0$, since each frequency component of the plane wave depends on the wave phase ($\boldsymbol{k}^0 \cdot \boldsymbol{r}^0 - \omega^0 t^0$) so that $e_k^0 \partial_k^0$ may be replaced by $-n\partial/(c\partial t^0)$. If we now insert the conditions (7.6) into the expression (7.2) for $R_{\mu\nu}$, we really find that $R_{\mu\nu}^0 = 0$.

So far we have only shown that the conditions (7.6) are *sufficient* to satisfy the transformation criterion; we have not verified that they are *necessary*. In fact, if we merely maintain the single restriction that S_{ik}^0 be proportional to $S_{i4}^0 e_k^0$, we find that the relation

$$S_{ik}^0 = -\frac{i}{c} \frac{|\boldsymbol{S}^0|}{W^0} S_{i4}^0 e_k^0 \tag{7.7}$$

is necessary to yield $R_{\mu\nu}^0 = 0$. Evidently eq. (7.7) becomes equal to the last of eqs. (7.6) when $|\boldsymbol{S}^0|/W^0 = c/n$. Note that the weak condition (7.7) does not even imply that $S_{\mu\nu}^0$ be divergence-free. We think that this condition is of minor physical interest, however, since it is preferable to construct the theory so as to conform to the equation (7.5) (or the wave equation) in a simple way, i.e. one should always take $|\boldsymbol{S}^0|/W^0 = c/n$.

It has been pointed out by G. MARX *et al*[3] that the radiation tensor $S_{\mu\nu}^S$ also obeys the transformation criterion. This feature can be explained on the basis of eqs. (7.6), since the radiation tensor satisfies these equations. On the contrary, both ABRAHAM's tensor and the DE GROOT-SUTTORP tensor (1.9) are incompatible with the condition (7.7) as well as the transformation criterion $R_{\mu\nu} = 0$.

Centre of mass

Let us now assume that the interior domain of the radiation field can be taken as a part of a *monochromatic* plane wave with wave vector $\boldsymbol{k}$. Similarly as in section 12 of I we further assume that the small boundary layer—in which the usual plane wave relations between the fields do not hold—contains negligible field energy and momentum.

The spatial coordinates $X_i(K)$ of the centre of mass of the field in K are defined by

$$X_i(K) = \frac{1}{\mathcal{H}} \int x_i W dV, \qquad (7.8)$$

whatever energy-momentum tensor is employed. Similarly as in the previous section it must however be borne in mind that in any case the localization of the field in K is determined by MINKOWSKI's tensor, i.e. one integrates over the volume of the field by integrating across the world lines corresponding to $\boldsymbol{S}^M$.

Let us first study the velocity of propagation of the centre of mass in K. From (7.8) we readily find the relation

$$\frac{d}{dt} X_i(K) = \frac{1}{\mathcal{H}} \int S_i dV - \frac{icX_i(K)}{\mathcal{H}} \int f_4 dV + \frac{ic}{\mathcal{H}} \int x_i f_4 dV, \qquad (7.9)$$

which in general shows a complicated behaviour for a non-closed system. Inserting ABRAHAM's tensor into the right hand side of eq. (7.9)—and assuming that corresponding world points in K and K^0 are connected by the invariant (MINKOWSKI) world lines—we find however that the two last terms in (7.9) fluctuate away. Moreover, since the field is homogeneous, we find from (7.9) the simple relation

$$\frac{d}{dt} \boldsymbol{X}^A(K) = \frac{\boldsymbol{S}^A}{W^A}. \qquad (7.10)$$

By taking into account the result obtained in the previous subsection, we thus find that the velocity $d\boldsymbol{X}^A(K)/dt$ is different from the velocity of propagation of the total field, i.e. the ray velocity $\boldsymbol{u}$. This feature severely limits the validity of the centre of mass as a representative point if ABRAHAM's tensor is used.

With the radiation tensor we get immediately

$$\frac{d}{dt} \boldsymbol{X}^S(K) = \frac{\boldsymbol{S}^S}{W^S} = \boldsymbol{u}, \qquad (7.11)$$

in accordance with the general equivalence between the radiation tensor and the MINKOWSKI tensor with regard to wave propagation properties.

So far having studied the *velocity* of propagation of the centre of mass we now turn our attention to its *localization*. From the sudy of MINKOWSKI's tensor in I, we recall that the different centres of mass we obtain by varying the reference frames K, do not in general coincide when considered simultaneously in one frame. In fact, we calculated the difference $\boldsymbol{X}^M(K) - \boldsymbol{X}^M$, where $\boldsymbol{X}^M$ denoted the simultaneous position in K of the *proper* centre of mass. The proper centre was defined as the centre of mass in the rest frame K^0, i.e. $\boldsymbol{X}^M(K^0) \equiv \boldsymbol{X}^{M0}$. Let us write down again the formula (I, 12.21)

$$\boldsymbol{a}^M(K) \equiv \boldsymbol{X}^M(K) - \boldsymbol{X}^M = \frac{1}{k^0} \frac{\boldsymbol{\beta} \times \boldsymbol{k}^0}{nk^0 + \boldsymbol{\beta} \cdot \boldsymbol{k}^0}, \tag{7.12}$$

where we now have added a superscript M.

Just the same procedure can now be applied to calculate the position $\boldsymbol{X}^A(K)$ when ABRAHAM's tensor is used for the field. In this context we stress that corresponding field points in K and K^0 are required to be connected by the MINKOWSKI world lines, i.e. we simply ignore for a moment the above result $d\boldsymbol{X}^A(K)/dt \neq \boldsymbol{u}$. Since the proper centres coincide in K^0, $\boldsymbol{X}^{A0} = \boldsymbol{X}^{M0}$, we evidently have also $\boldsymbol{X}^A = \boldsymbol{X}^M$ in K. We do not give the details of the calculation since it is just similar to the calculation carried through in I, section 12. The result is

$$\boldsymbol{a}^A(K) \equiv \boldsymbol{X}^A(K) - \boldsymbol{X}^A = \boldsymbol{a}^M(K), \tag{7.13}$$

showing that ABRAHAM's tensor yields the same position for the centre of mass as MINKOWSKI's tensor, $\boldsymbol{X}^A(K) = \boldsymbol{X}^M(K)$, if we integrate across the world lines determined by $\boldsymbol{S}^M$.

The radiation tensor exhibits very simple features with respect to the centre of mass. Since $\partial_\sigma(x_\mu S^S_{\nu\sigma} - x_\nu S^S_{\mu\sigma}) = 0$ it follows that the angular momentum quantities $M^S_{\mu\nu}$ constitute a tensor, and by calculating M^S_{i4} in K at $t = 0$ we readily find that

$$X^S_i(K) = -\frac{icM^S_{i4}}{\mathcal{H}^S} = X^M_i(K) \tag{7.14a}$$

$$\boldsymbol{a}^S(K) = \boldsymbol{a}^M(K). \tag{7.14b}$$

The equivalence we now have established between the three energy-momentum tensors with respect to the centre of mass is not accidental. It is connected with the fact that in (I, 12.12) we introduced the radiation tensor

as a *formal* remedy in order to extend certain volume integrals, taken over the internal, plane part of the field, into integrals taken over the *whole* field. In the case of the radiation tensor we could just take advantage of the tensor property of $M_{\mu\nu}^S$. It does not seem, however, that the equivalence could easily be foreseen.

The last point we shall dwell on in connection with the study of the centre of mass is a comment concerning a result obtained in a basic paper by C. Møller[43]. On the basis of some definite assumptions, Møller showed that the concept of mass centre for a non-closed system in general is incompatible with the equations of motion. This result seems to run into conflict with the result obtained in the present section, where we have defined the centre of mass even for the Abraham field. However, there is no real discrepancy between the results, since one of the assumptions inherent in Møller's proof does not apply to the present situation.

Let us point out in detail the mathematical reason for this circumstance. At an arbitrary point of the world line of the proper centre (with proper time τ) Møller assumes that the following relation can be written:

$$\frac{1}{c}\int S_{\mu\nu}d\sigma_\nu = M_0 \frac{d}{d\tau}X_\mu, \qquad (7.15)$$

where the integration is taken over a hyperplane σ which is normal to the world line. The surface pseudo four-vector $d\sigma_\nu$ is given by $d\sigma_\nu = -i\delta_{\nu\mu\sigma\varrho}dx_\mu \delta x_\sigma \varDelta x_\varrho$, $\delta_{1234} = 1$, where dx_μ, δx_σ and $\varDelta x_\varrho$ are four-vectors lying on σ. If σ is orthogonal to the x_4-axis, we choose the latter three vectors so that the non-vanishing component of $d\sigma_\nu$ is $d\sigma_4 = -idV$, when the outward normal lies in the direction of the positive x_4-axis. In (7.15) $M_0 = M_0(\tau)$ is a proportionality constant.

If we now insert Abraham's tensor into (7.15) in the frame K^* where the wave is at rest, we find for $\mu = 4$ the relation $\mathscr{H}^{A*} = M_0 c^2$, while for $\mu = i$ we find that M_0 becomes infinite. This discrepancy shows that an equation of the form (7.15) does not apply here. Hence Møller's proof does not come into conflict with the above results in this section. Nor does Minkowski's tensor satisfy the relation (7.15), while the radiation tensor does satisfy it.

The Čerenkov effect

As we already have noted, a study of the Čerenkov effect is very instructive for a comparison between the various energy-momentum tensors. In section 5 of the present paper we studied the Čerenkov effect in the case

that the emitting particle moves within a medium at rest, and in section 10
of I we considered the emitting particle in its own rest system from the point
of view of Minkowski's tensor. The reason why we shall here consider the
Čerenkov effect once more, it that we wish to point out how the relativistic
theory looks if Abraham's tensor is used for the field. This kind of analysis
is desirable, since I. Tamm in his famous paper[44] on the Čerenkov effect
studied the balance of momentum in the rest frame of the particle and came
to the conclusion that Minkowski's tensor, but not Abraham's tensor, is able
to give a satisfactory description. We shall thus discuss the momentum
balance in the Abraham case, since according to our general interpretation
Minkowski's and Abraham's tensors ought to be equivalent in such a case.

Consider then the same situation as in I: An electron is moving along
the x-axis with a uniform velocity which in K^0 is larger than c/n. The rest
frame of the particle is denoted by K; as shown by Tamm, $\boldsymbol{H} = 0$ in K, so
that there is no Minkowski energy current in this frame. We integrate the
differential conservation law for momentum over a volume which contains
the electron and which is enclosed by a cylindric surface S of small radius and
infinite length such that the axis of the cylinder coincides with the x-axis.
Since the field is stationary in K, one can thus write, in the case of Min-
kowski's tensor,

$$\int S_{ik}^M n_k \, dS = -\int f_i^M dV, \tag{7.16}$$

which is the same as (I, 10.3).

As Tamm points out, Minkowski's force must in any case represent the
force acting on the electric charge, because the terms which are added to
Minkowski's tensor in order to form Abraham's tensor will correspond to
additional forces acting on the *medium* itself, and not on the electric charge.
The total force on the electron as given by the right hand side of (7.16) can
thus be found by transforming the total force from K^0 using the usual
transformation formulas. Now Tamm evaluates the integral on the left hand
side of (7.16) and verifies that the two sides of the equation are equal.
Further, since $S_{ik}^M \neq S_{ki}^M$ for $i = 1$ and $k = 2, 3$, he concludes that a symme-
trical "Ansatz" for $S_{\mu\nu}$ would give a different result in disagreement with the
force expression on the right hand side of (7.16).

Let us now apply Abraham's tensor to the present case. It is instructive to
write the momentum balance in the form

$$\int S_{ik}^A n_k \, dS + \int (f_i^A - f_i^M) dV = -\int f_i^M dV, \tag{7.17}$$

and so it appears that the second integral on the left may represent a source (or sink) of electromagnetic momentum which also has to be taken into account. Since the force on the *matter* cannot make up an appreciable magnitude in a small volume element just enclosing the electron, we can exclude this element from the second integration in (7.17) and thus obtain

$$\int S^A_{ik} n_k \, dS + \int' f^A_i \, dV = - \int f^M_i \, dV, \qquad (7.18)$$

where $\int'$ means integration over the remaining part of the volume. However, also the second term on the left in (7.18) vanishes due to the rapid oscillation of the integrand, so that eqs. (7.18) and (7.16) become identical, i.e. $S^M_n = S^A_n$. In fact, the relation $S^M_{ik} = S^A_{ik}$, valid for all combinations of i, k that occur in (7,18), can be checked directly by expressing S^M_{ik} and S^A_{ik} in terms of the tensor components in K^0. Note that it is just the latter relation that represents the main reason why the (macroscopic) descriptions corresponding to Minkowski's and Abraham's tensors are identical in this case; properties of symmetry or asymmetry of the energy-momentum tensors are of no direct importance.

In the remainder of the present section we shall be concerned with a study of the so-called "principle of virtual power". Before embarking upon this subject, let us however pause to make the following brief remarks in connection with the topics considered in I: In sections 4 and 5 in I we gave two sets of conditions from which we showed that Minkowski's tensor is uniquely determined. It should be clear that both these sets of conditions automatically exclude from consideration the alternative tensor forms that we have been studying: The first set because eqs. (I, 4.1) and (I, 4.2) require the tensor to be asymmetric and divergence-free; the second set essentially because eq. (I, 5.1) requires the tensor not to contain the four-velocity V_μ explicitly (cf. (1.5), (1.7) and the fact that also $S^G_{\mu\nu}$ will contain V_μ in a complicated way).

In section 10 of I we discussed the negative field energy which appears with the use of Minkowski's tensor in a certain class of inertial systems due to the space-like character of the four-momentum G^M_μ. This property is peculiar to Minkowski's tensor and is not shared by the other tensor forms. We may check by direct calculation that $W^A > 0$ and $W^G > 0$ in any K, while the result $W^S > 0$ follows immediately from the fact that the four-momentum G^S_μ is time-like. If a plane wave moves parallel to the x-axis we may conveniently write the total energy density of matter and field as

$$W^{\text{tot}} = \gamma^2 (1 + 2n\beta + \beta^2) W^{A0} + \gamma^2 W^{\text{mech}\,0}, \tag{7.19}$$

where the contributions arising from $S_{\mu\nu}^{A0}$, $\boldsymbol{g}^{\text{mech}\,0}$ and $\boldsymbol{S}^{\text{mech}\,0}$ are collected in the first term.

Principle of virtual power

Quite recently, P. Penfield and H. A. Haus published a book [45] on the electrodynamics of moving media which is a synthesis of work they performed with various collaborators; especially the earlier article [46] by Chu, Haus and Penfield is of particular interest to us. The authors adopt a phenomenological point of view. In addition to employing the usual formulation (I, 1.1) of Maxwell's equations in a moving medium (the Minkowski formulation), which we also have employed throughout our work, they consider the so-called Chu formulation introduced in the book by Fano, Chu and Adler [39]. It is outside the scope of our work to go into a study of the Chu formulation. What really is of interest to us, is that the authors, within the frame of the Minkowski formulation, derive an expression for the electromagnetic energy-momentum tensor which is equal to Abraham's expression in an isotropic fluid, while Minkowski's tensor is claimed not to describe the electromagnetic system in a meaningful way. We find it therefore of interest to trace out the reason why the authors have arrived at this result. The keystone of the derivation presented is the "principle of virtual power", invented by the authors, so let us first sketch how the principle looks in the present case. An isotropic fluid is considered, where the fluid velocity $\boldsymbol{u}(\boldsymbol{r},t)$ may be a nonuniform function of the position at a certain time. We simplify the formalism (thereby ignoring the dependence of the field energy on the material density), and transform it to our notation.

Consider an arbitrary space-time point and denote by K^0 the inertial frame in which the velocity of a fluid element around this point momentarily is zero. Thus $\boldsymbol{u}^0 = 0$ for the element, but one assumes that virtual deformations can be applied to the material to produce arbitrary values of $\partial_k u_i^0$ and $\partial u_i^0/\partial t$.

Then let K denote the frame in which K^0 moves with a small velocity $\boldsymbol{u}$. To the first order in u/c we have

$$S_i = S_i^0 + u_k S_{ki}^0 + u_i W^0 \tag{7.20a}$$

$$W = W^0 + \boldsymbol{u} \cdot \boldsymbol{g}^0 + \frac{1}{c^2} \boldsymbol{u} \cdot \boldsymbol{S}^0, \tag{7.20b}$$

and these equations are introduced into the energy balance

$$\nabla \cdot \boldsymbol{S} + \partial W/\partial t = icf_4.$$ (7.21)

The authors then let K approach K^0 so that terms containing $\boldsymbol{u}$ (but not the derivatives of $\boldsymbol{u}$) vanish. The resulting equation is

$$\nabla \cdot \boldsymbol{S}^0 + \frac{1}{c^2} \boldsymbol{S}^0 \cdot \frac{\partial \boldsymbol{u}^0}{\partial t} + \frac{\partial W^0}{\partial t} + W^0 \nabla \cdot \boldsymbol{u}^0 - icf_4^0 = -S_{ik}^0 \partial_k u_i^0 - \boldsymbol{g}^0 \cdot \frac{\partial \boldsymbol{u}^0}{\partial t}$$ (7.22)

(note that the differential operators ∂_μ are not transformed). The essential point is now that a knowledge of the physical quantities appearing on the left hand side of (7.22), i.e. of $\boldsymbol{S}^0$, W^0 and f_4^0, is claimed to be sufficient to provide a determination of the remaining tensor components S_{ik}^0 and $\boldsymbol{g}^0$ appearing on the right hand side of (7.22). The following expressions are chosen:

$$\boldsymbol{S}^0 = c(\boldsymbol{E}^0 \times \boldsymbol{H}^0)$$ (7.23a)

$$\partial W^0/\partial t = \boldsymbol{E}^0 \cdot \partial \boldsymbol{D}^0/\partial t + \boldsymbol{H}^0 \cdot \partial \boldsymbol{B}^0/\partial t$$ (7.23b)

$$W^0 = \tfrac{1}{2}(\boldsymbol{E}^0 \cdot \boldsymbol{D}^0 + \boldsymbol{H}^0 \cdot \boldsymbol{B}^0), \quad f_4^0 = 0.$$ (7.23c)

The authors now argue that it is convenient to express the fields $\boldsymbol{E}^0$, $\boldsymbol{D}^0$, $\boldsymbol{H}^0$, $\boldsymbol{B}^0$ appearing in (7.23) in terms of the fields pertaining to the inertial frame K before inserting (7.23) into (7.22) (note again that K^0 means the frame where the fluid element momentarily is at rest). By inserting (7.23) into the expression on the left hand side of (7.22) they thus obtain

$$\left. \begin{array}{c} c\nabla \cdot (\boldsymbol{E} \times \boldsymbol{H}) + \boldsymbol{E} \cdot \dfrac{\partial \boldsymbol{D}}{\partial t} + \boldsymbol{H} \cdot \dfrac{\partial \boldsymbol{B}}{\partial t} \\[2mm] + [E_i D_k + H_i B_k - \tfrac{1}{2}\delta_{ik}(\boldsymbol{E} \cdot \boldsymbol{D} + \boldsymbol{H} \cdot \boldsymbol{B})]\partial_k u_i - \dfrac{1}{c}(\boldsymbol{E} \times \boldsymbol{H}) \cdot \dfrac{\partial \boldsymbol{u}}{\partial t}. \end{array} \right\}$$ (7.24)

The three first terms add up to zero because of MAXWELL's equations. By letting K approach K^0, identifying (7.24) with the right hand side of (7.22) and taking into account the arbitrariness of the derivatives of $\boldsymbol{u}^0$, the authors finally obtain

$$S_{ik}^0 = -E_i^0 D_k^0 - H_i^0 B_k^0 + \tfrac{1}{2}\delta_{ik}(\boldsymbol{E}^0 \cdot \boldsymbol{D}^0 + \boldsymbol{H}^0 \cdot \boldsymbol{B}^0)$$ (7.25a)

$$\boldsymbol{g}^0 = \frac{1}{c}(\boldsymbol{E}^0 \times \boldsymbol{H}^0).$$ (7.25b)

This is ABRAHAM's expression. (Actually, the expression given in ref. 46, containing the detailed derivation, was somewhat different from (7.25) but, according to a private communication by the authors, this difference is due to a printing error.)

If we now proceed to examine this principle of virtual power, we ought first to note that one must distinguish between the derivatives of the relative velocity v between the frames K^0 and K, and of the fluid velocity u. The formulas (7.20) relate the tensor components in the frame K to the tensor components in the momentary rest frame K^0 moving with the *constant* velocity v with respect to K; although $v = u$ at the space-time point considered the corresponding equality between the derivatives is generally not true. Thus each of the factors $\partial_\mu u^0$ in (7.22) should properly be replaced by $\partial_\mu v^0$, which is zero. In fact, by performing the transformation $K \to K^0$ the only result one can obtain is the covariant properties of the conservation equations $\partial_\nu S_{\mu\nu} = -f_\mu$. By starting from the relation (7.21), and assuming the velocity v to be small, one will thus end up with the same relation written in K^0. If we really subtract the equation $\nabla \cdot S^0 + \partial W^0/\partial t - ic f_4^0 = 0$ from eq. (7.22), we see that obvious inconsistencies will appear in the remaining equation if arbitrarily adjustable terms $\partial_\mu u^0$ are present.

However, the above remark does not elucidate the essential reason why a definite form of the electromagnetic energy-momentum tensor was obtained. To this end let us in the following simply *assume* the validity of eq. (7.22) as it stands. The essence of the principle of virtual power seems in reality to be that one starts from the energy balance (7.21) in K, then transforms the field quantities to K^0 and inserts some physical information in this frame, and finally transforms back to K. Within the frame of the physical information inserted in K^0 the formalism can therefore, if it is carried through consistently, yield only a mathematical *identity*. The reason why the authors instead obtained Abraham's expression in (7.25) is that they implicitly introduced into the formalism a physical assumption which is compatible with Abraham's tensor, but not with Minkowski's tensor. Let us go into some detail at this point. It is then necessary first to focus our attention on the force component f_4 in (7.21). In the conventional theory f_μ transforms like a four-vector, so that, in the limiting case of small u, $f_4 = f_4^0$. This equation was used by the authors in the construction of eq. (7.22). In particular, if $f_4^0 = 0$, as assumed in (7.23c), one should obtain $f_4 = 0$ also in K. However, if we use the covariant expression for $S_{\mu\nu}$ and calculate f_4 in K according to the basic equation $f_4 = -\partial_\nu S_{4\nu}$, we may obtain

a different result. For example, both in the Abraham case and the Minkowski case we know that $f_4^0 = 0$, while the covariant expressions (1.5) and (1.1) yield

$$f_4^A = 0, \qquad f_4^M = -i(n^2 - 1)(\boldsymbol{E} \times \boldsymbol{H}) \cdot \partial \boldsymbol{u}/\partial t \qquad (7.26)$$

to the lowest order. In the Minkowski case there is thus a conflict; it is incorrect to transform f_μ^M as if it were a four-vector.

Due to this peculiar transformation property of f_4 (which evidently is closely connected with the covariance problem of the conservation equations discussed above), it follows that f_4 should properly not have been replaced by f_4^0 in (7.22) but should rather have been retained unchanged. Accordingly, it follows that eq. (7.24) implies the relation $f_4 = 0$. This is a choice which, according to (7.26), implicitly singles out Abraham's tensor. The appearance of Abraham's expression in (7.25) is therefore what we should expect. It is also possible to make Minkowski's tensor emerge from the formalism; to this end we must insert the explicit expression for f_4^M, given by (7.26), into (7.22). Generally speaking, the introduction of a specific expression for f_4 implicitly implies the acceptance of a specific tensor, the remaining formalism thus effectively expressing an identity.

8. Analysis by Means of Curvilinear Coordinates

In connection with the study of the canonical procedure in section 8 of I we mentioned that it is possible, in the case of a *closed* field, to make the canonical energy-momentum tensor complete by means of a symmetrization procedure. Now it is well known that in the presence of a gravitational field one can obtain the complete energy-momentum tensor directly, without having to perform a symmetrization, by means of a variational method involving the variation of the metric tensor. Actually, and it is this case which is of interest to us, the variational method can be applied also in the absence of a gravitational field. Then the transition to curvilinear coordinates occurs formally as an intermediate step in the calculation.

Curvilinear coordinates have been used rather extensively in earlier studies of the electrodynamics of material media, although one here is confronted with a non-closed field. Incorrect use of the variational method caused a great deal of confusion in the literature some years ago. The

ambiguity inherent in the calculation seems first to have been pointed out by J. I. Horváth[47] (see also ref. 48). However, we think that it is still of interest to give a careful analysis of the electromagnetic field in terms of these coordinates, to point out the detailed reason why the power of the variational method is restricted, and to supplement with remarks pertaining to alternative variational methods. The main part of the present section is devoted to this task. In the last subsection we shall study again the Sagnac-type experiment from section 9 of I, in connection with an application of the various tensor forms. The cavity frame in this experiment is evidently non-inertial.

A variational method

Let us now leave out the imaginary x_4 coordinate and work with the real coordinates x^1, x^2, x^3, $x^0 = ct$. The square of the line element is $ds^2 = g_{\mu\nu}dx^\mu dx^\nu$ (μ, ν running over the numbers 1, 2, 3, 0), whence in Galilean coordinates

$$g_{11} = g_{22} = g_{33} = 1, \ g_{00} = -1$$
$$g = \det g_{\mu\nu} = -1, \ g_{\mu\nu} = 0 \ \text{for} \ \mu \neq \nu. \tag{8.1}$$

Further, in Galilean coordinates,

$$\boldsymbol{E} = (F_{10}, F_{20}, F_{30}), \ \boldsymbol{B} = (F_{23}, F_{31}, F_{12})$$
$$\boldsymbol{D} = (H_{10}, H_{20}, H_{30}), \ \boldsymbol{H} = (H_{23}, H_{31}, H_{12}), \tag{8.2}$$

and the connection between field and potentials is in general

$$F_{\mu\nu} = \nabla_\mu A_\nu - \nabla_\nu A_\mu = \partial_\mu A_\nu - \partial_\nu A_\mu, \tag{8.3}$$

as the covariant derivative ∇_μ can be replaced by the ordinary derivative when $F_{\mu\nu}$ is antisymmetric.

For a radiation field Maxwell's equations take the form

$$\nabla_\lambda F_{\mu\nu} + \nabla_\mu F_{\nu\lambda} + \nabla_\nu F_{\lambda\mu} = \partial_\lambda F_{\mu\nu} + \partial_\mu F_{\nu\lambda} + \partial_\nu F_{\lambda\mu} = 0 \tag{8.4a}$$

$$\nabla_\nu H^{\mu\nu} = \frac{1}{\sqrt{-g}}\partial_\nu(\sqrt{-g}\,H^{\mu\nu}) = 0. \tag{8.4b}$$

We have here assumed arbitrary coordinates where the $g_{\mu\nu}$ are given functions of the coordinates. Then proceed to determine the constitutive

relations. We shall keep the formalism so general that it includes the case of an anisotropic dielectric medium, but we shall assume magnetic isotropy with $\mu = 1$. (The procedure runs similarly, however, also if μ_{ik} is a tensor.) Introducing in the small region around each point a local rest system of inertia $\overset{\circ}{K}$ with the metric tensor given by (8.1), we may write

$$\overset{\circ}{H}_{i0} = \overset{\circ}{\varepsilon}{}_i^k \overset{\circ}{F}_{k0}. \tag{8.5}$$

Moreover, in $\overset{\circ}{K}$ we introduce the quantities

$$\overset{\circ}{\varepsilon}{}_0^\nu = \overset{\circ}{\varepsilon}{}_\nu^0 = 0 \; (\nu = 1, \, 2, \, 3, \, 0) \tag{8.6}$$

and let in the arbitrary coordinate system the symmetric tensor $\varepsilon^{\mu\nu}$ be defined in such a way that its mixed components in $\overset{\circ}{K}$ coincide with $\overset{\circ}{\varepsilon}{}_\nu^\mu$ given by (8.5) and (8.6). The constitutive relations written in covariant form are then

$$H^{\mu\nu} = F^{\mu\nu} + \frac{1}{c^2}(F^\mu - \varepsilon^{\mu\alpha}F_\alpha)V^\nu - \frac{1}{c^2}(F^\nu - \varepsilon^{\nu\alpha}F_\alpha)V^\mu, \tag{8.7}$$

where $F_\alpha = F_{\alpha\beta}V^\beta$, and V^β is the four-velocity of the medium. In isotropic media eq. (8.7) can be written

$$H^{\mu\nu} = F^{\mu\nu} - \varkappa(F^\mu V^\nu - F^\nu V^\mu), \; \varkappa = (\varepsilon - 1)/c^2. \tag{8.8}$$

This relation between (8.7) and (8.8) can readily be verified, since for an isotropic body in $\overset{\circ}{K}$

$$\overset{\circ}{\varepsilon}{}^{\mu\alpha} \overset{\circ}{F}_\alpha = \overset{\circ}{\varepsilon}{}_\alpha^\mu \overset{\circ}{F}{}^\alpha = \overset{\circ}{\varepsilon} \overset{\circ}{g}{}_\alpha^\mu \overset{\circ}{F}{}^\alpha = \overset{\circ}{\varepsilon} \overset{\circ}{F}{}^\mu. \tag{8.9}$$

Here g_α^μ is the metric tensor in GALILEAN form and $\overset{\circ}{\varepsilon}$ is the dielectric constant in $\overset{\circ}{K}$. Note that $\overset{\circ}{\varepsilon}{}_0^0 = 0$ according to (8.6) while $\overset{\circ}{g}{}_0^0 = 1$; however, this does not matter, since $\overset{\circ}{F}{}^0 = 0$. Writing (8.9) covariantly as $\varepsilon^{\mu\alpha}F_\alpha = \overset{\circ}{\varepsilon}F^\mu$, we obtain (8.8) from (8.7). Thus, while $\varepsilon^{\mu\alpha}$ in (8.7) is a tensor, the transformation (8.9) in the case of isotropic media causes the dielectric constant in (8.8) to be treated as a four-dimensional scalar.

It can be verified that an appropriate LAGRANGIAN is

$$\left. \begin{aligned} L &= -\tfrac{1}{4} F_{\mu\nu} H^{\mu\nu} \\ &= -\tfrac{1}{4} F_{\mu\nu} F^{\mu\nu} - \frac{1}{2c^2} F_\mu F^\mu + \frac{1}{2c^2} \varepsilon^{\mu\nu} F_\mu F_\nu = L_0 + L' + L''. \end{aligned} \right\} \tag{8.10}$$

Multiplying with the pseudo-invariant $\sqrt{-g}\,dx = \sqrt{-g}\,dx^1dx^2dx^3dx^0$ and integrating over a region Σ in four-space lying between two space-like surfaces and extending to infinity in the space directions, we get the action integral

$$J = \int_\Sigma L(x)\sqrt{-g}\,dx = \int_\Sigma \mathscr{L}(x)dx. \tag{8.11}$$

Since (8.10) corresponds to the field and its interaction with the matter, a variation of (8.11) with respect to the potentials will yield the field equations (8.4b). However, we are primarily interested in the invariance property of J under coordinate transformations.

Let an infinitesimal coordinate transformation be given by $x'^\mu = x^\mu + \delta x^\mu = x^\mu + \xi^\mu$, where the ξ^μ are small, but arbitrary functions of the coordinates, so that terms quadratic in ξ^μ may be neglected. The corresponding change of (8.11) is

$$\delta J = \int_{\Sigma'} \mathscr{L}'(x')dx' - \int_\Sigma \mathscr{L}(x)dx. \tag{8.12}$$

By transforming this expression and using the assumption that ξ^μ vanish on the boundary, we obtain[8]

$$\delta J = \int_\Sigma \delta^*\mathscr{L}(x)dx = 0, \tag{8.13}$$

where $\delta^*\mathscr{L}(x) = \mathscr{L}'(x) - \mathscr{L}(x)$ is the local variation. Eq. (8.13) has the form of a variational principle even though L does not correspond to a closed system; only it must be remembered that all variations are generated by the infinitesimal coordinate transformations.

We proceed then to calculate these variations. By a vector transformation we find

$$V'^\mu(x') = \partial_\nu x'^\mu V^\nu(x) = (\delta_\nu^\mu + \partial_\nu \xi^\mu)V^\nu(x), \tag{8.14}$$

whence

$$\delta^*V^\mu(x) = V^\nu(x)\partial_\nu\xi^\mu - \xi^\nu\partial_\nu V^\mu(x) = V^\nu\nabla_\nu\xi^\mu - \xi^\nu\nabla_\nu V^\mu. \tag{8.15}$$

Here we have for example $\nabla_\nu V^\mu = \partial_\nu V^\mu + \Gamma_{\nu\alpha}^\mu V^\alpha$, where $\Gamma_{\nu\alpha}^\mu$ is the CHRISTOFFEL symbol. It appears that δ^*V^μ is a four-vector, as should be the case, since this variation is the difference of the values of two four-vectors at the same point. Correspondingly for the potentials

$$\delta^*A_\mu(x) = -A_\nu\nabla_\mu\xi^\nu - \xi^\nu\nabla_\nu A_\mu. \tag{8.16}$$

The $g^{\mu\nu}$ will also be affected by the coordinate transformation, and we have

$$g'^{\mu\nu}(x') = g^{\alpha\beta}(x)\partial_\alpha x'^\nu \partial_\beta x'^\nu = g^{\mu\nu}(x) + g^{\mu\alpha}\partial_\alpha \xi^\nu + g^{\nu\alpha}\partial_\alpha \xi^\mu. \quad (8.17)$$

Thus

$$\delta^* g^{\mu\nu}(x) = g'^{\mu\nu}(x') - g^{\mu\nu}(x) - \xi^\alpha \partial_\alpha g^{\mu\nu}(x) = \nabla^\mu \xi^\nu + \nabla^\nu \xi^\mu. \quad (8.18)$$

Similarly

$$\delta^* \varepsilon^{\mu\nu} = \varepsilon^{\mu\alpha}\nabla_\alpha \xi^\nu + \varepsilon^{\nu\alpha}\nabla_\alpha \xi^\mu - \xi^\alpha \nabla_\alpha \varepsilon^{\mu\nu}. \quad (8.19)$$

The part J_0 of the action integral corresponding to L_0 in (8.10) is to be varied with respect to A_μ and $g^{\mu\nu}$. This term is present also in the case of an electromagnetic field in vacuum. One obtains after some calculation (for details, see FOCK[49], §§ 47, 48)

$$\left.\begin{aligned}
\delta J_0 = -\tfrac{1}{2}\int (F_{\mu\alpha}F_\nu^{\cdot\alpha} - \tfrac{1}{4}g_{\mu\nu}F_{\alpha\beta}F^{\alpha\beta})\delta^* g^{\mu\nu}\sqrt{-g}\,dx \\
-\int \nabla_\nu F^{\mu\nu}\delta^* A_\mu \sqrt{-g}\,dx.
\end{aligned}\right\} \quad (8.20)$$

Here use has been made of the relations $\delta^*\sqrt{-g} = -\tfrac{1}{2}\sqrt{-g}\,g_{\mu\nu}\delta^* g^{\mu\nu}$, $g^{\mu\nu}\delta^* g_{\mu\nu} = -g_{\mu\nu}\delta^* g^{\mu\nu}$. By virtue of (8.18) the first term in (8.20) can be transformed, so that

$$\delta J_0 = \int \nabla_\nu (F_{\mu\alpha}F^{\nu\alpha} - \tfrac{1}{4}g_\mu^\nu F_{\alpha\beta}F^{\alpha\beta})\xi^\mu \sqrt{-g}\,dx - \int \nabla_\nu F^{\mu\nu}\delta^* A_\mu \sqrt{-g}\,dx. \quad (8.21)$$

We shall now give the detailed calculation for the action term J' corresponding to L' in (8.10). Variations are here to be taken with respect to A^μ, $g^{\mu\nu}$ and V^μ. Let us first calculate the contribution from the potentials and write

$$\delta_A J' = -\frac{1}{c^2}\int F^\mu V^\alpha \delta^* F_{\mu\alpha}\sqrt{-g}\,dx = -\frac{1}{c^2}\int F^\mu V^\alpha(\partial_\mu \delta^* A_\alpha - \partial_\alpha \delta^* A_\mu)\sqrt{-g}\,dx,$$

since ∂_μ and δ^* commute. By partial integrations then

$$\delta_A J' = -\frac{1}{c^2}\int \nabla_\nu (F^\mu V^\nu - F^\nu V^\mu)\delta^* A_\mu \sqrt{-g}\,dx, \quad (8.22)$$

where we have exploited the antisymmetry property of the expression in the parenthesis.

The variation with respect to the metric tensor is handled in the same way, and we get by means of (8.18)

$$\delta_g J' \; = \; -\frac{1}{2c^2}\int F_\mu F_\nu (\sqrt{-g}\,\delta^* g^{\mu\nu} - \tfrac{1}{2}\sqrt{-g}\,g^{\mu\nu} g_{\alpha\beta}\delta^* g^{\alpha\beta})\,dx$$

$$= \; -\frac{1}{c^2}\int (F_\mu F - \tfrac{1}{2}g^\alpha_\mu F_\beta F^\beta)\nabla_\alpha \xi^\mu \sqrt{-g}\,dx \qquad\qquad (8.23)$$

$$= \; -\frac{1}{c^2}\int \{\nabla_\alpha[(F_\mu F^\alpha - \tfrac{1}{2}g^\alpha_\mu F_\beta F^\beta)\xi^\mu]$$

$$-\nabla_\alpha(F_\mu F^\alpha - \tfrac{1}{2}g^\alpha_\mu F_\beta F^\beta)\xi^\mu\}\sqrt{-g}\,dx.$$

Since the first term in this expression involves the covariant derivative of the product of a scalar and a four-vector, we can write this term as

$$-\frac{1}{c^2}\int \partial_\alpha[\sqrt{-g}\,(F_\mu F^\alpha - \tfrac{1}{2}g^\alpha_\mu F_\beta F^\beta)\xi^\mu]\,dx \qquad\qquad (8.24)$$

and transform into an integral over the boundary. Therefore this term vanishes. It remains

$$\delta_g J' \; = \; \frac{1}{c^2}\int \nabla_\nu(F_\mu F^\nu - \tfrac{1}{2}g^\nu_\mu F_\alpha F^\alpha)\xi^\mu \sqrt{-g}\,dx. \qquad\qquad (8.25)$$

Finally we consider the variations connected with the velocity. By means of (8.15) we have

$$\delta_V J' \; = \; -\frac{1}{c^2}\int F_{\alpha\mu} F^\alpha (V^\nu \nabla_\nu \xi^\mu - \xi^\nu \nabla_\nu V^\mu)\sqrt{-g}\,dx. \qquad\qquad (8.26)$$

Performing a partial integration we obtain, apart from an integral similar to (8.24)

$$\delta_V J' \; = \; -\frac{1}{c^2}\int [\nabla_\nu(F_{\mu\alpha}F^\alpha V^\nu) + F_{\nu\alpha}F^\alpha \nabla_\mu V^\nu]\xi^\mu \sqrt{-g}\,dx. \qquad\qquad (8.27)$$

Similarly we can evaluate the contributions from the term L'' in (8.10). We give the results:

$$\delta_A J'' \; = \; \frac{1}{c^2}\int \nabla_\nu[(\varepsilon^{\mu\alpha}V^\nu - \varepsilon^{\nu\alpha}V^\mu)F_\alpha]\delta^* A_\mu \sqrt{-g}\,dx \qquad (8.28a)$$

$$\delta_g J'' \; = \; \frac{1}{2c^2}\int \nabla_\mu(\varepsilon^{\alpha\beta}F_\alpha F_\beta)\xi^\mu \sqrt{-g}\,dx \qquad (8.28b)$$

$$\delta_V J'' \; = \; -\frac{1}{c^2}\int [\nabla_\nu(\varepsilon^{\alpha\beta}F_{\alpha\mu}F_\beta V^\nu) + \varepsilon^{\alpha\beta}F_{\alpha\nu}F_\beta \nabla_\mu V^\nu]\xi^\mu \sqrt{-g}\,dx \qquad (8.28c)$$

$$\delta_\varepsilon J'' = -\frac{1}{2c^2} \int [2\nabla_\nu (\varepsilon^{\nu\alpha} F_\mu F_\alpha) + F_\nu F_\alpha \nabla_\mu \varepsilon^{\nu\alpha}] \xi^\mu \sqrt{-g} \, dx. \qquad (8.28\mathrm{d})$$

In the last equation we have made use of (8.19).

Now we are able to write down the total variation δJ, where $\delta = \delta_A + \delta_g + \delta_V + \delta_\varepsilon$. We obtain

$$\left. \begin{aligned} 0 = \delta J = \delta J_0 + \delta J' + \delta J'' &= -\int \nabla_\nu \left[F^{\mu\nu} + \frac{1}{c^2}(F^\mu - \varepsilon^{\mu\alpha} F_\alpha) V^\nu \right. \\ \left. -\frac{1}{c^2}(F^\nu - \varepsilon^{\nu\alpha} F_\alpha) V^\mu \right] \delta^* A_\mu \sqrt{-g} \, dx &+ \int \left[\nabla_\nu (F_{\mu\alpha} H^{\nu\alpha} - \tfrac{1}{4} g_\mu^\nu F_{\alpha\beta} H^{\alpha\beta}) \right. \\ \left. -\frac{1}{c^2} F_{\nu\alpha}(F^\alpha - \varepsilon^{\alpha\beta} F_\beta)\nabla_\mu V^\nu - \frac{1}{2c^2} F_\nu F_\alpha \nabla_\mu \varepsilon^{\nu\alpha} \right] \xi^\mu \sqrt{-g} \, dx. \end{aligned} \right\} \quad (8.29)$$

In this relation $\delta^* A_\mu$ and ξ^μ are not independent, but related through (8.16). However, we do not have to express $\delta^* A_\mu$ by ξ^μ in (8.29) since we know that L is the LAGRANGIAN for the field in interaction with the medium. Therefore the coefficient of $\delta^* A_\mu$ must be equal to zero, as we also see by virtue of (8.7) and (8.4b).

Now the ξ^μ are arbitrary at each point. This means that during the displacement period the dielectric in general will not move as a rigid body, but the bulk density will vary throughout the body. However, even under this deformation process the LAGRANGIAN (8.10) is permitted, since MAXWELL's equations are assumed to be valid within the body also when it becomes inhomogeneous, with the small velocity changes that appear because of the deformations. So MAXWELL's equations do not restrict the variations ξ^μ, and we obtain from (8.29)

$$\nabla_\nu \overset{M}{S}{}_\mu^{\cdot\nu} = \frac{1}{c^2} F_{\nu\alpha}(F^\alpha - \varepsilon^{\alpha\beta} F_\beta)\nabla_\mu V^\nu + \frac{1}{2c^2} F_\nu F_\alpha \nabla_\mu \varepsilon^{\nu\alpha}, \qquad (8.30)$$

where

$$\overset{M}{S}{}_\mu^{\cdot\nu} = F_{\mu\alpha} H^{\nu\alpha} - \tfrac{1}{4} g_\mu^\nu F_{\alpha\beta} H^{\alpha\beta}$$

is MINKOWSKI's tensor. We now introduce GALILEAN coordinates and use that $\partial_\mu V^\nu = 0$ for the undisturbed body, whence

$$\partial_\nu \overset{M}{S}{}_\mu^{\cdot\nu} = \frac{1}{2c^2} F_\nu F_\alpha \partial_\mu \varepsilon^{\nu\alpha}. \qquad (8.31)$$

We should like to mention the possibility of requiring the body to move as a rigid body under the deformation period in some coordinate system. Then the variations of one world line can be chosen arbitrarily, but the variations on the surface t = constant will now be determined by the metric tensor. Because of the relativity of simultaneity however, deformations will in general occur in another coordinate system. Besides, this type of variation does not lead to the strong result (8.30). To see this, let us confine ourselves to GALILEAN coordinates, in which the restriction reads ξ^μ = constant on an arbitrary hypersurface t = constant in some inertial system. If we let χ_μ mean the difference between the left and the right sides of (8.31), we can write (8.29) as

$$0 = \int \chi_\mu \xi^\mu \, dx = \int dx^0 \xi^\mu \int d^3x \chi_\mu, \qquad (8.32)$$

from which we can only conclude that the volume integral $\int d^3x \chi_\mu = 0$.

Let us now return to the main result (8.31) emerging from the formalism. It should be clear that this result is only a certain combination of MAXWELL's equations. We could equivalently write eq. (8.31) in terms of ABRAHAM's tensor, or any other expression. Apart from the statement of the LAGRANGIAN (8.10), the subsequent calculation is of merely mathematical nature.

The present behaviour arises from the fact that the LAGRANGIAN (8.10) does not describe the total physical system. If the LAGRANGIAN had been complete, then we could further have reduced the expression for the variation of the action integral in view of the mechanical equations of motion, and would have been left with the total energy-momentum tensor as a result of the remaining variations. In some earlier treatments the electromagnetic energy-momentum tensor was claimed to be determined simply by the variation of the action integral with respect to the metric tensor. As mentioned above, HORVÁTH[47, 48] has emphasized the ambiguity of such a procedure. Further, H. G. SCHÖPF[50] has objected against certain calculational inconsistencies in the earlier attempts. The works of HORVÁTH and SCHÖPF contain references to the preceding literature.

In the treatment up till now we have generated all variations from *coordinate transformations*, since this seems to be the simplest kind of approach. However, one will commonly find another method used in order to calculate the variation of the velocity [3, 50, 51]. Namely to preserve the relation

$$V_\mu V^\mu = -c^2 \qquad (8.33)$$

also after the variation, one introduces LAGRANGE variables a^λ ($\lambda = 1, 2, 3, 0$) to describe the medium, where $a^0 = p$ is an arbitrary invariant parameter of the nature of a time. Then, writing

$$V^\mu = \frac{c\partial x^\mu/\partial p}{\sqrt{-g_{\alpha\beta}\,\partial x^\alpha/\partial p\,\partial x^\beta/\partial p}}, \qquad (8.34)$$

the relation (8.33) is identically satisfied. But when evaluating the variation of V^μ given by (8.34), the change in the $g_{\alpha\beta}$ must also be taken into account. In this way the ξ^μ are considered as arbitrary. However, we see that this procedure is necessary only if the LAGRANGIAN obeys an *action principle* with respect to the x^μ. In the case of an electromagnetic field in vacuum interacting with incoherent matter, as treated by FOCK[49] for example, the given LAGRANGIAN corresponds to the total system and must therefore yield the equations of motion of matter when the arbitrary ξ^μ-variations are taken in a *fixed* system of reference. Therefore one must take the restriction given by (8.33) into account, for instance by the parametrical representation (8.34). Another method has been given by L. INFELD[52, 53]; the method consists in introducing a LAGRANGIAN multiplier λ to take care of the degree of freedom being lost by (8.33).

In our case, the LAGRANGIAN L given by (8.10) obeys an action principle only with respect to the potentials; the ξ^μ-variations are consequences of coordinate transformations which preserve the condition (8.33) automatically. Therefore no attention was paid to the restriction (8.33) in the calculation above. But it is not incorrect to use the representation (8.34). We then obtain instead of (8.15) the velocity variation

$$\delta'^* V^\mu = V^\nu \nabla_\nu \xi^\mu - \xi^\nu \nabla_\nu V^\mu + \frac{1}{c^2} V^\mu V_\sigma V^\nu \nabla_\nu \xi^\sigma, \qquad (8.35)$$

when the change in the $g_{\alpha\beta}$ is taken into account. However when evaluating the δ_g^*-variations, we vary also the $g_{\alpha\beta}$ in (8.34), so that

$$\delta_g^* V^\mu = -\frac{1}{2c^2} V^\mu V_\sigma V_\nu \delta^* g^{\nu\sigma} = -\frac{1}{c^2} V^\mu V_\sigma V^\nu \nabla_\nu \xi^\sigma, \qquad (8.36)$$

where (8.18) has been inserted. We see that in the total velocity variation $(\delta'^* + \delta_g^*)V^\mu$ the expression (8.36) compensates the last term in (8.35), so that we end up with a certain combination of MAXWELL's equations, as before.

Similarly, by using INFELD's method, the multiplier λ drops out of the calculation.

We mention that in the case of isotropic media (fluids) some attempts[54, 50] have been made to complete the LAGRANGIAN so as to make the system closed. In such a case the LAGRANGIAN has to obey a variational principle also with respect to coordinate variations, so that one may use the representation (8.34). In this way the total energy-momentum tensor has been found to be given by ABRAHAM's tensor plus the hydrodynamical tensor.

The consistency of such a procedure may be illustrated by the following consideration. We first tentatively write the LAGRANGIAN density for the total system as

$$L^{\text{tot}} = -\tfrac{1}{4} F_{\mu\nu} F^{\mu\nu} + \frac{\varkappa}{2} F_\mu F^\mu - \mathring{\varrho}_m c^2, \tag{8.37}$$

where $\varkappa = (n^2 - 1)/c^2$, $F_\mu = F_{\mu\nu} V^\nu$, and $\mathring{\varrho}_m$ is the invariant rest mass density of the fluid. If we now perform coordinate variations (for fixed metric) and evaluate the contribution to the action integral which arises from the second term to the right in (8.37), we find the expression $\int f_\mu^A \xi^\mu \sqrt{-g} \, dx$ due to the velocity variations (8.35). Here f_μ^A means ABRAHAM's force density written in general coordinates. Therefore the coordinate variations, which effect only the two last terms in (8.37), lead to the hydrodynamical equations of motion with ABRAHAM's force as the external force. This result is compatible with the interpretation we found in section 3, and this is the crucial point, since it permits the adoption of (8.37) as the correct LAGRANGIAN density for the total system. If we then perform an infinitesimal coordinate transformation so that the action integral remains invariant, we see that the coefficients in front of $\delta^* A_\mu$ and ξ^μ vanish in view of the field equations and the equations of motion, so that we are left with a divergence-free total energy-momentum tensor in front of $\delta^* g^{\mu\nu}$ which is equal to the sum of ABRAHAM's tensor and the hydrodynamical tensor.

Note that the present direct connection between the variation of the metric tensor and the energy-momentum tensor, and between the remaining variations and the equations of motion, is lost if we employ our first method and generate all variations from coordinate transformations. Thus, if we use the LAGRANGIAN (8.10), a variation of the action integral (8.11) with respect to the metric tensor leads to ABRAHAM's tensor only if both (8.18) and (8.36) are taken into account. However, in order to analyse how the conservation equations emerge from the formalism when (8.10) is used, our first method is simpler.

Final remarks on the Sagnac-type experiment

The last task that we shall take up in our work is to give an extended analysis of the recent Sagnac-type experiment due to HEER, LITTLE and BUPP[55] which we considered in sect. 9 of I in connection with MINKOWSKI's tensor. We shall examine how this experiment is explained by the other tensors.

Let us briefly recall the essential features of the experiment. The apparatus is a triangular ring laser giving rise to two travelling electro-magnetic waves in the cavity, one circulating clockwise and the other counterclockwise. A dielectric medium is placed in the light path. When the system is at rest the photon frequencies in the two wave modes are equal. If the cavity is set into rotation with an angular velocity Ω, the photon frequencies of the two beams become different from each other and the beams interfere to produce beats which are counted. With MINKOWSKI's tensor the energy density W^M for one of the modes in the noninertial cavity frame is related to the energy density W^0 for this mode in an instantaneous inertial rest frame by

$$W^M = W^0 + \frac{1}{c}\Omega \cdot [\boldsymbol{r} \times (\boldsymbol{E} \times \boldsymbol{H})], \tag{8.38}$$

where the fields refer to the mode considered, and are evaluated for $\Omega = 0$ since only effects to the first order in Ω are investigated. Further, within this approximation the total field energy in the cavity frame is a conserved quantity, so that we obtain the formula (I, 9.6) for the relative frequency shift

$$\left(\frac{\Delta\nu}{\nu}\right)^M = \frac{4}{c}\frac{\Omega \cdot \int \boldsymbol{r} \times (\boldsymbol{E} \times \boldsymbol{H}) \, dV}{\int (\boldsymbol{E} \cdot \boldsymbol{D} + \boldsymbol{H} \cdot \boldsymbol{B}) \, dV}. \tag{8.39}$$

In the plane wave approximation the agreement between (8.39) and the observed data is excellent, and the authors conclude that their experiment supports the asymmetric MINKOWSKI's tensor.

As we shall see now, the above conclusion should be somewhat modified: The experiment represents a nice verification of the predictions of pheno-menological electrodynamics, but it is not a *critical* test of the convenience of MINKOWSKI's tensor as compared to all other tensor forms. In fact, both ABRAHAM's tensor and the radiation tensor give an equivalent description of the experiment. For we have in any case, to the first order in Ω, the following formula for the energy density in the cavity frame:

$$W = W^0 + \frac{g_{4k}}{g_{44}} \overset{\circ}{S}{}_4^{\cdot\,k}, \tag{8.40}$$

where $g_{\mu\nu}$ is the metric tensor in the cavity frame and the superscript zero refers to the instantaneous rest inertial frame. Since the tensor components $\overset{\circ}{S}{}_4^{\cdot\,\nu}$ are equal for MINKOWSKI's and ABRAHAM's tensors and also for the radiation tensor, we must obtain the same value for W. Therefore, in any of these cases, we can put the conserved total field energy of each mode proportional to the corresponding photon frequency, and obtain again the fundamental formula (8.39).

Note that the equivalence of the above three tensors with respect to the energy balance in the cavity frame holds for all participating terms. The energy balance reads in general

$$\nabla_\nu S_4^{\cdot\,\nu} = \frac{1}{\sqrt{-g}} \frac{\partial}{\partial x^\nu}(\sqrt{-g}\,S_4^{\cdot\,\nu}) - \Gamma_{\varrho,\,4\nu} S^{\varrho\nu} = -f_4, \tag{8.41}$$

but it can be verified that the term involving the CHRISTOFFEL symbol yields no contribution to the first order in Ω. Moreover, by performing a coordinate transformation between the inertial frame and the cavity frame we find that $f_4 = 0$, even in the ABRAHAM case, and that the components $S_4^{\cdot\,k}$ take on common values. In all the three cases considered we can thus write the energy balance as $\partial_\nu S_4^{\cdot\,\nu} = 0$, with common values for the tensor components.

Finally we note that with the DE GROOT-SUTTORP tensor (1.9), complications arise because the expression for W^0 is changed. In this case the force component f_4 is different from zero, yet the total field energy is a conserved quantity in the cavity frame since f_4 fluctuates away when integrated over the volume. However, we do not now obtain the expression (8.39) for the relative frequency shift; in fact, if we put the total energy proportional to the photon frequency for each mode we find the formula $(\Delta v/v)^G = (\mathscr{H}^{M0}/\mathscr{H}^{G0})(\Delta v/v)^M$, in disagreement with experiment. This tensor seems in general not to be suitable for the description of propagating waves, since in an inertial rest frame the magnitude of the quantity $\mathbf{S}^{G0}/W^{G0}$ is different from c/n.

Acknowledgements

Appendix

The table below gives a summary of the behaviour of the various energy-momentum tensors in those examined physical situations which are of experimental interest. References are given to those sections of Part I or Part II where the actual subject has been investigated. Cf. also the summaries in the introductory sections of I and II.

Situation considered	a) Minkowski	b) Abraham	c) Radiation tensor (Marx et al; Beck)	d) Einstein – Laub	e) de Groot-Suttorp (first version)
Dielectric isotropic or anisotropic body surrounded by a vacuum or isotropic liquid and acted upon by an electrostatic field: Measurement of force or torque.	Within an anisotropic body the tensor *asymmetry* is of main importance for the torque. I, sect. 3; II, sect. 2. No experimental distinction possible. II, sect. 2.	Torque always described in terms of the *force*. II, sect. 2.	Not defined in this case.	Same experimental result as in the cases a) and b). II, sect. 2.	
Excess pressure produced in a dielectric liquid by an electrostatic field: Hakim-Higham experiment.	In this case the electrostrictive terms must be taken into account. Thereby one obtains a tensor which yields Helmholtz' force, and which is in agreement with the second tensor form put forward by de Groot and Suttorp. Good agreement with experiment. II, sect. 2.		Not defined in this case.	Force density equal to Kelvin's force. Disagreement with experiment. II, sect. 2.	
Radiation pressure exerted by an electromagnetic wave travelling through a dielectric liquid: Jones-Richards experiment.	Good agreement with experiment. Simple interpretation. I, sect. 6; II, sect. 3.	Equivalent to case a), when the appropriate interpretation is imposed. II, sect. 3.	Disagreement with experiment. II, sect. 3.	Inconvenient.	
Dielectric isotropic or anisotropic body surrounded by a *vacuum* and acted upon by a high-frequency field: Measurement of force or torque (Barlow experiment, Beth experiment, etc.).	No experimental distinction possible. II, sect. 4.		Defined for isotropic media only. Same experimental result as in the cases a) and b), although the direction and magnitude of the surface force in general are different. II, sect. 4.	Same experimental result as in the cases a)-c).	
Dielectric isotropic or anisotropic body surrounded by a liquid and acted upon by a high-frequency field: Measurement of force or torque (experiment not performed).	No experimental distinction possible. II, sect. 4.		Experiment of the Barlow type should represent a critical test. II, sect. 4.	Experiment of the Barlow type should also here be critical. The torque formula is different from the formulas corresponding to the cases a)-c). II, sect. 4.	

Situation considered	a) Minkowski	b) Abraham	c) Radiation tensor (Marx et al; Beck)	d) Einstein-Laub	e) de Groot-Suttorp (first version)
Low-frequency variation of electric and magnetic fields: Measurement of oscillations of a suspended dielectric shell (experiment not performed).	Does not predict oscillations. The equivalence between the tensors does not apply to this case. An experimental distinction should be possible. II, sect. 4.	Predicts oscillations.	Same behaviour as in the case b). II, sect. 4.		
Čerenkov effect.	Good agreement with the experiments. Simple interpretation. I, sect. 10; II, sect. 5 and 7.	Equivalent to case a), when the appropriate interpretation is imposed. II, sect. 5 and 7.	Leads to unphysical value for the Čerenkov angle. II, sect. 5.	Inconvenient.	
Velocity of the energy of an optical wave in a uniformly moving body: Fizeau type experiments.	Good agreement with the experiments. The von Laue-Møller transformation criterion is fulfilled. I, sect. 9; II. sect. 7.	Equivalent to case a), when the appropriate interpretation is imposed, II, sect. 7.	Same behaviour as in the case a).	Inconvenient.	
Sagnac-type experiment performed by Heer, Little, Bupp.	Good agreement with experiment. I, sect. 9; II, sect. 8.			Inconvenient. II, sect. 8.	

References

1. I. BREVIK, Mat. Fys. Medd. Dan. Vid. Selsk. **37**, no. 11 (1970).
2. H. HERTZ, Ges. Werke II, 280.
3. G. MARX and G. GYÖRGYI, Ann. Physik **16**, 241 (1955).
4. F. BECK, Z. Physik **134**, 136 (1953).
5. A. EINSTEIN and J. LAUB, Ann. Physik **26**, 541 (1908).
6. S. R. DE GROOT and L. G. SUTTORP, Physica **39**, 28, 41, 61, 77, 84 (1968); *ibid.* **37**, 284, 297 (1967).
7. C. MØLLER, *The Theory of Relativity* (Oxford, 1952).
8. W. PAULI, *Theory of Relativity* (Pergamon Press, 1958).
9. G. MARX, Nuovo Cim. Suppl. **1**, 265 (1955).
10. WOLFGANG K. H. PANOFSKY and MELBA PHILLIPS, *Classical Electricity and Magnetism* (Addison-Wesley Publ. Comp., Inc., 1956), section 6–7.
11. S. S. HAKIM, Proc. IEE **109**, Part C, 158 (1962).
12. S. S. HAKIM and J. B. HIGHAM, Proc. Phys. Soc. **80**, 190 (1962).
13. P. MAZUR and S. R. DE GROOT, Physica **22**, 657 (1956).
14. ALLAN N. KAUFMAN, Phys. of Fluids **8**, 935 (1965).
15. R. V. JONES and J. C. S. RICHARDS, Proc. Roy. Soc. **221 A**, 480 (1954).
16. C. L. TANG and J. MEIXNER, Phys. Fluids **4**, 148 (1961).
17. S. R. DE GROOT and P. MAZUR, *Non-Equilibrium Thermodynamics* (North-Holland Publ. Comp., 1962), Ch. XIV.
18. N. L. BALAZS, Phys. Rev. **91**, 408 (1953).
19. E. G. CULLWICK, Proc. IEE **113**, 369 (1966).
20. P. PENFIELD, Proc. IEE **113**, 1875 (1966).
21. E. G. CULLWICK, Proc. IEE **113**, 1876 (1966).
22. GUY BARLOW, Proc. Roy. Soc. **87 A**, 1 (1912).
23. R. A. BETH, Phys. Rev. **50**, 115 (1936).
24. N. CARRARA, Nature **164**, 882 (1949).
25. A. RUBINOWICZ, Acta Phys. Polon. **14**, 209, 225 (1955).
26. O. COSTA DE BEAUREGARD, Nuovo Cim. **48 B**, 293 (1967).
27. C. GOILLOT, Phys. Letters **21**, 408 (1966).
28. O. COSTA DE BEAUREGARD, Phys. Letters **21**, 410 (1966).
29. J. M. JAUCH and K. M. WATSON, Phys. Rev. **74**, 950 (1948).
30. I. BREVIK and B. LAUTRUP, to be published in Mat. Fys. Medd. Dan. Vid. Selsk. (1970).
31. G. GYÖRGYI, Am. J. Phys. **28**, 85 (1960).
32. J. AGUDÍN, Phys. Letters **24 A**, 761 (1967).
33. R. GANS, Phys. Z. **12**, 806 (1911).
34. B. DE SA, The energy-momentum tensor in relativistic thermodynamics. Thesis, Aachen (1960).

35. G. A. KLUITENBERG and S. R. DE GROOT, Physica **21**, 148, 169 (1955).
36. G. MARX and G. GYÖRGYI, Acta Phys. Hung. **3**, 213 (1954).
37. G. MARX, Acta Phys. Hung. **2**, 67 (1952).
38. G. MARX and K. NAGY, Acta Phys. Hung. **4**, 297 (1955).
39. R. M. FANO, L. J. CHU and R. B. ADLER, *Electromagnetic Fields, Energy, and Forces* (John Wiley & Sons, Inc., 1960).
40. PAUL POINCELOT, C. R. Acad. Sc. Paris, **264 B**, 1064, 1179, 1225, 1560 (1967).
41. M. VON LAUE, *Die Relativitätstheorie*, bd. I (Fr. Vieweg, Braunschweig, 1961).
42. R. BECKER, *Theorie der Elektrizität*, bd. I (B. G. Teubner, Stuttgart, 1969).
43. C. MØLLER, Ann. Inst. Henri Poincaré **11**, 251 (1949).
44. I. TAMM, Journ. of Phys. USSR **1**, 439 (1939).
45. PAUL PENFIELD, jr., and HERMANN A. HAUS, *Electrodynamics of Moving Media* (Research monograph No 40, The M.I.T. Press, Cambridge, Mass.).
46. L. J. CHU, H. A. HAUS and P. PENFIELD, jr., Proc. IEEE **54**, 920 (1966).
47. J. I. HORVÁTH, Bull. l'Acad. Polon. (Cl.3) **4**, 447 (1956).
48. J. I. HORVÁTH, Nuovo Cim. **7**, 628 (1958).
49. V. FOCK, *The Theory of Space, Time and Gravitation* (Pergamon Press, second edition, 1964).
50. HANS-GEORG SCHÖPF, Ann. Physik **9**, 301 (1962).
51. HANS-GEORG SCHÖPF, Ann. Physik **13**, 41 (1964).
52. L. INFELD, Bull. l'Acad. Polon. (Cl.3) **5**, 491 (1957).
53. A. O. BARUT, *Electrodynamics and Classical Theory of Fields and Particles* (McMillan Comp., N.Y., 1964).
54. G. MARX, Bull l'Acad. Polon. (Cl.3) **4**, 29 (1956).
55. C. V. HEER, J. A. LITTLE and J. R. BUPP, Ann. Inst. Henri Poincaré **8 A**, 311 (1968).

K. B. WINTERBON, PETER SIGMUND
AND J. B. SANDERS

SPATIAL DISTRIBUTION OF ENERGY
DEPOSITED BY ATOMIC PARTICLES
IN ELASTIC COLLISIONS

Synopsis

Energetic atomic particles slowing down in a solid or a gas create cascades of atomic collisions. This paper deals with the spatial distribution of the energy dissipated within the cascades, at the end of the slowing-down process. This distribution is of central interest in the theory of radiation damage and sputtering. An integro-differential equation determining the distribution function is derived under the assumption of random slowing down in an infinite medium. A set of equations is derived determining spatial moments over the distribution functions, and the moment equations are solved explicitly under the assumption of elastic scattering with power-law cross sections. The theory applies to heavy ions or recoil atoms in the keV range (for lighter ions only in the lower keV range), slowing down in a (monatomic or polyatomic) target under conditions where crystal lattice effects may be neglected. Moments over the distribution are tabulated for a wide range of mass ratios and several exponents in the Lindhard power cross section, and are compared to corresponding moments over the distribution of ion ranges. Several methods of constructing distributions from spatial moments are discussed, and some typical energy and range distributions are presented, both in one dimension (depth distribution) and three dimensions. A brief discussion of the experimental situation concludes the paper.

TABLE OF CONTENTS

1. Introduction

This is the first of a series of papers dealing with the spatial extension of radiation damage induced by energetic atomic particles bombarding a random target. The term radiation damage is used in a rather general sense to comprise a number of changes in physical properties that may be considered stable on a time scale determined by the slowing down of the primary particle, such as lattice defects, disordering, ionization, dissociation, etc. The bombarding particles may come from an external source such as ions from an accelerator, or from internal sources such as recoil atoms from radioactive decays or collisions caused by fast neutrons in a reactor. The targets may be gases, liquids, amorphous solids and, with some restrictions, crystalline solids.

Since radiation damage is a consequence of the deposition of the energy of the bombarding particle in the target, the spatial distribution of deposited energy is of primary interest for all damage effects that are proportional to the amount of energy deposited, and for emission phenomena like sputtering and secondary electron emission.

In general the energy of the primary particle will be shared between atoms and electrons of the target. It is necessary to separate these two contributions since the slowing-down behaviour of electrons and atoms is different. A further separation may have to be made when the target consists of more than one kind of atom.

In this first paper we deal with the comparatively simple case of a heavy ion or atom slowing down by binary elastic collisions, i.e. slow enough that the energy dissipated among electrons may be neglected as a first approximation. This is a useful starting point since many calculations can be performed by exact methods. The results should be appropriate for keV ions, the actual energy limit being determined by the atomic numbers of the ion and the target.

It turns out that the equations governing the spatial distribution of deposited energy are much like those determining the distribution of ion ranges. Both sets of equations can be solved by applying the same methods, and sometimes even the quantitative results are rather similar. We shall compare ion ranges and damage distributions extensively. One major reason is that very accurate measurements of range distributions have been done, while existing measurements of damage distributions suffer from various kinds of uncertainties.

The basic physical assumptions entering the theory are essentially those formulated by LINDHARD and his colleagues in a series of three papers published in this journal (LINDHARD et al., 1963a, b, 1968). The mathematical formalism has been described in detail by one of us (SANDERS, 1968a, b, 1969). Parts of the present work have been presented at a recent conference (SIGMUND & SANDERS, 1967), and some results have been utilized in more specific applications (SIGMUND et al., 1968; SIGMUND, 1968, 1969a). In Section 2 we briefly summarize the scattering cross sections used in the present paper and discuss a zero order approximation to the damage distribution, based only on the specific energy loss. Integral equations determining energy distributions are derived in Section 3, and special care is taken to make the notation general enough to enable us to use the same equations under less restrictive assumptions. In Section 4 we consider equations determining moments over the damage distribution, and in Section 5 these equations are solved. While our previous calculations (SIGMUND & SANDERS, 1967) were done on a desk calculator, the present results were obtained by computer. This allows getting higher moments than previously and thus constructing distribution functions from the moments with more accuracy. Section 6 is devoted to this problem. Numerical results are presented in Section 7, and Section 8 contains a comparison with experimental and computer work.

2. Scattering & Stopping Cross Sections

Elastic Scattering

For screened Coulomb interaction between an ion and an atom or between two atoms LINDHARD et al. (1968) derived the following approximate form of the differential cross section:

$$d\sigma = \pi a^2 \frac{dt}{2\, t^{3/2}} f(t^{1/2}), \tag{1}$$

where

$$t = \varepsilon^2 T/T_m,$$
$$T_m = \gamma E,$$
$$E = \text{initial energy},$$
$$T = \text{recoil energy}, \; 0 \leq T \leq T_m,$$
$$\gamma = 4M_1 M_2/(M_1 + M_2)^2,$$
$$M_1 = \text{mass of scattered particle},$$
$$M_2 = \text{mass of recoiling particle},$$
$$\varepsilon = \left(\frac{M_2 E}{M_1 + M_2}\right)\left(\frac{Z_1 Z_2 e^2}{a}\right)^{-1},$$
$$Z_1 = \text{atomic number of scattered particle},$$
$$Z_2 = \text{atomic number of recoiling particle},$$
$$a = \text{screening radius},$$
$f(t^{1/2})$ is a function that depends on the assumed form of the screening function.

(1 a)

The last two quantities are not accurately known. We shall follow LINDHARD et al. (1968) and use the screening radius

$$a = 0.8853 \, a_0 \, Z^{-1/3} \tag{2}$$

where

$$Z^{2/3} = Z_1^{2/3} + Z_2^{2/3}, \tag{2a}$$

$$a_0 = \hbar^2/me^2 = 0.529 \text{ Å}.$$

The function $f(t^{1/2})$ has been calculated for the collision of neutral Thomas-Fermi atoms. Fig. 1 shows Lindhard's $f(t^{1/2})$ together with an analytical approximation

$$f_A(t^{1/2}) = \lambda' t^{1/6}[1 + (2\lambda' t^{2/3})^{2/3}]^{-3/2}, \tag{3}$$

where

$$\lambda' = 1.309.$$

We determined λ' by least-squares fit to the numerical curve. It is seen that the two curves agree to well within the accuracy of the Thomas-Fermi approximation.

At small t eq. (3) goes over into $f(t^{1/2}) = \lambda' t^{1/6}$, which is a special case of the power approximation (LINDHARD et al., 1968)

$$f(t^{1/2}) = \lambda_m t^{1/2 - m}. \tag{4}$$

Figure 1 also shows three examples of (4) for $m = 1/3, \; 1/2$ and 1 with

$$\lambda_{1/3} = \lambda' = 1.309; \; \lambda_{1/2} = 0.327; \; \lambda_1 = 0.5. \tag{4a}$$

It is seen that the case $m = 1/3$ is an excellent approximation at small values of t, $m = 1/2$ is a reasonable over-all approximation, and $m = 1$ (Rutherford scattering) is appropriate for $t \gg 1$. In general (4) describes approximately the scattering from a potential of the form $V(r) \propto r^{-1/m}$.

In the following paragraphs we work only with the cross sections of (4) for several values of m since they allow simple analytic solution of the integral equations for range and damage distributions. From (1), (1a) and (4) we obtain
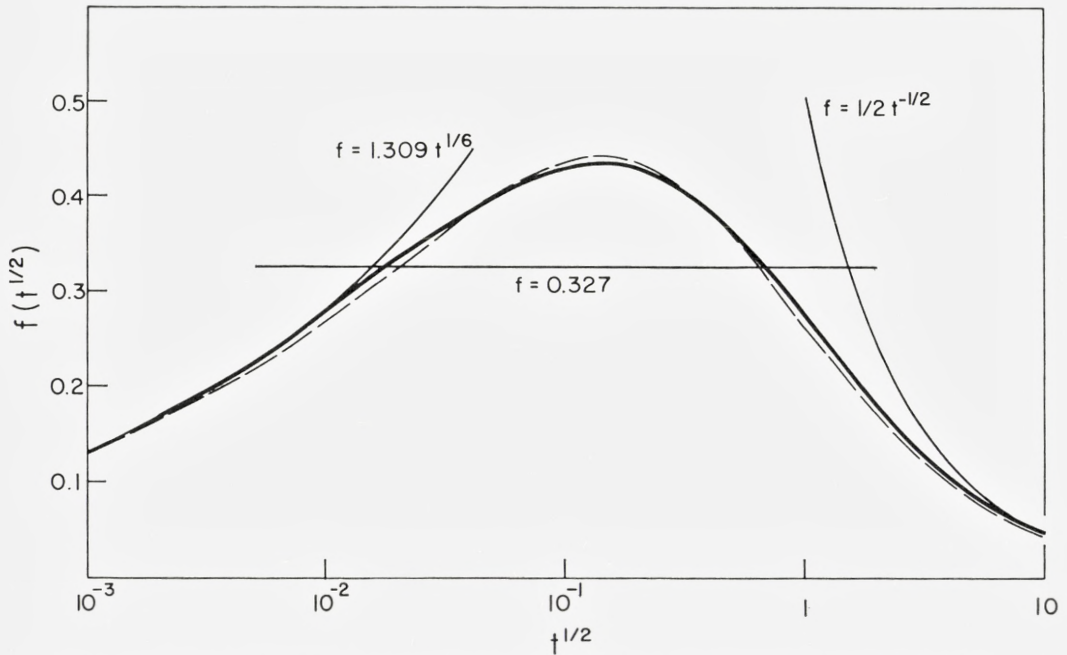
Fig. 1. Reduced Differential Cross Sections Calculated from Thomas-Fermi Potential. Thick solid line: Lindhard's numerical result. Dashed line: eq. (3). Thin solid lines: Power cross sections, eq. (4).

$$d\sigma = CE^{-m}T^{-1-m}dT, \tag{5}$$

where

$$C = \frac{\pi}{2}\lambda_m a^2 \left(\frac{M_1}{M_2}\right)^m \left(\frac{2Z_1 Z_2 e^2}{a}\right)^{2m}. \tag{5a}$$

Apart from the above three choices, we have made numerical calculations with $m = 2/3, 1/4, 1/8$, and $1/16$. While there is no specific energy region in Fig. 1 where any of these exponents would provide a particularly useful approximation to $f(t^{1/2})$ such calculations give an indication of how sensitive a quantity is to the shape of the differential cross section.

Calculations with the more accurate cross section (3) have also been performed. These can be done either analytically or numerically. In order that these results allow a more quantitative comparison with experiment than is possible on the basis of power cross sections it is necessary at the same time to include the effect of electronic energy loss. This work will be published separately.

To estimate the range of validity of the power cross sections it is convenient to consider the stopping cross section

$$S(E) = -\frac{1}{N}\frac{dE}{dR} = \int_0^{T_m} T d\sigma, \tag{6}$$
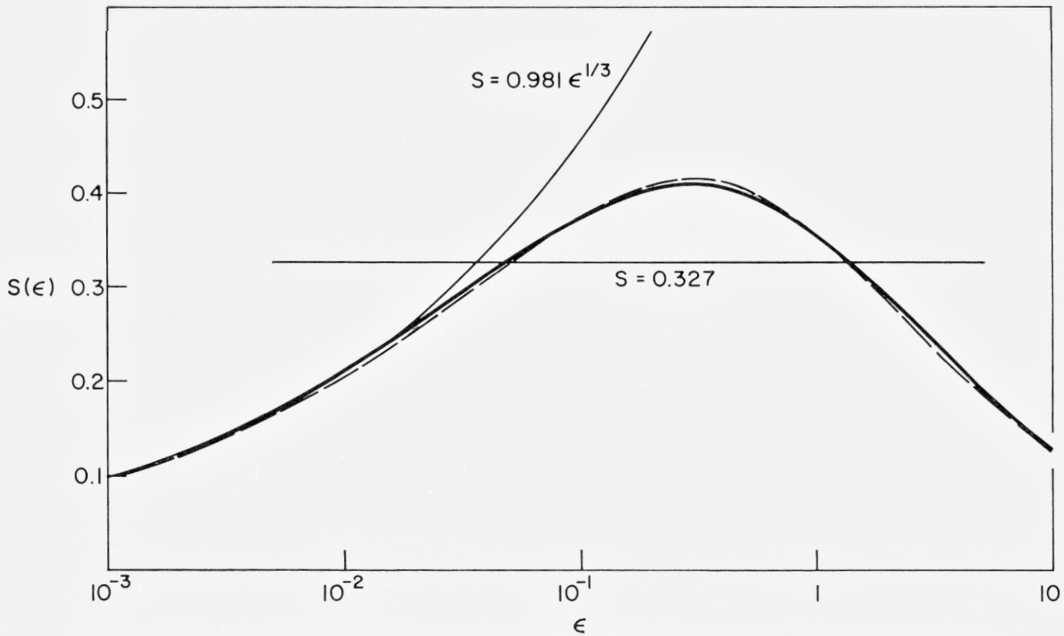
Fig. 2. Reduced Nuclear Stopping Cross Sections Calculated from Thomas-Fermi Potential.
Thick solid line: Lindhard's numerical result. Dashed line: Integrated from eq. (3). Thin solid
lines: eq. (10).

where dE/dR is the specific energy loss and N the density of atoms in the target,
and the path length,

$$R(E) = \int_0^E \frac{dE}{NS(E)}.$$

(7)

In dimensionless units (LINDHARD et al. 1968), these read

$$s(\varepsilon) = -\frac{d\varepsilon}{d\varrho} = \frac{1}{\varepsilon}\int_0^\varepsilon f(t^{1/2})dt^{1/2},$$

(8)

and

$$\varrho(\varepsilon) = \int_0^\varepsilon \frac{d\varepsilon}{s(\varepsilon)},$$

(9)

where

$$\varrho = RN\pi a^2\gamma.$$

(9a)

Fig. 2 compares Lindhard's numerical curve with the one following from (3)
by integration and the power laws
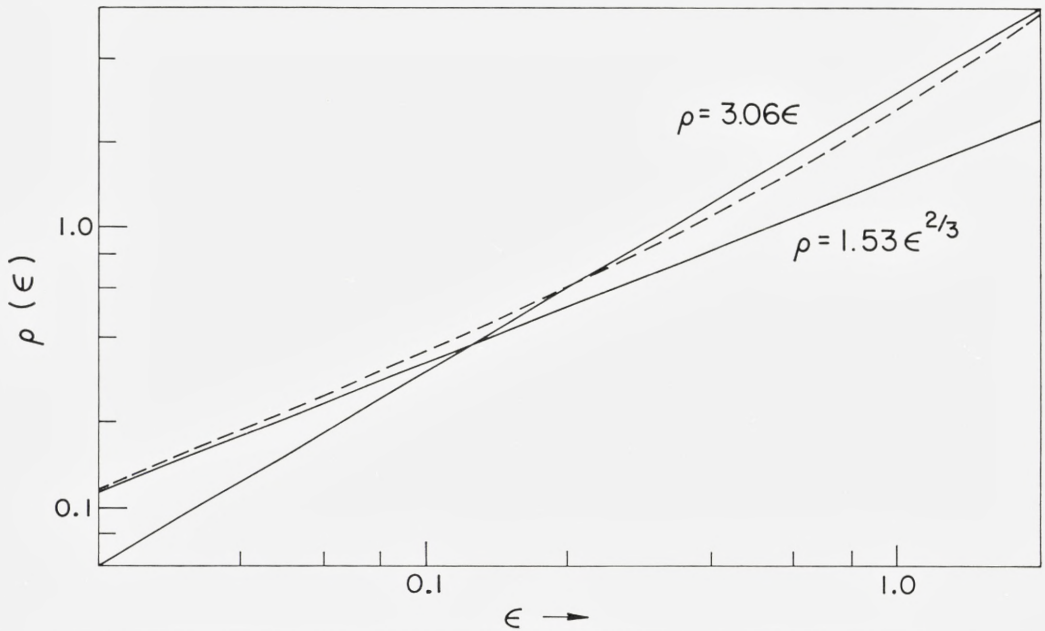
Fig. 3. Reduced Path Lengths. Dashed line: Integrated from eq. (3). Thin solid lines: eq. (11).

$$s(\varepsilon) \;=\; \frac{\lambda_m}{2(1-m)}\varepsilon^{1-2m} \tag{10}$$

corresponding to

$$S(E) \;=\; \frac{C}{1-m}\,\gamma^{1-m}E^{1-2m}. \tag{10a}$$

Fig. 3 compares the path length following from eq. (3) with the power law path lengths

$$\varrho(\varepsilon) \;=\; \frac{(1-m)}{m\cdot\lambda_m}\varepsilon^{2m}. \tag{11}$$

If $\sim 20\,{}^{0}/_{0}$ accuracy in both stopping and path length is required for the power cross-sections to be acceptable we obtain the following ranges of validity:

$$\left.\begin{array}{l} m \,=\, 1/3 \quad \text{for} \quad \varepsilon \lesssim 0.2 \\[4pt] m \,=\, 1/2 \quad \text{for} \quad 0.08 \lesssim \varepsilon \lesssim 2. \end{array}\right\} \tag{12}$$

Note also that the power law stopping with $m = 1/3$ is indistinguishable from the Lindhard stopping on the scale of the figure for $\varepsilon \lesssim 0.02$, while the path length figure indicates that the $m = 1/2$ stopping cross-section is a reasonable overall approximation. (BOHR 1948; NIELSEN, 1956). At very low energies all these cross

sections should be taken with caution since the Thomas-Fermi treatment becomes questionable.

It may be noted that in a previous communication (SIGMUND & SANDERS, 1967) we used a slightly different coefficient in the power cross section for $m = 1/3$ ($\lambda_{1/3} = 1.19$), and energy limits that differed from eq. (12). This is because both were determined only from the range-energy relationship.

Electronic Energy Loss

According to LINDHARD & SCHARFF (1961) electronic stopping can be approximated by

$$\left(\frac{d\varepsilon}{d\varrho}\right)_e = -k\varepsilon^{1/2} \quad \text{for} \quad E \lesssim Z_1^{4/3}A_1 \cdot 25 \,\text{keV}, \tag{13}$$

where k is of the order of 0.1 to 0.2 except for $Z_1 \langle\langle Z_2$ where k can become larger than 1. A_1 is the atomic weight of the ion. Thus, for $\varepsilon \lesssim 1$ electronic stopping is usually a minor correction, unless $Z_1 \lesssim 10 \, Z_2$, when it may not be neglected (SCHIØTT, 1966).

Deposited Energy: Simple Estimate

LINDHARD et al. (1963 b) established their basic range vs. energy relationship by evaluating the integral of eq. (9). This would be appropriate for continuous slowing down along a straight line. Subsequently they showed that (9) is a good approximation to the total travelled path length even when the slowing down is not continuous, and that the path length does not deviate much from the projected range as long as $M_1 > M_2$. It is tempting to make a similar estimate for the deposited energy. For purely elastic stopping the amount of energy deposited in *primary collisions* on the path element dx is given by

$$dE = N \, S(E(x)) \, dx = F(x) \, dx \tag{14}$$

where x is the path length travelled from the initial energy E down to energy $E(x)$. Eq. (14) defines a depth distribution function $F(x)$ of energy loss, which neglects the fact that energy is carried away by recoiling atoms.

For the case of the power cross section, equation (5), we obtain, by inserting (10 a) into (7),

$$R(E) = \frac{(1-m)}{2m} \frac{\gamma^{m-1}}{NC} E^{2m} \tag{15}$$

and, from (10 a) and (14),

$$F(x) = \begin{cases} \dfrac{E}{2mR}(1 - x/R)^{\frac{1}{2m}-1} & \text{for} \quad 0 \le x \le R \\ \\ 0 & \text{otherwise.} \end{cases} \tag{16}$$

It is easily verified from (16) that

$$\int_{-\infty}^{\infty} F(x)dx = E; \tag{17}$$

$$\langle x \rangle = \frac{1}{E}\int_{-\infty}^{\infty} x\,F(x)dx = \frac{2m}{1+2m}R; \tag{18}$$

$$\frac{\langle \Delta x^2 \rangle}{\langle x \rangle^2} = \frac{\langle x^2 \rangle - \langle x \rangle^2}{\langle x \rangle^2} = \frac{1}{1+4m}. \tag{19}$$

Eq. (17) states that the total amount of energy deposited along the whole trajectory is just the initially available kinetic energy, and (18, 19) determine the center and the width of the distribution. The path length $R(E)$ is an appropriate length unit to eliminate the explicit dependence on energy.

In fact, it will be seen in the following that, provided a number of simplifying assumptions can be made, the path length $R(E)$ as given by eq. (15) is a length unit that determines the energy dependence of the extension of the collision cascade in all three dimensions. Hence, within the limit of the power cross section the shape of the cascade can be considered independent of energy. This is one of the simplifying features of the power cross section.

The two major simplifications leading to eqs. (18) and (19) are the assumption of motion along a straight line, which breaks down for $M_1 \lesssim M_2$, and the neglect of energy transported a measurable distance away from the particle trajectory by energetic recoil atoms. Since the latter assumption becomes questionable for $M_1 \gtrsim M_2$ we have to conclude that (14) is probably less useful than eq. (7).

Estimates of the type discussed in this paragraph are more successful at high ion energies when the slowing down of the ion is governed by electronic stopping. Then, the ion trajectory becomes straightened out even for $M_1 \ll M_2$, and the recoil ranges tend to become relatively small as compared to ion ranges unless $M_1 \gg M_2$. Obviously, eq. (17) is no longer valid then. An estimate of this type has been made previously (SIGMUND & SAN-

DERS, 1967). BRICE (1970) improved the procedure by taking into account energy loss straggling and path length correction as well as electronic energy loss by recoil atoms. BRICE's approach is feasible if none of the three corrections has a dominating effect on the distribution. The finite range of recoiling atoms was neglected.*

3. Basic Integral Equations

It is well known that the distribution of ion ranges in a random medium is determined by an integro-differential equation of the transport type. The same is true for the distribution of deposited energy. There is, however, a major difference between the two distributions. For any *single* ion path the range distribution shrinks to one point, namely the end point of the ion's trajectory. The distribution is then *generated* by repeating the slowing-down process a sufficiently large number of times with the same initial conditions. For any single ion path however, the distribution of deposited energy extends over a region whose dimensions are expected to be of the order of the ion range. If we repeat the slowing down process many times with the same initial conditions, these distributions will be *superimposed* to create a distribution that, in general, extends over a larger region in space. Hence, while the range distribution contains all information that can possibly be obtained about the *end points* of the ion trajectories for random slowing down, the spatial distribution of deposited energy will in general *not* contain all *possible* information about the *location of energy* at the end of the slowing-down process: for example, one could also inquire about the energy distribution given the projectile's path, or end point. Whether the information contained in the distribution function of deposited energy is sufficient depends on the specific experimental situation. If it is not, one has to consider correlation functions. These will be investigated in another paper.

Average Deposited Energy

We first consider a monatomic, random, and infinite medium characterized by an atomic number Z_2, atomic mass M_2, density of atoms N; and a projectile of the same type (Z_2, M_2) starting its motion at a point $\vec{r} = 0$ with a velocity $\vec{v}$. Only binary collisions are considered. The energy or damage distribution function, $F(\vec{r}, \vec{v})$, is defined so that $F(\vec{r}, \vec{v})d^3r$ is the

---

*Note added in proof: Comparison with recent results of P. SIGMUND, M. T. MATTHIES, and D. L. PHILLIPS (to be publ.) shows that for equal masses of target and projectile, Brice's approach is valid for $\varepsilon \gg 1$.

average amount of energy located in the volume element $(\vec{r}, d^3r)$, after both the projectile and all recoiling atoms have slowed down below a certain energy limit that is very small compared to the initial energy. In most numerical calculations in this paper we take this limiting energy to be zero; we discuss this assumption in a subsequent paragraph. It is implied that the time after which the location of energy is determined is long enough to ensure that energy no longer propagates any appreciable distance via *collision* processes, but short enough to prevent sound waves from carrying the energy away. (The time constant for slowing-down is of the order of 10^{-13} seconds for keV ions, i.e. of the order of only one lattice vibrational period).

For the moment we neglect the binding forces acting on target atoms. Then, from the definition and energy conservation it follows that

$$\int F(\vec{r}, \vec{v}) d^3r = E. \tag{20}$$

$F(\vec{r}, \vec{v})$ satisfies the integral equation

$$-\frac{\vec{v}}{v} \frac{\partial}{\partial \vec{r}} F(\vec{r}, \vec{v}) = N \int d\sigma [F(\vec{r}, \vec{v}) - F(\vec{r}, \vec{v}') - F(\vec{r}, \vec{v}'')], \tag{21}$$

where

$$\left. \begin{array}{l} v = |\vec{v}| ; \\ \vec{v}' = \text{velocity of scattered particle}; \\ \vec{v}'' = \text{velocity of recoiling atom}; \\ d\sigma = \text{differential cross section} = K(\vec{v}, \vec{v}', \vec{v}'') d^3\vec{v}' d^3\vec{v}'' ; \end{array} \right\} \tag{21 a}$$

(21) is analogous to the integral equation for the vector range (SANDERS 1968a) and is also derived in the same way. The argument follows that of LINDHARD et al. (1963a, b), and, briefly, is this. The distribution F is that due to a particle starting at the origin with velocity $\vec{v}$. After this original particle has moved a short vector distance $\vec{\delta R}$ there is one particle at $\vec{\delta R}$ with velocity $\vec{v}$, if no scattering has taken place, or, if a collision has taken place, with probability $N|\vec{\delta R}|d\sigma$, two moving particles, with velocities $\vec{v}'$ and $\vec{v}''$. The original distribution must be the same as the superposition of distributions with these new initial conditions. Thus, to first order in $\vec{\delta R}$, and using the translational invariance of the medium,

$$F(\vec{r}, \vec{v}) = N|\vec{\delta R}| \int d\sigma [F(\vec{r}, \vec{v}') + F(\vec{r}, \vec{v}'')] + (1 - N|\vec{\delta R}| \int d\sigma) F(\vec{r} - \vec{\delta R}, \vec{v}) \tag{22}$$

where the integrations are over all possible (binary) collisions. Expanding the second term on the right to first order in $\vec{\delta R}$, and using $\vec{\delta R}/|\vec{\delta R}| = \vec{v}/v$, we obtain eq. (21).

We now proceed to the case of a monatomic medium, characterized by Z_2, M_2, N, and bombarded by a projectile with atomic number Z_1 and mass M_1. We have to distinguish between the function $F(\vec{r},\vec{v})$ defined as before (i.e., for a bombarding *target* atom) and a new function $F_{(1)}(\vec{r},\vec{v})$ that determines the spatial distribution of energy as a consequence of the projectile ion (Z_1,M_1) slowing down from velocity $\vec{v}$. Collisions between the ion and target atoms are described by a cross section $d\sigma_{(1)}$, while $d\sigma$ still describes collisions between target atoms. By the same argument as previously we obtain

$$\int F_{(1)}(\vec{r},\vec{v})d^3r = E; \tag{23}$$

and

$$-\frac{\vec{v}}{v}\frac{\partial}{\partial \vec{r}}F_{(1)}(\vec{r},\vec{v}) = N\int d\sigma_{(1)}[F_{(1)}(\vec{r},\vec{v}) - F_{(1)}(\vec{r},\vec{v}') - F(\vec{r},\vec{v}'')]. \tag{24}$$

The essential difference between (21) and (24) is that the former is homogeneous while the latter contains $F(\vec{r},\vec{v}'')$ as an inhomogeneity. This is a major complication of the computational work as compared to the range distribution $F_{(R)}(\vec{r},\vec{v})$ where we have (SANDERS, 1968a)

$$\int F_{(R)}(\vec{r},\vec{v})d^3r = 1 \tag{25}$$

$$-\frac{\vec{v}}{v}\frac{\partial}{\partial \vec{r}}F_{(R)}(\vec{r},\vec{v}) = N\int d\sigma_{(1)}[F_{(R)}(\vec{r},\vec{v}) - F_{(R)}(\vec{r},\vec{v}')] \tag{26}$$

for either equal or unequal masses.

Next, we consider the case of a polyatomic medium containing atoms of type j (Z_j,M_j), $(j = 2,3,4..)$, where collisions between atoms i (striking) and j (struck) are described by a cross section $d\sigma_{(ij)}$. We define $F_{(ij)}(\vec{r},\vec{v})d^3r$ as the average amount of energy located in the volume element d^3r as kinetic energy of atoms of type j, as a consequence of an atom of type i slowing down from a point $\vec{r} = 0$ with initial velocity $\vec{v}$. By generalizing the previous argument we obtain

$$\sum_j \int F_{(ij)}(\vec{r},\vec{v})d^3r = E; \tag{27}$$

and

$$-\frac{\vec{v}}{v}\frac{\partial}{\partial\vec{r}}F_{(ij)}(\vec{r},\vec{v}) = \sum_k N_k \int d\sigma_{(ik)}[F_{(ij)}(\vec{r},\vec{v}) - F_{(ij)}(\vec{r},\vec{v}') - F_{(kj)}(\vec{r},\vec{v}'')]. \quad (28)$$

Eqs. (27) and (28) are in general not sufficient to determine $F_{(ij)}(\vec{r},\vec{v})$ uniquely. Also, the sharing of energy between the various components of the system may lead to conceptual difficulties, especially in solids. In many practical problems $F_{(ij)}(\vec{r},\vec{v})$ may not even be of interest. One may need only the simpler energy distribution functions

$$F_{(i)}(\vec{r},\vec{v}) = \sum_j F_{(ij)}(\vec{r},\vec{v})$$

that determine the location of energy irrespective of its distribution among the constituent atoms. These satisfy the following equations:

$$\int F_{(i)}(\vec{r},\vec{v})d^3r = E \qquad (27a)$$

and

$$-\frac{\vec{v}}{v}\frac{\partial}{\partial\vec{r}}F_{(i)}(\vec{r},\vec{v}) = \sum_k N_k \int d\sigma_{(ik)}[F_{(i)}(\vec{r},\vec{v}) - F_{(i)}(\vec{r},\vec{v}') - F_{(k)}(\vec{r},\vec{v}'')] \qquad (28a)$$

which follow immediately from (27) and (28). Eq. (28 a) represents a system of as many coupled integro-differential equations as there are components in the system. Once all $F_{(i)}(\vec{r},\vec{v})$ have been determined—which may be a cumbersome procedure—it is relatively easy to determine the function $F_{(1)}$ determining the deposited energy in a poly-atomic medium bombarded by an ion (Z_1, M_1) that is different from any of its components. We obtain

$$\int F_{(1)}(\vec{r},\vec{v})d^3r = E, \qquad (27b)$$

$$-\frac{\vec{v}}{v}\frac{\partial}{\partial\vec{r}}F_{(1)}(\vec{r},\vec{v}) = \sum_k N_k \int d\sigma_{(1k)}[F_{(1)}(\vec{r},\vec{v}) - F_{(1)}(\vec{r},\vec{v}') - F_{(k)}(\vec{r},\vec{v}'')], \quad (28b)$$

i.e. only one additional equation containing all $F_{(k)}$ as inhomogeneities.

The corresponding equations for the ion range are

$$\int F_{(R)}(\vec{r},\vec{v})d^3r = 1, \qquad (25a)$$

$$-\frac{\vec{v}}{v}\frac{\partial}{\partial\vec{r}}F_{(R)}(\vec{r},\vec{v}) = \sum_k N_k \int d\sigma_{(1k)}[F_{(R)}(\vec{r},\vec{v}) - F_{(R)}(\vec{r},\vec{v}')]. \qquad (26a)$$

Special cases of (26 a) have been considered by SANDERS (1968 a), SCHIØTT (1968), and BAROODY (1969).

A number of other authors have used integral equations of this type to investigate ion ranges (HOLMES & LEIBFRIED, 1960; LEIBFRIED, 1962, 1963; BAROODY, 1964, 1965; LEIBFRIED & MIKA, 1965) and damage distributions (CORCIOVEI et al., 1962, 1963, 1966; v. JAN., 1964; DEDERICHS, 1965; DEDERICHS et al., 1966). All the work on damage distributions and part of the range work dealt only with the equal mass case. Furthermore, all of these investigations except the one by BAROODY (1965) used hard-sphere or hard-sphere-like scattering in the numerical work. We have shown in an earlier communication (SIGMUND & SANDERS, 1967) that hard-sphere scattering is too poor an approximation to allow quantitative conclusions, and sometimes even produces results that differ qualitatively from those obtained with the (more accurate) power cross sections.

Finally we mention that the integral equations derived in this paragraph are rather general and apply also to situations other than heavy ions slowing down by elastic collisions. As long as the cross sections are not specified the equations apply as well to moving electrons, neutrons, etc., and the different components of the system in (28) may also be electrons on the one side and atoms on the other. In this case, of course, the conventional picture of a series of successive two-particle collisions is not necessarily applicable. For example, from one impact of an ion on an atom there may arise several energetic electrons. In such a case the recoil term $F(\vec{r}, \vec{v}'')$ in (24) or any equivalent equation has to be replaced by $\sum_{\nu} F_{(\nu)}(\vec{r}, \vec{v}_{\nu}'')$ which is the sum of the contributions to $F(\vec{r}, \vec{v})$ of all particles originating from a collision (LINDHARD et al., 1963 a, b). These more general cases will be dealt with in a later paper.

Deposited Energy: Relation to Damage Effects

In the foregoing paragraph we assumed that the process of dissipation of kinetic energy can continue to arbitrarily low particle energies, via binary collisions between freely moving atoms. Obviously, at low particle energies the effects of atomic binding have to be considered. We limit our discussion to a solid target, which may be amorphous or crystalline, the effects of regular lattice structure on slowing down being neglected. Two effects of potential energy appear to be dominant.

a) There will be a certain minimum energy W for a particle either to get displaced "permanently" from its original position or to displace other

atoms. This has the immediate consequence that the quantity E^{2m}/NC is no longer a universal length unit, since e.g. W^{2m}/NC also has the dimension of a length. W may be a function of the position of the atom and its direction of motion. In the bulk, W is the order of the radiation damage threshold energy E_d ($\sim 10 - 100$ eV), while considerably smaller values of W are expected at and near the surface. The energy lost in subthreshold collisions ($T < W$) will normally be converted into heat and thus not be of interest to radiation damage (except that subthreshold collisions may cause annealing of existing radiation damage). From the theory of displacement cascades it is well known that the number $N(E)$ of permanently displaced atoms is of the order of $N(E) \approx E/2W$ for $E \gg W$, W now being a suitable average threshold energy (Lehmann, 1961, Sigmund, 1969 b, c). Thus, one would expect that, in the average, one atom will be displaced for each volume element containing an amount of $\sim 2W$ of deposited energy. Provided that the initial energy $E \gg 2W$, this volume element is much smaller than the total extension of the collision cascade. Hence, in the limit of $E \gg W$, the introduction of a finite threshold energy W should not affect the gross spatial distribution of deposited energy. This will be formulated more quantitatively in sect. 5. The close similarity to the spatial distribution of interstitials or vacancies can be formulated more quantitatively, too, if certain additional assumptions are made concerning the displacement process (Dederichs, 1965; v. Jan, 1964; Sigmund et al., 1968).

b) Upon leaving its rest position, an atom will in general lose an amount of energy U that may depend on position, energy, and direction of motion of the atom. U may be of the order of the cohesive energy or less. Also, the lattice may be left in an excited state, so that some of the lattice potential energy is converted into kinetic energy of the atoms surrounding the initial position of the displaced atom. Although one could in principle define the deposited energy function $F(\vec{r}, \vec{v})$ in such a way that energy is conserved, so eq. (20) holds, it is more convenient not to include the above amounts of potential energy in the energy balance. Then, of course, eq. (20) does not hold. The energy defect can be found by counting the number of recoil events in which potential energy is converted. For example, let us assume a sharp threshold energy W as defined above, and let a particle stop dissipating energy as soon as its energy is below W. Let us further assume that a recoiling atom loses a fixed amount of energy U upon leaving its initial position. Then, the total number of atoms that recoil with an energy in the interval (E_0, dE_0) in a collision cascade initiated by an atom of energy E is given by (Sigmund, 1969c).

$$F(E, E_0) dE_0 = \frac{m}{\psi(1) - \psi(1-m)} \frac{E}{(E_0 + U)^{1-m} E_0^{1+m}} dE_0, \qquad (29)$$

for $E \gg E_0 \gg U$ assuming the scattering to be described by the power cross section eq. (5). The function $\psi(x) = (d/dx) \ln \Gamma(x)$ is the digamma function.

The total amount of kinetic energy lost during slowing down to W is then given by

$$\Delta E = U \cdot \int_W^E F(E, E_0) dE_0 = \frac{(1 + U/W)^m - 1}{\psi(1) - \psi(1-m)} E. \qquad (29\,\mathrm{a})$$

Depending on the ratio of U/W, ΔE can be a sizable fraction of E. If U/W is small, the fraction $\Delta E/E$ is of the order of U/W. However, even though this energy defect may not be negligible when the *amount* of deposited energy is considered, the *spatial distribution* is hardly affected at all, since eq. (29) clearly shows that the great majority of these energy quanta U are lost by atoms recoiling with very low energy E_0, i.e. that do not affect the spatial distribution. In fact, for $E_0 \gg U$ we have an $\sim E_0^{-2}$ recoil density. This point also will be elucidated more quantitatively in sect. 5.

Apart from the effects of potential energy, another limit is imposed on the energy dissipation when essentially every atom within the cascade volume is set in motion with a sizable energy. This defines a limiting energy E^* of the order of $\sim E/N\Omega$, where Ω is the volume covered by the cascade. Rough estimates indicate that E^* is usually small compared with W, so this effect will be assumed negligible in the following.*

The above discussion concentrated on the spatial distribution of *displaced* atoms, as characterized by a threshold energy W. Obviously, the argument also applies to the spatial distribution of recoils with energies different from W, for example, those described by the recoil density $F(E, E_0)$ of eq. (29), and to the slowing-down-density that dominates the numbers of atoms *moving* in a certain energy interval under steady-state conditions. The latter quantity is of great use in sputtering theory (SIGMUND, 1969a). In fact, the number of atoms moving with an energy greater than the sputtering threshold energy is proportional to the total energy, but the fraction of those that are close enough to the target surface to be sputtered is determined by the energy deposition function. Also the spatial distribution of the *collision density* can be reduced to the deposited energy distribution, provided that

---

*Note added in proof: E^* can become comparable to W for very heavy ions in the lower keV region. Presumably, this affects the number of atoms set in motion (recoil density) but hardly the spatial distribution.

the collision density is defined to count all collision products in suitable energy intervals (SANDERS, 1966, 1968b; ROBINSON, 1965b; KOSTIN, 1965; FELDER & KOSTIN, 1966). Various concepts of collision density have been introduced in the literature; a discussion of their physical significance is a delicate task, but not the subject of this paper.

Finally, we mention that the assumption of complete randomness of the system under consideration is not necessarily applicable to crystalline targets. The assumption is not valid when single crystals are bombarded under channelling conditions, and even in polycrystals, or single crystals bombarded in a "random" direction, there is a possibility for scattering of ions and recoil atoms into a channel, and of linear collision chains travelling over a distance exceeding that for random slowing down at the same energy. It is implied that random-slowing-down theory holds approximately only when these lattice effects are rare, or when the corresponding ranges are small compared with the total extension of the collision cascade. Obviously, the significance of these lattice effects depends on the target, damage state, ion dose, and irradiation temperature.

Probability Distribution of Deposited Energy

It was mentioned earlier that the distribution function $F(\vec{r},\vec{v})$ and related quantities do not contain all possible information on the distribution of deposited energy. At present we go only one step further and derive an equation for the probability distribution of deposited energy, of which $F(\vec{r},\vec{v})$ is the average. We define the function $G(\vec{r},\vec{v},P)$ in the following way.

$G(\vec{r},\vec{v},P)\,dP$ is the probability that an amount of energy between Pd^3r and $(P+dP)d^3r$ is deposited in the volume element $(\vec{r},d^3r)$, by a projectile starting with velocity $\vec{v}$ at $\vec{r}=0$, and all generations of recoiling particles.

Obviously G has to be normalized:

$$\int_0^\infty G(\vec{r},\vec{v},P)dP = 1. \tag{30}$$

The average energy deposited in $(\vec{r},d^3r)$ is then

$$\int_{P=0}^\infty (Pd^3r)G(\vec{r},\vec{v},P)dP = F(\vec{r},\vec{v})d^3r,$$

so

$$F(\vec{r},\vec{v}) = \int_0^\infty PG(\vec{r},\vec{v},P)dP \tag{31}$$

where $F(\vec{r},\vec{v})$ is the function defined by (20) and (21) with W finite or zero.

By use of the argument leading to (22) we obtain the following equation for $G(\vec{r},\vec{v},P)$:

$$G(\vec{r},\vec{v},P) = N|\vec{\delta R}| \int d\sigma \int_0^P dQ G(\vec{r},\vec{v}',Q)G(\vec{r},\vec{v}'',P-Q)$$

$$+ (1 - N|\vec{\delta R}| \int d\sigma)G(\vec{r} - \vec{\delta R},\vec{v},P). \tag{32}$$

The first term on the right side expresses the fact that the total energy deposited in $(\vec{r},d^3r)$ by the scattered projectile and the recoiling particle must sum to P. Letting δR go to zero we obtain

$$-\frac{\vec{v}}{v}\frac{\partial}{\partial \vec{r}}G(\vec{r},\vec{v},P) = N \int d\sigma \left[G(\vec{r},\vec{v},P) - \int_0^P dQ G(\vec{r},\vec{v}',Q)G(\vec{r},\vec{v}'',P-Q) \right]. \tag{33}$$

We want to derive eq. (21) from (33). Multiplying (33) by P and integrating over P we obtain, by use of (31)

$$-\frac{\vec{v}}{v}\frac{\partial}{\partial \vec{r}}F(\vec{r},\vec{v}) = N \int d\sigma \left[F(\vec{r},\vec{v}) - \int_0^\infty dP \int_0^P dQ \cdot P G(\vec{r},\vec{v}',Q)G(\vec{r},\vec{v}'',P-Q) \right]. \tag{34}$$

Substituting $P \to P + Q$ in the second term on the right side in (34) we obtain

$$-\int_0^\infty dP \int_0^\infty dQ(P+Q)G(\vec{r},\vec{v}',Q)G(\vec{r},\vec{v}'',P) = -F(\vec{r},\vec{v}') - F(\vec{r},\vec{v}''), \tag{35}$$

using (30) and (31). Inserting (35) into (34) we arrive at (21).

Eq. (33) could easily be generalized to all the cases discussed at the beginning of this section. This is merely a matter of notation.

4. Equations for Spatial Averages

There are several methods available to find approximate solutions of integral equations of the type derived in the preceding section. These are reviewed in textbooks and review articles on slowing down of neutrons, penetration of X-rays, etc. But even in the highly simplified case of hard-sphere scattering it has not been possible to find the exact solutions. It is, however, possible to calculate exact expressions for *averages* over the distribution functions, for a certain class of cross sections including the power cross sections specified in (5). We shall, therefore, calculate averages first, in order to have a solid basis for comparison with experiments, and try to construct distribution functions from the averages, rather than attack directly the equations for the distribution functions. The derivations in the present section are based on standard methods developed several decades

ago in other penetration problems and used also in the theory of ion ranges. We sketch the derivations for completeness and because of some slight differences from the equations occurring in other problems.

Plane Monodirectional Source

In experiments with ion beams one has a more or less monodirectional source of projectiles, hitting a target with a more or less planar surface. It is convenient to solve the integral equations for planar geometry. This determines the depth distribution of the deposited energy.

Let us assume a coordinate system with the x-axis perpendicular to the surface of the target, and a plane monodirectional source at $x = 0$. Then $F(\vec{r}, \vec{v})$ does not depend on y and z so (20) and (21) read

$$\int_{-\infty}^{\infty} F(x, \vec{v}) \, dx = E, \tag{36}$$

$$-\cos\theta \, \frac{\partial}{\partial x} F(x, \vec{v}) = N \int d\sigma [F(x, \vec{v}) - F(x, \vec{v}\,') - F(x, \vec{v}\,'')], \tag{37}$$

where $F(x, \vec{v}) dx = dx \int F(\vec{r}, \vec{v}) dy dz$ is the energy deposited in the layer (x, dx) on the average by *one* projectile starting in the plane $x = 0$ with velocity $\vec{v}$, and $\cos\theta = \eta$ is the directional cosine of $\vec{v}$ with respect to the x-axis. Note that (37) still requires the medium to be infinite, and that the "surface" at $x = 0$ is only a reference plane. Whether our results apply to a target with a real surface depends on the importance of scattering back and forth through the plane $x = 0$.

For an isotropic medium, $F(x, \vec{v})$ cannot depend on the azimuth of $\vec{v}$ with respect to the x-axis. Hence

$$F(x, \vec{v}) \equiv F(x, E, \eta) = \sum_{l=0}^{\infty} (2l + 1) F_l(x, E) P_l(\eta), \tag{38}$$

after changing from velocity to energy variables, and expanding F in terms of Legendre polynomials. The factor $(2l + 1)$ is included for convenience. The coefficients $F_l(x, E)$ are then given by

$$F_l(x, E) = \frac{1}{2} \int_{-1}^{1} d\eta \, F(x, E, \eta) P_l(\eta) \tag{38a}$$

Integrating (38a) over x, and taking into account eq. (36), we obtain

$$\int_{-\infty}^{\infty} dx F_l(x, E) = \delta_{l0} E. \qquad (39)$$

Eq. (37) will now be reduced to a set of equations for the $F_l(x,E)$. On the left side we employ the recurrence formula for Legendre polynomials, so that

$$\left. \begin{aligned} -\eta \frac{\partial}{\partial x} F(x, \vec{v}) &= -\sum_l \frac{\partial}{\partial x} F_l(x, E) \cdot [(l+1)P_{l+1}(\eta) + lP_{l-1}(\eta)] \\ &= -\sum_l \left[l \frac{\partial}{\partial x} F_{l-1}(x, E) + (l+1) \frac{\partial}{\partial x} F_{l+1}(x, E) \right] P_l(\eta). \end{aligned} \right\} \quad (40\,\text{a})$$

The first integral on the right of (37) is given by

$$N \int d\sigma F(x, \vec{v}) = \sum_l (2l+1) N \int d\sigma(E, T) F_l(x, E) P_l(\eta), \qquad (40\,\text{b})$$

while the second,

$$-N \int d\sigma F(x, \vec{v}') = -\sum_l (2l+1) N \int d\sigma(\vec{v}, \vec{v}') F_l(x, E - T) P_l(\eta'),$$

has to be transformed in such a way that η, not η', is the variable in $P_l(\eta)$. η' is the directional cosine of $\vec{v}'$ with respect to the x-axis. We can express the cross section for elastic collisions by

$$d\sigma(\vec{v}, \vec{v}') = d\sigma(E, T) \frac{d\vec{e}'}{2\pi} \delta(\vec{e} \cdot \vec{e}' - \cos\varphi'), \qquad (41)$$

where $\vec{e} = \vec{v}/v$, $\vec{e}' = \vec{v}'/v'$ and φ' is the laboratory scattering angle of the projectile, a function of E and T. We expand the δ-function,

$$\delta(\vec{e} \cdot \vec{e}' - \cos\varphi') = \sum_{l=0}^{\infty} \frac{2l+1}{2} P_l(\vec{e} \cdot \vec{e}') P_l(\cos\varphi'),$$

and insert the addition theorem for spherical harmonics,

$$P_l(\vec{e} \cdot \vec{e}') = \sum_{\mu=-l}^{l} \frac{4\pi}{2l+1} Y_{l\mu}(\vec{e}) Y_{l\mu}^*(\vec{e}'),$$

where $Y_{l\mu}(\vec{e})$ are spherical harmonics in the notation of SCHIFF (1955). With the x-axis as a reference axis, the integral over $\vec{e}'$ can be performed and yields

$$-N\int d\sigma F(x,\vec{v}') = -\sum_l (2l+1)N\int d\sigma(E,T)P_l(\cos\varphi')F_l(x,E-T)P_l(\eta). \quad (40\,c)$$

A similar calculation for the third integral in (37) yields

$$-N\int d\sigma F(x,\vec{v}'') = -\sum_l (2l+1)N\int d\sigma(E,T)P_l(\cos\varphi'')F_l(x,T)P_l(\eta), \quad (40\,d)$$

where φ'' is the laboratory scattering angle of the recoiling atom. Collecting equations (40 a–d) we obtain

$$\left. \begin{aligned} -l\frac{\partial}{\partial x}F_{l-1}(x,E) - (l+1)\frac{\partial}{\partial x}F_{l+1}(x,E) &= (2l+1)N\int d\sigma(E,T) \\ \cdot[F_l(x,E) - P_l(\cos\varphi')F_l(x,E-T) &- P_l(\cos\varphi'')F_l(x,T)]. \end{aligned} \right\} \quad (42)$$

Spatial averages over the distribution function $F(x,\vec{v})$ are obtained by integration of (38),

$$\int_{-\infty}^{\infty} x^n dx\, F(x,\vec{v}) = \sum_{l=0}^{\infty} (2l+1)\, F_l{}^n(E)\, P_l(\eta), \quad (43)$$

where

$$F_l{}^n(E) = \int_{-\infty}^{\infty} dx\, x^n\, F_l(x,E). \quad (43\,a)$$

So, by integrating (42),

$$\left. \begin{aligned} nlF_{l-1}^{n-1}(E) + n(l+1)F_{l+1}^{n-1}(E) &= (2l+1)N\int d\sigma \\ \cdot[F_l{}^n(E) - P_l(\cos\varphi')F_l{}^n(E-T) &- P_l(\cos\varphi'')F_l{}^n(T)]. \end{aligned} \right\} \quad (44)$$

Using the notation of (43 a), (39) reads

$$F_l{}^0(E) = \delta_{l0}E. \quad (45)$$

Thus (44) represents a system of integral equations that can be solved stepwise with increasing n, the case $n = 1$ being defined by (45). Obviously, for $n = 1$ only the moment $F_1^1(E)$ is different from zero since, because of eq. (45), eq. (44) is homogeneous for $n = 1$ and $l \neq 1$. Similar arguments

apply to higher order moments. It turns out that $F_l^n \neq 0$ only for $l \leq n$ and $l + n$ even. Thus, the sum (43) is always finite.

Eq. (44) has been derived from (21) for the simplest of the distribution functions discussed in the previous section. Generalization to other functions is a matter only of adding the right indices. For example, (23) reduces to

$$
\left.
\begin{aligned}
nl\, F_{(1)}{}_{l-1}^{n-1}(E) + n(l+1)F_{(1)}{}_{l+1}^{n-1}(E) &= (2l+1)N\int d\sigma_{(1)} \\
\cdot\,[F_{(1)}{}_l^n(E) - P_l(\cos\varphi'_{(1)})F_{(1)}{}_l^n(E-T)& \\
- P_l(\cos\varphi''_{(1)})F_l^n(T)],&
\end{aligned}
\right\} \quad (46)
$$

where $\varphi'_{(1)}$ and $\varphi''_{(1)}$ are laboratory scattering angles for $M_1 \neq M_2$, and $F_{(1)}{}_l^n(E)$ derives from $F_{(1)}(\vec{r},\vec{v})$ in the same way as $F_l^n(E)$ from $F(\vec{r},\vec{v})$. Furthermore, from (22) and (45),

$$
F_{(1)}{}_l^0(E) = \delta_{l0}E. \quad (47)
$$

If the last term on the right side of (46) is omitted one obtains the equation for the moments of the projected range distribution. Eq. (47) has then to be replaced by $F_{(1)}{}_l^0(E) = \delta_{l0}$. This system of equations has been studied by BAROODY (1964, 1965).

Point Monodirectional Source

If one is interested in the extension in three dimensions of collision cascades it may be more convenient to consider a point source. This case has been studied by CORCIOVEI et al. (1962, 1963, 1966), v. JAN (1964), DEDERICHS (1965), and SANDERS (1968), as well as in our previous communication (SIGMUND & SANDERS, 1967), and in all the range work quoted previously, with the exception of BAROODY (1964, 1965, 1969). A general relation between the solutions for plane and point sources has been derived by BERGER & SPENCER (1959), and is quoted in Appendix C. We remind the reader that $F(\vec{r},\vec{v})$ does not in general determine the dimensions of a single cascade but those of the region covered by a great number of cascades with the same initial conditions.

With a point source at $\vec{r} = 0$, the initial velocity vector $\vec{v}$ is used as a reference axis X. The Y and Z axes are perpendicular to $\vec{v}$.

We expand

$$
F(\vec{r},\vec{v}) \equiv \sum_l (2l+1)f_l(r,E)P_l(\zeta), \quad (48)
$$

where $\zeta = (\vec{r}\cdot\vec{v})/(rv)$. For the moments

$$f_l^n(E) = 4\pi \int_0^\infty r^{2+n} dr f_l(r, E) \tag{49}$$

we obtain the following set of equations:

$$l(l+n+1)f_{l-1}^{n-1}(E) + (l+1)(n-l)f_{l+1}^{n-1}(E) = (2l+1)N\int d\sigma$$
$$[f_l^n(E) - P_l(\cos\varphi')f_l^n(E-T) - P_l(\cos\varphi'')f_l^n(T)], \left.\right\} \tag{50}$$

and the normalization condition

$$f_0^0(E) = E. \tag{51}$$

The $f_l^0(E)$, $l \neq 0$ are not prescribed, in contrast to (45). However, those moments $f_l^n(E)$ that can be calculated recursively from $f_0^0(E)$ determine the spatial averages $\int X^i Y^j Z^k F(\vec{r}, \vec{v})d^3r$ for integer $i,j,k \geq 0$. From (48) we obtain

$$\int X^i Y^j Z^k F(\vec{r}, \vec{v})d^3r = \sum_l (2l+1)f_l^{i+j+k}(E)\frac{1}{2}\int_{-1}^1 d\zeta \zeta^i(1-\zeta^2)^{\frac{j+k}{2}} P_l(\zeta)$$
$$\times \frac{1}{2\pi}\int_0^{2\pi} d\chi \cos^j\chi \sin^k\chi \left.\right\} \tag{52}$$

which can be readily evaluated. The resulting general expression looks more complicated than it is so we list the first few examples:

$$\int X F(\vec{r}, \vec{v})d^3r = f_1^1(E); \tag{53a}$$

$$\int Y F(\vec{r}, \vec{v})d^3r = \int Z F(\vec{r}, \vec{v})d^3r = 0; \tag{53b}$$

$$\int X^2 F(\vec{r}, \vec{v})d^3r = \tfrac{1}{3}f_0^2(E) + \tfrac{2}{3}f_2^2(E); \tag{53c}$$

$$\int Y^2 F(\vec{r}, \vec{v})d^3r = \int Z^2 F(\vec{r}, \vec{v})d^3r = \tfrac{1}{3}f_0^2(E) - \tfrac{1}{3}f_2^2(E); \tag{53d}$$

$$\int XY F(\vec{r}, \vec{v})d^3r = 0; \tag{53e}$$

$$\int X^3 F(\vec{r}, \vec{v})d^3r = \tfrac{3}{5}f_1^3(E) + \tfrac{2}{5}f_3^3(E); \tag{53f}$$

$$\int XY^2 F(\vec{r}, \vec{v})d^3r = \tfrac{1}{5}f_1^3(E) - \tfrac{1}{5}f_3^3(E); \tag{53g}$$

etc.

Again, of course, by adding a number of indices we could easily generalize these results to the more complex cases of an impurity ion or a polyatomic medium.

5. Evaluation for Power Cross Sections

LINDHARD et al. (1963 b) have shown that moments over the range distribution can be calculated by exact integration if the power cross section (5) is used. SANDERS (1968) has shown that the same is true for moments over the damage distribution, and some numerical results have been presented in an earlier communication (SIGMUND & SANDERS, 1967). In this section we first discuss the method and then present some numerical results.

First Order Moments: Equal Mass Case

Equation (44) reads, for $n = l = 1$,

$$F_0^0(E) + 2F_2^0(E) = 3N \int d\sigma \left[F_1^1(E) - \cos\varphi' F_1^1(E - T) - \cos\varphi'' F_1^1(T) \right]$$

or, after inserting the cross section $d\sigma$ from (5), the zero order moments from (45) and the laboratory scattering angles

$$\cos\varphi' = (1 - T/E)^{1/2}, \cos\varphi'' = (T/E)^{1/2}, \tag{54}$$

$$\left. \begin{array}{l} E = 3NCE^{-m} \displaystyle\int_0^E T^{-1-m} dT \left[F_1^1(E) - (1 - T/E)^{1/2} F_1^1(E - T) \right. \\[2mm] \qquad\qquad \left. - (T/E)^{1/2} F_1^1(T) \right]. \end{array} \right\} \tag{55}$$

Before solving (55) we investigate the boundary conditions imposed by a threshold energy W, as introduced in sect. 3. For planar geometry, and neglecting the energy loss U for the moment, we have

$$F(x, \vec{v}) = E\delta(x) \quad \text{for} \quad E \le W, \tag{56}$$

so, by use of (38) and (43),

$$F_l^n(E) = \delta_{l0}\delta_{n0} E \quad \text{for} \quad E \le W, \tag{57}$$

i.e. $F_1^1(E) = 0$ for $E \le W$.

We first treat the case $W = 0$. With the *ansatz*

$$F_1{}^1(E) = \frac{A_1{}^1}{NC} E^{1+2m} \tag{58}$$

where $A_1{}^1$ is a constant, we obtain from (55)

$$1 = 3A_1{}^1 \int_0^1 t^{-1-m} dt \left[1 - (1-t)^{3/2+2m} - t^{3/2+2m}\right],$$

where now

$$t = T/E. \tag{59}$$

The integrals are easily evaluated and yield

$$3A_1{}^1 = \left[-\frac{1}{m} - B(-m, 5/2 + 2m) - \frac{1}{3/2+m}\right]^{-1} \tag{60}$$

$B(x,y)$ is the beta function (ABRAMOWITZ & STEGUN, 1964),

$$B(x,y) = \int_0^1 dt\, t^{x-1}(1-t)^{y-1} = \frac{\Gamma(x)\,\Gamma(y)}{\Gamma(x+y)}. \tag{61}$$

Because of (45) all other moments $F_l{}^1(E)$ are zero so, by use of (43) and (36), we obtain the "average damage depth"

$$\langle x \rangle = \frac{\int x\, dx\, F(x, \vec{v})}{\int dx\, F(x, \vec{v})} = \frac{3A_1{}^1}{NC} E^{2m} \cos\theta, \tag{62}$$

where θ is the angle between the beam and the x-axis.

This is to be compared with the average projected range that was first calculated by LINDHARD et al. (1963b) and is, in the present notation,

$$\langle x \rangle_{(R)} = \frac{3A_{(R)1}{}^1}{NC} E^{2m} \cos\theta,$$

where

$$3A_{(R)1}{}^1 = \left[-\frac{1}{m} - B(-m, 3/2 + 2m)\right]^{-1}$$

Note that, because of the different normalization condition of the range distribution, we have

$$F_{(R)1}{}^1(E) = \frac{A_{(R)1}{}^1}{NC} E^{2m},$$

i.e. an energy dependence that is different from that in (58).

We now consider the case $W > 0$. It is then no longer possible to calculate the complete $F_1{}^1(E)$ explicitly, but the asymptotic form for $E \gg W$ can be found by Laplace transform, as was shown by ROBINSON (1965a) on a similar integral equation. Introducing the logarithmic variable $u = \ln E/W$ in (55) we obtain, by following Robinson's method, the following expression for the Laplace transform $\bar{F}_1^1(s)$ of $F_1^1(E(u))$ with respect to u:

$$\bar{F}_1^1(s) = -\frac{mW^{1+2m}}{3NC} \frac{1}{(s-1-2m)(1-2\bar{g}(s+1/2))}, \tag{63}$$

where

$$\bar{g}(s) = -\frac{m}{2} \cdot \frac{1}{s-m} + \frac{1}{2} \frac{\Gamma(1-m)\,\Gamma(s+1)}{\Gamma(s+1-m)}.$$

It appears difficult to express the inverse Laplace transform of (63) in terms of elementary functions, but it is easy to evaluate the first two terms in an asymptotic expansion in powers of E/W. These arise from the two poles at $s = 1 + 2m$ and $s = 1/2$ in (63). We then obtain

$$F_1^1(E) \sim \frac{A_1^1}{NC} E^{1+2m} - \frac{\tilde{A}_1^1}{NC} E^{1/2}W^{1/2+2m} \quad \text{for} \quad E \gg W, \tag{64}$$

where A_1^1 is identical with the expression calculated before, eq. (60), and

$$3\tilde{A}_1^1 = \frac{m(1-m)}{1/2+2m} \cdot \frac{1}{\psi(1)-\psi(1-m)}, \tag{64a}$$

$\psi(x) = \dfrac{d}{dx} \ln \Gamma(x)$. Thus the first correction term for $W \neq 0$ is smaller where than the main term by a factor of the order of $(W/E)^{1/2+2m}$. For $m > 1/4$ this factor goes more rapidly to zero than W/E. This means that W can usually be neglected when E is in the keV region, and the error made can be estimated from eq. (64).

A similar calculation shows that the correction in the average projected range due to a threshold W is proportional to $E^{-1/2}$, i.e. again smaller by a factor of the order of $(W/E)^{1/2+2m}$ than the leading term. Of course the numerical factor $\tilde{A}_1^1$ is different from the one given by (64a).

Introduction of an energy loss U of the recoiling atoms, as discussed in § 3, has two consequences. First, since energy is not conserved, the left-hand side of eq. (55) is replaced by $E - \Delta E$. Because of eq. (29 a), this means that for $E \gg U, W$, the left-hand side of eq. (55) remains linear in E. Hence, because of eq. (62), the average $\langle x \rangle$ is not affected. Second, the recoil term $F_1^1(T)$ in eq. (55) is replaced by $F_1^1(T - U)$. It is, then, possible to establish an asymptotic expansion of $F_1^1(E)$ in powers of U/E, where (62) is the leading term. Higher terms can be neglected for $E \gg U$.

First Order Moments: Nonequal Mass Case

Equation (46) reads, for $n = l = 1$,

$$E = 3N \int d\sigma_{(1)} [F_{(1)1}{}^1(E) - \cos\varphi_{(1)}{}' F_{(1)1}{}^1(E - T) - \cos\varphi_{(1)}{}'' F_1{}^1(T)], \quad (65)$$

where (47) has been inserted on the left side. The laboratory scattering angles $\varphi_{(1)}{}'$ and $\varphi_{(1)}{}''$ are given by

$$\cos\varphi_{(1)}{}' = (1 - T/E)^{1/2} + \alpha \frac{T}{E}(1 - T/E)^{-1/2} \quad (66\,a)$$

and

$$\cos\varphi_{(1)}{}'' = \gamma^{-1/2}(T/E)^{1/2} \quad (66\,b)$$

for elastic collisions, where

$$\alpha = \frac{1}{2}(1 - M_2/M_1). \quad (66\,c)$$

The cross section $d\sigma_{(1)}$ is given by

$$d\sigma_{(1)} = C_{(1)} E^{-m}{}_{(1)} T^{-1-m}{}_{(1)} dT, \quad 0 \le T \le \gamma E \quad (67)$$

where in general, $C_{(1)}$ and $m_{(1)}$ are different from C and m. We shall assume in the following that

$$m_{(1)} = m, \quad (68)$$

i. e. the same power in the cross section for both types of interaction. This is a gross simplification, the validity of which will be discussed in the following chapter. Accepting (68) for the moment, we can make the *ansatz*

$$F_{(1)1}{}^1(E) = \frac{A_{(1)1}{}^1}{NC_{(1)}} E^{1+2m} \quad (69)$$

and, inserting both (58) and (69) into (65), we obtain

$$1 + \frac{3}{3/2 + m} A_1^1 \frac{C_{(1)}}{C} \gamma^{1+m} = 3A_{(1)1}^1 \int_0^\gamma \frac{dt}{t^{1+m}} [1 - \cos\varphi_{(1)}'(1 - t)^{1+2m}]. \quad (69\,a)$$

The integral is easily evaluated after inserting (66a) and we get

$$1 + \frac{3}{3/2 + m} A_1^1 \frac{C_{(1)}}{C} \gamma^{1+m} = 3A_{(1)1}^1 \left\{ -\frac{\gamma^{-m}}{m} - B_\gamma(-m, 5/2 + 2m) \right. $$
$$\left. - \alpha B_\gamma(1 - m, 3/2 + 2m) \right\}, \quad (70$$

where B_γ is the incomplete beta function,

$$B_\gamma(x, y) = \int_0^\gamma dt\, t^{x-1}(1 - t)^{y-1}. \quad (71)$$

Eq. (70) determines $A_{(1)1}^1$, since A_1^1, $C_{(1)}$, and C are known. We note that from (5a)

$$\frac{C_{(1)}}{C} = \left(\frac{M_1}{M_2}\right)^m \left(\frac{Z_1}{Z_2}\right)^{2m} \left(\frac{a_{12}}{a_{22}}\right)^{2(1-m)}$$

or, with the approximation $Z_2/Z_1 = M_2/M_1 = \mu$,

$$\frac{C_{(1)}}{C} = \mu^{-3m} \left(\frac{2}{1 + \mu^{-2/3}}\right)^{1-m}. \quad (72)$$

It may be appropriate to make a remark on the convergence of the above integrals. Eq. (70) follows directly from (69a) provided $m < 0$ so that each term in the integral converges. For $0 < m < 1$, it is readily verified that the integral as a whole converges, while divergences occur in two terms at $t = 0$. The divergence can easily be removed by partial integration, but this would make (70) look more complicated. Instead we understand (70) for $0 < m < 1$ as the analytical continuation from the region $m < 0$.

First Order Moments: Two Different Power Cross Sections

There is no basic obstacle against treating the case $m \neq m_{(1)}$, and in fact, the solutions of (65) can be found by straightforward calculation. However, it is highly desirable to make use of the simple power laws of the type of (69), as long as this can be justified. The main advantage is, as has been seen, that *all lengths* are proportional to $E^{2m}/NC_{(1)}$ and there is complete similarity of all distributions over the

energy range where the power cross section in question is valid, so that the only numerical work to be done is the calculation of various factors. In the case $m \neq m_{(1)}$, (69) is no longer valid.

Let us assume a primary particle 1 with energy E that slows down by a power cross section characterized by $m_{(1)}$. Recoil atoms have energies T up to $T_m = \gamma E$. There is formally no lower limit for T, but for the stopping only recoils with, say $T \gtrsim \frac{1}{100} T_m$ are important. Thus

$$\frac{1}{100}\gamma E \; < \; T \; < \; \gamma E \tag{73}$$

is the energy range of interest for recoiling atoms whose scattering is characterized by a power m in the cross section. Whether eq. (68) is a reasonable assumption depends on the values of T and E in dimensionless units. We introduce two different energy units,

$$\varepsilon \; = \; E\, \frac{M_2}{M_1 + M_2} \frac{a_{12}}{Z_1 Z_2 e^2}; \quad \tau \; = \; T\frac{1}{2}\frac{a_{22}}{Z_2^2 e^2}, \tag{73a}$$

which both follow from (1a), τ applying to the equal-mass case. Hence (73) reads

$$\frac{1}{100}\varepsilon \varkappa(\mu) \; < \; \tau \; < \; \varepsilon \cdot \varkappa(\mu), \tag{74}$$

where

$$\varkappa(\mu) \; \approx \; \frac{2}{\mu(1 + \mu)} \sqrt{\tfrac{1}{2}(1 + \mu^{-2/3})} \tag{74a}$$

and $\mu = M_2/M_1 \approx Z_2/Z_1$. Figure 4 shows that the function $\varkappa(\mu)$ varies rapidly with μ, so that primary and recoil energies can differ by several orders of magnitude when measured in dimensionless units. Now, let us first assume that $M_2/M_1 < 1$, say $M_2/M_1 = 1/4$ so $\varkappa(\mu) = 8.5$, according to Fig. 4. Then $0.1\,\varepsilon \lesssim \tau < 8.5\,\varepsilon$. Hence the distribution of τ values centres around ε on a logarithmic scale, with a spread of a factor of 10 to both sides. Thus one seems justified in assuming that primary and secondary particles obey similar scattering laws, $m \approx m_{(1)}$. If M_2/M_1 is considerably smaller than $1/4$ the ratio τ/ε will be greater. Thus in extreme cases it may become necessary to assume $m > m_{(1)}$. Let us now assume $M_2/M_1 > 1$, say $M_2/M_1 = 4$, or $\varkappa(\mu) = 0.083$. Obviously the distribution of τ values ranges from $\sim 0.1\,\varepsilon$ down to $\sim 0.001\,\varepsilon$, i.e. we will have in general $m < m_{(1)}$ for $M_1 \ll M_2$. However for $M_1 \ll M_2$ the ranges of recoiling atoms are small, so the recoil term is negligible. This can be seen from the fact that the term containing the factor $C_{(1)}/C$ in (69a) goes to zero as μ^{-1-4m} for $\mu \gg 1$.

We conclude that assumption (68) is justified for $M_1 \gg M_2$, while for $M_1 \ll M_2$ the choice of m does not affect the calculated quantities. For $M_1 \approx M_2$ neither argument applies. Therefore we consider the case $M_1 = M_2$ more quantitatively. Going back to (55), one way to solve the problem would be to assume that the primary particle of energy E has a scattering law with $m = m_1$, and secondary particles, with energy T, have $m = m_2$, where $m_2 < m_1$ since $T < E$. This is, however, unsatisfactory, because a measurable fraction of all recoil atoms do have energies of the order of E. Instead, we assume the following consistent picture: introduce an arbitrary energy E_1 and assume that whenever an atom (primary or secondary)
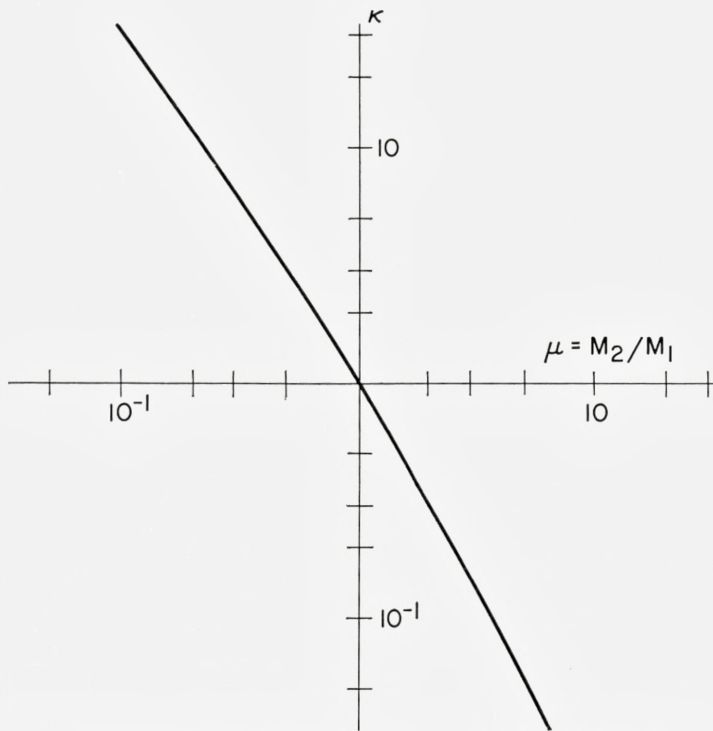
Fig. 4. The function $\varkappa(\mu)$ defined in (74a), as a function of mass ratio.

has an energy below E_1 the cross section is given by $m = m_1$, while for energies $> E_1$ we have $m = m_2$ ($> m_1$). Then, of course, $F_1{}^1(E)$ is given by (58) for $E < E_1$, with $C = C_1$ and $m = m_1$ in (60). For $E > E_1$, the integrations in (55) have to be split into the regions $E \gtrless E_1$, and $F_1{}^1(E)$ inserted as a known inhomogeneity for $E \leq E_1$. Eq. (55) can then be solved by Laplace transform, just as in the first chapter of this section, with E_1 substituted for W. The resulting expression contains (58) as the leading term with the highest power of E with $m = m_2$ and $C = C_2$, while the first correction term goes as $E^{1/2}$, i.e. can usually be neglected in comparison with E^{1+2m_2}. Thus (58) holds both for $E < E_1$ and $E > E_1$, with the respective value of m inserted in each energy region. Since this is just what was assumed above we conclude that even in the case $M_1 = M_2$, where the assumption (68) was least justified, one is indeed allowed to make it. The result of this paragraph may seem trivial to the reader, but one should be cautious. There are other, similar integral equations (SIGMUND, 1969a, 1969b) where exactly the opposite result is true. The choice of the power m is a major problem that has to be considered with great care whenever power cross sections are used.

Higher Order Moments

Higher order moments ($n \geq 2$) can be calculated in a similar way as first order ones. We set $W = U = 0$ from the beginning—which choice could be justified in the same way as for $n = 1$—and also choose a single power m in the cross sections $d\sigma$ and $d\sigma_{(1)}$.

Equal-Mas Case

Equation (44) reads, with the cross section (5),

$$\Delta F_l{}^n(E) = (2l+1)NC\,E^{-2m}\int_0^1 \frac{dt}{t^{1+m}}\,[F_l{}^n(E) - P_l(\cos\varphi')F_l{}^n(E(1-t)) \\ \left. - P_l(\cos\varphi'')F_l{}^n(Et)], \right\} \quad (75)$$

where

$$\Delta F_l{}^n(E) = nl F_{l-1}^{n-1}(E) + n(l+1)F_{l+1}^{n-1}(E). \quad (75\,a)$$

With the *ansatz*

$$F_l{}^n(E) = A_l{}^n E\left(\frac{E^{2m}}{NC}\right)^n, \quad (76)$$

(45) becomes

$$A_l{}^0 = \delta_{l0}, \quad (76a)$$

and (75) gives

$$A_l{}^n = \frac{\Delta A_l{}^n}{(2l+1)I_l{}^n}, \quad (77)$$

where

$$I_l{}^n = \int_0^1 \frac{dt}{t^{1+m}}\,[1 - P_l(\sqrt{1-t})(1-t)^{2mn+1} - P_l(\sqrt{t})\,t^{2mn+1}]. \quad (77\,a)$$

$\Delta A_l{}^n$ is defined in analogy to (75 a),

$$\Delta A_l{}^n = nl A_{l-1}^{n-1} + n(l+1)A_{l+1}^{n-1}. \quad (77b)$$

Thus it depends only on the $A_{l'}^{n-1}$. Hence the problem has been reduced to evaluating the integrals $I_l{}^n$. As before it is easily verified that $I_l{}^n$ as a whole is convergent for $m < 1$, so it is legitimate to evaluate $I_l{}^n$ first for $m < 0$, where each of the three terms is finite, and then continue the result to the region $0 \leq m < 1$.

For $m < 0$ we can write

$$I_l{}^n = -\frac{1}{m} - J_l{}^n - K_l{}^n \qquad (78)$$

where

$$J_l{}^n = \int_0^1 \frac{dt}{t^{1+m}} P_l(\sqrt{1-t})(1-t)^{2mn+1}, \qquad (78a)$$

and

$$K_l{}^n = \int_0^1 \frac{dt}{t^{1+m}} P_l(\sqrt{t}) t^{2mn+1}. \qquad (78b)$$

The two integrals are reduced to readily calculable forms in Appendix A. It should be mentioned that in a previous communication (SIGMUND & SANDERS, 1967) we evaluated $J_l{}^n$ and $K_l{}^n$ in "the pedestrian way", i.e. by inserting P_l, and evaluating the resulting beta functions, first for $n \leq 3$ and later for $n \leq 5$. This is perfectly justified for small n. In the present work we evaluate $A_l{}^n$ up to $n = 20$ and in this case one has to make the accumulation of errors in the recurrence procedure as small as possible. The method described in Appendix A is one of several procedures that have been tried. Since it is the simplest one, we have confidence that the results are accurate. In the most important lower moments ($n \leq 3$) agreement is found between the results computed by various methods and our previous results obtained with the desk calculator.

Non-Equal Masses

   With the cross section $d\sigma_{(1)} = C_{(1)}E^{-m}T^{-1-m}dT$, (46) reads

$$\left. \begin{aligned} \Delta F_{(1)l}{}^n(E) = (2l+1)NC_{(1)}E^{-2m} \int_0^\gamma \frac{dt}{t^{1+m}} [F_{(1)l}{}^n(E) - P_l(\cos\varphi_{(1)}') \times \\ \times F_{(1)l}{}^n(E(1-t)) - P_l(\cos\varphi_{(1)}'') F_l{}^n(Et)] \end{aligned} \right\} \qquad (79)$$

Inserting (76) in the last term on the right side we obtain, with the *ansatz*

$$F_{(1)l}{}^n(E) = A_{(1)l}{}^n E\left(\frac{E^{2m}}{NC_{(1)}}\right)^n, \qquad (80)$$

$$d_l{}^n A_{(1)l}{}^n = \frac{\Delta A_{(1)l}{}^n}{2l+1} + A_l{}^n \left(\frac{C_{(1)}}{C}\right)^n \mathscr{K}_l{}^n, \qquad (81)$$

3*

where

$$d_l{}^n = -\frac{\gamma^{-m}}{m} - \mathscr{J}_l{}^n, \tag{81a}$$

$$\mathscr{J}_l{}^n = \int_0^\gamma \frac{dt}{t^{1+m}} P_l(\cos\varphi_{(1)}{}')(1-t)^{2mn+1}, \tag{81b}$$

and

$$\mathscr{K}_l{}^n = \int_0^\gamma dt\, t^{m(2n-1)} P_l(\cos\varphi_{(1)}{}''). \tag{81c}$$

From (78b) and (81c), (75b) and (79a), we get

$$\mathscr{K}_l{}^n = \gamma^{1+m(2n-1)} K_l{}^n. \tag{82}$$

Also, from (47)

$$A_{(1)l}{}^0 = \delta_{l0}. \tag{83}$$

Thus, given the $A_l{}^n$, the computation of $A_{(1)l}{}^n$ is reduced to evaluating integrals. The $\mathscr{J}_l{}^n$ are evaluated in Appendix A.

Range Calculations

Moments over the ion range are calculated with the same program, the differences being the following:

i) There are no $K_l{}^n$ or $\mathscr{K}_l{}^n$ terms, since the recoil term is absent in (25). Hence it is not necessary first to evaluate the equal-mass case.

ii) Because of the different normalization condition (24), the exponents of $(1-t)$ in (78a) and (81b) are $2mn$, instead of $2mn+1$. The extra factor E in (76) and (80) disappears.

Polyatomic Targets

The extension to polyatomic targets is easily done by adding the appropriate indices and summing over the various components. Because of the difference in the values of ε, power cross sections are not applicable when the constituents of the target have extremely different masses. Consider (28a). We define

$$N_i = \alpha_i N, \tag{84}$$

so that α_i is the fraction of atoms of type i $(i = 2, 3\ldots)$. Following the procedure of the previous sections we obtain the following expression for the moments over the function $F_{(i)}(\bar{r}, \bar{v})$:

TABLE I. Coefficients A_l^n, defined by (76), for $M_1 = M_2$ and various values of m. (Note that in case of the *range* distribution the extra factor E in (76) has to be dropped).

(Ia) Deposited Energy: Nonvanishing Coefficients A_l^n for $n \leq 5$.

	$m = 2/3$	$m = 1/2$	$m = 1/3$	$m = 1/4$	$m = 1/8$	$m = 1/16$
A_0^0	1.000	1.000	1.000	1.000	1.000	1.000
A_1^1	5.199_{10-2}	9.831_{10-2}	1.685_{10-1}	2.188_{10-1}	3.307_{10-1}	4.170_{10-1}
A_0^2	1.297_{10-2}	4.916_{10-2}	1.572_{10-1}	2.871_{10-1}	8.777_{10-1}	2.149
A_2^2	3.921_{10-3}	1.419_{10-2}	4.043_{10-2}	6.563_{10-2}	1.349_{10-1}	1.958_{10-1}
A_1^3	1.880_{10-3}	1.415_{10-2}	7.813_{10-2}	1.830_{10-1}	8.195_{10-1}	2.517
A_3^3	3.404_{10-4}	2.420_{10-3}	1.153_{10-2}	2.320_{10-2}	6.275_{10-2}	1.017_{10-1}
A_0^4	6.100_{10-4}	9.583_{10-3}	9.911_{10-2}	3.203_{10-1}	2.689	$1.485_{10 1}$
A_2^4	2.644_{10-4}	4.021_{10-3}	3.815_{10-2}	1.126_{10-1}	6.853_{10-1}	2.408
A_4^4	3.158_{10-5}	4.530_{10-4}	3.662_{10-3}	9.162_{10-3}	3.254_{10-2}	5.880_{10-2}
A_1^5	1.275_{10-4}	4.169_{10-3}	7.686_{10-2}	3.217_{10-1}	3.979	$2.763_{10 1}$
A_3^5	3.615_{10-5}	1.132_{10-3}	1.856_{10-2}	6.857_{10-2}	5.513_{10-1}	2.145
A_5^5	3.031_{10-6}	8.992_{10-5}	1.256_{10-3}	3.933_{10-3}	1.852_{10-2}	3.765_{10-2}

(Ib) Range: Nonvanishing Coefficients A_l^n, for $n \leq 5$.

	$m = 2/3$	$m = 1/2$	$m = 1/3$	$m = 1/4$	$m = 1/8$	$m = 1/16$
A_0^0	1.000	1.000	1.000	1.000	1.000	1.000
A_1^1	6.799_{10-2}	1.229_{10-1}	1.991_{10-1}	2.500_{10-1}	3.562_{10-1}	4.336_{10-1}
A_0^2	2.072_{10-2}	7.374_{10-2}	2.168_{10-1}	3.750_{10-1}	1.031	2.352
A_2^2	5.881_{10-3}	1.993_{10-2}	5.229_{10-2}	8.077_{10-2}	1.519_{10-1}	2.089_{10-1}
A_1^3	3.339_{10-3}	2.331_{10-2}	1.166_{10-1}	2.561_{10-1}	1.010	2.840
A_3^3	5.559_{10-4}	3.650_{10-3}	1.574_{10-2}	2.984_{10-2}	7.251_{10-2}	1.101_{10-1}
A_0^4	1.211_{10-3}	1.755_{10-2}	1.626_{10-1}	4.889_{10-1}	3.533	$1.748_{10 1}$
A_2^4	5.044_{10-4}	7.051_{10-3}	5.986_{10-2}	1.645_{10-1}	8.698_{10-1}	2.770
A_4^4	5.468_{10-5}	7.167_{10-4}	5.176_{10-3}	1.211_{10-2}	3.815_{10-2}	6.415_{10-2}
A_1^5	2.706_{10-4}	8.110_{10-3}	1.329_{10-1}	5.145_{10-1}	5.414	$3.333_{10 1}$
A_3^5	7.258_{10-5}	2.073_{10-3}	3.010_{10-2}	1.030_{10-1}	7.125_{10-1}	2.497
A_5^5	5.476_{10-6}	1.472_{10-4}	1.818_{10-3}	5.291_{10-3}	2.190_{10-2}	4.123_{10-2}

TABLE II. Coefficients $A_{(1)l}^n$, defined by (80), as functions of mass ratio M_2/M_1.

(IIa) Deposited Energy: $m = 1/2$.

M_2/M_1	1/10	1/4	1/2	1	2	4	10
$A_{(1)0}^0$	1.000	1.000	1.000	1.000	1.000	1.000	1.000
$A_{(1)1}^1$	2.305_{10-1}	1.630_{10-1}	1.254_{10-1}	9.831_{10-2}	8.020_{10-2}	6.588_{10-2}	4.761_{10-2}
$A_{(1)0}^2$	2.905_{10-1}	1.434_{10-1}	7.978_{10-2}	4.916_{10-2}	3.801_{10-2}	3.376_{10-2}	3.077_{10-2}
$A_{(1)2}^2$	8.032_{10-2}	4.008_{10-2}	2.328_{10-2}	1.419_{10-2}	9.266_{10-3}	5.929_{10-3}	2.890_{10-3}
$A_{(1)1}^3$	2.374_{10-1}	7.864_{10-2}	3.009_{10-2}	1.415_{10-2}	9.386_{10-3}	7.001_{10-3}	4.601_{10-3}
$A_{(1)3}^3$	3.521_{10-2}	1.216_{10-2}	5.180_{10-3}	2.420_{10-3}	1.236_{10-3}	5.967_{10-4}	1.911_{10-4}
$A_{(1)0}^4$	5.923_{10-1}	1.231_{10-1}	2.802_{10-2}	9.583_{10-3}	6.256_{10-3}	4.976_{10-3}	3.911_{10-3}
$A_{(1)2}^4$	2.137_{10-1}	4.591_{10-2}	1.148_{10-2}	4.021_{10-3}	2.196_{10-3}	1.288_{10-3}	5.693_{10-4}
$A_{(1)4}^4$	1.833_{10-2}	4.257_{10-3}	1.283_{10-3}	4.530_{10-4}	1.776_{10-4}	6.348_{10-5}	1.321_{10-5}

(IIb) Deposited Energy: $m = 1/3$.

M_2/M_1	1/10	1/4	1/2	1	2	4	10
$A_{(1)0}^0$	1.000	1.000	1.000	1.000	1.000	1.000	1.000
$A_{(1)1}^1$	3.776_{10-1}	2.678_{10-1}	2.123_{10-1}	1.685_{10-1}	1.338_{10-1}	1.074_{10-1}	8.056_{10-2}
$A_{(1)0}^2$	6.347_{10-1}	3.573_{10-1}	2.382_{10-1}	1.572_{10-1}	1.142_{10-1}	1.002_{10-1}	1.055_{10-1}
$A_{(1)2}^2$	2.078_{10-1}	1.032_{10-1}	6.468_{10-2}	4.043_{10-2}	2.529_{10-2}	1.605_{10-2}	8.842_{10-3}
$A_{(1)1}^3$	6.364_{10-1}	2.701_{10-1}	1.468_{10-1}	7.813_{10-2}	4.742_{10-2}	3.504_{10-2}	2.764_{10-2}
$A_{(1)3}^3$	1.387_{10-1}	4.790_{10-2}	2.359_{10-2}	1.153_{10-2}	5.632_{10-3}	2.805_{10-3}	1.127_{10-3}
$A_{(1)0}^4$	1.359	4.911_{10-1}	2.246_{10-1}	9.911_{10-2}	5.755_{10-2}	4.713_{10-2}	4.987_{10-2}
$A_{(1)2}^4$	6.473_{10-1}	2.046_{10-1}	8.983_{10-2}	3.815_{10-2}	1.878_{10-2}	1.111_{10-2}	6.325_{10-3}
$A_{(1)4}^4$	1.048_{10-1}	2.507_{10-2}	9.650_{10-3}	3.662_{10-3}	1.390_{10-3}	5.413_{10-4}	1.583_{10-4}

$$F_{(i)l}^n(E) = G_{(i)l}^n E \left(\frac{E^{2m}}{N\overline{C}}\right)^n, \tag{85}$$

where $\overline{C}$ is an average C value defined in some arbitrary way, and the $G_{(i)l}^n$ are found from the following system of equations:

$$\frac{\Delta G_{(i)l}^n}{2l + 1} = \sum_k \alpha_k \frac{C_{(ik)}}{\overline{C}} \left\{ G_{(i)l}^n d_{(ik)l}^n - G_{(k)l}^n \mathscr{K}_{(ik)l}^n \right\}. \tag{85a}$$

TABLE II (continued). Coefficients $A_{(1)l}{}^{n}$, defined by (80), as functions of mass ratio M_2/M_1.

(IIc) Range, $m = 1/2$.

M_2/M_1	1/10	1/4	1/2	1	2	4	10
$A_{(1)0}{}^{0}$	1.000	1.000	1.000	1.000	1.000	1.000	1.000
$A_{(1)1}{}^{1}$	2.805_{10-1}	1.922_{10-1}	1.511_{10-1}	1.229_{10-1}	9.904_{10-2}	7.623_{10-2}	5.090_{10-2}
$A_{(1)0}{}^{2}$	2.582_{10-1}	1.345_{10-1}	9.404_{10-2}	7.374_{10-2}	6.166_{10-2}	5.333_{10-2}	4.684_{10-2}
$A_{(1)2}{}^{2}$	9.840_{10-2}	4.794_{10-2}	3.031_{10-2}	1.993_{10-2}	1.255_{10-2}	7.226_{10-3}	3.154_{10-3}
$A_{(1)1}{}^{3}$	1.454_{10-1}	5.743_{10-2}	3.433_{10-2}	2.331_{10-2}	1.655_{10-2}	1.162_{10-2}	7.109_{10-3}
$A_{(1)3}{}^{3}$	3.838_{10-2}	1.362_{10-2}	6.963_{10-3}	3.650_{10-3}	1.759_{10-3}	7.457_{10-4}	2.106_{10-4}
$A_{(1)0}{}^{4}$	1.479_{10-1}	4.769_{10-2}	2.644_{10-2}	1.755_{10-2}	1.275_{10-2}	9.649_{10-3}	7.229_{10-3}
$A_{(1)2}{}^{4}$	8.062_{10-2}	2.443_{10-2}	1.237_{10-2}	7.051_{10-3}	4.044_{10-3}	2.179_{10-3}	8.829_{10-4}
$A_{(1)4}{}^{4}$	1.605_{10-2}	4.212_{10-3}	1.739_{10-3}	7.167_{10-4}	2.602_{10-4}	8.050_{10-5}	1.463_{10-5}

(IId) Range, $m = 1/3$.

M_2/M_1	1/10	1/4	1/2	1	2	4	10
$A_{(1)0}{}^{0}$	1.000	1.000	1.000	1.000	1.000	1.000	1.000
$A_{(1)1}{}^{1}$	6.511_{10-1}	3.821_{10-1}	2.685_{10-1}	1.991_{10-1}	1.520_{10-1}	1.170_{10-1}	8.384_{10-2}
$A_{(1)0}{}^{2}$	1.394	5.402_{10-1}	3.123_{10-1}	2.168_{10-1}	1.768_{10-1}	1.653_{10-1}	1.795_{10-1}
$A_{(1)2}{}^{2}$	5.226_{10-1}	1.852_{10-1}	9.388_{10-2}	5.229_{10-2}	3.046_{10-2}	1.805_{10-2}	9.315_{10-3}
$A_{(1)1}{}^{3}$	1.795	4.523_{10-1}	2.045_{10-1}	1.166_{10-1}	7.872_{10-2}	5.945_{10-2}	4.670_{10-2}
$A_{(1)3}{}^{3}$	4.609_{10-1}	1.009_{10-1}	3.747_{10-2}	1.574_{10-2}	6.995_{10-3}	3.200_{10-3}	1.194_{10-3}
$A_{(1)0}{}^{4}$	4.194	7.552_{10-1}	2.978_{10-1}	1.626_{10-1}	1.146_{10-1}	9.926_{10-2}	1.092_{10-1}
$A_{(1)2}{}^{4}$	2.250	3.735_{10-1}	1.314_{10-1}	5.986_{10-2}	3.206_{10-2}	1.888_{10-2}	1.060_{10-2}
$A_{(1)4}{}^{4}$	4.318_{10-1}	5.946_{10-2}	1.631_{10-2}	5.176_{10-3}	1.758_{10-3}	6.226_{10-4}	1.682_{10-4}

The quantities $d_{(ik)l}{}^{n}$ and $\mathcal{K}_{(ik)l}{}^{n}$ are defined in (81 a) and (81 c), the pair of indices (ik) indicating the projectile and the target in the specific collision integral. $C_{(ik)}$ is the corresponding constant in the cross section given by (5). Obviously $G_{(i)l}{}^{n}$ for any specific pair of values (l,n) must be calculated from a set of inhomogeneous linear equations.

Equation (27b), representing the distribution of energy deposited by an ion (1) in a polyatomic medium $(2,3....)$ is solved in a similar way. With the *ansatz*

$$F_{(1)\text{poly}} l^n(E) = G_{(1)} l^n E \left(\frac{E^{2m}}{N\overline{C}}\right)^n \tag{86}$$

we obtain

$$\frac{\Delta G_{(1)} l^n}{2l+1} = G_{(1)} l^n \cdot \sum_k \alpha_k \frac{C_{(1k)}}{\overline{C}} d_{(1k)} l^n - \sum_k \alpha_k \frac{C_{(1k)}}{\overline{C}} G_{(k)} l^n \mathscr{K}_{(1k)} l^n, \tag{86a}$$

where the notation is the same as in (85a).

If the $G_{(k)} l^n$ are known from (85a) for $k = 2,3..$, then (86a) is easy to solve recursively.

The ion *range* equation in a polyatomic target is found from (86a) by discarding the last term on the right. Substituting (81), with $\mathscr{K}_l^n = 0$, into (86a) with $\mathscr{K}_{(1k)} l^n = 0$ we obtain

$$G_{(1)} l^n = \frac{\Delta G_{(1)} l^n}{\sum_k \alpha_k \dfrac{C_{(1k)}}{\overline{C}} \cdot \dfrac{\Delta A_{(1k)} l^n}{A_{(1k)} l^n}}. \tag{87}$$

This equation relates the moments over the range distribution in a polyatomic target t othe moments $A_{(1k)} l^n$ over the range distribution of the ion in the constituents. In this case the most natural choice of the constant $\overline{C}$ is $\overline{C} = \sum_k \alpha_k C_{(1k)}$, but the result,

$$F_{(1)} l^n(E) = G_{(1)} l^n \left(\frac{E^{2m}}{N\overline{C}}\right)^n, \tag{87a}$$

is of course independent of the choice of $\overline{C}$.

The results of this section allow us to calculate a great variety of moments over range and damage distributions, some of which are listed in Tables I–II. The calculations were done on the CDC G-20/3100 computer system at Chalk River Nuclear Laboratories.

6. Construction of Distributions

While an infinite set of moments uniquely determines a distribution (with certain restrictions; see below) it is a rather delicate task to construct a good approximation to a distribution from a finite number of moments. Various procedures have been used in the slowing-down theory of neutrons, electrons, X-rays etc. The present approach is based on the assumption that the depth distribution of ion ranges and deposited energy is close to gaussian when the medium is random and infinite.

An alternative approach, using Chebyshev inequalities (FELLER, 1966) to obtain bounds on the integrated density, will be discussed by one of us in a subsequent paper (WINTERBON, 1970).

We follow customary usage in this field and use the term 'distribution' in the following where a statistician would say 'density'. This should not cause confusion here because we have no occasion in this work to refer to a statistician's 'distribution', which is an integrated density.

The gaussian or normal distribution is in many ways the simplest starting point. For ion ranges there appears to be experimental evidence that the gaussian is an adequate approximation, in the sense that the distribution appears to decrease like $\exp(-x^2)$ at large distances, but for deposited energy distributions there is no sufficiently accurate experimental information. There are indications from computer simulation work of Pavlov et al. (1966) that distributions of vacancies or interstitials are close to gaussian shape, but it is felt that the number of runs made in that work is too small to permit definite statements.

Given a set of moments v_n of an unknown distribution f and an initial approximation $\psi = \psi_0$, there is a well-defined procedure for making successive approximations ψ_n to f as follows. Let the polynominals p_n be orthogonal polynomials associated with the weight function ψ. Then

$$\psi_n = \sum_{m=0}^{n} c_m p_m \psi, \tag{88}$$

where c_m is chosen so that the mth moment of ψ_m $(m \leq n)$ is equal to v_m. The p_m are orthogonal polynomials so the value of c_m does not depend on n.

This procedure has the disadvantage that the approximants ψ_n are not necessarily everywhere positive. In fact if the interval is $(-\infty, +\infty)$, as it is here, then each odd approximant is negative for sufficiently large (absolute) values of the argument in one direction or the other.

If ψ_0 is a gaussian, the polynominals p_m are Hermite polynomials, and the approximants are partial sums of an Hermite polynomial series. If ψ_0 has the same mean and variance as f, we deal with a Gram-Charlier series. If the terms of the Gram-Charlier series are rearranged in a certain way, we obtain an Edgeworth series. (See, for example, Cramer, 1945; Feller, 1966; Kendall & Stuart, 1958).

Baroody (1965) used Edgeworth's expansion to approximate range distributions. Sanders (1968a, 1968b) used the same procedure, and Sigmund (1968, 1969a) applied it to distributions of deposited energy. Pringle (1968), by analyzing accurate experimental range distributions, found that the best gaussian fit to his distributions was not necessarily centered around the average projected range, nor was the width of it the same as the straggling. Similar observations were made with calculated distribu-

tions in the present work. Hence it was decided to examine various other methods for determining the parameters of the gaussian. These are described in this section. Also we consider a class of series with a non-gaussian $\psi_0 \sim \exp(-\lambda|x-a|^\beta)$.

At present, we deal exclusively with planar geometry. From (43), (36), and (76) we have

$$\langle x^n \rangle = \frac{1}{E} \sum_{l=0}^{\infty} (2l+1) F_l^n(E) P_l(\eta) = \left(\frac{E^{2m}}{NC}\right)^n \sum_{l} (2l+1) A_l^n P_l(\eta), \qquad (89)$$

for $M_1 = M_2$, and

$$\langle x^n \rangle = \left(\frac{E^{2m}}{NC_{(1)}}\right)^n \sum_{l} (2l+1) A_{(1)l}^n P_l(\eta) \qquad (89\,a)$$

for $M_1 \neq M_2$. Eq. (89 a) and the last part of (89) hold for both range and damage distributions, with different values for the A_l^n and $A_{(1)l}^n$. Similar relations hold for polyatomic targets. Hence, for any value of $\eta = \cos\theta$, θ being the angle of the beam with the direction in which the depth distributions are measured, we obtain a set of averages $\langle x^n \rangle$ over these depth distributions. We define

$$\langle x^n \rangle = \nu_n \left(\frac{E^{2m}}{NC}\right)^n. \qquad (90)$$

so that ν_n is dimensionless. C stands for either C, $C_{(1)}$, or $\overline{C}$, depending on the specific problem. Thus the distribution functions depend on energy only in the length unit, E^{2m}/NC. This, again, is a specific feature of power cross sections, for $W = U = 0$. When reconstructing $F(x)$ in the following, x will also have units of E^{2m}/NC.

Introducing the new variable

$$\xi = \alpha(x - a), \qquad (91)$$

where a and α are not yet specified, we can write

$$F(x) = F(x(\xi)) = f(\xi) = \psi(\xi) \sum_{m=0}^{\infty} c_m \mathrm{He}_m(\xi) \qquad (92)$$

where

$$\psi(\xi) = (2\pi)^{-1/2} \exp(-\xi^2/2) \qquad (92\,a)$$

and $\mathrm{He}_m(\xi)$ are Hermite polynominals (ABRAMOWITZ & STEGUN, 1964).

A word should be said about convergence. The set of moments need not define the distribution uniquely (see for example, FELLER, 1966): the moments must satisfy certain restrictions in the rate of growth for there to be uniqueness. From the footnote in FELLER, p. 224, it can be seen that if the density is $0(\exp(-\lambda|x|))$ for some $\lambda > 0$, then it is uniquely determined by its moments. Since the mere existence of the moments suffices for the convergence (in the mean) of the Hermite series, and since $F(x)$ is expected to be continuous, it follows that if $F(x) = 0(\exp(-\lambda|x|))$ then the series in (92) converges to F. We expect $F(x) = 0(\exp(-\lambda x^2))$, so we assume convergence of (92). Since we have been unable to obtain asymptotic limits on the ν_n, we can of course not prove either convergence or the stronger estimate $F(x) = 0(\exp(-\lambda x^2))$.

An expression for the c_m in terms of the ν_r is derived in Appendix B, eq. B6,

$$c_m = \frac{\alpha}{m!} \sum_{r=0}^{m} \binom{m}{r} \alpha^r \nu_r \operatorname{He}_{m-r}(-a\alpha) \tag{93}$$

For the Gram-Charlier or Edgeworth series the parameters a and α are chosen so that

$$c_1 = c_2 = 0, \tag{94}$$

whence

$$a = \nu_1, \quad \alpha = (\nu_2 - a^2)^{-1/2}. \tag{94a}$$

To try to improve apparent convergence, higher order moments were used in determining a and α. The first method tried used second and third or third and fourth moments. Thus we require

$$c_2 = c_3 = 0 \tag{95}$$

or

$$c_3 = c_4 = 0. \tag{95a}$$

Appropriate values of a and α in terms of the ν_r are given in Appendix B. Such a procedure could in principle be continued indefinitely, but the amount of labour required increases rapidly. *In these two cases we could consider ψ_0 to be a gaussian times a linear or quadratic polynomial*, so we call them "linear" and "quadratic" fits.

Another possible fitting criterion is that the c_n should decrease rapidly. This may be satisfied by minimizing

$$c_0^{-2} \sum_{n=0}^{N} c_n^2 \omega_n,$$

with the weight ω_n a rapidly increasing function of n. We have used $\omega_n = n!$ and $(n!)^2$, and got apparently good results, but have not investigated this procedure fully.

Besides the gaussian base, some fits were tried with a more general form,

$$\psi_0 = N' \exp(-\lambda |\xi|^\beta). \tag{96}$$

Only one class of fit was tried, that with

$$c_1 = c_2 = c_4 = 0 \tag{96 a}$$

(ψ_0 is symmetric in ξ, so it is not possible in general to make $c_1 = c_3 = 0$). Details are reported in Appendix B.

7. Results & Discussion

Table III and Figures 5–7 show up to fourth order moments of the damage and range distributions for the case of the point source, where the distribution is considered both parallel (X) and perpendicular (Y, Z) to the initial velocity $\vec{v}$. As a length unit we use either the quantity $E^{2m}/NC_{(1)}$ or the average path length in the LSS approximation, $R(E)$, as given by eq. (15). The latter length unit is convenient for comparison with those calculations of LINDHARD et al. (1963b) that are based on the accurate Thomas-Fermi cross section. Note that all but first-order moments are given in *relative* units so that the dependence on ion energy is eliminated for $n \geq 2$.

Table III contains results for the case $M_1 = M_2$ for several values of the exponent m in the cross section. This table shows how sensitive the distributions are to the choice of the differential scattering cross section. Table III a indicates that for the damage distribution there are no large variations with m over the most important range, $m = \frac{2}{3}, \frac{1}{2}, \frac{1}{3}$ and $\frac{1}{4}$, except that the distribution broadens in the Y, Z plane with decreasing m (decreasing energy), as seen in $\langle \varrho^2 \rangle / \langle X \rangle^2$, and that the skewness in the X direction, as measured by $\langle \Delta X^3 \rangle / \langle \Delta X^2 \rangle^{3/2}$ has a maximum for $m \sim \frac{1}{3}$. The average damage depth $\langle X \rangle$ is always smaller than the path length R of the ion. Table III b shows similar results for the range distribution. Note that both ratios $\langle X \rangle / R$ and $\langle \Delta X^2 \rangle / \langle X \rangle^2$ are slightly more sensitive to changes in m than they are for the damage distributions.

For $M_1 \neq M_2$ we consider only the most important cases, $m = \frac{1}{2}$ and $m = \frac{1}{3}$. Fig. 5 shows the various first and second moments as functions of mass ratio $\mu = M_2/M_1$. For $\mu \gtrsim \frac{1}{2}$ the results appear to be insensitive to m. This is also true for higher moments (Figs. 6 & 7). The ratio $\langle X \rangle / R$ decreases with increasing μ, since for $M_1 \ll M_2$ ions undergo many large-

TABLE III. Moments over the damage and range distribution, $M_1 = M_2$. X = direction of initial velocity; Y, Z = directions perpendicular to initial velocity; $\varrho^2 = Y^2 + Z^2$; R = path length = $\int_0^E dE/NS_n(E)$.

(IIIa) Damage.

m	2/3	1/2	1/3	1/4	1/8	1/16
$\langle X \rangle / \left(\dfrac{E^{2m}}{NC} \right)$	0.1560	0.2949	0.5054	0.6563	0.9922	1.251
$\langle X \rangle / R$	0.6239	0.5899	0.5054	0.4375	0.2835	0.1668
$\langle \varDelta X^2 \rangle / \langle X \rangle^2$	0.3388	0.3807	0.4070	0.4286	0.5766	0.9989
$\langle \varrho^2 \rangle / \langle X \rangle^2$	0.2601	0.3146	0.4397	0.5714	1.098	2.121
$\langle \varDelta X^3 \rangle / \langle \varDelta X^2 \rangle^{3/2}$	0.4930	0.7333	0.8468	0.8263	0.5412	0.2260
$\langle X\varrho^2 \rangle / (\langle X \rangle \langle \varrho^2 \rangle)$	1.394	1.406	1.332	1.261	1.119	1.041
$\langle \varDelta X^4 \rangle / \langle \varDelta X^2 \rangle^2$	2.807	3.373	3.782	3.853	3.623	3.310
$\langle X^2\varrho^2 \rangle / (\langle X^2 \rangle \langle \varrho^2 \rangle)$	1.663	1.723	1.608	1.485	1.234	1.096
$\langle \varrho^4 \rangle / \langle \varrho^2 \rangle^2$	3.706	3.773	3.402	3.073	2.478	2.186

(IIIb) Range.

| m	2/3	1/2	1/3	1/4	1/8	1/16
$\langle X \rangle / \left(\dfrac{E^{2m}}{NC} \right)$	0.2040	0.3687	0.5973	0.7500	1.069	1.301
$\langle X \rangle / R$	0.8159	0.7374	0.5973	0.5000	0.3053	0.1734
$\langle \varDelta X^2 \rangle / \langle X \rangle^2$	0.2050	0.2756	0.3405	0.3846	0.5682	1.007
$\langle \varrho^2 \rangle / \langle X \rangle^2$	0.2895	0.3519	0.4825	0.6154	1.1410	2.163
$\langle \varDelta X^3 \rangle / \langle \varDelta X^2 \rangle^{3/2}$	0.2602	0.5456	0.6868	0.6800	0.4522	0.1962
$\langle X\varrho^2 \rangle / (\langle X \rangle \langle \varrho^2 \rangle)$	1.134	1.195	1.196	1.168	1.086	1.031
$\langle \varDelta X^4 \rangle / \langle \varDelta X^2 \rangle^2$	2.733	3.134	3.503	3.597	3.486	3.258
$\langle X^2\varrho^2 \rangle / (\langle X^2 \rangle \langle \varrho^2 \rangle)$	1.219	1.341	1.357	1.313	1.173	1.076
$\langle \varrho^4 \rangle / \langle \varrho^2 \rangle^2$	2.480	2.729	2.742	2.638	2.338	2.144
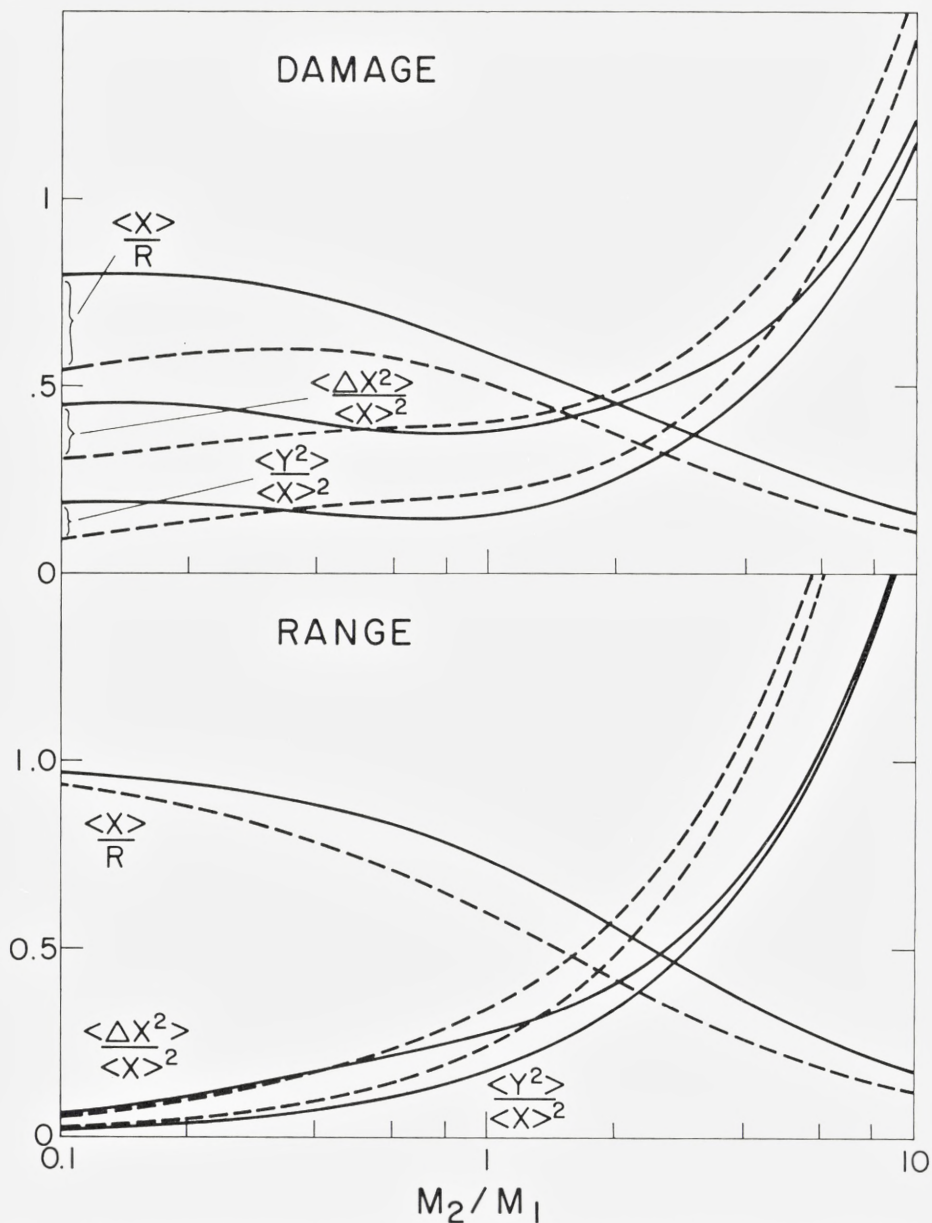
Fig. 5. First and second order averages over damage and range distribution as functions of mass ratio M_2/M_1; R = path length = $\int_0^E dE/(NS_n(E))$; X-direction parallel to initial velocity; $\Delta X = X - \langle X \rangle$. Dashed line, $m = 1/3$; solid line $m = 1/2$.
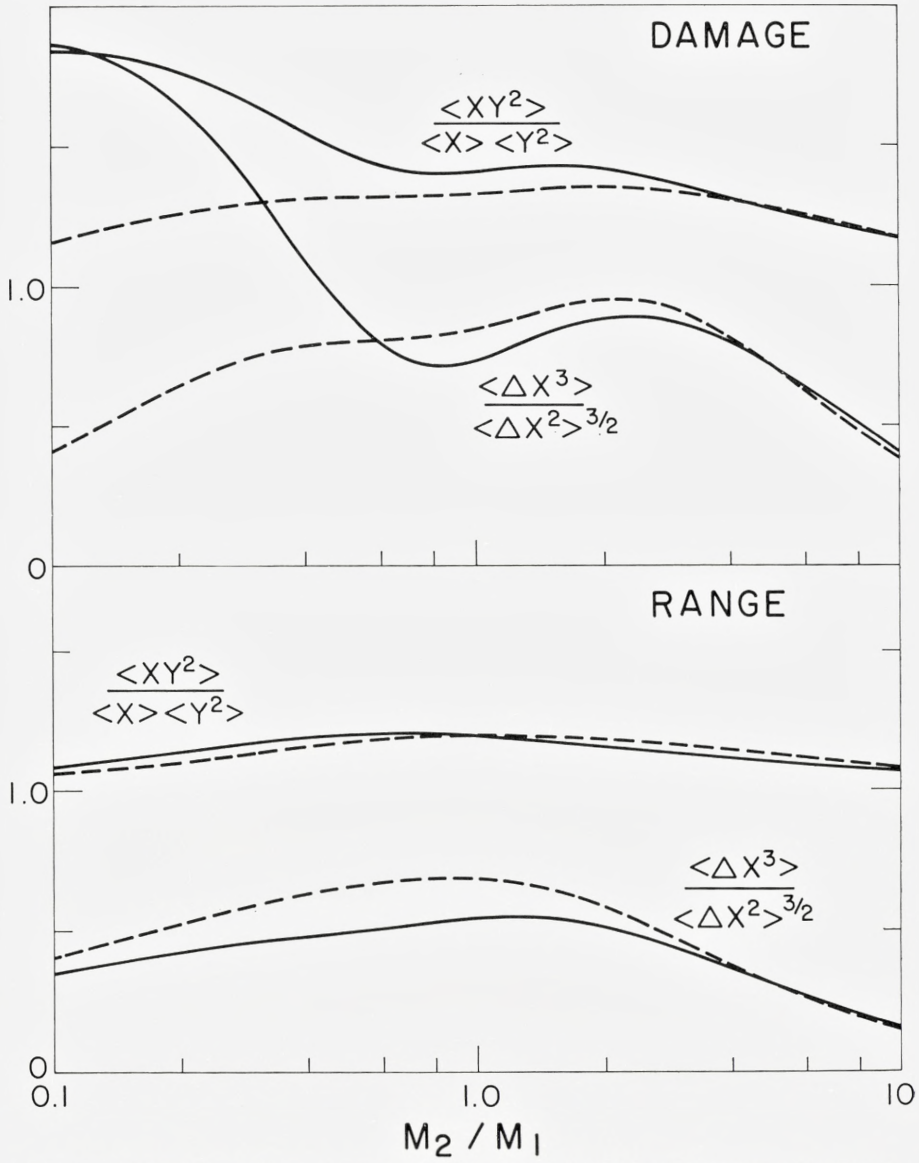
Fig. 6. Third order averages over damage and range distribution. Definitions as in Fig. 5.
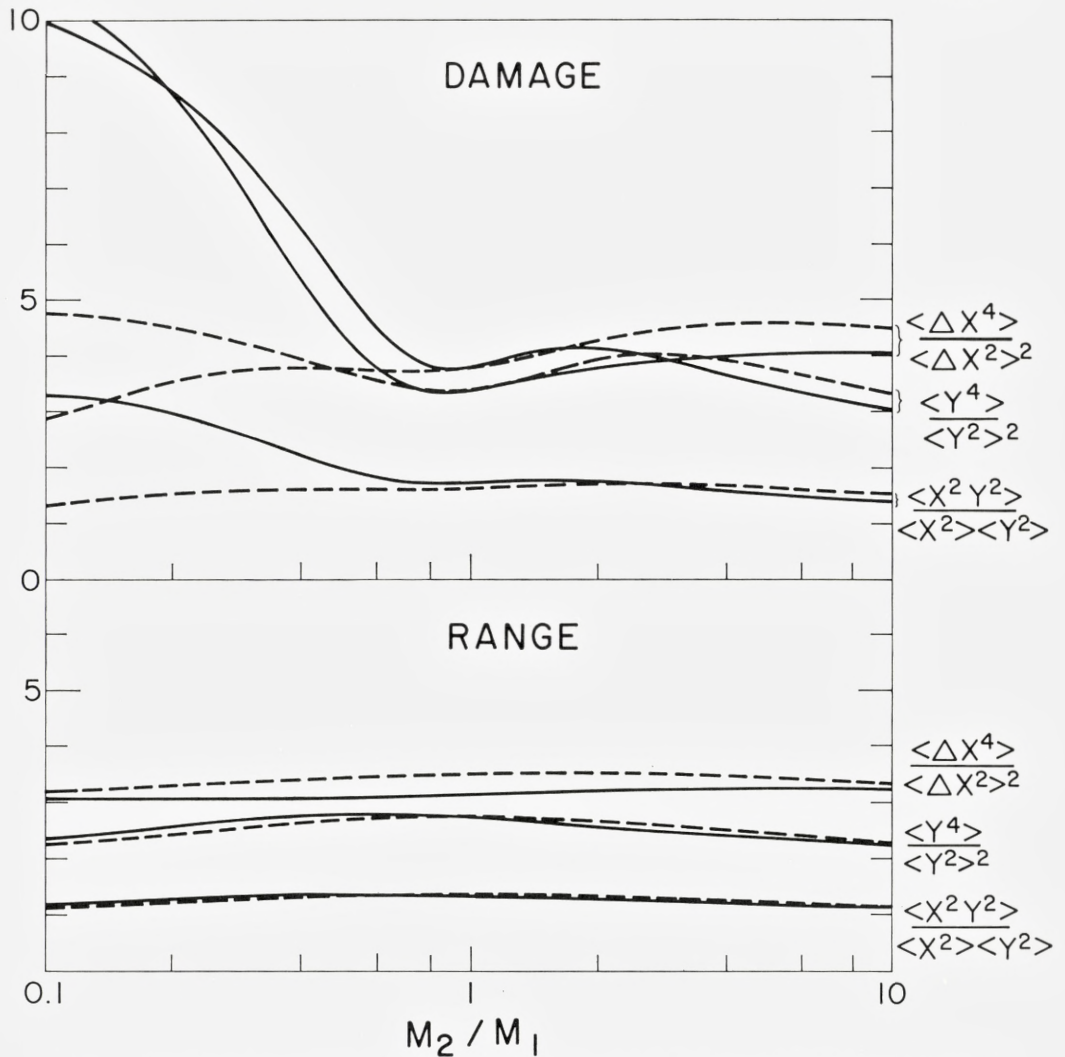
Fig. 7. Fourth order averages over damage and range distributions. Definitions as in Fig. 5.

angle deflections. Similarly, the distributions broaden in each dimension when μ increases.

The distributions are slightly prolate at all mass ratios considered, most pronouncedly so for $\mu < 1$. For $\mu \gg 1$ the distributions are practically spherical.

The simple stopping vs. path length argument of (18, 19) gives $\langle X \rangle / R = 0.5$ and 0.4, and $\langle \Delta X^2 \rangle / \langle X \rangle^2 = 0.333$ and 0.429, for $m = \frac{1}{2}$ and $\frac{1}{3}$ respectively. Comparison with Fig. 5 shows that this approach gives rather poor results at all mass ratios.

Figure 6 shows third order moments. For a purely gaussian distribution the ratio $\langle \Delta X^3 \rangle / \langle \Delta X^2 \rangle^{3/2}$ would be zero and $\langle X Y^2 \rangle / (\langle X \rangle \langle Y^2 \rangle) = 1$. The range distribution appears to be more nearly gaussian than the damage distribution, especially for $\mu \lesssim 1$. The same conclusion can be drawn from an inspection of fourth order moments, Fig. 7. For a gaussian, one would obtain $\langle \Delta X^4 \rangle / \langle \Delta X^2 \rangle^2 = \langle Y^4 \rangle / \langle Y^2 \rangle^2 = 3$, and $\langle X^2 Y^2 \rangle / (\langle X^2 \rangle \langle Y^2 \rangle) = 1$. The most pronounced deviations from these relations occur in the damage density for $\mu \ll 1$ and $m = \frac{1}{2}$.

In Figs. 8 a–c we compare range moments with the corresponding damage moments. Fig. 8 a shows that the mean damage depth is consistently smaller than the mean projected range. The difference is small except for $\mu \ll 1$ and $m = \frac{1}{3}$ where it is a factor of ~ 2. In this case heavy damage is created all over the ion path, so that despite energy transport of recoiling atoms the ion comes to rest essentially at the far end of the damage cloud, while $\langle X \rangle$ is in the center. This picture is consistent with Fig. 8 b that shows that the damage distribution is much broader than the range distribution for $\mu \ll 1$. It may be surprising to see that the opposite is true for $\mu \gtrsim 1$. This is obviously because we are considering the damage distribution of *many events*. For $\mu \gtrsim 1$, the ion undergoes large deflections, but mainly those in the beginning, where the ion still has much energy to share with its collision partners, determine the region where the energy is located, while those collisions undergone by the ion toward the end of its slowing down still may contribute to range straggling, but not to a broadening of the damage distribution. Note that the effect is not very pronounced, about a factor of 1.3 in the linear dimensions at the highest mass ratios considered. Fig. 8 c shows the same qualitative effect for the transverse extension $\langle Y^2 \rangle$, except that $\langle Y^2 \rangle_R / \langle Y^2 \rangle_D$ goes through a maximum near $\mu = 2$.

Some approximate damage and range distributions are plotted in Figs. 9–11. Fig. 9 (damage, $m = \frac{1}{3}$, $\mu = 1$) compares various methods of fitting. Case 1 is the Edgeworth expansion, cases 2 and 3 the linear and quadratic fits, and case 4 the non-gaussian. (In this case the exponent $\beta = 1.49$). For the Edgeworth and non-gaussian cases the heavy line is ψ_0, the initial approximation. In the other two it includes the linear or quadratic polynomial as well. The two to four lightly drawn lines include the first correction terms. The Gram-Charlier expansion is not shown. In it the density
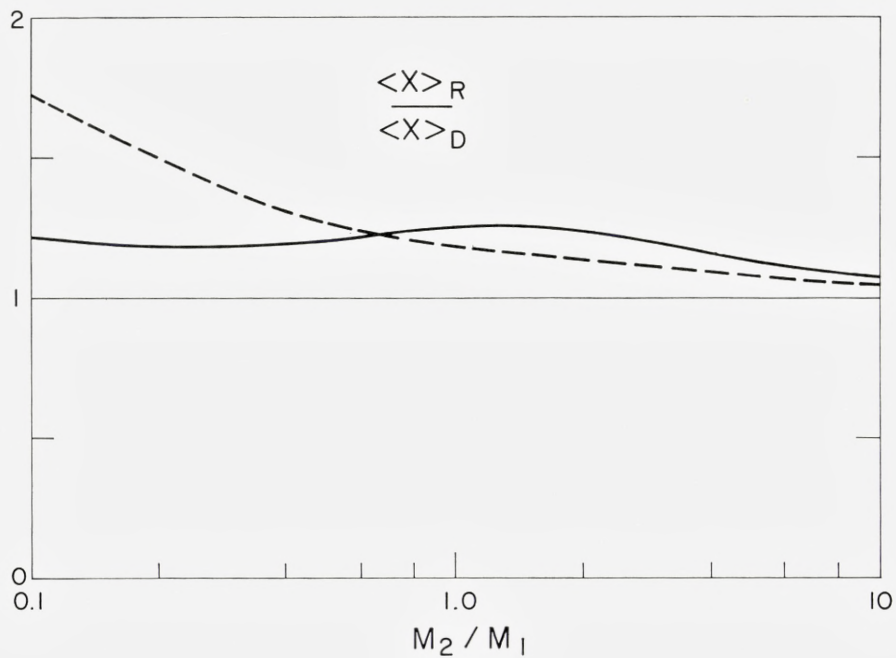
Fig. 8 a.
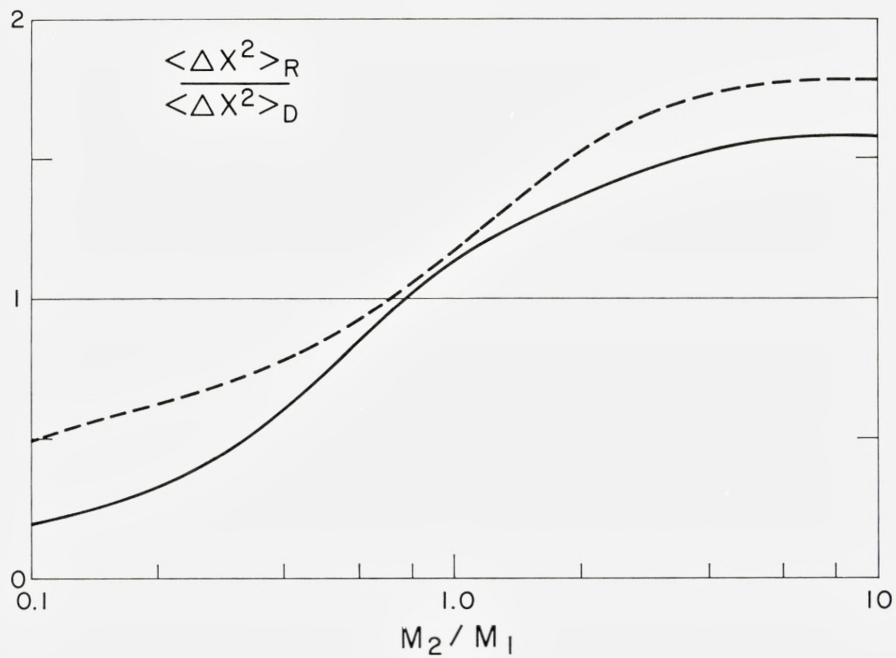
Fig. 8 b.
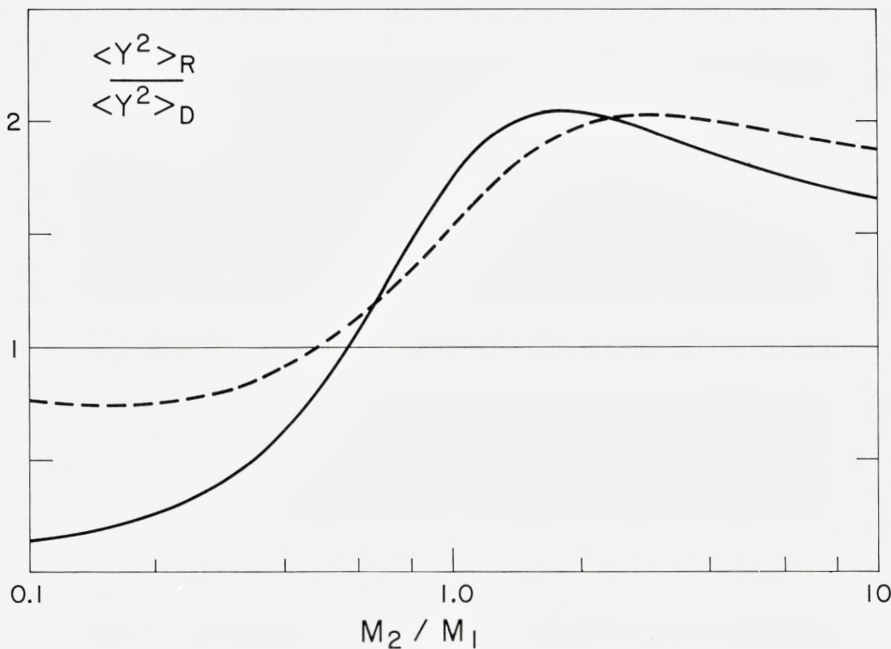
Fig. 8 c.

Fig. 8. Ratio between averages over range and damage distributions as a function of mass ratio. Dashed line, $m = 1/3$; Solid line, $m = 1/2$.

a) First order averages. $\langle X \rangle_R$ = average projected range; $\langle X \rangle_D$ = average damage depth.
b) Second order averages. $\langle \Delta X^2 \rangle_R$ = straggling of projected range; $\langle \Delta X^2 \rangle_D$ = width of the damage depth distribution.
c) Second order averages. $\langle Y^2 \rangle_R$ = transverse straggling of range distribution; $\langle Y^2 \rangle_D$ = transverse width of damage distribution.

had pronounced oscillations, indicating that the fit was poor. In the Edgeworth expansion the minimum outside the surface deepens and approaches the surface as the order of approximation increases, and the tail within the target is not well fitted. In the linear and quadratic fits the tail does not appear to change with the order of approximation and the minimum outside the surface is farther out. Again this minimum moves in with increasing order. The non-gaussian curve, case 4, has a narrower peak because with $\beta = 1.49$, the tails have greater weight.

Range distributions were all fitted well with the Edgeworth expansion, and the exponents β of case 4 were close to 2.

Figure 10 compares damage and range distributions ($m = \frac{1}{2}$). The Edgeworth expansion for damage in 10a ($\mu = 4$) converges reasonably

4*

Fig. 9. Damage distribution as a function of depth. In units of $R(E)$. $m = \frac{1}{3}$, $\mu = 1$. Heavy line, initial approximation Light lines, higher approximations.

1) Edgeworth series.
2) $\psi_0 =$ Gaussian times linear function.
3) $\psi_0 =$ Gaussian times quadratic.
4) Non-gaussian, $\psi_0 = N' \exp(-\lambda |\xi|^\beta)$, $\beta = 1.49$.

well; for $\mu = \frac{1}{4}$ (Fig. 10b) the Edgeworth expansion gave no signs of convergence. The gaussian parameters plotted here were obtained by minimizing

$$c_0^{-2} \sum_{n=0}^{20} c_n^2 (n!)^2.$$

Approximants ψ_0 (the heavy line), ψ_1, ψ_2, and ψ_{20} are plotted.

Figure 11 shows isodensity contours (contour interval 10% of max-. imum density) in the $X-Y$ plane of range and damage for $m = \frac{1}{2}$, $\mu = 1$, The distributions were constructed using the formalism of Appendix C with parameters chosen to minimize

$$c_{00}^{-2} \left(\sum_{m=0}^{20} c_{m0}^2 (m!)^2 + \sum_{n=0}^{10} c_{0n}^2 (2n)! \right).$$

At high densities both distribution functions narrow toward the rear, but at low densities they appear to broaden. The maximum of both distributions occurs closer to the surface than the maximum of the corresponding depth distributions, especially in case of the range plot. This is consistent with increasing lateral spread with increasing depth, as evident from fig. 11.

8. Comparison with Experiment & Computer Simulation

Radiation Damage Measurements

In a previous communication (SIGMUND & SANDERS, 1967) we attempted to compare some results of the theory with experimental radiation damage distributions. Sufficient evidence was found to support one of the main results of the theory, namely that the average damage depth does not differ very much from the average projected ion range (Fig. 8a). There are as yet few experimental results on damage distributions*, and several problems occur when these are compared with theory.

a) Some experimental techniques, such as those based on the orientation dependence of Rutherford scattering (BøGH, 1968), the change in optical reflection (HINES et al., 1960), and the dependence of the sputtering yield on prebombardment (MACDONALD et al., 1966a, b) can be used only on single crystals. Therefore low-dose bombardment may lead to damage distributions that are more or less influenced by channeling effects. High-dose bombardment, on the other hand, leads to saturation effects of bombardment damage and, in some cases, the distributions

---

* Note added in proof: Substantial progress has been made since the submission of this paper. The reader is referred to the Proceedings of an Int. Conf. on Ion Implantation in Semiconductors, Thousand Oaks, Calif., 1970, to be published in Radiation Effects.

M = .5000, M₂/M₁ = 4.000, CASE I, DAMAGE

RANGE

0   1   2
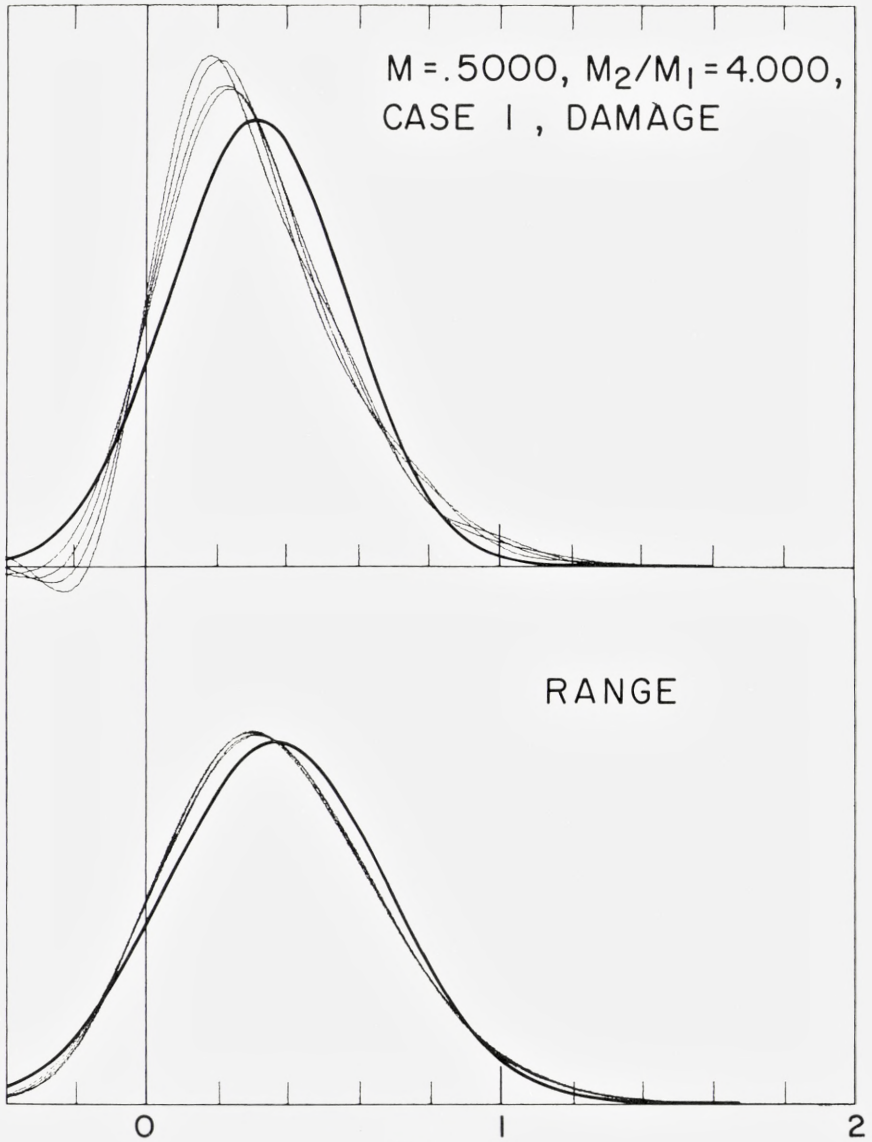
Fig. 10a.

M = .5000,   M$_2$/M$_1$ = $\frac{1}{4}$, CASE I

DAMAGE

RANGE

0   1   2
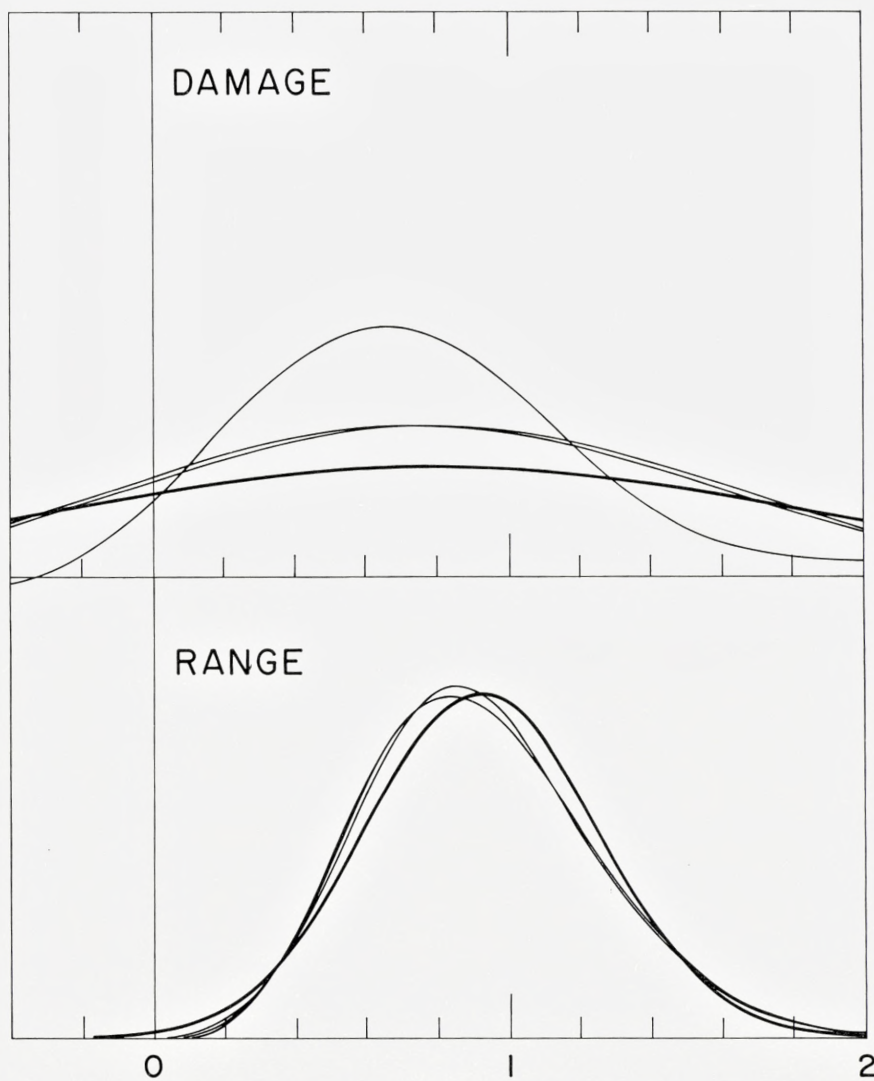
Fig. 10b.

Fig. 10. Damage and Range Distributions. Depth in units of $R(E)$. $m = \frac{1}{2}$. Heavy line, initial approximation. Edgeworth series, except 10b, damage
     Gaussian parameters for damage density in Fig. 10b chosen by minimizing weighted sum of squares of the c_n. Base density ψ_0, ψ_1, ψ_2 and ψ_{20} shown.
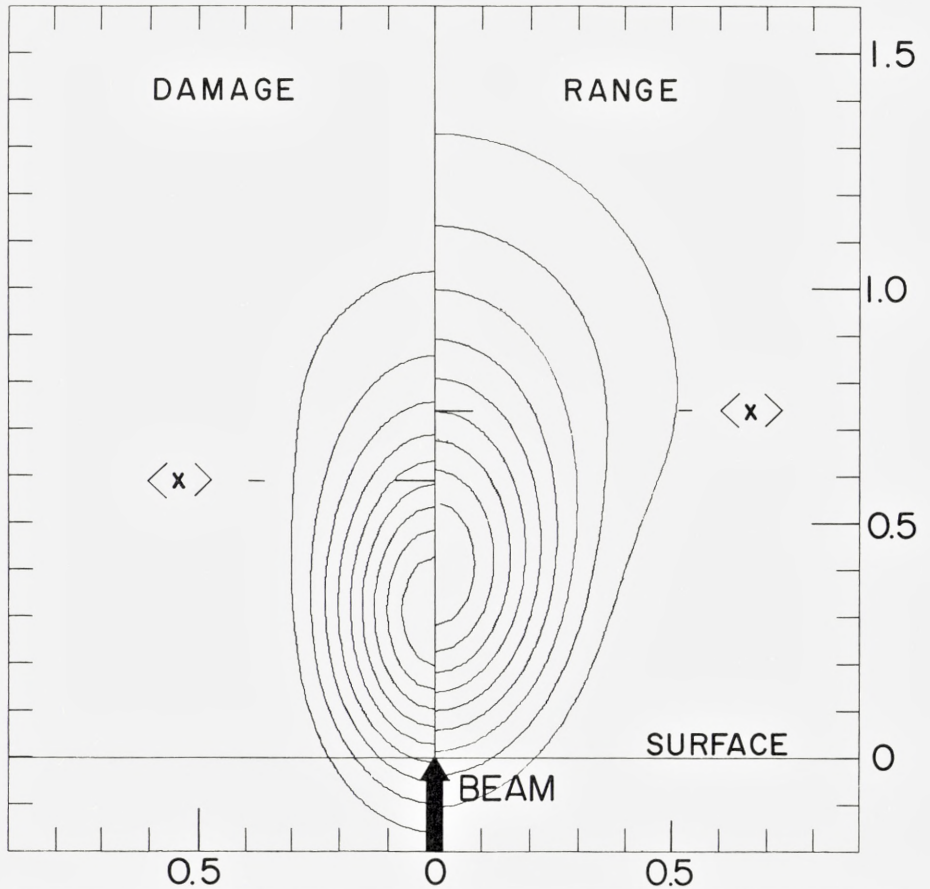
Fig. 11. Damage and Range isodensity Contours. $m = \frac{1}{2}$, $\mu = 1$. Contour interval 10% of maximum. Length in units of $R(E)$.

might change because of radiation-enhanced diffusion. Therefore experiments on single crystals can be used for quantitative comparison only when done at sufficiently low doses to prevent saturation effects and when the ion beam has not been aligned with a channeling direction.

b) Physical properties that are affected by ion bombardment damage may also be affected by implanted ions. The distinction between the ion range and damage distributions appears most direct with the orientation dependence of Rutherford scattering (DAVIES et al., 1967).

c) Electron microscopy of large defects (PARSONS et al., 1964; MERKLE, 1966; THOMAS et al., 1969) leads to results that are not necessarily comparable with the present theory. First, not all deposited energy leads to visible damage. There may be a threshold energy for creating visible damage clusters, the value of which is probably in the keV region but is not accurately known (MERKLE, 1966; THOMAS et al., 1969; HÖGBERG et al., 1969 a, b). Consequently, the region where visible damage is created need not coincide with the actually damaged region. Second, even when polycrystalline samples are irradiated the part of the target that is investigated under the microscope is often a crystallite of definite (low index) orientation, so that channeling may play a role. Third, image-size distributions of damage clusters, which are measured more easily than depth distributions (PARSONS et al., 1964; THOMAS et al., 1969), are not comparable to the quantities discussed in the present paper, since they concern properties of *single* collision cascades.*

With these reservations in mind, we find that none of the existing experimental data can be used for quantitative comparison with our theory. However, depth distribution measurements by use of Rutherford scattering are being performed currently by several groups.** For a more qualitative comparison, we discuss the work of HINES et al. (1960); MACDONALD et al. (1966 a, b), and NORRIS (1969).

HINES et al. bombarded quartz, with keV heavy rare gas ions at doses around 10^{14} ions/cm^2. The effective thickness of the damaged layer was determined from optical reflexion measurements and turned out to be largely independent of ion dose. One would expect, therefore, that neither saturation effects nor diffusion played a significant role. Table IV shows experimental results and several calculated range and damage quantities. The effective layer depth can be estimated from the sum $\{\langle x \rangle + a \langle \Delta x^2 \rangle^{1/2}\}_{\text{damage}}$, where a is a number of the order of 1 to 2. There is good agreement between measured and calculated depths for Ne$^+$ and A$^+$ bombardment, while the calculated depths are much smaller than the measured ones for Kr$^+$ and Xe$^+$ bombardment. This discrepancy is probably caused by channeling of

---

* Note added in proof: Average cluster size is discussed in a forthcoming paper by J. E. WESTMORELAND & P. SIGMUND (Radiation Effects, 1970).

** Note added in proof. In three recent papers on damage-depth distributions measured by Rutherford-scattering, comparison is made with results of the present paper (E. BØGH, P. HØGILD, & I. STENSGAARD, Rad. Eff. 1970; L. C. FELDMAN & J. W. RODGERS, J. Appl. Phys. 1970; F. H. EISEN, B. WELCH, J. E. WESTMORELAND, & J. W. MAYER; Atomic Collision Phenomena in Solids (ed. by D. W. PALMER et al.) North Holland 1970 p. 111). We also refer to a forthcoming paper on depth distributions in the electronic-stopping region by P. SIGMUND, M. T. MATTHIES, & D. L. PHILLIPS.

TABLE IV. Range and Damage Quantities for Quartz Bombarded with Rare Gas Ions. Measured Layer Depth from Measurements of HINES and ARNDT (1960). In the calculations, SiO_2 has been approximated by a monatomic target with the same density, atomic number 10 and atomic weight 20.

Ion	E keV	ε	$\langle X \rangle$ Damage Å	$\langle \Delta X^2 \rangle^{1/2}$ Damage Å	$\langle X \rangle$ Range Å	$\langle \Delta X^2 \rangle^{1/2}$ Range Å	Measured Layer Depth Å
Ne+	38.3	1.14	372	229	450	236	740
($m = 1/2$)	43.9	1.31	428	264	518	272	850
	51.8	1.55	504	310	610	320	950
A+	22.9	0.422	215	150	259	114	600
($m = 1/2$)	38.4	0.706	360	251	434	191	700
	59.0	1.087	554	386	666	293	1000
Kr+	20.3	0.094	84	50	123	41	500
($m = 1/3$)	39.7	0.183	131	78	193	64	600
	59.0	0.272	171	101	251	83	670
Xe+	20.3	0.039	75	43	119	32	470
($m = 1/3$)	39.4	0.075	117	67	185	50	530
	59.0	0.113	154	88	243	65	580

the ions. Note, however, that in pure silicon a dose of 10^{14} Xe+ ions would be sufficient to suppress channeling almost completely (DAVIES et al., 1964).

MacDONALD et al. (1964 a, b) measured the sputtering yield of germanium for low energy A+ ions (100–200 eV) as a function of the sputtered layer thickness. The targets were pre-bombarded with 500–1000 eV rare gas ions, and the sputtering yield was enhanced over the layer thicknesses that corresponded to the penetration depths of the pre-bombarded ions. Typical pre-bombardment doses were 10^{16} to 10^{17} ions/cm², enough to make the target surface amorphous (PARSONS, 1965; MAYER et al., 1968). Also, with a range of about 20 Å the (calculated) dopant concentration is of the order of 1 dopant ion/atom within the penetration depth and, finally, the layer thickness sputtered by the pre-bombardment may well be greater than the range of the ions. All these factors indicate that the measurements can provide only a very rough estimate of the damage and penetration depth of the pre-bombarded ions, and the good agreement with the calculated depths (SIGMUND et al., 1967) confirms this. A distinction between range and damage distributions does not appear feasible.

NORRIS (1969) measured depth distributions of vacancy clusters observed by stereo electron microscopy in gold and nickel bombarded with 80 to

150 keV gold and mercury ions at doses of the order of 10^{15} ions/cm². Channeling of the ions plays a role but does not appear to be dominant, at least not in the target of (112) orientation. The results were compared to measured and calculated ion range distributions (for random slowing down) and it was found that the average depth of vacancy clusters was smaller than one would expect from our Fig. 7a. The difference is not very pronounced, possibly still within the experimental accuracy. Note that less than one cluster is observed per incident ion, and that the average cluster diameter is of the order of the average damage depth.

A similar investigation has been carried out by THOMAS et al. (1969) at lower ion energies (5 to 40 keV) and much smaller ion doses (10^9 to 10^{12} ions/cm²). The measured depth distributions appear to be dominated by channeling and dechanneling of the bombarding ions. A comparison with these results is, therefore, outside the scope of this paper.

Range Measurements

Although a considerable amount of information on range distributions is contained in Tables I–III we do not make a comparison with measured range distributions in this paper. There are several reasons for this. First, ion ranges are not a main subject of this paper. Second, it has been well documented that random-slowing-down theory with the Thomas-Fermi cross section predicts ion ranges accurately (LINDHARD et al., 1963b; SCHIØTT, 1966, 1968). Third, contrary to radiation damage distributions, range distributions can be measured very accurately (for recent reviews see MAYER & MARSH, 1969; MAYER et al., 1969), and for a quantitative comparison an accuracy of at least $10^0/_0$ in calculated average range and straggling is required. Fig. 4b shows that the difference betweem the two representative cases $m = \frac{1}{2}$ and $\frac{1}{3}$ is usually larger than this limit and, more important, electronic stopping is usually not negligible at energies where measurements of high relative accuracy can be made. Some results, however, mainly on very heavy ions in the elastic stopping region, will be compared with experimental results elsewhere (WINTERBON, 1970).

Computer Simulation

Computer simulation has been used occasionally to calculate ion ranges and collision cascades. In the present context we are mainly concerned with Monte-Carlo-type computer codes, where collisions are governed by a cross section. These calculations are essentially equivalent to ours, provided that the cross sections are similar.

TABLE V. Comparison Between Range Quantities Found from Computer Simulation (OEN et al., 1964) and Analytic Calculation (present work).

a) Straggling in Projected Range, $\langle \Delta X^2 \rangle^{1/2} / \langle X \rangle$.

Ion-Target	M_2/M_1	Energy Range (keV)	Computed Straggling	From Fig. 5 $m = 1/2$	From Fig. 5 $m = 1/3$
Xe$^+$ – Al	0.20	5 –250	0.25–0.30	0.33	0.30
K$^+$ – Al	0.64	5 –100	0.42–0.47	0.47	0.50
Cu$^+$ – Cu	1.0	1.75–250	0.47–0.54	0.52	0.59
Kr$^+$ – W	2.16	4.5 –250	0.57–0.63	0.66	0.78

b) Transverse Spread $\langle \varrho^2 \rangle / \langle X^2 \rangle$

Ion-Target	Mass Ratio	Computed	From Fig. 5 $m = 1/2$	From Fig. 5 $m = 1/3$
Xe$^+$ – Al	0.20	0.08	0.07	0.09
K$^+$ – Al	0.64	0.18–0.23	0.18	0.24
Cu$^+$ – Cu	1.0	0.28–0.34	0.27	0.36
Kr$^+$ – W	2.16	0.50–0.56	0.48	0.65

The most extensive study of this type has been done by OEN et al. (1963, 1964), but only range distributions were investigated. It was already pointed out in these papers that *average* ranges calculated for purely elastic scattering agree well with experimental results at sufficiently low ion energies, and also with the range-energy formula of LINDHARD et al. (1963b), in those cases where good agreement is expected. Table V shows a comparison between computed *straggling* data (both longitudinal and transverse) with our analytical results. The computer data are based on Thomas-Fermi interaction with neglect of electronic stopping. Most of the computed straggling parameters depend slightly on energy, because they are not based on a power cross section. One recognizes that this variation with ion energy has about the same magnitude as the difference between our results for $m = \frac{1}{2}$ and $\frac{1}{3}$, and the general agreement is excellent. We made this comparison only to give an indication of the accuracy with which analytical and Monte-Carlo range calculations can agree with each other, provided the input parameters are in close enough agreement. Note that a slight difference is always expected, especially at low energies, since the interaction potential has to be truncated at some finite distance in a Monte-Carlo simulation of binary collision events.

Quite recently, PAVLOV et al. (1967) made a series of Monte-Carlo simulations to get both range and damage depth distributions for several ions implanted in silicon, for applications in ion-implanted semi-conductors. Ion doses were about the same (400–1000 ions for each energy and ion-target combination) as those of OEN et al. Mostly light ions were used in the medium and upper keV region, so that electronic stopping (which was taken into account) dominated. While some runs have been made simulating arsenic ions bombarding silicon, where electronic stopping is only a minor correction at $E \lesssim 50$ keV, damage distributions were not recorded in just these runs. Hence, only a qualitative comparison is possible for the $Al^+ - Si$ bombardments, where the ratio between the median ion range and the median damage depth turned out to decrease from 1.52 to 1.44 from $E = 25$ to 150 keV. This is to be compared with our calculated ratio $\langle x \rangle_R / \langle x \rangle_D = 1.25$ for $\mu \approx 1$ and $m = \frac{1}{2}$ (Fig. 8 a). The difference may be caused by the difference between median and average penetration depths and/or the fact that hard-sphere scattering was assumed in the computations to simulate low-energy collisions. The difference between vacancy and interstitial distributions is considered to be insignificant (SIGMUND et al., 1968).

Backscattering of Ions

A very sensitive check on the validity of calculated range distributions is the backscattering coefficient α of the implanted ions. Preliminary calculations (SIGMUND, 1968) show that α depends very sensitively on the mass ratio μ. The results are in qualitative agreement with experimental data of BROWN et al. (1963). A joint experimental and theoretical effort to establish back-scattering coefficients for a number of ion-target combinations has been started.

Sputtering Measurements

The distribution of deposited energy is a key quantity in the theory of sputtering. First, the amount of energy deposited *outside* a target surface determines the sputtered *energy* (SIGMUND, 1968) and can be measured thermometrically (ANDERSEN, 1968). Second, the energy deposited *in* the target surface is converted into kinetic energy of a number of slowly moving atoms, part of which can get sputtered. The general formula for the sputtering yield is (SIGMUND, 1969 a)

$$S(x, E, \eta) = \Lambda F(x, E, \eta), \qquad (97)$$

where Λ is a material constant, x the distance between the bombarded and the sputtered surface (for backsputtering $x = 0$), E the ion energy and η the cosine of the angle of incidence of the beam. $F(x,E,\eta)$ is the deposited energy distribution for either equal or unequal masses, in the notation of eq. (38).

It was shown that eq. (97) can be used successfully to predict sputtering ratios for a great number of ion-target combinations and to obtain good agreement with experimental results. While extensive use has been made of the results of the present paper in the sputtering work, there is no need for repeating the results here.

In view of recent thermometric measurements of ANDERSEN (1968, 1970), a detailed discussion of the sputtered energy would be desirable. While several qualitative predictions of the theory (SIGMUND, 1968) were confirmed by the experiments, the quantitative agreement is satisfactory for only a limited range of mass ratios. More accurate estimates of the sputtering efficiency on the basis of the results of the present paper will be reported elsewhere (WINTERBON, 1970).

APPENDIX A

Moment Integrals

The first integral in eq. (78) in the equal mass case, has the form

$$I(a,b,l) = \int_0^1 dt\, t^{-1+a}(1-t)^{-1+b} P_l((1-t)^{1/2}) \tag{A1}$$

so that $I(a,b,0) = B(a,b)$, the beta function and $I(a,b,1) = B(a,b+\frac{1}{2})$. Using the Legendre polynominal recurrence relation we find

$$(l+1)I(a,b,l+1) = (2l+1)I(a,b+\tfrac{1}{2},l) - lI(a,b,l-1). \tag{A2}$$

To evaluate the I's from this, the beta functions $B(a,b)$ and $B(a,b+\frac{1}{2})$ are calculated, and from these the quantities $B(a,b+1)$, $B(a,b+\frac{3}{2})$, $B(a,b+2), \ldots$ are obtained using the recursion relation

$$B(a,b+1) = \frac{b}{a+b} B(a,b). \tag{A3}$$

In the unequal-mass case, the first integral is

$$I_\gamma(a,b,l) = \int_0^\gamma dt\, t^{-1+a}(1-t)^{-1+b} P_l((1-t)^{1/2} + \alpha t(1-t)^{-1/2}) \tag{A4}$$

Now $I_\gamma(a,b,o) = B_\gamma(a,b)$, the incomplete beta function. From the Legendre polynominal recurrence relation, and the obvious relation

$$I_\gamma(a,b,l) = I_\gamma(a,b-1,l) - I_\gamma(a+1,b-1,l), \tag{A5}$$

we find

$$\left.\begin{aligned}(l+1)I_\gamma(a,b,l+1) &= (2l+1)[(1-\alpha)I_\gamma(a,b+\tfrac{1}{2},l) + \\ \alpha I_\gamma(a,b-\tfrac{1}{2},l)] &- lI_\gamma(a,b,l-1).\end{aligned}\right\} \tag{A6}$$

The required values of the incomplete beta function are generated from the initial values $B_\gamma(a,b), B_\gamma(a,b+\frac{1}{2})$ with the recursion relation

$$\left.\begin{aligned}B_\gamma(a,b+1) &= \gamma^a(1-\gamma)^b/(a+b) + bB_\gamma(a,b)/(a+b) \\ (b &\neq 0)\end{aligned}\right\} \tag{A7}$$

(this may be derived by integration by parts and using $B_\gamma(a,b+1) = B_\gamma(a,b) - B_\gamma(a+1,b)$ and, if necessary, $B_\gamma(a,o) = \frac{\gamma^a}{a} F(1,a;a+1;\gamma)$, where F is the hypergeometric function.

The second integral in eq. (78) is essentially the same in both equal-mass and unequal-mass cases:

$$K_l{}^n(a) = \int_0^1 dt\, t^{a-1} P_l(t^{1/2}) = 2 \int_0^1 dx\, x^{2a-1} P_l(x).$$ (A8)

From ERDELYI et al. (1954), p. 313, we have

$$K_l = \frac{2\pi^{1/2}\Gamma(2a)}{2^{2a}\,\Gamma\!\left(a + \dfrac{1-l}{2}\right)\Gamma(a+1+l/2)}.$$ (A9)

We use the duplication formula for Γ-functions, (ABRAMOWITZ & STEGUN, 1964),

$$\Gamma(2a) = 2^{2a-1}\pi^{-1/2}\Gamma(a)\,\Gamma(a + \tfrac{1}{2}),$$

to get

$$K_l(a) = \frac{\Gamma(a)\,\Gamma(a+1/2)}{\Gamma\!\left(a + \dfrac{1-l}{2}\right)\Gamma(a+1+l/2)}$$ (A10)

from which

$$K_0(a) = 1/a$$

$$K_1(a) = 1/(a + \tfrac{1}{2})$$

and

$$K_{l+2}(a) = \frac{a - (l+1)/2}{a + 1 + l/2}\, K_l(a).$$ (A11)

APPENDIX B

Expansions of the Distributions

In this paragraph we derive the coefficients for expansion of depth distribution functions in terms of Hermite or more general orthogonal polynomials. Let the (unknown) distribution function be $F(x)$, and introduce the new variable

$$\xi = \alpha(x - a),$$ (B1)

so we can write

$$F(x) \equiv f(\xi) = \psi(\xi) \sum_{m=0}^{\infty} c_m He_m(\xi),$$ (B2)

where

$$\psi(\xi) = (2\pi)^{-1/2}\exp(-\xi^2/2).$$ (B3)

We still have the freedom of choosing the parameters α and a in (B1).

We wish to express the c_m in terms of the moments v_r of F,

$$v_r = \int_{-\infty}^{\infty} dx\, x^r F(x). \tag{B4}$$

Using the orthogonality of the Hermite polynomials we have

$$
\left.
\begin{aligned}
n!\,c_n &= \int d\xi He_n(\xi) f(\xi)\\[4pt]
&= \alpha \int dx He_n(\alpha(x-a)) F(x)\\[4pt]
&= \alpha \sum_{m=0}^{[n/2]} \frac{n!(-)^m \alpha^{n-2m}}{m!\,2^m(n-2m)!} \sum_{r=0}^{n-2m} \binom{n-2m}{r} (-a)^{n-2m-r} \int dx\, x^r F(x)
\end{aligned}
\right\} \tag{5B}
$$

The integral is v_r. Interchanging the order of summation and recognizing the inner sum as a Hermite polynomial, we have

$$c_n = \frac{\alpha}{n!} \sum_{r=0}^{n} \binom{n}{r} \alpha^r v_r He_{n-r}(-a\alpha). \tag{B6}$$

The conditions $c_i = 0$ reduce to the following:

c_1: $a - v_1 = 0$

c_2: $(a^2 - 2av_1 + v_2)\alpha^2 - 1 = 0$

c_3: $(a^3 - 3a^2v_1 + 3av_2 - v_3)\alpha^2 - 3(a - v_1) = 0$

c_4: $\alpha^4(a^4 - 4a^3v_1 + 6a^2v_2 - 4av_3 + v_4) - 6\alpha^2(a^2 - 2av_1 + v_2) + 3 = 0.$

In the usual Gram-Charlier expansion one chooses $c_1 = c_2 = 0$ and therefore $a = v_1$ and $\alpha = b^{-1/2}$, where $b = v_2 - v_1^2$. In the $c_2 = c_3 = 0$ case,

$$a = v_1 + (d/2)^{1/3}, \quad \text{and}$$

$$\alpha^{-2} = b + (d/2)^{2/3},$$

where

$$d = v_1^3 + 3bv_1 - v_3.$$

In the $c_3 = c_4 = 0$ case,

$$
\left.
\begin{aligned}
a &= v_1 + (d/2)^{1/3} - z, \quad \text{and}\\[4pt]
\alpha^{-2} &= b + (d/2)^{2/3} + e, \quad \text{say,}
\end{aligned}
\right\} \tag{B7}
$$

where

$$e = z^2((d/2)^{1/3} + z/3)/((d/2)^{1/3} + z)$$

and z is a root of

$$h(1+z)^2 - 2z^3(d/2)^{4/3}(4 + 5z + 2z^2 + z^3/3) = 0 \tag{B7a}$$

with $h = v_4 - 4v_3v_1 - 3v_2^2 + 12v_2v_1^2 - 6v_1^4 + 6(d/2)^{4/3}.$

There are two real roots of (B7a), only one of which is useful.

Consider now a non-gaussian distribution:
Let

$$\psi(\xi) = N' \exp(-\lambda|\xi|^\beta). \tag{B8}$$

The moments of ψ are ($\nu = (2n+1)/\beta$)

$$\left.\begin{aligned}
M_{2n} &= \int_{-\infty}^{\infty} d\xi\, \xi^{2n} \psi = \frac{2N'}{\beta} \frac{\Gamma(\nu)}{\lambda^\nu} \\
M_{2n+1} &= 0.
\end{aligned}\right\} \tag{B9}$$

We take $N' = \beta\lambda^{1/\beta}/2\Gamma(1/\beta)$, so that $M_0 = 1$. We can again write the density as

$$f(\xi) = \sum_{m=0}^{\infty} c_n H_n(\xi)\psi,$$

where the $H_n(\xi)$ are a set of polynomials orthogonal on $(-\infty,\infty)$, with the weight function $\psi(\xi)$, chosen so that

$$\left.\begin{aligned}
H_0 &= 1, \\
H_1 &= \xi, \\
H_{n+1} &= \xi H_n - r_n H_{n-1}.
\end{aligned}\right\} \tag{B10}$$

The recurrence coefficients r_n are equal to quotients of Gram determinants, as discussed in ERDELYI et al., 1963.

The norm of the polynomials H_n is (ERDELYI et al., 1963)

$$\int d\xi\, H_n^2(\xi)\psi(\xi) = \prod_{i=1}^{n} r_i \int d\xi\, \psi(\xi) = \prod_{i=1}^{n} r_i. \tag{B11}$$

Write

$$H_n(\xi) = \sum_{m=0}^{[n/2]} h_m{}^n \xi^{n-2m};$$

from (B10) we have

$$h_m{}^n = 0, \quad m < 0 \quad \text{or} \quad m > n/2$$

$$h_0{}^n = 1$$

$$h_m^{n+1} = h_m{}^n - r_n h_{m-1}^{n-1},$$

so that

$$h_m{}^n = (-)^m \sum_{i_m=2m-1}^{n-1} \sum_{i_{m-1}=2m-3}^{i_m-2} \cdots \sum_{i_1=1}^{i_2-2} r_{i_m} \cdots \cdots r_{i_1}. \tag{B12}$$

The expression for the c_n cannot be expressed as concisely as in the gaussian case. Proceeding as before, we obtain

$$\left(\prod_{i=1}^{n} r_i\right) c_n = \alpha \sum_{m=0}^{[n/2]} h_m{}^n \alpha^{n-2m} y_{n-2m}, \tag{B13}$$

where

$$y_n = \sum_{i=0}^{n} \binom{n}{i} (-a)^{n-i} \nu_i. \tag{B14}$$

We now have three parameters, a, β, and $\lambda \alpha^\beta$. λ may without loss of generality be chosen to satisfy some criterion of computational ease, but should reduce to $\lambda = \frac{1}{2}$ for $\beta = 2$; in all the calculations done here, λ was chosen so that $r_1 = 1$.

The distribution ψ_0 is unskewed, so we can not demand that $c_1 = c_3 = 0$, or, more generally, that any two odd coefficients vanish simultaneously.

The only fitting that has been done is the simplest case,

$$c_1 = c_2 = c_4 = 0.$$

These conditions are

$$c_1: \quad y_1 = 0 \tag{B15a}$$

$$c_2: \quad \alpha^2 y_2 - r_1 = 0 \tag{B15b}$$

$$c_4: \quad \alpha^4 y_4 - (r_1 + r_2 + r_3)\alpha^2 y_2 + r_1 r_3 = 0, \tag{B15c}$$

so that

$$\frac{r_2}{r_1} = \frac{y_4}{y_2^2} - 1, \tag{B16}$$

with

$$r_2/r_1 = \Gamma(1/\beta)\Gamma(5/\beta)/\Gamma^3(3/\beta), \quad \text{from (B14)}. \tag{B16a}$$

We want also the integral of f outside the target:

$$\int_{-\infty}^{0} dx f(x) = \frac{1}{\alpha} \int_{-\infty}^{-a\alpha} d\xi \sum_{n=0}^{\infty} c_n H_n(\xi)\psi = \frac{1}{\alpha} \sum_{n=0}^{\infty} c_n \sum_{m=0}^{[n/2]} h_m{}^n I_{n-2m} \tag{B17}$$

where

$$I_n = \int_{-\infty}^{-a\alpha} d\xi \, \xi^n N' e^{-\lambda|\xi|^\beta} = \frac{(-1)^n \Gamma(n+1/\beta, \lambda(a\alpha)^\beta)}{2\Gamma(1/\beta)\lambda^{n/\beta}} \tag{B17a}$$

and the Γ in the numerator is the incomplete gamma function (ABRAMOWITZ & STEGUN, 1964).

APPENDIX C

Point-Source distributions

For a point source the distribution function can be studied in three dimensions. We begin by comparing moments of the distribution in various co-ordinate systems (Fig. 12). We have been calculating the moments

$$\nu_n = \int dx \, dy \, dz \, x^n F(\vec{r}), \tag{C1}$$
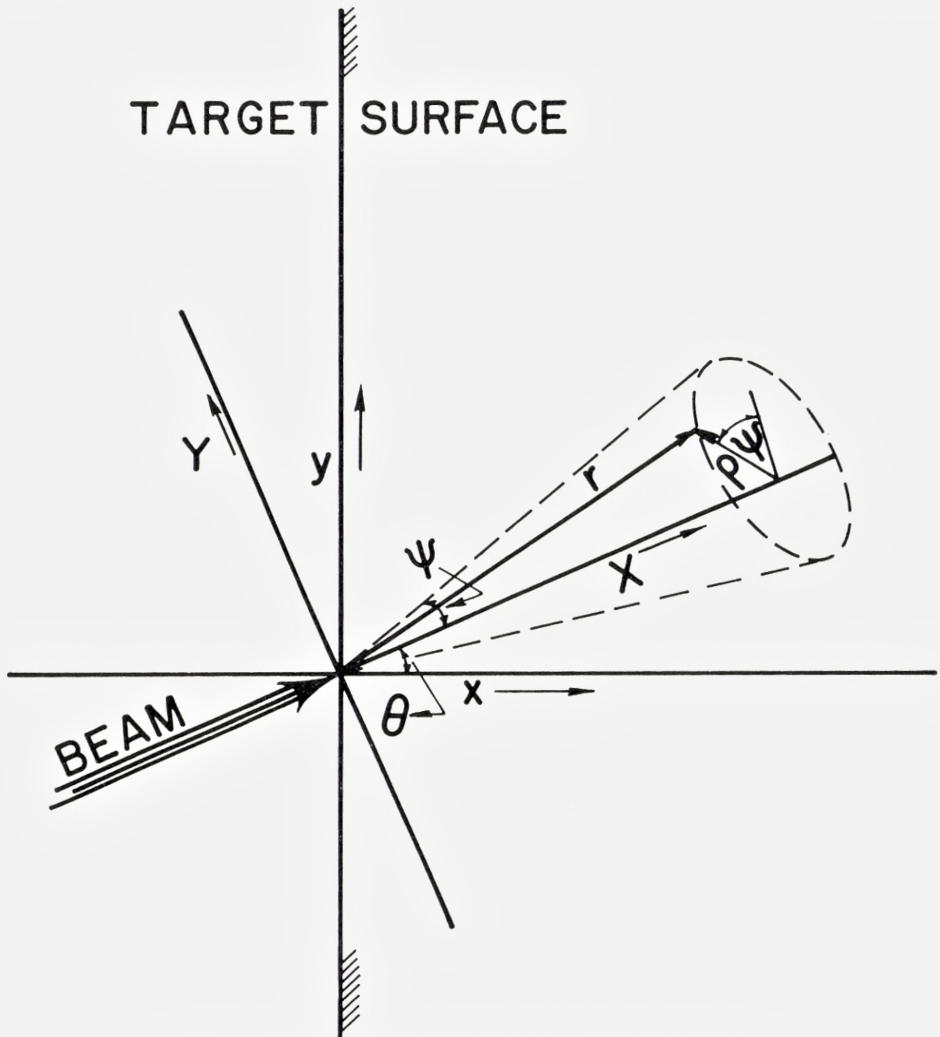
Fig. 12. Plane-source and Point-source coordinates (see text).

dropping the velocity variable $\vec{v}$ for the moment. We have written (C1) as a Legendre polynomial series in the angle θ between beam and surface normal:

$$\nu_n = \nu_n(\theta) = \sum (2l + 1) A_l^n P_l(\cos\theta) = \sum_{m=0}^{[n/2]} (2n - 4m + 1) A_{n-2m}^n P_{n-2m}(\cos\theta) \quad (C2)$$

Moments in the following beam-centred coordinate systems are also used:

1) rectangular coordinates XYZ:

$$f_{n,2m,2l} = \int dX dY dZ X^n Y^{2m} Z^{2l} F(\vec{r}) \qquad (C3)$$

2) cylindrical coordinates X, ϱ, ψ:

$$\omega_{n,2m} = 2\pi \int dX d\varrho \varrho X^n \varrho^{2m} F(\vec{r}) \qquad (C4)$$

3) spherical coordinates r, φ, ψ:

$$f_m{}^n = 2\pi \int dr r^2 d(\cos\varphi) r^n P_m(\cos\varphi) F(\vec{r}). \qquad (C5)$$

One relation is trivial:

$$f_{n,2m,2l} = \frac{\binom{2m}{m}\binom{2l}{l}}{2^{2m+2l}\binom{m+1}{m}} \omega_{n,2m+2l}. \qquad (C6)$$

Another is given by BERGER and SPENCER (1959); in our notation,

$$f_{n-2m,2m,0} = \frac{1}{\binom{n}{2m}} \sum_{l=0}^{[n/2]} (2n-4l+1) A^n_{n-2l} \beta_{nml}. \qquad (C7)$$

By similar methods one can show

$$A^n_{n-2m} = \sum_{l=0}^{[n/2]} \binom{n}{2l} f_{n-2l,2l,0} \alpha_{nml}, \qquad (C8)$$

$$\omega_{n-2m,2m} = \sum_{l=0}^{[n/2]} f^n_{n-2l}(2n-4l+1)\alpha_{nlm} \qquad (C9)$$

$$f^n_{n-2m} = \sum_{l=0}^{[n/2]} \omega_{n-2l,2l} \beta_{nlm}, \qquad (C10)$$

and

$$A^n_{n-2m} = \sum_{l=0}^{[n/2]} (2n-4l+1) f^n_{n-2l} \sum_{k=0}^{[n/2]} \alpha_{nmk} \alpha_{nlk}, \qquad (C11)$$

where we have written

$$\alpha_{nml} = 2^{n-2m} \sum_{k=0}^{k_1} \binom{l}{k} \frac{(-)^{l-k}(n-2k)!(n-m-k)!}{(m-k)!(2n-2m-2k+1)!} \qquad (C12)$$

and

$$\beta_{nml} = \frac{1}{2^{n-2l}} \sum_{k=k_0}^{[n/2]} \binom{k}{m} \frac{(-)^{k-l}(2n-2l-2k)!}{(k-l)!(n-l-k)!(n-2k)!}, \qquad (C13)$$

with k_0 equal to the larger, and k_1 the smaller, of m and l.

From these moments, for example the $\omega_{n,2j}$, we can construct the density in three dimensions, as in Fig. 11, in much the same way as was done in one dimension.

References

M. ABRAMOWITZ & I. A. STEGUN, 1964. Handbook of Mathematical Functions. Nat. Bur. Stand., Washington, D.C.

H. H. ANDERSEN, 1968. The Energy Efficiency of Lead Self-Sputtering, Appl. Phys. Letters, **13**, 85.

H. H. ANDERSEN, 1970. The Sputtering Efficiency of Polycrystalline Solids. Rad. Eff. **3**, 51,

E. M. BAROODY, 1964. Stopping by Elastic Collisions of Particles from a Unidirectional Plane Source. J. Appl. Phys. **35**, 2074.

E. M. BAROODY, 1965. Influence of Anisotropic Scattering on Stopping by Elastic Collisions. J. Appl. Phys. **36**, 3565.

E. M. BAROODY, 1969. Stopping by Elastic Collisions of Kilovolt Ions in Gaseous Mixtures and Amorphous Compounds. J. Appl. Phys. **40**, 2555.

M. J. BERGER & L. V. SPENCER, 1959. General Relation Between Fluxes from Collimated Point and Plane Sources of Radiation. Phys. Rev. **113**, 408.

E. BØGH, 1968. Defect Studies by Means of Channeling. Can. J. Phys. **46**, 653.

N. BOHR, 1948. The Penetration of Atomic Particles Through Matter. Mat. Fys. Medd. Dan. Vid. Selsk. **18**, No. 8.

D. K. BRICE, 1969. Implantation Depth Distributions: Energy Deposition into Atomic Processes and Ion Locations. Appl. Phys. Lett.. **16,** 103.

F. BROWN & J. A. DAVIES, 1963. The Effect of Energy and Integrated Flux on the Retention and Range of Inert Gas Ions Injected at keV Energies in Metals. Can. J. Phys. **41**, 844.

A. CORCIOVEI, G. GHIKA, & D. GRECU, 1962. La Fonction de Distribution des Atomes Déplacés dans un Solide Produits par des Irradiations. Rev. de Physique ((Bucharest) **7**, 227.

A. CORCIOVEI, A. BABCENKO, & D. GRECU, 1963. Fonction de Distribution des Atomes Interstitiels et des Lacunes d'une Cascade de Déplacements produite par Irradiation. Rev. de Physique (Bucharest) **8**, 445.

A. CORCIOVEI & M. CROITORU, 1966. Integral Equation for the Distribution of Interstitial Atoms of a Cascade Produced by Irradiation. Rev. Roum. Phys. **11**, 317.

H. CRAMÉR, 1945. Mathematical Methods of Statistics, Princeton, University Press.

J. A. DAVIES, G. C. BALL, F. BROWN, & B. DOMEIJ, 1964. Range of Energetic ^{125}Xe Ions in Monocrystalline Silicon. Can. J. Phys. **42**, 1070.

J. A. DAVIES, J. DENHARTOG, L. ERIKSSON, & J. W. MAYER, 1967. Ion Implantation of Silicon. I. Atom Location on Lattice Disorder by Means of 1.0 MeV Helium Ion Scattering. Can. J. Phys. **45**, 4053.

P. H. DEDERICHS, 1965. Die räumliche Struktur einer Defektkaskade im Gasmodell. Phys. Stat. Sol. **10**, 303.

P. H. DEDERICHS, G. LEIBFRIED, & K. MIKA, 1966. Näherungslösungen einer Boltzmann-Gleichung für Primäratome und Defekte. Nukleonik **8**, 80.

A. ERDELYI, W. MAGNUS, F. OBERHETTINGER, & F. G. TRICOMI, 1953. Higher Transcendental Functions, Vol. II, Chapter X, McGraw-Hill, New York.

A. Erdelyi, W. Magnus, F. Oberhettinger, & F. G. Tricomi, 1954. Tables of Integral Transforms, Vol. II, McGraw-Hill, New York.

R. M. Felder & M. D. Kostin, 1966. Energy Distribution of Energetic Atoms in an Irradiated Medium. II. Single Species Case: Application to Radiation Damage Calculations. J. Appl. Phys. **37**, 791.

W. Feller, 1966. An Introduction to Probability Theory and its Applications, Vol. II, Wiley, New York.

R. L. Hines & R. Arndt, 1960. Radiation Effects of Bombardement of Quartz & Vitreous Silica by 7.5 keV to 59 keV Positive Ions, Phys. Rev. **119**, 623.

G. Högberg & H. Nordén, 1969a. Damage in Gold Bombarded with Medium Mass Ions. Forskningsrådens Laboratorium, Studsvik, Sweden. Unpublished Report LF-24.

G. Högberg & H. Nordén, 1969b. The Energy Dependence of Krypton Ion Damage in Gold. Phys. Stat. Sol. **33**, K 71.

D. K. Holmes & G. Leibfried, 1960. Range of Radiation Induced Primary Knock-ons in the Hard Core Approximation. J. Appl. Phys. **31**, 1046.

R. v. Jan, 1964. Defektverteilung in Verlagerungskaskaden. I. Phys. Stat. Sol. **6**, 925.

M. G. Kendall & A. Stuart, 1958. The Advanced Theory of Statistics, Vol. I, Griffin, London.

M. D. Kostin, 1965. Energy Distribution of Energetic Atoms in an Irradiated Medium. J. Appl. Phys. **36**, 850.

C. Lehmann, 1961. Zur Bildung von Defektkaskaden in Kristallen beim Beschuss mit energiereichen Teilchen. Nukleonik **3**, 1.

G. Leibfried, 1962. Calculation of Averages for Primary Recoil Distributions. J. Appl. Phys. **33**, 1933.

G. Leibfried, 1963. Higher Order Averages of Primary Recoil Distributions. Z. Physik **171**, 1.

G. Leibfried & K. Mika, 1965. Boltzmann-Gleichungen für die Verteilung von Primäratomen. Nukleonik **7**, 309.

J. Lindhard & M. Scharff, 1961. Energy Dissipation by Ions in the keV Region, Phys. Rev. **124**, 128.

J. Lindhard, V. Nielsen, M. Scharff, & P. V. Thomsen, 1963a. Integral Equations Governing Radiation Effects (Notes on Atomic Collisions III). Mat. Fys. Medd. Dan. Vid. Selsk. **33**, No. 10.

J. Lindhard, M. Scharff, & H. E. Schiøtt, 1963b. Range Concepts & Heavy Ion Ranges (Notes on Atomic Collisions II). Mat. Fys. Medd. Dan. Vid. Selsk. **33**, No. 14.

J. Lindhard, V. Nielsen, & M. Scharff, 1968. Approximation Method in Classical Scattering by Screened Coulomb Fields (Notes on Atomic Collisions I). Mat. Fys. Medd. Dan. Vid. Selsk. **36**, No. 10.

R. J. MacDonald & D. Haneman, 1966a. Depths of Low-Energy Ion Bombardment Damage in Germanium. J. Appl. Phys. **37**, 1609.

R. J. MacDonald & D. Haneman, 1966b. Low-Energy-Ion-Bombardment Damage in Germanium. J. Appl. Phys. **37**, 3048.

J. W. Mayer, L. Eriksson, S. T. Picraux, & J. A. Davies, 1968. Ion Implantation of Silicon & Germanium at Room Temperature. Analysis by Means of 1.0 – MeV Helium Ion Scattering. Can. J. Phys. **46**, 663.

J. W. Mayer, L. Eriksson, & J. A. Davies, 1969. Ion Implantation of Semi-
    conductors; Academic Press, New York

J. W. Mayer & O. J. Marsh, 1969. Ion Implantation in Semiconductors, Applied
    Solid State Science **1**, 239.

K. L. Merkle, 1966. Radiation-Induced Point Defect Clusters in Copper & Gold.
    I. Clusters Produced in Energetic Displacement Cascades, Phys. Stat. Sol. **18**,
    173.

K. O. Nielsen, 1956. The Range of Atomic Particles with Energies about 50 keV,
    in "Electromagnetically Enriched Isotopes & Mass Spectrometry", Acad. Press,
    New York, p. 68.

D. I. R. Norris, 1969. Depth Distributions of Vacancy Clusters in Ion Bombarded
    Gold & Nickel. Phil. Mag. **19**, 653.

O. S. Oen, D. K. Holmes, & M. T. Robinson, 1963. Ranges of Energetic Atoms
    in Solids, J. Appl. Phys. **34**, 302.

O. S. Oen & M. T. Robinson, 1964. Monte Carlo Range Calculations for a Thomas-
    Fermi Potential, J. Appl. Phys. **35**, 2515.

J. R. Parsons, 1965. Conversion of Crystalline Germanium to Amorphous Ger-
    manium by Ion Bombardment. Phil. Mag. **12**, 1159.

J. R. Parsons & R. W. Balluffi, 1964. Displacement Spike Crystallization of
    Amorphous Germanium during Irradiation. J. Phys. Chem. Solids **25**, 263.

P. V. Pavlov, D. I. Tetel'baum, E. I. Zorin, & V. I. Alekseev, 1966. Distribution
    of Implanted Atoms and Radiation Defects in the Ion Bombardment of Silicon
    (Monte Carlo Method). Fizika Tverdogo Tela **8**, 2679 (Engl. Transl. in Sov.
    Phys. Solid State **8**, 2141 (1967)).

J. S. Pringle, 1968. Private Communication.

M. T. Robinson, 1965a. The Influence of the Scattering Law on the Radiation
    Damage Displacement Cascade. Phil. Mag. **12**, 741.

M. T. Robinson, 1965b. The Energy Spectra of Atoms Slowing Down in Structure-
    less Media. Phil. Mag. **12**, 145.

J. B. Sanders, 1966. Recoil Numbers in Crystalline Structures. Physica **32**, 2197.

J. B. Sanders, 1968a. Ranges of Projectiles in Amorphous Materials. Can. J. Phys.
    46, 455.

J. B. Sanders, 1968b. On Penetration Depths & Collision Cascades in Solid Ma-
    terials. Thesis, University of Leiden.

J. B. Sanders, 1969. On the Spatial Distribution of Recoil Atoms, Created in a
    Collision Cascade in Crystalline Material. Physica **41**, 353.

L. I. Schiff, 1955. Quantum Mechanics, McGraw-Hill, New York.

H. E. Schiøtt, 1966. Range-Energy Relations for Low-Energy Ions. Mat. Fys.
    Medd. Dan. Vid. Selsk. **35**, No. 9.

H. E. Schiøtt, 1968. Projected Ranges of Light Ions in Heavy Substances. Can.
    J. Phys. **46**, 449.

P. Sigmund & J. B. Sanders, 1967. Spatial Distribution of Energy Deposited by
    Ionic Bombardment. Proc. Int. Conf. on Application of Ion Beams to Semi-
    conductor Technology, ed. P. Glotin, Editions Ophrys, p. 215.

P. Sigmund, G. P. Scheidler, & G. Roth, 1968. Spatial Distribution of Defects
    in Cascades. Black Spot Defects in Electron-Bombarded Copper. Proc. Conf.
    on "Solid State Research with Accelerators", ed. A. N. Goland, BNL-50083
    (C-52), p. 374.

P. Sigmund, 1968. Sputtering Efficiency of Amorphous Substances. Can. J. Phys.
    46, 731.

P. Sigmund, 1969a. Theory of Sputtering I. Sputtering Yield of Amorphous & Polycrystalline Targets. Phys. Rev. **184**, 383.

P. Sigmund, 1969b. A Note on Integral Equations of the Kinchin-Pease Type. Rad. Eff. **1**, 15.

P. Sigmund, 1969c. On the Number of Atoms Displaced by Implanted Ions or Energetic Recoil Atoms. Appl. Phys. Letters, **14**, 114.

L. E. Thomas, T. Schober, & R. W. Balluffi, 1969. Defects Observed by Electron Microscopy in Gold Bombarded with Gold Ions. I–III. Rad. Eff. **1**, 257, 269, & 279.

K. B. Winterbon, 1970. To be published.

K. B. Winterbon*
Chalk River Nuclear Laboratories
Chalk River, Ontario, Canada.

Peter Sigmund†*
Argonne National Laboratory
Argonne, Illinois, U.S.A.

J. B. Sanders*
F.O.M. Institute for Atomic & Molecular Physics
Amsterdam, Netherlands.

† Work performed under the auspices of the U.S. Atomic Energy Commission.
* Present address: Institute of Physics, University of Aarhus, Denmark.